On the role of the carbohydrate vs the lipid moieties in neoglycolipid self-organisation : Synthesis and liquid crystalline properties of two new families of carbohydrate-based amphiphiles

Rui Xu

▶ **To cite this version:**

Rui Xu. On the role of the carbohydrate vs the lipid moieties in neoglycolipid self-organisation : Synthesis and liquid crystalline properties of two new families of carbohydrate-based amphiphiles. Other. INSA de Lyon, 2013. English. NNT : 2013ISAL0001 . tel-00940381

HAL Id: tel-00940381

https://theses.hal.science/tel-00940381

Submitted on 31 Jan 2014

HAL is a multi-disciplinary open access archive for the deposit and dissemination of scientific research documents, whether they are published or not. The documents may come from teaching and research institutions in France or abroad, or from public or private research centers.

L'archive ouverte pluridisciplinaire **HAL**, est destinée au dépôt et à la diffusion de documents scientifiques de niveau recherche, publiés ou non, émanant des établissements d'enseignement et de recherche français ou étrangers, des laboratoires publics ou privés.

THESE

Présentée devant

L'INSTITUT NATIONAL DES SCIENCES APPLIQUEES DE LYON

Pour l'obtention du
DIPLOME DE DOCTORAT

Ecole Doctorale de Chimie de Lyon
Spécialité Chimie

Par

XU Rui

Sur le rôle de la partie glucidique ou de la partie lipidique dans l'auto-organisation des neoglycolipides : Synthèse de deux nouvelles familles de glycoamphiphiles et étude de leur comportement liquide cristallin

On the role of the carbohydrate vs the lipid moieties in neoglycolipid self-organisation: synthesis and liquid crystalline properties of two new families of carbohydrate-based amphiphiles

Directeur de thèse	Co-directeur de thèse
Dr. Yves QUENEAU	**Dr. Stéphane CHAMBERT**

Jury :

M. Bruno ANDRIOLETTI, Professeur à l'Université Claude Bernard-Lyon 1	**Examinateur**
M. Jacques AUGE, Professeur à l'Université de Cergy-Pontoise	**Rapporteur**
M. Grahame MACKENZIE, Professeur à l'Université de Hull, Royaume Uni	**Rapporteur**
M. Stéphane CHAMBERT, Maitre de Conférences à l'INSA de Lyon	**Invité**
M. Yves QUENEAU, Directeur de Recherche CNRS à l'INSA de Lyon	**Examinateur**

Cette thèse est accessible à l'adresse : http://theses.insa-lyon.fr/publication/2013ISAL0001/these.pdf
© [R. Xu], [2013], INSA de Lyon, tous droits réservés

Cette thèse est accessible à l'adresse : http://theses.insa-lyon.fr/publication/2013ISAL0001/these.pdf
© [R. Xu], [2013], INSA de Lyon, tous droits réservés

INSA Direction de la Recherche - Ecoles Doctorales – Quinquennal 2011-2015

*ScSo : Histoire, Geographie, Aménagement, Urbanisme, Archéologie, Science politique, Sociologie, Anthropologi

SIGLE	ECOLE DOCTORALE	NOM ET COORDONNEES DU RESPONSABLE
CHIMIE	**CHIMIE DE LYON** **http://www.edchimie-lyon.fr** Insa : R. GOURDON	M. Jean Marc LANCELIN Université de Lyon – Collège Doctoral Bât ESCPE 43 bd du 11 novembre 1918 69622 VILLEURBANNE Cedex Tél : 04.72.43 13 95 directeur@edchimie-lyon.fr
E.E.A.	**ELECTRONIQUE, ELECTROTECHNIQUE, AUTOMATIQUE** **http://edeea.ec-lyon.fr** Secrétariat : M.C. HAVGOUDOUKIAN eea@ec-lyon.fr	M. Gérard SCORLETTI Ecole Centrale de Lyon 36 avenue Guy de Collongue 69134 ECULLY Tél : 04.72.18 60 97 Fax : 04 78 43 37 17 Gerard.scorletti@ec-lyon.fr
E2M2	**EVOLUTION, ECOSYSTEME, MICROBIOLOGIE, MODELISATION** **http://e2m2.universite-lyon.fr** **Insa : H. CHARLES**	Mme Gudrun BORNETTE CNRS UMR 5023 LEHNA Université Claude Bernard Lyon 1 Bât Forel 43 bd du 11 novembre 1918 69622 VILLEURBANNE Cédex Tél : 04.72.43.12.94 e2m2@biomserv.univ-lyon1.fr
EDISS	**INTERDISCIPLINAIRE SCIENCES-SANTE** **http://ww2.ibcp.fr/ediss** Sec : Safia AIT CHALAL Insa : M. LAGARDE	M. Didier REVEL Hôpital Louis Pradel Bâtiment Central 28 Avenue Doyen Lépine 69677 BRON Tél : 04.72.68 49 09 Fax :04 72 35 49 16 Didier.revel@creatis.uni-lyon1.fr
INFOMATHS	**INFORMATIQUE ET MATHEMATIQUES** **http://infomaths.univ-lyon1.fr**	M. Johannes KELLENDONK Université Claude Bernard Lyon 1 LIRIS - INFOMATHS Bâtiment Nautibus 43 bd du 11 novembre 1918 69622 VILLEURBANNE Cedex Tél : 04.72. 43.19.05 Fax 04 72 43 13 10 infomaths@bat710.univ-lyon1.fr
Matériaux	**MATERIAUX DE LYON** Secrétariat : M. LABOUNE PM : 71.70 –Fax : 87.12 Bat. Saint Exupéry	M. Jean-Yves BUFFIERE INSA de Lyon MATEIS Bâtiment Saint Exupéry 7 avenue Jean Capelle 69621 VILLEURBANNE Cédex Tél : 04.72.43 83 18 Fax 04 72 43 85 28 Jean-yves.buffiere@insa-lyon.fr
MEGA	**MECANIQUE, ENERGETIQUE, GENIE CIVIL, ACOUSTIQUE** Secrétariat : M. LABOUNE PM : 71.70 –Fax : 87.12 Bat. Saint Exupéry mega@insa-lyon.fr	M. Philippe BOISSE INSA de Lyon Laboratoire LAMCOS Bâtiment Jacquard 25 bis avenue Jean Capelle 69621 VILLEURBANNE Cedex Tél :04.72.18.71.70 Fax : 04 72 43 72 37 Philippe.boisse@insa-lyon.fr
ScSo	**ScSo*** M. OBADIA Lionel Sec : Viviane POLSINELLI Insa : J.Y. TOUSSAINT	M. OBADIA Lionel Université Lyon 2 86 rue Pasteur 69365 LYON Cedex 07 Tél : 04.78.69.72.76 Fax : 04.37.28.04.48 Lionel.Obadia@univ-lyon2.fr

Cette thèse est accessible à l'adresse : http://theses.insa-lyon.fr/publication/2013ISAL0001/these.pdf
© [R. Xu], [2013], INSA de Lyon, tous droits réservés

Cette thèse est accessible à l'adresse : http://theses.insa-lyon.fr/publication/2013ISAL0001/these.pdf
© [R. Xu], [2013], INSA de Lyon, tous droits réservés

Acknowledgement

Three years ago, I packed my luggage and took the plane from Shanghai to Paris. I was nervous at that time. I seldom travelled abroad and rarely on my own, even in China. I had a very basic knowledge of the French language and I didn't know whether I could express myself correctly. When I landed at the airport, after the long queue to show my passport to the officer, he replied in French "Merci". At this moment I finally realized that I had arrived in France. Now I am on the stage to finish all my work here, looking backwards and finding that this three-year experience is a big treasure in my life, which in fact is accompanied with a lot of help from known or unknown people.

I will firstly express my appreciation to my supervisor, Dr. Yves QUENEAU, Directeur de Recherche CNRS à l'INSA de Lyon, who kindly accepted me as the PhD student in the lab. He helped me, from the very first day when picking me up at the rail station in Lyon, waiting for me with my name written in Chinese on a paper. He also showed me all along my thesis how it is important to be strict and curious in science, always thinking about new aspect of the subject, and inspiring me a lot on my work. Thanks to his generous help, I could gradually establish my sense as a glycochemist.

Dr. Stéphane CHAMBERT, Maitre de Conférences à l'INSA de Lyon, who accompanies with my bench work for all these years, has been very patient and kind on me. His suggestions were very helpful to pull me out of the problems I had met with in my experiments. He was always very kind to receive me although I kept bothering him. I am also very happy that we have spent a great time in the CANOE during the drifting in Ardèche. His precious piloting helped us finish the drifting with a lot of fun.

I also thank Prof. Jacques AUGE, from Université de Cergy-Pontoise and Prof. Grahame MACKENZIE, from University of Hull**,** for spending time on examining my manuscript. As well as to Prof. Bruno ANDRIOLETTI, from Université Claude Bernard-Lyon 1, who accepted the additional task to be president of the jury for my defense.

I would like to thank to Prof. John GOODBY, Dr. Stephen COWLING and the fellows in the lab for their warm welcome at the University of York, where I have spent two fruitful weeks discussing the subject of glycolipidic liquid crystal with them. There I have learned how wide the field of liquid crystalline materials which I found fascinating was.

I also owe my thank to Dr. David GUEYRARD, Prof. Peter GOEKJIAN, from LCO-2 in Lyon 1 and Dr. Olivier MARCILLAT, Prof. René BUCHET from ODMB in Lyon 1 for their kind advice on developing the glycoprobes along with the fluorescence tests of them.

Many thanks to my colleagues in the lab who have accompanied with me for these years. Their help from many aspects has made my life in the lab full of happiness. Particular thanks

Cette thèse est accessible à l'adresse : http://theses.insa-lyon.fr/publication/2013ISAL0001/these.pdf
© [R. Xu], [2013], INSA de Lyon, tous droits réservés

to Dr. Nuno XAVIER and Dr. Madan SINGH for their kind guide around Lyon when I just arrived, and Dr. Mohamad SABBAH for his delicious Lebanese flavor which I quite miss right now, and Dr. Sebastien REDON for his kind invitation to the rugby match which was excellent. I will also thank Lucie GRAND for her super French courses where I got a lot of progress. I am also grateful to Professor DOUTHEAU, then to Professor POPOWYCZ, for the kind interest they have expressed to my work and to myself.

Particular thanks to China Scholarship Committee (CSC), who supported my life in France so that I could have a better life condition and undergo my research calmly. I also thank my friends in Lyon with whom I spent the unforgettable period on travelling around, cooking, sporting and so on.

To close this little piece, I have to say I owe a lot to my parents and my family. Thanks to their backing and comprehension, I could come to France and proceed on my subject without much care. You are the best.

非常感谢！！

Cette thèse est accessible à l'adresse : http://theses.insa-lyon.fr/publication/2013ISAL0001/these.pdf
© [R. Xu], [2013], INSA de Lyon, tous droits réservés

Résumé

INTRODUCTION

Les amphiphiles à base de glucides représentent une importante classe de molécules non seulement parce qu'ils sont largement présents dans la Nature (glycolipides) mais aussi du fait de leur propriétés physico-chimiques liées à leur aptitude à l'auto-assemblage et l'auto-organisation. Ces propriétés sont aussi celles qui donnent aux amphiphiles glucidiques leur intérêt industriel, avec par exemple des tensioactifs tels que les esters de saccharose et les alkylpolyglycosides.

Les glycolipides sont largement distribués dans les membranes, et participent à de nombreux mécanismes biologiques. Compte tenu du caractère organisé de la membrane cellulaire, l'aptitude physicochimique des glycolipides à établir ou s'insérer dans des édifices supramoléculaires est nécessairement un paramètre clé dans leur possibilité de remplir leur rôle biologique. L'état physique en question est celui de cristal liquide, aussi dénommé le quatrième état de la Nature (avec l'état solide, l'état liquide et l'état gazeux), et c'est ce qui donne son importance au domaine des cristaux liquides glucidiques**.**

Par le processus d'auto-assemblage et/ou d'auto-organisation, ces molécules s'associent pour former les mésophases possédant l'état cristal liquide. De tels amphiphiles peuvent former des phases thermotropes (état pur) ou lyotropes (en présence d'eau). La formation des phases thermotropes dépend beaucoup de la structure des molécules, alors que pour les phases lyotropes, c'est surtout la concentration dans l'eau qui est le paramètre le plus important. Les forces qui conduisent à l'établissement de ces phases sont notamment les interactions polaires (liaisons hydrogène) et les interactions hydrophobes (liaisons de van der Waals). Des phases lamellaires, hexagonales, cubiques sont communément observées. Les paramètres qui orientent vers telle ou telle géométrie de phase sont notamment les surfaces de section respectives des têtes polaires sucre et des chaines hydrophobes, la balance hydrophile-lipophile globale de la molécule, et les éléments qui affectent la forme de la molécule tels que le degré de substitution ou la position de la chaine hydrophobe sur le sucre.

Notre laboratoire s'est impliqué dans le domaine des cristaux liquides glycoamphiphiliques depuis plusieurs années, dans le cadre d'une collaboration avec le Professeur John Goodby à l'Université de York, et précédemment, à l'Université de Hull au Royaume-Uni, impliquant

Cette thèse est accessible à l'adresse : http://theses.insa-lyon.fr/publication/2013ISAL0001/these.pdf
© [R. Xu], [2013], INSA de Lyon, tous droits réservés

aussi le Professeur Grahame Mackenzie. L'objectif était en particulier d'apporter des éléments sur la relation entre la structure des molécules et leurs propriétés, grâce à la conception et la synthèse de diverses familles d'amphiphiles glucidiques. Le travail présenté dans cette thèse est une nouvelle contribution à ce thème de recherche collaboratif qui vise à une meilleure compréhension des aspects moléculaires des processus d'auto-assemblage et auto-organisation des amphiphiles glucidiques.

Dans ce travail, on a développé deux nouvelles familles de molécules : une série de n-*O*-(2-hydroxylalkyl)-α-D-glucopyranosides de méthyle (1) et une série de glucostéroides (2) comportant un motif espaceur de type alkyle et pouvant présenter une deuxième substitution par une chaîne hydrophobe en position O-2 (figure 1).

La première famille (1) est une série d'hydroxyalkylethers de l'α-D-glucoside de méthyle possédant des chaines alkyle de différentes longueurs, monosubstitutués sur l'une des 4 positions disponibles sur le squelette sucre. Les comportements thermotrope et lyotrope de ces produits ont été étudiés. Après nos travaux qui avaient porté sur un système disaccharidique (saccharose), et qui avaient mis en évidence l'influence des interactions entre les deux parties du disaccharide lui-même, l'objectif avec cette nouvelle série monosaccharidique était d'établir des relations structure-propriété liées exclusivement à la position de la chaine et à ces conséquences sur la compétition entre liaisons hydrogène inter- et intra-moléculaires.

Le cholestérol est un des lipides les plus fréquemment rencontrés, notamment au sein des membranes, où il coexiste avec d'autres types de lipides et glycolipides. De nombreuses molécules possédant un sucre et un stéroïde comme éléments structuraux principaux existent également dans la Nature. Malgré cette occurrence, la physicochimie des amphiphiles glycostéroidiques a été relativement peu étudiée, et en particulier le comportement cristal liquide. C'est ce qui nous a guidés dans la conception de la deuxième famille de dérivés étudiés dans ce travail, mettant à profit une stratégie de synthèse basée sur l'utilisation de synthons bicyclolactoniques (CMGLs), développée dans notre laboratoire. Comme illustré dans la figure 1, les glycostéroides (2) qui ont été préparés sont en fait constitués de quatre éléments, le sucre, le stéroïde, un espaceur de type alkyle de différentes longueurs, et la position O-2 du sucre substituée ou non par une chaine grasse de différentes longueurs. L'objectif était dans ce cas d'établir une voie d'accès aussi modulable que possible pour faire varier la flexibilité du système et la nature des interactions

Cette thèse est accessible à l'adresse : http://theses.insa-lyon.fr/publication/2013ISAL0001/these.pdf
© [R. Xu], [2013], INSA de Lyon, tous droits réservés

lipide-lipide, et observer les conséquences de ces variations sur le comportement thermotrope.

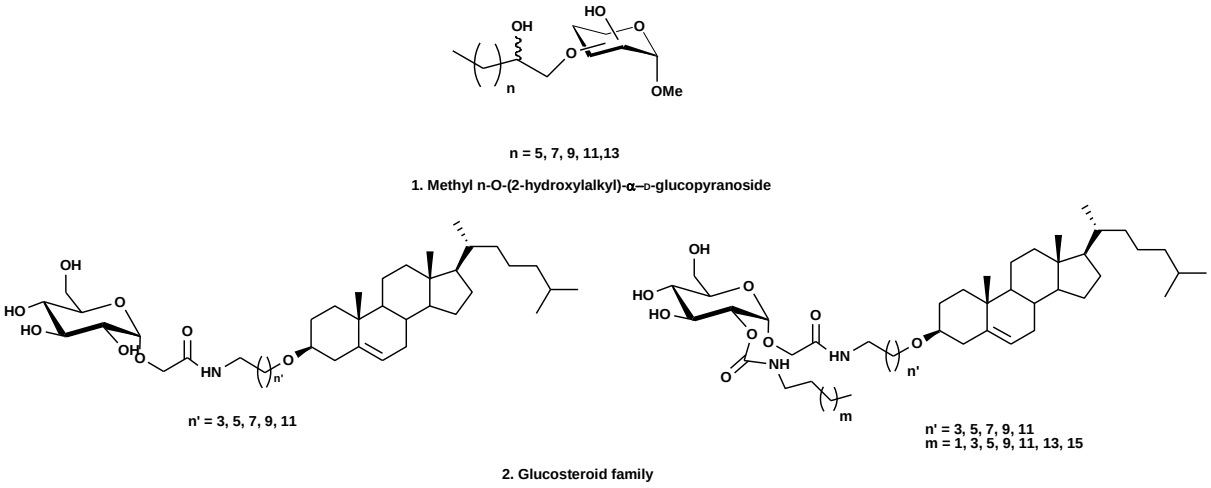

Fig. 1 : Structures des produits ciblés dans ce travail

RESULTATS ET DISCUSSION

Hydroxyalkylethers du méthyl glucoside

La première famille de glycoamphiphiles est une série de mono-hydroxyalkyléthers du glucoside de méthyle sur les 4 positions possibles, et possédant des longueurs de chaine de 8 à 16 atomes de carbone, préparés par réaction d'un groupe hydroxy du sucre avec des 1, 2-epoxyalkanes. Dans des études précédentes sur le saccharose, il avait été mis en évidence la difficulté de contrôler à la fois le degré de substitution et la régiochimie de la réaction, nécessitant des étapes de purification très délicates et rendant difficile l'obtention de composés parfaitement purs au niveau régioisomérique. C'est pourquoi il a été préféré une stratégie totalement contrôlée basée sur la préparation préalable des substrats partiellement protégés du glucoside de méthyle possédant un seul groupe hydroxy libre. Elle est décrite dans la figure 2.

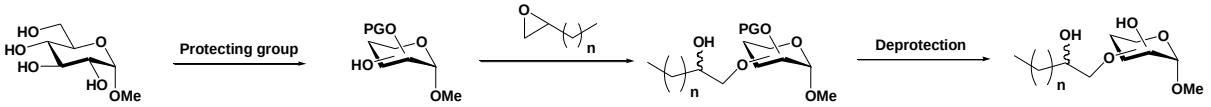

Figure 2 : Synthèse contrôlée des hydroxyalkyléthers du glucoside de méthyle.

Cette thèse est accessible à l'adresse : http://theses.insa-lyon.fr/publication/2013ISAL0001/these.pdf
© [R. Xu], [2013], INSA de Lyon, tous droits réservés

Pour les séries substituées sur 2-*O* et 3-*O* (Figure 3), le glucopyranoside de méthyle est d'abord protégé en 4,6 par un acétal benzylidene, puis la monobenzylation conduit à un mélange des deux produits possibles ayant soit OH-2 soit OH-3 comme seule position libre. Celle-ci peut être alors éthérifiée par réaction avec les 1,2-epoxyalkanes en présence de DMAP et de DABCO dans le DMSO. Après purification par chromatographie sur colonne de gel de silice, les produits ont été traités avec l'acide *p*-toluène sulfonique pour couper le 4,6-acétal, puis débenzylés par hydrogénolyse en présence de palladium sur charbon. Cette séquence a été appliquée à partir des époxydes en C8, C10, C12, C14 et C16, et les produits finaux correspondants ont été purifiés et parfaitement caractérisés. Rappelons que chaque composé est en fait un mélange de deux isomères au niveau de l'OH sur la chaine éther, dans un rapport 1 :1 comme démontré par la RMN du carbone 13.

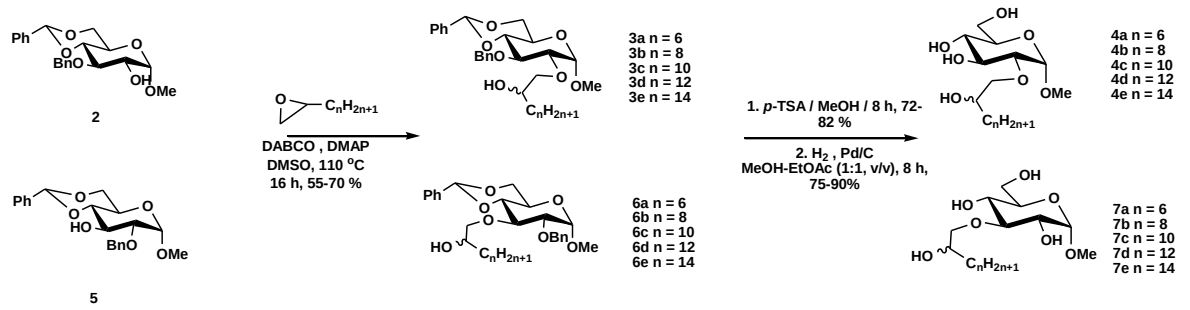

Figure 3 : Obtention des éthers en position 2 et 3

Pour la série avec la chaine en position 4-*O*, le 4,6-benzylidene déjà employé auparavant est dibenzylé en position 2 et 3, puis l'acétal est ouvert en conditions réductrices, libérant ainsi la position 4 et conservant la position 6 protégée par un éther benzylique. Les 4-*O*-(2-hydroxylalkyl)-2, 3, 6-tri-*O*-benzyl-α-D-glucopyranosides de méthyle sont ensuite obtenus par la même réaction avec les époxydes terminaux, qui sont ensuite débenzylés (Figure 4).

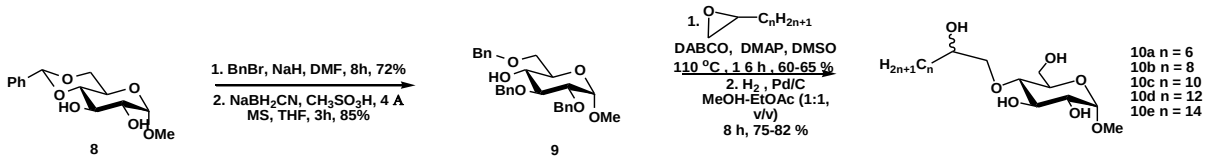

Figure 4 : Obtention des éthers en position 4

Cette thèse est accessible à l'adresse : http://theses.insa-lyon.fr/publication/2013ISAL0001/these.pdf
© [R. Xu], [2013], INSA de Lyon, tous droits réservés

Pour la dernière série substituée en O-6, OH-6 est d'abord protégé par un groupe trityle. Puis, les autres groupes hydroxy sont benzylés et le trityle est déprotégé en conditions acides. Le produit résultant est alors éthérifié avec les 1, 2-epoxyalkanes puis les groupes benzyles sont hydrogénolysés (Figure 5).

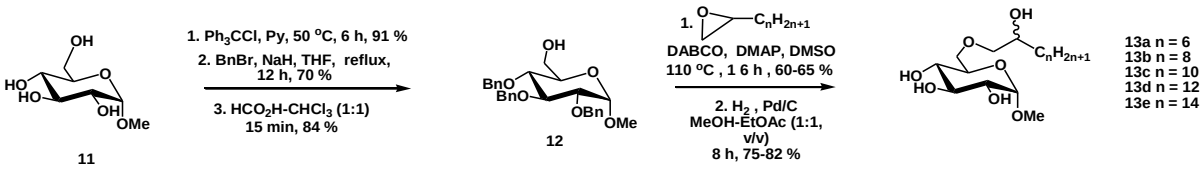

Figure 5 : Obtention des éthers en position 6

Les propriétés thermotropes de ces éthers ont été étudiées par microscopie optique polarisée et par calorimétrie différentielles (DSC). Les phases lamellaires (smectiques) de type Sm A* sont l'unique type de phase observé pour toute la famille de molécules, ce qui signifie que les tailles respectives de la partie sucre et de la partie aliphatique est de l'ordre de 1 :1 pour ce système. La longueur de chaine C12 est la limite à partir de laquelle les molécules sont capables de former les mésophases. Pour les séries qui ont les chaines les plus longues (14 et 16), les températures de transition entre la phase organisée et le liquide isotrope (clearing point) varient avec la position de la chaine, diminuant quand la chaine est déplacée de O-2 vers O-6. Pour la série en C12, les températures de transition sont plus irrégulières, avec le composé substitué en O-3 était ayant la plus haute température de transition, et aucune mésophase observée pour de dérivé en O-4. Les études de modélisation moléculaires et l'analyse des enthalpies et entropies de transition de phase, permettent d'interpréter les variations de comportement en termes de capacité des différents groupes hydroxyéther de s'associer de manière intramoléculaire avec les autres OH du motif sucre, ce qui modifie donc la compétition entre liaisons intra et intermoléculaires des têtes polaires entre elles.

Les propriétés lyotropes ont été aussi étudiées, montrant successivement, quand on augmente la quantité d'eau, des phases lamellaires, cubiques puis hexagonales, comme il est attendu pour ce type de molécules.

Cette thèse est accessible à l'adresse : http://theses.insa-lyon.fr/publication/2013ISAL0001/these.pdf
© [R. Xu], [2013], INSA de Lyon, tous droits réservés

Glucostéroides

Pour la famille de glucostéroïdes, on a utilisé les synthons carboxymethyl glycosyl lactones (CMGL) pour attacher la partie sucre au système. Il a été montré que ces synthons, qui ont été développés par notre groupe, peuvent être facilement ouverts par divers types de nucléophiles, notamment possédant une fonction amine. L'ouverture de la lactone conduit à l'obtention d'un OH libre sur position 2 qui peut être alors sélectivement fonctionnalisé. Cette méthode a permis d'obtenir divers types de pseudo glycoconjugués, tels que des pseudodisaccharides, des glycosondes fluorescentes, des monomères pour polymérisation, *etc*. Notamment, des travaux préliminaires avaient permis d'obtenir des composés dans lesquels un stéroïde et le sucre étaient couplés directement, mais ces produits étaient quasiment incapables de former des mesophases. C'est pourquoi on s'est intéressé dans cette thèse à une nouvelle gamme de glycostéroides comportant un espaceur entre la partie sucre et la partie stéroïde. La substitution en position 2 a ensuite conduit à de nouveaux bolaphiles. La séquence synthétique est illustrée dans la figure 6.

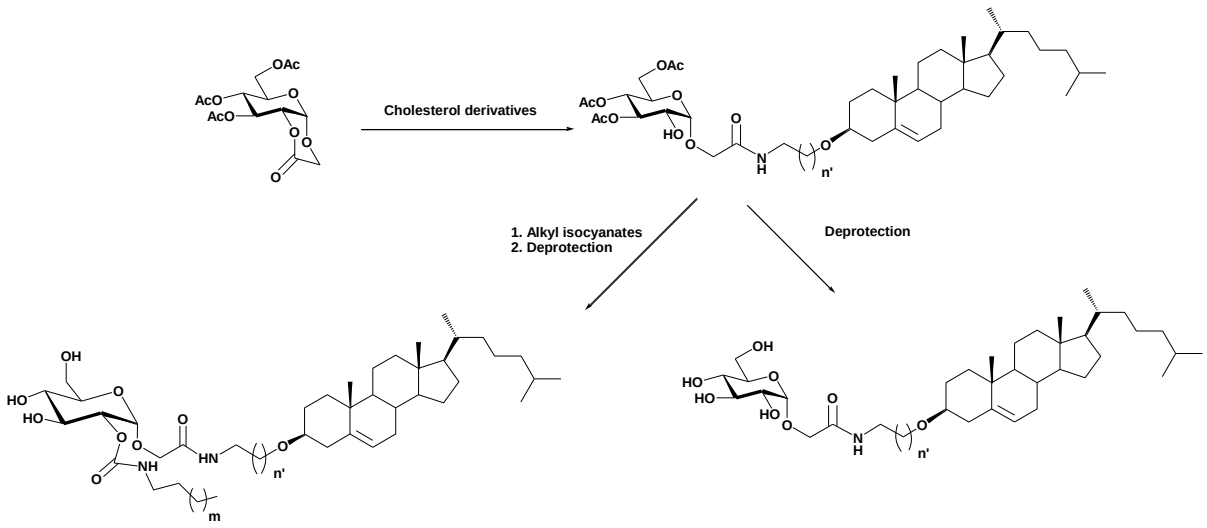

Figure 6 : Synthèse pour obtenir des glucostéroïdes

Pour la série avec l'espaceur en C4, l'étape de couplage se fait par réaction de métathèse entre l'allylamide issu de l'ouverture de la lactone par l'allylamine et l'allylether du cholestérol, suivie d'une hydrogénation sélective de la double liaison isssue de la métathèse par l'hydrogène en présence de Pd. La séquence synthétique est illustrée dans la figure 7.

Cette thèse est accessible à l'adresse : http://theses.insa-lyon.fr/publication/2013ISAL0001/these.pdf
© [R. Xu], [2013], INSA de Lyon, tous droits réservés

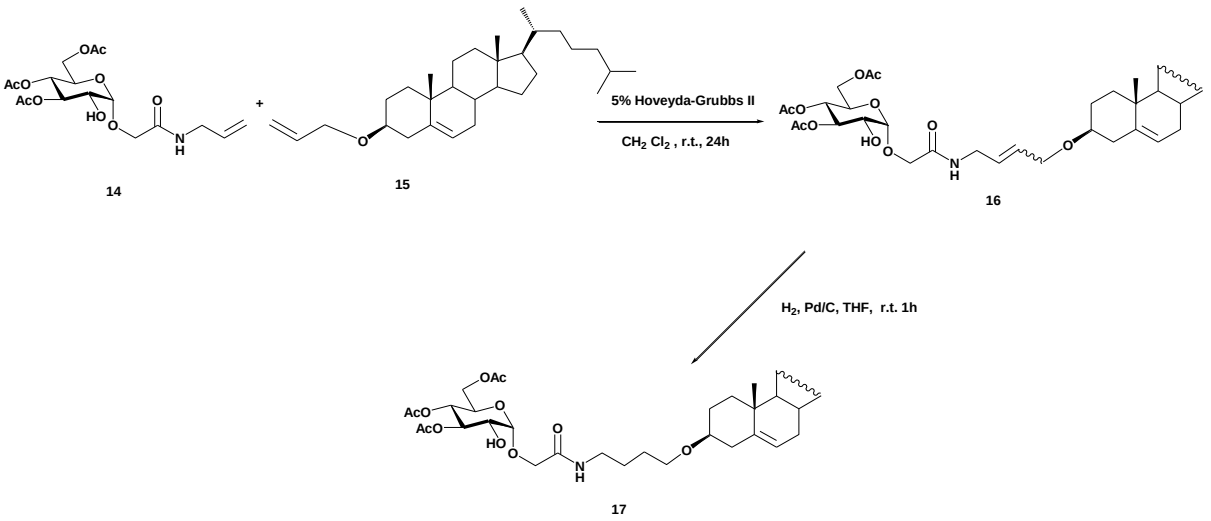

Figure 7 : Séquence de synthèse des glucostéroïdes avec espaceur en C4

Pour les séries avec les espaceurs plus longs (C6, C8, C10, C12) une autre séquence a été utilisée, basée sur l'ouverture de la lactone par des éthers de cholestérol possédant une fonction terminale amino sur la chaine. Comme indiqué dans la figure 7, l'éthérification du tosylcholestérol par les 1,ω–diols de longueurs variées est suivie par la transformation de l'OH terminal en amine via le mésylate, puis l'azido correspondant.

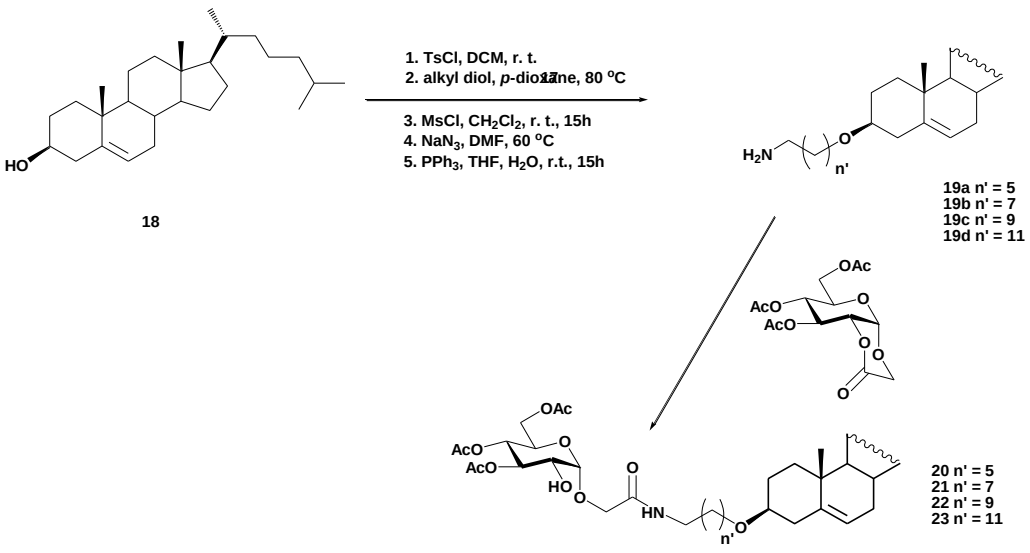

Figure 8. Séquence vers les glycostéroides avec espaceurs 6, 8, 10 et 12

Cette thèse est accessible à l'adresse : http://theses.insa-lyon.fr/publication/2013ISAL0001/these.pdf
© [R. Xu], [2013], INSA de Lyon, tous droits réservés

L'ouverture de la CMGL par cette amine conduit aux produits de couplage qui peuvent être ensuite fonctionnalisés sur la position 2 par réaction avec des alkylisocyanates de diverses longueurs soit dans le dichloromethane avec NEt_3 comme catalyseur basique, soit dans le THF avec 1, 8-diazabicycloundec-7-ene (DBU) comme catalyseur. La deuxième méthod a permis d'utiliser moin d'isocyanate et de temp pour purifier des produits loin d'urée. La déprotection finale des groupes acétyles par NEt_3 dans un mélange d'eau et de MeOH conduit aux nouveaux produits qui ont tous été parfaitement caractérisés.

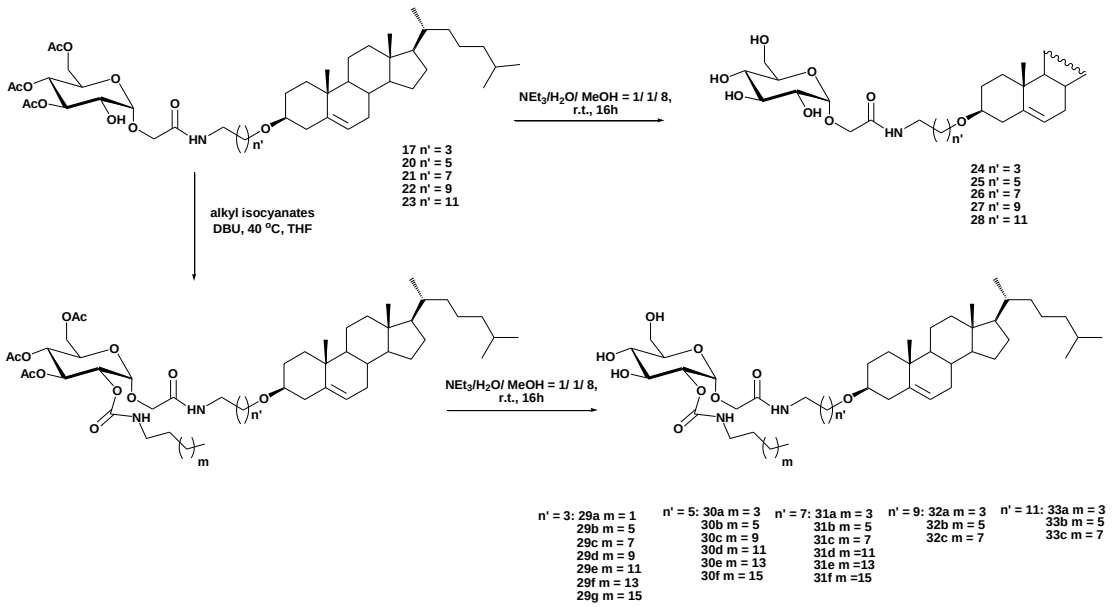

Figure 9 : Séquence vers les glycostéroides finaux

Les propriétés liquides cristallines de ces produits ont été étudiées. En premier lieu, il ressort que les températures de transition entre la phase liquide cristalline et le liquide isotrope décroit à mesure que la longueur de l'espaceur entre le sucre et le cholestérol augmente, en raison de la plus grande flexibilité que cela apporte dans le système.

Pour ce qui concerne l'effet de la variation de la longueur de la chaine latérale en O-2, quand cette chaine est courte, on observe des phases lamellaires (Sm A*) indiquant un équilibre entre les tailles relatives de la tête sucre et de la partie hydrophobe (quand cette chaine latérale passe de C4 à C12, on observe une diminution du clearing point). Dès la chaine latérale est en C14 ou plus longue, une autre mésophase se forme, identifiée comme colonnaire (hexagonale), avec augmentation de la température de transition vers le liquide isotrope, signalant une stabilisation de la phase hexagonale à mesure que la chaine latérale

Cette thèse est accessible à l'adresse : http://theses.insa-lyon.fr/publication/2013ISAL0001/these.pdf
© [R. Xu], [2013], INSA de Lyon, tous droits réservés

augmente en taille. L'analyse par modélisation moléculaire indique que dans ces cas, les molécules adoptent une forme de coin (wedge-shape), expliquant la préférence de l'architecture hexagonale au niveau supramoléculaire. Les mésophases Sm A* sont observées clairement dans la série avec espaceur en C4, elles persistent déjà moins dans le cas de la série avec espaceur en C6, alors que pour la série avec espaceur en C8, seule la phase hexagonale est observée, sans passer par la phase SmA*. Toutes ces variations de comportement illustrent les divers types d'interactions qui existent entre le cholestérol et la chaine latérale, et ce en fonction de la flexibilité du système apportée par un espaceur plus ou moins long.

Glycosondes fluorescentes

A la fin de cette thèse, nous avons abordé brièvement la synthèse, par la voie CMGL, d'autres dérivés possédant un motif sucre et une partie hydrophobe fluorescente, dans l'idée d'obtenir des glycosondes destinées à l'imagerie. Le motif fluorescent est le laurdan (6-dodecanoyl-2-(dimethylamino) naphthalene) (Figure 8). Le laurdan permet la fluorescense à deux photons, mais sa faible solubilité dans l'eau peut être une cause de mauvaise performance. La modification par greffage d'une partie sucre peut apporter cette solubilité et une aptitude à l'insertion membranaire.

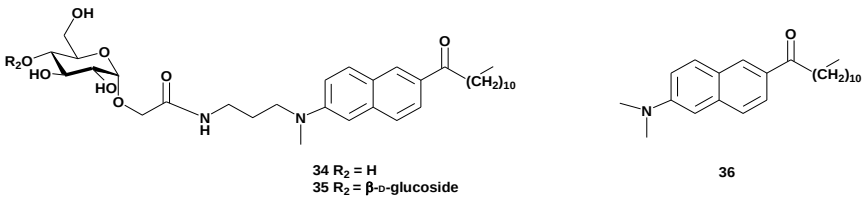

Figure 10 : Structures des glycosondes preparées.

Pour obtenir ces sondes (Figure 9), on a d'abord préparé le 6-dodecanoyl-2-bromo-naphthalene par couplage du 2-bromonaphthalene avec le chlorure de dodecacanoyle, puis le produit résultant a été couplé avec la (N-Boc-aminopropyl)méthylamine par amination de Buchwald–Hartwig. L'amine terminale est ensuite déprotégée par le TFA et est alors disponible pour ouvrir le cycle des CMGLs, conduisant aux glycosondes dont il reste à déprotéger les groupes acetates (NEt_3/ H_2O/MeOH, 1/1/8 , v /v), pour obtenir les produits finaux dont la structure a été parfaitement caractérisée. Les sondes sont maintenant dans

Cette thèse est accessible à l'adresse : http://theses.insa-lyon.fr/publication/2013ISAL0001/these.pdf
© [R. Xu], [2013], INSA de Lyon, tous droits réservés

les mains des collègues biochimistes qui procèderont aux évaluations physicochimiques et biologiques.

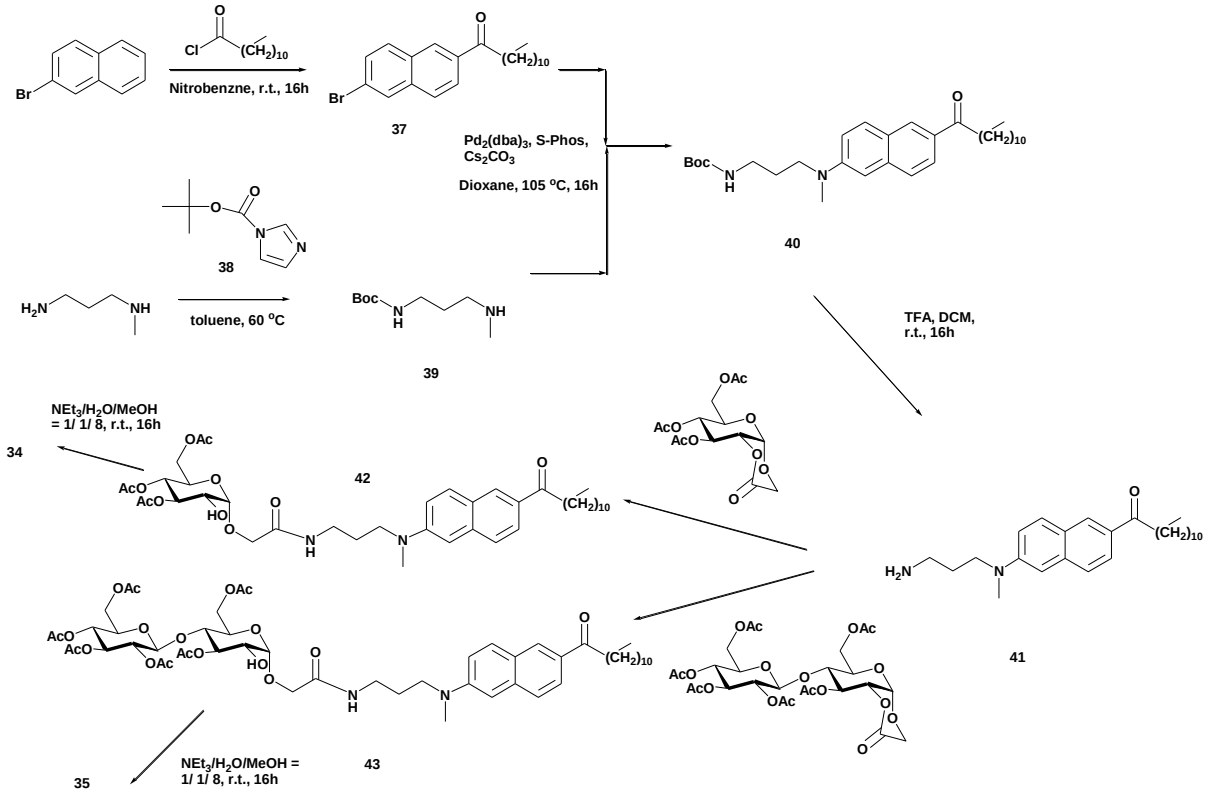

Figure 11 : Synthèse des nouvelles glycosondes

CONCLUSION

En conclusion, dans ce travail, on a synthétisé trois familles de neoglycolipides, deux familles principalement destinées à apporter des éléments sur l'état liquide cristallin des glycolipides, et une troisième famille permettant d'aborder l'étude de nouvelles glycosondes fluorescentes. Plus de 50 produits finaux ont été synthétisés (et donc leurs très nombreux précurseurs) et caractérisés structuralement par spectroscopie RMN, de masse, et par analyse élémentaire. Les propriétés liquides cristallines de ces nouveaux produits ont été ensuite étudiées par microscopie optique et DSC.

L'étude des propriétés liquides cristallines de la famille d'éthers montrent que la localisation de la chaine sur le squelette sucre modifie la répartition entre liaisons hydrogène inter- ou intra moléculaires entre têtes polaires sucres. L'analyse du comportement thermotrope des

Cette thèse est accessible à l'adresse : http://theses.insa-lyon.fr/publication/2013ISAL0001/these.pdf
© [R. Xu], [2013], INSA de Lyon, tous droits réservés

glucostéroïdes, notamment ceux qui sont disubstitués, montre que les interactions lipide-lipide sont également très importantes. Il a été observé que ces systèmes complexes pouvaient adopter deux types d'architectures au niveau supramoléculaire en fonction de la flexibilité du système, laissant plus ou moins aux trois motifs présents dans la molécule la liberté de choisir leur préférence d'autoassociation. Les glycostéroïdes étant largement rencontrés dans la Nature, on peut considérer que ces observations nouvelles qui ont été apportées signalent que le comportement supramoléculaire de telles molécules est potentiellement multiple. Enfin, une brève exploration d'une nouvelle famille de glycosondes fluorescentes a été abordée.

Cette thèse est accessible à l'adresse : http://theses.insa-lyon.fr/publication/2013ISAL0001/these.pdf
© [R. Xu], [2013], INSA de Lyon, tous droits réservés

Cette thèse est accessible à l'adresse : http://theses.insa-lyon.fr/publication/2013ISAL0001/these.pdf
© [R. Xu], [2013], INSA de Lyon, tous droits réservés

Key words

Carbohydrates

Liquid crystals

Self-assembly, self-organisation

Glycolipids

Steroids

Glycoamphiphiles

Sugar lactones

Cette thèse est accessible à l'adresse : http://theses.insa-lyon.fr/publication/2013ISAL0001/these.pdf
© [R. Xu], [2013], INSA de Lyon, tous droits réservés

Cette thèse est accessible à l'adresse : http://theses.insa-lyon.fr/publication/2013ISAL0001/these.pdf
© [R. Xu], [2013], INSA de Lyon, tous droits réservés

Abbreviations

ABS	Alkylbenzene sulfonates
Ac	Acetyl
APGs	Alkyl polyglucosides
ASG	Acyl steryl glycosides
BbGL-I	Cholesteryl 6-*O*-acyl-β-D-galactopyranoside
BbGL-II	1,2-di-*O*-acyl-3-*O*-α-D-galactopyranosyl-*sn*-glycerol
Bn	Benzyl
Boc	*tert*-butoxycarbonyl
Bz	Benzoyl
CMC	Critical micelle concentration
CMG	Carboxymethyl glycoside
CMGL	Carboxymethyl glycoside lactone
CNTs	Carbon nanotubes
Col_h	Hexagonal columnar phases
Col_o	Oblique columnar phases
Col_r	Rectangular columnar phases
Col_s	Square columnar phases
COSY	Correlation spectroscopy
DABCO	1,4-Diazabicyclo[2.2.2]octane
DCM	Dichloromethane
DEPT	Distortionless Enhancement by Polarization Transfer

Cette thèse est accessible à l'adresse : http://theses.insa-lyon.fr/publication/2013ISAL0001/these.pdf
© [R. Xu], [2013], INSA de Lyon, tous droits réservés

ABBREVIATIONS

DGDG	Digalactosyl-diacylglycerol
DMAP	4-Dimethylaminopyridine
DMF	Dimethylformamide
DMPC	1,2-dimyristoyl-sn-glycero-3-phosphocholine
DMSO	Dimethyl sulfoxide
DSC	Differential scanning calorimetry
FITC	Fluorescein isothiocyanate
FRET	Fluorescence resonance energy transfer
FTIR	Fourier transform infrared spectroscopy
GGLs	Glycoglycerolipids
GPPPs	Glycosyl phosphopolyprenols
GSLs	Glycosphingolipids
HLB	Hydrophilic/lipophilic balance
HMBC	Heteronuclear multiple-bond correlation
HSQC	Heteronuclear single-quantum correlation spectroscopy
LABS	Linear alkylbenzene sulfonates
LMWGs	Low molecular weight gelators
MELs	Mannosylerithritol lipids
MeOH	Methanol
MGDG	Monogalactosyl diacylglycerol
MWCNTs	Multi-walled carbon nanotubes
NEt_3	Triethylamine
OSW-1	3β,16β,17α-trihydroxycholest-5-en-22-one 16-*O*-(2-*O*-4-methoxybenzoyl-β-D-xylopyranosyl)-(1→3)-(2-*O*-acetyl-α-l-

Cette thèse est accessible à l'adresse : http://theses.insa-lyon.fr/publication/2013ISAL0001/these.pdf
© [R. Xu], [2013], INSA de Lyon, tous droits réservés

	arabinopyranoside)
PDT	Photodynamic therapy
Piv	Pivaloyl
POM	Polarized optical microscopy
PPh_3	Triphenylphosphine
p-TSA	*p*-Toluenesulfonic acid
RAFT	Reversible addition fragmentation chain transfer
SEC	Size exclusion chromatography
SGs	Steroid glycosides
Sm A*	Smectic A*
S-Phos	2-Dicyclohexylphosphino-2′,6′-dimethoxybiphenyl
TBAI	Tetrabutylammonium iodide
TFA	Trifluoroacetic acid
THF	tetrahydrofuran
TLC	Thin layer chromatography
TPEF	two-photon excitation fluorescence
TrCl	Triphenylmethyl chloride
XRD	X-ray diffraction
α-CAG	Cholesteryl 6'-O-acyl-α-glucopyranoside
H-bonding	Hydrogen bonding

Cette thèse est accessible à l'adresse : http://theses.insa-lyon.fr/publication/2013ISAL0001/these.pdf
© [R. Xu], [2013], INSA de Lyon, tous droits réservés

Cette thèse est accessible à l'adresse : http://theses.insa-lyon.fr/publication/2013ISAL0001/these.pdf
© [R. Xu], [2013], INSA de Lyon, tous droits réservés

CONTENTS

Acknowledgement 1

Résumé 3

Key words 15

Abbreviations 17

General introduction 25

Chapter 1 Carbohydrate based amphiphiles 27

1.1. Introduction 27

1.2. Surfactants 28

1.2.1. General aspects 28

1.2.2. Classification and applications 30

1.3. Carbohydrate Based amphiphiles 33

1.3.1 Introduction 33

1.3.2 Industrial manufacturing carbohydrate surfactants for consumer products 34

1.3.3. Glycolipids and glycolipid biosurfactants 36

1.4. Carbohydrate-based liquid crystals 42

1.4.1 Introduction 42

1.4.2 Mesophase behavior based on the structure of the glycolipids 44

1.4.3 Methods to identify the liquid crystalline behavior 60

1.4.4 Conclusion 63

Chapter 2 Carbohydrate Bicyclic Lactones and Their Applications 65

2.1 Introduction 65

2.2. Development of carboxymethyl glycoside lactones (CMGLs) 69

2.3 Conclusion 83

Chapter 3 Study on the liquid crystalline behavior of methyl n-*O*-(2-hydroxyalkyl)-glucopyranosides 85

Cette thèse est accessible à l'adresse : http://theses.insa-lyon.fr/publication/2013ISAL0001/these.pdf
© [R. Xu], [2013], INSA de Lyon, tous droits réservés

3.1 Introduction 85

3.2 Synthesis procedure 86

3.2.1 Synthesis of methyl 2-*O*-(2-hydroxyalkyl)-α-D-glucopyranosides 86

3.2.2 Synthesis of methyl 3-*O*-(2-hydroxyalkyl)-α-D-glucopyrano-sides 92

3.2.3 Synthesis of methyl 4-O-(2-hydroxyalkyl)-α-D-glucopyranosides 97

3.2.4 Synthesis of methyl 6-*O*-(2-hydroxyalkyl)-α-D-glucopyranosides 101

3.2.5 Synthesis of methyl 6-O-octyl- and dodecyl-α-D-glucopyranosides 105

3.3 Study on the thermotropic liquid crystalline behavior of the methyl glucoside hydroxyalkyl ethers 106

3.3.1 DSC and polarized light microscopy results of these ether compounds 106

3.3.2 The effects of aliphatic chain and the substituted position on the liquid crystalline behavior of the series 111

3.3.3 Structure study by modeling 114

3.4 Lyotropic study 117

3.5 Conclusions 119

Chapter 4 Synthesis and thermotropic liquid crystalline behavior of new glycosteroidic amphiphiles 121

4.1 Introduction 121

4.2 Synthesis of monosubstituted glycosteroids 124

4.2.1 Synthesis of C4 spacer 124

4.2.2 Synthesis of C6 and longer spacers 129

4.3 Synthesis of disubstituted glycosteroids by O-2 carbamatation 135

4.4 Thermotropic liquid crystalline behavior study of the glucosteroid 139

4.4.1 Phases identification and transition behaviors 139

4.4.2 Effect of the length of linker and side chain on the liquid crystalline behaviors 148

4.4.3. Molecular modeling study 149

4.4. Conclusion 151

Chapter 5 Synthesis of neoglucosyl laurdans and their evaluation in fluorescence microscopy 153

Cette thèse est accessible à l'adresse : http://theses.insa-lyon.fr/publication/2013ISAL0001/these.pdf
© [R. Xu], [2013], INSA de Lyon, tous droits réservés

5.1. Introduction 153

5.2. Synthesis procedure 156

5.2.1. Synthesis of 6-dodecanoyl-2-bromonaphthalene 157

5.2.2. Synthesis of the N^1-Boc-N^2-methyl-1,3-diaminopropane 158

5.2.3. Amination of 6-dodecanoyl-2-bromonaphthalene and N^1-Boc-N^2-methyl-1,3-diaminopropane 158

5.2.4. Synthesis of CMG derived probes 160

5.3 Fluorescence properties 163

5.3.1 Characterization of fluorescence in various solvents. 163

5.3.2 Fluorescent tests of probes in model membrane 165

5.4 Conclusion 168

General conclusion 169

Experimental section 171

A. General aspect 171

B. Characterizations of liquid crystalline behaviors 172

C. Fluorescent properties of probes 172

D. Synthetic procedures and characterizations of all the products studied 173

D. 1 Methyl n-*O*-(2-hydroxyalkyl)-α-D-glucopyranosides 173

D. 2 Glucosteroids 188

D.3 Synthesis of glucosyl and cellobiosyl probes 231

Appendix 239

A. DSC curves of n-*O*-(2-hydroxyalkyl)-α-D-glucopyranosides 239

B. DSC curves of glucosteroids 249

B. 1 Glucosteroidic amphiphiles 249

B. 2 Glucosteroidic bolaphiles 252

References 265

Cette thèse est accessible à l'adresse : http://theses.insa-lyon.fr/publication/2013ISAL0001/these.pdf
© [R. Xu], [2013], INSA de Lyon, tous droits réservés

Cette thèse est accessible à l'adresse : http://theses.insa-lyon.fr/publication/2013ISAL0001/these.pdf
© [R. Xu], [2013], INSA de Lyon, tous droits réservés

General introduction

Carbohydrate-based amphiphiles are important molecules not only because they are widely distributed in nature (glycolipids), but also because they often behave as materials which show specific physicochemical properties due to their self-assembling and self-organizing ability. The mesophases shown by these amphiphiles were observed in the early age of glycochemistry, but this liquid crystalline behavior was recognized as one of their major properties only many years later. Nowadays, it is believed that this liquid crystalline state, referred to as the fourth state of matter, has some relationships with the biological properties shown by glycolipids. Also, glycoamphiphilicity is a basis for developing biobased surfactants having interest in industry or biology.

This is why our laboratory has been involved in this topic for several years, in particular trying to provide information of the structure-property relationships by designing and synthesizing various series of sugar-based amphiphiles. This has been the object of collaboration with the group of Pr. J. Goodby at the University of York, and prior to this, at the University of Hull. The work achieved in this thesis which relates to two new families of glycoamphiphiles is a new contribution to this collaborative project dedicated to understanding better the molecular aspects of the self-organisation of carbohydrate-based amphiphiles.

The first family is a series of monosubstituted hydroxyalkylethers of α-methyl-D-glucoside (**1** shown in Fig. 1) having alkyl chains of different lengths at one of four possible positions on the sugar backbone. The liquid crystalline study of these compounds was performed in terms of thermotropic and lyotropic aspects. After some previous work on a disaccharidic system (sucrose), the present study on monosaccharidic ethers aimed at establishing some structure-property relationships that would not relate to the intersaccharidic interactions (as it happened in the disaccharidic series), but only to the positioning of the chain and the resulting balance between intermolecular and intramolecular hydrogen bonding.

Among key lipidic compounds is cholesterol. Despite the extremely important presence of cholesterol in supramolacular biological systems and the numerous natural products which possess a sugar and a steroid as their main building blocks, very little has been reported about glycoseroidic amphiphiles, notably in terms of liquid crystalline behavior. This has

Cette thèse est accessible à l'adresse : http://theses.insa-lyon.fr/publication/2013ISAL0001/these.pdf
© [R. Xu], [2013], INSA de Lyon, tous droits réservés

inspired the second family of compounds studied in this work, prepared using carboxymethyl glycoside lactones (CMGLs) synthons, a strategy developed in our group which allows straightforward preparation of disubstituted sugar derivatives. As depicted **2** in Fig 1, the glycosteroids which have been prepared and studied involve actually four building blocks, namely the sugar, the steroid, an alkyl chain spacer, and an optional alkyl side chain of different length at O-2.The aim was here to elaborate a versatile strategy for reaching compounds with variable flexibility and level of lipid-lipid interactions, and observing the consequences on their thermotropic properties.

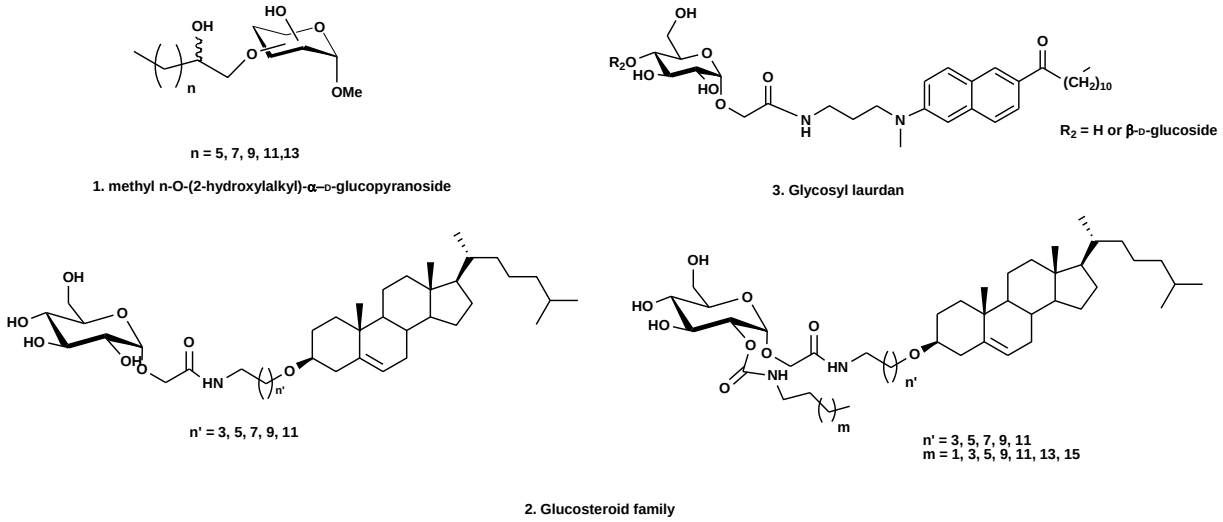

Fig. 1: Chemical structures of desired compounds

In this document, a bibliographic section is firstly given, illustrating the basic aspects of amphiphilicity, followed by focus on glycoamphiphiles and more specifically on carbohydrate-based liquid crystals. Also, the scope of the CMGL synthon strategy is rapidly overviewed.

In the second “result and discussion” part, is described the synthesis and the study of the liquid crystalline properties of the two series of new carbohydrate-based amphiphiles above mentioned. Also in this part, it is included a short chapter dealing with some preliminary work using the CMGLs strategy to prepare other carbohydrate-based amphiphiles, designed in the context of a project aimed at developing new fluorescent probes, **3** in Fig 1.

In the final part of this thesis, we will document the experimental section, including the experimental procedures, spectroscopic and physical data, and the references.

Cette thèse est accessible à l'adresse : http://theses.insa-lyon.fr/publication/2013ISAL0001/these.pdf
© [R. Xu], [2013], INSA de Lyon, tous droits réservés

Chapter 1

Carbohydrate based amphiphiles

1.1. Introduction

An amphiphilic molecule is constructed by two blocks with different affinities, where one affinity, *hydrophilic head,* is towards the water and the other, *hydrophobic tail*, towards the organic solvent, as illustrated in Fig. 1.1. The hydrophilic head could be charged, such as those bearing a sulfate ion (anionic amphiphiles) or quaternary ammonium ion (cationic amphiphiles), or uncharged, such as those involving a carbohydrate moiety (nonionic type). The hydrophobic tail could be a long straight chain or branched alkyl groups with the chain length ranging from 8 to 22 carbon atoms with possible unsaturations, like those coming from vegetable oils, or alkyl substituted aromatic groups, or polymeric blocks, etc. [1]

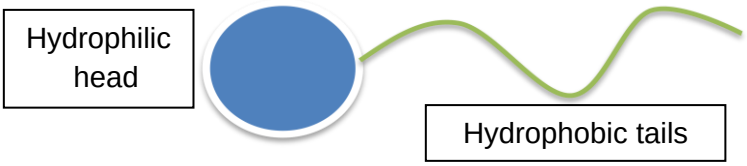

Fig. 1.1: Schematic illustration of an amphiphilic molecule

Among properties of amphiphiles there is the ability to self-assemble and self-organize through specific interactions between polar heads, on one hand, and between non polar tails,

Cette thèse est accessible à l'adresse : http://theses.insa-lyon.fr/publication/2013ISAL0001/these.pdf
© [R. Xu], [2013], INSA de Lyon, tous droits réservés

on the other hand, either in solution (formation of micelles) or as pure materials forming liquid crystalline assemblies.

In this section, after a short basic overview on surfactants, we will focus on those who possess a carbohydrate moiety, and develop particularly the specific field of liquid crystalline glycolipids.

1.2. Surfactants

1.2.1. General aspects

Surfactants are used in every corner in daily life. Fig. 1.2 shows surfactant market demand in the US in 2007.[2] Although the detergents and industrial areas remain two predominant parts in surfactant consumptions, some other applications, like cosmetics,[3] oil recovery process,[4, 5] medicine,[6-8] have seen rapid development recently. Special uses are also explored.[9, 10] Fig. 1.3 shows a more detailed diversity of applications of surfactants.[1] Referring to requirements for surfactant performance, besides some traditional ones, like stability, foaming power, detergency, solubility, etc, other more specific properties have been emphasized, like toxicity, skin irritability, and environmental performance. The requirements of some important applications are listed in Table 1.1.[1] These diverse functionalities may in turn demand for diverse chemical building blocks and synthetic strategies.

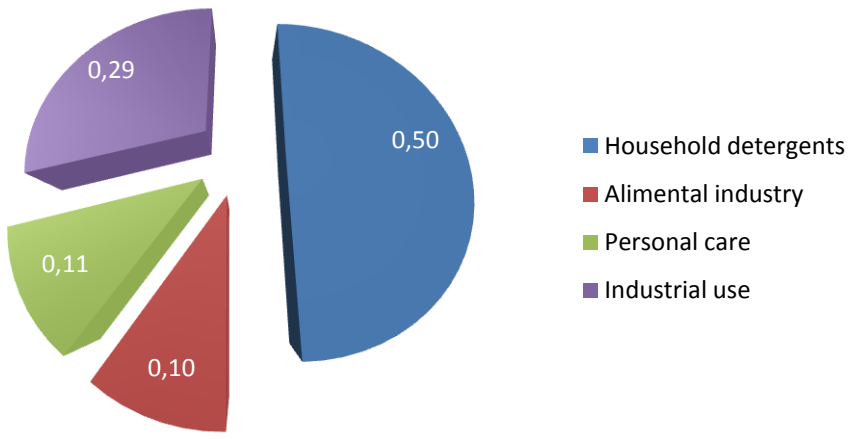

Fig.1.2: US surfactants market demand in 2007[2]

Cette thèse est accessible à l'adresse : http://theses.insa-lyon.fr/publication/2013ISAL0001/these.pdf
© [R. Xu], [2013], INSA de Lyon, tous droits réservés

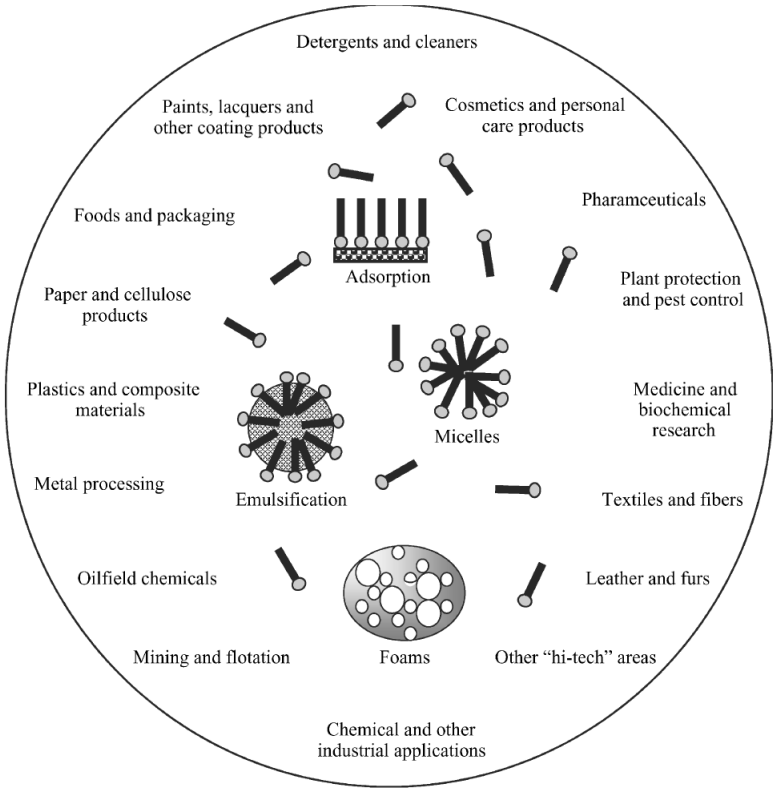

Fig.1.3: Some important surfactant applications[1]

Application	Characteristics
Detergency	Low CMC, good salt and pH stability, biodegradability, desirable foaming properties
Emulsification	Chemical stability, adsorption at surfaces
Mineral flotation	Proper adsorption characteristics on the ore(s) of interest, low cost
Petroleum recovery	Proper wetting of oil-bearing formations, microemulsion formation and solubilization properties, ease of emulsion breaking after oil recovery
Pharmaceuticals	Biocompatibility, low toxicity, proper emulsifying properties
Lubrication	Chemical stability, adsorption at surface

Table 1.1: Typical characteristics for surfactants that must be evaluated for various applications[1]

Soaps are a kind of surfactant that have been involved in human`s history for a long time. In China, the first record of manufacturing soap is in the Song Dynasty. At that time, people smashed the seeds from *Gleditsia sinensis*, mixed with some perfume to form spherical

Cette thèse est accessible à l'adresse : http://theses.insa-lyon.fr/publication/2013ISAL0001/these.pdf
© [R. Xu], [2013], INSA de Lyon, tous droits réservés

pieces of matter, and sold to be used for personal care. In western history, the Phoenicians were the first to be documented to sell the alkali metal soaps as early as 600 BC. The Romans developed the manufacture process, which is, however, generally considered to be from the Celts or some Mediterranean culture.[1]

In the modern time, with the development of science and technology, people began to think about using chemical synthetic methods to design and manufacture useful surfactants. The early example was the short-chain alkylnaphthalene sulfonates, created by the Germans, during the World War I, showing a good wetting property. Then the surfactant industry has seen a rapid growth that new surfactants emerged one after another, like long-chain alkyl alcohol sodium sulfates, long-chain alkylaryl sulfonates, alkylbenzene sulfonates (ABS), and linear alkylbenzene sulfonates (LABS). They are widely used in routine life at present.[1] Nowadays, the ecological harmony has become an important issue in the world, as well as the as limitation of fossil fuel reserves, an alternative resource to replace the petrochemical feedstocks must be identified. Thus the oleochemical feedstocks and a variety of other renewable substrates have been of increasing interest as feedstocks for surfactant production. Some research revealed that if the petro-originated surfactants were replaced by renewable surfactants, the resulting reduction of CO_2 emission generated from the production and utilization of surfactants could be up to 37%.[11] Meanwhile, some unique properties directed by oleochemical feedstocks, like versatile self-assembling and biochemical properties, have been found one after another, providing some very interesting applications in ecological and biological fields.

1.2.2. Classification and applications

Surfactants may be classified in several ways, either in terms of properties (emulsifier, wetting agent…) or in terms of structure, in particular with respect to the type of hydrophilic moiety, as it is done below.[1]

1.2.2.1. ANIONIC SURFACTANTS

As the only available for thousands of years, the anionic surfactants are the kind received most attention. In 2012, the production of anionic surfactants in European Union is 1.219 million tons, nearly half in whole surfactant industry.[12] The major head group of this class could be constructed by the alkali carboxylates or soaps, sulfates, sulfonates, and phosphates, as shown in Table 1.2.

Cette thèse est accessible à l'adresse : http://theses.insa-lyon.fr/publication/2013ISAL0001/these.pdf
© [R. Xu], [2013], INSA de Lyon, tous droits réservés

Type name	Formula	Representative	Characteristic
Sulfate esters	$ROSO_3^-M^+$ (R is aliphatic chain)	Sodium dodecylsulfate (SDS)	Good water solubility and surface activity, reasonable chemical stability; easy-made, low-cost, easy acess
Sulfonic acid salts	$R\text{-}SO_3^-M^+$	alkylbenzene sulfonates (ABS), linear alkylbenzene sulfonates (LABS)	Good pH stability, excellent water solubility, good wetting properties, low cost
Carboxylate soaps	$R\text{-}COO^-M^+$ (R is tallow, fatty acid condensed with amino derivatives)	Classical soaps	Less sensible to hard water and low pH, low skin irritability, low toxicity
Phosphoric acid esters	$RO\text{-}PO_3^-M^+$ (R is long-chain alcohol or phenol)	Lecithin, glyceryl esters containing one phosphate ester	Low foaming, good water solubility, resistant to high pH

Table 1.2: Major types of anionic surfactants (M could be alkali metal or ammonium ion)

1.2.2.2. CATIONIC SURFACTANTS

There are two types of cationic surfactants based on the nitrogen-containing group, the first is the alkyl nitrogen compounds, as shown in Fig. 1.4, and the second is the heterocyclic amine surfactants, as shown in Fig. 1.5.

$$C_nH_{2n+1}NHR_2^+X^-$$
$$C_nH_{2n+1}NR_3^+X^-$$
$$C_nH_{2n+1}N^{\delta+}R_2 \rightharpoonup O^{\delta-}$$

Fig. 1.4: Structures of alkyl nitrogen compounds (R is H or low-molecular -weight alkyl groups, X could be halide, sulfate, acetate, etc)

Cette thèse est accessible à l'adresse : http://theses.insa-lyon.fr/publication/2013ISAL0001/these.pdf
© [R. Xu], [2013], INSA de Lyon, tous droits réservés

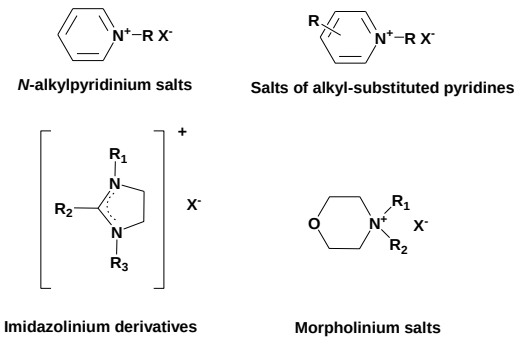

Fig. 1.5: Schematic representatives of heterocylic amino compounds (R is H or low-molecular -weight alkyl groups, X could be halide, sulfate, acetate, etc)

They are used as fabric softeners in textile industry, modifiers for controlling the surface tribological properties in the mineral flotation process, are also extremely important.

1.2.2.3. NONIONIC SURFACTANTS

Different from two types above with the head group charged, the nonionic surfactants are the neutral kinds driven by hydrogen bondings (H-bondings) between the polar groups with the solvent, particularly the water. These materials have some advantages such as lower sensitivity to the electrolytes and pH, and easy designed properties. The most widely produced and used non ionic surfactants are based on polyoxyethylene (POE). The general formula for this type is:

$$\mathbf{RX(CH_2CH_2O)_nH} \quad \mathbf{X = O, N, functional\ group}$$
$$\mathbf{n > 6}$$

Fig. 1.6: Formula of polyoxyethelene

For these compounds, a characteristic is the inverse temperature-solubility relationship, that is to say, when the temperature increases, the solubility of the molecule in the water decreases. This phenomenon is mainly due to the change of hydrogen bonding interactions between the molecules and the water.

Another source in this category is the derivatives of polyols, in which renewable hydrophilic moieties are included, for example, glycerol or carbohydrates. Due to their low toxicity and

Cette thèse est accessible à l'adresse : http://theses.insa-lyon.fr/publication/2013ISAL0001/these.pdf
© [R. Xu], [2013], INSA de Lyon, tous droits réservés

biocompatibility, they are found use in foods and food emulsions, pharmaceuticals, cosmetics, and agricultural applications of pesticides and herbicides. A more extended discussion on the carbohydrate-based amphiphiles is given in the next section.

1.3. Carbohydrate Based amphiphiles

1.3.1 Introduction

Sugar-based amphiphiles rank high among compounds that are designed according to the principles of green chemistry.[13] The raw materials for producing sugar-based amphiphiles, such as monosaccharides, disaccharides are abundant in the nature and of easy access, for example for sucrose, by crystallization from concentrated sugarcane or sugar beet juice. [] Though plenty of methods have been tried out to bind the carbohydrate moiety to the hydrophobic tails, in the industrial point of view, such as price and quality, only a few carbohydrates derived surfactants could be brought into commercial. Thus, more convenient and economically acceptable manufacturing procedures in industrial scale are still under research. Nowadays, the best-known carbohydrate based surfactants are alkyl polyglycosides (APGs), sorbitan esters, and sucrose esters.[13-16] Table 1.3 shows a survey on the production volume and cost of three big families in the carbohydrate surfactants, exhibiting comparative counterparts towards the petroleum based surfactants in the industrial perspective. [13]

	Production Volume[t/a]	Average Price[euro/kg]
Sucrose	150,000,000	0.25
Glucose	30,000,000	0.30
Sorbitol	650,000	1,80

Source: Lichtentaler, F. W., Methods and Reagents for Green Chemistry, Wiley-Interscience, 2007. (Price here could only be indications)

Table 1.3: Availability of Carbohydrate Raw Materials[13]

Another rich resource of carbohydrate amphiphiles is found in the natural organisms,[17-20] these glycolipids, the biological name of carbohydrate amphiphiles, are known to play key roles in immune and endocrine systems, fertilization, brain development, prevation of

Cette thèse est accessible à l'adresse : http://theses.insa-lyon.fr/publication/2013ISAL0001/these.pdf
© [R. Xu], [2013], INSA de Lyon, tous droits réservés

pathogenesis and blood clotting.[21, 22] The glycolipid biosurfactants discovered as the metabolic compounds from fermentation of microorganisms are also found very important in some specific domains. Owing to their biocompatibility and some ecological advantages, they were firstly considered as the alternatives to chemical surfactants, but as their unique properties explored recently and optimized conditions for large scale manufacturing, they will be seen in great growth in the cosmetic, medical domains.[19] Some examples will be shown in the following sections.

Self-assembling and self-organizing mechanism is considered as the main theory to explain the formation of liquid crystals,[23-26] gelators,[27-30] and nanotubes[31-33] by the carbohydrate amphiphiles. The resulting supramolecules will exhibit some interesting properties as not possible for the individual molecules. Some pioneering work will be described, too.

1.3.2 Industrial manufacturing carbohydrate surfactants for consumer products

1.3.2.1 Sorbitan esters

Known under the trade name of Span™ (sorbitan alkanoates) and Tween™ (ethoxylated sorbitan alkanoates),[16] the sorbitan esters find main applications in pharmaceuticals,[34] cosmetic products,[35] latex polymerization.[36, 37]

There are two main processes to fabricate the sorbitan esters: batch and continuous processes. Both processes employ the acid (NaH_2PO_3 or *p*-TSA) as catalyst.[13] Since the easy-controlled conditions for continuous process, the appearance of resulting product would be better.[38] Scheme 1.1 shows the general process of continuous process.

Cette thèse est accessible à l'adresse : http://theses.insa-lyon.fr/publication/2013ISAL0001/these.pdf
© [R. Xu], [2013], INSA de Lyon, tous droits réservés

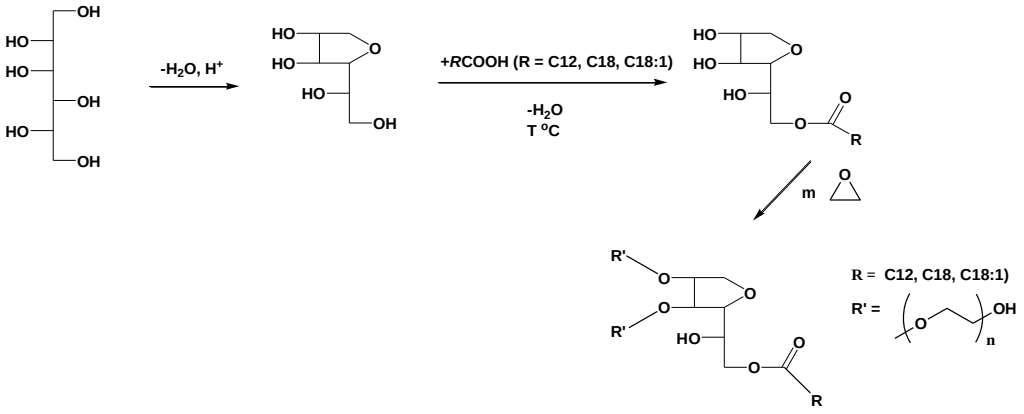

Scheme 1.1: Industrial synthetic procedure for obtaining sorbitan esters

1.3.2.2 Sucrose esters

The only commercially available surfactants using sucrose as the polar head are the sucrose esters, which are found in the food emulsification, personal care and pharmaceutical domains. Because of multifunctionalities as three primary alcohols, five secondary alcohols, and two anomeric carbons on the sucrose matrix,[13, 15] it is difficult to control the degrees of substitution: 255 distinct possible isomers with varying degrees of substitution can be obtained from acylation with a single fatty acid. However, due to rapid acyl group migration towards primary positions,[39] fatty chains are essentially found at the primary position in the final products.

Early condensed process was performed in DMSO or DMF, [13-15] in which the sucrose could be dissolved, with K_2CO_3 as the basic catalyst, shown in Scheme 1.2. But the problematic removal of solvent made it not easy to conduct, so an important know-how has been developed to have this reaction optimized for industrial production, for example, transesterification and solvent-free process. These methods have been proved to have a good yield and facile workup.

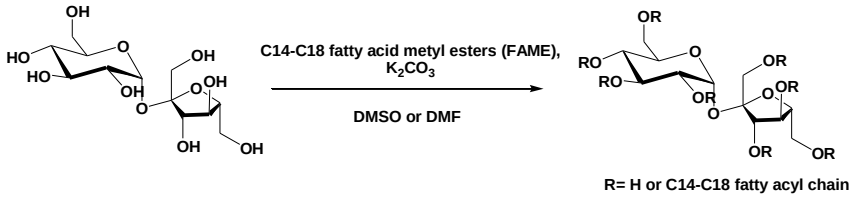

Scheme 1.2: Industrial manufacturing procedure for obtaining sucrose esters

Cette thèse est accessible à l'adresse : http://theses.insa-lyon.fr/publication/2013ISAL0001/these.pdf
© [R. Xu], [2013], INSA de Lyon, tous droits réservés

1.3.2.3 Alkyl polyglucosides (APGs)

APGs are the most extensively studied carbohydrate based surfactants.[40] As the starting materials are from fatty alcohol and glucose or starch, they are the first commercial series to offer a variety of properties based on the green chemistry concept.[13] The synthesis method is known as the Fischer glycosydation reaction. Currently, the industrial available processes are the direct glycosydation and double alcohol exchange.[14] The double alcohol exchange process employs short chain alcohol, like butanol, as reagent to convert glucose into *O*-alkylglucoside at the first step, which is the solvent in the following transglycosidation with long chain fatty alcohol (C8~C16), as shown in Scheme 1.3. This process is not as popular as direct glycosydation since the latter process could save time and control the selectivity. An alternative is enzymatic synthesis, using β-glucosidase as catalyst which yields only the β-anomer though such processes are less easy to be used in large scale syntheses.

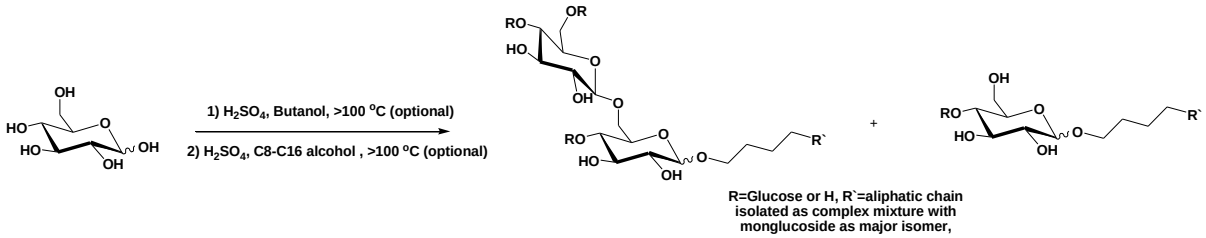

Scheme 1.3: Industrial manufacturing procedure for obtaining alkyl polyglucosides

APGs are widely used as the liquid dishwashing agents and personal care products for C12/14 series, cleaners for hard surface and industrial cleaning for C8/10 series.[13]

1.3.3. Glycolipids and glycolipid biosurfactants

1.3.3.1 Biologically occurring carbohydrate amphiphiles - glycolipids

Glycolipids are widely found in the cell membranes.[22] The most common seen glycolipids in the organisms are glycosphingolipids (GSLs), glycoglycerolipids (GGLs) and glycosyl phosphopolyprenols (GPPPs).[41] Among them, GSLs and GGLs are those which are the most studied. GSLs are widely distributed in the eukaryotes, some prokaryotes and

Cette thèse est accessible à l'adresse : http://theses.insa-lyon.fr/publication/2013ISAL0001/these.pdf
© [R. Xu], [2013], INSA de Lyon, tous droits réservés

viruses,[42, 43] containing a hydrophobic ceramide anchor N-acylsphingosine and a hydrophilic head group composed of sugars, which could be sorted into three subgroups: cerebrosides, globosides, and gangliosides.[44] Since many important biological behaviors like cell-cell recognition, [15, 45, 46] membrane transport,[47-51] are related to the activity of this species, thousands of studies have been dedicated to this type of glycolipids. It was found that absence or a too low level of GSLs may cause some physiological problems.[43] GM1 (Fig. 1.7), a kind of GSLs, is found to one of important components forming a microdomain, “lipid raft”, in the membranes for selective membrane transport.[47, 49-53]

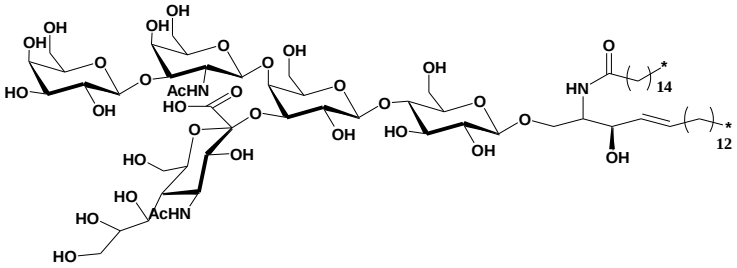

Fig. 1.7: Chemical structure of GM1 ganglioside

Glycoglycerolipids are found in chloroplasts of plants and eukaryotic algae and in cyanobacteria.[54, 55] Monogalactosyl- and digalactosyl-diacylglycerol (MGDG and DGDG) are two major glycoglycerolipids found. The DGDGs are found to play a crucial role in plant growth, thylakoid function and protein import into chloropalsts.[56, 57] One of this kind of compound digalactosyldiacylglycerol mono-estolides, isolated from oat seeds, is shown in Fig. 1.8.[58]

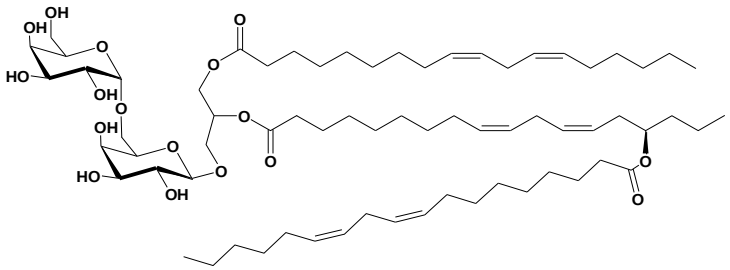

Fig. 1.8: Digalactosyldiacylglycerol mono-estolides were reported in oat kernels [58]

Cette thèse est accessible à l'adresse : http://theses.insa-lyon.fr/publication/2013ISAL0001/these.pdf
© [R. Xu], [2013], INSA de Lyon, tous droits réservés

Other glycolipids like steroid glycosides (SGs) are also found in many plants and fungi, some animals and bacteria.[59] Some of SGs are considered as an active component in Chinese traditional medicine.[60-62] One such example, 3β, 16β, 17α-trihydroxycholest-5-en-22-one 16-*O*-(2-*O*-4-methoxybenzoyl-β-D-xylopyranosyl)-(1 → 3)-(2-*O*-acetyl-α-l-arabinopyranoside), **1**, (OSW-1) is illustrated in Fig. 1.9.[63] It was found in bulbs of *Ornithogalum saudersiae,* which showed high antitumor activities. Acyl steryl glycosides (ASG) are usually referred to the SGs where a monoglycoside conjugates with sterol in 3β-*O* position while an additional acyl long fatty chain attached in the position 6 of a glycoside.[64] For most compounds of this kind, they are found in plants, while two kinds of cholesteryl glucosides were just reported recently from some bacteria: one is the cholesteryl 6-*O*-acyl-β-D-galactopyranoside (BbGL-I),[65], **3**, which is from *Borrelia burgdorferi*. Accompanied with another glycolipid 1, 2-di-*O*-acyl-3-*O*-α-D-galactopyranosyl-*sn*-glycerol (BbGL-II), they were found to have activities towards Lyme disease; the other kind is cholesteryl 6'-O-acyl-α-glucopyranoside (α-CAG), **2**, which is from *H. pylori*.[66, 67] It is thought to be synthesized by the taking up cholesterol from the stomach cells to couple with glucose moiety via a bacterial glucosyltransferase, Hp0421, the resulting compounds of which are further enzymatically acylated. [59]

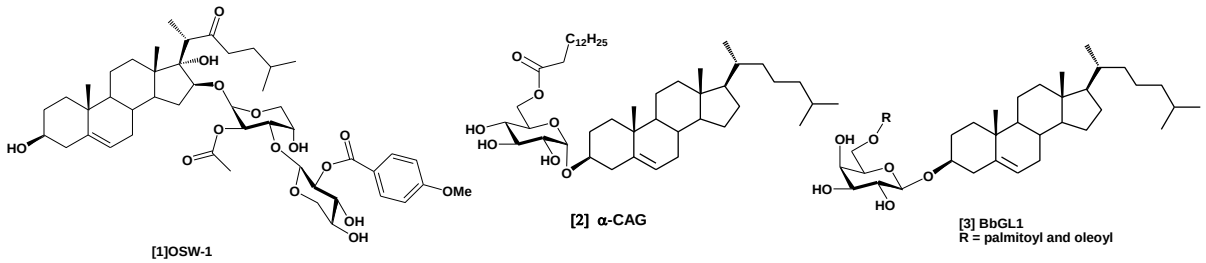

Fig. 1.9: Chemical structures of some steroid glycosides

1.3.3.2 Biotechnologically-produced carbohydrate-based surfactants [68]

Another source for the glycolipids relies on the fermentation of microorganisms. Up to now, the glycolipid biosurfactant categories include the mannosylerithritol lipids (MELs) mainly from the genus *Pseudozyma,*[69] sophorolipids from the genus *Candida*,[70] rhamnolipids from the genus *Pseudomonas aeruginosa*,[71] trehalose lipids from the genus *Rhodococcus*,[72] succinoyl trehalose lipids, cellobiose lipids, and oligosaccharide lipids. The Fig. 1.10 shows the general structure of each glycolipids.

Cette thèse est accessible à l'adresse : http://theses.insa-lyon.fr/publication/2013ISAL0001/these.pdf
© [R. Xu], [2013], INSA de Lyon, tous droits réservés

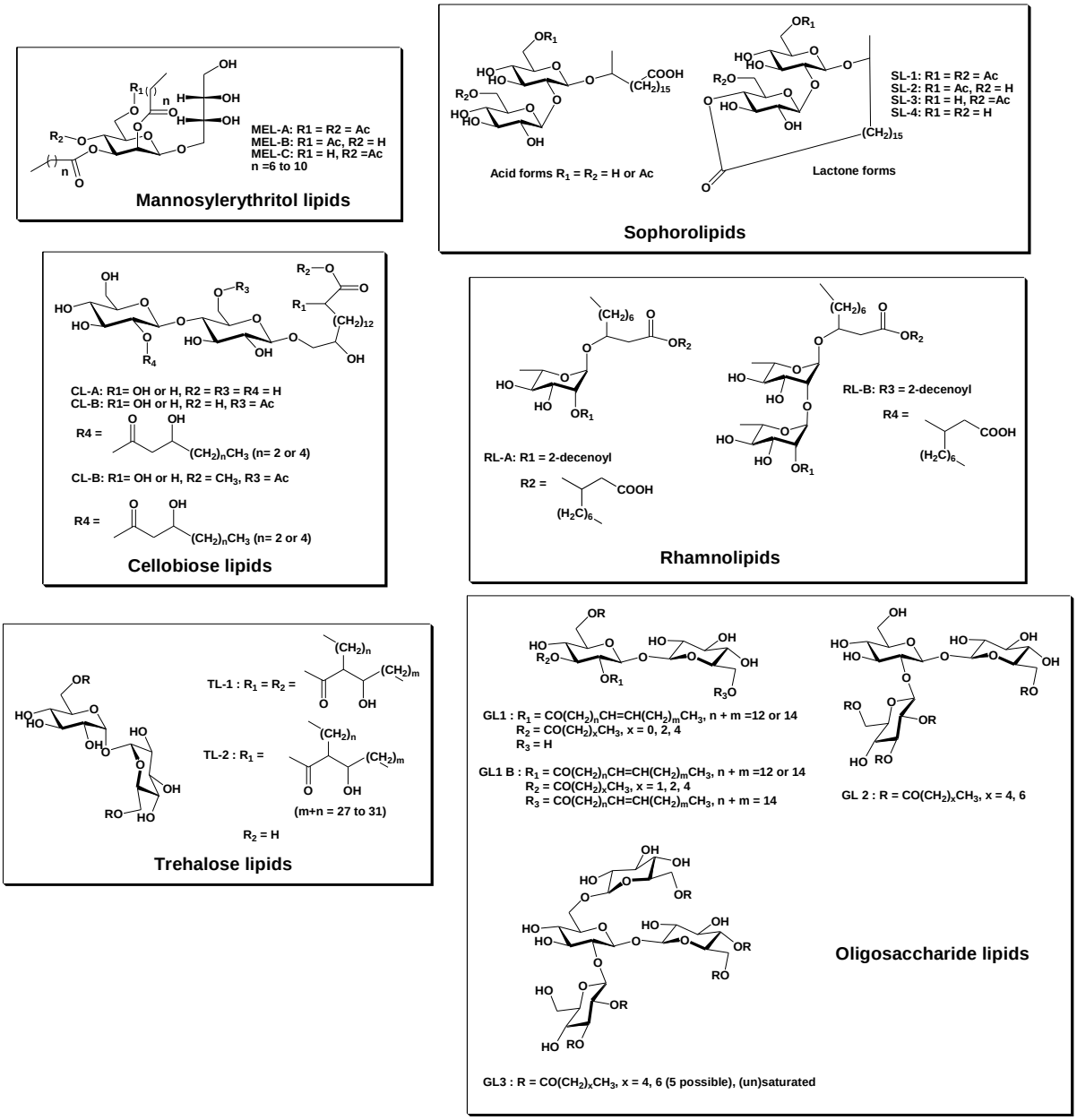

Fig. 1.10: Chemical structures of glycolipd biosurfactants available in the market

They could be produced from some renewable resources and even waste materials, like the byproducts of biodiesel production.[71] For example, RL-1 and -2, two kinds of rhamonlipid, could be produced from vegetable oils, like soybean oil, or corn oil. As the development of biological technology, the yield of some types could surpass 100g l^{-1}, like MELs and rhamnolipids, though that for some other glycolipid surfactants is still less. Another problematic issue in the industrial scale is the downstream processing since the isolation of the products is not economic.[17]

Cette thèse est accessible à l'adresse : http://theses.insa-lyon.fr/publication/2013ISAL0001/these.pdf
© [R. Xu], [2013], INSA de Lyon, tous droits réservés

In the traditional surfactant domain, studies showed that these biosurfactants could reduce the surface tension of water from 72 mN/m to less than 25 mN/m. Further comparison showed that STL-1, a kind of trehalose lipid, is highly efficient with a low critical micelle concentration (CMC) at 5.6×10^{-6} M, which reduces the tension to 19 mN/m.[19] Extensive applications of this kind could be found in the food additive industry,[73] enhancing hydrocarbon degradation[17, 20, 72, 74, 75] formation and disruption of biofilm,[76] nanotechnologies,[77-79] gene transfection, [68, 80, 81] enhancing oil recovery.[82, 83] One interesting application involving such glycolipids is towards wound healing, as some researches indicated that the additions of rhamnolipids may help the recovery in the treatments of burns and ulcers. [84, 85]

1.3.4. Supramolecular systems

Self assembling and self organizing properties of glycolipids have attracted intense attention. In such systems, non-covalent interactions drive these units to cluster together to form supramolecular moieties. The forces vary in strength from hydrogen-bonding, CH-π, $\pi-\pi$ stacking to weak van der Waals attractions.

1.3.4.1. Hydrogel and organogels

Low molecular weight gelators (LMWGs) are an interesting family of small molecules which could form reversible supramolecular gels to immobilize the organic fluids. The resulting soft matters could be used in the field of drug delivery [86-88], enzyme immobilization [89, 90], *etc.*. A recent study showed that the galactoside amphiphile shown in Fig. 1.11, was very effective to make gelation of various organic liquids, fuel oils, vegetable oils. Interestingly, it also showed selective affinity towards organic phase against aqueous phase, as it could gel the organic liquid, fuel oils in the mixture with water. In addition to this, it was found to remove crystal violet as efficiency up to 97%, found to be very useful for the water purification.[91]

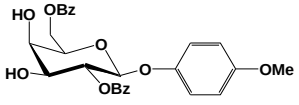

Fig.1.11: Chemical structure of *p*-methyoxylbenze-2, 6-di-benzoyl-β-D-galactopyranoside

Cette thèse est accessible à l'adresse : http://theses.insa-lyon.fr/publication/2013ISAL0001/these.pdf
© [R. Xu], [2013], INSA de Lyon, tous droits réservés

1.3.4.2. Modified nanotubes

The carbon nanotubes (CNTs) have a wide range of biomedical applications,[92] including biosensing,[93] imaging,[94] drug delivery and specifically targeting and killing of cancer cells.[95] However, their poor solubility in most solvents, above all water, has hindered the CNTs from practical uses. Thus some modifications on the CNTs sidewalls introduced by covalent and non-covalent bonds have been developed.[96] The non-covalent method is preferred as the covalent method may disrupt the π-network in the CNTs leading to the loss of electrical, mechanical and biosensing properties.[97] In addition, the π–π stacking strategy proved itself as an efficient method to combine the functionalities onto the surface of carbon nanotubes. One such example was carried out by Assali, M. *et al.*.[33] The compounds have shown a stronger interaction with the multi-walled carbon nanotubes (MWCNTs) comparing with that baring the conventional pyrene as an anchor group. By the test of affinity towards *Arachis hypogeal* (peanut) lectin, compound **4** showed a positive action, while compound **5** was negative, demonstrating the selectivity of ligand-lectin interactions simulating the situation of glycoconjugates on a cell membrane, shown in Fig. 1.12.

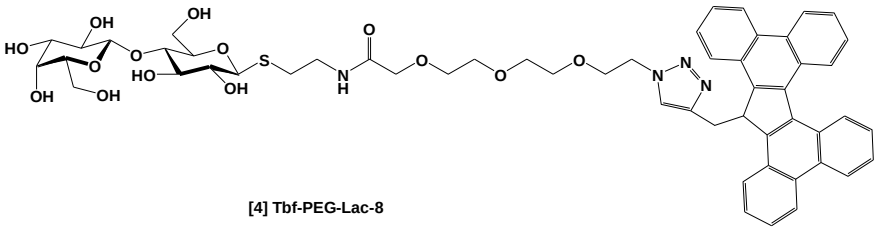

[4] Tbf-PEG-Lac-8

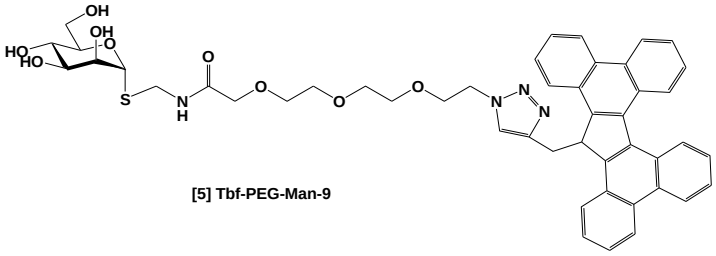

[5] Tbf-PEG-Man-9

Cette thèse est accessible à l'adresse : http://theses.insa-lyon.fr/publication/2013ISAL0001/these.pdf
© [R. Xu], [2013], INSA de Lyon, tous droits réservés

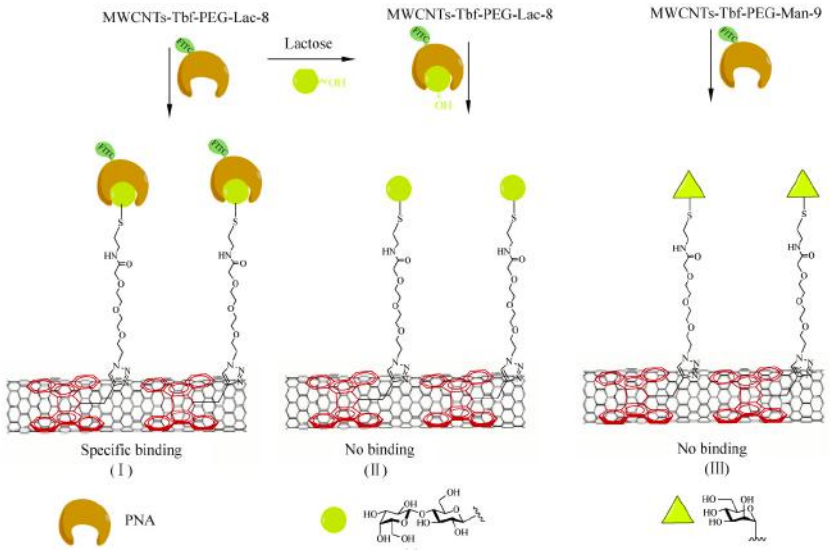

Fig 1.12: Schematic representation of (I) specific binding of peanut agglutin (PNA) to the MWCNT-Tbf-PEG-Lac-8 surface, (II) inhibition of the specific binding by soluble lactose, (III) absence of binding of PNA to mannose coated nanoglycoarrays MWCNT-Tbf-PEG-Man-9. [33]

1.3.4.3. Liquid crystals

Another consequence of the self-assembling and self-organizing properties of carbohydrate-based amphiphiles is their ability to exist in the physical state of liquid crystal. Lamellar, columnar, cubic mesophases are three main liquid crystalline behaviors for carbohydrate-based amphiphiles in a pure state, while in the solution state, a sequence of mesophases will be observed according to the concentration. An extensive discussion on the carbohydrate-based liquid crystal materials is given in the next section.

1.4. Carbohydrate-based liquid crystals

1.4.1 Introduction

“Carbohydrates are remarkable as a source of mesogens.”[25]Commented by Jeffrey G. A., who was respected as a pioneer in the field of carbohydrate-based liquid crystal, as there are not only a great variety of carbohydrate moiety itself, but also the versatility of possibilities to access to polyfunctionality and adjustable degree of polymerization from mono-, di- to oligo- and polymer. On the other hand, a growing knowledge on the mechanism of carbohydrate-based amphiphiles in their biological activities makes people think that their physical state

Cette thèse est accessible à l'adresse : http://theses.insa-lyon.fr/publication/2013ISAL0001/these.pdf
© [R. Xu], [2013], INSA de Lyon, tous droits réservés

like liquid crystal should be argued as a factor responsible for these functionalities, too.[98] For example, the disease caused by *tubercle* bacteria, was believed to have connections with "Cord factor" appearance of extracted materials under the microscope, which was actually related to their lyotropic liquid crystalline behaviors.[23]

The first synthesized carbohydrate derivative observed to show liquid crystalline behavior was hexadecyl β-D-glucoside **6** (Fig. 1.13), which was prepared by E. Fischer *et al.* around 1911. In their report, the unusual melting behavior of this compound as it softened near 78 ^{o}C and finally melted to the fluid at around 145 ^{o}C confused them.[99] A similar melting pattern was observed on a same polar head with longer aliphatic chain, named ceryl β-D-glucopyranoside **7** (Fig. 1.13) two years later.[100] It was not until 1938 that people began to realize this "double melting" behavior was due to the ability of alkyl β-D-glucopyranoside to exhibit liquid crystalline behavior.[101] Besides the synthetic sugar derivatives, the nature-occurred glycolipids are also found to exhibit liquid crystalline phases. For instance, the 6, 6`-dimycolic ester of α, α–trehalose **8** (Fig. 1.13), which possesses immunostimulant properties and antitumour activity in cluster, exhibits a thermotropic cubic liquid crystal phase.[23] But in many cases, these experiments are taken in the aqueous condition, since the functionalities of glycolipids are more related to the water atmosphere. For example, the MEL-A mentioned above was observed to show sponge, bicontinuous cubic, and lamellar phases according to different concentrations.[102]

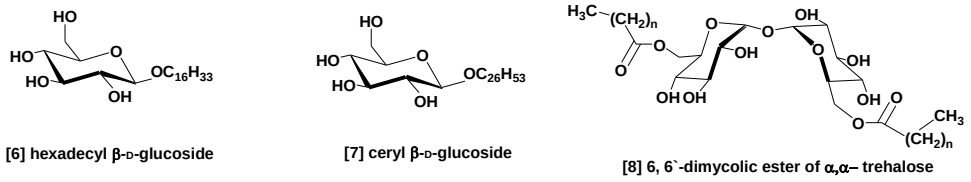

Fig. 1.13: Chemical structures of β-D-glucoside lipids **6, 7** and 6, 6`-dimycolic ester of α, α–trehalose **8**

Today, as thousands of works contributed in this area, the mesogenic behavior has been regarded as a common property of sugar amphiphilic derivatives.[24]

Cette thèse est accessible à l'adresse : http://theses.insa-lyon.fr/publication/2013ISAL0001/these.pdf
© [R. Xu], [2013], INSA de Lyon, tous droits réservés

1.4.2 Mesophase behavior based on the structure of the glycolipids

There are plenty of reviews dealing with the carbohydrate-based thermotropic and lyotropic liquid crystalline behaviors.[23, 25, 26, 99, 100, 103-105] An early point of view towards these behaviors relies on the microphase separation caused by the fact of amphiphilic structure, owing to the different melting behaviors and affinities of sugar head and hydrophobic tails.[98, 103] Nowadays, based on the more broadened category of amphiphilic carbohydrate derivatives, a modern attitude to examine these mesophases is the self assembling and self organizing mechanism,[23] which could be expressed in the terms that the units in the system communicate with each other to found some ordered state under certain conditions.[106] This mechanism could be used to explain the mesomorphic behaviors and to predict the possibilities of mesophases formed by amphiphiles, as shown in Fig. 1.14.

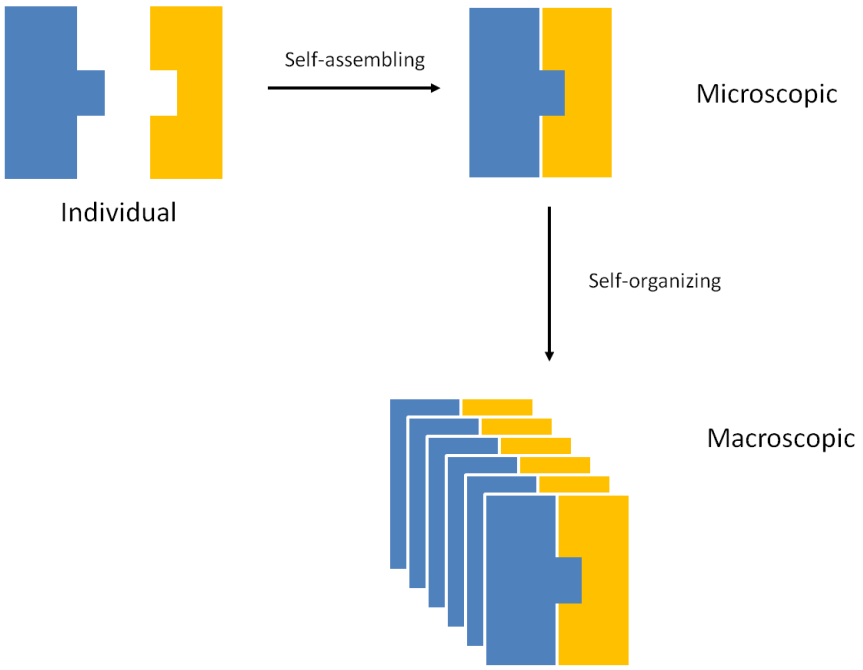

Fig. 1.14: The structure formed by self-organizing and self-assembling liquid crystals

The means for these amphiphilic molecules to communicate with each other are the non-covalent forces, like hydrogen bondings (H-bondings), CH-π, π–π (T-stacking), or van der Waals attractions, where the H-bondings is caused by the interactions of sugar head and others are by those of hydrophobic tails. In the traditional view of the requirements for

Cette thèse est accessible à l'adresse : http://theses.insa-lyon.fr/publication/2013ISAL0001/these.pdf
© [R. Xu], [2013], INSA de Lyon, tous droits réservés

mesogens, the structure of carbohydrate-based amphiphilic molecules seems to be softer than the rod-like mesogen in monophilic systems. However, with the fact that the hydroxyl groups of sugar head could be packed together via the intermolecular H-bondings to form the hard core moiety as the benzyl groups do in the monophilic system, and a flexible counterpart provided by the self-assembly of hydrophobic tails, the mesophases could be induced in the carbohydrate-base amphiphilic system.

At this point, according to the competition between the hydrophilic and hydrophobic parts during the self-assembling and self-organizing process, a tendency to form the layer or to create the curvature to bend into other dimensions will affect the packing strategy, which will be eventually observed in the different types of mesophases. Normally, this tendency could be examined in terms of comparing the relative sizes of cross-sectional area of head group to aliphatic chains and the resulting curvature, which refers to the molecular structure and interactions with outer environment.

The effect of molecular structure could be seen in the thermotropic liquid crystalline behaviors, since it is tested in the pure state of compound. According to the structure of compound, they may show 1D, 2D, 3D molecular topology as will be shown in the following discussions, thus the possible connections between structure and performance could be built up.

In low curvature occasion, as the carbohydrate derivatives own competitive amounts of sugar heads and hydrophobic tails, a lamellar mesophase is preferred. In this case, the relative sizes of hydrophilic to hydrophobic parts in this system are nearly equal, leading to a rod-like topological structure. These calamitic mesogens then aggregate paralleling to each other to form the layers where the head groups self-assemble together via the intermolecular H-bondings. These mesophases possess high viscosity, since the closely packing of layers. Normally, the lamellar mesophases observed by the glycolipids are Sm A*, where the average of the long molecular axes parallels to normal (n) of layers, as shown A in Fig. 1.15 . A typical defect texture is shown B in Fig. 1.15 under transmission optical microscope, which shows the elliptical and hyperbolic lines. Some models of the possible packing styles were proposed to support the experimental results in Fig. 1.16. The difference between these two models is whether the H-bondings or van der Waals attractions devote more to the stabilization of mesophases. As indicated in this figure, in the first model the H-bondings are more important whereas in the second the hydrophobic parts stay inside the bilayer, the mesophases are more stabilized by the interactions of fatty chains. In the case of the carbohydrate-based amphiphiles showing regular and small changes in transition

Cette thèse est accessible à l'adresse : http://theses.insa-lyon.fr/publication/2013ISAL0001/these.pdf
© [R. Xu], [2013], INSA de Lyon, tous droits réservés

temperatures, the second model would be preferred. This might be due to the sensitivity of H-bonding towards the increase of thermal energy than the van der Waals forces.

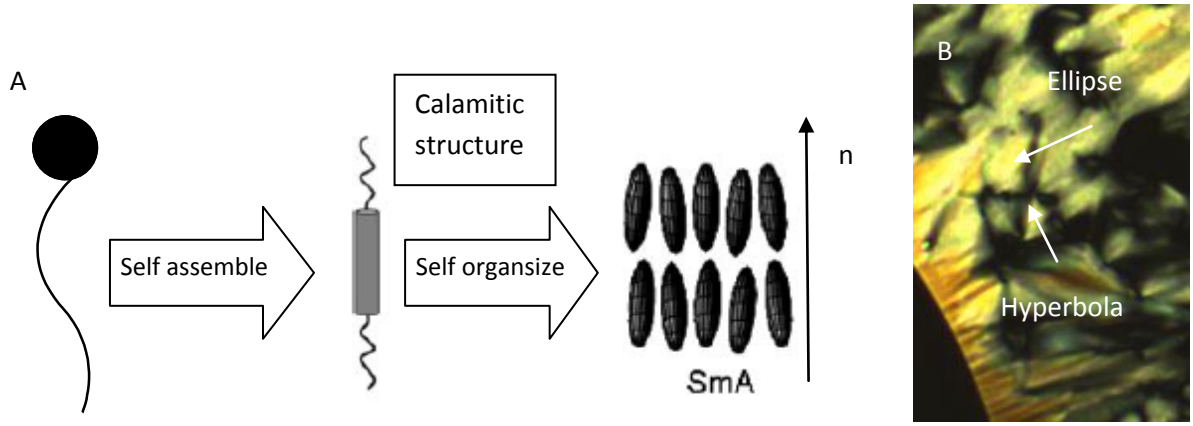

Fig. 1.15: A: Illustration of molecular structure and the packing type for lamellar (Sm A*) phase;[103] B: Typical defect image of lamellar phases (Sm A*) under light polarized microscope[23]

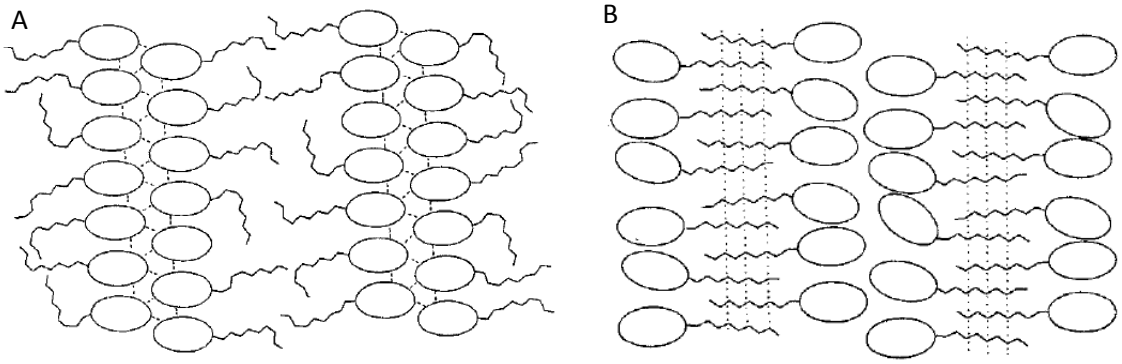

Fig. 1.16: Proposed models for lamellar phases: A) the sugar heads stay inside of the bilayer, the dashed lines stand for static H-bondings; B) the hydrophobic chains stay inside, the dotted lines represent optimum van der Waals attractions[25]

If the ratios of relative sizes lean to either hydrophilic or hydrophobic fraction, for instance, two sugar heads to one aliphatic chain or for an inverse construction, a wedge-shape topology of molecule will be created (A, Fig. 1.17). Thus, assembling of these compounds will lead to disc-like supra-structures or a lamellar structure formed by inserting alternatively, B, Fig. 1.17. For glycolipids, the disc-like supra-structure is preferred. And the resulting disc-

Cette thèse est accessible à l'adresse : http://theses.insa-lyon.fr/publication/2013ISAL0001/these.pdf
© [R. Xu], [2013], INSA de Lyon, tous droits réservés

like group will be packed into columns, which will be further aggregated paralleling into 2D mesophases, like hexagonal (Col_h), rectangular (Col_r), oblique (Col_o) or square (Col_s), as shown in Fig. 1.18. As the packing forces between and within the columns are from the interactions of the hydrophobic fraction of molecules, these disc-groups are easy to diffuse, leading to the low viscosity. In the case of carbohydrate-based amphiphiles, the hexagonal mesophases are normally observed compared to other columnar phases, the schematic representation is shown in Fig. 1.18.

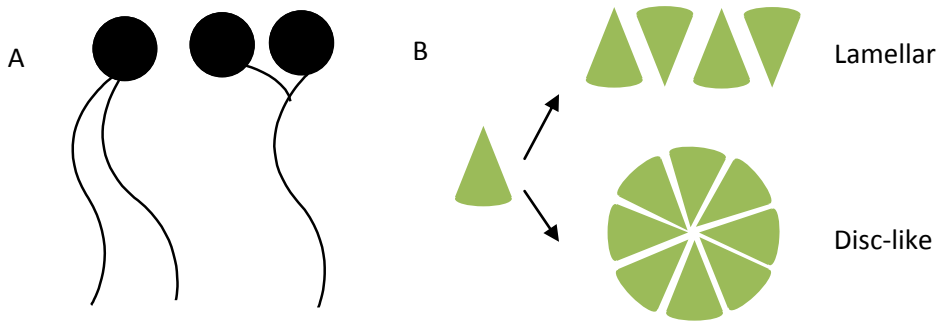

Fig. 1.17: Illustration of molecular structure (A) and the packing type for hexagonal mesophases (B) [23]

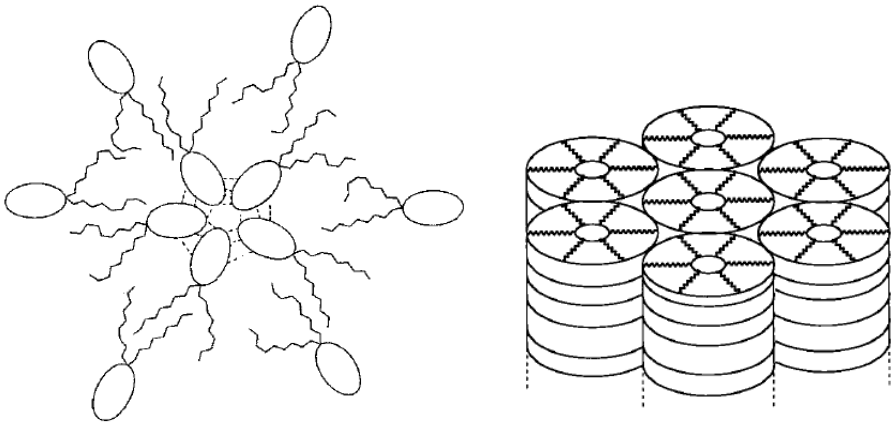

Fig. 1.18: Schematic representation of packing style of hexagonal phases[25, 99]

Cubic phases are less commonly observed in pure state of these amphiphiles. These phases are shown when the molecular topology has a conical or bowlic shape, which will require the molecular structure to be highly unbalanced to hydrophilic or hydrophobic part, as illustrated in Fig. 1.19. These cones pack together to form objects, like micelles, possessing curvature

Cette thèse est accessible à l'adresse : http://theses.insa-lyon.fr/publication/2013ISAL0001/these.pdf
© [R. Xu], [2013], INSA de Lyon, tous droits réservés

in three dimensions. The organization of this type of compounds will form a cubic array, which expresses the discontinuous cubic phases. Cubic phases are highly viscous and they don`t show the birefringent property under the transmission light microscope, however, which makes its identification very problematic. Thus, a supplementary dyeing technology or X-ray diffraction experiment is needed to study these mesophases.

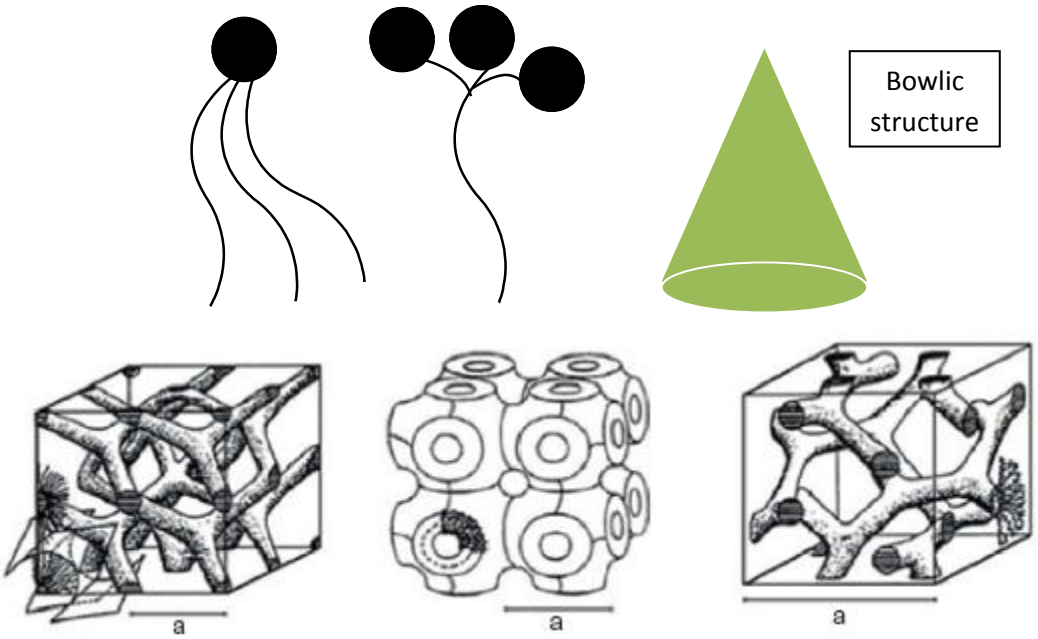

Fig. 1.19: Illustration of molecular structure (up) and the packing type for cubic mesophases (down) [23, 105]

The effect of molecular structure on the lyotropic behaviors of amphiphiles could still be seen, but the effect of outer environment, in most cases the water, plays a key role in the formation of mesophases. The curvature here will change rapidly according to concentration as well as temperature, as a result a sequence of phases could be observed. For example, the alkyl β-D-glucopyranoside,[107] with one single thermotropic phase as lamellar, shows a sequence of mesophases in aqueous conditions, shown in Fig. 1.20.

Cette thèse est accessible à l'adresse : http://theses.insa-lyon.fr/publication/2013ISAL0001/these.pdf
© [R. Xu], [2013], INSA de Lyon, tous droits réservés

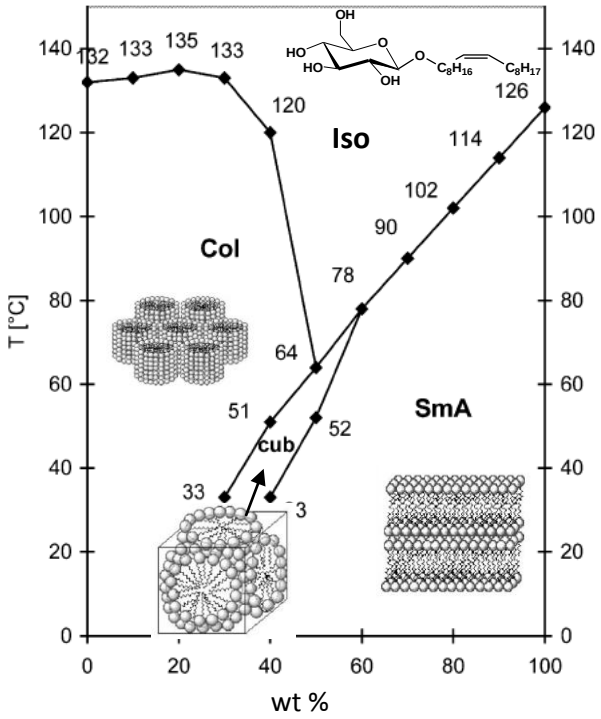

Fig 1.20: Phase diagram of alkyl β-D-glucopyranoside in water solution[107]

In addition, some rare phases which could not be observed in pure state can be observed under lyotropic conditions, like nematic, cholesteric and blue phase. This is because these phases are very sensitive to small modifications of the curvature which are easier to provoke by modification of solvation than by modifying the structure of the molecules.

From the discussion above, a schematic representation of relationship between curvature and mesophase type could be drawn, as shown in Fig. 1.21. In the following section, these models will be detailed into the discussion of different effects on the formation of mesophases. Here we will mainly talk about the molecular structural diversities in the study of thermotropic liquid crystalline behaviors, in which we are more interested in our studies.

Cette thèse est accessible à l'adresse : http://theses.insa-lyon.fr/publication/2013ISAL0001/these.pdf
© [R. Xu], [2013], INSA de Lyon, tous droits réservés

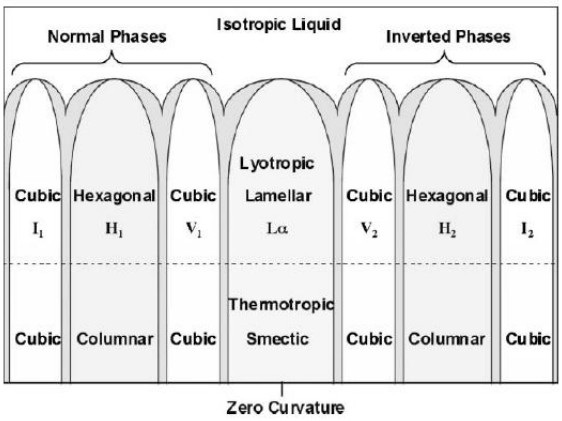

Fig. 1.21: The relation of curvature and mesophase types in thermotropic and lyotropic liquid crystalline behaviors[108]

1.4.2.1 Hydrophilic/hydrophobic balance

The hydrophilic/hydrophobic balance (or hydrophilic/lipophilic, HLB) plays a core role in surfactant performances of amphiphiles, and it is also an important factor in the liquid crystalline behaviors. It could be examined in terms of ratio of head groups to tails and the degree of substitution.

Many systematic studies employed a gradual increase of the number of methylene groups to study the effect of HLB on the liquid crystalline behavior. For example, the thermotropic liquid crystalline behaviors of alkyl β-D-glucopyranosides,[24] shown in Fig. 1.22, were found an increase of clearing point as the chain length increased.

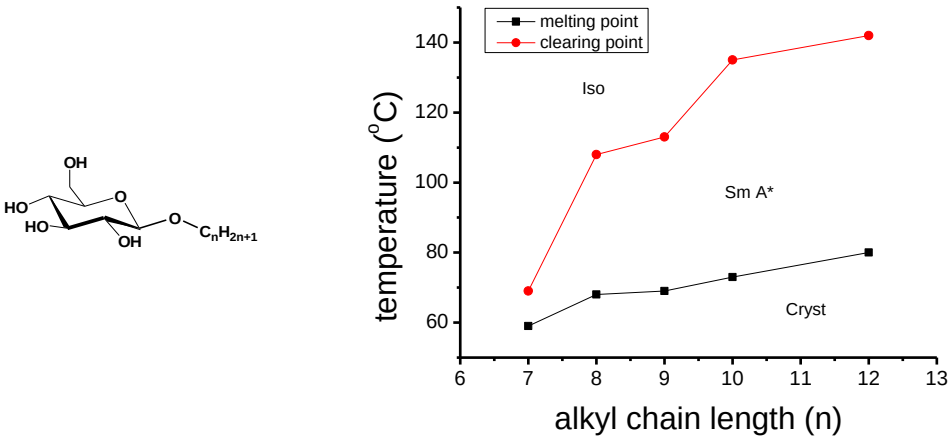

Fig. 1.22: The transition temperatures of alkyl β-D-glucopyranosides[24]

Cette thèse est accessible à l'adresse : http://theses.insa-lyon.fr/publication/2013ISAL0001/these.pdf
© [R. Xu], [2013], INSA de Lyon, tous droits réservés

By summarizing the data obtained from these systematic observations, a general tendency of transition temperatures depending on the aliphatic chains could be drawn,[109] Fig. 1.23 : with short chain length, there are no mesophases; once the chain in long enough (thus bringing equilibrium to the hydrophilic hydrophobic balance of the molecule, the mesophases are observed, and as the chain extends, the transition temperature increases, as indicated in A; And this tendency will meet a critical proportion B, from which the transition temperature begins to decrease, as C, due to the randomization of increasing aliphatic chain length.

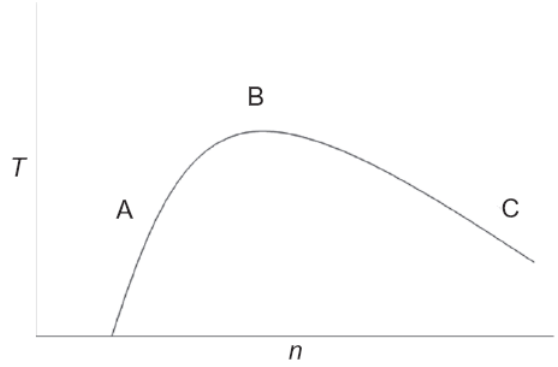

Fig. 1.23: Transition temperature (T) dependency on the aliphatic chain length (n) of homologous series[109]

Interestingly, the odd-even effects were found their influence on the clearing point, as shown in the 6-*O*-alkyl-D-galactitols system, Fig.1.24.[110] The reason for this phenomenon is still unknown. On the other hand, this effect is obvious on the system with shorter aliphatic chain.

Cette thèse est accessible à l'adresse : http://theses.insa-lyon.fr/publication/2013ISAL0001/these.pdf
© [R. Xu], [2013], INSA de Lyon, tous droits réservés

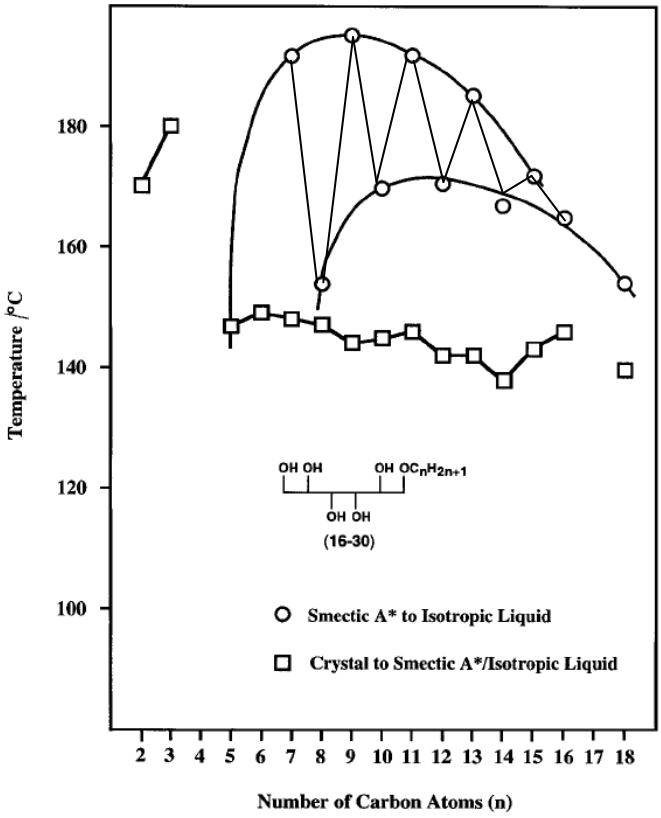

Fig. 1.24: The transition temperatures of 6-*O*-alkyl-D-galactitols as function of chain length[110]

The effect of the degree of substitution has been discussed in the previous section. Here we will examine some examples. The psychosine, (1-β-D-galactosphingosine), exhibits the Sm A* phase,[44] but if a second long chain was attached on the amine group, like palmitoyl, stearoyl, oleoyl and nervonoyl galactocerebrosides,[111] they show thermotropic columnar phases (Fig. 1.25).

Cette thèse est accessible à l'adresse : http://theses.insa-lyon.fr/publication/2013ISAL0001/these.pdf
© [R. Xu], [2013], INSA de Lyon, tous droits réservés

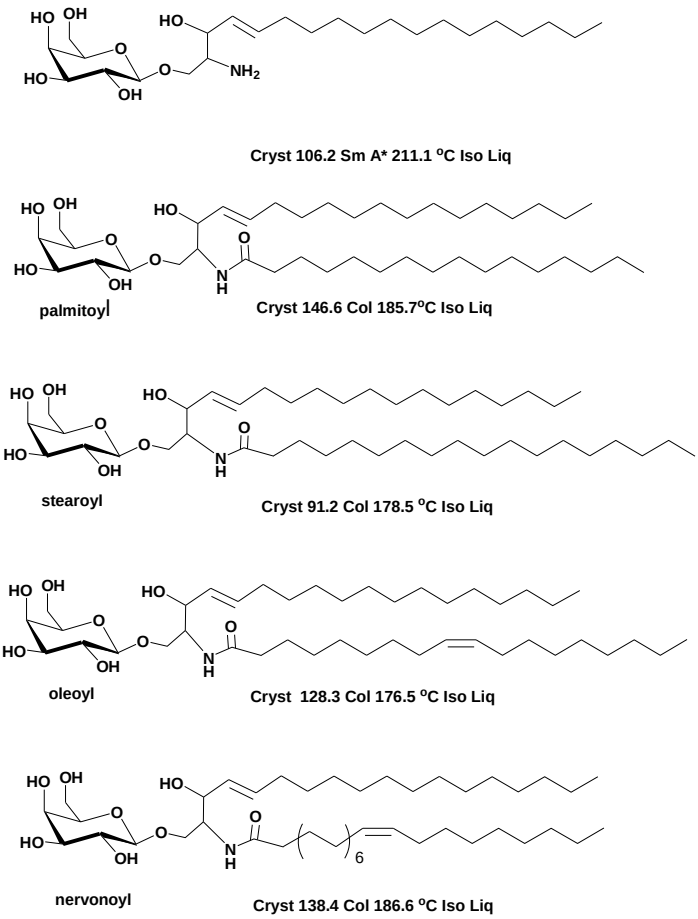

Fig.1.25: The chemical structures and liquid-crystalline properties of psychosine and its cerebrosides derivatives[111]

Some of the glycolipids consisting of triple substituted aliphatic chain show double mesophases during heating process. Like compound *O*-β-D-galactopyranosyl-tri-*O*-alkyl pentaerythritols,[108] it was composed of three aliphatic chains and one galactose head. Its decyl derivative show a passage from crystal-columnar-cubic-isotropic liquid phases across the phase diagram as the temperature increases. The transition temperatures of the *O*-β-D-galactopyranosyl-tri-*O*-alkyl pentaerythritols derivatives with different alkyl chain lengths are shown in Table 1.4. At low temperature, the energy is not enough for the aliphatic chain to move, they are more restricted to vibrate within a certain space; thus the topology of this compound is wedge-like, a columnar phase was expected to adopt, the mesogenic units self-organize into a cylindrical columnar arrangement. When the temperature goes up, the chains could take up more dynamical motion, they were much expanded at this time. As a result, the compound showed a conical shape, which was able to support the formation of the cubic mesophase.

Cette thèse est accessible à l'adresse : http://theses.insa-lyon.fr/publication/2013ISAL0001/these.pdf
© [R. Xu], [2013], INSA de Lyon, tous droits réservés

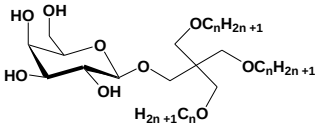

n	Cryst	Col	Cub	Iso Liq
6		62.3		
7	44.0	72.1	82.3	
9	36.0	59.4	76.2	
10	37.0	53.3	63.8	
11	30.0	38.3	43.4	
12	37.5	(32.0)		
14	52.7			
16	58.2			

Table 1.4: Transition temperatures (^{o}C) and phase classifications for *O*-β-D-galactopyranosyl-tri-*O*-alkyl pentaerythritols[108]

1.4.2.2 Location of substitution

For the non-cyclic system, the family of x-*O*-dodecyl-(D or L)-xylitols was tested as the dodecyl chain moved from position 1 to 3. The melting and clearing points increased as the order of position 1 < 2, 4 < 3, sequentially, see Table 1.5.[112] The explanation to this behavior could be as the dodecyl chain moved from outer position inward, the ratio of the cross-sectional area of hydrophilic to hydrophobic part increased, increasing the curvature during the formation of mesophase. Another reason is that the flexibility of compound reduced as the motion of aliphatic chain was disturbed by the steric hindrance.

Compound	Cryst	Sm A*	Iso Liq
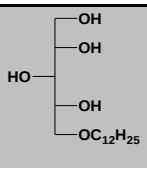	49.5	114.7	
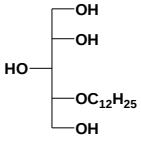	69.1	123.1	

Cette thèse est accessible à l'adresse : http://theses.insa-lyon.fr/publication/2013ISAL0001/these.pdf
© [R. Xu], [2013], INSA de Lyon, tous droits réservés

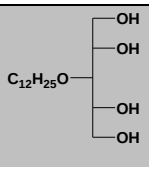	101.3	138.0
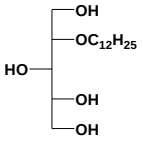	67.8	123.8

Table 1.5: Transition temperatures (^{o}C) and phase classifications for x-*O*-dodecyl-(D or L)-xylitols[112]

A similar study was carried out on the cyclic glucosyl derivatives, the dodecyl glucopyranoside and x-*O*-dodecyl α, β-D-glucopyranoses family, see Fig. 1.26. They showed Sm A* phases, with a wide range of transition temperature, which was influenced by the location of substitution.

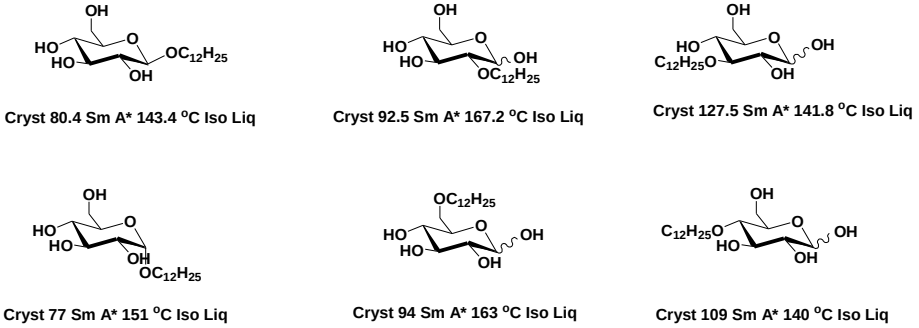

Fig 1.26: Thermotropic liquid crystalline behaviors of dedecyl glucopyranoside and x-*O*-dodecyl α, β-D-glucopyranoses

An example of study on the sucrose showed that the location of substituent may eventually change the molecular topology shape, thus two kinds of mesophases were observed.[113] The thermotropic liquid crystalline behaviors of this family were shown in Table 1.6. From the study of molecule modeling, Fig. 1.27, the compounds substituted at the position of **a** and **f** were more wedge-like, thus they could show the cubic and the columnar phases, thus the observations were confirmed.

Cette thèse est accessible à l'adresse : http://theses.insa-lyon.fr/publication/2013ISAL0001/these.pdf
© [R. Xu], [2013], INSA de Lyon, tous droits réservés

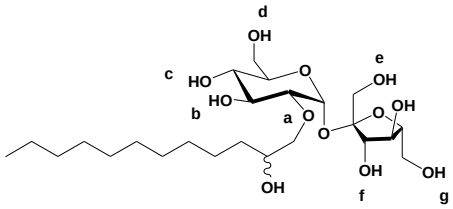

position	Cryst	Sm A*	Cub	Col	Iso Liq
a	132		135.9	147	
b	125	176.5			
c	125	167.3			
d	134	186.9			
e	154	171.1			
f	125			147.3	
g	174	190.7			

Table 1.6: Transition temperatures (^{o}C) and phase classifications for the mono-*O*-(2-hydroxydodecyl) sucroses[113]

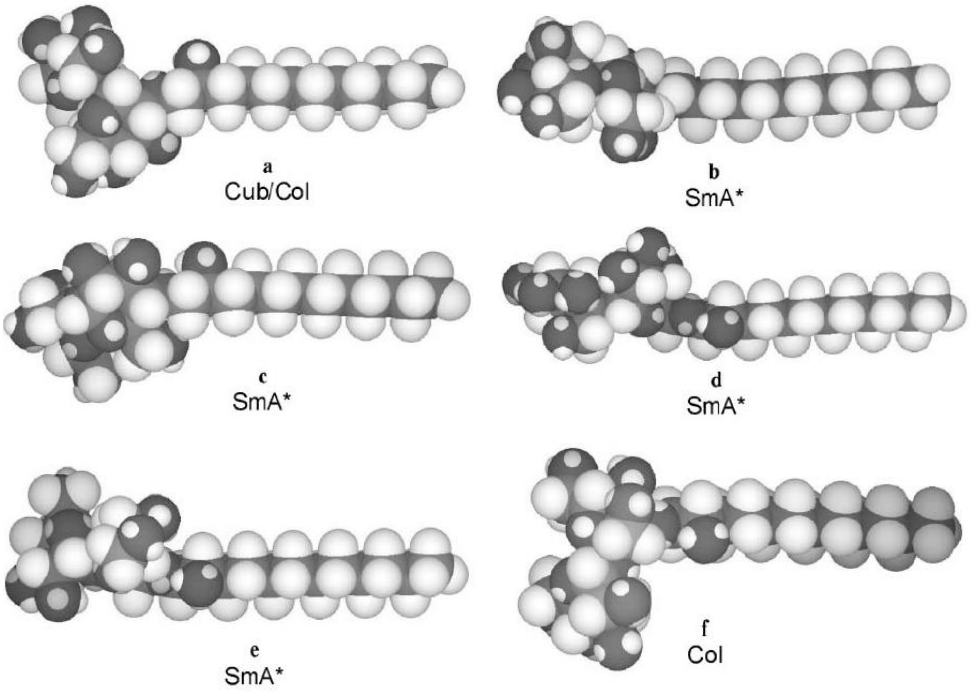

Cette thèse est accessible à l'adresse : http://theses.insa-lyon.fr/publication/2013ISAL0001/these.pdf
© [R. Xu], [2013], INSA de Lyon, tous droits réservés

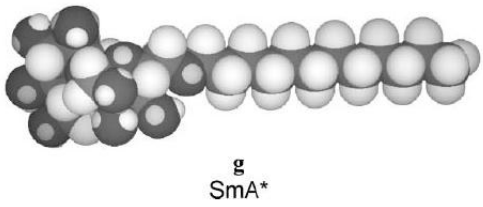

Fig. 1.27: Molecular modelings on the effect of substitutions of n-*O*-(2-hydroxyldodecyl)-sucroses[113]

1.4.2.3 Orientation of hydroxyl groups

As the carbohydrate units are full of chiral centers, one could expect cholesteric mesophases to show up in this category like monophilic chiral compounds do. However, so far these mesophases induced by the orientation of hydroxyl groups on the sugar head have not been observed yet. In many cases, the effect of chirality in the category could be regarded as the effect of conformation of hydroxyl groups on the sugar moiety. But still, the data obtained is confusing.

For some systems, this effect on clearing point is not significant. For example, in the non-cyclic polyol with mono-aliphatic chain system, the compound **9** and **10**, **11** and **12** (Fig. 1.28), showed the similar clearing points. But this factor did affect the melting behaviors, just as the diversity of melting points of sugars.

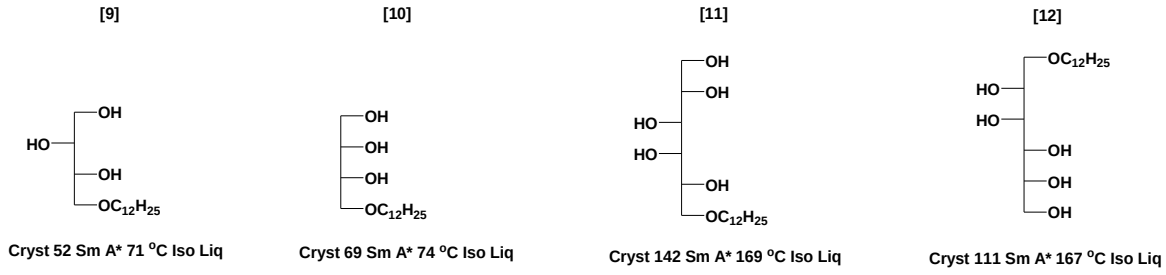

Fig. 1.28: Thermotropic behaviors of acyclic polyols lipids

But for some systems, the conformation of hydroxyl group will change the cross-sectional area of hydrophilic moiety, influencing the packing style of molecules; thus, a different mesophase will be observed. A study was conducted on the 4'-*N, N*-didodecylaminophenylazo) phenyl as the hydrophobic tail coupling with different sugar heads, gluocopyranoside, galactopyranoside, lactose, xylopyranoside, and mannopyranoside,[114]

Cette thèse est accessible à l'adresse : http://theses.insa-lyon.fr/publication/2013ISAL0001/these.pdf
© [R. Xu], [2013], INSA de Lyon, tous droits réservés

in which the glucose derivative showed columnar mesophases whereas galatose and mannose derivatives showed lamellar phases, no mesophases observed for the other two series. Compared the structures of these amphiphiles showing the mesophases, the hydroxyl groups are all in equatorial position for glucose while there is one of the hydroxyl groups stands in the axial position for the others. Thus, the head group of **14** is smaller than the others, resulting in a larger relative size of hydrophobic to that of sugar head. In consequence, the topological shape of glucose derivative is more wedge-like, inducing a rectangular columnar, as shown in Fig. 1.29.

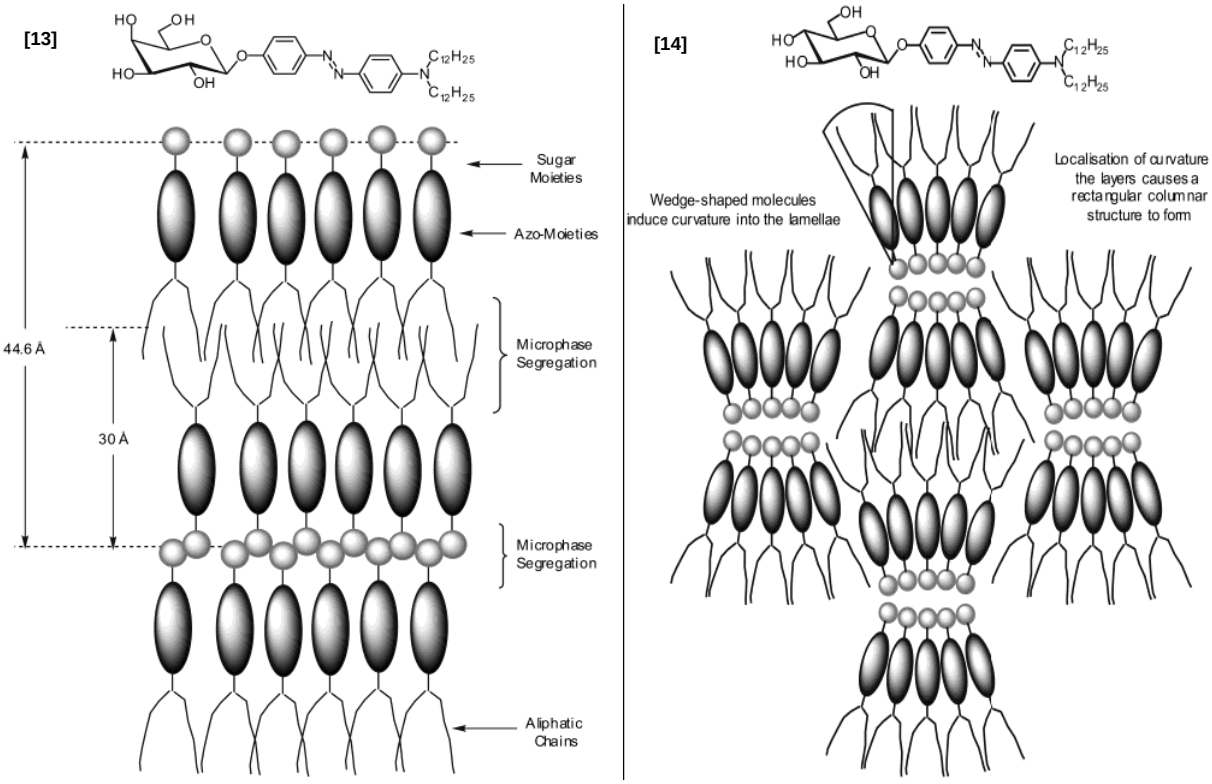

Fig. 1.29: Proposed schematic representations of arrangements in the mesophases of 4-(4'-*N, N*-didodecylaminophenylazo) phenyl β-D-galactopyranoside and 4-(4'-*N, N*-didodecylaminophenylazo) phenyl β-D-glucopyranoside[114]

1.4.2.4 Other effects

The configuration of the head group may see its effect in the thermotropic transition behavior of homologue, e.g. the α- and β- octyl D-glucopyranoside and furanoside.[115] Fig. 1.30 showed that clearing point of this array followed this order α-pyranoside > β-pyranoside > β-

Cette thèse est accessible à l'adresse : http://theses.insa-lyon.fr/publication/2013ISAL0001/these.pdf
© [R. Xu], [2013], INSA de Lyon, tous droits réservés

furanoside > α-furanoside. But this pattern is not universal, since the formation of liquid crystal phases depends strongly on balance of hydrophilic and hydrophobic parts, the order could not be easily obeyed in other sugar systems.

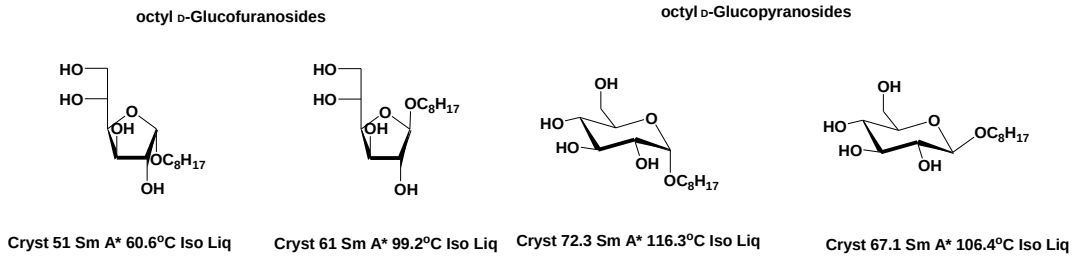

Fig 1.30: Thermotropic behaviors of octyl D-glucofuranoside and octyl D-glucopyranoside[115]

Besides the effect of molecular nature on the packing process, small modifications on the structure may have impact, too. One example of this kind is the linkage between the carbohydrate matrix and the hydrophobic part.[116] The comparison work was carried out on the mono-substituted xylitol system with linkage of ether, thioether ester and amide, respectively. The transition temperatures of these molecules as a function of alkyl chain length are shown in Fig. 1.31, where it was found the efficiency of these functional groups to stabilize the mesophases was shown as the order of RS->RCOO->RO-.

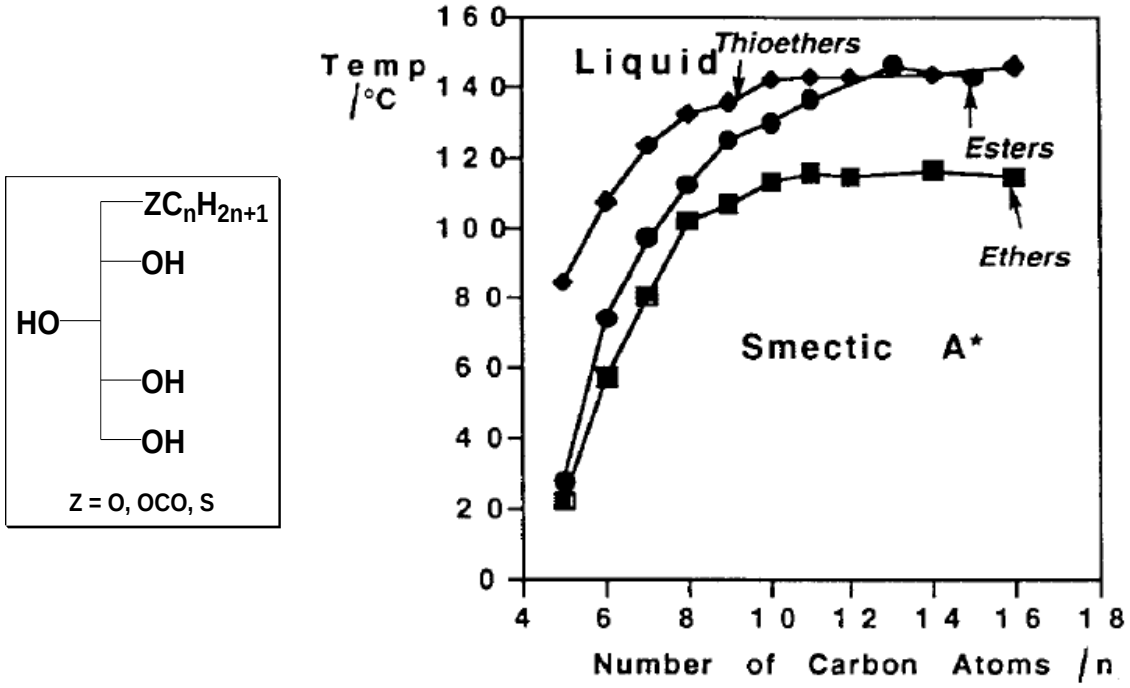

Fig. 1.31: The transition temperature of mono-substituted xylitol system with linkage of ether, thioether ester and amide as the function of aliphatic chain length[116]

Cette thèse est accessible à l'adresse : http://theses.insa-lyon.fr/publication/2013ISAL0001/these.pdf
© [R. Xu], [2013], INSA de Lyon, tous droits réservés

Even the pattern of attached aliphatic chain may affect the formation of mesophases. The archaeal lipid mimics with two linear chains showed defined melting and clearing behavior, shown in Fig. 1.32, while in the case of two branched aliphatic chains, the crystal state was replaced by glassy state a very low temperature. In addition, it showed a lower the isotropization point. These phenomena could be due to the steric hindrance by the additional methyl groups which disturbed ordered packing of aliphatic chains.[117]

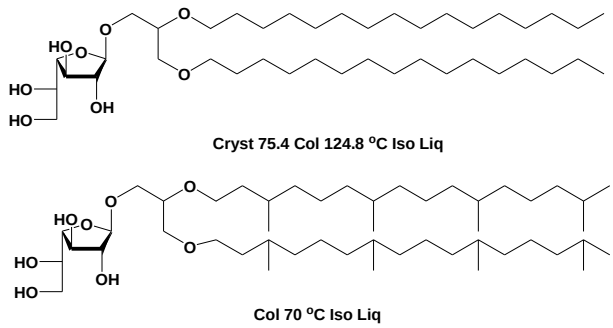

Fig. 1.32: Chemical structures of archaeal lipid mimics with linear and branched aliphatic substituents[117]

1.4.3 Methods to identify the liquid crystalline behavior

1.4.3.1 Polarized optical microscopy (POM)

For most of liquid crystalline materials, they possess a birefringent property, meaning that if the polarized light enters these materials the orientation of light wave will be change, thus some exotic images which are the reflection of the defects occurring during the formation of mesophases could be observed. This method which was found by Friedel in 1922[24] is the most widely used in identifying the type of liquid crystalline phases. The images, Fig. 1.33-1.35, below show some conventional mesophases exhibited by carbohydrate-based amphiphiles. Recent equipments include rather precise heating plates which allow estimating the transition temperatures with 0.1 to 1°C accuracy.

Cette thèse est accessible à l'adresse : http://theses.insa-lyon.fr/publication/2013ISAL0001/these.pdf
© [R. Xu], [2013], INSA de Lyon, tous droits réservés

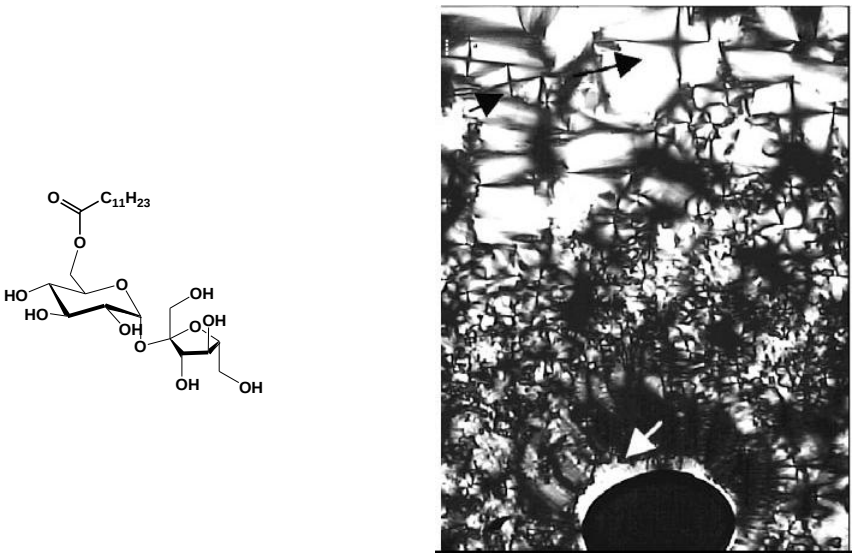

Fig. 1.33: Defect texture of lamellar mesophases with hyperbolic and elliptical lines (black arrows) and oily streaks and fringes around air bubbles (here a Sm A* lamellar phase is shown) [39]

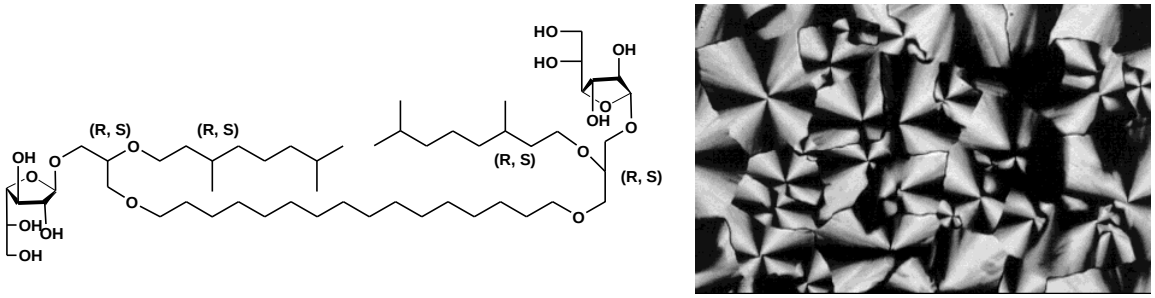

Fig. 1.34: Fan-like region defects texture of columnar phases [117]

Fig. 1.35: Transition from cubic to columnar phases,[108] where the cubic phases were black and the normal of columnar phases could be seen as the long rang of extension of long rod

Cette thèse est accessible à l'adresse : http://theses.insa-lyon.fr/publication/2013ISAL0001/these.pdf
© [R. Xu], [2013], INSA de Lyon, tous droits réservés

1.4.3.2 Differential scanning calorimetry (DSC)

DSC is another useful tool to identify the transition temperatures. Since this method is very sensitive to the heat absorption and emission, it gives a more precise data for the transition temperatures, with accuracy close to 0.01°C. In addition, by measuring heat absorption and emission, it also allows to calculate the corresponding transition enthalpies ΔH and entropies ΔS. Melting point and clearing point are normally reported from the first heating cycle, as possible hysteresis during the test can occur. In some cases, some transitions like crystal-crystal which were not seen under the polarized light microscope can be identified here.

Fig. 1.36 shows a DSC curve for the first heating cycle of 6-*O*-tetradecyl-α-D-galactopyranose, where the melting point is 114 ^{o}C and clearing point is 169 ^{o}C.[110]

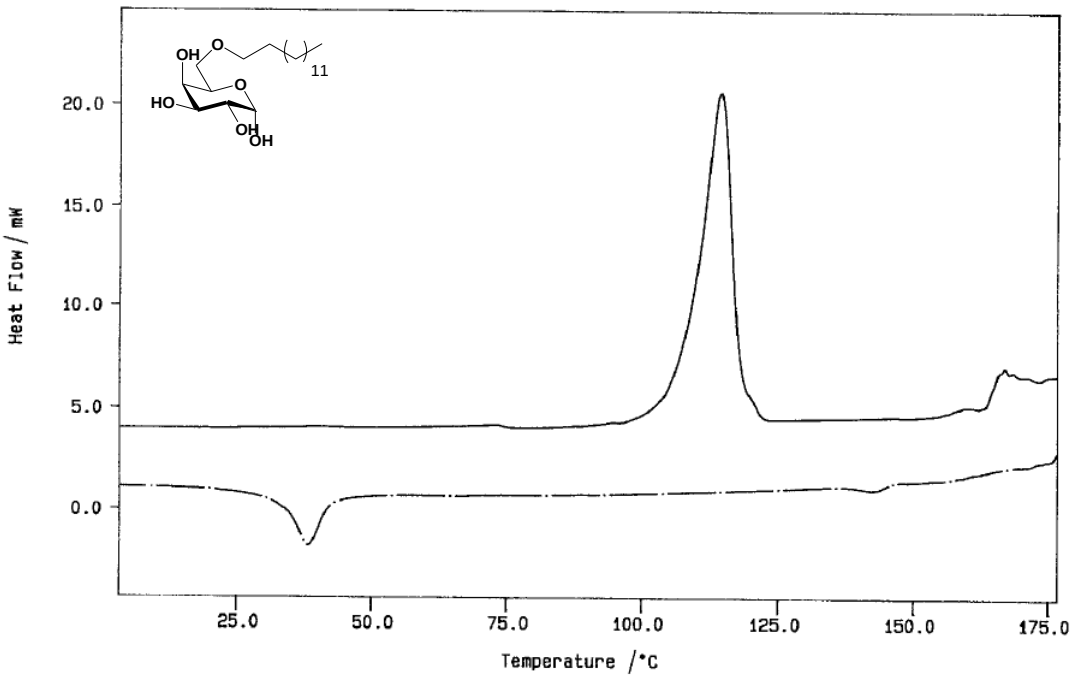

Fig.1.36: DSC thermogram for the first heating cycle of 6-*O*-tetradecyl-α-D-galactopyranose, scan rate 10 ^{o}C min^{-1}[110]

Cette thèse est accessible à l'adresse : http://theses.insa-lyon.fr/publication/2013ISAL0001/these.pdf
© [R. Xu], [2013], INSA de Lyon, tous droits réservés

1.4.3.3. X-ray diffraction spectroscopy (XRD)

When unclear or insufficient information is provided by microscopy when identifying the type of mesophase, X-ray diffraction can be used as a supplementary means, as it could give some information by providing diagnostic diffraction patterns. [118] The relation between the first reflections for different liquid crystalline phases could be shown as below:

Cubic: 1:1/√2:1/√3:1/√4:1/√5:1/√6:1/√8...

Lamellar: 1:1/2:1/3:1/4...

Hexagonal: 1:1/√3:1/√4:1/√7...

1.4.4 Conclusion

In this section, we briefly described the carbohydrate-based liquid crystals, their self-assembling and self-organizing properties and the effects that induce different formations of mesophases. The intermolecular H-bondings and the relative cross-sectional area of sugar heads to aliphatic tails are considered as two essential factors that govern the formation of mesophases. Van der Waals and other types of interactions also contribute to the stability of such mesophases. Though carbohydrates are chiral molecules, no cholesteric phases, like chiral smectic, chiral discotic, have been yet discovered in the family of carbohydrate surfactants. Elaboration of more complex systems involving sugar and lipidic moieties can still enrich the field of carbohydrate based liquid crystals.

Such studies contribute to the understanding of the relationships between structures and properties, which eventually can provide insights in their possible roles in some biological processes.

Cette thèse est accessible à l'adresse : http://theses.insa-lyon.fr/publication/2013ISAL0001/these.pdf
© [R. Xu], [2013], INSA de Lyon, tous droits réservés

Cette thèse est accessible à l'adresse : http://theses.insa-lyon.fr/publication/2013ISAL0001/these.pdf
© [R. Xu], [2013], INSA de Lyon, tous droits réservés

Chapter 2

Carbohydrate Bicyclic Lactones and Their Applications

2.1 Introduction

During the last decade, our group has been involved in developing a new synthon based on glycosyl lactones, namely carboxymethyl glycosyl lactones (CMGLs). Over the years, we have widened the scope of this synthetic strategy and applied it to several intermediates towards functional compounds such as probes for fluorescent imaging, monomers for polymerization, mesogens for carbohydrate liquid crystals, pseudoglycoconjugates and so on. These efforts proved it to be a general and useful way to couple carbohydrate moieties with other specific systems. What follows aims at reviewing briefly the field of carbohydrate lactones with a focus on bicyclic ones.

Carbohydrate-based lactones are interesting compounds which have been used in many fields and a topic for several reviews.[119-124]

Monocyclic and bicyclic lactones are two main streams in the carbohydrate derived lactones. The former ones are found to be in 1,4- (γ) or 1,5- (δ) configurations. In the latter system, the lactones could be fused or linked to the sugar moiety. Both families contain α, β-unsaturated examples.

Monocyclic lactones, or aldonolactones, from the carbohydrate resources are usually prepared by the selective oxidation on the anomeric hydroxyl group. The resulting γ and

Cette thèse est accessible à l'adresse : http://theses.insa-lyon.fr/publication/2013ISAL0001/these.pdf
© [R. Xu], [2013], INSA de Lyon, tous droits réservés

δ lactones, under certain conditions, could be reversed, Fig. 2.1. Using traditional method, for example, oxidized by bromine, the majority of resulting lactones will be aldono-1,4-lactones (γ–lactones), which are thermodynamic more stable, except for D-glucose.

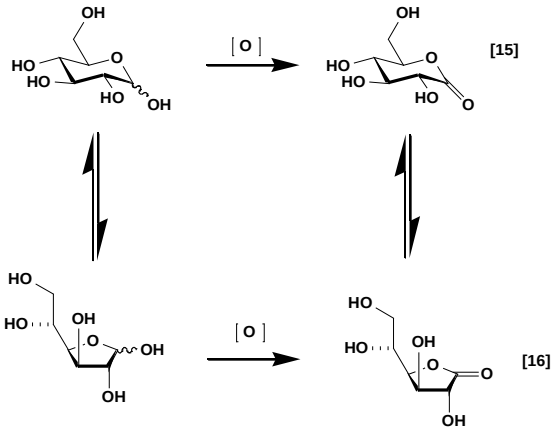

Fig. 2.1: Formation of D-glucono-1,4-lactone and 1,5-lactone

In order to obtain the 1,5-lactones as major products, some efforts have been carried out. By using the Schvo`s catalytic system, where dimeric ruthenium complex $[(C_4Ph_4CO)(CO)_2Ru]_2$, **18**, as catalyst, cyclohexanone as hydrogen acceptor, the selectivity ratio in δ-D-galactonolactone reached 93%, whereas the δ-D-mannonolactone reached to 94%.[125] Scheme 2.1 and Table 2.1 show the results.

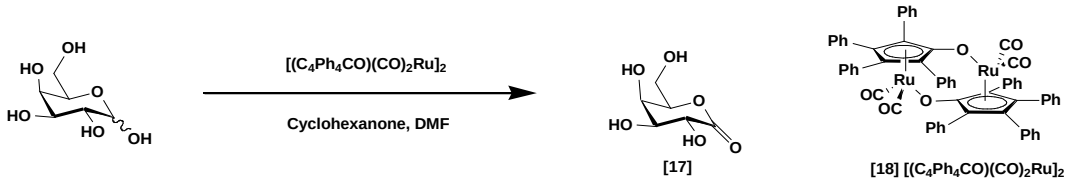

Scheme 2.1: Synthesis of δ-D-galactonolactone **17** catalyzed by dimeric ruthenium complex $[(C_4Ph_4CO)(CO)_2Ru]_2$ **18** in DMF[125]

	Time	T	Conversion	Isolated yield	γ/δ□ratio of isolated produc
Glucose	16	45	98	86	99.9 :0.1
Mannose	87	21	91	41	94 :6

Cette thèse est accessible à l'adresse : http://theses.insa-lyon.fr/publication/2013ISAL0001/these.pdf
© [R. Xu], [2013], INSA de Lyon, tous droits réservés

Galactose	87	21	92	54	93 :7

Table 2.1: Yields in lactones resulting from different sugars[125]

Whereas a similar system, where $[RuH_2(PPh_3)_4]$ as catalyst and benzalacetone (*trans*-4-phenylbut-3-en-2-one) as hydrogen acceptor, showed a reversed results. In this condition, aldono-1,4-lactones were the major products, where even for the D-gluocose, no δ-lactone was obtained. [126]

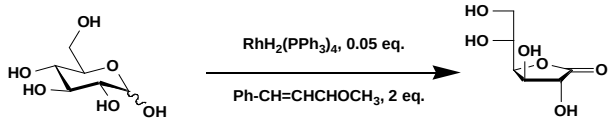

Scheme 2.2: Synthetic path for 1,4-D-gluconolatone[126]

Substrates	Products	Isolated yield (%)
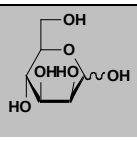	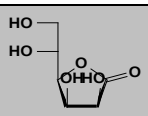	90
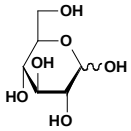	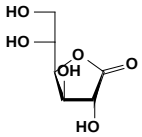	90
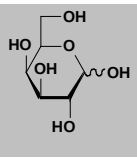	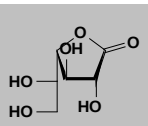	90
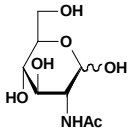	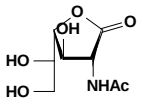	62
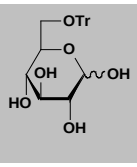	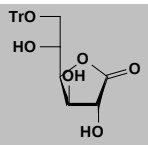	73
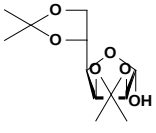	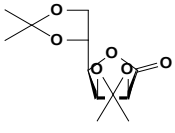	93

Table 2.2: Results obtained from a variety of sugars and protected sugars in this condition[126]

Cette thèse est accessible à l'adresse : http://theses.insa-lyon.fr/publication/2013ISAL0001/these.pdf
© [R. Xu], [2013], INSA de Lyon, tous droits réservés

Another method by the ring-closed reaction of dihydroxyenoate was achieved. In this method, 2, 4-hexadienoates were employed as the starting materials, of which the second double bond was dihydroxylation by Sharpless AD-mix reagents, followed by either direct ring-closed reaction to obtain the γ- L-galactonolactone or further protected to obtain the δ- L-galactonolactone, as shown in Scheme 2.3. [127, 128]

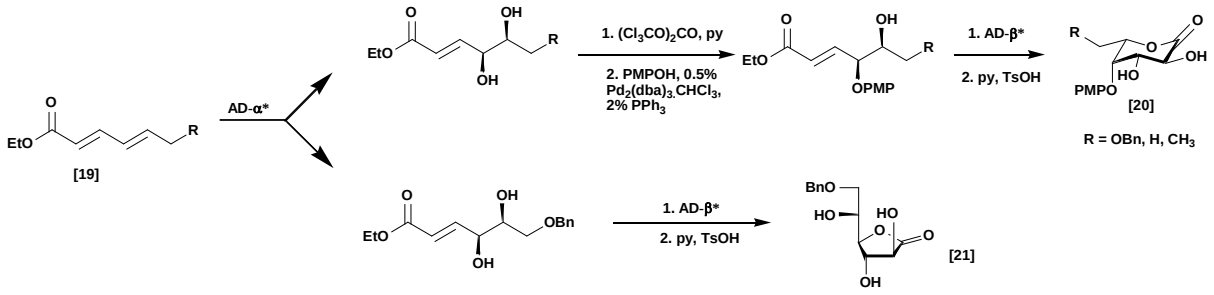

Scheme 2.3: Synthetic paths for 1,5- and 1,4- L-galctonolactones **20** and **21** [127, 128]

The microorganisms are also employed to produce to aldonolactones. For example, the δ-D-gluconolactone could be largely manufactured by oxidation of glucose associated by the enzymes form bacteria of *Pseudomonas* and fungi of *Asperigillus niger*.[129] In this case, a lactonase enzyme is also needed for preventing further opening of lactone (Scheme 2.4).

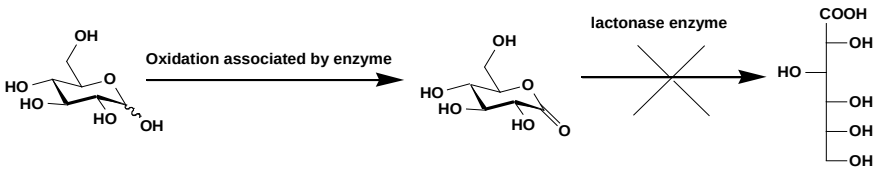

Scheme 2.4: Oxidation of D-glucose by *Aspergillus niger*

More elaborated systems which are bicyclic though still including a carbohydrate lactone have also been reported。When opened by a nucleophile, they offer the possibility to conserve the skeleton of the carbohydrate-head in the resulting products, which can be necessary for some biological purposes. Some efforts have thus been dedicated to investigating possibilities of making the bicyclic carbohydrate-based lactones. In Fig. 2.2,

Cette thèse est accessible à l'adresse : http://theses.insa-lyon.fr/publication/2013ISAL0001/these.pdf
© [R. Xu], [2013], INSA de Lyon, tous droits réservés

several examples are shown, such as the uronic acid derived lactones, compounds **22,**[130] **23**[131] and **24;**[132] fused C-branched lactones **25**[133] and **26**[134]; lactonized carboxyalkyl ether **27** and **28**,[135] and the CMGLs. The synthesis and the uses of this latter family are further detailed in the next section.

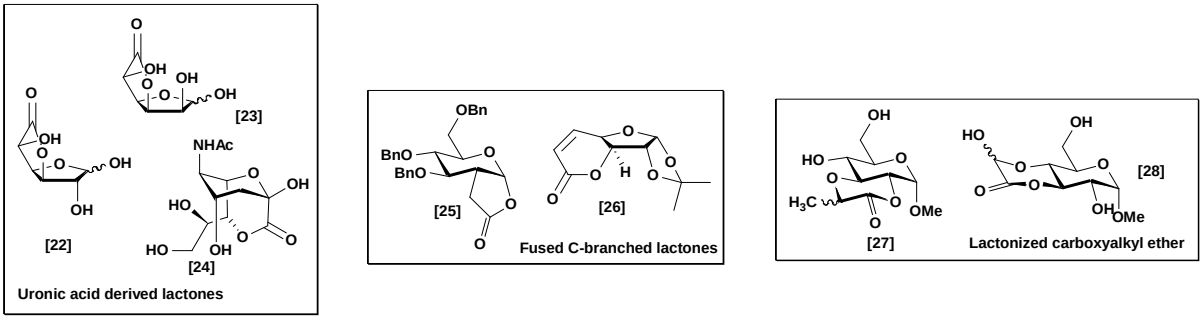

Fig. 2.2: Chemical structures of representations of several bicyclic carbohydrate lactones

2.2. Development of carboxymethyl glycoside lactones (CMGLs)

2.2.1 Synthesis of the CMGLs

The interest of our group for this topic originated from some work on the reactivity of sucrose. Looking for new oxidation products by reaction with hydrogen peroxide and sodium tungstate, a clean and efficient method already applied to the preparation of adipic acid from cyclohexene via cylohehane diol, the low stability of sucrose in acidic conditions appeared as an absolute drawback. However, we knew that isomaltulose, (6-α-D-glucopyranosyl-D-fructofuranose), was significantly more stable under acidic conditions and we switched to this other substrate, also a cheap and available sugar interesting starting material for sucrochemistry, obtained by bioconversion from sucrose. It was found that the oxidation of isomaltulose could lead to a glucopyranoside derived carboxylate, which was identified as carboxymethyl α-D-glucopyranoside (α-CMG) (Scheme 2.5).[136, 137] Further reaction with acetic anhydride led to the 3, 4, 6-tri-*O*-acetyl-α-D-glucopyranoside 2-*O*-lactone (α-CMGL) by a ring-closure reaction. Trehalulose, (1-α-D-glucopyranosyl-D-fructopyranose), a less available other disaccharide also obtained from sucrose by bioconversion, could also be used in this reaction.

Cette thèse est accessible à l'adresse : http://theses.insa-lyon.fr/publication/2013ISAL0001/these.pdf
© [R. Xu], [2013], INSA de Lyon, tous droits réservés

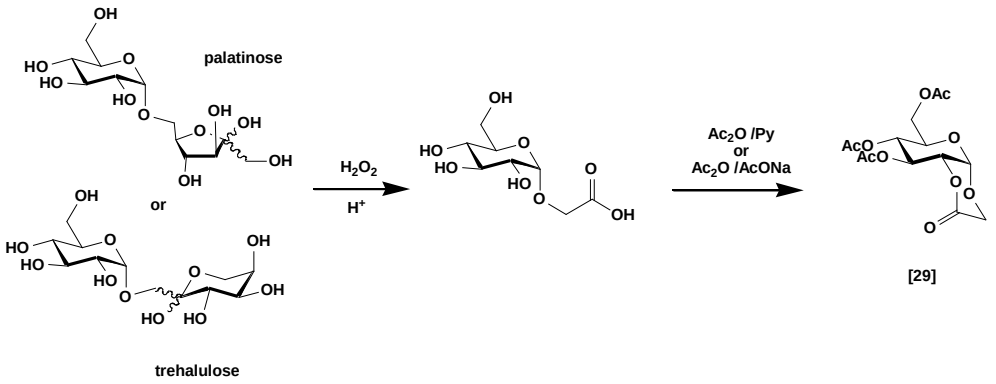

Scheme 2.5: Synthesis for α-CMGL **29** originated from palatinose or trehalose

Various parameters affecting this oxidation reaction were studied. The results showed that the pH value was essential. In the case of palatinose, at high pH, the yield of α-CMG was very low, below 15%; but when the reaction took place at pH 2, the reaction took less time and the yield was improved up to 35%. The effect of catalyst was investigated, too. The presence of sodium tungstate (Na_2WO_4) would shorten the reaction time, but increasing amount of tungstate was not found to help increase the yield of α-CMG. The result obtained from trehalulose was better, where the yield of α-CMG could be up to 59% based on recovery of starting material. However, thehalulose is not as available. Despite the modest yield of this reaction, it appeared as a simple and direct method compared to multistep selective construction by classical glycosylation sequences.

In the next step, the obtained α-CMG was subjected to the reaction with acetic anhydride in pyridine, and underwent ring-closure. A possible mechanism of this step is proposed in Scheme 2.6

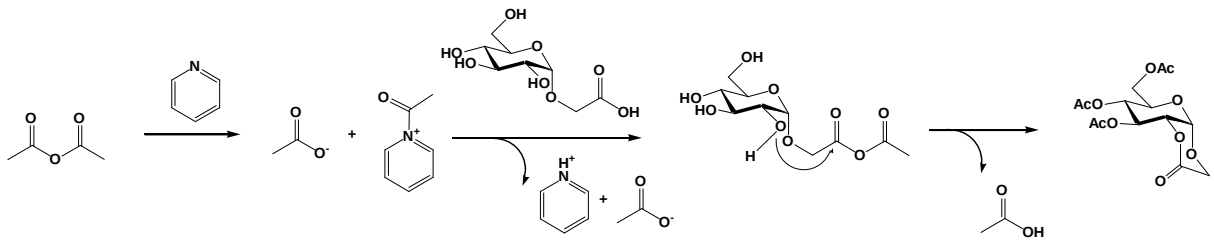

Scheme 2.6: Mechanism of ring closed to form the α-CMG lactone

Cette thèse est accessible à l'adresse : http://theses.insa-lyon.fr/publication/2013ISAL0001/these.pdf
© [R. Xu], [2013], INSA de Lyon, tous droits réservés

To examine the factors affecting the oxidation of the disaccharides and optimize the conditions for increasing the yield of lactones, a close supervision on each step was carried out.[138] By monitoring the resulting byproducts, the study showed that a stable pH value at 4 where the glycosidic linkage was stable for preventing the hydrolysis to glucose and higher temperature for complete oxidation of the fructose moiety were needed. Since the obtained lactone was sensitive to the conditions, careful handling was needed for storage and use. Before purification by silica gel column chromatography, the residue was washed by ammonium chloride solution and dried over the sodium sulfate (Na_2SO_4) carefully. After gaining the pure compound, a precipitation in pentane was needed to yield a white solid which could be stored at 4 ^oC for months. Different protecting groups, like chloroacetyl, pivaloyl and benzoyl, were used to yield the corresponding α-CMGLs with more or less stable protecting groups, as shown in Fig. 2.3.

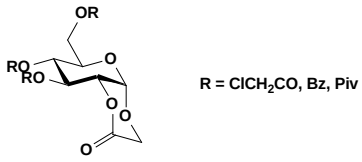

Fig. 2.3: Chemical structures of obtained α-CMGLs by different protecting group

Besides this straightforward oxidative degradation from disaccharides, other efforts by modifications on the anomeric position have also been developed, from which the list of sugars converted into lactones expanded. A first synthetic sequence was involved allyl glycosides which were oxidized by sodium periodate ($NaIO_4$) using ruthenium trichloride ($RuCl_3$) as catalyst, followed by treating the resulting product with triethylamine (TEA) to yield corresponding CMG residue.[139] The ring closed reaction was also carried out with acetic anhydride in pyridine. The whole procedure is shown in Scheme 2.8. An alternative oxidation can be ozonolysis to the aldehyde which is further oxidized in the presence of sodium chlorite ($NaClO_2$) to the carboxylic acid. This method offers a more straightforward sequence to the desired lactones, without purifying the intermediates. The procedure is shown in Scheme 2.9.

Cette thèse est accessible à l'adresse : http://theses.insa-lyon.fr/publication/2013ISAL0001/these.pdf
© [R. Xu], [2013], INSA de Lyon, tous droits réservés

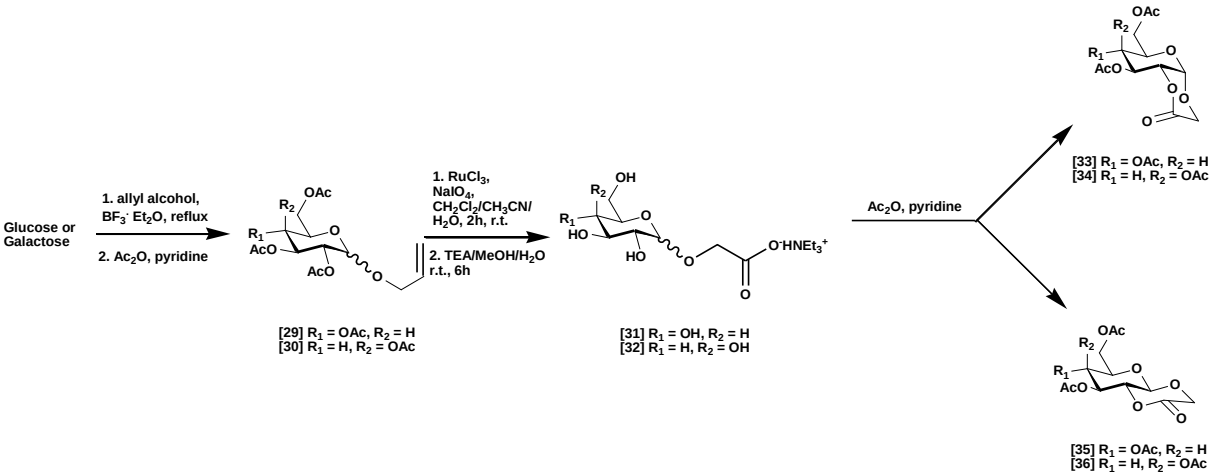

Scheme 2.8: Synthesis of α- and β- glucopyranoside lactones **33** and **35**, and α- and β-galactopyranoside lactones **34** and **36** [139]

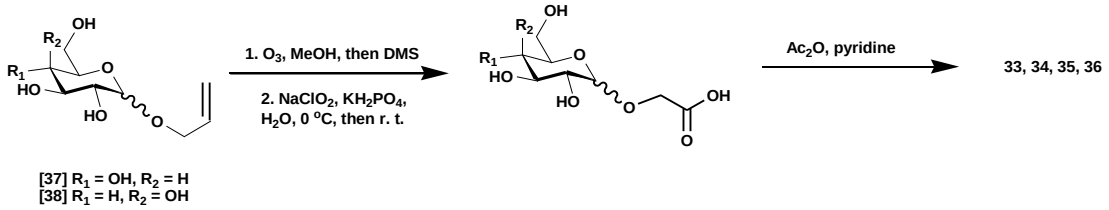

Scheme 2.9: Synthesis of the lactones **33, 34, 35, 36** via oxidation using O_3

A Koenigs-Knorr-type reaction was tried to obtain the lactones with benzyl groups protected. These lactones are less stable than the acetylated ones, however. For the β conformation, the procedure went through a orthoester strategy to yield the resulting OH-2 free compounds with benzyl groups protected in 3, 4, 6 position, which followed by the same route of previous ozonolysis process, shown in Scheme 2.10.

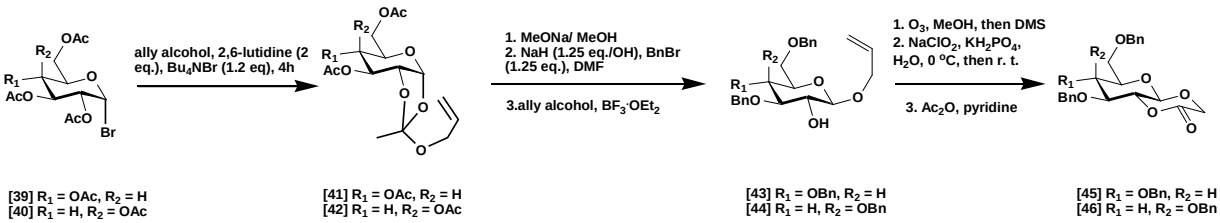

Scheme 2.10: Synthetic process for benzylated β-D-glucopyranoside lactone **45,** and β-D-galatopyranoside lactone **46**

Cette thèse est accessible à l'adresse : http://theses.insa-lyon.fr/publication/2013ISAL0001/these.pdf
© [R. Xu], [2013], INSA de Lyon, tous droits réservés

The α lactones were prepared in a different way, where the 2-*O*-benzyl of allyl 2,3,4,6-tetra-benzyl-*O*-α-D-glucopyranoside **49** and α-D-galatopyranoside **50** were cleaved by triisobutylaluminium (TIBAL) to yield 2-OH, as shown in Scheme 2.11. This method was applied to glucofuranoside, where the α-lactone **51** was obtained while β one was not. This might due to the instability of these benzylated compounds.

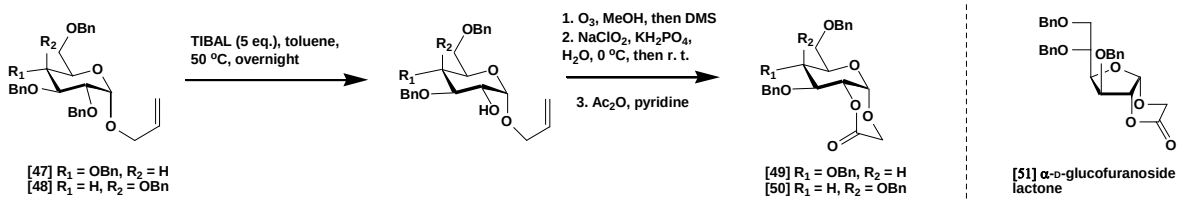

Scheme 2.11: Synthetic process for benzylated α-D-glucopyranoside and α-D-galatopyranoside lactones **49** and **50,** and the chemical structure of α-D-glucofuranside lactone **51**

A modified option is based on an anomeric alkylation with *tert*-butyl bromoacetate, which proved to be very convenient and general in terms of starting carbohydrate (Scheme 2.12).[140] Firstly, the peracetylated glucopyranoside was treated with NH_2NH_3OAc to deprotect the anomeric OH, which was further reacted with *tert*-butyl bromoacetate in the presence of K_2CO_3 to yield the acetal ether **48**. At this stage, the α and β anomers were obtained. The α anomer was preferred with the ratio α: β = 6.1: 1. After, the *tert*-butyl group was selectively removed by TFA to the carboxymethyl acid. The lactones were obtained in the same ring-closed conditions as described. This procedure was applied on other mono- and di- saccharides and proved to be successful. (Table 2.3)

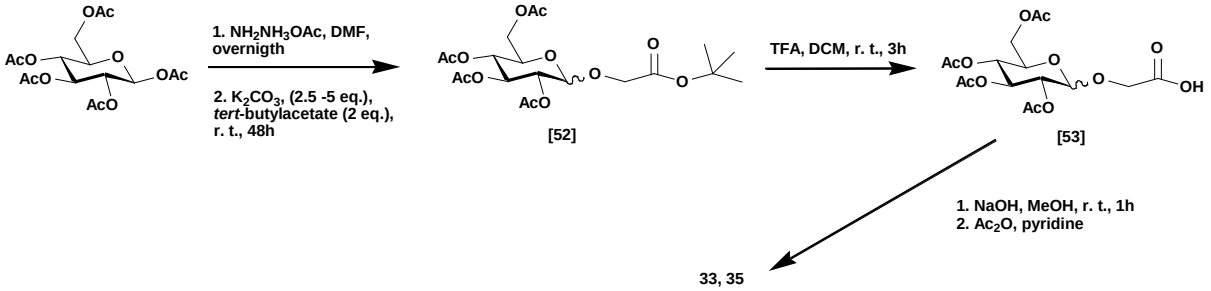

Scheme 2.12 Synthetic process of α- and β-D-glucopyronside lactones by using the *tert*-butyl bromoacetate[140]

Cette thèse est accessible à l'adresse : http://theses.insa-lyon.fr/publication/2013ISAL0001/these.pdf
© [R. Xu], [2013], INSA de Lyon, tous droits réservés

Product	Yield (%)	Product	Yield (%)
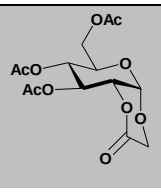	83	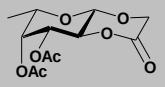	60
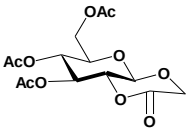	71	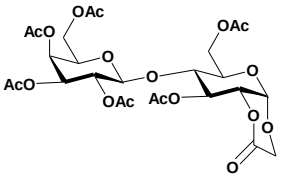	70
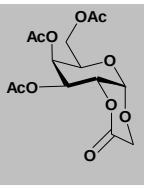	87	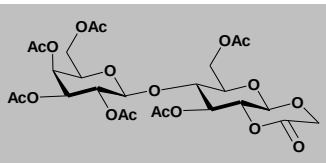	60
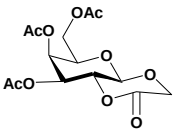	64	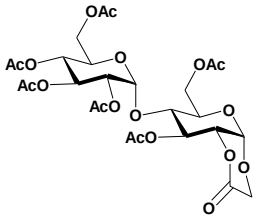	80
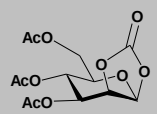	74	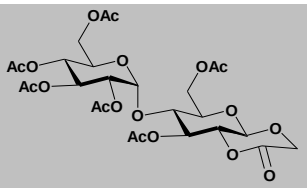	64
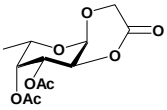	84	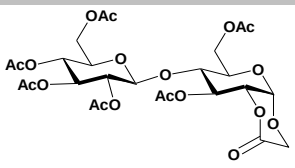	73

Table 2.3 List of sugars formed CMGLs[140]

The conditions for starting from fully unprotected sugars were also studied. The glucose, mannose, N-acetyl glucosamine, maltose, and lactose were treated with NaH in DMF (Scheme 2.13). The yield was low compared with the corresponding acetylated ones, but the reaction showed preference towards β conformation, as shown in Table 2.4.

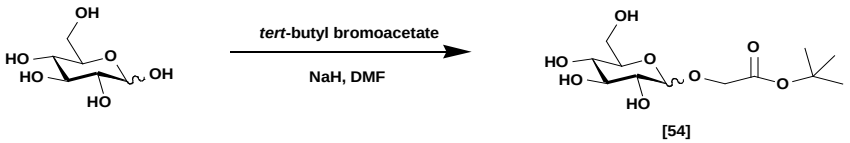

Scheme 2.13: Synthetic process of glucose with *tert*-butyl bromoacetate[140]

Cette thèse est accessible à l'adresse : http://theses.insa-lyon.fr/publication/2013ISAL0001/these.pdf
© [R. Xu], [2013], INSA de Lyon, tous droits réservés

	Yield (%)	α : β
Glucose	50	1:2.8
Mannose	55	1:1
N-acetyl glucosamine	77	2.8:1
Maltose	49	1:1.8
Lactose	57	1:2

Table 2.4: Yields and α: β conformation ratios obtained by different sugars[140]

2.2.2 Construction and applications of conjugates obtained from CMGLs

The lactones are known to be readily opened by nucleophiles, such as amines and alcohols. Via this strategy, pseudo disaccharides, sugar amino acids, surfactants and monomers and so on can be prepared. Using these bicyclic lactones, since the attack by nucleophiles would not affect the sugar ring, the opening of lactone ring offers a convenient method for conserving the cyclic pyranose or furanose skeleton into the target molecules, which could be useful for bringing some biological function or at least some biocompatibility.

At first, this research started with amino acids, and simple alcohols, amines. With alcohols, the reaction can be either promoted by acid or base catalysis. The reaction was applied to a great variety of alcohols, Scheme 2.13. However, the newly created ester function is just as unstable as other acetyl groups on the sugar, therefore making difficult subsequent deprotection of adducts without cleaving as well the new connection. Using chloroacteyl protected lactones, selective de protection of the sugar could be achieved.[137]

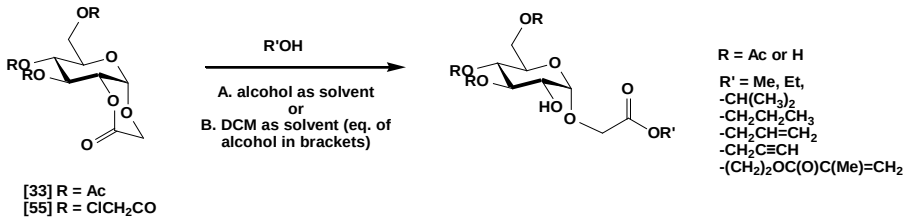

Scheme 2.14: Reactions of lactones **33** and **55** with alcohols[137]

Cette thèse est accessible à l'adresse : http://theses.insa-lyon.fr/publication/2013ISAL0001/these.pdf
© [R. Xu], [2013], INSA de Lyon, tous droits réservés

The reaction proved to be much more general and useful using amines as nucleophiles. The results showed that with amines the obtained yields were much higher than alcohols with a short reaction time, and the resulting compounds were stable which could be further deacetylated to yield the glucopyranoside derivatives. The conditions and types of amine used are shown in Scheme 2.14. Starting from amino acid, an extended reaction time was needed and the yields were fair, Scheme 2.15.

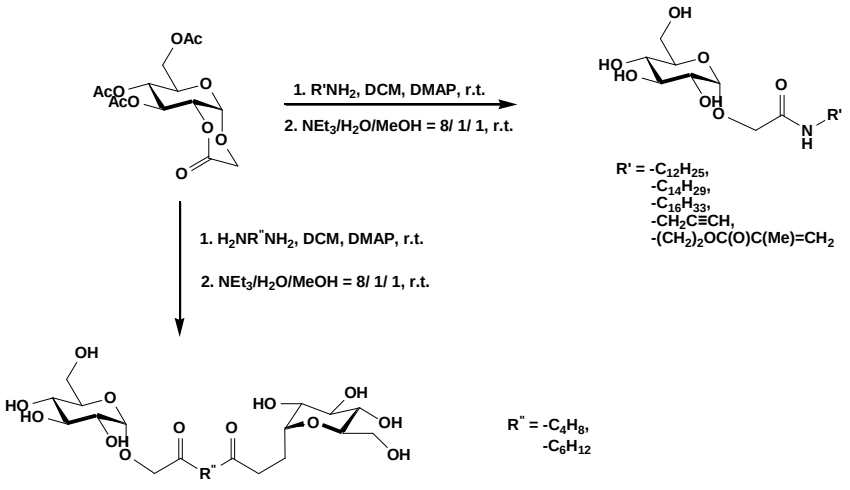

Scheme 2.15: Reactions of α-CMGL with amine and diamines[137]

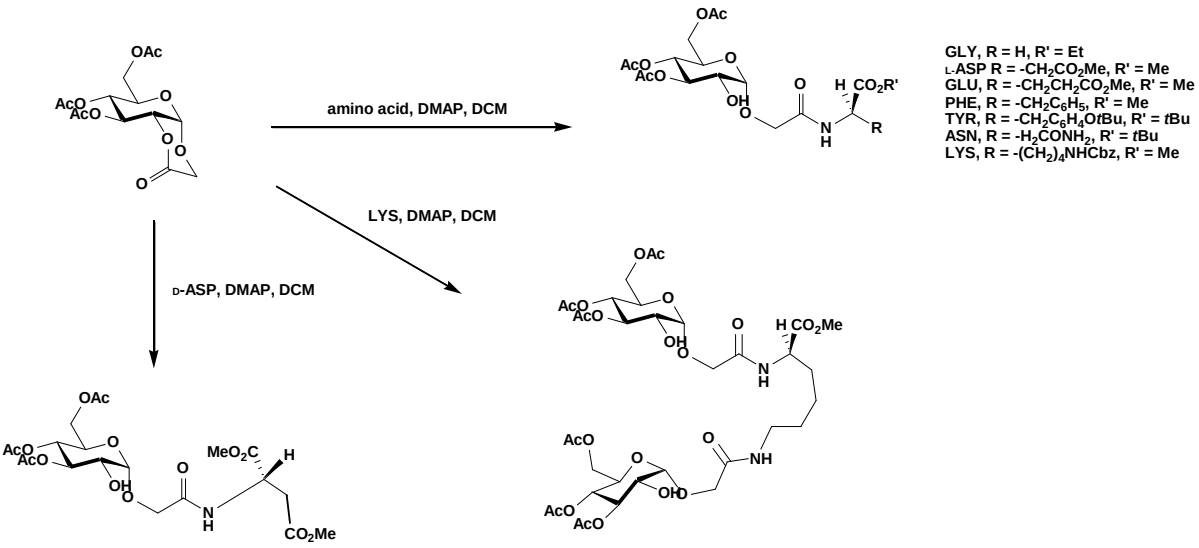

Scheme 2.16: Reactions of α-CMGL with amino acids[137]

Cette thèse est accessible à l'adresse : http://theses.insa-lyon.fr/publication/2013ISAL0001/these.pdf
© [R. Xu], [2013], INSA de Lyon, tous droits réservés

Some pseudodisaccharides of glucose-glucose, glucose-galactose, and glucose-uridine were formed by the amide linkage by ring-opening of α-CMGL.[141] The yields of final product were 72% **56**, 72% **57**, and 60% **58**, respectively, as shown in Fig. 2.4.

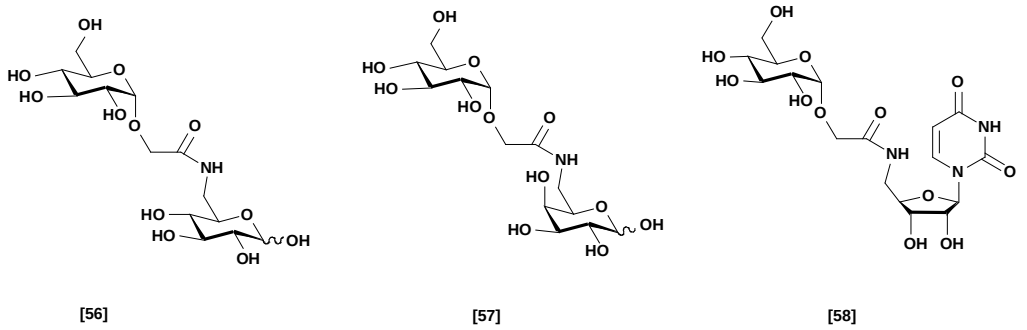

Fig. 2.4: Chemical structures of pseudodisaccharides of glucose-glucose **56**, glucose-galactose **57**, glucose-uridine **58** by amide linkage

Some functional groups were also introduced on the sugar moieties via this strategy, like **59**, **63**, and the resulting OH-2 could be further functionalized, as shown in Fig. 2.5. For example, **59** could be used in Huisgen cycloaddition (‘click’ chemistry).[139] The compound was anchored to the 5`-azido-5` deoxyuridine in the presence of Cu (I) catalysis. The procedure is shown in Scheme 2.17.

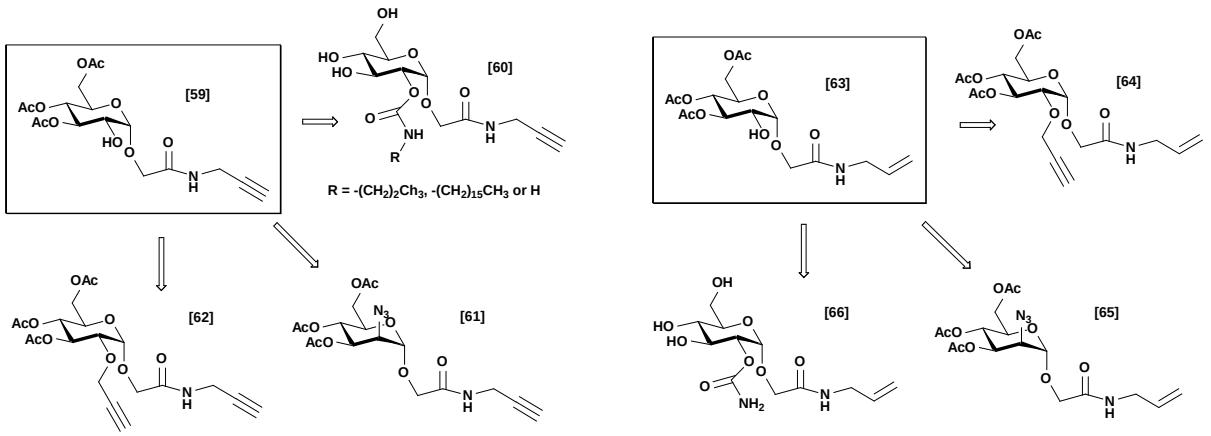

Fig. 2.5: The resulting compounds bearing the functional groups and possibilities of functionnalizations on OH-2

Cette thèse est accessible à l'adresse : http://theses.insa-lyon.fr/publication/2013ISAL0001/these.pdf
© [R. Xu], [2013], INSA de Lyon, tous droits réservés

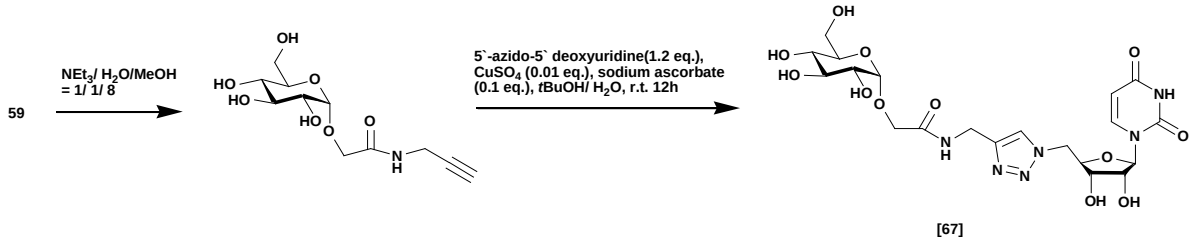

Scheme 2.17: An example of applications in 'click' chemistry[139]

In the field of biological applications, the CMGLs were used to couple sugars with some hydrophobic functional groups to improve their solubility in water along with biological compatibility. For example, compound **68** was synthesized as a photosensitizer in the field of photodynamic therapy (PDT)[142] and fluorescent probes **69**, **70** showed a good an affinity towards membranes, as shown in Fig. 2.6.[143]

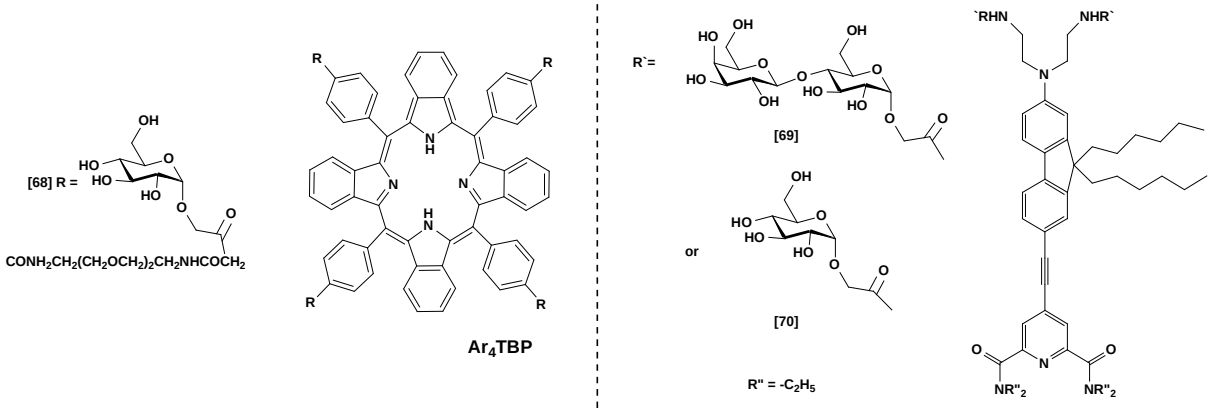

Fig. 2.6: Chemical structures of α-CMG amide probes[142, 143]

By further oxidation at O-2 after lactone opening, a series of α, β- unsaturated carbonyl compounds derived from the CMGLs were synthesized.[144] Their structures were shown in Fig. 2.7. Among them, the compounds bearing dodecyl chain show the activity in the antifungal and antibacterial tests, and interestingly compound **73** showed a low toxicity while its α-isomer **76** was toxic.

Cette thèse est accessible à l'adresse : http://theses.insa-lyon.fr/publication/2013ISAL0001/these.pdf
© [R. Xu], [2013], INSA de Lyon, tous droits réservés

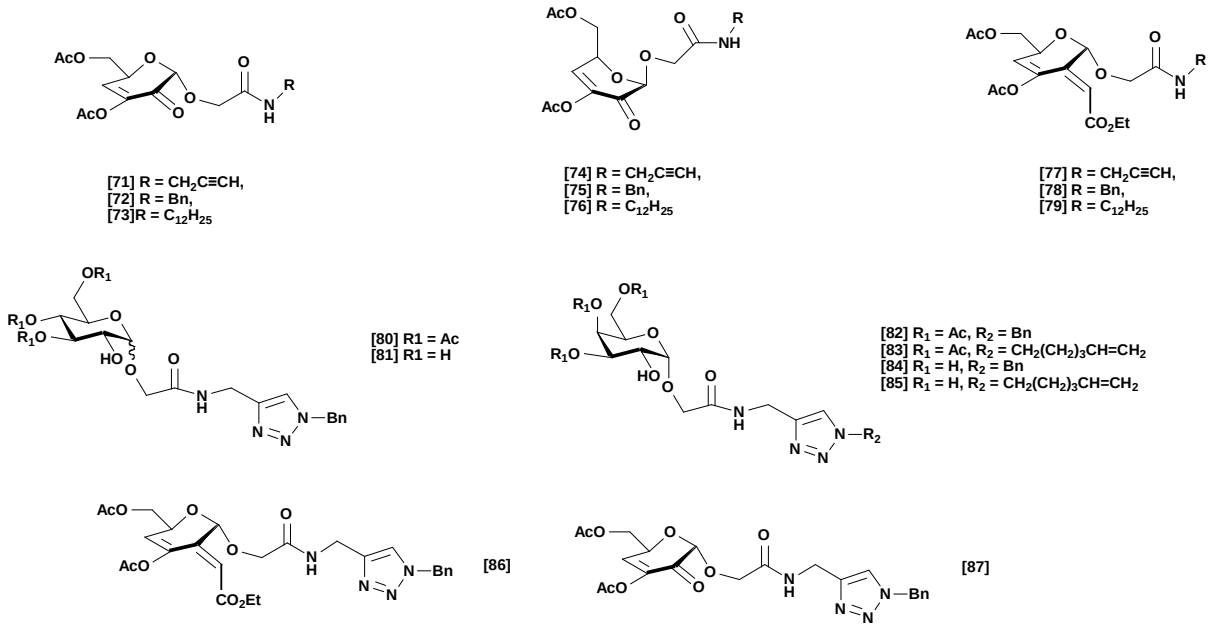

Fig. 2.7: Chemical structures of α, β-unsaturated carbonyl compounds derived from CMGLs[144]

"Living" polymerization using monomers arising from α-CMGL derivatives has also been explored.[145] The obtained monomers **88** and **89** (Scheme 2.18) show a good ability to form the polymers via the reversible addition fragmentation chain transfer (RAFT) polymerization. They also showed a great trend in the "living" polymerization, as indicated in the size exclusion chromatography (SEC) spectra that the elution volume continued to grow.

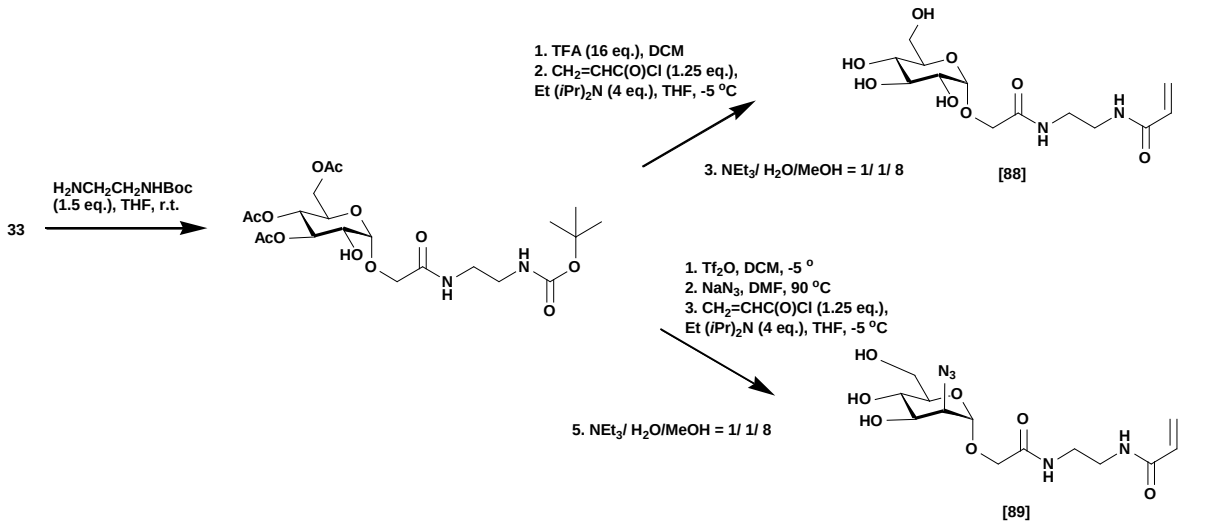

Scheme 2.18: Synthesis for glycomonomers **88** and **89**[145]

Cette thèse est accessible à l'adresse : http://theses.insa-lyon.fr/publication/2013ISAL0001/these.pdf
© [R. Xu], [2013], INSA de Lyon, tous droits réservés

Further study on the post-modification on the resulting glycopolymer **89** gained some exciting results. With the azido group on the carbohydrate group, the possibility of bridging other functional group bearing the triple bond became available. This work is the first time showing that the preformed glycopolymer could afford a post modification (Scheme 2.19).

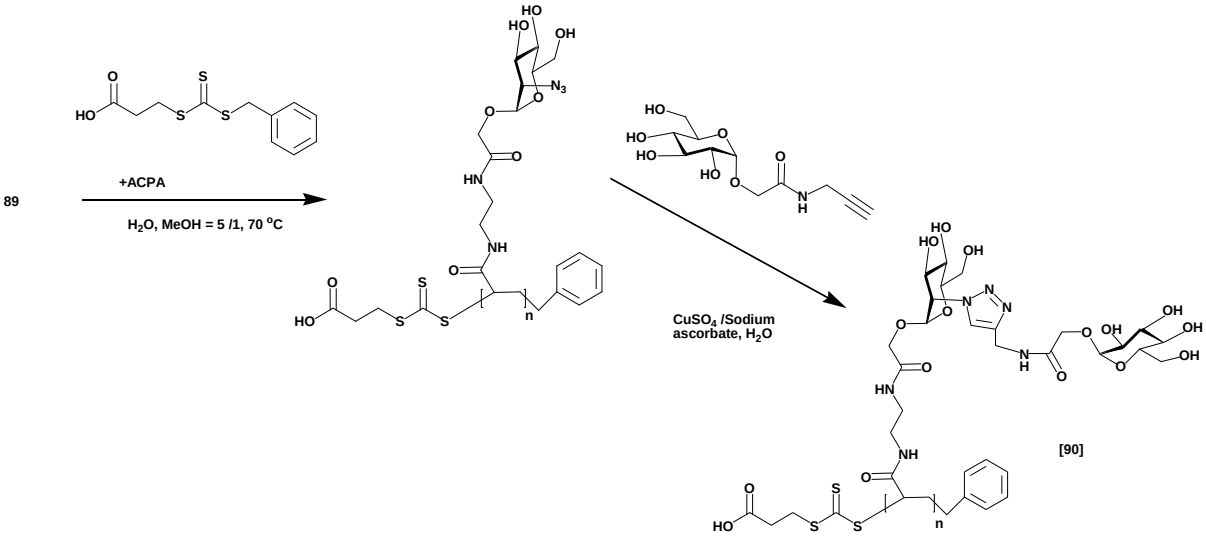

Scheme 2.19: Polymerization of monomer **89** and post modification by CuAAC reaction[145]

The possibility of trying polymerizations through this strategy was also studied by introducing both the azido and alkynyl groups on the glucosyl matrix.[146] The monomers were derived from α- and β-CMGLs, whose structures were shown in Scheme 2.19. The polymerization of these monomers was performed in the DMSO-d_6, monitored by ^{1}HNMR. They all showed a good ability to polymerize, and an example of polymerization of monomer **91** is shown in Scheme 2.19.

Cette thèse est accessible à l'adresse : http://theses.insa-lyon.fr/publication/2013ISAL0001/these.pdf
© [R. Xu], [2013], INSA de Lyon, tous droits réservés

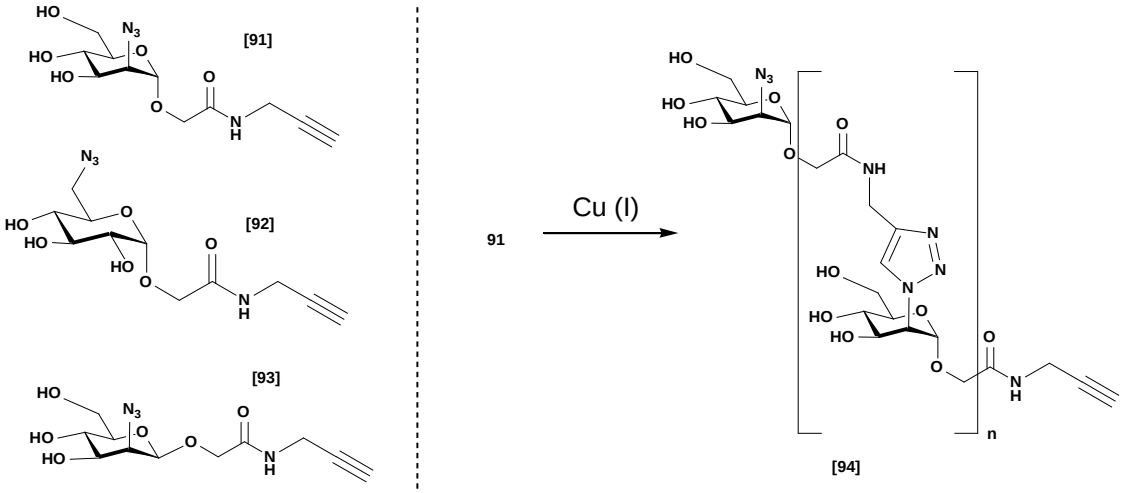

Scheme 2.20: Chemical structures of azido alkynyl compounds derived from CMGL and the polymerization of compound **91**[146]

The long time interest of the collaborative project gathering the teams in Lyon, Hull then York in the field of carbohydrate based liquid crystals led us to explore the application of the glucoconjugates prepared by CMGLs strategy in this area. In order to study the effect of relative cross-sectional areas of sugar head to aliphatic tails on the thermotropic liquid crystalline behavior, glucopyranoside derivatives of a series of aliphatic amines (C6, C8, C10, C12, C14, C16) and aminocholesterol, amino steroid with α and β conformations were prepared.[147] Table 2.5 shows the results observed by aliphatic series, Fig. 2.7 is the defect texture of Sm A* phases shown by dodecyl amide methylcarboxyl glucopyranoside under polarized light microscope.

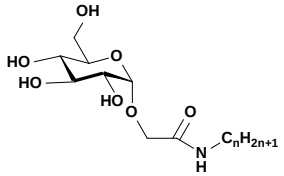

Chain length (n)	Melting point (^{o}C)	Clearing point (^{o}C)
6	63	/
8	74	/
10	81	94
12	89	122
14	92	178
16	100	192

Table 2.6: Transition temperatures of alkyl amide methylcarboxyl glucopyranoside[147]

Cette thèse est accessible à l'adresse : http://theses.insa-lyon.fr/publication/2013ISAL0001/these.pdf
© [R. Xu], [2013], INSA de Lyon, tous droits réservés

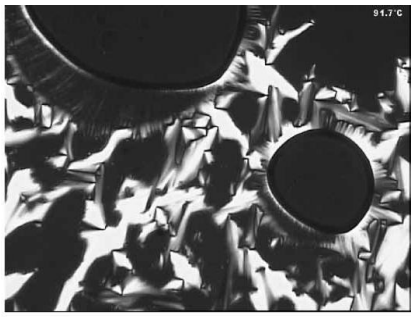

Fig. 2.8: Sm A* defect textures of dodecyl amide methylcarboxyl glucopyranoside at 91.1 ^{o}C (× 100) [147]

For steroidal series, structures of which were shown in Fig 2.9. Unlike the systems with the fatty chain, the steroid moieties are bulky and rigid units, thus the transition temperature for two cholestanyl compounds are very high while no mesophases were observed on the cholesteryl derivatives, since the double bonds brought more rigidity to the system compared to the cholestanyl mimics.

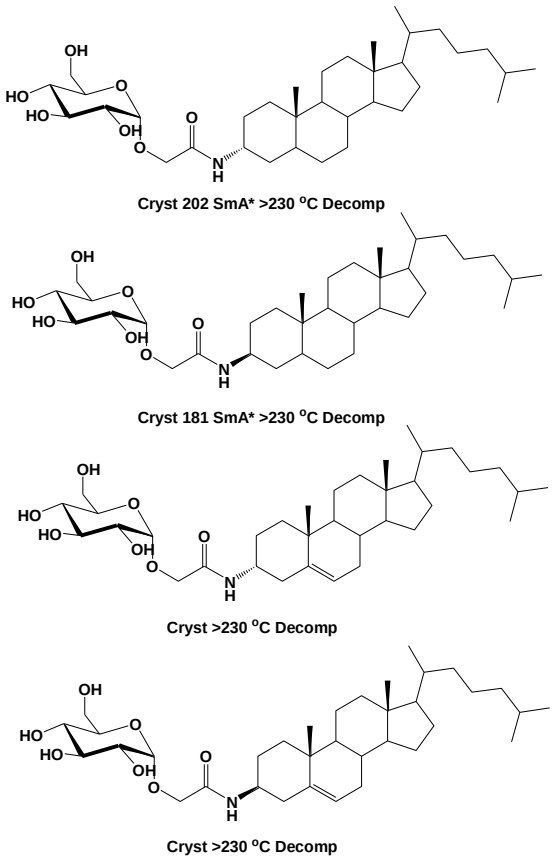

Fig. 2.9: Chemical structure of glucosteroid analogs and their transition temperatures[147]

Cette thèse est accessible à l'adresse : http://theses.insa-lyon.fr/publication/2013ISAL0001/these.pdf
© [R. Xu], [2013], INSA de Lyon, tous droits réservés

2.3 Conclusion

Carbohydrate-based lactones are important synthons not only in the aspect of their easy way to be introduced into the systems, but also in some special abilities they could bring, like chirality, biocompatibility and water solubility and so on. The CMGLs were found to be a useful type of synthons with various preparations, with versatile sources of sugars, and with wide applications.

Cette thèse est accessible à l'adresse : http://theses.insa-lyon.fr/publication/2013ISAL0001/these.pdf
© [R. Xu], [2013], INSA de Lyon, tous droits réservés

Cette thèse est accessible à l'adresse : http://theses.insa-lyon.fr/publication/2013ISAL0001/these.pdf
© [R. Xu], [2013], INSA de Lyon, tous droits réservés

Chapter 3

Study on the liquid crystalline behavior of methyl n-*O*-(2-hydroxyalkyl)-glucopyranosides

3.1 Introduction

In previous investigations of our group on sucrose hydroxyalkylethers, it was observed that different topological shapes, as the 2-hydroxyldodecyl chain switched sequentially around the sucrose moiety, led to different types of mesophases. (see page 52 in the first section) This phenomenon was found to have a relation with the modification of the intramolecular hydrogen bonding between the two monosaccharide moieties of the sucrose. The focus was made on changes in the sucrose conformation, precisely on the way the two monosaccharidic moieties of sucrose arrange spatially, but neither the role of the additional hydroxyl group in the hydroxyalkyl ether linkage, nor the effect of the length of the alkyl chain on the hydrophilic hydrophobic balance were studied. Thus, a systematical study with respect to the aliphatic chain length and substitution position on a simple glucidic head was undertaken for this purpose.

At this point, in this study, the simplest monosaccharide glucopyranose was chosen; and, as to prevent conformational variations due to anomeric equilibrium, the system was locked as a

Cette thèse est accessible à l'adresse : http://theses.insa-lyon.fr/publication/2013ISAL0001/these.pdf
© [R. Xu], [2013], INSA de Lyon, tous droits réservés

methyl α-glucoside throughout the study. The hydrophobic reagents used were 1,2-epoxyalkanes with alkyl chain length from 8 to 16 carbon atoms. As a matter of comparison, two compounds having simple linear alkyl chains of 8 and 12 carbons atoms at the position 6 were also prepared.

Some of the compounds in this series were synthesized by Mr. Madan Kumar Singh during his post-doc stay in the laboratory.

3.2 Synthesis procedure

The general scheme for the preparation of the desired monosubstituted hydroxyalkylethers is shown in Scheme 3.1. It relies on the preparation of partially protected methyl glucoside derivatives which have only one define hydroxyl group available for etherification. Indeed, attempts for making directly the mono-substituted ether products from methyl glucoside proved unsuccessful. After etherification by reaction with 1,2-epoxyalkane, deprotection led to final monosubstituted ethers.

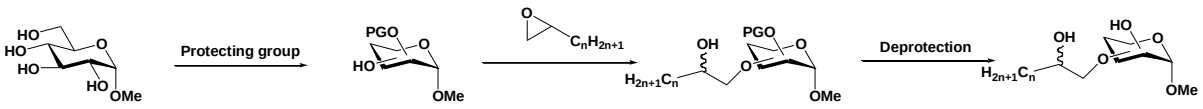

Scheme 3.1: General synthetic procedure leading to the monosbstituted hydroxyalkylethers

Since the etherification reaction by base catalyzed opening of the 1,2-epoxyalkanes requires rather high temperature and the presence of base, protecting groups having high stability in such conditions were chosen, namely benzyl ethers and benzylidene acetal. The starting materials with OH-2, OH-3, OH-4, and OH-6 as only hydroxyl group were obtained following classical synthetic sequences, which proved to be convenient. The details of their syntheses are shown in the sections below.

3.2.1 Synthesis of methyl 2-*O*-(2-hydroxyalkyl)-α-D-glucopyranosides

The method we adapted for the OH-2 compound is by J. Xue *et al.*.[148] In this method, the methyl α-D-glucopyranoside was firstly reacted with benzaldehyde dimethylacetal and

Cette thèse est accessible à l'adresse : http://theses.insa-lyon.fr/publication/2013ISAL0001/these.pdf
© [R. Xu], [2013], INSA de Lyon, tous droits réservés

catalytic amount of camphorsulfonic acid in acetonitrile to get the methyl 4,6-*O*-benzylidene-α-D-glucopyranoside, then the diol OH-2-OH-3 was monobenzylated via the intermediate tin acetal obtained by reaction with dibutyltin oxide, using benzyl bromide and tetrabutylammonium iodide in toluene, as shown in Scheme 3.2. The resulting product was a mixture of ethers at O-2 and O-3 compounds. The major product **96**, which has its OH-2 free, was obtained in 42% yield, and easily separated by chromatography.

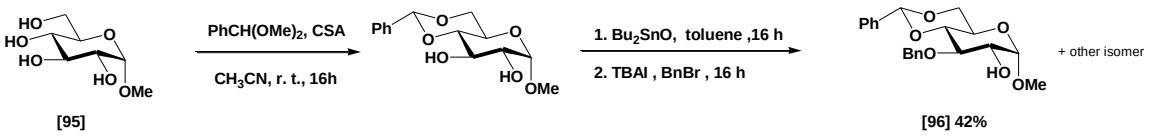

Scheme 3.2: The synthetic procedure for obtaining the methyl 3-*O*-benzyl-4,6-*O*-benzylidene-α-D-glucopyranoside **96**

The structure of the obtained product was is agreement with published data, and was also confirmed by analyzing the COSY, HSQC, and HMBC spectra, as shown in the Fig. 3.1-3.3

Using the COSY spectrum, the signal of proton on the H-2 of the glucopyranoside merges at around δ 3.75 ppm, with a shape of dd, and the signals of protons on the methylene of benzyl group are at δ 4.80 ppm and 5.00 ppm with a pattern of AB system. The proton of H-2 is corresponding to the δ 75 ppm on the carbon spectrum via the HSQC experiment, which indicated the C-2. If the Bn group was attached on the C-2, then in the HMBC experiment, the protons on the methylene group of the Bn substituent would have a response to the carbon signal of δ 75 ppm. However, this response was not found. Instead, these protons reply to the signal at δ 80 ppm, which reflects C-3 carbon.

Cette thèse est accessible à l'adresse : http://theses.insa-lyon.fr/publication/2013ISAL0001/these.pdf
© [R. Xu], [2013], INSA de Lyon, tous droits réservés

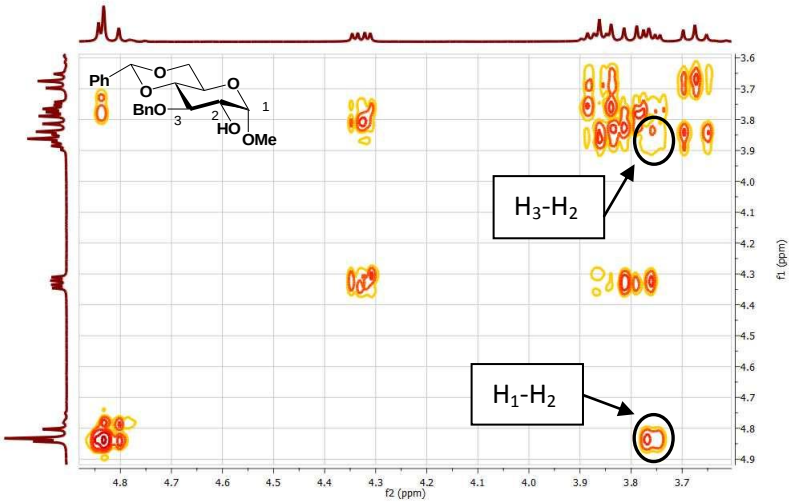

Fig. 3.1: ^{1}H-^{1}H COSY spectrum of methyl 3-*O*-benzyl-4,6-*O*-benzylidene-α-D-glucopyranoside **96**

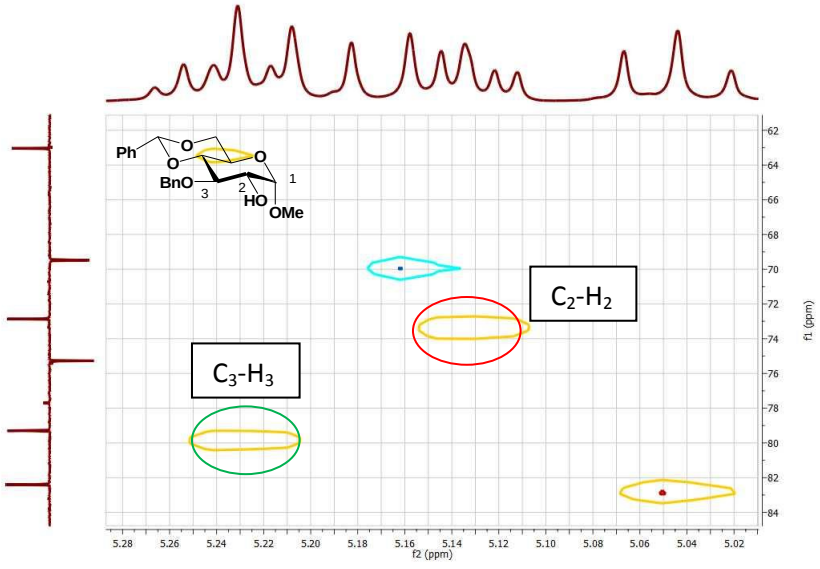

Fig. 3.2: ^{1}H-^{13}C HSQC spectrum of methyl 3-*O*-benzyl-4,6-*O*-benzylidene-α-D-glucopyranoside **96**

Cette thèse est accessible à l'adresse : http://theses.insa-lyon.fr/publication/2013ISAL0001/these.pdf
© [R. Xu], [2013], INSA de Lyon, tous droits réservés

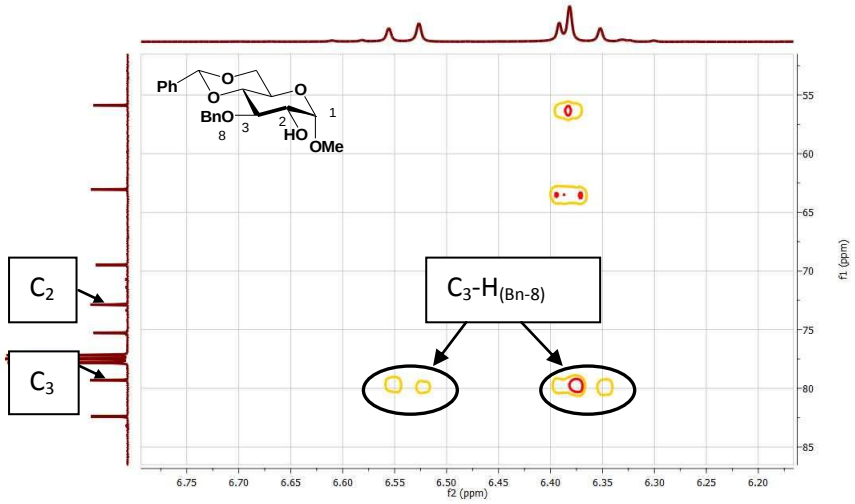

Fig. 3.3: ^{1}H-^{13}C HMBC spectrum of methyl 2-*O*-benzyl-4,6-*O*-benzylidene-α-D-glucopyranoside **96**

The 2-OH of the compound reacted with 1,2-epoxyalkanes of various chain lengths in the presence of DABCO/DMAP. The reaction took place in DMSO at 110 ^{o}C. After 16H, the starting materials were converted into the corresponding methyl 2-*O*-(2-hydroxyalkyl)-3-*O*-benzyl-4,6-*O*-benzylidene-α-D-glucopyranosides **97**, with consistent yields between 65% and 70%. The deprotection of aromatic group was achieved in two steps: firstly, *p*-Toluenesulfonic acid (*p*-TSA) was added to cleave the benzylidene group and then Pd-catalyzed hydrogenolysis of the benzyl group in MeOH-EtOAc, as shown in Scheme 3.3. Thus, methyl 2-*O*-(2-hydroxyalkyl)-α-D-glucopyranosides were obtained.

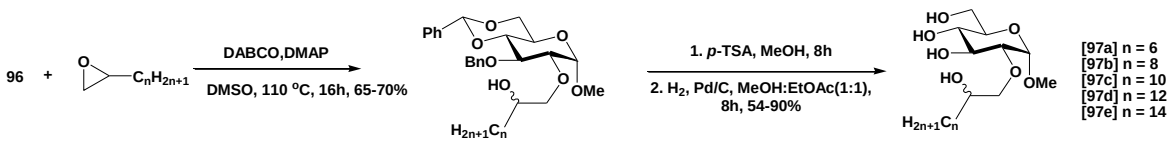

Scheme 3.3: The synthetic path for the synthesis of methyl 2-*O*-(2-hydroxyalkyl)-α-D-glucopyranosides **97**

Cette thèse est accessible à l'adresse : http://theses.insa-lyon.fr/publication/2013ISAL0001/these.pdf
© [R. Xu], [2013], INSA de Lyon, tous droits réservés

As the resulting compounds are amphiphilic, a mixture of $CDCl_3$ and MeOD at the ratio of 9 to 1 was used to dissolve them. Fig. 3.4 shows the ^{13}C NMR spectrum of methyl 2-*O*-(2-hydroxydodecyl)-α-D-glucopyranoside **97c**. It is observed that some peaks appear as pairs of two peaks. The reason is that the etherification product is a mixture of two epimers, because the configurations of the hydroxyl group resulting from the epoxy ring opening reaction either upside or downside, as indicated in the Scheme 3.4. Separation of these two epimers was not feasible in view of the very close R_f on the thin layer chromatography (TLC). According to this ^{13}C NMR, their proportion in the two products was close to 1:1, showing that the chance of forming the two isomers was equal. Through the whole series of compounds studied, the same thing was observed and the ratios of the two isomers in these series were nearly the same. Thus, the mesomorphic behaviors of these compounds were studied as the state of mixture at this hydroxyalkylether position.

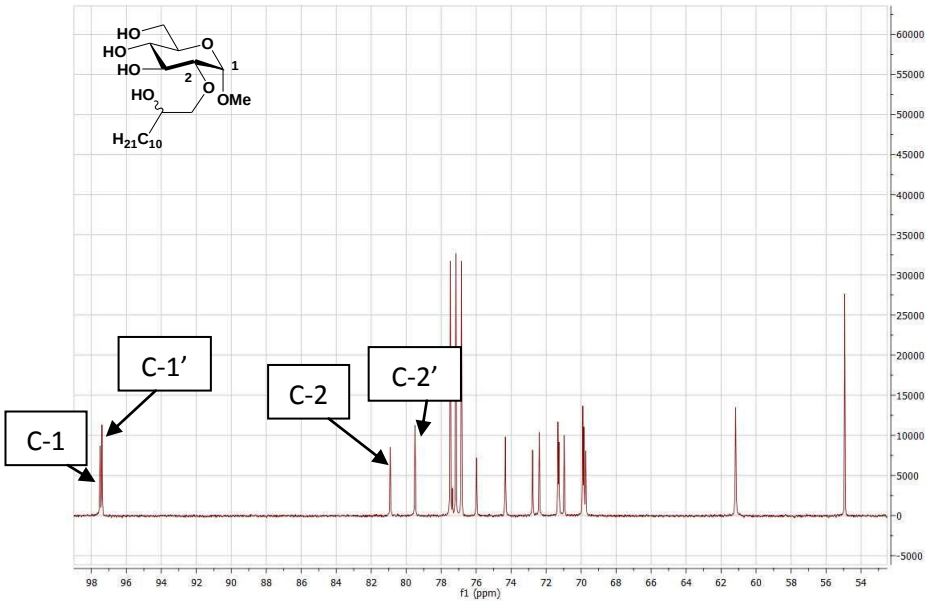

Fig. 3.4: ^{13}C NMR spectrum of methyl 2-*O*-(2-hydroxydodecyl)-α-D-glucopyranoside **97c**

Scheme 3.4: The two epimers arising from the ring-opening of epoxyalkanes

Cette thèse est accessible à l'adresse : http://theses.insa-lyon.fr/publication/2013ISAL0001/these.pdf
© [R. Xu], [2013], INSA de Lyon, tous droits réservés

The structure of the compounds with the ether at position 2 and varying in chain lengths was studied by COSY, HSQC, and HMBC. Since all the structures of this series are very similar, here we show only the detailed spectroscopic study of methyl 2-*O*-(2-hydroxydodecyl)-α-D-glucopyranoside **97c**, Fig. 3.6-3.8. As shown in the ^{1}HNMR, the proton of H-2 appeared at δ 3.25 ppm, corresponding to C-2 signals of two epimers found at δ 81.3 and 79.9 ppm by HSQC method. These signals are found to interact with δ 3.65-3.51 ppm and δ 3.42-3.23 ppm of the proton signals of H-8 on the aliphatic chain in HMBC spectrum. Thus, the structure of the compound **97c** could be confirmed.

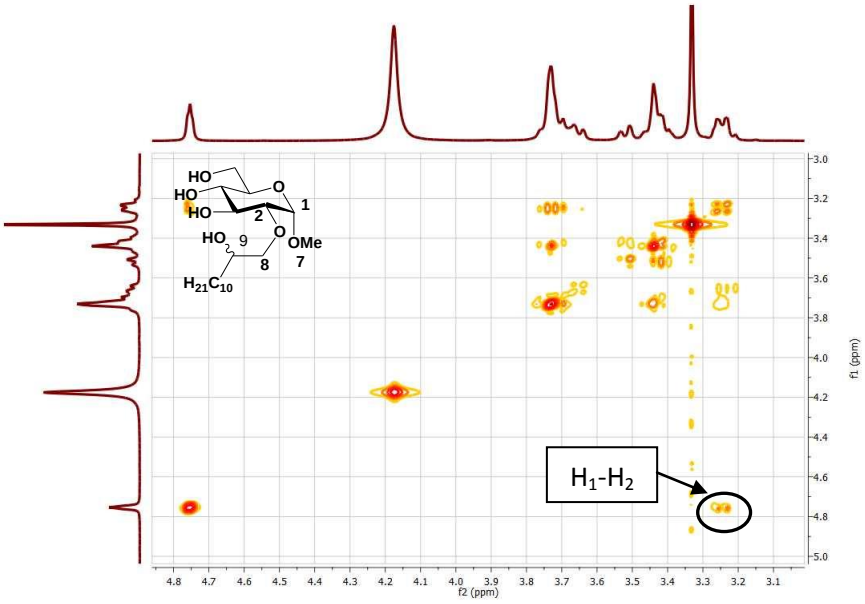

Fig. 3.5: ^{1}H-^{1}H COSY spectrum of methyl 2-*O*-(2-hydroxydodecyl)-α-D-glucopyranoside **97c**

Cette thèse est accessible à l'adresse : http://theses.insa-lyon.fr/publication/2013ISAL0001/these.pdf
© [R. Xu], [2013], INSA de Lyon, tous droits réservés

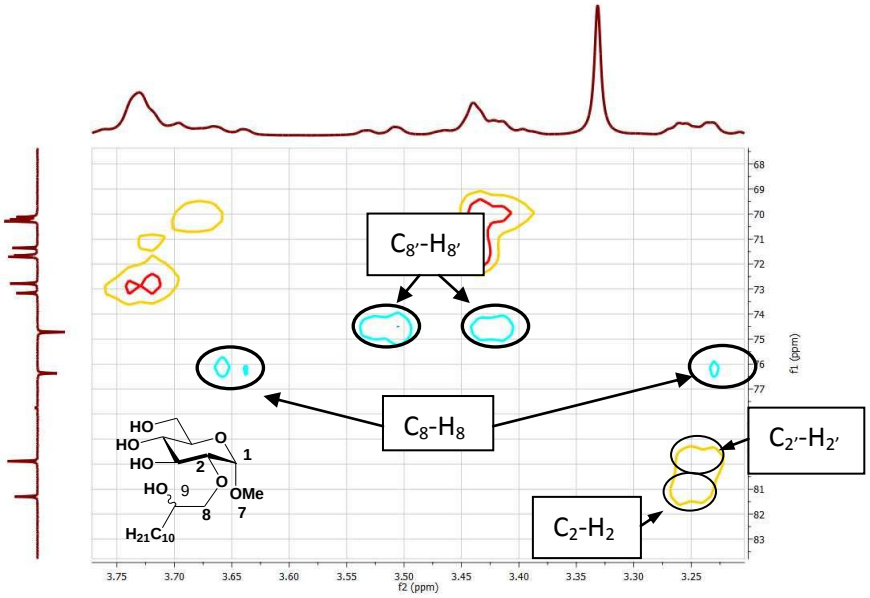

Fig. 3.6: ^{1}H-^{13}C HSQC spectrum of methyl 2-*O*-(2-hydroxydodecyl)-α-D-glucopyranoside **97c**

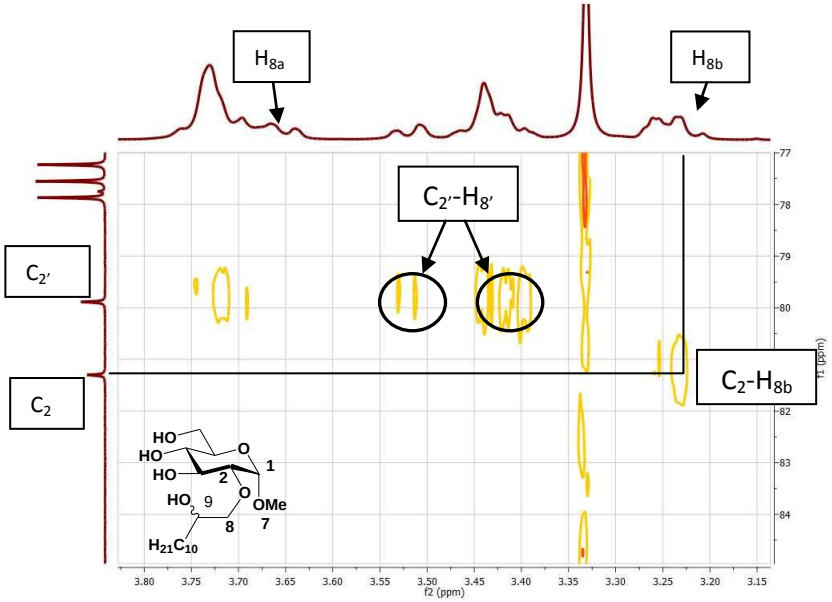

Fig. 3.7: ^{1}H-^{13}C HMBC spectrum of methyl 2-*O*-(2-hydroxydodecyl)-α-D-glucopyranoside **97c**

3.2.2 Synthesis of methyl 3-*O*-(2-hydroxyalkyl)-α-D-glucopyrano-sides

For methyl 3-*O*-(2-hydroxyalkyl)-α-D-glucopyranosides, the method introduced by Murphy *et al.* was used.[149] An intermediate in the previous synthesis, methyl 4,6-*O*-benzylidene-α-D-

Cette thèse est accessible à l'adresse : http://theses.insa-lyon.fr/publication/2013ISAL0001/these.pdf
© [R. Xu], [2013], INSA de Lyon, tous droits réservés

glucopyranoside, was also used as starting material. It was reacted with benzyl bromide (BnBr), tetrabutylammonium iodide (TBAI) and aqueous NaOH in DCM at room temperature, as shown in Scheme 3.5. Again both regioisomers were obtained, but this time, the product with OH-3 free was the major one.

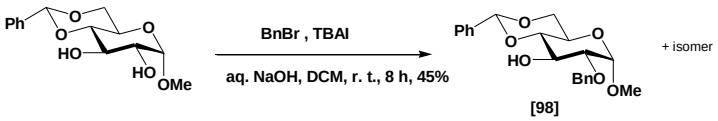

Scheme 3.5: Synthesis of methyl 2-*O*-benzyl-4,6-*O*-benzylidene-α-D-glucopyranoside **98**

The structure of methyl 2-*O*-benzyl-4,6-*O*-benzylidene-α-D-glucopyranoside **98** was also studied by COSY, Fig. 3.8, HSQC, Fig. 3.9, and HMBC, Fig. 3.10. For this compound, the anomeric proton appears at δ 4.51 ppm in the ^{1}HNMR. The nearby proton in C-2 could be found at δ 3.36 ppm from the connection of C-1, as a shape of dd, followed by C-3 at δ 4.06 ppm, triplet shape. Their carbon signals could be identified as δ 80.2 ppm for C-2 and δ 70.7 ppm for C-3 by HSQC. The protons of the methylene unit on the Bn group are found at δ 4.70 and 4.60 ppm, respectively, which is because of AB system. From the HMBC, these protons are found to have interaction with the signal at δ 80.2 ppm, which proves that the OH-2 was protected.

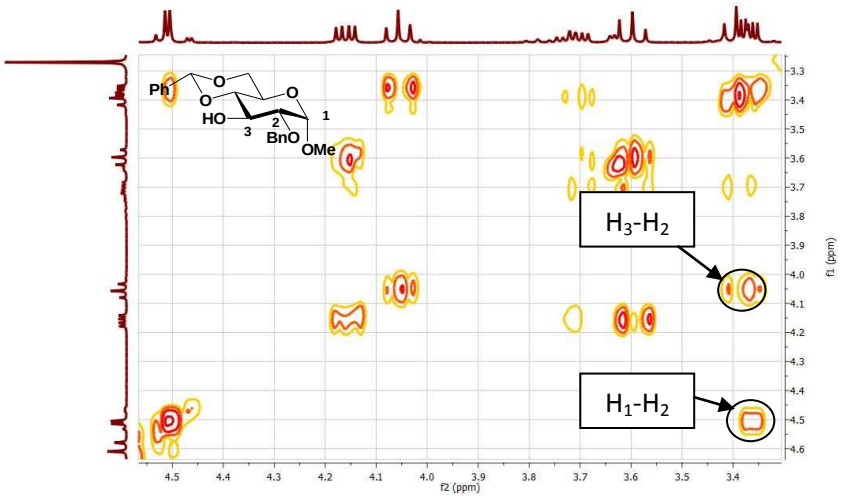

Fig. 3.8: ^{1}H-^{1}H COSY spectrum of methyl 2-*O*-benzyl-4,6-*O*-benzylidene-α-D-glucopyranoside **98**

Cette thèse est accessible à l'adresse : http://theses.insa-lyon.fr/publication/2013ISAL0001/these.pdf
© [R. Xu], [2013], INSA de Lyon, tous droits réservés

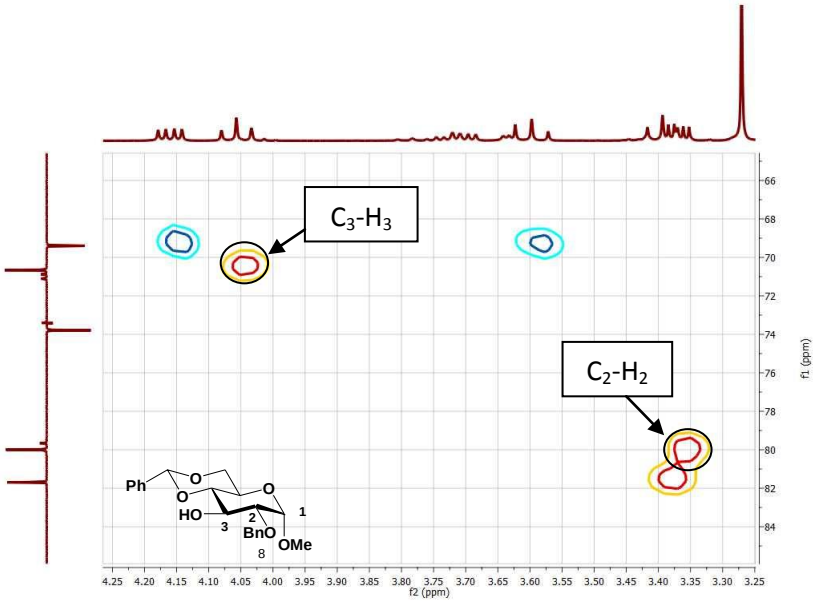

Fig. 3.9: ^{1}H-^{13}C HSQC spectrum of methyl 2-*O*-benzyl-4,6-*O*-benzylidene-α-D-glucopyranoside **98**

Fig. 3.10: ^{1}H-^{13}C HMBC spectrum of methyl 2-*O*-benzyl-4,6-*O*-benzylidene-α-D-glucopyranoside **98**

Cette thèse est accessible à l'adresse : http://theses.insa-lyon.fr/publication/2013ISAL0001/these.pdf
© [R. Xu], [2013], INSA de Lyon, tous droits réservés

The etherification of OH-3 with 1,2-epoxyalkanes was achieved under the same conditions as for the 2-*O*-(2-hydroxyalkyl)-α-D-glucopyranosides, as shown in Scheme 3.6.

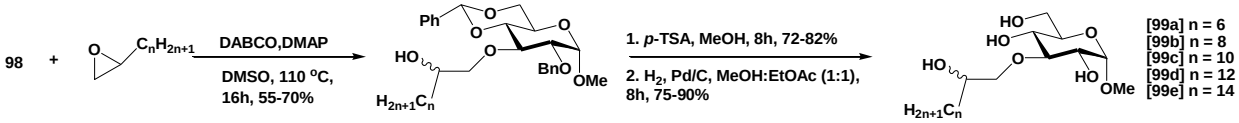

Scheme 3.6: Synthetic procedure of methyl 3-*O*-(2-hydroxyalkyl)-α-D-glucopyranosides **99**

The structures of final compounds were also confirmed by spectroscopic studies. The methyl 3-*O*-(2-hydroxydodecyl)-α-D-glucopyranoside **99c** is detailed below as an example, Fig. 3.11-3.13. From the COSY spectrum, the proton signal of H-3 could be identified at δ 3.86 ppm. And their corresponding carbon signals are at δ 84.3, 83.6 ppm. They have been found from HMBC spectrum to be related with δ 3.85-3.83 ppm and 3.50-3.48 ppm, where the protons of H-7 and H7', respectively in the ^{1}H NMR. Thus, the structure of the resulting compound **99c** is confirmed.

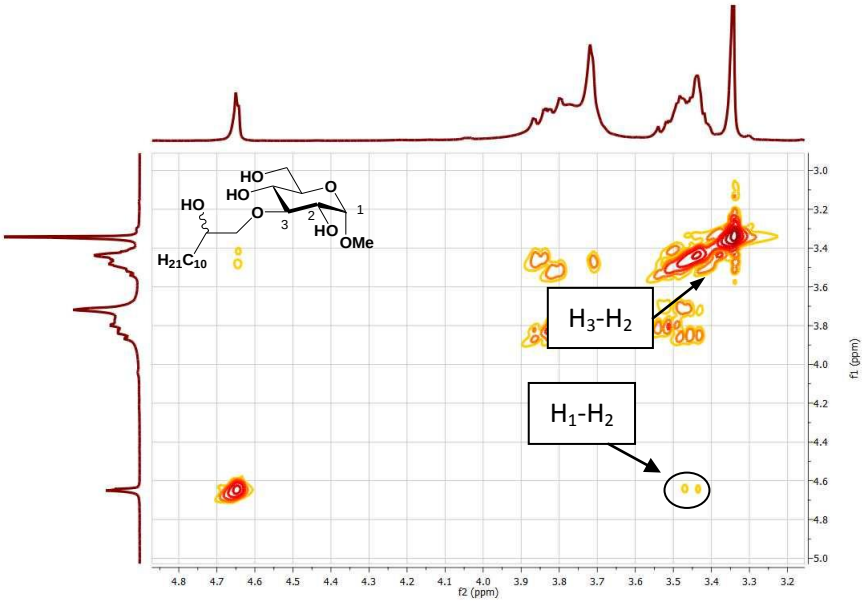

Fig. 3.11: ^{1}H-^{1}H COSY spectrum of methyl 3-*O*-(2-hydroxydodecyl)-α-D-glucopyranoside **99c**

Cette thèse est accessible à l'adresse : http://theses.insa-lyon.fr/publication/2013ISAL0001/these.pdf
© [R. Xu], [2013], INSA de Lyon, tous droits réservés

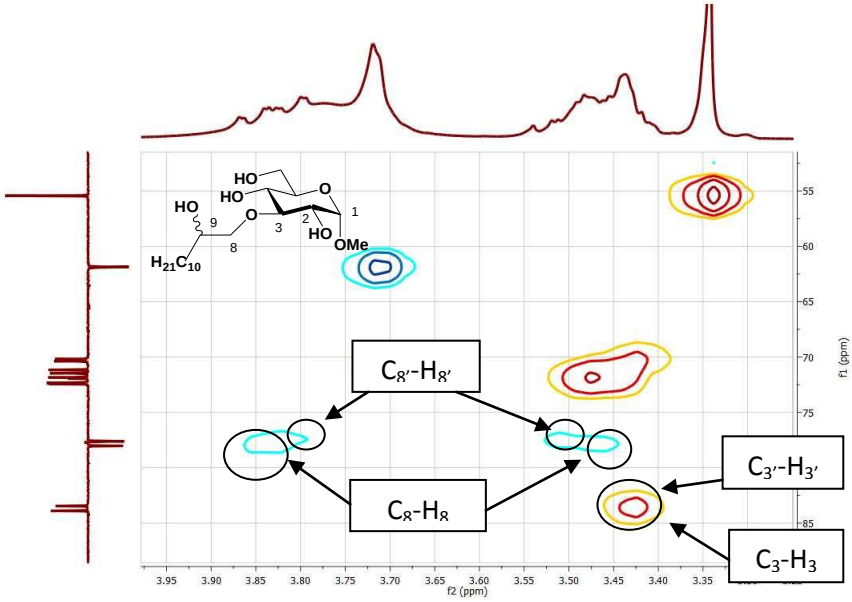

Fig. 3.12: ^{1}H-^{13}C HSQC spectrum of methyl 3-*O*-(2-hydroxydodecyl)-α-D-glucopyranoside **99c**

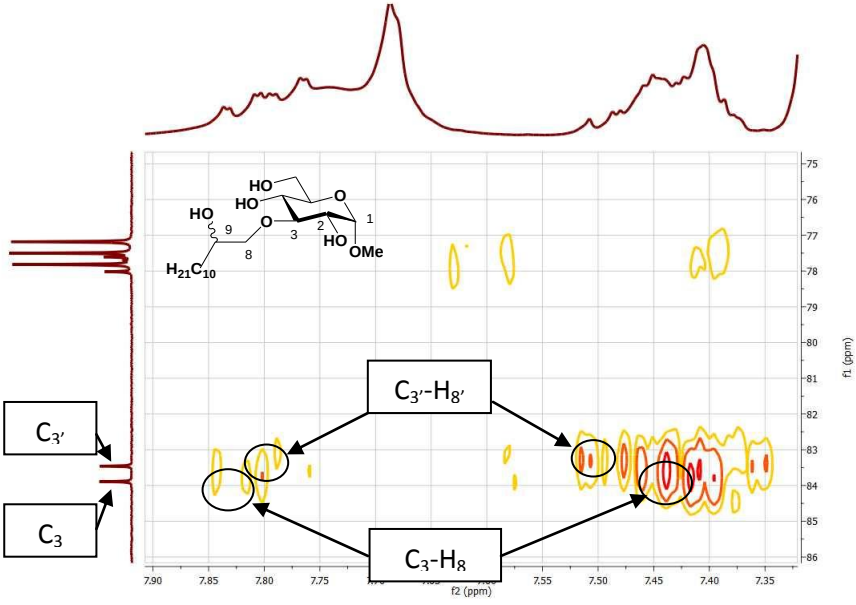

Fig. 3.13: ^{1}H-^{13}C HMBC spectrum of methyl 3-*O*-(2-hydroxydodecyl)-α-D-glucopyranoside **99c**

Cette thèse est accessible à l'adresse : http://theses.insa-lyon.fr/publication/2013ISAL0001/these.pdf
© [R. Xu], [2013], INSA de Lyon, tous droits réservés

3.2.3 Synthesis of methyl 4-O-(2-hydroxyalkyl)-α-D-glucopyranosides

The synthetic sequence toward this series was adapted from T. Nobuo *et al*..[150] Firstly, the 4,6-*O* benzylidene-α-D-glucopyranoside reacted with benzyl bromide at the presence of NaH to obtain the methyl 4,6-*O*-benzylidene-2,3-di-*O*-benzyl-α-D-glucopyranoside. The resulting compound was then treated with $NaBH_3CN/CH_3SO_3H$ in THF, to promote reductive selective opening of the acetal, leading to methyl 2,3,6-tri-*O*-benzyl-α-D-glucopyranoside **100**, as shown in Scheme 3.7.

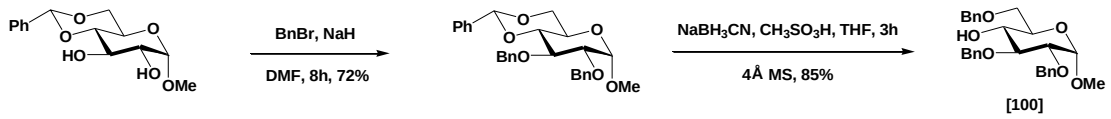

Scheme 3.7: Synthetic procedure for methyl 2,3,6-tri-*O*-benzyl-α-D-glucopyranoside **100**

From the COSY spectrum, Fig. 3.14, we can easily identify the glucoside carbon atoms by the H-H coupling. Here, the anomeric H is at δ 4.66 ppm, which links the H-2 at the δ 3.55 ppm. Followed by this way, the H-4 could be identified at δ 3.63 ppm with a shape of triple. Combining with the data on the HSQC spectrum, Fig. 3.15, the C-4 was found at δ 70.49 ppm on the carbon spectrum. As the signals of the protons on the methylene groups of the Bn groups show themselves at around δ 5.05 to 4.53 ppm, having no relations with C-4 on the HMBC spectrum, Fig. 3.16, where they are seen to be connected with C-2, C-3, and C-6. Thus, we confirm that the obtained molecule was the methyl 2,3,6-tri-*O*-benzyl-α-D-glucopyranoside.

Cette thèse est accessible à l'adresse : http://theses.insa-lyon.fr/publication/2013ISAL0001/these.pdf
© [R. Xu], [2013], INSA de Lyon, tous droits réservés

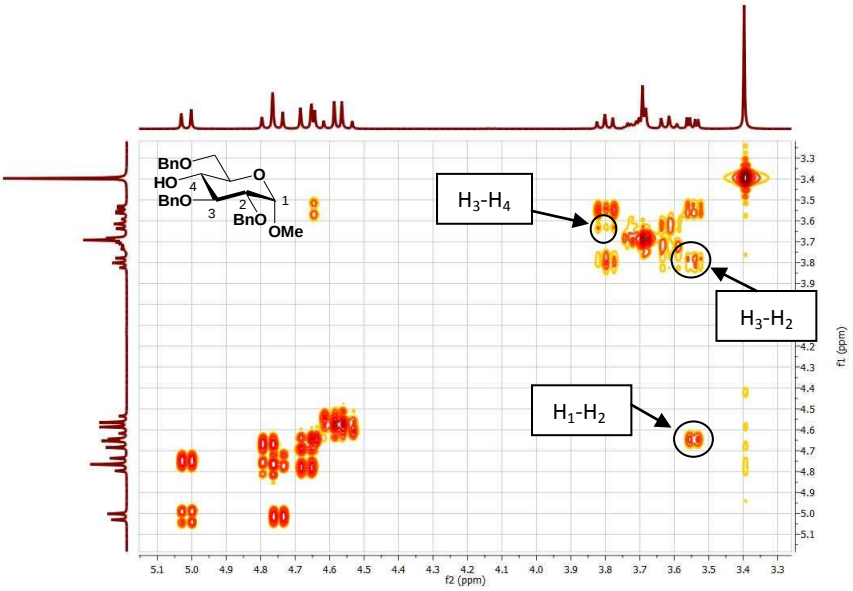

Fig. 3.14: ^{1}H-^{1}H COSY spectrum of methyl 2,3,6-tri-*O*-benzyl-α-D-glucopyranoside **100**

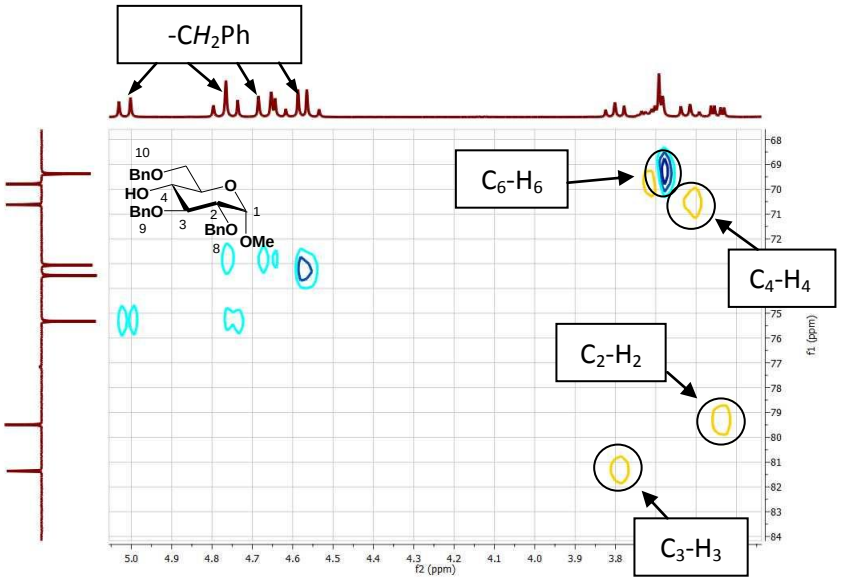

Fig. 3.15: ^{1}H-^{13}C HSQC spectrum of methyl 2,3,6-tri-*O*-benzyl-α-D-glucopyranoside **100**

Cette thèse est accessible à l'adresse : http://theses.insa-lyon.fr/publication/2013ISAL0001/these.pdf
© [R. Xu], [2013], INSA de Lyon, tous droits réservés

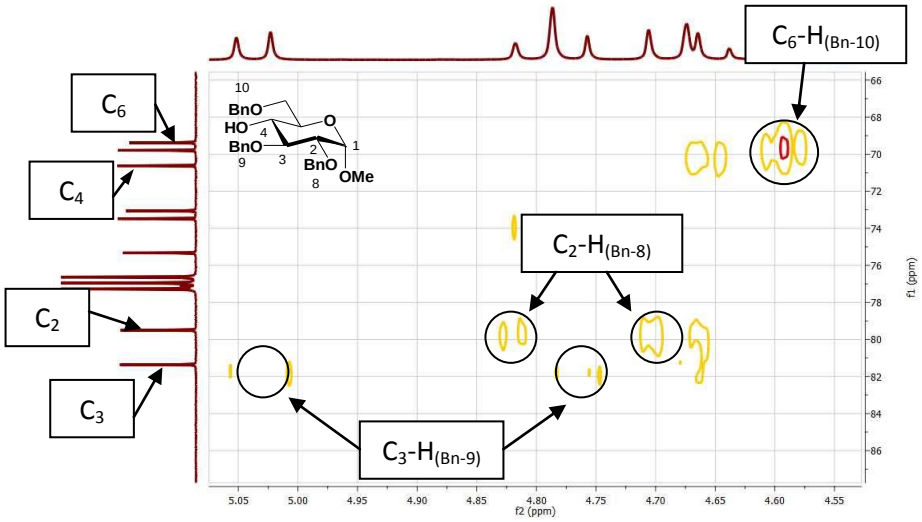

Fig. 3.16: ^{1}H-^{13}C HMBC spectrum of methyl 2,3,6-tri-*O*-benzyl-α-D-glucopyranoside **100**

Having the pure methyl 2,3,6-tri-*O*-benzyl-α-D-glucopyranoside **100** in hands, it was reacted with 1,2-epoxyalkanes under the same conditions as previously. The resulting ethers were then treated with H_2/Pd to yield the desired deprotected products.

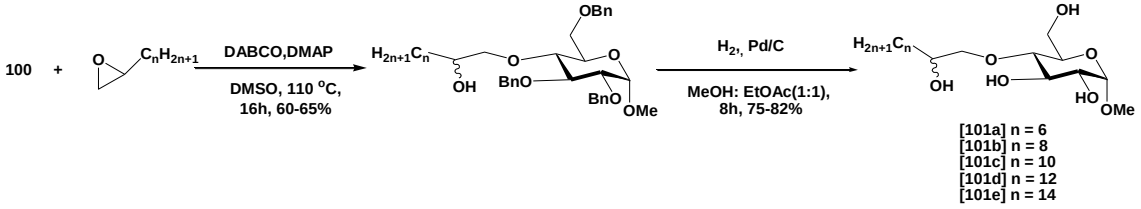

Scheme 3.8: The synthetic procedure for methyl 4-*O*-(2-hydroxyalkyl)-α-D-glucopyranosides **101**

The structure of compounds is studied by the means of NMR spectroscopy. The example is shown of methyl 4-*O*-(2-hydroxydodecyl)-α-D-glucopyranoside **101c**. From the COSY spectrum, Fig. 3.17, the proton of H-4 could be identified at δ 3.28 ppm. And their corresponding carbon signals are found at δ 78.4, 79.9 ppm, Fig. 3.18. These peaks are seen from HMBC spectrum, Fig. 3.19, having relations with δ 3.74-3.68 ppm, 3.50-3.48 ppm, where the protons of H-8 and H-8' of aliphatic chain respectively in the ^{1}HNMR.

Cette thèse est accessible à l'adresse : http://theses.insa-lyon.fr/publication/2013ISAL0001/these.pdf
© [R. Xu], [2013], INSA de Lyon, tous droits réservés

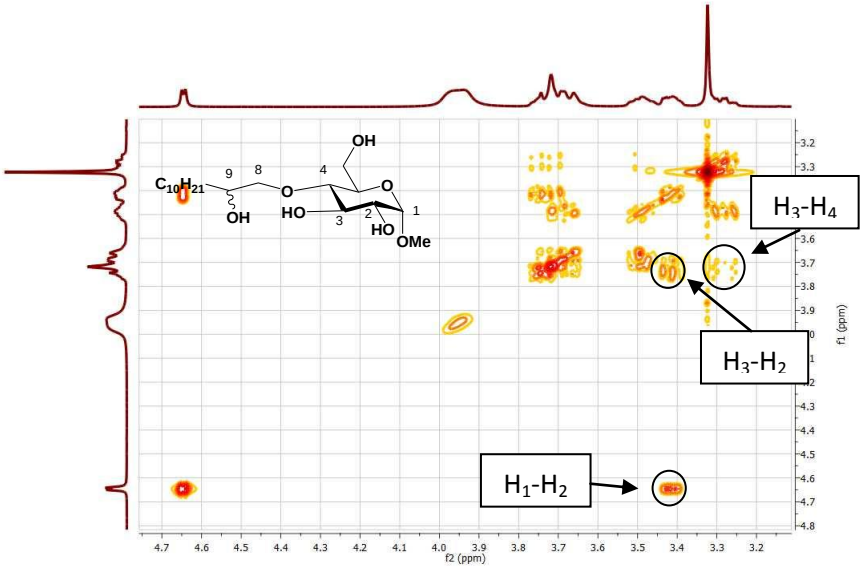

Fig. 3.17: ^{1}H-^{1}H COSY spectrum of methyl 4-*O*-(2-hydroxydodecyl)-α-D-glucopyranoside **101c**

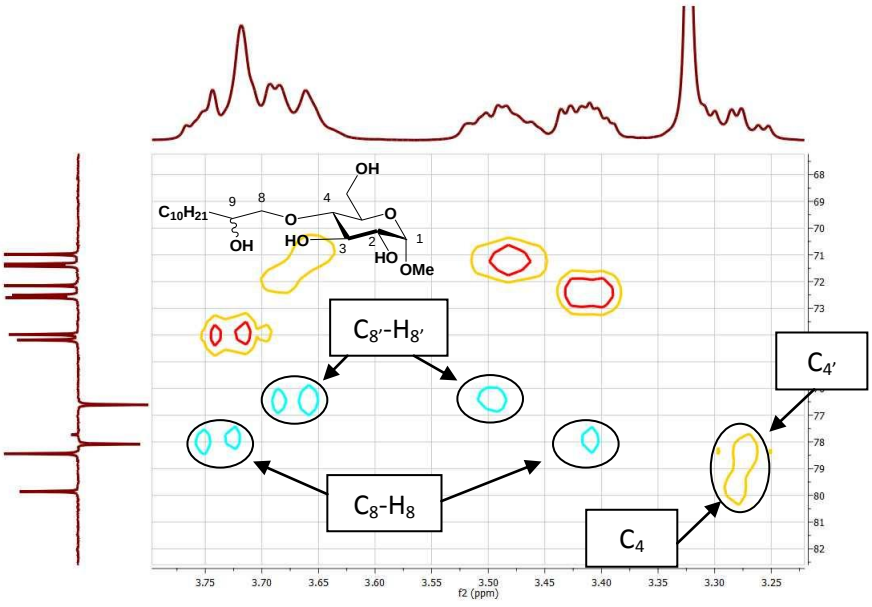

Fig. 3.18: ^{1}H-^{13}C HSQC spectrum of methyl 4-*O*-(2-hydroxydodecyl)-α-D-glucopyranoside **101c**

Cette thèse est accessible à l'adresse : http://theses.insa-lyon.fr/publication/2013ISAL0001/these.pdf
© [R. Xu], [2013], INSA de Lyon, tous droits réservés

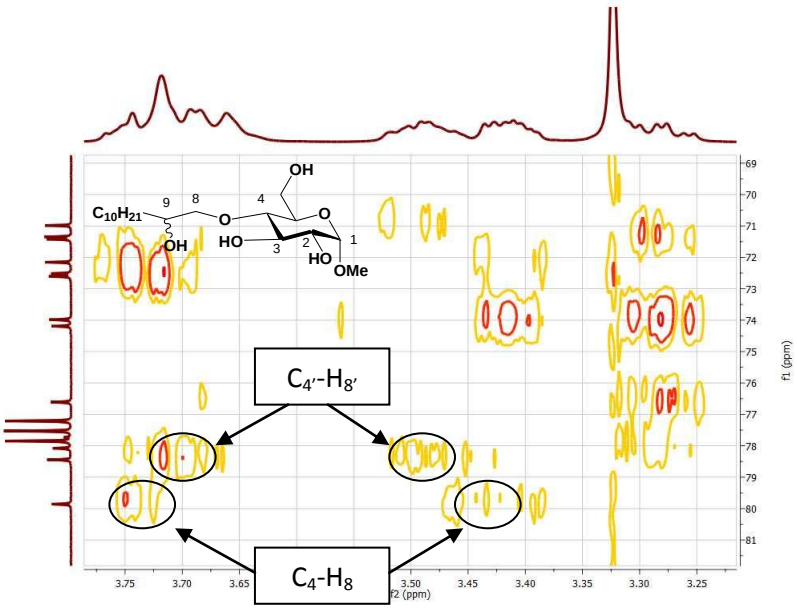

Fig. 3.19: ^{1}H-^{13}C HMBC spectrum for methyl 4-*O*-(2-hydroxyldodecyl)-α-D-glucopyranoside **101c**

3.2.4 Synthesis of methyl 6-*O*-(2-hydroxyalkyl)-α-D-glucopyranosides

In this procedure, the methyl α-D-glucopyranoside was reacted with triphenylmethyl chloride (TrCl), which shows a preference for reacting with primary alcohols.[151] The obtained compound was further protected by benzyl groups to afford methyl 2,3,4-tri-*O*-benzyl-6-trityl-α-D-glucopyranoside **104**. Detritylation was then achieved in the presence of formic acid in Et_2O in order to get the OH-6 compound. The scheme is shown as Scheme 3.8.

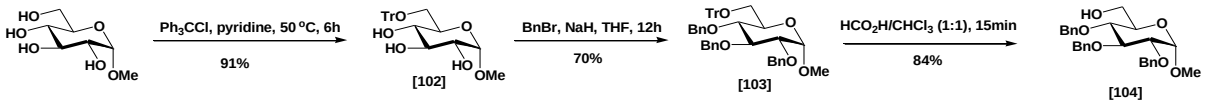

Scheme 3.9: Synthetic procedure for methyl 2,3,4-tri-*O*-benzyl-α-D-glucopyranoside **104**

From the NMR spectra, Fig. 3.20 and Fig. 3.21, the H-2, H-3, H-4 could be traced in the ^{1}HNMR spectrum as the δ 3.60, 4.11 and 3.64 ppm, respectively. Their corresponding C-2,

Cette thèse est accessible à l'adresse : http://theses.insa-lyon.fr/publication/2013ISAL0001/these.pdf
© [R. Xu], [2013], INSA de Lyon, tous droits réservés

C-3, C-4 are also identified as δ 80.5, 82.4 and 77.9 ppm. Since these three positions were substituted by Bn, they may have responses to the proton signals of the methylene units, which could be found in the HMBC spectrum. (Fig. 3.22)

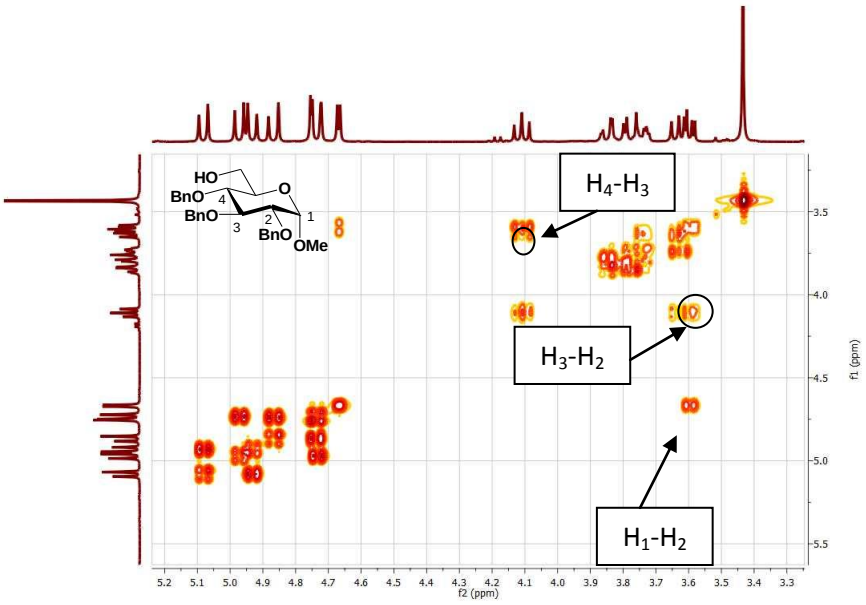

Fig. 3.20: ^{1}H-^{1}H COSY spectrum of methyl 2,3,4-tri-*O*-benzyl-α-D-glucopyranoside **104**

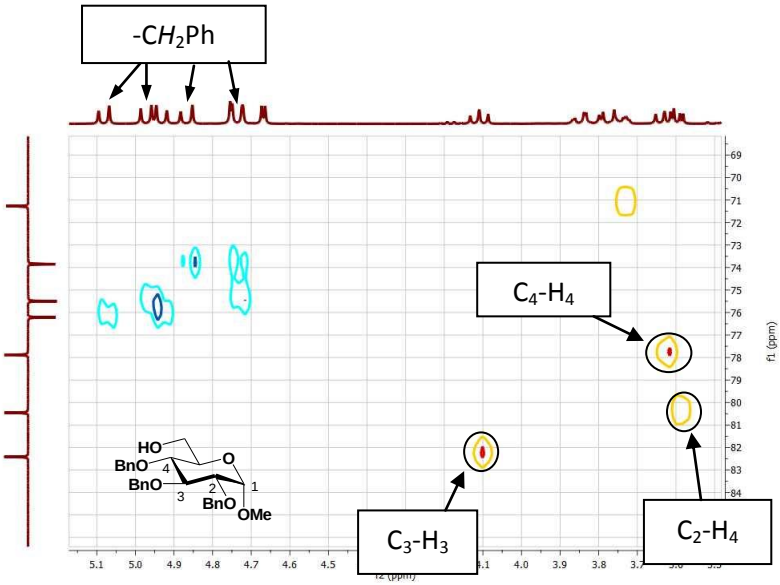

Fig. 3.21: ^{1}H-^{13}C HSQC spectrum of methyl 2,3,4-tri-*O*-benzyl-α-D-glucopyranoside **104**

Cette thèse est accessible à l'adresse : http://theses.insa-lyon.fr/publication/2013ISAL0001/these.pdf
© [R. Xu], [2013], INSA de Lyon, tous droits réservés

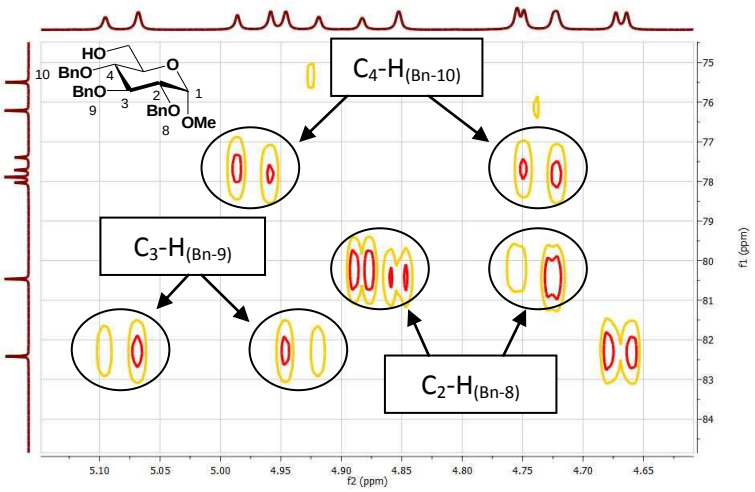

Fig. 3.22: ^{1}H-^{13}C HMBC spectrum of methyl 2,3,4-tri-*O*-benzyl-α-D-glucopyranoside **104**

From this 6-OH derivative, the same etherification reaction was carried out with the 1,2-epoxyalkanes. The procedure is shown in Scheme 3.10.

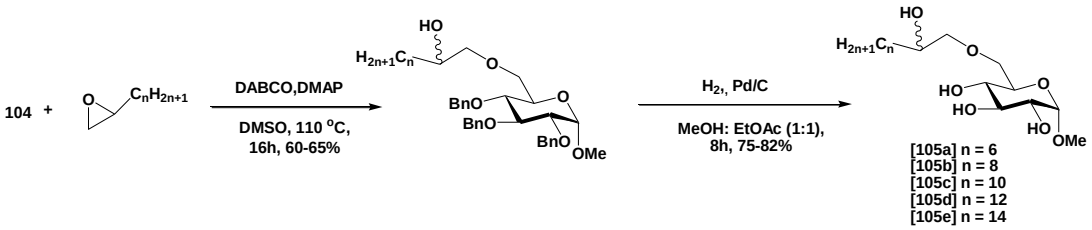

Scheme 3.10: Synthetic procedure for methyl 6-*O*-(2-hydroxyalkyl)-α-D-glucopyranosides **105**

The structural identification resulted again from studies of the NMR spectroscopy data. It is easy to identify the carbon signals of C-6, C-6' at δ 70.1, 70.1 ppm and the C-7, C-7' at δ 76.2, 76.0 ppm in the DEPT spectrum, Fig. 3.23. By analyzing the HSQC, Fig. 3.24 and HMBC, Fig. 3.25 spectra, it is observed that these signals have relation with δ 3.66-3.73 ppm, 3.43-3.50 ppm in the ^{1}HNMR, corresponding to the hydrogen atoms on the C-8 position of aliphatic chain. This correlation could be interpreted as a proof for attachment of the aliphatic chain on the position 6.

Cette thèse est accessible à l'adresse : http://theses.insa-lyon.fr/publication/2013ISAL0001/these.pdf
© [R. Xu], [2013], INSA de Lyon, tous droits réservés

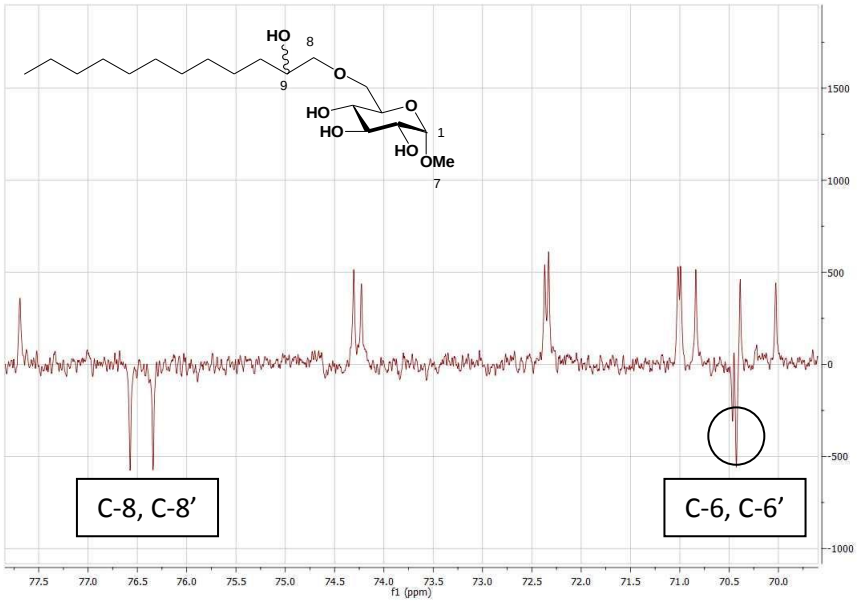

Fig. 3.23: DEPT spectrum of methy 6-*O*-(2-hydroxydodecyl)-α-D-glucopyranoside **105c**

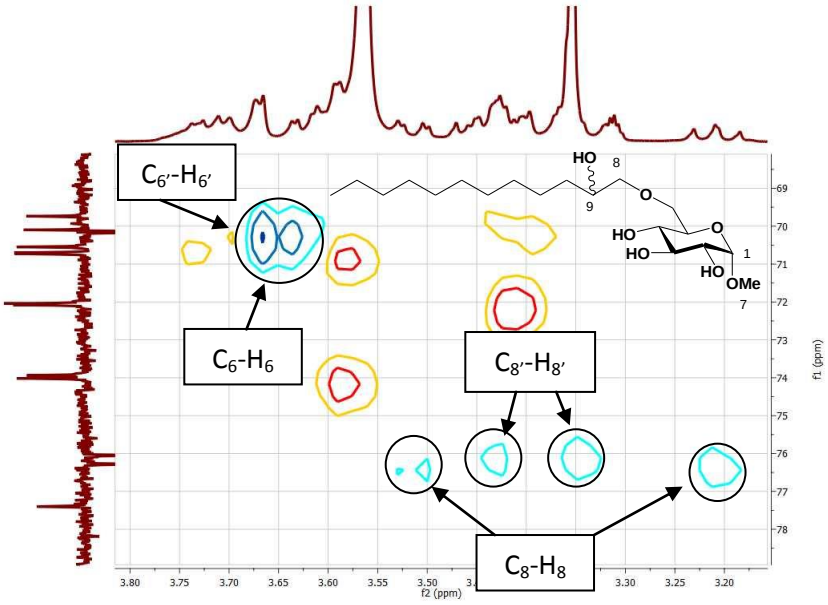

Fig. 3.24: ^{1}H-^{13}C HSQC spectrum of methy 6-*O*-(2-hydroxydodecyl)-α-D-glucopyranoside **105c**

Cette thèse est accessible à l'adresse : http://theses.insa-lyon.fr/publication/2013ISAL0001/these.pdf
© [R. Xu], [2013], INSA de Lyon, tous droits réservés

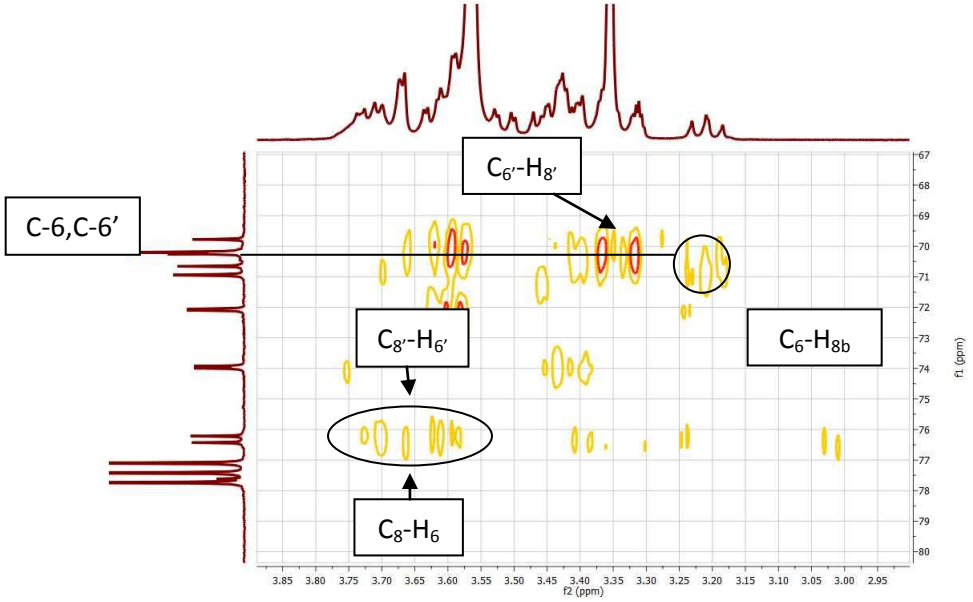

Fig. 3.25: ^{1}H-^{13}C HMBC spectrum of methyl 6-*O*-(2-hydroxydodecyl)-α-D-glucopyranoside **105c**

3.2.5 Synthesis of methyl 6-O-octyl- and dodecyl-α-D-glucopyranosides

1-bromooctane and 1-bromododecane were selected to react with methyl 2,3,4-tri-*O*-benzyl -α-D-glucopyranoside **104** to yield non-functional aliphatic chain systems for comparison. The procedure followed the Scheme 3.11.

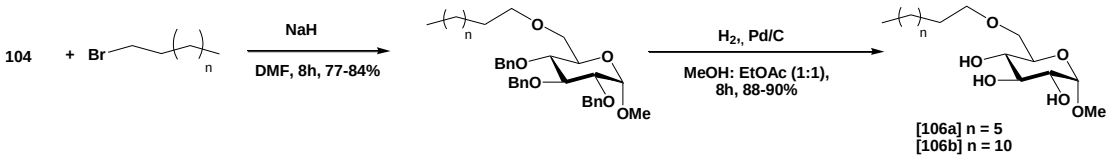

Scheme 3.11: Synthetic procedure of methyl 6-*O*-alkyl-α-D-glucopyranosides **106**

The resulting products **106a**, **106b** were examined by NMR, and their structure was confirmed by comparison with the data reported in literature.[152-154]

Cette thèse est accessible à l'adresse : http://theses.insa-lyon.fr/publication/2013ISAL0001/these.pdf
© [R. Xu], [2013], INSA de Lyon, tous droits réservés

3.3 Study on the thermotropic liquid crystalline behavior of the methyl glucoside hydroxyalkyl ethers

The studies of thermotropic liquid crystalline behavior were carried out in collaboration of J. W. Goodby's group in the University of York. They were examined in three aspects: the mesophases, the transition temperature, the transition ΔH and ΔS. The methods using for the tests were polarized light microscopy and differential scanning calorimetry (DSC). Since the mesophases were very characteristic in all series and easily identified with microscopy, the X-ray diffraction (XRD) was not used.

3.3.1 DSC and polarized light microscopy results of these ether compounds

The DSC tests were performed at the scan rate of 10 ^{o}C min^{-1}, and the heating and cooling processes were repeated twice. Fig. 3.26 shows the DSC curves of methyl 3-O-(2-hydroxyalkyl)-α-D-glucopyranosides **98**:

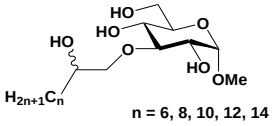

n = 6, 8, 10, 12, 14

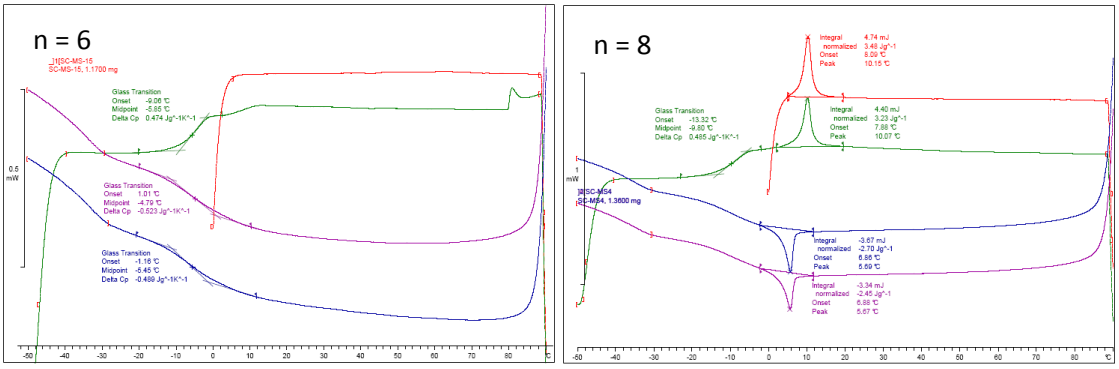

Cette thèse est accessible à l'adresse : http://theses.insa-lyon.fr/publication/2013ISAL0001/these.pdf
© [R. Xu], [2013], INSA de Lyon, tous droits réservés

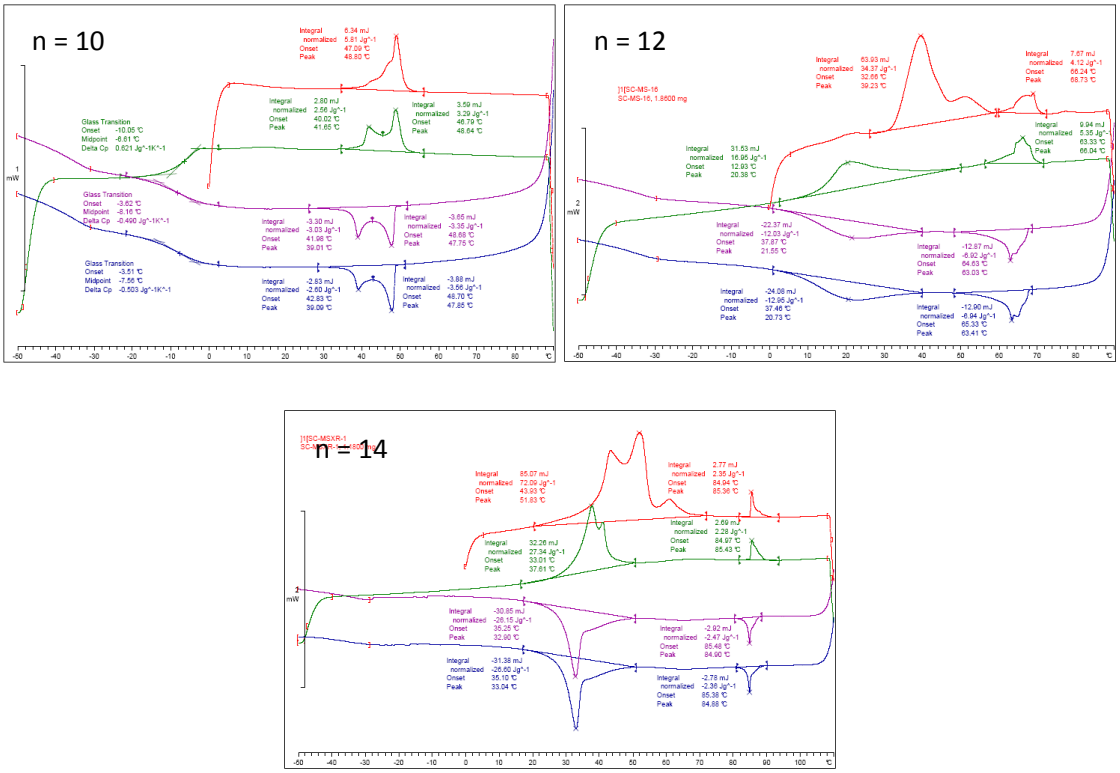

Fig. 3.26: DSC curves of methyl 3-*O*-(2-hydroxyalkyl)-α-D-glucopyranosides **98**

In this series, the shortest aliphatic chain with 8 carbon atoms was not observed to form a mesophase. It was found to form a glassy state at -5.4 ^{o}C and melt into liquid at higher temperature. The formation of glassy state, which is a typical state of sugar, indicates that intermolecular H-bondings of the head groups are the main interactions in this system. As the chain extended to 10 and 12 carbon atoms, the crystalline state appeared whereas the glassy state could still be seen at low temperatures, which were higher than the shortest C8 chain. This behavior suggests that as the increase of hydrophobic proportion in the system, the van der Waals interactions of the hydrocarbon chain began to compete with the intermolecular H-bondings. Eventually, with the longer aliphatic chains of 14 and 16 carbon atoms, the glassy state was replaced by the crystalline state. And a new heat absorbing peak was observed, which indicated a mesophase was formed between the crystalline state and isotropic liquid.

This result fits with the results observed by transmission polarized light microscopy as the Smectic A* (Sm A*) phase. The compounds of all the series bearing longer chain were found to show this mesophase, indicating that the topological shape of these molecules is rod-like. Fig. 3.27 shows the defect image of compound **97e** at 90 ^{o}C of the identical focal-conic defects of elliptical and hyperbolic lines (which are inside the white circle). The formation of

Cette thèse est accessible à l'adresse : http://theses.insa-lyon.fr/publication/2013ISAL0001/these.pdf
© [R. Xu], [2013], INSA de Lyon, tous droits réservés

this defect is due to the fact that the aligning of the molecules was perpendicular to the plane of the microscope slide. That is because of hydroxyl groups of glucoside head preferring to interact with the glass surface while the aliphatic chain didn`t.

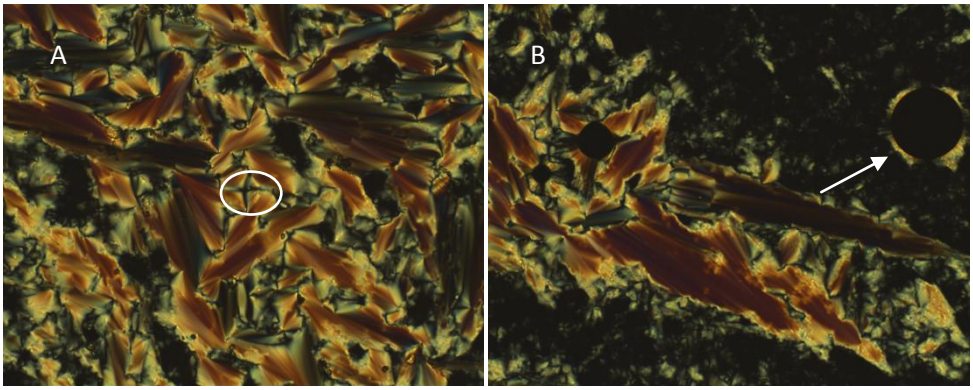

Fig. 3.27: Defect texture of compound **97e** at 90 ^{o}C showing A) focal-conic domains and the elliptical and hyperbolic lines (in the white circle); B) oily streaks and fringes around air bubbles (arrow)

Combining the results from the DSC experiments and observations from transmission light microscopy, the following tables (Table 3.1 to Table 3.5) summarize the thermotropic behaviors of these series. The melting points and the clearing points are recorded in the first heating and first cooling section, since these temperatures are sensitive to thermal history of sample and possibility of decomposition during the heating.[24] For example, the melting points of methyl 3-*O*-(2-hydroxydodecyl)-α-D-glucopyranosides **99c** in the first heating was 32.7 ^{o}C while that in the second heating was 12.9 ^{o}C. This is due to the fact that the crystal melting in the first heating is from the solution whereas the crystal in the second heating is from the crystallization in the bulk sample which follows a different energetical and structural mechanism. The clearing points of some compounds are in the brackets, which is because these transition temperatures were observed during the cooling process.

Cette thèse est accessible à l'adresse : http://theses.insa-lyon.fr/publication/2013ISAL0001/these.pdf
© [R. Xu], [2013], INSA de Lyon, tous droits réservés

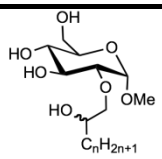

Cpd No	n	K		Sm A*		Iso	Tg
97a	6	•	49.4 [127.57]	—	—	•	-11.5
97b	8	•	33.0 [21.90]	—	—	•	-11.5
97c	10	•	59.7 [87.39]	(•	39.8) [1.54]	•	8.2
97d	12	•	62.8 [71.69]	•	73.7 [1.78]	•	—
97e	14	•	69.2/78.2 [54.75/31.17]	•	94.8 [2.21]	•	—

Table 3.1: Transition temperatures (^{o}C) and enthalpies (J g^{-1}) of transition shown in square bracket for the O-2 series

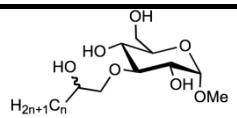

Cpd No	n	K		Sm A*		Iso	Tg
99a	6	—	—	—	—	•	-5.4
99b	8	•	8.1 [3.48]	—	—	•	-9.8
99c	10	—	—	•	48.7§ [3.35]	•	-6.6
99d	12	•	32.7 [34.37]	•	66.2 [5.35]	•	—
99e	14	•	43.9 [72.09]	•	85.0 [2.35]	•	—

Table 3.2: Transition temperatures (^{o}C) and enthalpies (J g^{-1}) of transition shown in square bracket for the O-3 series (§ there is a second peak at 42.0 ^{o}C)

Cette thèse est accessible à l'adresse : http://theses.insa-lyon.fr/publication/2013ISAL0001/these.pdf
© [R. Xu], [2013], INSA de Lyon, tous droits réservés

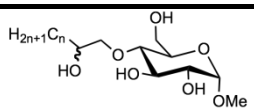

Cpd No	n	K		Sm A*		Iso	Tg
101a	6	•	25.2/31.3 [2.46/6.75]	—	—	•	-14.7
101b	8	•	64.2 [26.21]	—	—	•	-1.3
101c	10	•	33.7 [55.77]	—	—	•	-4.2
101d	12	•	34.5 [53.02]	•	62.6 [0.27]	•	—
101e	14	•	39.7 [57.81]	•	81.3 [1.68]	•	—

Table 3.3: Transition temperatures (^{o}C) and enthalpies (J g^{-1}) of transition shown in square bracket for the O-4 series

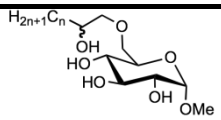

Cpd No	n	K		Sm A*		Iso	Tg
105a	6	—	—	—	—	•	—
105b	8	•	47.9 [55.51]	—	—	•	-2.1
105c	10	•	64.8 [81.1]	(•	37.9) [1.97]	•	0.3
105d	12	•	71.3 [83.64]	(•	58.5) [2.19]	•	—
105e	14	•	72.8 [75.05]	•	79.0 [1.60]	•	—

Table 3.4: Transition temperatures (^{o}C) and enthalpies (J g^{-1}) of transition shown in square bracket for the O-6 series

Cette thèse est accessible à l'adresse : http://theses.insa-lyon.fr/publication/2013ISAL0001/these.pdf
© [R. Xu], [2013], INSA de Lyon, tous droits réservés

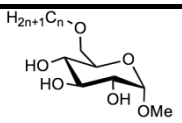

Cpd No	n	K		SmA		Iso	Tg
106a	8	•	28.9	(•	20.1)	•	-22.6
			[0.82]		[2.52]		
106b	12	•	56.5	(•	33.3)	•	
			[98.99]		[2.48]		

Table 3.5: Transition temperatures (^{o}C) and enthalpies (J g^{-1}) of transition shown in square bracket for the regular chains

For these 6-alkyl ethers (**106**), the Sm A* phase showed up when the aliphatic chains consisted of 8 carbon atoms, where the equivalent of **105a** was not observed. And with longer chain, the two counterparts acted in a similar manner, the transition temperatures were all at around 35 ^{o}C along with a very close enthalpy values.

Comparing these two distant results, the additional hydroxyl group may have a relatively stronger impact on the shorter aliphatic to the longer ones. This result may be due to the hydrophilic/ hydrophobic balance of the system. In the case of regular aliphatic chain, the number of carbon atoms of 8 was enough to be competitive to the H-bondings induced by the glucoside head group; but for the family with the additional hydroxyl group, the hydrophilic/ hydrophobic balance at this stage was not enough to stabilize the mesophases at this stage. Once the hydrophilic/ hydrophobic balance rebuilt where the effect of the hydroxyl group was not significant, the liquid crystalline behavior may more rely on the interaction of the hydrophobic part rather than the intermolecular H-bondings.

3.3.2 The effects of aliphatic chain and the substituted position on the liquid crystalline behavior of the series

Fig. 3.28-3.31 illustrate the melting point and the clearing point as the function of chain length of all the series. Examining these curves, we could find an increase of the clearing point relative to the increasing methylene groups. This kind of behavior is similar with other carbohydrate based liquid crystals, for example, the alkyl α-D-glucosides with short aliphatic chains,[24] indicating that the van der Waals attractions also have effects on the formation of thermotropic liquid crystalline phases.

Cette thèse est accessible à l'adresse : http://theses.insa-lyon.fr/publication/2013ISAL0001/these.pdf
© [R. Xu], [2013], INSA de Lyon, tous droits réservés

The substitution position has a significant effect on the melting points. The O-3 and O-4 series had relative lower melting points compared to O-2 and O-6 families. This kind of behavior was also observed in other systems, for example the series of mono-O-dodecyl-pyranoses, where the two middle positions showed higher melting points than the other outer two positions.[154]

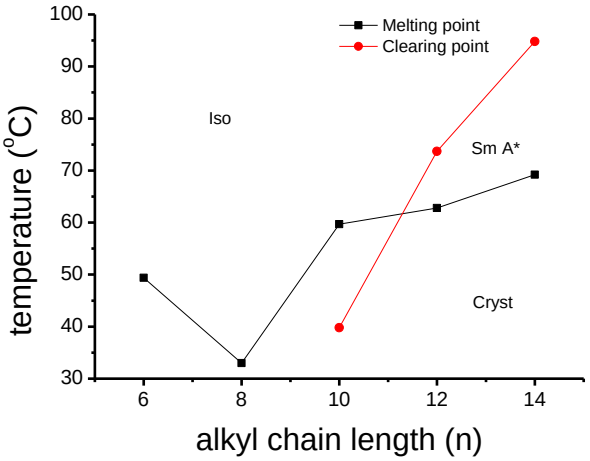

Fig. 3.28: The melting points and the clearing points as a function of chain length (n) of 2-*O*-(2-hydroxyalkyl)-α-D-glucopyranosides **97**

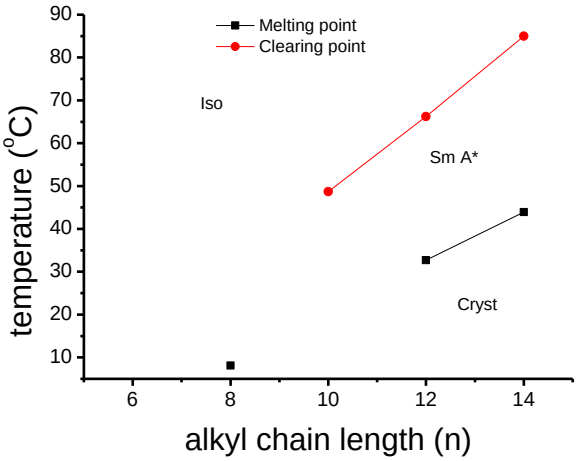

Fig. 3.29: The melting points and the clearing points as a function of chain length (n) of 3-*O*-(2-hydroxyalkyl)-α-D-glucopyranosides **99**

Cette thèse est accessible à l'adresse : http://theses.insa-lyon.fr/publication/2013ISAL0001/these.pdf
© [R. Xu], [2013], INSA de Lyon, tous droits réservés

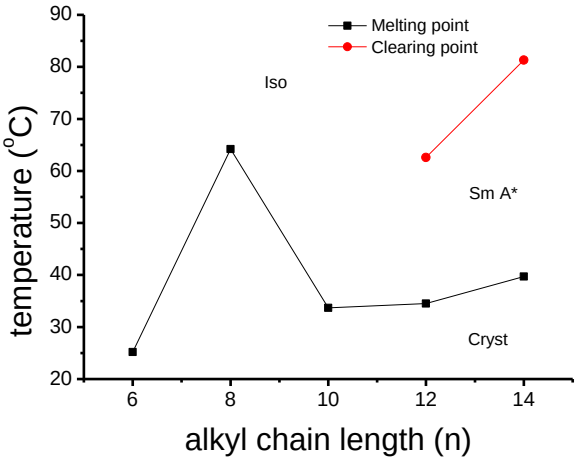

Fig. 3.30: The melting points and the clearing points as a function of chain length (n) of 4-*O*-(2-hydroxyalkyl)-α-D-glucopyranosides **101**

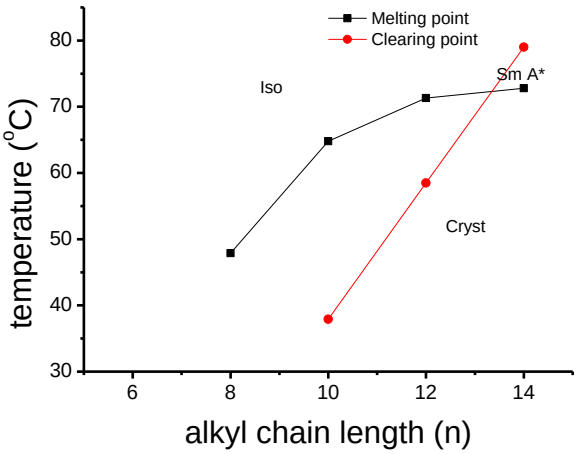

Fig. 3.31: The melting points and the clearing points as a function of chain length (n) of 6-*O*-(2-hydroxyalkyl)-α-D-glucopyranosides **105**

For the clearing points, the effect of substitution positions is not as significant as that on the melting points, but it conveys some interesting information. As shown in Fig. 3.32, for the longer chains (14, 16), these compounds behaved a consistent decreasing manner as the order of **97** > **99** > **101** > **105**. But the equivalents bearing the chain length of 12 carbons behaved a strange manner. At this chain length, the **99c** showed the highest clearing point, no mesophases were observed in the **101c** compound, and **97c** and **105c** compounds had a similar isotropization temperature which was lower than the **99c**. This unusual manner could

Cette thèse est accessible à l'adresse : http://theses.insa-lyon.fr/publication/2013ISAL0001/these.pdf
© [R. Xu], [2013], INSA de Lyon, tous droits réservés

be regarded as the boundary where the hydrophilic/hydrophobic balance met its limit. At this point, the inter- and intra-molecular H-bond played a central role in the formation of mesophases. And this difference of the interaction may eventually enhance the liquid crystalline behavior for O-3, or suppress the liquid crystalline behavior in the case of O-4.

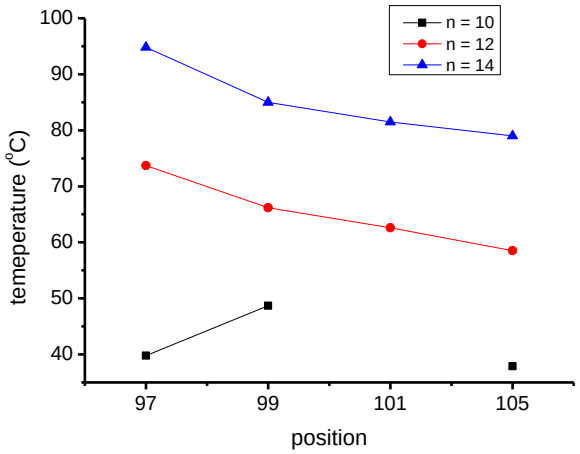

Fig. 3.32: The clearing points as a function of substitution positions

3.3.3 Structure study by modeling

In order to understand the possible structure-properties relationships in these series, the energy minimized models of the molecules with C8 chain, **97a**, **99a**, **101a**, **105a**, were examined in the gas phase at absolute zero, as shown in Fig. 3.33, with two epimers respectively. The effect of intra- and inter-molecular H-bondings was investigated in terms of effective distance between the hydroxyl group on the aliphatic chain and the neighboring hydroxyl groups on the sugar head. The closest interaction distances are shown in the models. For **97a**, the hydroxyl group in the alkyl chain has one possible interaction with the OH-3 with an effective H-bonding distance of 4.2 Å for one epimer and 5.0 Å for the other. A similar situation was detected in the case of compound **105a** where the possible interaction is at 4.2 Å and 3.6 Å, respectively. Since the aliphatic chain of **99a** is located inbetween the O-2 and O-4 position, the possibility of the additional hydroxyl group interacting with the OH-2 and OH-4 is largely increased, with the effective distance at 3.0 Å and 5.6 Å for one epimer, 5.3 Å and 3.9 Å for the other. In this case, a preference of forming the intramolecular H-bondings is much higher than the **97a** and **105a**. A similar conclusion could also be drawn for

Cette thèse est accessible à l'adresse : http://theses.insa-lyon.fr/publication/2013ISAL0001/these.pdf
© [R. Xu], [2013], INSA de Lyon, tous droits réservés

the compound **101a**. As a consequence, these configurations may employ a more rigid structure, where the alkyl chain and glucoside unit are more likely to fixed together, compared to the **97a** and **105a**.

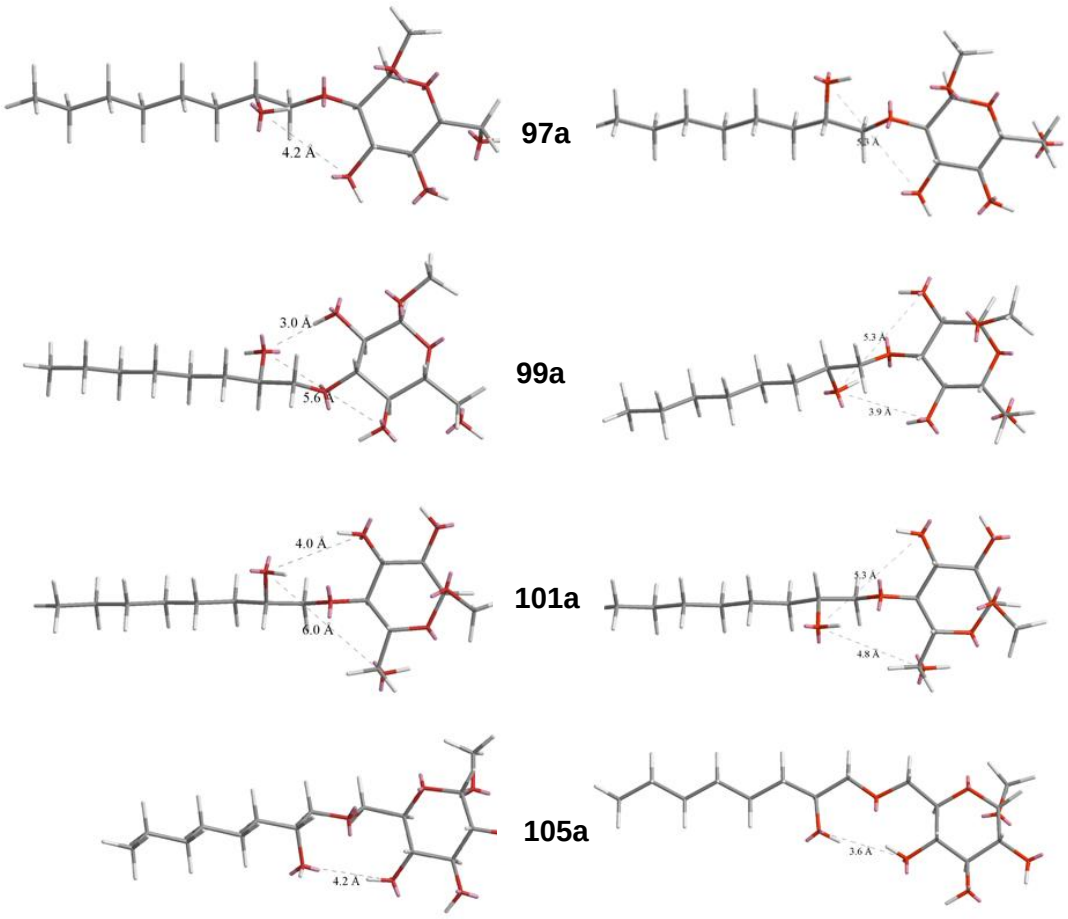

Fig. 3.33: Energy minimized models of **97a**, **99a**, **101a** and **105a**

So in the **99** and **101** series, which kind of H-bonding will be preferred in the system? To answer this, an insight study on enthalpies and entropies of the transition for the compounds showing the liquid crystalline behaviors was carried out. The investigation was focused on comparing the enthalpies as function of aliphatic chain length and substitution position, along with the $\Delta S/R$, where R is the constant value of 8.314 J K^{-1} mol $^{-1}$. The results are listed in Table 3.6. Observed in other systems, the enthalpy of transition increases as the chain length extends, which indicates that the mesophase is becoming more organized and less like the liquid, the rule could also be applied for these series as the methylene groups

Cette thèse est accessible à l'adresse : http://theses.insa-lyon.fr/publication/2013ISAL0001/these.pdf
© [R. Xu], [2013], INSA de Lyon, tous droits réservés

increased. When comparing with these values in regarding of substitution positions, the compound **101d** possesses a lowest enthalpy value, along with the ΔS/R, which could be interpreted as that the compound is more disorganized than the others. This may be the reason for why the Sm A* was not observed for the **101c**. And it also suggests that the H-bondings in this system is intra- rather than inter-, that is to say, the additional hydroxyl group would have more chance to interact with the hydroxyl groups inside the molecule. Once this intramolecular H-bonding was formed, the compound may create a pseudo-six member ring, which reduces the hydrophilic /hydrophobic balance. As a result, the msophase stability was reduced. And for the longer chain, since the hydrocarbon chain began to dominate the transition behavior, the formation of pseudo-six ring would be interrupted by the flexibility of aliphatic chain.

In contrast, the **99** series exhibited relative high enthalpy values, which met their summit at chain length of C14. This array of values indicate that hydroxyl groups in this series are preferred the intermolecular H-bondings, suggesting that the mosophase is formed easily and stabilized well.

Compound	ΔH / J mol^{-1}	T / K	ΔS / J mol^{-1}K^{-1}	DS/R
97c	617.93	312.8	1.9755	0.2376
97d	764.12	346.7	2.204	0.2651
97e	1010.66	367.8	2.7479	0.3305
99c	1344.19	321.7	4.1784	0.5025
99d	2296.66	339.2	6.7708	0.8143
99e	1074.69	358	3.0019	0.361
101d	115.91	335.6	0.3454	0.0415
101e	768.29	354.3	2.1685	0.2608
105c	790.46	310.9	2.5425	0.3058
105d	940.13	331.5	2.836	0.3411
105e	731.7	352	2.0787	0.25

Table 3.6: Enthalpies (J mol^{-1}) and entropies for compounds showing liquid crystalline mesophases

The effective H-bondings could also be used to explain the melting behaviors of these compounds. An obvious explanation could be given as the additional hydroxyl group in the aliphatic chain substituted in the middle positions of the sugar has more chance to form

Cette thèse est accessible à l'adresse : http://theses.insa-lyon.fr/publication/2013ISAL0001/these.pdf
© [R. Xu], [2013], INSA de Lyon, tous droits réservés

intramolecular H-bonding than the outer couples. At lower temperature, the effective hydroxyl groups in these compounds to bridge with other molecules are less, thus the ratio of intermolecular H-bonding is low, leading to less stable crystal state. As a result, the melting points of compounds of **99** and **101** are lower than that of **97** and **105**. A more insightful comment stands on the global structure of the molecule. In the **97** and **105** series, since the orientations of hydroxyl groups on the sugar head are the same, they could take part in building up the interactions with other molecules. This process might not be disturbed as the aliphatic chain could be packed aside. In other two systems, because of the location of substitution is inbetween those with hydroxyl groups, the opportunities of disturbing the intermolecular H-bonding by the alkyl chain is much higher, leading to the lower melting points.

3.4 Lyotropic study

The lyotropic liquid crystalline behaviors of these compounds were also investigated. The experiments were carried out by examining contact preparations, which is designed as a small amount of water is added into the space by the coverslip and glass plate where the sample is. As a result, from contact frontier to inside solid, the glucoside sample forms a gradient of concentration from high to low. The plate is then examined under the transmission light microscope. The results are listed in Table 3.7.

	97	**99**	**101**	**105**
b	Cubic Hexagonal	Lamellar Cubic Hexagonal	Cubic Hexagonal	Lamellar Cubic Hexagonal
c	Cubic Hexagonal	Lamellar Cubic	Lamellar Cubic Hexagonal	Lamellar Cubic Hexagonal
d	Cubic	Lamellar Cubic	Lamellar Cubic	Lamellar Cubic
e	Insoluble	Insoluble	Insoluble	Insoluble

Table 3.7: Lyotropic behaviors of compounds **97**, **99**, **101**, **105**

Cette thèse est accessible à l'adresse : http://theses.insa-lyon.fr/publication/2013ISAL0001/these.pdf
© [R. Xu], [2013], INSA de Lyon, tous droits réservés

As observed, according to different concentrations, the molecules formed hexagonal, cubic and lamellar mesophases, which are similar to some simple sugar head derivatives.[155, 156] The Fig.3.34 shows the defect images of lyotropic liquid crystalline mesophases as lamellar, cubic, and hexagonal of compound **101c**.

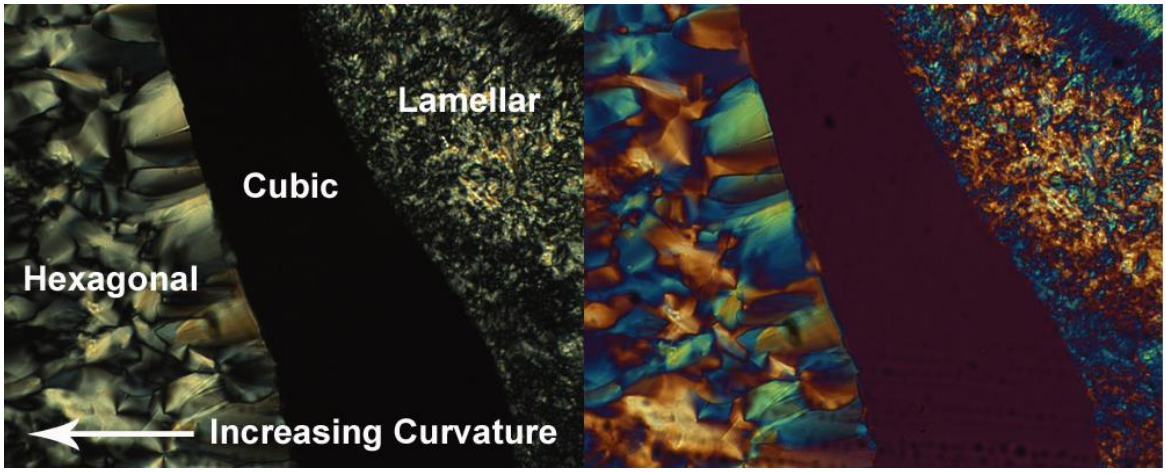

Fig. 3.34: Defect textures of mesophases shown by compound **101c**: A) view from the microscope; B) view from microscope with a waveplate (X100 magnification)

A general tendency for these compounds is that as the aliphatic chain length increased, the types of mesophases were limited. For example, for the compounds **101b** with the shorter chain, the molecule showed hexagonal and cubic phases. When the chain extended for 14, **101d**, the mesophases observed was just the cubic, Fig. 3.35. These phenomena indicate that as the alkyl chain extended, the relative cross-sectional area of the sugar head to the alkyl chain decreased, resulting that the curvature of the system was not sufficient to support the formation of mesophases.

Cette thèse est accessible à l'adresse : http://theses.insa-lyon.fr/publication/2013ISAL0001/these.pdf
© [R. Xu], [2013], INSA de Lyon, tous droits réservés

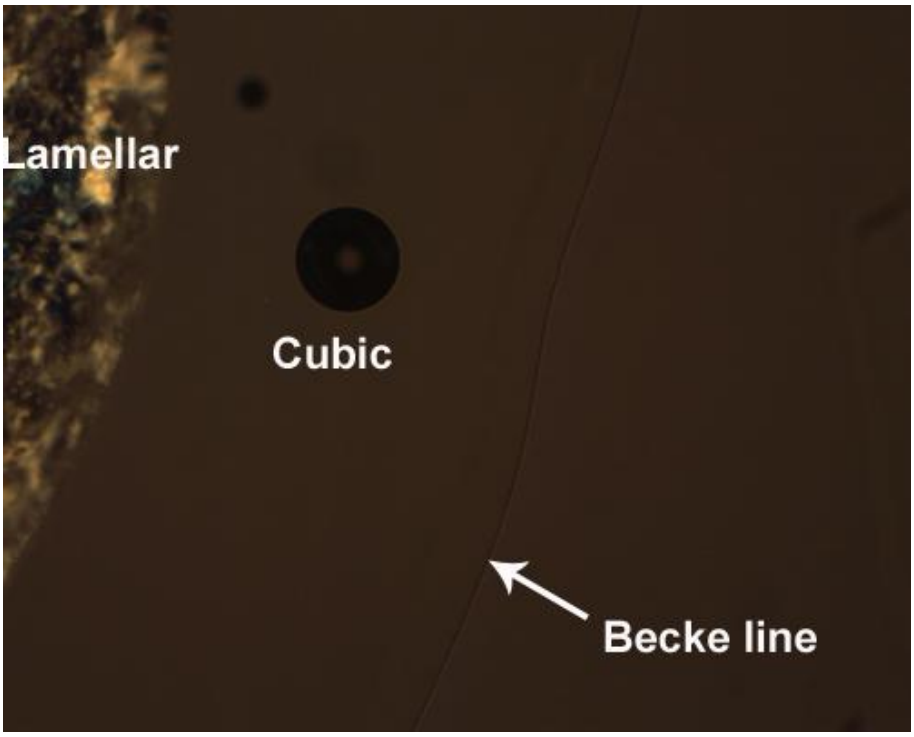

Fig. 3.35: Lamellar and cubic phases of compound **101d** (X100 magnification)

And since the aliphatic chain became to dominate the portion of molecule, the compound was turned to be hydrophobic which was not soluble in water.

Interestingly, compounds where the alkyl chain is attached in the O-2 position exhibited increased curvature compared to the other compounds. This indicates that the cross-sectional area of the sugar is larger for these materials in comparison to the other homologous series. The **99** series showed a tendency for lower curvature than the other analogues, where the hexagonal phase was only observed for the shortest chain lengths, which disappeared the chain length reached C10**.**

3.5 Conclusions

A new family of methyl n-*O*-(2-hydroxylalkyl)-α-D-glucopyranosides have been synthesized and characterized. The synthesis methods involved partially protecting the hydroxyl groups on the glucopyranoside head to make target position available, followed by being etherified with different chain lengths of 1,2-epoxyalkanes. The final products were obtained by removing the protecting groups. The structures of final products were identified by NMR and mass spectroscopy to be the desired compounds.

Cette thèse est accessible à l'adresse : http://theses.insa-lyon.fr/publication/2013ISAL0001/these.pdf
© [R. Xu], [2013], INSA de Lyon, tous droits réservés

Their thermotropic liquid crystalline behaviors were investigated by means of transmission light microscopy and DSC experiment. As observed, the Sm A* phases are the dominant phases. Comparing with our previous investigation of similar systems based on sucrose, [113] these compounds show relatively low transition temperatures. The substitution position has little effect on the mesophase formation, yet a significant one on the melting points.

The clearing point increases as the aliphatic chain extends. When the chain length is 14 or 16, the transition temperature decreases as the substituted chain moved from O-2 to O-6. For the C12 series, the effect of position is different, possibly due to a preference for intermolecular H-bonding, as indicated by significantly higher transition enthalpies for all O-3 compounds, while in the case of O-4 compounds, intramolecular H-bondings would be the dominant factor. Moreover, for these latter O-4 compounds, modeling shows that the hydroxyl group of the aliphatic chain and the sugar hydroxyl groups may have a very approaching distance.

Cette thèse est accessible à l'adresse : http://theses.insa-lyon.fr/publication/2013ISAL0001/these.pdf
© [R. Xu], [2013], INSA de Lyon, tous droits réservés

Chapter 4

Synthesis and thermotropic liquid crystalline behavior of new glycosteroidic amphiphiles

4.1 Introduction

Cholesterol is abundant in the membranes of most mammalian cells.[157] For example, it covers 15% of total weight of skin surface lipids.[158] The role of cholesterol associating with sphingolipids in the concept of “lipid rafts” is well known.[47, 159, 160] Cholesterol’s unique structure, where two different facial geometrical graphs as the hydroxyl group on the C-3 and methyl substituents on the C-10, C-13, and C-17 are orientated in β face, is considered to be responsible for these properties. Molecular modeling is shown as A in Fig. 4.1.[161]

Cholesterol is also an important mesogen in the liquid crystal domain. It is a topic of several reviews recently.[162, 163] Over 3300 cholesterol-based LCs with a variety of structures have been tested and studied. Due to its chirality with 8 chiral centers on the moiety and rigid structure, the cholesterol-based LCs could form cholesteric mesophases, showing unique optical properties in the forms of helical supra-structure, shown as B in Fig. 4.1.

Cette thèse est accessible à l'adresse : http://theses.insa-lyon.fr/publication/2013ISAL0001/these.pdf
© [R. Xu], [2013], INSA de Lyon, tous droits réservés

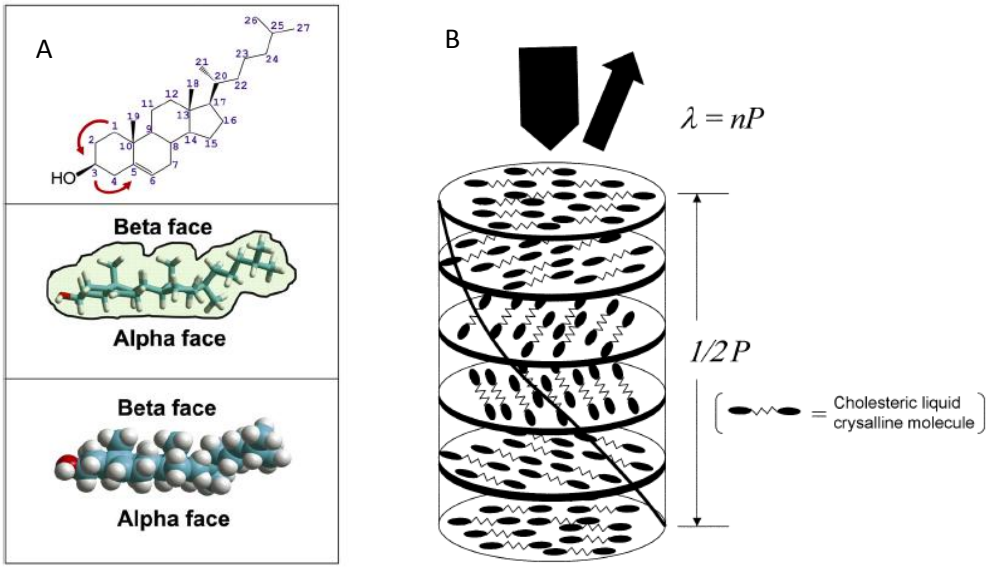

Fig. 4.1: (A) The molecular structure (upper), molecular modeling (middle), and space-filling of cholesterol;[161] (B) Helical structure of cholesteric liquid crystal[162]

Its conjugates with carbohydrates, in the big family namely steroidal glycosides, are ubiquitous compounds. The structures of two recently found compounds in this family are shown in Fig. 1.9.[65, 67] Some efforts have been dedicated to investigating the ability of synthetic glycosyl cholesterol to show the liquid crystalline phases. Like compound GlcNAc-E_4-cholesterol, Fig. 4.2, it was found to show Sm A* in pure state and an array of phases according to the concentrations, illustrated in B in Fig. 4.2, under lyotropic conditions.[164]

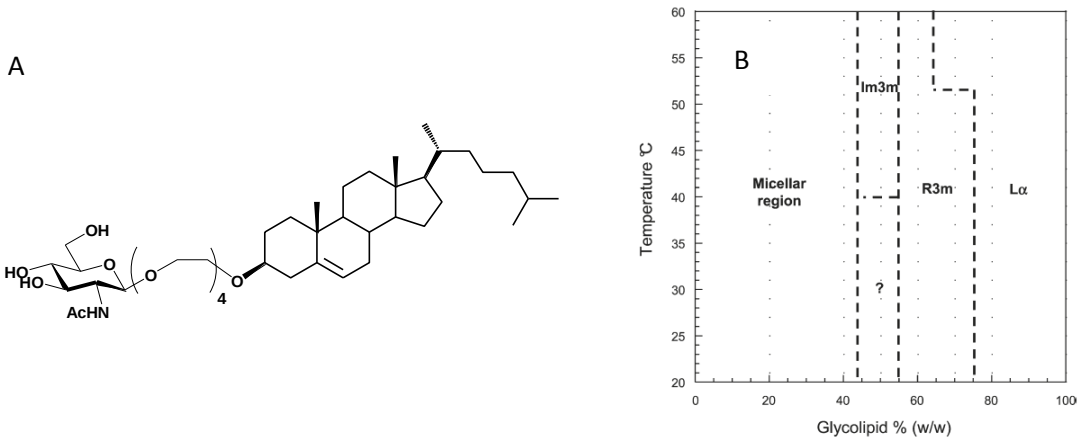

Fig. 4.2: A) Chemical structure of GlcNAc-E_4-cholesterol and B) its performance in water solution according to the concentration (lines are guides for the eyes, but the error of their positions in terms of glycolipids percentage is ±5%)[164]

Cette thèse est accessible à l'adresse : http://theses.insa-lyon.fr/publication/2013ISAL0001/these.pdf
© [R. Xu], [2013], INSA de Lyon, tous droits réservés

Our lab being involved in projects dedicated to the study of glycolipidic liquid crystalline materials, and taking into account these natural compounds and their importance in terms of biological functions, it was thus interesting to include cholesterol among hydrophobic moieties used in such systems.

A first series of compounds coupling a sugar to a cholesterol moiety (Fig 4.3) was prepared via the CMGLs in 2007 (see bibliographic section). The connection between the two moieties was directly achieved by reaction of aminocholesterol with CMG lactone. However their liquid crystalline behavior was very limited because of decomposition at high temperature and also attributed to a lack of flexibility of the system.

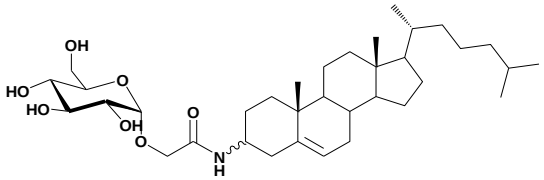

Fig. 4.3: Chemical structures of cholesteryl amide glucosides

In the present work, we prepared a series of novel glycosteroidic systems with an alkyl chain spacer between the sugar and the cholesterol varying from 4 to 12 carbon atoms. For C4 spacer, we used the olefin metathesis; whereas for the other four spacers 6, 8, 10, 12, we introduced a terminal amino group on the steroid alkylether for opening the α-CMGLs. The procedure is indicated in Scheme 4.1. In this aspect, we could get the information about the effect of flexibility on the liquid crystalline behaviors. Taking advantage of the CMGL strategy, it was also easy to add a second chain into these glycosteroid systems, by reaction of OH-2 with alkylisocyanates. These disubstituted compounds, named as bolaphiles, having two hydrophobic moieties connected through a polar head, might convey other information how the interactions of lipids might affect the liquid crystalline behaviors. The schematic representation of the whole synthetic procedures is shown in Scheme 4.1. Mrs Fahima Alirachedi and Mr Nuno Xavier contributed to this part of the work during their internships in the lab by preparing compounds in the the C4 linker series.

Cette thèse est accessible à l'adresse : http://theses.insa-lyon.fr/publication/2013ISAL0001/these.pdf
© [R. Xu], [2013], INSA de Lyon, tous droits réservés

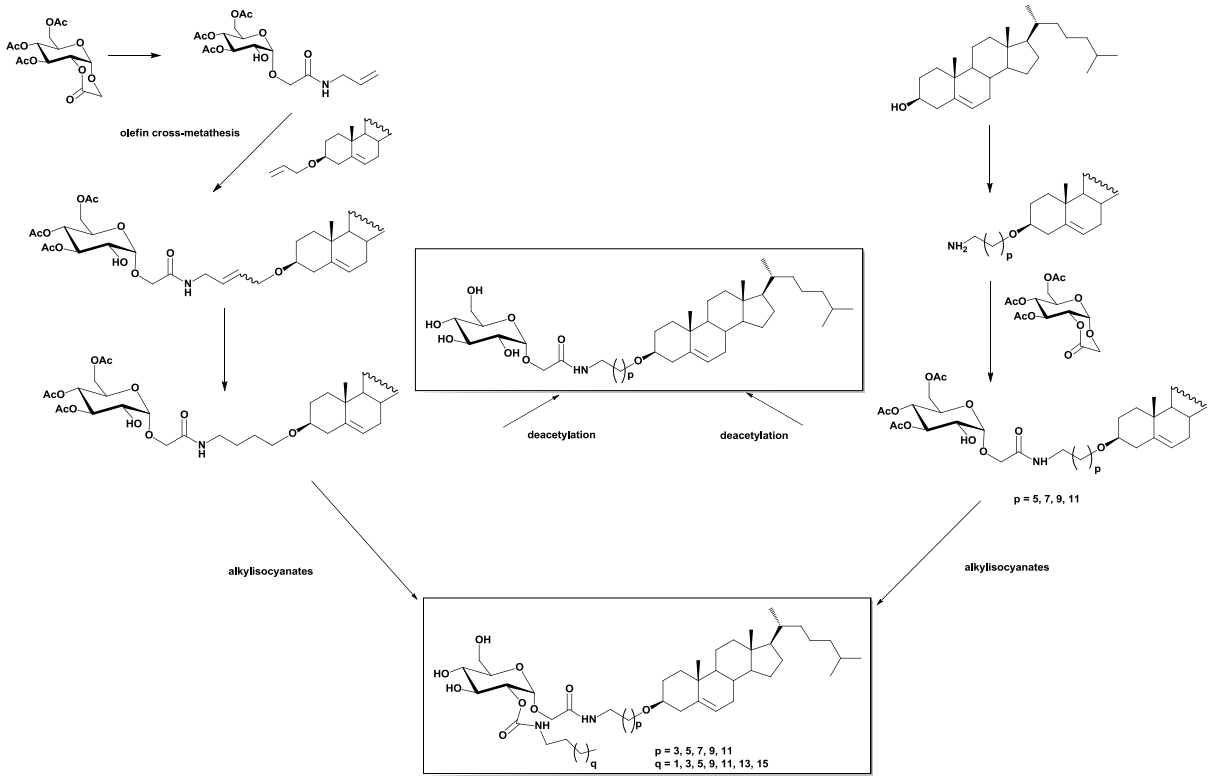

Scheme 4.1: Schematic representation of the synthetic procedures

4.2 Synthesis of monosubstituted glycosteroids

4.2.1 Synthesis of C4 spacer

The key step towards the C4 linker compound is the olefin cross-metathesis between the allyamide obtained from CMGL, and the allyl cholesteryl ether. This metathesis reaction was discovered around the 1950s, and the main contributors to the discovery, Yves Chauvin, Robert H. Grubbs, and Richard R. Schrock, received the Nobel Prize in 2005. The accepted mechanism of this reaction is shown in Fig. 4.4, as the olefin being firstly coordinated with a metal alkylidene to form a metallacyclobutane intermediate, which further exchanges with the other olefins to generate the more entropic stable product. [165]

Cette thèse est accessible à l'adresse : http://theses.insa-lyon.fr/publication/2013ISAL0001/these.pdf
© [R. Xu], [2013], INSA de Lyon, tous droits réservés

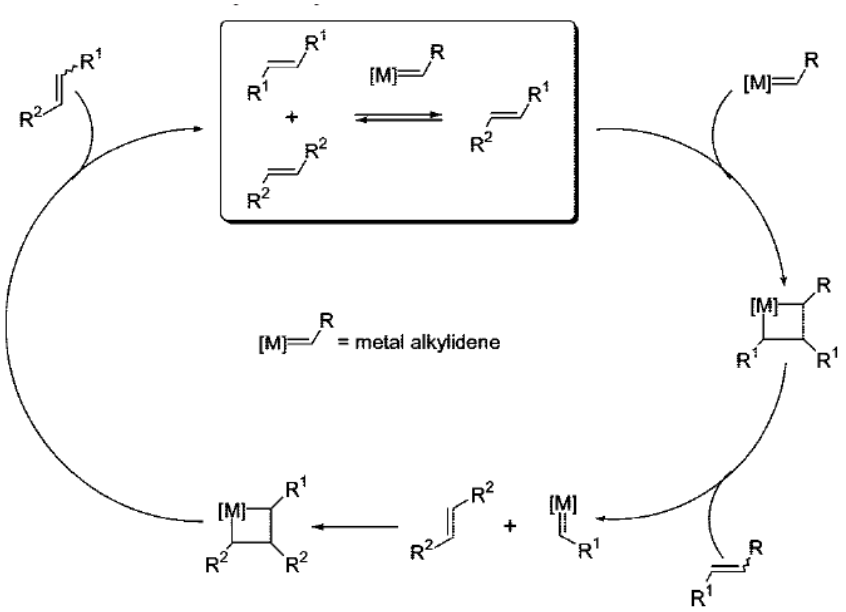

Fig. 4.4: Catalystic cycle of olefin metathesis[165]

Nowadays, the ruthenium-based catalysts are the most widely used in olefin metathesis, since they show a good tolerance towards oxygen, water and functional groups and a good catalytic activity. In this synthesis, we employed the Grubbs-Hoveyda catalyst 2nd generation. The structure is shown in Fig. 4.5.

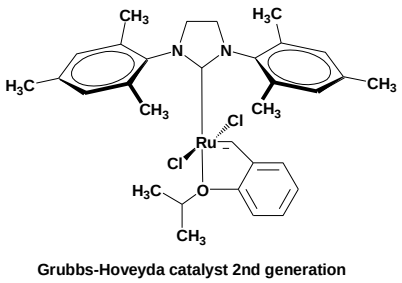

Fig. 4.5: Chemical structure of olefin metathesis catalyst

The starting material **107** was synthesized by the reaction of allyl amine and the α-CMG lactone. Evidence for the lactone ring opening is that the H-2 at 4.40 ppm in the lactone ^{1}HNMR disappears to the benefit of a signal at 3.78 ppm. Also, in carbon spectrum, the C-2 appears at 70.3 ppm instead of 76.3 ppm. The compound **108** was synthesized by reaction of allyl bromide with cholesterol in the presence of NaH, the yield of which was 72 to 80%.

Cette thèse est accessible à l'adresse : http://theses.insa-lyon.fr/publication/2013ISAL0001/these.pdf
© [R. Xu], [2013], INSA de Lyon, tous droits réservés

The NMR data fits with what was reported in literature.[166] Coupling of carbohydrate olefin **107** and cholesteryl olefin **108** was carried out in DCM in the presence of Grubbs-Hoveyda catalyst, and the desired glycosteroid was obtained in 72% yield, Scheme 4.2.

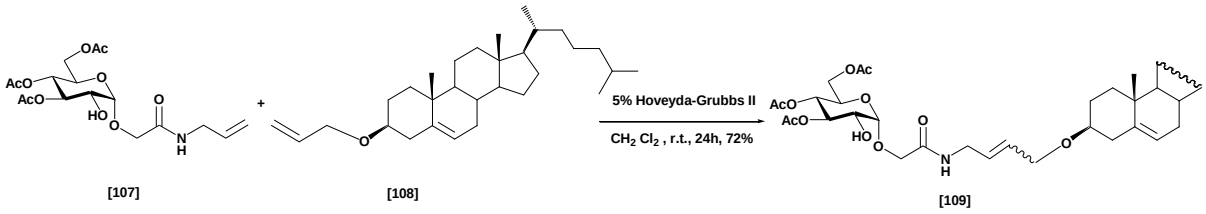

Scheme 4.2: Synthetic procedure for spacer 4 with double bonds

In proton NMR spectrum, Fig. 4.6, the realization of coupling is identified by the disappearance of multiplet peaks of double bond of cholesteryl olefin disappears at δ 5.85 ppm to the benefit of a signal around 5.68 ppm, indicating a new double bond was formed. And the corresponding carbon signals are found at δ 129.7 and 128.2 ppm.

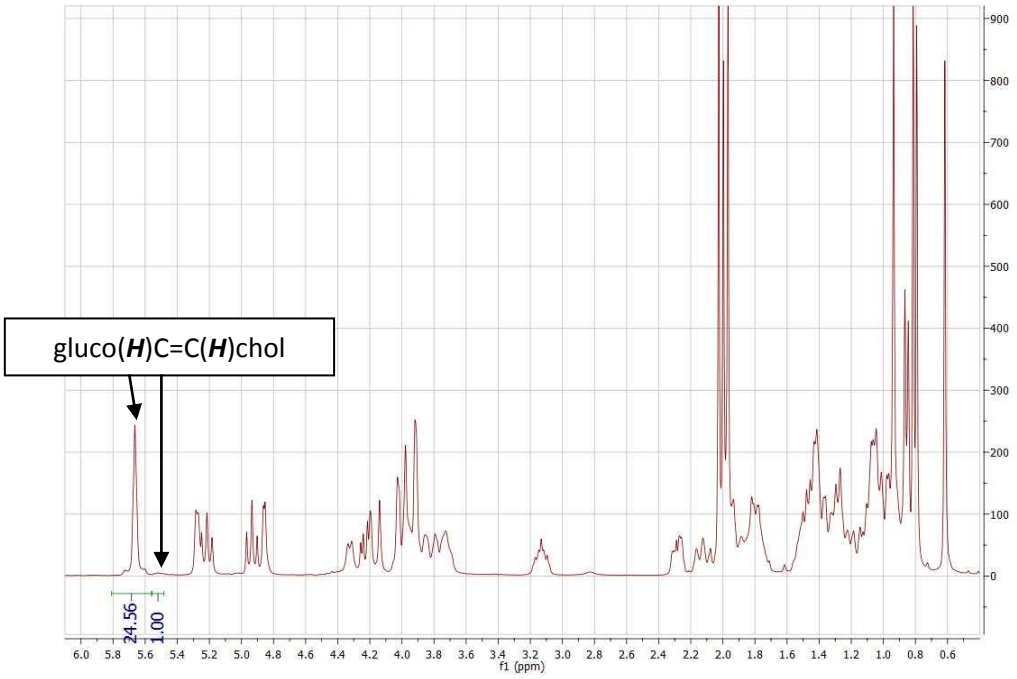

Fig. 4.6: ^{1}HNMR spectrum of compound **109**

Cette thèse est accessible à l'adresse : http://theses.insa-lyon.fr/publication/2013ISAL0001/these.pdf
© [R. Xu], [2013], INSA de Lyon, tous droits réservés

At δ 5.54 ppm, there is a small peak indicating that the resulting product was a mixture of two epimers. Further investigation concerning the structure and the ratio of these two epimers was carried out by the NMR experiment. The process is shown in Fig. 4.7. Firstly the peak at around 5.54 ppm was selectively excited. As shown in Fig 4.7.B, a tocsy 1D experiment was carried out to identify the nearby proton signals. The peak at 5.68 ppm could be identified as the other proton on the double bond, meaning that the integration of this peak in Fig. 4.7 contains part of this compound. Homodecoupling of CH_2 gives the coupling constant of these two protons as 10 Hz, showing in C, which confirms this configuration is Z. As a result, the ratio of E/Z could be calculated as 23/2.

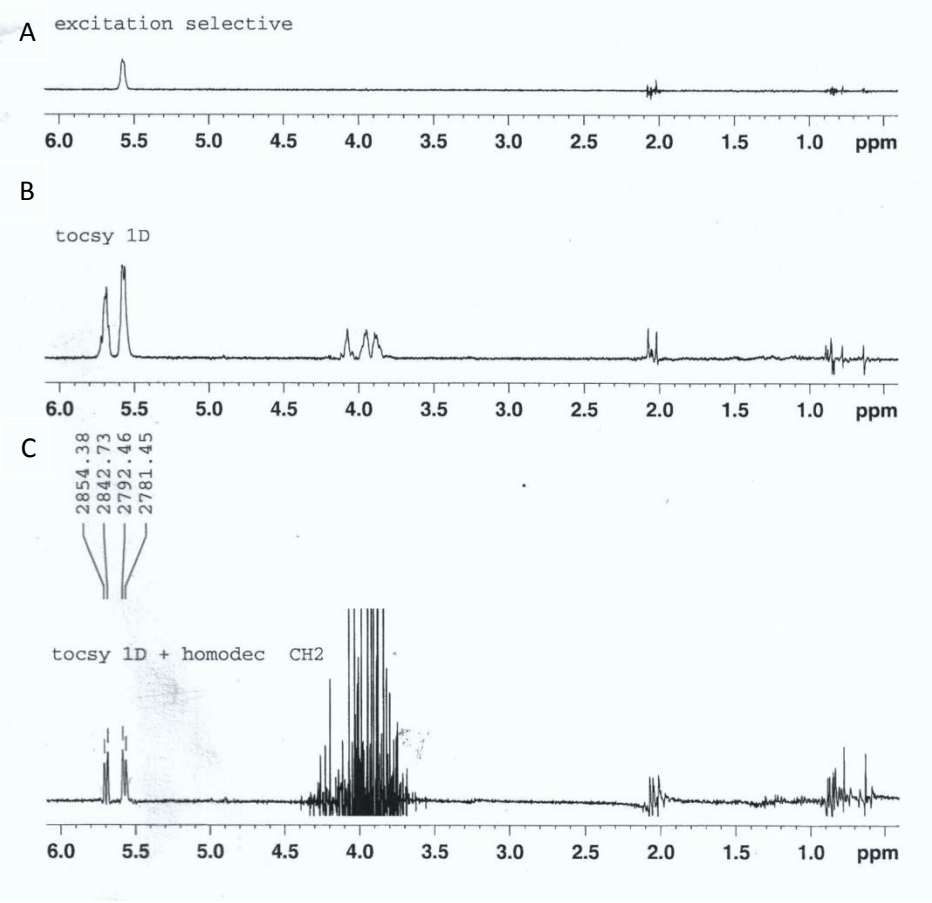

Fig. 4.7: Identification of Z configuration by NMR spectroscopy: A) selective excitation of peak at 5.54 ppm; B) tocsy 1D spectrum to find the nearby =***C***H; C) homodecoupling of CH_2 to identify the coupling constant

Then the hydrogenation of double bond was treated with hydrogen in the presence of Pd/C led to the C-4 spacer system, as shown in Scheme 4.3. In this condition, the double bond of

Cette thèse est accessible à l'adresse : http://theses.insa-lyon.fr/publication/2013ISAL0001/these.pdf
© [R. Xu], [2013], INSA de Lyon, tous droits réservés

the cholesterol would be also affected, thus a careful following of the reaction by TLC was applied. The product was purified on the silica gel with the eluent of toluene/acetone (7/3) with a yield of 82%.

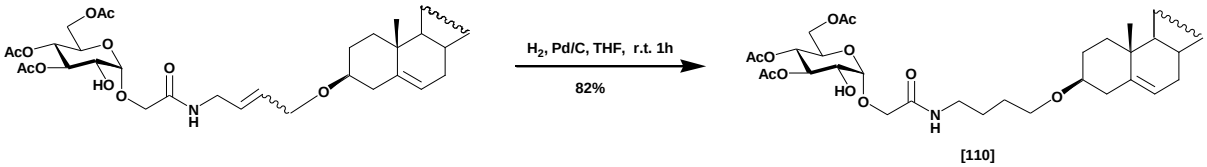

Scheme 4.3: Selective hydrogenation on the double bond of spacer

The reduction of the double bond was confirmed in proton spectrum (Fig. 4.8) by the disappearance of the peak at δ 5.68 ppm of protons on the double bond whereas two new peaks appeared at around 3.30-3.52 ppm. The peak at 5.22 ppm belonging to H-6" indicating that the intracyclic double bond still existed in the compound.

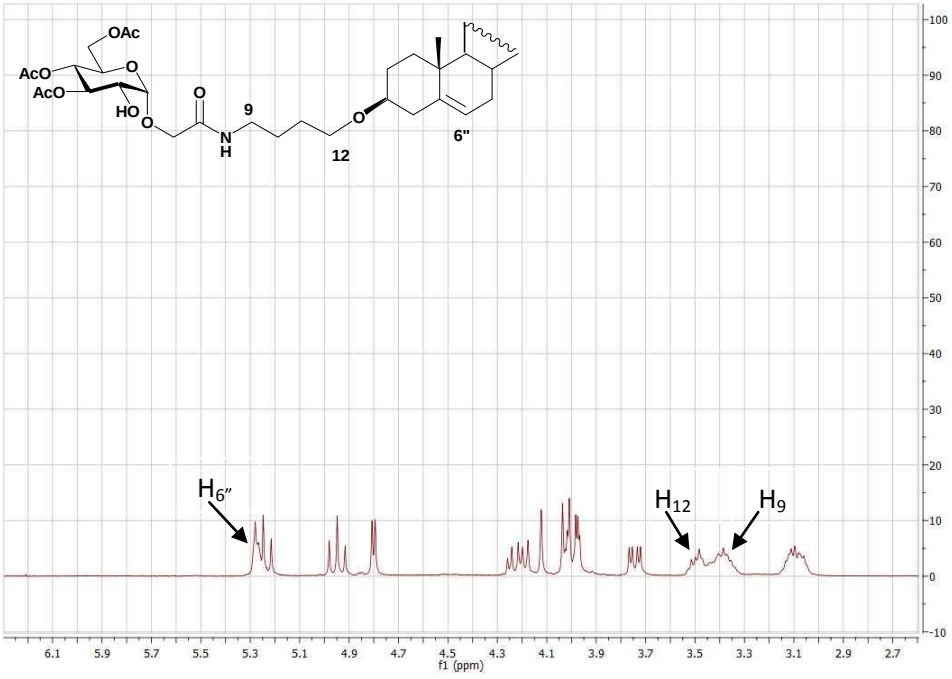

Fig. 4.8: ^{1}HNMR spectrum of compound **110**

Cette thèse est accessible à l'adresse : http://theses.insa-lyon.fr/publication/2013ISAL0001/these.pdf
© [R. Xu], [2013], INSA de Lyon, tous droits réservés

The acetyl groups were then removed by NEt_3 in a mixture of MeOH and H_2O, Scheme 4.4. The reaction was monitored by TLC using the eluent of. Removal of acetyl groups could be seen in the ^1H NMR and ^{13}C NMR. In the proton NMR, the three single peaks around δ 2.03 ppm belonging to CH_3 of acetyl group in the spectrum of starting material disappeared in that of the final compound, while in carbon NMR, the disappearing of three peaks around 174.5 ppm belonging to ***C***=O also indicated the cleavage of ester bond. All other H and C atoms were found in the spectra. The mass measured by mass spectrometry of the resulting compound at 678.2 (M+ H) confirmed the structure of the compound.

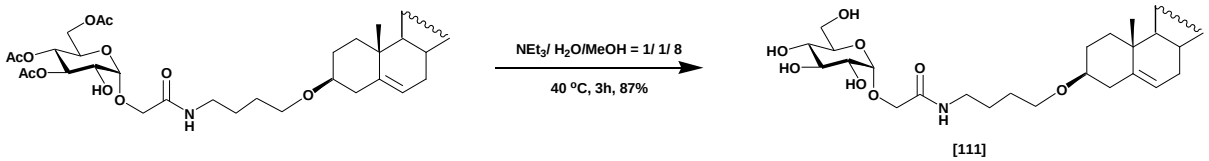

Scheme 4.4: Removing acetyl groups on the sugar head

4.2.2 Synthesis of C6 and longer spacers

When applying the same method using olefin metathesis for synthesizing the longer linkers series, the attempts failed as the reaction outcome was in favor of the homocoupling process and not the desired cross-coupling one. This might be due to the loss of electronic effects on the carbohydrate olefin where the nitrogen of amide group could no longer improve the activity of double bonds since more carbon atoms were set between them. Thus, we developed an alternative synthetic strategy, which relied on the connection of ω-aminoalkylethers of cholesterol with α-CMGL.

This necessitated the prior synthesis of these ω-aminoalkylethers of cholesterol. Firstly we followed a method reported by Cha S.W *et al.*[167] to get the ω-hydroxyalkylethers of cholesterol. The tosylated cholesterol **112** was reacted with a large amount of 1, ω-akyldiol (30 eq.) in anhydrous 1,4-dioxane leading to the cholest-5-en-3β-yl ω-hydroxyalkyl ether **113**. The diols were soluble in dioxane at the reaction temperature, thus the reaction was carried out in the homogeneous atmosphere. After the reaction, since the diols were not well soluble in cool dioxane, the excess diol would precipitate. As a result, a large amount of excess diols would be separated from the product by filtration. The desired compound was then purified

Cette thèse est accessible à l'adresse : http://theses.insa-lyon.fr/publication/2013ISAL0001/these.pdf
© [R. Xu], [2013], INSA de Lyon, tous droits réservés

by column chromatography with the eluent of DCM/ acetone (9.8/ 0.2). The procedure is shown in Scheme 4.5.

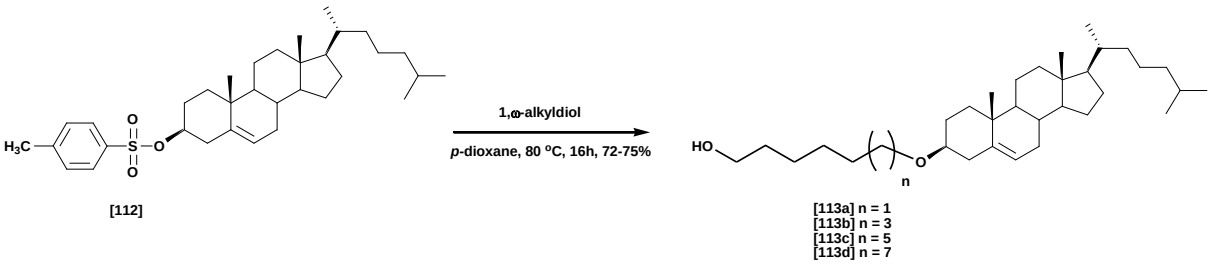

Scheme 4.5: Synthetic procedure giving cholest-5-en-3β-yl ω-hydroxyalkyl ethers **113**

The structure of these compounds were confirmed by NMR spectroscopy and by comparing the data with the ones reported in literature.[167] The product had only the β configuration at the C-3 of cholesterol, owing to the mechanism of the reaction. As indicating in Fig. 4.9, the bond between tosyl group and the steroid is easily broken by the presence of a proton, generating the carbocation at the C-3 of cholesterol. Then the nearby double bond is cleaved and an intermediate with the carbocation at the C-6 position is formed. This mechanism is called "mesomerical stabilization" in steroid chemistry.[168] Since the reaction is thermodynamically controlled, the nucleophiles will attack at the C-3; and for stereoelectronic reasons, the bond will be exclusively formed from the upper side (β) of the steroid molecule.

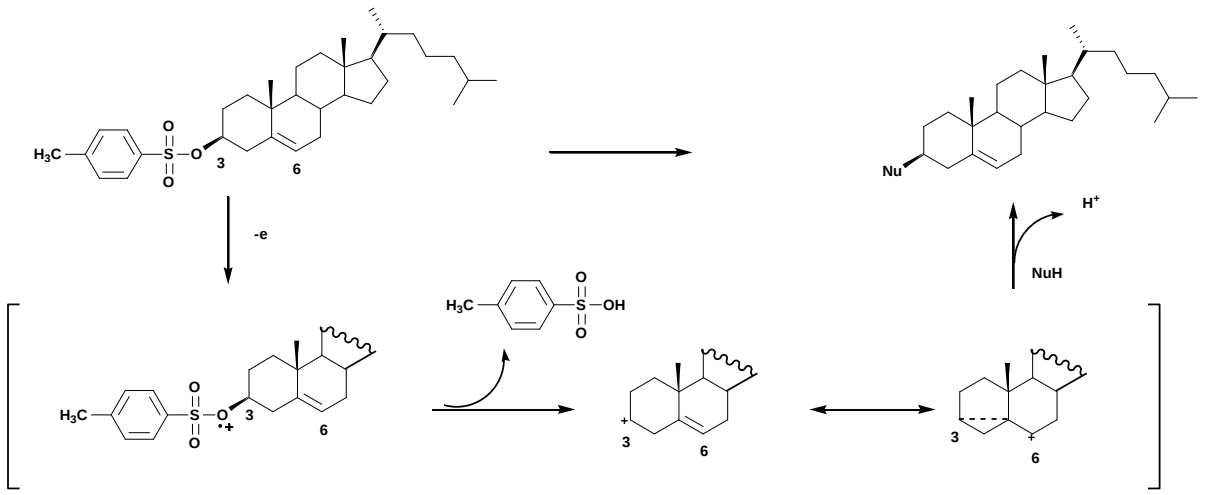

Fig. 4.9: Mechanism explaining the retention of coupling[168]

Cette thèse est accessible à l'adresse : http://theses.insa-lyon.fr/publication/2013ISAL0001/these.pdf
© [R. Xu], [2013], INSA de Lyon, tous droits réservés

The next step is to convert the terminal OH group to an amino group. This was accomplished in three steps. First, the hydroxyl was treated with methanesulfonyl chloride (MsCl) to obtain the mesylate, which is a very good leaving group. The resulting compound was washed with saturated NaCl solution several times until the solution was neutral. Solvents were evaporated off and the residue was used directly with sodium azide (NaN_3) in DMF to get the corresponding azido compound, as shown in Scheme 4.6.

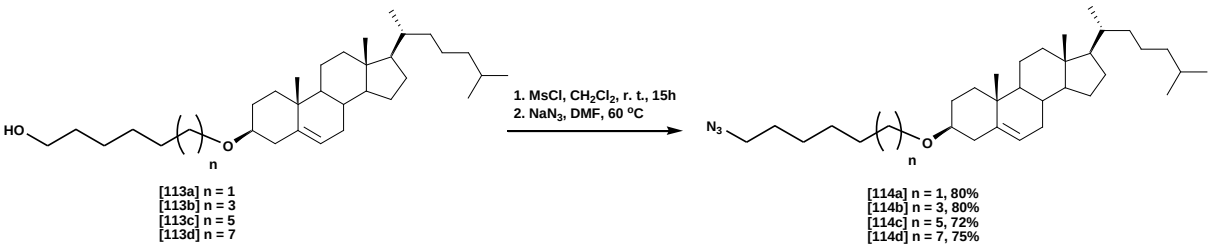

[113a] n = 1
[113b] n = 3
[113c] n = 5
[113d] n = 7

[114a] n = 1, 80%
[114b] n = 3, 80%
[114c] n = 5, 72%
[114d] n = 7, 75%

Scheme 4.6: Synthetic procedure giving cholest-5-en-3β-yl ω-azidoalkyl ethers **114**

The information provided by ^{1}HNMR showed some traces of the newly formed structure as the proton signal of the methylene next to the OH group of the starting material at δ 3.63 ppm disappeared to the benefit of a signal at 3.24 ppm. The existence of the azido group was confirmed by Fourier transform infrared spectroscopy (FTIR), as it has a diagnostic absorption peak at 2095 cm^{-1}. The Fig. 4.10 shows the FTIR spectrum of cholest-5-en-3β-yl 6-azidohexyl ether **114a**. The high resolution mass spectroscopy confirms this where the highest peak at 534.4398 ($M + Na^+$) indicating the cholest-5-en-3β-yl 6-azidohexyl ether.

Cette thèse est accessible à l'adresse : http://theses.insa-lyon.fr/publication/2013ISAL0001/these.pdf
© [R. Xu], [2013], INSA de Lyon, tous droits réservés

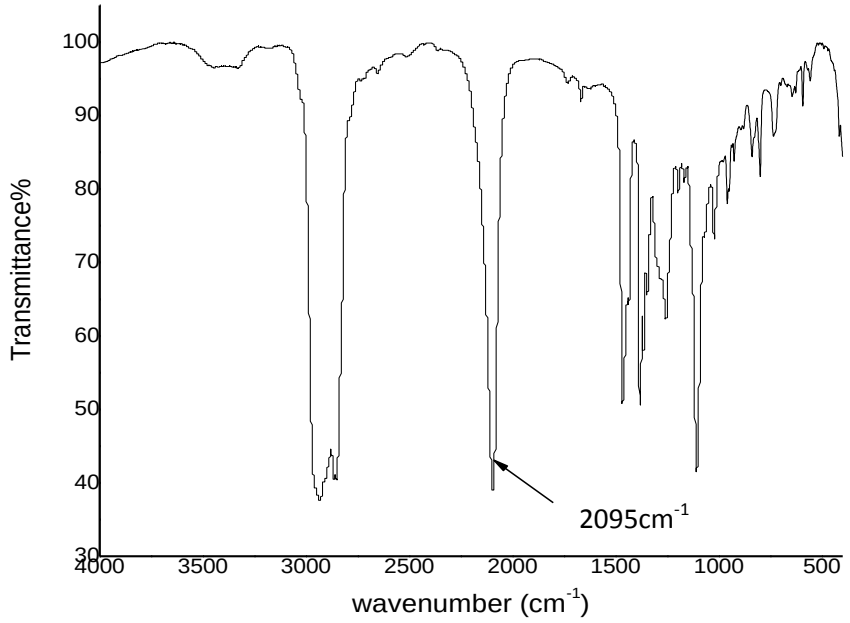

Fig. 4.10: FTIR spectrum of cholest-5-en-3β-yl 6-azidohexyl ether **114a**

With azido compounds in hands, the amino analogues were obtained by treatment with triphenylphosphine (PPh_3) and water in THF, the standard conditions for the Staudinger reaction, shown in Scheme 4.7. From the TLC plate, the R_f of the resulting amino compounds were near 0.3 using the eluent of DCM/ MeOH (9/1 vol.), and the spot shape was not a dot but an ellipse, typical of amino compounds which have strong interaction with the silica gel. Thus a small amount of NEt_3 was added (0.5 % vol.) to improve the alkalinity of the eluent. The residue was then submitted to column chromatography using the same condition to get the pure compound, and the yields of amino compounds were up to 96%.

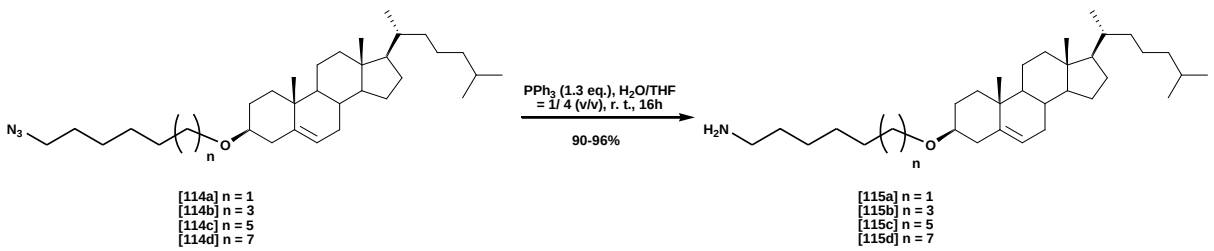

Scheme 4.7: Synthetic procedure giving cholest-5-en-3β-yl ω-aminoalkyl ethers **115**

Cette thèse est accessible à l'adresse : http://theses.insa-lyon.fr/publication/2013ISAL0001/these.pdf
© [R. Xu], [2013], INSA de Lyon, tous droits réservés

In the proton NMR of the amino analogues, the H of the methylene group near the amino appeared around δ 2.71 ppm instead of δ 3.25 ppm in the spectrum of starting azido compounds. Also in carbon NMR, the signal of ***C***H_2NH_2 appeared at δ 39.9 ppm when compared to 51.6 ppm of ***C***H_2N_3. Fig. 4.11 shows proton and carbon NMR spectra of cholest-5-en-3β-yl 6-aminohexyl ether **115a**. The mass data of 486.3 ($M+H^+$) for cholest-5-en-3β-yl 6-aminohexyl ether also confirms the formation of amino group, which fits with the data described in the literature.[169]

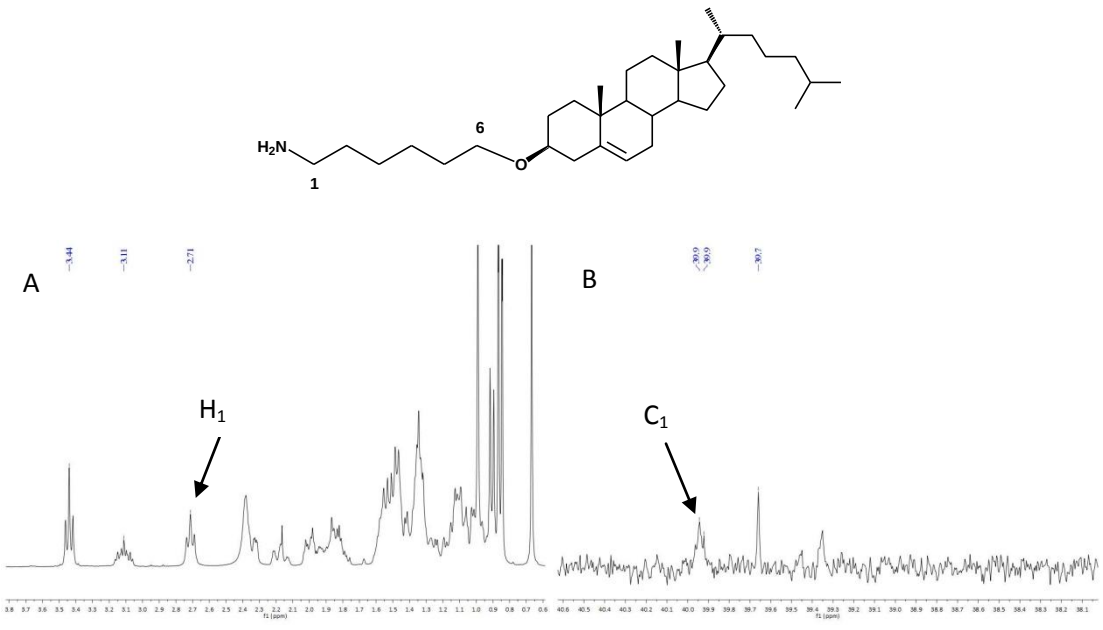

Fig. 4.11: NMR spectra of cholest-5-en-3β-yl 6-aminohexyl ether **115a**. A) ^{1}HNMR; B) ^{13}CNMR

Carboxymethyl tri-*O*-acteyl-α-D-glucopyranoside 2-*O*-lactone (CMGL), prepared by the procedure described in the literature,[137, 138] was added to a solution of cholesteryl ω-aminoalkyl ethers in anhydrous DCM. The mixture was stirred under Ar at room temperature overnight. After the reaction, the solution was concentrated under vacuum and purified by the column chromatography using the eluent of DCM/ acetone (9/1).

Cette thèse est accessible à l'adresse : http://theses.insa-lyon.fr/publication/2013ISAL0001/these.pdf
© [R. Xu], [2013], INSA de Lyon, tous droits réservés

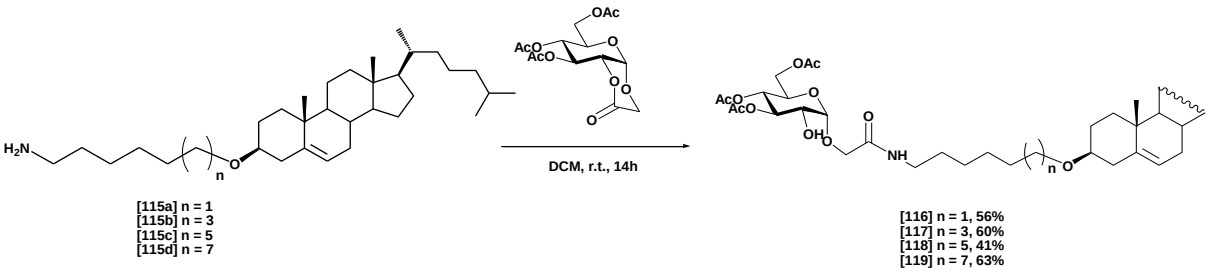

Scheme 4.8: Ring opening reaction of CMGL by cholesteryl ω-aminoalkyl ethers

The proof of opening of the lactone ring could be seen in NMR spectroscopy. Fig. 4.12 shows the examples of the C6 linker series. In the ^{1}H NMR, the signal of H-2 appeared at δ 3.81 ppm instead of 4.40 ppm for the starting lactone whereas the C-2 at δ 70.4 ppm instead of 76.3 ppm in lactone in the ^{13}C NMR. A signal of N***H***C=O is also seen in δ 7.44 ppm indicating that the cholestryl ω-aminoakyl ether was attached to the carboxyl group of lactone. Other peaks were just similar to the spectrum of C4 linker compound. The high resolution mass of 832.5540, 860.5852, 888.6162, and 916.6475 (M + H^{+}) for spacers of C6, 8, 10, 12, respectively, indicated the products to be the desired ones.

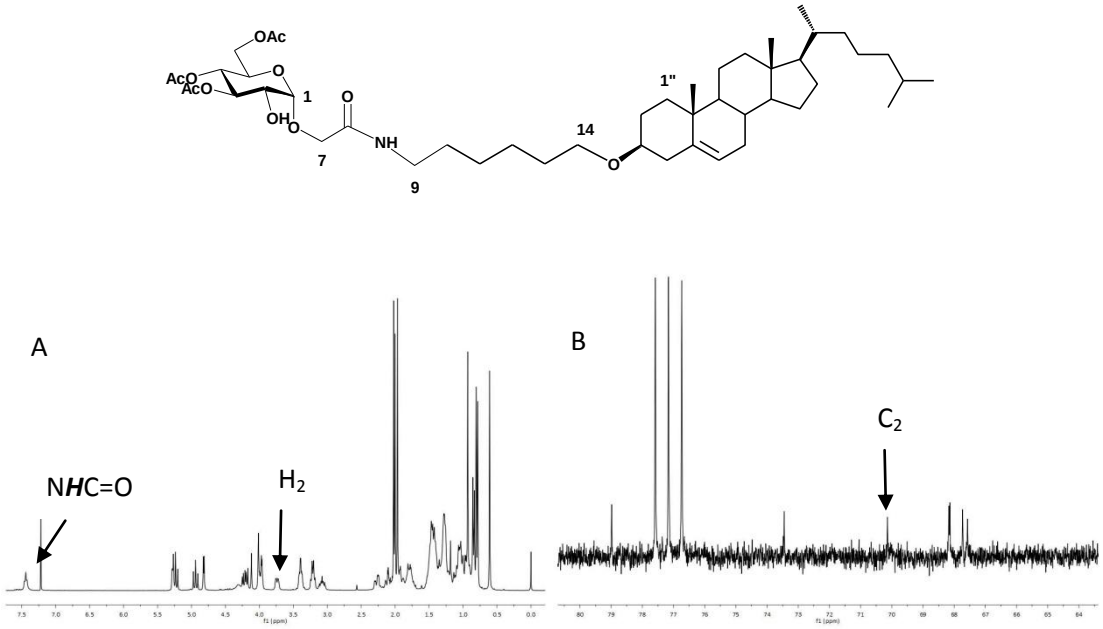

Fig. 4.12: NMR spectra of compound **116**. A) ^{1}HNMR; B) ^{13}CNMR

Cette thèse est accessible à l'adresse : http://theses.insa-lyon.fr/publication/2013ISAL0001/these.pdf
© [R. Xu], [2013], INSA de Lyon, tous droits réservés

The procedure of using the amino products without purification to open the lactone ring was also tried. In this procedure, the cholest-5-en-3β-yl 8-azidooctyl ether was employed. After reduction of the azido to an amino group, the solvent was evaporated under vacuum and the residue was dried over the pump. Then it was dissolved in DCM and reacted with the lactone (1.3 eq.) to get the final product in nearly 50% yield from the starting azido compound, similarly to the previous examples.

The same reaction conditions as the one used for the C4 linker compound was employed for the deacetylation of these longer linkers, as shown in scheme 4.9. The disappearance of 3 singlet peaks of C***H***$_3$ around 1.99 ppm in ^{1}H NMR and 3 peaks of ***C***=O of acetyl group around 170 ppm in the ^{13}C NMR indicates the deprotection of hydroxyl groups on the sugar head, whereas all other C and H atoms were identified in the spectra.

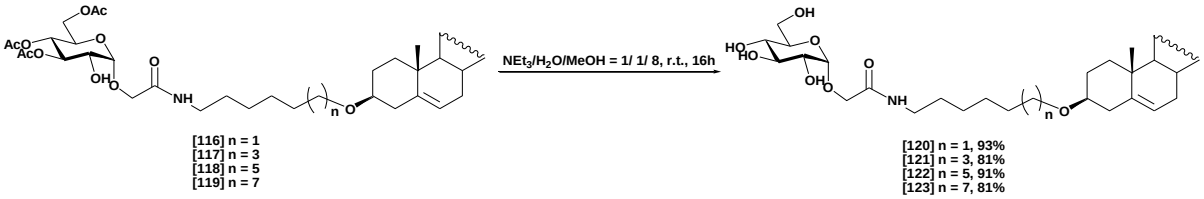

Scheme 4.9: Deacetylation of compounds with C6, C8, C10, and C12 spacers

4.3 Synthesis of disubstituted glycosteroids by O-2 carbamatation

The tri-*O*-acetyl protected glycosteroids, having their OH-2 as the only free OH, were submitted to reaction with alkyl isocyanates of different chain lengths. The final glucosteroidic bolaphiles were then obtained by deacetylation with NEt_3 in the condition previously described. Scheme 4.10 shows the procedure of this step. Table 4.1 lists the yields of final compounds with different n and m values. Compounds will be referred to as LnSm in the following sections.

Cette thèse est accessible à l'adresse : http://theses.insa-lyon.fr/publication/2013ISAL0001/these.pdf
© [R. Xu], [2013], INSA de Lyon, tous droits réservés

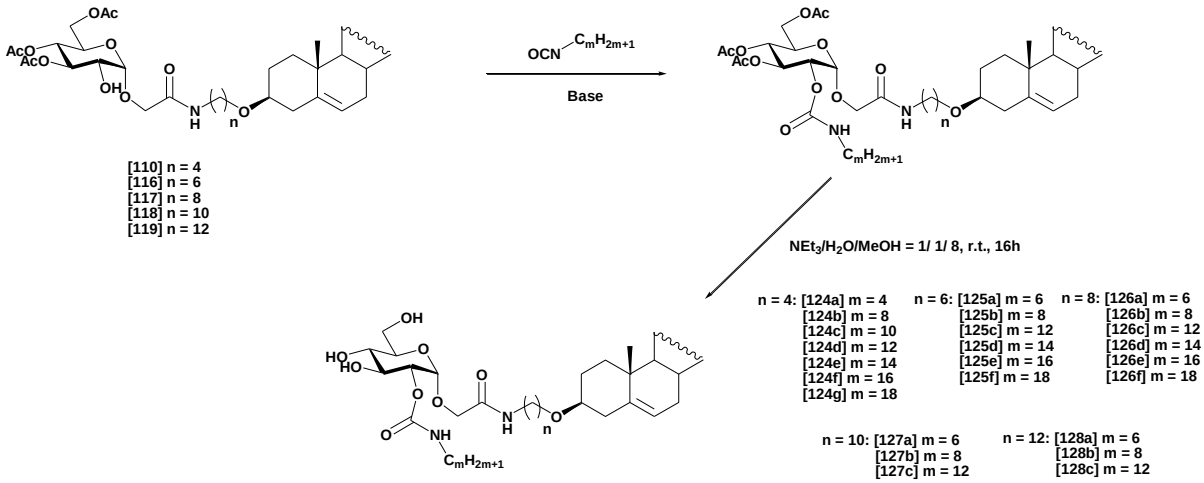

Scheme 4.10: Synthetic procedure of glucosteroidic bolaphiles

(n = 4, 6, 8, 10, 12 and m = 4, 6, 8, 10, 12, 14, 16, 18)

Linker (n) / Side (m)	6	8	10	12
6	50%	61%	75%	69%
8	61%	61%	66%	70%
12	87%	67%	80%	67%
14	52%	52%		
16	53%	41%		
18	50%	52%		

Table 4.1: The yields of glucosteroidic bolaphiles with different spacers and side chains after two steps

In order to attach the alkyl isocyanates, two methods were employed. One was at room temperature in the presence of NEt_3 as the catalyst and the other one was at 45 ^oC with 1,8-diazabicycloundec-7-ene (DBU). By applying these two methods on a same compound, it was found that the yields from these two methods were competitive. Table 4.2 shows the yields of some examples obtained by both methods.

Cette thèse est accessible à l'adresse : http://theses.insa-lyon.fr/publication/2013ISAL0001/these.pdf
© [R. Xu], [2013], INSA de Lyon, tous droits réservés

	NEt_3	DBU
L (linker)6 S (side chain) 8	70%	61%
L12S8	64%	70%

Table 4.2: Yields of L6S8 and L12S8 obtained by two methods

However, the first method using NEt_3 used 10 equivalents of isocyanate against 1.5 eq. in the one using DBU, and the urea formed by excess isocyanates is problematic for the purification of final products. This urea was formed by undesired hydrolysis of isocyanates which was difficult to prevent even though being careful to exclude water from the solvents and reagents. It was found that the urea was not well soluble in the organic solvents, such as DCM, EtOAc, toluene or pentane, or their binary mixtures. This allowed the removal of a large amount of urea by filtration. However, after the purification on silica gel column, some urea was still present as an impurity, detected by mass spectroscopy.

It has also been tried to get rid of urea by combining the attaching of alkyl isocyanates and deactetylation steps together, where large proportion of urea was filtered after the first step. After the deacetylation, as the polarity of eluent using for purifying the final products was much higher than that used in the first step, it was thought that the urea might come before the product so that the separation could be done. But it did not allow to excluding all the urea impurity easily. Thus several successive chromatography columns were necessary to finally get the pure desired disubstituted compounds which were free of urea as demonstrated by absence of the typical urea peak in mass spectroscopy.

When we switched to the method using the DBU as the base for synthesizing the linker 6 and 8 series with longer side chains, from 14 to 18 carbon atoms, it was found that though the urea was still a problem in this method, less time was needed to get the pure final compounds.

When the final molecule was not well soluble in $CDCl_3$, a mixture of $CDCl_3$ and MeOD was used for the NMR characterization. Here shows the example of compound **125e** (L6S16). In the proton spectrum, Fig. 4.13, the signal of H-2 appears at δ 4.43 ppm instead of 3.81 ppm in the starting **116**, indicating that a substitution did occur in the position 2. And the new peak of 156.3 ppm in the ^{13}CNMR belongs to the ***C***=O in the carbamate group. By analyzing HMBC spectrum, Fig. 4.14, this peak is found to be related to the H-2, confirming that the attachment of hexadecyl isocyanate happened uniquely on the position 2. The peaks of 973.8 ($M+H^+$) and 995.8 ($M+Na^+$) in mass spectrum fit with the desired molecular weight of product.

Cette thèse est accessible à l'adresse : http://theses.insa-lyon.fr/publication/2013ISAL0001/these.pdf
© [R. Xu], [2013], INSA de Lyon, tous droits réservés

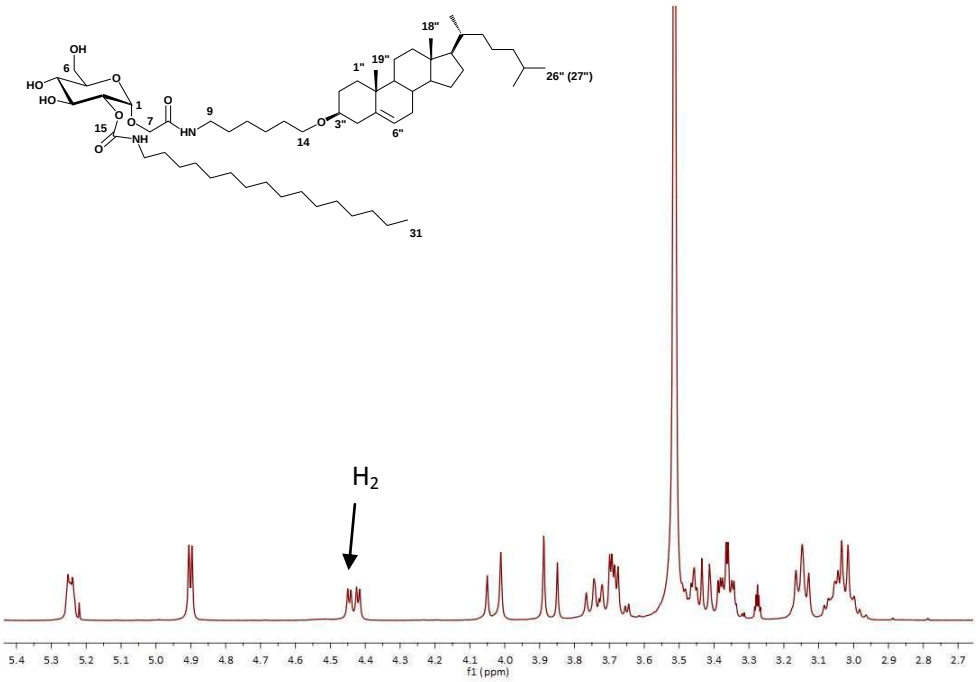

Fig. 4.13: ^{1}HNMR spectrum of compound **125e** (L6S16)

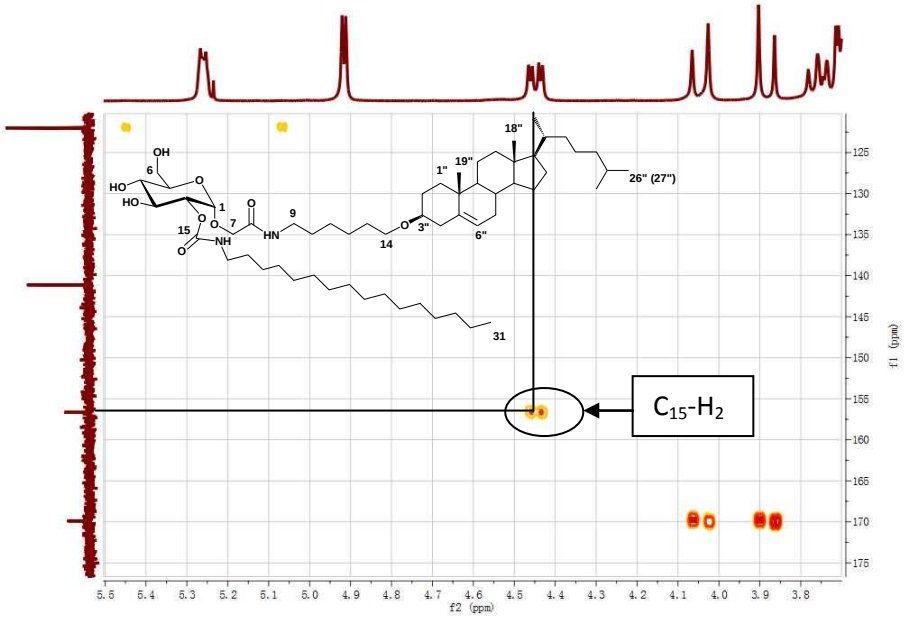

Fig. 4.14: ^{1}H-^{13}C HMBC spectrum of compound **125e** (L6S16)

Cette thèse est accessible à l'adresse : http://theses.insa-lyon.fr/publication/2013ISAL0001/these.pdf
© [R. Xu], [2013], INSA de Lyon, tous droits réservés

4.4 Thermotropic liquid crystalline behavior study of the glucosteroid

4.4.1 Phases identification and transition behaviors

The thermotropic liquid crystalline behaviors of these compounds were studied by polarized light microscopy and DSC.

As observed under polarized optical microscope, upon heating the glucosteroid amphiphiles (without side chains) Sm A* mesophases were observed, which were identified by the streak textures and homeotropic regions, image A in Fig. 4.15. Once the compounds were heated to the isotropic liquid and cooled slowly, the Sm A* phase was primarily observed in a homeotropic orientation where the sugar moiety is orienting with the surface due to hydrogen bonding, see image B in Fig. 4.15.

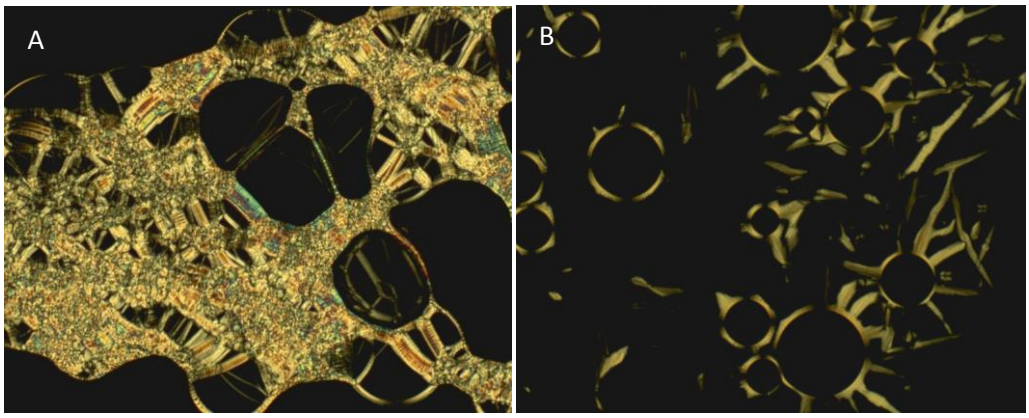

Fig. 4.15: Defect textures (×100 magnification) of Sm A* phases showing by A) **111** at 200 ^{o}C and B) **124b** at 170 ^{o}C

In the bolaphiles series, a same type of thermotropic behaviors was observed by the compounds with short side chains, 6, 8, 12 carbon atoms, while for compounds bearing longer side chains of 14, 16, 18 carbon atoms in the series of linker 4, 6, 8, a new type of mesophases were observed. These phases are classified as hexagonal columnar phases and appear from the isotropic liquid as large platelets, image A in Fig. 4.16. The platelets have well defined boundaries and do not contain any striations which would indicate rectangular columnar phases. Upon cooling from the columnar to Sm A* phase transition the

Cette thèse est accessible à l'adresse : http://theses.insa-lyon.fr/publication/2013ISAL0001/these.pdf
© [R. Xu], [2013], INSA de Lyon, tous droits réservés

platelet texture collapses rapidly and many parabolic defects appear, image B in Fig. 4.16. The optical texture continues to become more homeotropic once into the Sm A* phase and this is accompanied by a fan texture, image C in Fig. 4.16. Due to the nature of the phase transition it is not possible to observe the typical ellipse and hyperbola defects normally associated with focal conics. Interestingly, the appearance of the columnar phase changes dramatically as the side-chain length is increased and the platelet domains become less well defined.

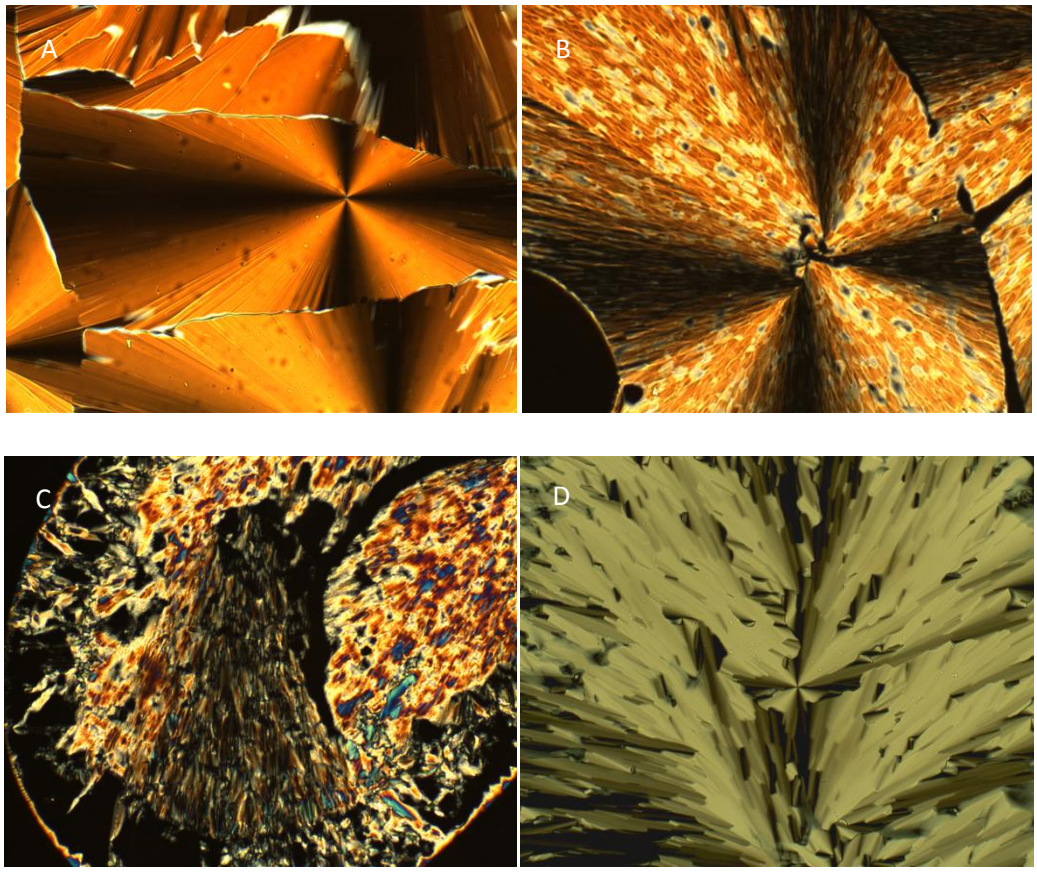

Fig 4.16: Defect textures (×100 magnification) of **124e** A) Col_h phase at 158 ^oC; B) phase transition Col_h to Sm A*; C) Sm A* phase at 140 ^oC. D) Col_h phases of **124f** at 164 ^oC

The (DSC) measurements were then carried out to study these molecules. The resulting DSC curves of these compounds are listed in Appendix. The transition temperatures and the transition enthalphies of the compounds are summarized in the following tables and curves. The corresponding curves based on these data are drawn after each table.

Cette thèse est accessible à l'adresse : http://theses.insa-lyon.fr/publication/2013ISAL0001/these.pdf
© [R. Xu], [2013], INSA de Lyon, tous droits réservés

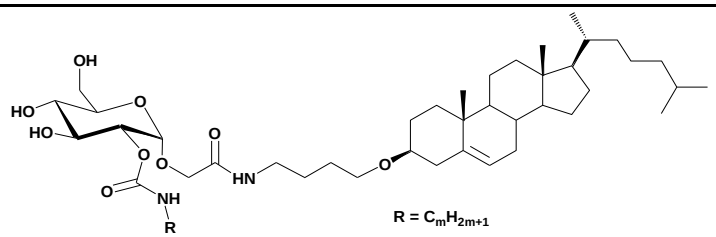

Cpd	m	K		Sm A*		Col_h		Iso. Liq.
111	–	•	50 [188.34]	•	290 [9.57]	–	–	•
124a	4	•	96 [10.21]	•	251 [0.29]	–	–	•
124b	8	•	94 [21.51]	•	178 [1.19]	–	–	•
124c	10	•	115 [9.50]	•	164 [0.75]	–	–	•
124d	12	•	110 [26.59]	•	159 [0.70]	–	–	•
124e	14	•	128 [29.89]	•	142 [0.56]	•	165 [0.72]	•
124f	16	•	124 [14.13]	•	150 [1.51]	•	176 [1.15]	•
124g	18	•	103, 126 [9.39, 9.82]	•	146 [2.47]	•	183 [1.25]	•

Table 4.3: Phase transitions temperature (°C) and enthalpies (J g^{-1}) of transition shown in square bracket for L4 linker series

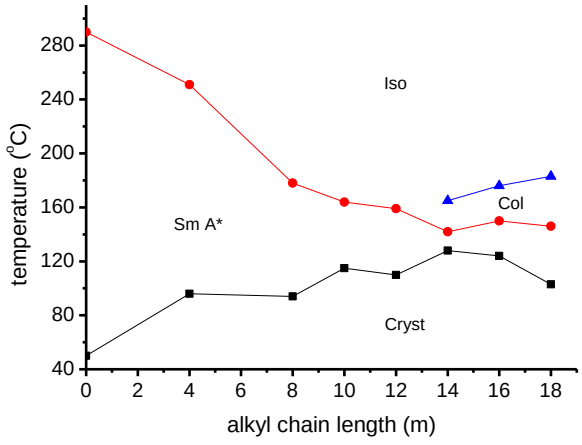

Fig. 4.17: Thermotropic behaviors for L4 series as function of side chain lengths

Cette thèse est accessible à l'adresse : http://theses.insa-lyon.fr/publication/2013ISAL0001/these.pdf
© [R. Xu], [2013], INSA de Lyon, tous droits réservés

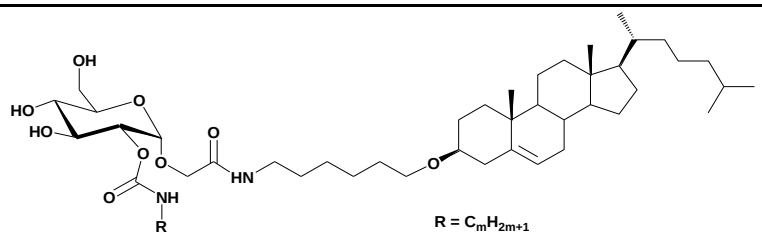

Cpd	m	K		Sm A*		Col_h		Iso. Liq.
120	-	•	50 [20.45]	•	269 [5.54]			•
125a	6	•	123 [31.91]	•	193 [2.66]			•
125b	8	•	109 [17.61]	•	178 [2.03]			•
125c	12	•	127 [26.30]	•	145 [0.40]			•
125d	14	•	132 [24.43]	•	126 [0.44]	•	155 [0.53]	•
125e	16	•	138 [29.94]	•	129 [0.31]	•	170 [1.07]	•
125f	18	•	138 [22.23]	•	138 [3.48]	•	180 [1.08]	•

Table 4.4: Phase transitions temperature (°C) and enthalpies (J g^{-1}) of transition shown in square bracket for L6 linker series

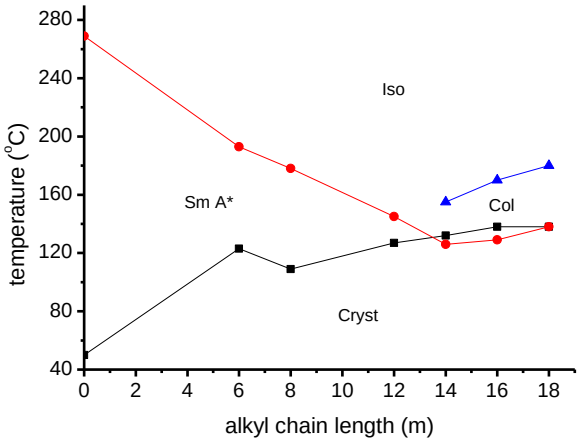

Fig. 4.18: Thermotropic behaviors for L6 series as function of side chain lengths

Cette thèse est accessible à l'adresse : http://theses.insa-lyon.fr/publication/2013ISAL0001/these.pdf
© [R. Xu], [2013], INSA de Lyon, tous droits réservés

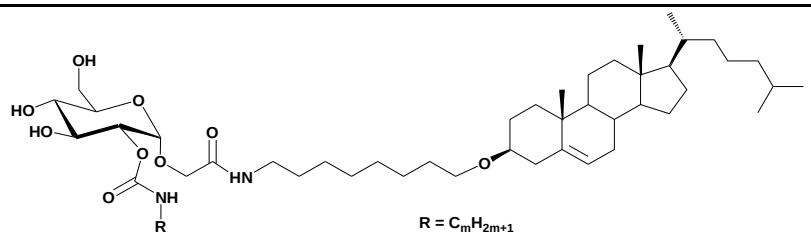

Cpd	m	K		Sm A*		Col_h		Iso. Liq.
121	–	•	60 [48.84]	•	244 [3.43]	–	–	•
126a	6	•	154 [37.22]	•	192 [3.81]			•
126b	8	•	126 [33.02]	•	188 [3.28]			•
126c	12	•	131 [16.92]	•	156 [0.86]			•
126d	14	•	123 [23.05]	–	–	•	144 [0.47]	•
126e	16	•	125 [18.41]	–	–	•	150 [0.89]	•
126f	18	•	131 [23.15]	–	–	•	170 [1.22]	•

Table 4.5: Phase transitions temperature (°C) and enthalpies (J g^{-1}) of transition shown in square bracket for L8 linker series

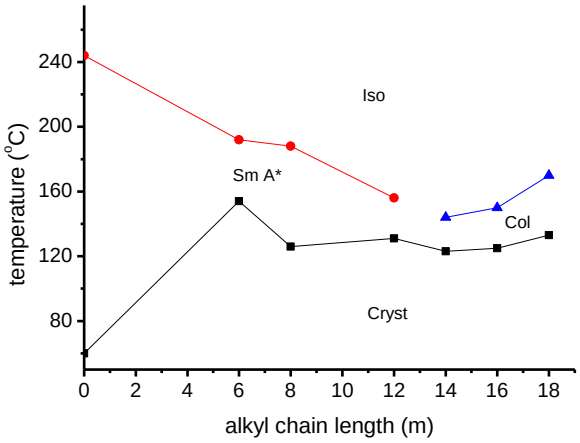

Fig. 4.19: Thermotropic behaviors for L8 series as function of side chain lengths

Cette thèse est accessible à l'adresse : http://theses.insa-lyon.fr/publication/2013ISAL0001/these.pdf
© [R. Xu], [2013], INSA de Lyon, tous droits réservés

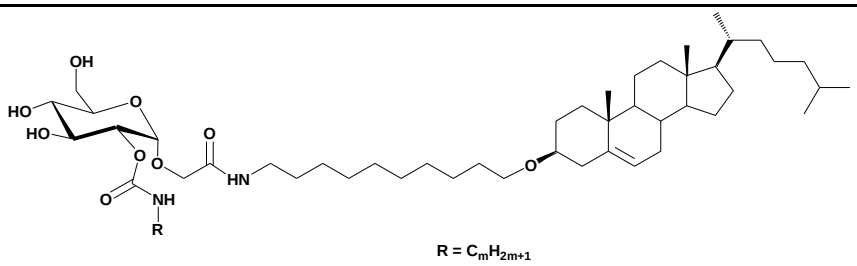

Cpd	m	K		Sm A*		Iso. Liq.
122	–	•	75 [52.49]	•	246 [5.90]	•
127a	6	•	137 [34.39]	•	194 [5.11]	•
127b	8	•	152 [36.40]	•	181 [4.71]	•
127c	12	•	117 [21.53]	•	160 [2.36]	•

Table 4.6: Phase transitions temperature (°C) and enthalpies (J g^{-1}) of transition shown in square bracket for L10 linker series

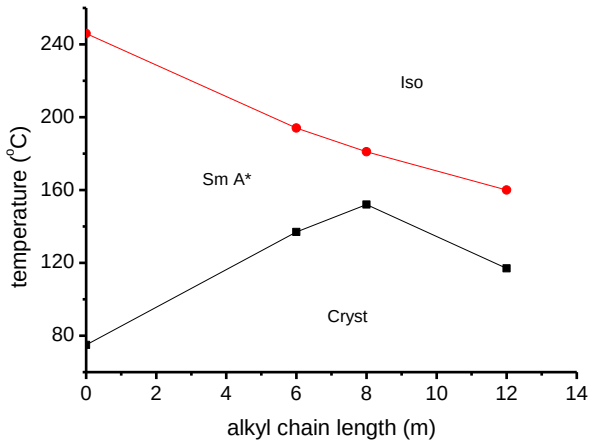

Fig. 4.20: Thermotropic behaviors for L10 series as function of side chain lengths

Cette thèse est accessible à l'adresse : http://theses.insa-lyon.fr/publication/2013ISAL0001/these.pdf
© [R. Xu], [2013], INSA de Lyon, tous droits réservés

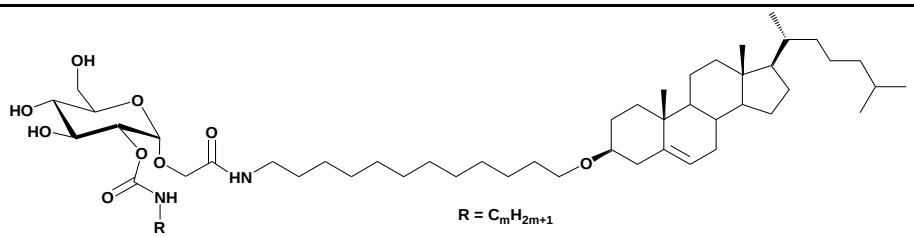

Cpd	m	K		Sm A*		Iso. Liq.
123	–	•	100 [13.50]	•	239 [6.33]	•
128a	6	•	136 [35.49]	•	192 [6.45]	•
128b	8	•	118 [23.29]	•	177 [5.82]	•
128c	12	•	118 [30.96]	•	159 [4.23]	•

Table 4.7: Phase transitions temperature (°C) and enthalpies (J g^{-1}) of transition shown in square bracket for L12 linker series

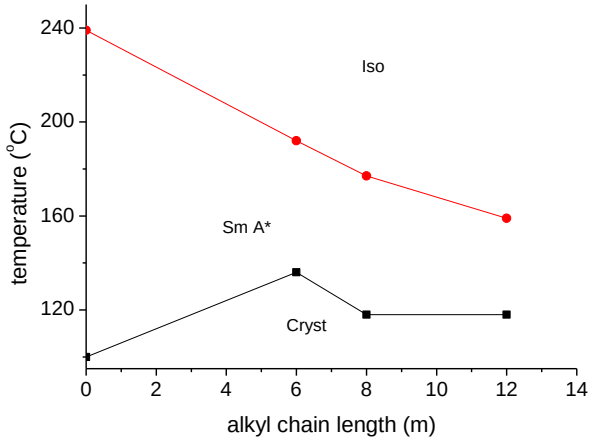

Fig. 4.21: Thermotropic behaviors for L12 series as function of side chain lengths

As observed from these tables and curves, a decrease of transition temperatures from Sm A* to isotropic liquid was observed when a side chain is present, and consistent decrease of this transition temperature upon increasing side chain length. At the same time, the margins between the melting points and the clearing points are narrowing, as shown in Fig. 4.17 to Fig. 4.21. Since the O-2 was not substituted, the relative sizes of hydrophilic to hydrophobic

Cette thèse est accessible à l'adresse : http://theses.insa-lyon.fr/publication/2013ISAL0001/these.pdf
© [R. Xu], [2013], INSA de Lyon, tous droits réservés

were much bigger than those of the substituted ones. It could also be considered as the molecules without side chain are more rod-like than those of substituted ones where the addition of side chains hindered the tendency of molecules to close packing. Thus, the transition temperatures of Sm A* to isotropic liquid of the amphiphiles are the highest. For the bolaphiles, as the side chain extends, the increasing carbon atoms make the molecules more difficult to pack together, leading to the decrease of stability of Sm A*. As a result, the transition temperatures decreased. During cooling processes, the compounds bearing the side chains of 4, 6, 8 carbon atoms were found to transform from a liquid crystalline state to a glassy state, which was a typical sugar behavior. The glassy state disappeared as the side chain extended to 12 carbon atoms, where Sm A* would transform to a crystal state. At this stage, the hydrophobic part of the system became to be dominated in the crystallization process. A hexagonal columnar phase appeared during the heating process for the homologues bearing side chain of 14, 16, and 18 carbon atoms, as a result of increasing space of two lipid parts in the system. At this point, the topological shapes of the molecules are more wedge-like, leading to the curvature to stabilize the columnar phases. And an increase manner of clearing points was observed as the chain extended. Compared the thermotropic behaviors of these compounds showing the columnar phases in terms of linkers, the Sm A* phase was clearly observed during the heating process for L4 series and this phases were just observed during the cooling process for L6 series, while no Sm A* phases were observed for L8 series.

The melting point enthalpies, which are large compared with the clearing point enthalpies, indicate that these values correspond to the breaking of a three dimensional crystal lattice primarily held together by intermolecular H-bondings between the carbohydrate moieties. The small clearing point enthalpies indicate that the Sm A* phase is less order than the crystal, and the forces to stabilize Sm A*, which are the van der Waals forces, are relative small in comparison with intermolecular hydrogen bonding. The values of the transition enthalpies are agreed with the conventional Sm A* to isotropic liquid transitions, although the variations are quite large (0.37~7.031 J mol^{-1}). The high enthalpies may be due to the residual H-bondings in the system.

Cette thèse est accessible à l'adresse : http://theses.insa-lyon.fr/publication/2013ISAL0001/these.pdf
© [R. Xu], [2013], INSA de Lyon, tous droits réservés

S (m) \ L (n)	4	6	8	10	12
0	14.116	7.847	4.673	7.742	8.011
6	0.37 (S4)	3.193	4.424	5.746	7.031
8	1.428	2.357	3.688	5.134	6.156
12	0.787	0.436	0.91	2.424	4.224
14	0.61	0.465			
16	1.597	0.318			
18	2.537	3.475			

Table 4.8: Transition enthalpies (J mol^{-1}) of Sm A* to liquid or columnar phases of all the series

The transition enthalpies of columnar to isotropic liquid are small as shown in Table 4.9. They are weak which indicates that the hexagonal columnar phase is disordered. If the phase was more ordered (crystal like), a much higher lattice enthalpy would show. The polar interactions of the head groups are contributing to the centre of the column but the phase is being driven by steric factors which occur because the side-chain is filling space making the molecule appear wedge-like. For the L4 and L6 series, the transition enthalpies with side chain of 16 were the highest, while for the L8, an increasing manner of enthalpies as the side chain extends were found. These results may be due to the interactions of additional aliphatic chain and the cholesterol moiety.

S (m) \ L (n)	4	6	8
14	0.785	0.561	0.483
16	1.597	1.099	0.889
18	1.284	1.078	1.185

Table 4.9: Transition enthalpies (J mol^{-1}) of columnar phases to liquid of compounds bearing long side chains

Cette thèse est accessible à l'adresse : http://theses.insa-lyon.fr/publication/2013ISAL0001/these.pdf
© [R. Xu], [2013], INSA de Lyon, tous droits réservés

4.4.2 Effect of the length of linker and side chain on the liquid crystalline behaviors

Comparing the transition temperatures of non substitution homologues, they firstly decrease rapidly as the linker extends from L4 to L8, and then the decrease goes by a slower manner as the chain extends further. This kind of behavior could be seen in the many carbohydrate-based liquid crystals of a long chain substitution like 18 to 26, where the aliphatic moiety dominates the transition behavior as hydrophilic/hydrophobic balance leans towards the hydrophobic part of the system. The increasing amount of carbon atoms also brought into the system more flexibility, which decoupled the effects of the sugar group from the cholesteryl moiety. Thus, the role of bulky cholesterol moiety in this system is more like a long aliphatic chain with a very rigid level, which is the reason of the high transition temperature.

Interestingly, when the side chain was attached, the resulting clearing point was shown to depend more on the length of the side chain rather than the linker. The transition temperature decreases as the side chain extends. With the same side chain, the transition temperatures of different linkers did not change with very rough increase or decrease manner, rather fluctuating within a small range. For the side chain S6 series, this range is even at 2 ^{o}C, however, a dramatic increase of transition enthalpies (>1 J mol^{-1}) as a function of linker lengths could be seen from the DSC experiments, shown in Table 4.8.

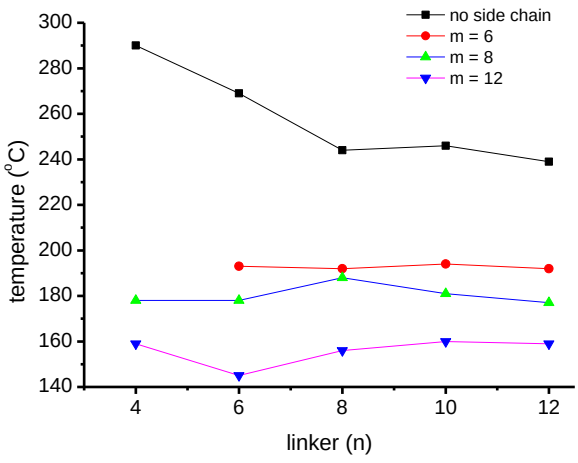

Fig. 4.22: The clearing points of different side chains as function of the length (n) of linkers

Cette thèse est accessible à l'adresse : http://theses.insa-lyon.fr/publication/2013ISAL0001/these.pdf
© [R. Xu], [2013], INSA de Lyon, tous droits réservés

Another interesting manner could be seen as the length of side chain and the linker has an inverse effect on the formation of columnar phase. The trend of transition temperature as the function of linker with different side chain length is shown in Fig. 4.23. In this figure, we can see that the increasing side chain may bring the transition temperature to go up while the extension of linker lowers down the transition temperature.

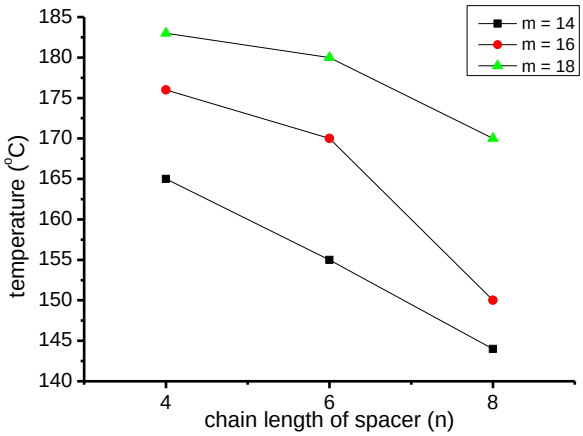

Fig. 4.23: The transition temperatures of columnar phases to isotropic liquid with different side chains as function of the length (n) of linkers

4.4.3. Molecular modeling study

In order to well understand the structure/performance relation in the glucosteroid series, the molecular modeling study could offer some structural information to support the previous observations.

As shown above, for the C4, C6, C8 linker, the side chain with 14 carbons is the limit where the columnar phases are formed. This indicates that at this stage the molecular shape begins to change. The following study was based on the C4 linker. At no or short chain length (C4-C12) only a Sm A* phase is evident which indicates that the molecule is rod-like in shape and the alkyl chain must occupy space alongside the spacer and cholesterol unit, Fig. 4.24. However, once the chain length is increased (C14-C18) the chain is now large enough that at higher temperatures where the chain has more dynamic freedom to move it prefers to orient away from the spacer and cholesterol unit and hence the molecular shape changes from rod-like to wedge-like and a phase transition from Sm A* to hexagonal columnar occurs. The energy minimised molecular model shown in Fig. 4.25 for compound **124e** demonstrates how

Cette thèse est accessible à l'adresse : http://theses.insa-lyon.fr/publication/2013ISAL0001/these.pdf
© [R. Xu], [2013], INSA de Lyon, tous droits réservés

the spacer overlaps with terminal alkyl chain of the cholesteryl unit in a rod-like shape whereas when the chain is allowed greater freedom for motion the molecular shape becomes more wedge-like than rod-like. It is expected that the structure of the hexagonal columnar phase consists of several molecules orienting together to form discs and these discs form the column where the centres of the columns are occupied by the sugar units and the outer parts are filled with the cholesteryl and alkyl moieties. When this shape change occurs there is a stabilisation of the columnar liquid crystal mesophase and instead of a decrease in clearing point an increase with chain length is now observed.

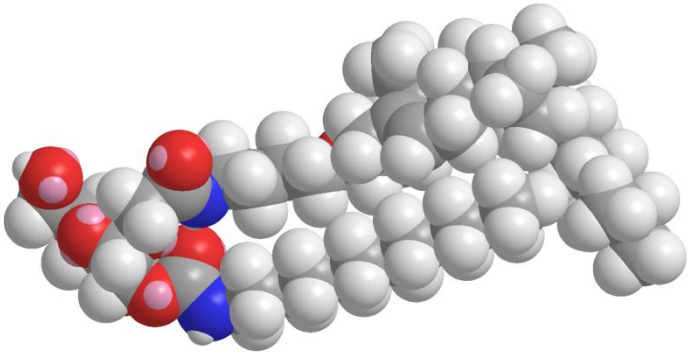

Fig. 4.24: Minimum energy molecular model showing the rod-like appearance for compound **124d**

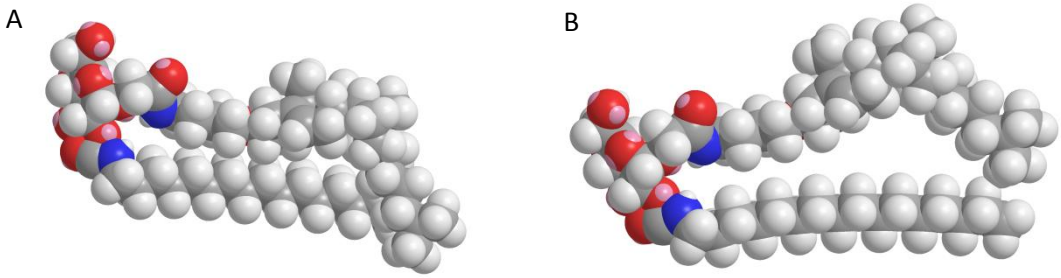

Fig. 4.25: Minimum energy molecular model for compound **124e** showing A) the rod-like appearance; B) the wedge-like appearance at higher temperature

Cette thèse est accessible à l'adresse : http://theses.insa-lyon.fr/publication/2013ISAL0001/these.pdf
© [R. Xu], [2013], INSA de Lyon, tous droits réservés

For C8 linker, as the aliphatic chain bearing the cholesteryl moiety was long enough to minimize the effect of the cholestryl part as the bulky rigid moiety which covered the side chain in shorter linker system, the Sm A* phase was not observed while the columnar phase was the unique liquid crystalline phase shown in this chain length.

4.4. Conclusion

In this chapter, we described the synthesis of a family of glucosteroids with a spacer which is of different length of 4, 6, 8, 10 and 12 carbon atoms between the carbohydrate ring and the cholesterol moiety. Also 2-O derivatives from these compounds of an aliphatic side chain length varying from 4 to 18 carbon atoms were synthesized taking advantage of CMGLs strategy. For the spacer C4, it was adapted by olefin cross-metathesis to couple the allyl glucoside and allyl cholesteryl blocks together. For other lengths of spacers, the aliphatic chains were first etherified with the cholesterol, followed by being converted the terminal group into amino group, which were further used to open the lactone ring. The combination of aliphatic side chains are conducted by the carbamation of alkyl isocyantes with OH-2. The structures of compounds of each step were characterized by NMR spectroscopy, mass spectroscopy and for some special compounds, for example the azido intermediates, the FTIR spectroscopy was used to identify the structure.

Their thermotropic liquid crystalline behaviors were investigated by the means of polarized optical microscopy, and DSC. The results of this studied could be summarized in two aspects, no or the short side chain species and long side chain species.

For the no side chain or short side chain species, where the length of side chain is within 12 carbons, the Sm A* phases were dominated, indicating these compounds owned a rod-like shape. The clearing points of these compounds were decreasing as the chain length extended. In comparison of the compounds with no side chains, the clearing points also showed a decrease tendency as the chain length extended. Both of these observations could be explained by the flexibility brought by the increasing carbon atoms or the randomization during the packing of aliphatic chains.

For long side chain species, where the lengths of side chain are from 14 to 18, the exhibition of Sm A* mesophases was observed in a more limited temperature range as the spacer extended, and finally at C8, no Sm A* mesophases were observed. These observations could be related to a less rod-like structure shown with longer spacer series. Also in these species, a second hexagonal columnar mesophases were shown, indicating the topology structures of these compounds are wedge-like. Structural modeling study showed an

Cette thèse est accessible à l'adresse : http://theses.insa-lyon.fr/publication/2013ISAL0001/these.pdf
© [R. Xu], [2013], INSA de Lyon, tous droits réservés

expanded structure was formed by the lipid and steroid parts. And the transition temperatures of columnar phases to isotropic liquid increased as the side chain length extended.

Cette thèse est accessible à l'adresse : http://theses.insa-lyon.fr/publication/2013ISAL0001/these.pdf
© [R. Xu], [2013], INSA de Lyon, tous droits réservés

Chapter 5

Synthesis of neoglucosyl laurdans and their evaluation in fluorescence microscopy

5.1. Introduction

Fluorescent technology is widely used nowadays as an efficient approach to study the live routine of the organisms.[170-173] This technology has several advantages over the traditional way of studying the cell biology, for example, it could be used to observe the events in the cells *in situ*[174, 175] and follow the molecular dynamics in the functional area, like “lipid raft”, with a minimization of impact of the probe itself on the studied phenomena.[47, 176, 177] Many probes have been developed for this purpose, which could be categorized into some types with respect to their brightness and emission wavelength, as shown in Fig. 5.1. Some microscopic technologies are developed, too, to reveal better image, like fluorescence resonance energy transfer (FRET), fluorescence lifetime microscopy, two-photon excitation fluorescence (TPEF) microscopy.[174, 178] Several requirements are needed for the probe applied, like wavelength, brightness, stability, and pharmacokinetics. [170]

Cette thèse est accessible à l'adresse : http://theses.insa-lyon.fr/publication/2013ISAL0001/these.pdf
© [R. Xu], [2013], INSA de Lyon, tous droits réservés

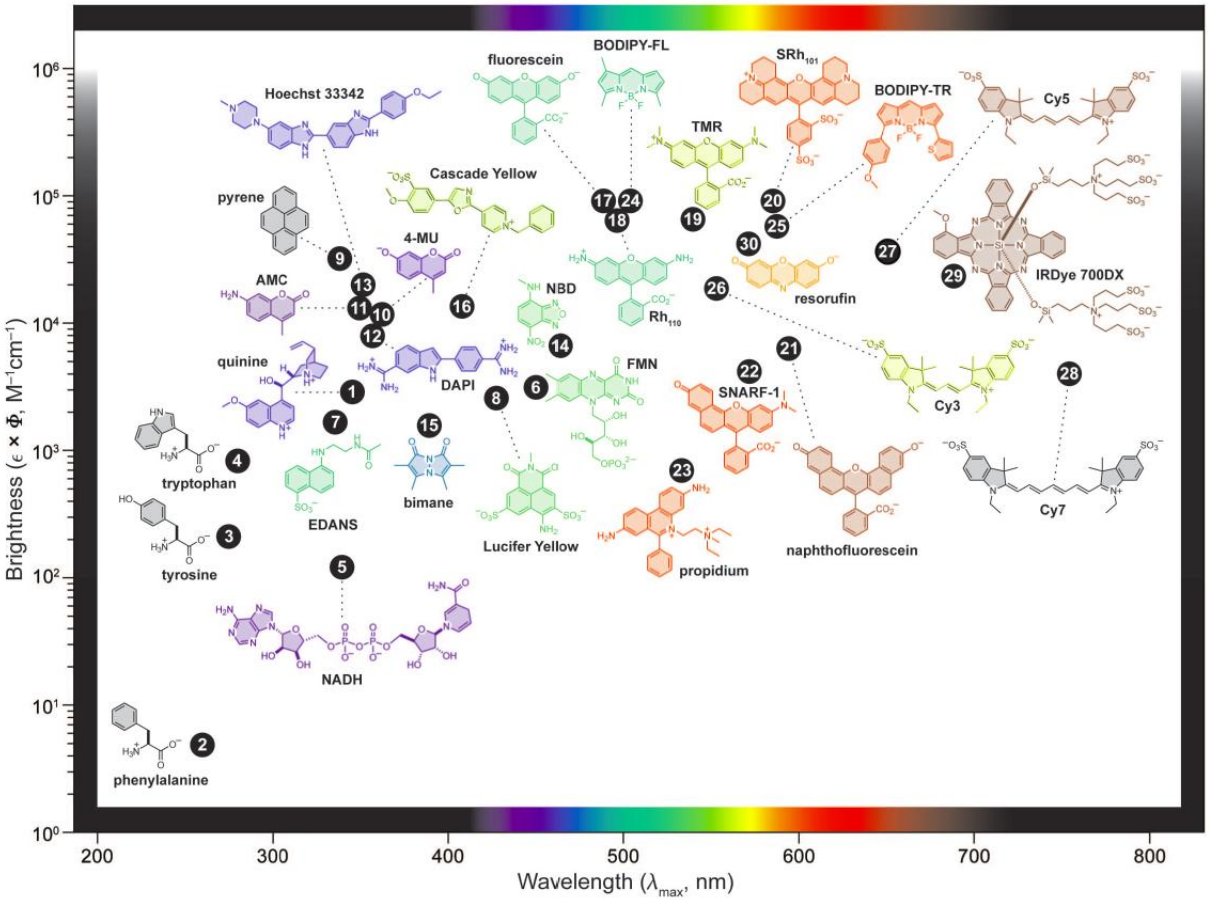

Fig. 5.1: Standard fluorescent probes ranked according to brightness and maximum emission wavelength (color of the compounds)[179]

Since some probes are hydrophobic, the introduction of hydrophilic moiety to make it soluble in water is necessary. Among the choices, the carbohydrate moiety is very ideal, since it enhances the solubility of the final compound.

Our initial idea of developing the new probe is to investigate the microdomain in the membranes, referring to “lipid raft”. The structure of this new probe was adapted of the previous glucosteroid studied in this thesis. Since a cholesterol moiety was in the structure, we expected it would have some interactions towards this microdomain rich in the cholesterols. The fluorescent probe we chose was the fluorescein isothiocyanate (FITC),

Cette thèse est accessible à l'adresse : http://theses.insa-lyon.fr/publication/2013ISAL0001/these.pdf
© [R. Xu], [2013], INSA de Lyon, tous droits réservés

taking advantage of its high quantum yield and good water solubility. The structure of target molecule is shown in Fig. 5.2.

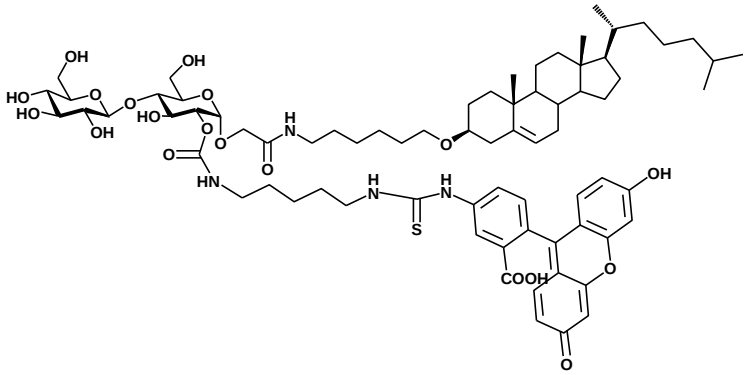

Fig. 5.2: Chemical structure of designed compound

The synthesis involved the ring opening of α-cellobioside lactone and the linker to attach the fluorescein. The final compound was achieved. However, the condition for coupling the probe and the sensitivity of final compound to the environment made it not ideal. As a consequence, we switched to a more stable fluorescent moiety. This was achieved within a new collaboration with the teams ODMB and CO2GLYCO of ICBMS, under the leadership of Prof Buchet and Goekjian, together with Dr Marcillat and Dr Gueyrard. This project is dedicated to the synthesis of new laurdan containing probes, and our part is to propose a glycolipidic type of compounds in this series.

Laurdan, commercial name for 6-dodecanoyl-2-(dimethylamino) naphthalene, compound **129** in Fig. 5.3, was found to have very good quantum yield in TPEF microscopy.[178, 180, 181] However, its hydrophobic property made it less efficient for this study. A recent attempt by modifying the laurdan by introducing a hydrophilic carboxylic acid was performed,[182, 183] compound **130** in Fig. 5.3, and received a good result in solubility and stronger two-photon excited fluorescence emission. A first series of probes was prepared in Professor Peter Goekjian`s lab with hydrophilic parts introduced such as sarcosine ethyl ester **131,** *N*-methylpiperazine **132**, aminoacetaldehyde **133** *N*-methyl aminoacetaldehyde dimethylacetal **134,** and *N*-methylallylamine **135**,. In the light of previous studies on carbohydrate-based fluorescent probes in our lab,[143] we thought that combining a sugar moiety to the laurdan part, taking advantage of water solubility and fluorescent stability, would be an interesting modification of the system.

Cette thèse est accessible à l'adresse : http://theses.insa-lyon.fr/publication/2013ISAL0001/these.pdf
© [R. Xu], [2013], INSA de Lyon, tous droits réservés

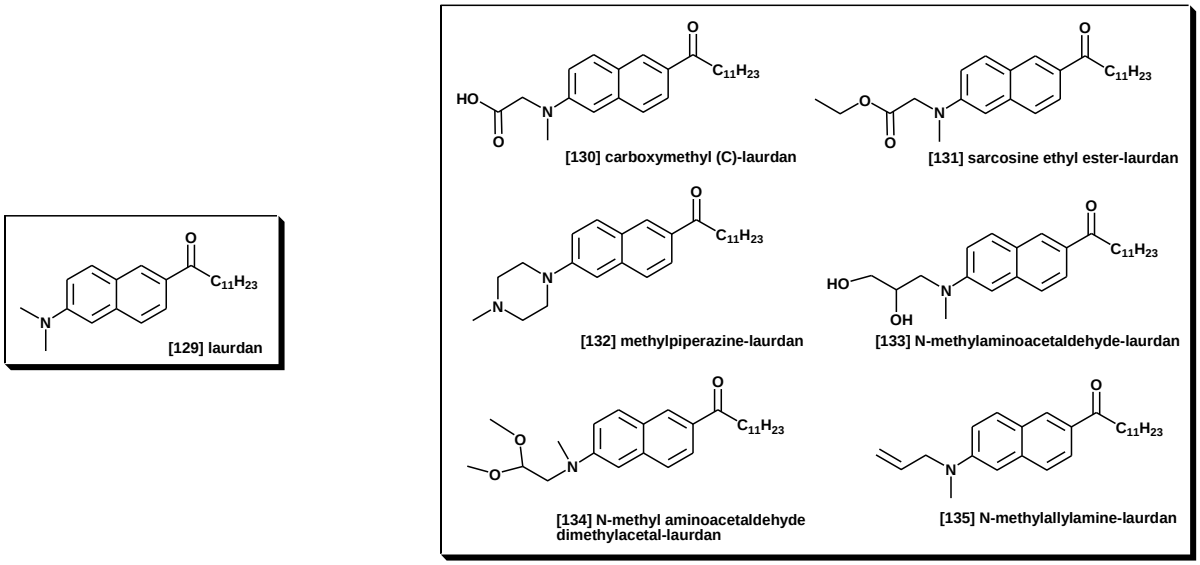

Fig. 5.3: Chemical structures of laurdan and modified laurdan derivatives

5.2. Synthesis procedure

To achieve this goal, two structures bearing the carbohydrate moieties were proposed firstly to be tested, one was based on glucose **136** and the other was based on cellobiose **137**, Fig. 5.4.

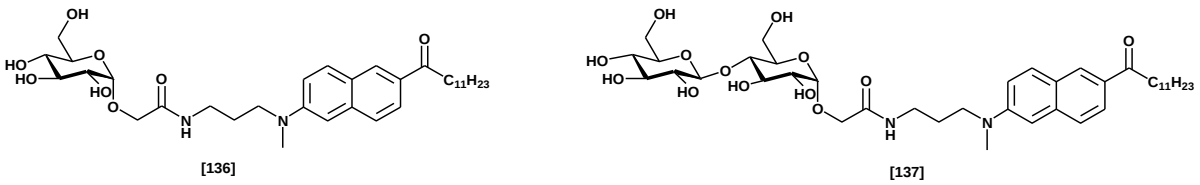

Fig. 5.4: Chemical structures of desired probes based on glucose and cellobiose scaffolds **136** and **137**

To realize this, we proposed a synthetic path as described here. 6-dodecanoyl-2-bromide naphthalene was obtained by the Friedel-Crafts coupling of 2-bromonaphthalene with 6-dodecacyl chloride, followed by reaction with the N^1-Boc-N^2-methyl-1,3-diaminopropane via Buchwald–Hartwig amination. The resulting compound was then deprotected to yield the amine, which was further used to open the lactone ring. For the final step, the obtained

Cette thèse est accessible à l'adresse : http://theses.insa-lyon.fr/publication/2013ISAL0001/these.pdf
© [R. Xu], [2013], INSA de Lyon, tous droits réservés

compounds were deacetylated to get the desired products. The whole procedure is shown in Scheme 5.1.

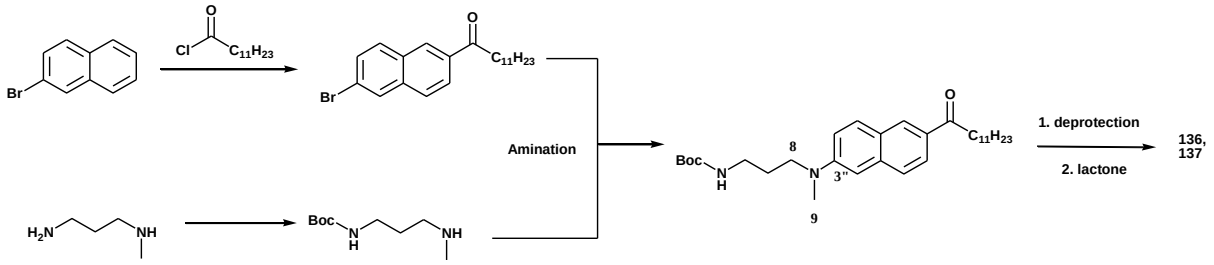

Scheme 5.1: General procedure for obtaining carbohydrate-based laurdans

5.2.1. Synthesis of 6-dodecanoyl-2-bromonaphthalene

The synthesis of this compound was adapted the method explored by Kim, H. M *et al.*[183]. The compound they reported was 6-hexanoyl-2-methoxynaphthalene, but we found that bromide has a same localized effect like methyoxyl group which resulted in a same substitution position of dodecanoyl group.

The synthesis was using the typical Friedel-Crafts reaction catalyst, $AlCl_3$, and nitrobenzene as the solvent. After the reaction, the nitrobenzene was removed in vacuum, and the final product was purified by crystallization from the cold MeOH.

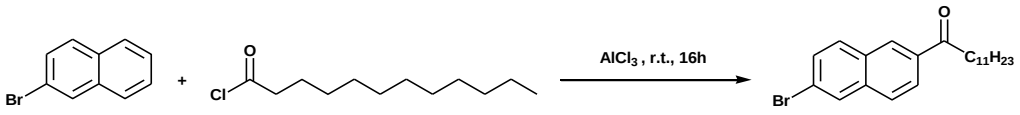

Scheme 5.2: Synthetic procedure of 6-dodecanyol-2-bromoanphthalene

The structure of the compound was confirmed by M. Mouhdine CHENIOUR in his thesis.[184]

Cette thèse est accessible à l'adresse : http://theses.insa-lyon.fr/publication/2013ISAL0001/these.pdf
© [R. Xu], [2013], INSA de Lyon, tous droits réservés

5.2.2. Synthesis of the N^1-Boc-N^2-methyl-1,3-diaminopropane

Inspired by the work of Rannard S. P. *et al.* [185] the Boc anhydride was firstly reacted with imidazole to obtain Boc-imidazole, followed by the selectively coupling with primary amine of *N*-methyl 1,3-diaminopropane. The synthetic procedure is shown in Scheme 5.3.

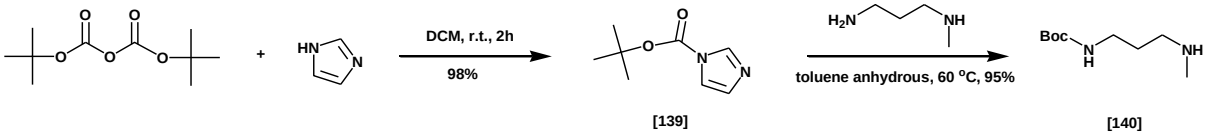

Scheme 5.3: Synthetic procedure for N^1-Boc-N^2-methyl-1,3-diaminopropane **140**

Compared to the process described in the paper, the condition of present first step was mild. After 2h, the reaction was finished as only one spot was shown by thin layer chromatography (TLC). The solution was then washed with the saturated NaCl solution. Then the obtained organic phase was dried and filtered, followed by the evaporation of the solvent to get the white solid. The yield of this step was high, up to 98%.

With this intermediate in hands, we went through the second step where the Boc group went to protect the primary amine of *N*-methyl-1,3-diaminopropane, following the literature procedure. Since the bond of the imidazole and the carboxyl group is fragile, water at high temperature might cleave this bond, which would result in imidazole, *t*-butanol and CO_2.[185] Thus, anhydrous toluene was used and the compound **139** was carefully dried under the pump. With careful handling, the yield of final compound **140** was up to 95% according to ^{1}HNMR. The signals are agreed with the data reported in the literature.[186]

5.2.3. Amination of 6-dodecanoyl-2-bromonaphthalene and N^1-Boc-N^2-methyl-1,3-diaminopropane

The palladium-involved C-N cross coupling, or Buchwald-Hartwig amination, has become very popular as it offers a great efficiency towards the constitution of aromatic C-N bonds, which is widely used in the pharmaceutical field.[187] This system commonly consists of four

Cette thèse est accessible à l'adresse : http://theses.insa-lyon.fr/publication/2013ISAL0001/these.pdf
© [R. Xu], [2013], INSA de Lyon, tous droits réservés

components: ligands; palladium precursors; base; solvents. A possible mechanism of this reaction is shown in Fig. 5.5.

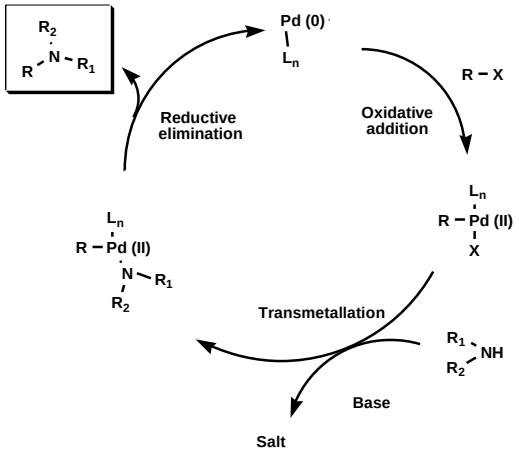

Fig. 5.5: Proposed mechanism of C-N coupling [188]

In this experiment, the tris(dibenzylideneacetone)dipalladium(0)[$Pd_2(dba)_3$] was used as the catalyst, along with 2-dicyclohexylphosphino-2′,6′-dimethoxybiphenyl **(**S-Phos) as the ligand. The reaction took place at 105 ^{o}C in the anhydrous *p*-dioxane in the Schlenk flask. The yield of **141** was 64%. The procedure is shown in Scheme 5.4.

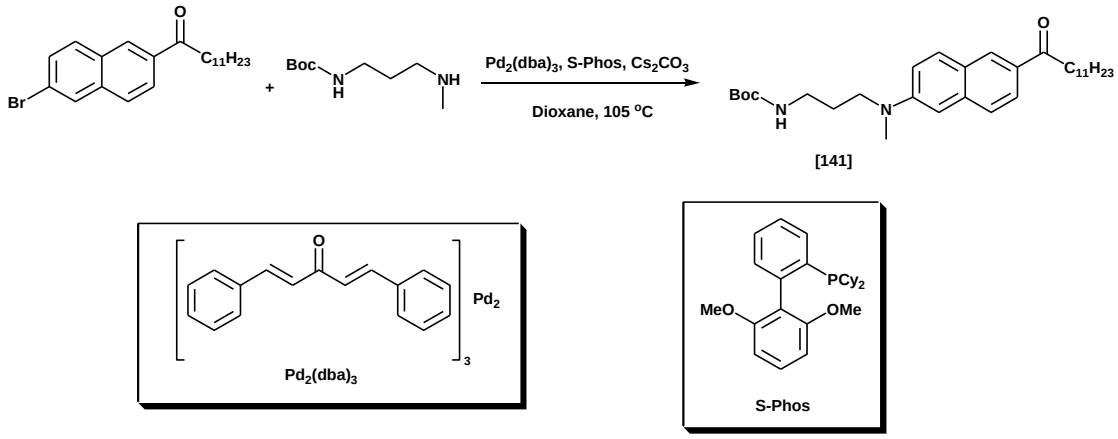

Scheme 5.4: Synthetic procedure of amination and the chemical structure of $Pd_2(dba)_3$ and S-Phos

Cette thèse est accessible à l'adresse : http://theses.insa-lyon.fr/publication/2013ISAL0001/these.pdf
© [R. Xu], [2013], INSA de Lyon, tous droits réservés

For this reaction, a careful control was needed. Though some reports demonstrated that water might improve the reaction performance,[189] it was found to hinder the reaction in this experiment. Thus, the dried amino product was crucial to this reaction.

From the ^{13}C NMR spectrum, we could see a significant shift of C-3'' from δ 136.4 ppm of the original to 148.8 ppm in the product. And this peak could also be found to have relation with H-9 and H-8 in the HMBC spectrum, Fig. 5.6.

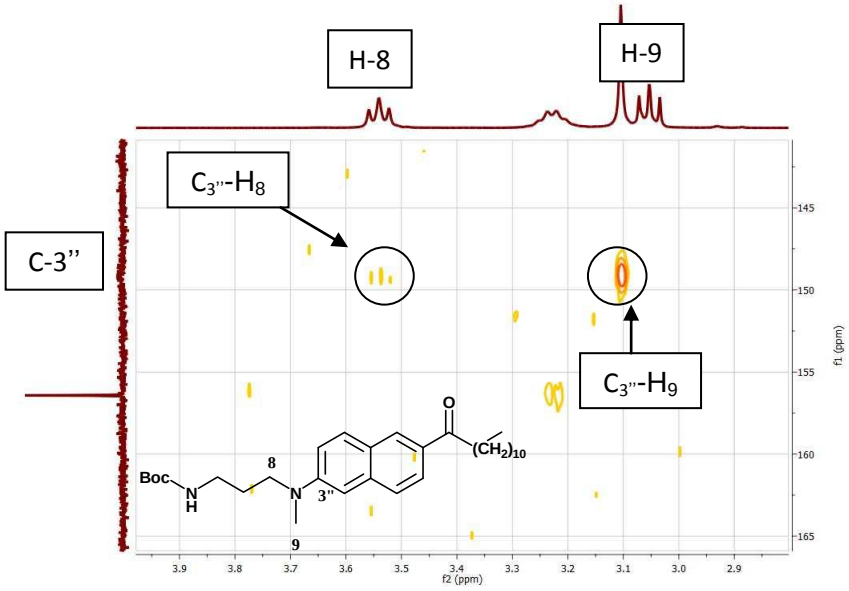

Fig. 5.6: ^{1}H-^{13}C HMBC spectrum of compound **141**

5.2.4. Synthesis of CMG derived probes

The compound **141** was then *N*-deprotected in the presence of TFA for 16h. After removal of excess TFA under the vacuum, the amino compound was then reacted with glucose and cellobiose derived lactones, followed by the deacetylation in the mixture of MeOH/ H_2O/ NEt_3 at the ratio of 8/1/1. The target compounds were obtained. The procedure is shown in Scheme 5.5.

Cette thèse est accessible à l'adresse : http://theses.insa-lyon.fr/publication/2013ISAL0001/these.pdf
© [R. Xu], [2013], INSA de Lyon, tous droits réservés

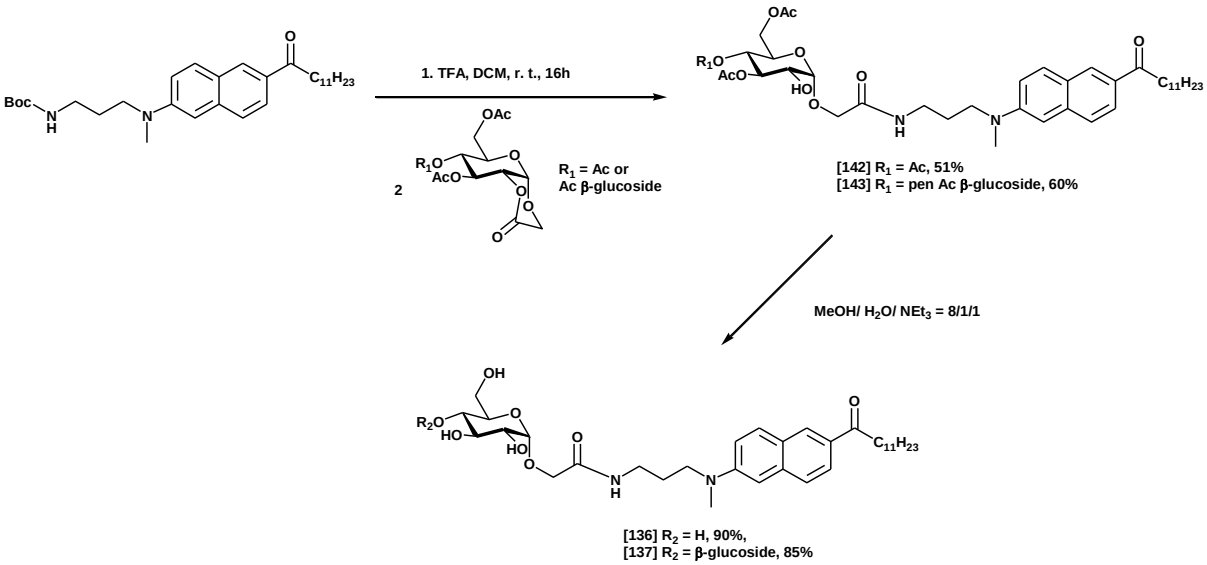

Scheme 5.5: Synthesis of glucosyl and cellobiosyl laurdan derivatives **136** and **137**

The structure of the resulting compound was studied by NMR spectroscopy. Here we show the example of compound **143**. The spectra firstly shown are the acetylated one. Compared with the proton NMR spectrum of cellobioside derived lactone, the signals of H-2, H-7 of the product are shifted. H-2 has moved from δ 4.28 ppm of the lactone to δ 3.61 ppm of the compound as well as that of H-7 is from 4.62 and 4.42 to 4.13 and 3.97, as indicated in the Fig. 5.7.

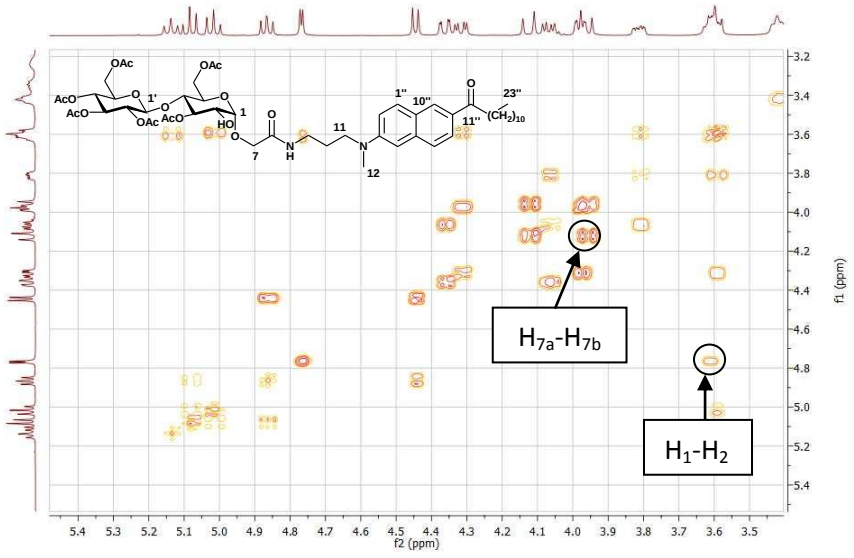

Fig. 5.7: ^{1}H-^{1}H COSY spectrum of compound **143**

Cette thèse est accessible à l'adresse : http://theses.insa-lyon.fr/publication/2013ISAL0001/these.pdf
© [R. Xu], [2013], INSA de Lyon, tous droits réservés

Changes also could be found in carbon spectra, as the C-2 is d 76.1 ppm and C-7 is δ 67.4 ppm, where C-2 is δ 72.0 ppm and C-7 is δ 64.5 ppm for the lactone, Fig. 5.8.

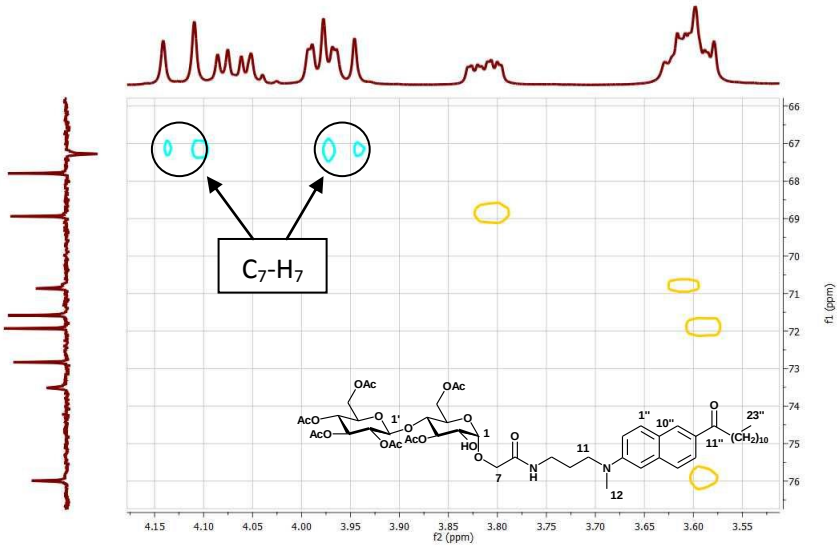

Fig. 5.8: ^{1}H-^{13}C HSQC spectrum of compound **143**

The carbon signal of carboxyl group C-8 of amide also shifted from δ 163.6 ppm of lactone to δ 169.0 ppm, which could be found in response to H-9 on the linker, Fig. 5.9. Upon these observations, the structure of compound **143** was approved.

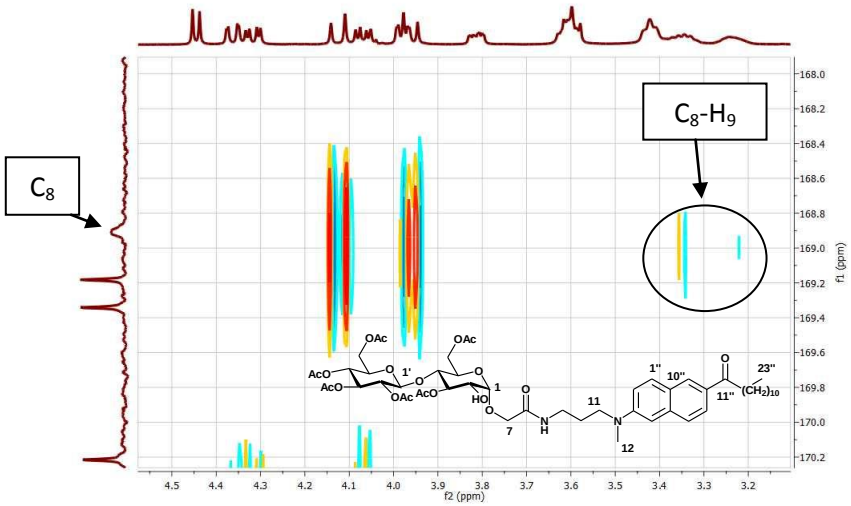

Fig. 5.9: ^{1}H-^{13}C HMBC spectrum of compound **143**

Cette thèse est accessible à l'adresse : http://theses.insa-lyon.fr/publication/2013ISAL0001/these.pdf
© [R. Xu], [2013], INSA de Lyon, tous droits réservés

After deacetylation, the disappeared proton signals around δ 1.90 to 2.08 ppm of C*H*$_3$ of acetyl groups are very obvious in product ^{1}HNMR spectrum. Another proof could be seen as the carbon signals of *C*=O of acetyl groups around δ 174.5 ppm disappeared in the ^{13}C NMR.

5.3 Fluorescence properties

The fluorescence properties of two compounds were studied first by measuring the fluorescence in various solvents of different polarities and then when included in liposomes in order to have a preliminary information of their behavior within a supramolecular system considered as a membrane model.

5.3.1 Characterization of fluorescence in various solvents.

Since the environments in which the probes should be used are complex in terms of polarity, a series of solvents having various polarities was chosen for mimicking this situation, namely from low to high polarity THF, DMF, DMSO, ethanol, and water. The excitation wavelength was set at 385 nm, while the emission wavelengths were detected in the range of 400 nm to 600 nm. The normalized emission curves of these two probes are shown in Fig. 5.10 and 5.11, respectively.

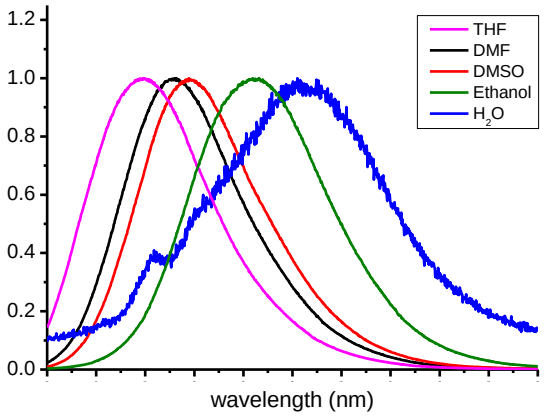

Fig. 5.10: Normalized emission spectra of **136** in different solvents

Cette thèse est accessible à l'adresse : http://theses.insa-lyon.fr/publication/2013ISAL0001/these.pdf
© [R. Xu], [2013], INSA de Lyon, tous droits réservés

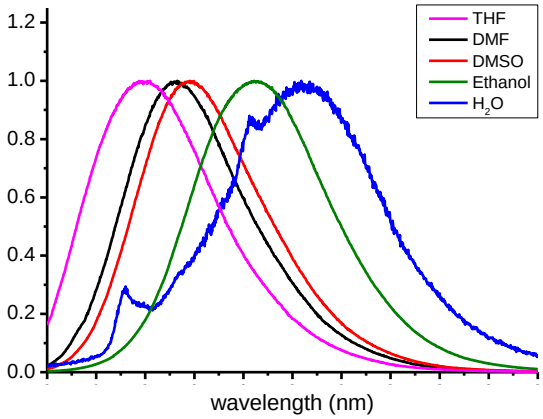

Fig. 5.11: Normalized emission spectra of **137** in different solvents

As seen in the figures above, the spectra of these probes show gradual bathochromic shifts as the polarity of solvent increases. The λ^{fl}_{max} of water is the highest while that of THF is the lowest, and the difference between the two is nearly 70 nm, showing that these two probes have a high sensitivity to the polarity of environment. The spectra of the probes in water contain a lot of noise, because of the very low fluorescence intensities detected by the equipment. The probes were found to be well soluble in water at this concentration, so this low intensity is not the result of a low concentration, but the classical consequence of the high polarity of the solvent. The un-normalised fluorescence intensities for probe **136** are shown in Fig. 5.12, where the curve in purple is the solution in water with the highest intensity at 549.574. In contrast, the fluorescence intensities shown in other solvents were within the same order of magnitude which is more than 40000 and relatively high compared to water. A similar result was also obtained for probe **137**. These results indicate that since the probes would be applied to the membrane whose condition is hydrophobic, they should be useful because of providing a good contrast under the microscope.

Cette thèse est accessible à l'adresse : http://theses.insa-lyon.fr/publication/2013ISAL0001/these.pdf
© [R. Xu], [2013], INSA de Lyon, tous droits réservés

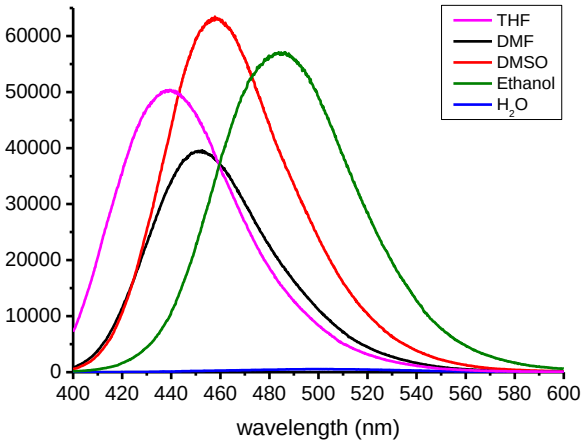

Fig. 5.12: The fluorescent intensities of probe **136** of same concentration in different solvents

5.3.2 Fluorescent tests of probes in model membrane

Liposomes constructed by bilayer association of dimyristoylphosphatidylcholine (DMPC), as shown in Fig. 5.13, were prepared by extrusion according to a standard procedure.[190] In this experiment, the liposome of LUV (large unilamellar vesicles) was selected, whose diameter is ranging from 80 to 800 nm. The probes were firstly dissolved in ethanol and mixed with the DMPC at the concentration of 1/400 molar ratio (probe/lipid). After the hydration and extrusion of lipids, the fluorescence performance of labeled liposomes was measured in terms of emission wavelengths recorded in the range of 420 to 550 nm under the condition of a scanning excitation wavelength from 300 and 420 nm. The data were obtained at every 5 degree in the range of temperature of 15 to 45 ^{o}C, based on which a 3D spectrum could be drawn. Two examples of probe **136** at different temperatures are shown Fig. 5.14, where a shift of the maximum emission wavelength from low to high temperature is seen.

Cette thèse est accessible à l'adresse : http://theses.insa-lyon.fr/publication/2013ISAL0001/these.pdf
© [R. Xu], [2013], INSA de Lyon, tous droits réservés

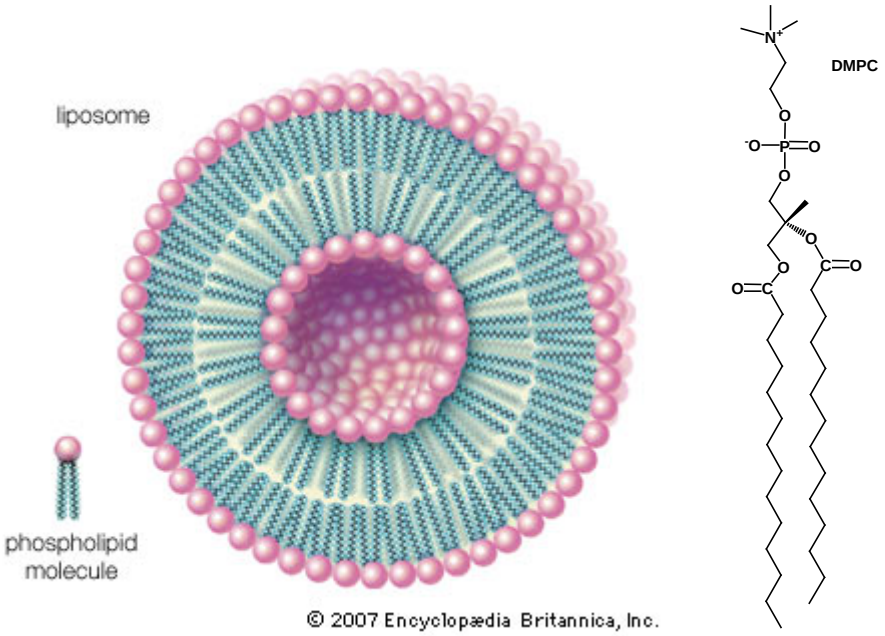

Fig. 5.13: Schematic presentation of LUV bilayer and the structure of DMPC

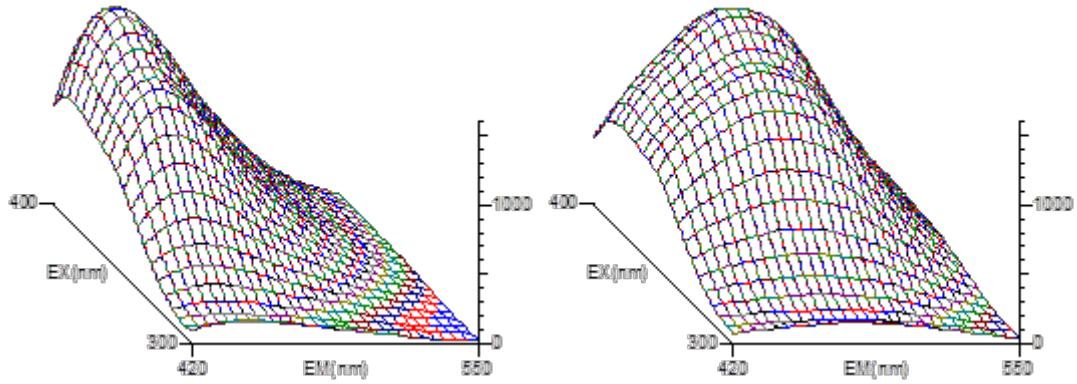

Fig. 5.14: 3D spectra of excitation and emission properties of probe **136** in DMPC liposomes at A) 20 ^{o}C and B) 45 ^{o}C

From these spectra, the maximum excitation and emission wavelengths were obtained. It was observed that by increasing the temperature, the excitation wavelength decreased on a small range (<10 nm) whereas the emission wavelength increased on a larger range (30 nm). A similar behavior was observed for probe **137**. The maximum emission wavelengths of these probes were investigated as a function of temperatures, as shown in Fig. 5.15 and 5.16. At low temperature, the liposomes were tightly packed, forming a hydrophobic environment, as a result the maximal emission wavelength was low; whereas at high

Cette thèse est accessible à l'adresse : http://theses.insa-lyon.fr/publication/2013ISAL0001/these.pdf
© [R. Xu], [2013], INSA de Lyon, tous droits réservés

temperature, the alkyl chain of DMPC had more freedom to fluid around, the space between the lipids expanded where more water had penetrated into the liposome. At this stage, the λ^{em}_{max} was found red shifted. These results show that these probes are sensitive to their environment, in agreement with the observations in the solvents of different polarities.

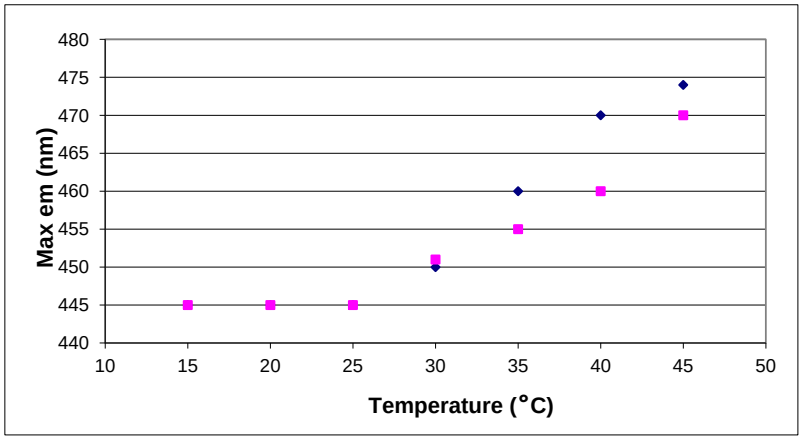

Fig. 5.15: Performance of probe **136** in DMPC liposomes (purple for first trial; dark blue for second trial)

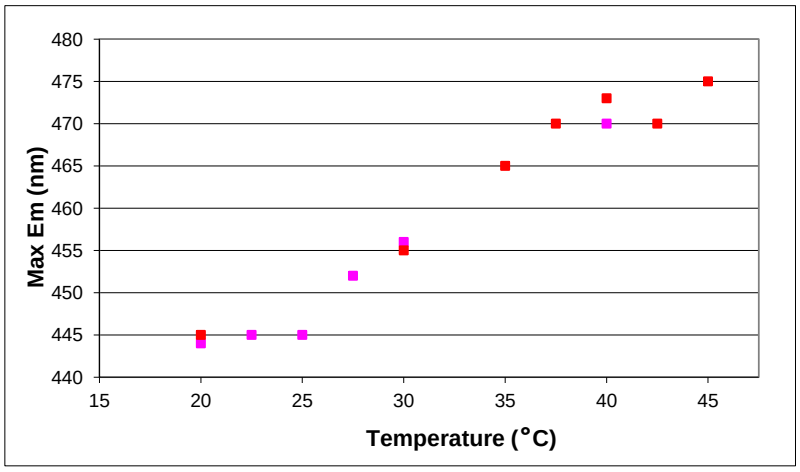

Fig. 5.16: Performance of probe **137** in DMPC liposomes (pink for first trial; red for second trial)

According to the preliminary results recorded above, the transition temperatures of liposomes in these experiments were around 34 ^{o}C. This is higher than the transition temperature of this model membrane for which the transition temperature is normally of 23 ^{o}C based on literature

Cette thèse est accessible à l'adresse : http://theses.insa-lyon.fr/publication/2013ISAL0001/these.pdf
© [R. Xu], [2013], INSA de Lyon, tous droits réservés

and previous experiments in the ODMB team. Further work is needed to understand this behavior and estimate how much the characteristics of the liposomes are affected by the inserted probes.

5.4 Conclusion

In this chapter, we reported two new neogluco-laurdan probes for the purposes of detecting microdomains in the membrane. The synthesis involved Buchwald amination and CMGLs strategy, which were well performed. The products were characterized by NMR and mass spectroscopy to be the desired compounds.

The fluorescence properties of the probes were investigated in different solvents and when applied to liposomes, unveiling their sensitivity to the environment. In polar solvents, corresponding to the high temperature in liposomes experiments, the max emission wavelength was higher than that in unpolar solvents or liposomes at low temperatures.

Further investigations by preparing other liposomes system involving phospholipids will be conducted, and investigations on the fluorescent efficiency of the probes in real cells are also scheduled.

Cette thèse est accessible à l'adresse : http://theses.insa-lyon.fr/publication/2013ISAL0001/these.pdf
© [R. Xu], [2013], INSA de Lyon, tous droits réservés

General conclusion

In this study, we have synthesized two families of new carbohydrate-based amphiphilic derivatives: a series of alkyl glucoside ethers varying in terms of chain length and position on the sugar, and a series of glucosteroids varying in terms of alkyl spacer and, for the disubstituted systems, in terms of alkyl side chain length. By the means of analytical methods, such as NMR spectroscopy, mass spectroscopy and elementary analysis, the structure of all the compounds was carefully established, as well as their purity. Their liquid crystalline behaviors were studied by the means of transmission light microscopy and differential scanning calorimetry.

The liquid crystalline studies of these two families showed that the formation of mesophases were strongly dependent on the structural factors, such as hydrophilic/hydrophobic balance, intra-and inter-molecular H-bondings and relative cross-sectional area of sugar head to aliphatic tails.

For the methyl glucoside ethers family, the Sm A* phases were the unique thermotropic mesophases observed by these compounds, indicating that the cross-sectional areas of hydrophobic part relative to that of sugar head approached to 1:1. The C12 chain length was found to be the limit where the molecules could form the mesophases. For chain length C14 and longer, the clearing points show a consistent decrease as the aliphatic chain moved from O-2 to O-6, sequentially. The C12 series, the behavior was more irregular: the clearing point for the O-3 ether was the highest, and no mesophases was observed for O-4. Structural modeling studies allowed to discuss these observations, notably with respect to possible inter- or intramolecular H-bonding interactions.

The lyotropic liquid crystalline behaviors of these compounds were also studied. Upon increasing the amount of water added to the compounds, a sequence of mesophases, from lamellar, cubic and hexagonal, was observed, which was expected for such monosubstituted systems.

For the thermotropic behaviors of the glucosteroids, as the spacer length extended, where more flexibility was introduced in the systems, the clearing points decreased. This tendency was enhanced as the additional side chain was attached. With a short side chain, the Sm A* phases were observed due to the similar relative cross-sectional areas of sugar head to hydrophobic moieties. For the C-4 spacer series, when the side chain extended to C14, a

Cette thèse est accessible à l'adresse : http://theses.insa-lyon.fr/publication/2013ISAL0001/these.pdf
© [R. Xu], [2013], INSA de Lyon, tous droits réservés

second type of mesophases appeared, which were identified as hexagonal columnar phases. Modeling suggested that partition of the lipidic moieties, either showing cholesterol- alkyl chain interactions, or preferring cholesterol – cholesterol and alkyl chain – alkyl chain packing could be the main driving force for this behavior.

In the case of the C6 spacer series, same observations were made however with Sm A* phases showing more limited temperature range. For the C8 spacer series, only the columnar phase was observed. All these observations were discussed in terms of interactions between cholesterol and the aliphatic chain.

The two families of compounds which have been studied illustrate how much the behavior can be essentially related to polar interactions (H-bonding), therefore to the sugar moiety, for the ether series, or to hydrophobic interactions (lipid-lipid) in the glucosteroid series. In this latter series, preference for either steroid-steroid or steroid alkyl packing appears as an insight in understanding the behavior of complex lipids, showing potentially more than one conformational structure with important consequences on the supramolecular level, therefore to their potential biological role. This could be regarded as “lipid denaturation” by analogy to the protein denaturation. Also, when we see that compounds like the glycosteroids having an long chain ester α-CAG, BbGL-I, are found to exist in Nature, and how much glycolipid-cholesterol interactions were recently shown to be critical in some biological processes, it is hoped that our observations can provide a new vision angle for the study of complex lipids and glycolipids.

As a start to develop new probes targeting the “lipid raft” microdomain in membranes, we also explored a sequence towards carbohydrate laurdan hybrids. Further development of this strategy and evaluation of the biological properties is programmed within new collaborative projects.

Cette thèse est accessible à l'adresse : http://theses.insa-lyon.fr/publication/2013ISAL0001/these.pdf
© [R. Xu], [2013], INSA de Lyon, tous droits réservés

Experimental section

A. General aspect

The solvents used for reactions and chromatography were bought from SDS, Carolo Erba, and Sigma-Aldrich. Most of the solvents used in the syntheses were distilled before use, dichloromethane over the P_2O_5, THF over Na and benzophenone, and DMF over CaH_2.

The reagents used in this thesis were bought from Aldrich and used directly without purification.

The TLC plates are from Merck 60F, coated with silica gel GF_{254} (0.25 mm).

The purification using the chromatographies is by column of silica gel flash Merck (60, 40-63 μm)

NMR spectroscopy: Bruker AC or DRX spectrometers at 75.47 MHz (100.61 MHz, or 125.77 MHz) for ^{13}C NMR and 300.13 MHz (or 400.13 MHz, or 500.13 MHz) for ^{1}H NMR. Chemical shifts (δ) are given in parts per million (ppm) and were measured relative to the signal of tetramethylsilane ($\delta = 0$)

The peak of remaining chloroform is at 7.26 ppm, which was used as a calibration of spectra using $CDCl_3$ as the uniqud solvent. In case of mixture, the peak of TMS was used as calibration. The chemical shift was determined in ppm. The abreviations used in the list of NMR characterization are: s (singulet); ls (large singulet); d (doublet); t (triplet); dt (doublet and triplet); dd (doublet of doublet); q (quadruplet); m (multiplet).

Mass spectroscopy: The spectra were recorded by Centre de Spectrométrie de Masse of the Université Claude Bernard (Villeurbanne) using electrospray (ESI) technique

Optical rotation: Perkin Elmer 241 polarimeter at 589 nm (sodium D line). The measurements were carried out at 20 ^{o}C and the concentrations are reported in g/100 mL

Elementary analysis: The measurements were performed by the Service Central d'Analyse of CNRS (Vernaison)

Cette thèse est accessible à l'adresse : http://theses.insa-lyon.fr/publication/2013ISAL0001/these.pdf
© [R. Xu], [2013], INSA de Lyon, tous droits réservés

B. Characterizations of liquid crystalline behaviors

Polarized optical microscopy: Phase identification and determination of melting point and transition temperatures were carried out by thermal polarized light microscopy using a Zeiss Axioskop 40 polarizing transmitted light microscope equipped with a Mettler FP82HT microfurnace in conjunction with a FP90 Central Processor.

Differential scanning calorimetry: Differential scanning thermograms (scan rate 10° min-1) were obtained using a Mettler DSC822^e operating on the Star^e software. The results obtained were standardized to indium (measured onset 156.68 °C, ΔH 28.47 Jg^{-1}, lit. value 156.60 °C, ΔH 28.45 Jg^{-1}).

C. Fluorescent properties of probes

Probes features in solvents: Absorption spectra were recorded on a Hewlett-Packard 8453 diode array spectrophotometer. Fluorescence measurements (excitation and emission spectra) were performed with a Hitachi F4500 fluorometer. The spectra were recorded at 25 ^oC using a 1 cm path length thermostated quartz micro-cuvette.

Probes features in LUV (Large Unilamellar Vesicles) at different temperatures: Liposomes were prepared by pure DMPC according to a standard procedure. Fluorescence data were obtained using a Hitachi F4500 fluorometer. Emission spectra were recorded between 420 and 550 nm for each excitation wavelength between 300 and 400 nm and at several temperatures between 15 to 45 ^oC. The probes were initially dissolved in ethanol and were added to the liposomes to reach a 3 μM final concentration, corresponding to a 1:400 (probe: phospholipids) molar ratio.

Cette thèse est accessible à l'adresse : http://theses.insa-lyon.fr/publication/2013ISAL0001/these.pdf
© [R. Xu], [2013], INSA de Lyon, tous droits réservés

D. Synthetic procedures and characterizations of all the products studied

D. 1 Methyl n-*O*-(2-hydroxyalkyl)-α-D-glucopyranosides

D. 1.1 Synthesis of 2-*O*-(2-hydroxylalkyl)-α-D-glucopyranosides and 3-*O*-(2-hydroxylalkyl)-α-D-glucopyranosides

Monobenzylated methyl 4, 6-*O*-benzylidene-α-D-glucopyranoside can be obtained by two methods, either via the stannylene by reaction with dibutyltin oxide or in the presence of tetrabutylammonium iodide and aqueous NaOH in DCM at room temperature.Both methods give mixtures of the two possible monobenzylated products at O-2 (major compound for the first method) or at O-3 (major compound for the second method). Reaction of 1,2-epoxyalkanes with methyl 2- or 3-*O*-benzyl-4,6-*O*-benzylidene-α-D-glucopyranosides, in the presence of DABCO/DMAP/DMSO yielded methyl 3-*O*-benzyl-2-*O*-(2-hydroxyalkyl)-4,6-*O*-benzylidene-α-D-glucopyranosides or 2-*O*-benzyl-3-*O*-(2-hydroxyalkyl)-4,6-*O*-benzylidene-α-D-glucopyranosides in 55-70% yield. Deprotection by acidic treatment (cat. *p*-toluenesulphonic acid in methanol) followed by Pd-catalyzed hydrogenation in MeOH-EtOAc afforded methyl 2-*O*-(2-hydroxyalkyl)-α-D-glucopyranosides and 3-*O*-(2-hydroxyalkyl)-α-D-glucopyranosides

Methyl 2-O-(2-hydroxyoctyl)-α-D-glucopyranoside (97a)

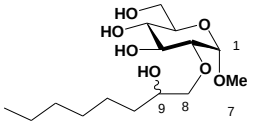

White solid

^{1}HNMR (400 MHz, $CDCl_3$) :

Cette thèse est accessible à l'adresse : http://theses.insa-lyon.fr/publication/2013ISAL0001/these.pdf
© [R. Xu], [2013], INSA de Lyon, tous droits réservés

δ: 4.82 (d, 1H, *J* = 3.6 Hz, H-1), 3.88-3.68 (m, 4H, H-3, H-9, H-6), 3.60-3.10 (m, 6H, H-2, H-4, H-5, H-8a, H-8b, H-8a', H-8b'), 3.43 (s, 3H, OCH_3), 1.41-1.26 (m, 10 H, H-octyl ether), 0.87 (t, 3H, *J* = 7.2 Hz, CH_3)

^{13}CNMR (100 MHz, $CDCl_3$) :

δ: 97.9 (C1+C1'), 81.3 (C2+C2'), 76.3 (C8), 73.2 (C3), 71.5 (C5), 71.2 (C9), 70.1 (C4), 61.7 (C6+C6'), 55.3 (OCH_3), 33.0, 31.9, 29.5, 25.6, 22.8, 14.2

m/z (HRMS) :

calcd for $C_{15}H_{30}O_7Na$: 345.1884; found: 345.1878

Methyl 2-O-(2-hydroxydecyl)-α-D-glucopyranoside (97b)

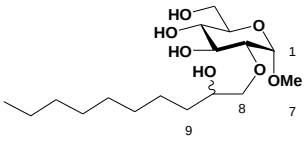

White solid

^{1}HNMR (400 MHz, $CDCl_3$) :

δ: 4.82 (s, 1H, H-1), 4.24 (s, 4H, OH), 3.88-3.65 (m, 4.5H, H-3, H-9, H-6, H-8a), 3.58-3.40 (m, 3H, H-4, H-5, H-8a', H-8b'), 3.40 (s, 3H, OCH_3), 3.30 (m, 1.5H, H-2, H-8b), 1.42-1.25 (m, 14H, H-decyl ether), 0.87 (t, 3H, *J* = 7.2 Hz, CH_3)

^{13}CNMR (100 MHz, $CDCl_3$) :

δ: 97.8 (C1), 97.7 (C1'), 81.1 (C2), 79.6 (C2'), 76.2 (C8), 74.2 (C8'), 73.1 (C3), 72.6 (C3'), 71.4 (C5), 71.3 (C5'+C9), 70.2 (C9'), 70.0 (C4), 69.8 (C4'), 61.5 (C6), 61.4 (C6'), 55.3 (OCH_3), 33.0, 32.0, 29.9, 29.8, 29.7, 29.5, 25.9, 25.7, 22.8, 14.2

m/z (HRMS) :

calcd for $C_{17}H_{34}O_7Na$: 373.2197; found: 373.2193

Cette thèse est accessible à l'adresse : http://theses.insa-lyon.fr/publication/2013ISAL0001/these.pdf
© [R. Xu], [2013], INSA de Lyon, tous droits réservés

Methyl 2-O-(2-hydroxydodecyl)-α-D-glucopyranoside (97c)

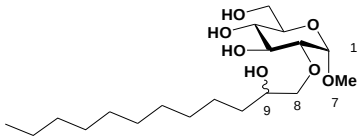

White solid

^{1}HNMR (300 MHz, $CDCl_3$) :

δ: 5.59 (s, 1H, OH), 5.11 (s, 1H, OH), 4.77 (m, 1H, H-1), 4.35 (m, 1H, OH), 3.88-3.65 (m, 4.5H, H-3, H-9, H-6, H-8a), 3.60-3.45 (m, 3H, H-4, H-5, H-8a', H-8b'), 3.35 (s, 3H, OCH_3), 3.26 (m, 1.5H, H-2, H-8b), 1.37-1.21 (m, 18H, H-dodecyl ether), 0.83 (t, 3H, *J* = 6.9 Hz, CH_3)

^{13}CNMR (75 MHz, $CDCl_3$) :

δ: 97.7 (C1), 97.6 (C1'), 81.0 (C2), 79.5 (C2'), 76.1 (C8), 74.2 (C8'), 73.0 (C3), 72.5 (C3'), 71.4 (C5), 71.2(C5'), 70.1 (C9), 69.9 (C9'), 69.8 (C4), 69.7 (C4'), 61.4 (C6), 61.3 (C6'), 55.2 (OCH_3), 32.9, 32.0, 29.9, 29.8, 29.7, 25.8, 25.6, 22.7, 14.1

m/z (HRMS) :

calcd for $C_{19}H_{38}O_7Na$: 401.2510; found: 401.2506

Methyl 2-O-(2-hydroxytetradecyl)-α-D-glucopyranoside (97d)

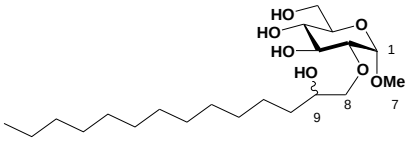

White solid

^{1}HNMR (400 MHz, $CDCl_3$) :

Cette thèse est accessible à l'adresse : http://theses.insa-lyon.fr/publication/2013ISAL0001/these.pdf
© [R. Xu], [2013], INSA de Lyon, tous droits réservés

δ: 4.82 (s, 1H), 3.88-3.70 (m, 4.5H, H-3, H-9, H-6, H-8a), 3.61-3.43 (m, 3H, H-4, H-5, H-8a', H-8b'), 3.68-3.31(m, 5.5H, H-2, H-8b, 4OH), 3.40 (s, 3H, OCH_3), 1.40-1.25 (m, 22H, H-tetradecyl ether), 0.86 (t, 3H, *J* = 6.8 Hz, CH_3)

^{13}CNMR (100 MHz, $CDCl_3$) :

δ: 97.8 (C1), 97.6 (C1'), 81.3 (C2), 79.6 (C2'), 76.3 (C8), 74.3 (C8'), 73.1 (C3), 72.6 (C3'), 71.4 (C5), 71.2 (C5'+C9), 70.2 (C9'), 70.1 (C4), 69.9 (C4'), 61.7 (C6+C6'), 55.3 (OCH_3), 32.9, 32.1, 29.9, 29.8, 29.8, 29.7, 29.5, 25.9, 25.7, 22.8, 14.3

m/z (HRMS) :

calcd for $C_{21}H_{42}O_7Na$: 429.2823; found: 429.2815

Methyl 2-O-(2-hydroxyhexadecyl)-α-D-glucopyranoside (97e)

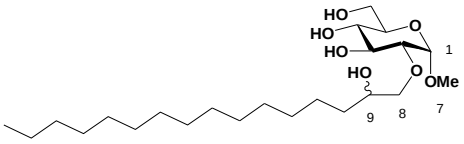

White solid

^{1}HNMR (400 MHz, $CDCl_3$) :

δ: 4.82 (m, 1H, H-1), 3.90-3.73 (m, 4.5H, H-3, H-9, H-6, H-8a),3.61-3.43 (m, 7H, H-4, H-5, H-8a', H-8b', 4OH), 3.40 (s, 3H, OCH_3), 3,31 (m, 1.5H, H-2, H-8b), 1.40-1.25 (m, 26H, H-hexadecyl ether), 0.88 (t, 3H, *J* = 7.2 Hz, CH_3)

^{13}CNMR (100 MHz, $CDCl_3$) :

δ: 97.8 (C1), 97.6 (C1'), 81.3 (C2), 79.6 (C2'), 76.3 (C8), 74.3 (C8'), 73.1 (C3), 72.6 (C3'), 71.4 (C5), 71.2 (C5'+C9), 70.2 (C9'), 70.1 (C4), 69.9 (C4'), 61.7 (C6+C6'), 55.3 (OCH_3), 32.9, 32.1, 29.9, 29.8, 29.8, 29.7, 29.5, 25.9, 25.7, 22.8, 14.3

m/z (HRMS) :

calcd for $C_{23}H_{46}O_7Na$: 457.3136; found: 457.3130.

Cette thèse est accessible à l'adresse : http://theses.insa-lyon.fr/publication/2013ISAL0001/these.pdf
© [R. Xu], [2013], INSA de Lyon, tous droits réservés

Methyl 3-O-(2-hydroxyoctyl)-α-D-glucopyranoside (99a)

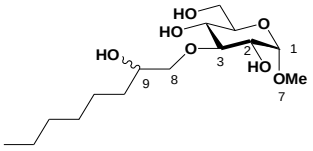

Colorless soft matter

^{1}HNMR (400 MHz, $CDCl_3$) :

δ: 4.75 (d, 1H, *J* = 3.6 Hz, H-1), 3.88 (m, 0.5H, H-8a), 3.79 -3.69(m, 3.5H, H-6, H-9, H-8a'), 3.68-3.38 (m, 5H, H-2, H-3, H-4, H-5, H-8b, H8b'), 3.42 (s, 3H, OCH_3), 1.40-1.27 (m, 10H, H-octyl ether), 0.87 (t, 3H, *J* = 7.2 Hz, CH_3)

^{13}CNMR (100 MHz, $CDCl_3$) :

δ: 99.8 (C1+C1'), 84.4(C3), 83.8 (C3), 78.1 (C8), 72.6 (C2), 72.4 (C2'), 71.7 (C5+C5'), 71.4 (C9), 71.1 (C9'), 70.4 (C4), 70.0 (C4'), 62.2 (C6), 62.1 (C6'), 55.5 (OCH_3), 33.1, 31.9, 29.5, 25.7, 25.6, 22.7, 14.2

m/z (HRMS) :

calcd for $C_{15}H_{30}O_7Na$: 345.1884; found: 345.1881

Methyl 3-O-(2-hydroxydecyl)-α-D-glucopyranoside (99b)

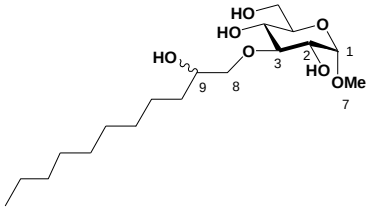

Cette thèse est accessible à l'adresse : http://theses.insa-lyon.fr/publication/2013ISAL0001/these.pdf
© [R. Xu], [2013], INSA de Lyon, tous droits réservés

White solid

^{1}HNMR (300 MHz, $CDCl_3$) :

δ: 4.73 (d, 1H, *J* = 3.3 Hz, H-1), 3.90 (d, 0.5H, *J* = 9.1Hz, H-8a), 3.85-3.71 (m, 3.5H, H-6, H-9, H-8a'), 3.65-3.40 (m, 5H, H-2, H-3, H-4, H-5, H-8b, H8b'), 3.39 (s, 3H, OCH_3), 1.37-124 (m, 14H, H-decyl ether), 0.86 (t, 3H, *J* = 6.9 Hz, CH_3)

^{13}CNMR (100 MHz, $CDCl_3$) :

δ: 99.8 (C1+C1'), 84.1 (C3), 83.3 (C3'), 78.0 (C8), 72.4 (C2), 72.3 (C2'), 71.6 (C5), 71.5 (C5'), 71.4 (C9), 70.9 (C9'), 70.0 (C4), 69.6 (C4'), 61.7 (C6+C6'), 55.4 (OCH_3), 33.1, 32.0, 29.9, 29.8, 29.7, 29.4, 25.7, 25.6, 22.8, 14.2.

m/z (HRMS) :

calcd for $C_{17}H_{34}O_7Na$: 373.2197; found: 373.2189

Methyl 3-O-(2-hydroxydodecyl)-α-D-glucopyranoside (99c)

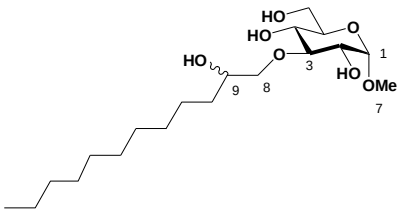

Colorless soft matter

^{1}HNMR (300 MHz, $CDCl_3$) :

δ: 4.73 (d, 1H, *J* = 2.7 Hz, H-1), 3.93 (d, 0.5H, *J* = 10.8Hz, H-8a), 3.86-3.70 (m, 3.5H, H-6, H-9, H-8a'), 3.65-3.40 (m, 5H, H-2, H-3, H-4, H-5, H-8b, H8b'), 3.40 (m, 3H, OCH_3), 1.37-1.24 (m, 18H, H-dodecyl ether), 0.86 (t, 3H, *J* = 6.9 Hz, CH_3)

^{13}CNMR (75 MHz, $CDCl_3$) :

Cette thèse est accessible à l'adresse : http://theses.insa-lyon.fr/publication/2013ISAL0001/these.pdf
© [R. Xu], [2013], INSA de Lyon, tous droits réservés

δ: 99.8 (C1+C1'), 84.1 (C3), 83.4 (C3'), 78.0 (C8), 72.4 (C2), 72.3 (C2'), 71.6 (C5), 71.5 (C5'), 71.0 (C9+C9'), 70.0 (C4), 69.6 (C4'), 61.8 (C6), 61.7 (C6'), 55.4 (OCH_3), 33.1, 32.0, 29.9, 29.8, 29.5, 25.8, 25.7, 22.8, 14.2

m/z (HRMS) :

calcd for $C_{19}H_{38}O_7Na$: 401.2510; found: 401.2498

Methyl 3-O-(2-hydroxytetradecyl)-α-D-glucopyranoside (99d)

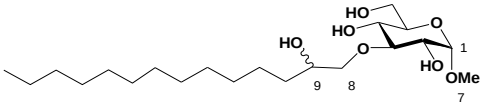

White solid

^{1}HNMR (300 MHz, $CDCl_3$) :

δ: 4.72 (d, 1H, *J* = 3.3 Hz, H-1), 3.93 (d, 0.5H, *J* = 9.3Hz, H-8a), 3.85-3.70 (m, 3.5H, H-6, H-9, H-8a'), 3.63-3.43 (m, 5H, H-2, H-3, H-4, H-5, H-8b, H8b'), 3.40 (m, 3H, OCH_3), 1.35-1.22 (m, 22H, H-tetradecyl ether), 0.86 (t, 3H, *J* = 6.9 Hz, CH_3)

^{13}CNMR (75 MHz, $CDCl_3$) :

δ: 99.8 (C1+C1'), 83.9 (C3), 83.2 (C3'), 78.0 (C8), 72.3 (C2), 72.2 (C2'), 71.6 (C5), 71.4 (C5'), 71.0 (C9+C9'), 69.8(C4), 69.4 (C4'), 61.6 (C6), 61.5 (C6'), 55.3 (OCH_3), 33.0, 32.0, 29.9, 29.8, 29.7, 29.5, 25.8, 25.7, 22.8, 14.2

m/z (HRMS) :

calcd for $C_{21}H_{42}O_7Na$: 429.2823; found: 429.2811

Methyl 3-O-(2-hydroxyhexadecyl)-α-D-glucopyranoside (99e)

Cette thèse est accessible à l'adresse : http://theses.insa-lyon.fr/publication/2013ISAL0001/these.pdf
© [R. Xu], [2013], INSA de Lyon, tous droits réservés

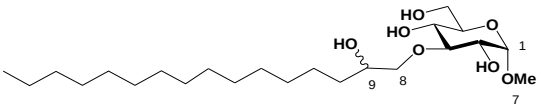

White solid

^{1}HNMR (300 MHz, $CDCl_3$) :

δ: 4.75 (d, 1H, *J* = 3,4 Hz, H-1), 3.97 (d, 0.5H, *J* = 9.1Hz, H-8a), 3.88-3.70(m, 3.5H, H-6, H-9, H-8a'), 3.68-3.40 (m, 5H, H-2, H-3, H-4, H-5, H-8b, H8b') 3.35 (m, 3H, OCH_3), 3.21 (s, 4H, OH), 1.40-1.25 (m, 26H. H-hexadecyl ether), 0.87 (t, 3H, *J* = 6.8 Hz, CH_3)

^{13}CNMR (75 MHz, $CDCl_3$) :

δ: 99.8 (C1+C1'), 84.3 (C3), 83.6 (C3'), 78.0 (C8), 72.5 (C2), 72.4 (C2'), 71.6 (C5), 71.4 (C5'), 71.1 (C9+C9'), 70.3 (C4), 69.9 (C4'), 62.1 (C6), 62.0 (C6'), 55.5 (OCH_3), 33.1, 32.1, 29.9, 29.7, 29.5, 25.7, 25.6, 22.8, 14.3

m/z (HRMS) :

calcd for $C_{23}H_{46}O_7Na$: 457.3136; found: 457.3128

D. 1. 2 Synthesis of 4-*O*-(2-hydroxyalkyl)-α-D-glucopyranosides

Methyl 4,6-*O*-benzylidene-α-D-glucopyranoside was reacted with benzyl bromide in the presence of NaH/DMF followed by selective reductive opening of the benzylidene ring with $NaBH_3CN/CH_3SO_3H$/THF to give methyl 2,3,6-tri-*O*-benzyl-α-D-glucopyranoside**.** It was reacted with 1, 2-epoxyalkanes in the presence of DABCO/DMAP/DMSO to yield benzylated 4-*O*-(2-hydroxyalkyl)-ethers of methyl glucoside, which were deprotected by Pd-catalysed hydrogenation in MeOH-EtOAc to afford methyl 4-*O*-(2-hydroxyalkyl)-α-D-glucopyranosides

Methyl 4-O-(2-hydroxyoctyl)-α-D-glucopyranoside (101a)

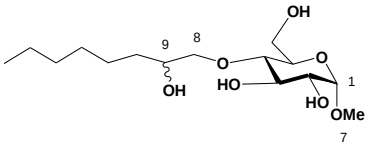

Cette thèse est accessible à l'adresse : http://theses.insa-lyon.fr/publication/2013ISAL0001/these.pdf
© [R. Xu], [2013], INSA de Lyon, tous droits réservés

Colorless soft matter

^{1}HNMR (300 MHz, $CDCl_3$) :

δ: 4.72 (d, 1H, *J* = 3.6Hz, H-1), 4.08 (s, 4H, OH), 3.86-3.64 (m, 5H, H-3, H-6, H-8a, H-8a', H-9), 3.60-3.45 (m, 3H, H-2, H-5, H-8b, H-8b'), 3.42-3.39 (m, 1H, H-4), 3.36 (m, 3H, OCH_3), 1.39-1.24 (m, 10H, H-octyl ether), 0.85 (t, 3H, *J* = 6.9 Hz, CH_3)

^{13}CNMR (75 MHz, $CDCl_3$) :

δ: 99.7 (C1+C1'), 79.5 (C4), 78.0 (C4'), 77.9 (C8), 76.2 (C8'), 74.0 (C3), 73.8 (C3'), 72.4 (C2), 72.3 (C2'), 72.1 (C9), 71.2 (C5), 71.1 (C5'), 70.9 (C9'), 61.5 (C6+C6'), 55.3 (OCH_3), 33.1, 32.9, 31.9, 29.5, 25.8, 25.6, 22.8, 14.1

m/z (HRMS) :

calcd for $C_{15}H_{30}O_7Na$: 345.1884; found: 345.1881

Methyl 4-O-(2-hydroxydecyl)-α-D-glucopyranoside (101b)

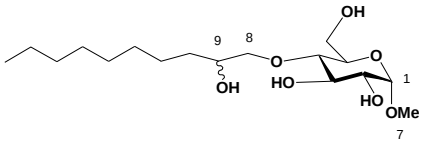

Colorless soft matter

^{1}HNMR (400 MHz, $CDCl_3$) :

δ: 4.76 (d, 1H, *J* = 3.6 Hz, H-1), 3.90 (s, 4H, OH), 3.88-3.65 (m, 5H, H-3, H-6, H-8a, H-8a', H-9), 3.61-3.45 (m, 3H, H-2, H-5, H-8b, H-8b'), 3.46-3.38 (m, 1H, H-4), 3.39 (s, 3H, OCH_3), 1.41-1.25 (m, 14H, H-decyl ether), 0.86 (t, 3H, *J* = 6.8 Hz, CH_3)

^{13}CNMR (100 MHz, $CDCl_3$) :

Cette thèse est accessible à l'adresse : http://theses.insa-lyon.fr/publication/2013ISAL0001/these.pdf
© [R. Xu], [2013], INSA de Lyon, tous droits réservés

δ: 99.4 (C1), 99.3 (C1'), 79.6 (C4), 78.1 (C4'), 77.4 (C8), 76.4 (C8'), 74.5 (C3), 72.8 (C3'), 72.7 (C2), 72.6 (C2'), 72.3 (C9), 71.2 (C5), 71.1 (C5'), 70.9 (C9'), 61.7 (C6), 61.6 (C6'), 55.5 (OCH_3), 33.1, 32.9, 32.0, 29.8, 29.7, 29.4, 25.8, 25.6, 22.8, 14.2

m/z (HRMS) :

calcd for $C_{17}H_{34}O_7Na$: 373.2197; found: 373.2188

Methyl 4-O-(2-hydroxydodecyl)-α-D-glucopyranoside (101c)

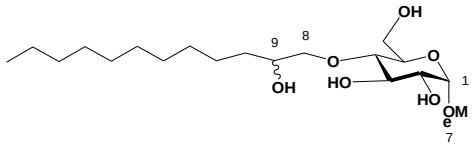

White solid

^{1}HNMR (300 MHz, $CDCl_3$) :

δ: 4.72 (d, 1H, *J* = 3.6 Hz, H-1), 3.85-3.67 (m, 5H, H-3, H-6, H-8a, H-8a', H-9), 3.63-3.45 (m, 3H, H-2, H-5, H-8b, H-8b'), 3.46-3.28 (m, 1H, H-4), 3.39 (s, 3H, OCH_3), 1.40-1.23 (m, 18H, H-dodecyl ether), 0.86 (t, 3H, *J* = 6.9 Hz, CH_3)

^{13}CNMR (75 MHz, $CDCl_3$) :

δ: 99.6 (C1), 79.7 (C4), 78.0 (C4'), 76.2 (C8'), 74.2 (C3), 73.9 (C3'), 72.5 (C2), 72.4 (C2'), 72.2 (C9), 71.2 (C5), 71.1(C5'), 70.9 (C9'), 61.6 (C6+C6'), 55.4 (OCH_3), 33.1, 32.9, 32.0, 29.9, 29.8, 29.5, 25.9, 25.7, 22.8, 14.2

m/z (HRMS) :

calcd for $C_{19}H_{38}O_7Na$: 401.2510; found: 401.2525

Methyl 4-O-(2-hydroxytetradecyl)-α-D-glucopyranoside (101d)

Cette thèse est accessible à l'adresse : http://theses.insa-lyon.fr/publication/2013ISAL0001/these.pdf
© [R. Xu], [2013], INSA de Lyon, tous droits réservés

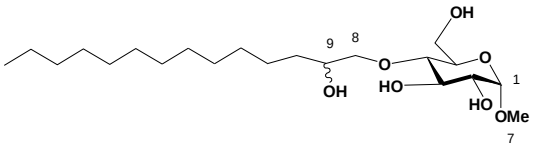

White solid

^{1}HNMR (400 MHz, $CDCl_3$) :

δ: 4.75 (d, 1H, *J* = 3.1Hz, H-1), 3.88-3.67 (m, 5H, H-3, H-6, H-8a, H-8a', H-9), 3.62-3.50 (m, 3H, H-2, H-5, H-8b, H-8b'), 3.45 (m, 1H, H-4), 3.40 (s, 3H, OCH_3), 3.35 (s, 4H, OH), 1.42-1.25 (m, 22H, H-tetradecyl ether), 0.87 (t, 3H, *J* = 6.9 Hz, CH_3)

^{13}CNMR (100 MHz, $CDCl_3$) :

δ: 99.6 (C1), 99.5 (C1'), 79.7 (C4), 78.8 (C4'), 77.9 (C8), 76.3 (C8'), 74.5 (C3), 74.2 (C3'), 72.7 (C2), 72.6 (C2'), 72.3 (C9), 71.2 (C5), 71.1 (C5'), 70.9 (C9'), 61.8 (C6), 61.7 (C6'), 55.5 (OCH_3), 33.1, 32.9, 29.9, 29.8, 29.5, 25.8, 25.7, 22.8, 14.3

m/z (HRMS) :

calcd for $C_{21}H_{42}O_7Na$: 429.2823; found: 429.2823

Methyl 4-O-(2-hydroxyhexadecyl)-α-D-glucopyranoside (101e)

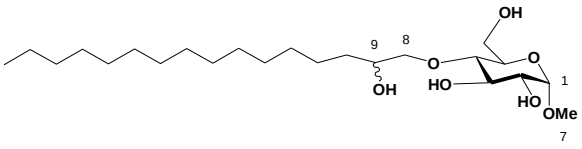

Colorless soft matter

^{1}HNMR (400 MHz, $CDCl_3$) :

δ: 4.75 (d, 1H, *J* = 3.6 Hz, H-1), 3.88-3.68 (m, 5H, H-3, H-6, H-8a, H-8a', H-9), 3.63-3.45(m, 3H, H-2, H-5, H-8b, H-8b'), 3.45-3.38 (m, 1H, H-4), 3.40 (s, 3H, OCH_3), 3.22 (s, 4H, OH), 1.42-1.25 (m, 26H, H-hexadecyl ether), 0.87 (t, 3H, *J* = 6.8 Hz, CH_3)

Cette thèse est accessible à l'adresse : http://theses.insa-lyon.fr/publication/2013ISAL0001/these.pdf
© [R. Xu], [2013], INSA de Lyon, tous droits réservés

^{13}CNMR (75 MHz, $CDCl_3$) :

δ: 99.5 (C1), 99.4 (C1'), 79.7 (C4), 78.2 (C4'), 77.9 (C8), 76.3 (C8'), 74.6 (C3), 74.3 (C3'), 72.7 (C2), 72.6 (C2'), 72.3 (C9), 71.2 (C5), 71.1 (C5'), 70.9 (C9'), 61.8 (C6), 61.7 (C6'), 55.5 (OCH_3), 33.1, 32.9, 32.1, 29.9, 29.8, 29.7, 29.5, 25.9, 25.7, 22.8, 14.3

m/z (HRMS) :

calcd for $C_{23}H_{46}O_7Na$: 457.3136; found: 457.3128

D. 1. 3 Synthesis of 6-*O*-(2-hydroxyalkyl)-α-D-glucopyranosides

Tritylation and subsequent benzylation of methyl α-D-glucopyranoside afforded methyl 2,3,4-tri-*O*-benzyl-6-trityl-α-D-glucopyranoside which was deprotected under acidic conditions to give compound (only OH-6 is available). The structure of this compound was confirmed by comparison to an identical compound obtained from an alternative reductive opening of the benzylidene. It was reacted with 1,2-epoxyalkanes in presence of DABCO and DMAP in DMSO at 110 ^{o}C for 16 h followed by catalytic hydrogenation to give the desired methyl 6-*O*-(2-hydroxyalkyl)-α-D-glucopyranosides

Methyl 6-O-(2-hydroxyoctyl)-α-D-glucopyranoside (105a)

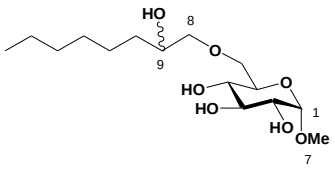

Colorless soft matter

^{1}HNMR (400 MHz, $CDCl_3$) :

δ: 4.76 (d, 1H, *J* = 2.4 Hz, H-1), 3.80-3.63 (m, 2.5H, H-6, H-9,), 3.63-3.55 (m, 2H, H-3,H-5), 3.55-3.47 (m, 1.5H, H-8a, H-4), 3.47-3.32 (m, 2.5H, H-2, H-8a', H-8b', H9'), 3.40 (s, 3H, OCH_3), 3.27 (t, 0.5H, *J* = 9.3Hz, H-8b), 1.41 -1.22 (m, 10H, H-octyl ether), 0.87 (t, 3H, *J* = 7.2 Hz, CH_3)

Cette thèse est accessible à l'adresse : http://theses.insa-lyon.fr/publication/2013ISAL0001/these.pdf
© [R. Xu], [2013], INSA de Lyon, tous droits réservés

^{13}CNMR (100 MHz, $CDCl_3$) :

δ: 99.9 (C1), 99.8 (C1'), 76.5 (C8), 76.2 (C8'), 74.8 (C3), 74.3 (C3'), 72.1 (C2+C2'), 70.9 (C5), 70.8 (C5'), 70.8 (C9), 70,3 (C9), 70,3 (C6), 70.2 (C4), 70.2 (C6'), 69.7 (C4'), 55.4 (OCH_3), 33.2, 31.9, 29.5, 25.7, 25.6, 22.8, 14.2

m/z (HRMS) :

calcd for $C_{15}H_{30}O_7Na$: 345.1884; found: 345.1886

Methyl 6-O-(2-hydroxydecyl)-α-D-glucopyranoside (105b)

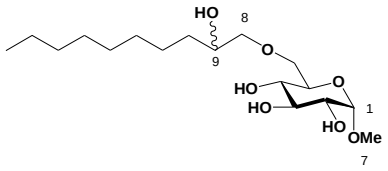

White solid

^{1}HNMR (300 MHz, $CDCl_3$) :

δ: 4.75 (m, 1H, H-1), 3.80-3.63 (m, 2.5H, H-6, H-9,), 3.63-3.55 (m, 2H, H-3, H-5), 3.55-3.47 (m, 1.5H, H-8a, H-4), 3.47-3.32 (m, 2.5H, H-2, H-8a', H-8b', H9'), 3.33 (s, 3H, OCH_3), 3.27 (t, 0.5H, *J* =9.3Hz, H-8b), 1.40-1.20 (m, 14H, H-dectyl ether), 0.85 (t, 3H, *J* = 6.3 Hz, CH_3)

^{13}CNMR (75 MHz, $CDCl_3$) :

δ: 99.9 (C1), 99.8 (C1'), 76.4 (C8), 76.2 (C8'), 74.1 (C3), 74.0 (C3'), 71.9 (C2), 70.9 (C5), 70.8 (C5'), 70.6 (C9), 70.1 (C9'+C6+C6'+C4), 69.5 (C4'), 55.3 (OCH_3), 33.2, 32.0, 29.8, 29.7, 29.4, 25.8, 25.7, 22.7, 14.2

m/z (HRMS) :

calcd for $C_{17}H_{34}O_7Na$: 373.2197; found: 373.2199

Methyl 6-O-(2-hydroxydodecyl)-α-D-glucopyranoside (105c)

Cette thèse est accessible à l'adresse : http://theses.insa-lyon.fr/publication/2013ISAL0001/these.pdf
© [R. Xu], [2013], INSA de Lyon, tous droits réservés

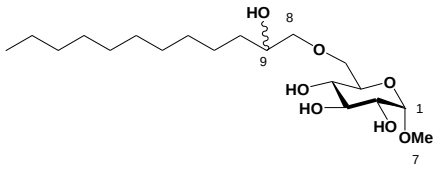

Colorless soft matter

^{1}HNMR (300 MHz, $CDCl_3$) :

δ: 4.74 (m, 1H, H-1), 3.85-3.63 (m, 2.5H, H-6, H-9,), 3.63-3.55 (m, 2H, H-3, H-5), 3.55-3.47 (m, 1.5H, H-8a, H-4), 3.47-3.32 (m, 2.5H, H-2, H-8a', H-8b', H9'), 3.36 (s, 3H, OCH_3), 3.23 (t, 0.5H, *J* = 9.3 Hz, H-8b), 1.40-1.20 (m, 18H, H-dodecyl ether), 0.84 (t, 3H, *J* = 6.9 Hz, CH_3)

^{13}CNMR (75 MHz, $CDCl_3$) :

δ: 99.9 (C1), 99.8 (C1'), 76.4 (C8), 76.2 (C8'), 74.1 (C3), 74.0 (C3'), 71.9 (C2+C2'), 70.9 (C5), 70.8 (C5'), 70.6 (C9), 70.2 (C9'+C6+C6'), 69.5 (C4+C4'), 55.3 (OCH_3), 33.2, 32.0, 29.9, 29.7, 29.4, 25.8, 25.7, 22.7, 14.2

m/z (HRMS) :

calcd for $C_{19}H_{38}O_7Na$: 401.2510; found: 401.2504

Methyl 6-O-(2-hydroxytetradecyl)-α-D-glucopyranoside (105d)

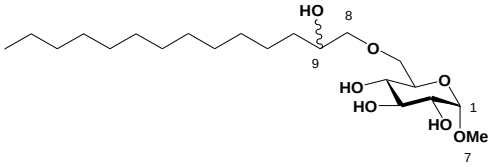

White solid

^{1}HNMR (300 MHz, $CDCl_3$) :

Cette thèse est accessible à l'adresse : http://theses.insa-lyon.fr/publication/2013ISAL0001/these.pdf
© [R. Xu], [2013], INSA de Lyon, tous droits réservés

δ: 4.74 (m, 1H, H-1), 3.90-3.63 (m, 2.5H, H-6, H-9), 3.63-3.55(m, 2H, H-3, H-5), 3.55-3.47 (m, 1.5H, H-8a, H-4), 3.47-3.30 (m, 2.5H, H-2, H-8a', H-8b', H9'), 3.36 (s, 3H, OCH_3), 3.25 (t, 0.5H, *J* = 9.3 Hz, H-8b), 1.42-1.20 (m, 22H, H-tetradecyl ether), 0.87 (t, 3H, *J* = 6.9 Hz, CH_3)

^{13}CNMR (75 MHz, $CDCl_3$) :

δ: 100.0 (C1), 99.9 (C1'), 76.5 (C8), 76.3 (C8'), 74.2 (C3), 74.1 (C3'), 72.0 (C2+C2'), 71.0 (C5), 70.9 (C5'), 70.7(C9), 70.3 (C9'+C6), 70.2 (C6'), 69.6 (C4+C4'), 55.4 (OCH_3), 33.3, 32.1, 30.0, 29.9, 29.8, 29.5, 25.8, 25.7, 22.8, 14.2

m/z (HRMS) :

calcd for $C_{21}H_{42}O_7Na$: 429.2823; found: 429.2804

Methyl 6-O-(2-hydroxyhexadecyl)-α-D-glucopyranoside (105e)

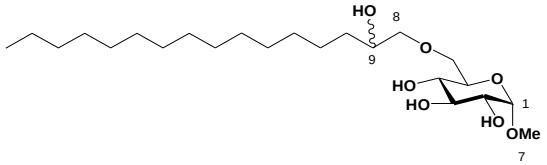

Colorless soft matter

^{1}HNMR (300 MHz, $CDCl_3$) :

δ: 4.75 (s, 1H, H-1), 3.85-3.63 (m, 2.5H, H-6, H-9), 3.63-3.55 (m, 2H, H-3, H-5), 3.55-3.47 (m, 1.5H, H-8a, H-4), 3.47-3.32 (m, 2.5H, H-2, H-8a', H-8b', H9'), 3.40 (s, 3H, OCH_3), 3.26 (t, 0.5H, *J* = 9.3 Hz, H-8b), 1.41-1.20 (m, 26H, H-hexadecyl ether), 0.87 (t, 3H, *J* = 6.9 Hz, CH_3)

^{13}CNMR (75 MHz, $CDCl_3$) :

δ: 100.0 (C1), 99.9 (C1'), 76.5 (C8), 76.3 (C8'), 74.2 (C3), 74.1 (C3'), 72.1 (C2+C2'), 70.9 (C5+C5'), 70.7 (C9), 70.3 (C9'+C6), 70.2 (C6'), 69.7 (C4+C4'), 55.4 (OCH_3), 33.3, 32.1, 29.9, 29.8, 29.5, 25.8, 25.7, 22.8, 14.3

m/z (HRMS) :

calcd for $C_{23}H_{46}O_7Na$: 457.3136; found: 457.3121

Cette thèse est accessible à l'adresse : http://theses.insa-lyon.fr/publication/2013ISAL0001/these.pdf
© [R. Xu], [2013], INSA de Lyon, tous droits réservés

D. 2 Glucosteroids

D. 2. 1 Synthesis for the C4 linker compound

To a solution of (*N*-Allylcarbamoyl) methyl 3,4,6-tri-*O*-acetyl-α-D-glucopyranoside (100 mg, 0.24 mmol) and allyl cholesteryl ether (530 mg, 1.24 mmol) in dichloromethane (1.5 mL), Grubbs-Hoveyda 2nd generation catalyst (5%, 0.0078 g, 0.0124 mmol) was added. The reaction was stirred under nitrogen at RT for 24h to be directly chromatographied on silica gel using a toluene/acetone (7:3) eluting mixture and gave compound **109** (0.143 g, 72%, E:Z = 23:2) as a yellow foam

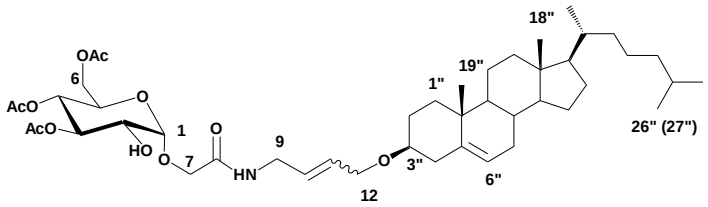

Yellow foam

^{1}HNMR (500 MHz, $CDCl_3$) :

δ: 7.36 (t, 1 H, *J* = 5.4 Hz, N-H), 5.74 (m, 2H, H-10, H-11), 5.33 (m, 1H, H-6”), 5.26 (t, 1H, *J* = 9.6 Hz, H-3), 5.00 (t, 1H, *J* = 9.6 Hz, H-4), 4.89 (t, 1H, *J* = 9.4 Hz, H-3), 4.89 (d, 1H, *J* = 3.0 Hz, H-1), 4.28 (dd, 1H, *J* = 4.6 and 12.3 Hz, H-6a), 4.22 (d, 1H, *J* = 15.9 Hz, H-7a), 4.09-3.96 (m, 6H, H-6b, H-7b, H-5, CH_2-12, H-9a), 3.80-3.77 (m, 3H, H-9b, H-2, OH), 3.10 (m, 1H, H-3”), 2.34 (m, 1H, H-4”a), 2.19 (m, 1H, H-4”b), 2.08, 2.06, 2.02 (3s, 9 H, 3 x CH_3-Ac), 2.01-0.84 (m, 38 H, H-Cholesterol), 0.66 (s, 1H, CH_3-18”)

^{13}CNMR (125 MHz, $CDCl_3$) :

δ: 171.4, 170.7, 169.7, 168.7 (3xC=O in Ac, C8), 140.7 (C5”), 128.8, 129.9 (C10, C11), 122.0 (C6”), 99.2 (C1), 79.1 (C3”), 73.4 (C3), 70.3 (C2), 68.2 (C5), 68.0 (C4), 67.9 (C12), 67.4 (C7), 61.9 (C6), 56.8 (C14”), 56.2 (C17”), 50.2 (C19”), 42.4 (C13”), 40.3 (C9), 39.8 (C16”), 39.6 (C24”), 39.1 (C4”), 37.2 (C1”), 36.9 (C10”), 36.3 (C22”), 35.9 (C20”), 32.1 (C7”), 32.0 (C8”), 28.5 (C2”), 28.3 (C12”), 28.1 (C25”), 24.4 (C15”), 23.9 (C23”), 22.9 (C26”), 22.6 (C27”), 21.2 (C11”), 21.0, 20.8, 20.7 (3***C***H_3CO), 19.4 (C19”), 18.8 (C21”), 11.9 (C18”)

Cette thèse est accessible à l'adresse : http://theses.insa-lyon.fr/publication/2013ISAL0001/these.pdf
© [R. Xu], [2013], INSA de Lyon, tous droits réservés

Elemental analysis:

Found: C, 67.24; H, 9.22; N, 2.03. $C_{45}H_{71}O_{11}N$ requires C, 67.39; H, 8.92; N, 1.75

m/z (ESI) :

824.4 ($M + Na^+$)

$[\alpha]_D^{20}$

+52 (c 0.9 in $CHCl_3$)

To a solution of neoglucolipid **109** (420 mg, 0.52 mmol) in THF (5 mL), 10% Pd on charcoal (60 mg) was added. The suspension was stirred under H_2 and the reaction was carefully monitored by TLC. The reaction was stopped after 2 hours when only one spot remained on the TLC. The suspension was filtrated over a silica gel pad and the solvent was evaporated. The obtained crude residue was chromatographied on silica gel using a toluene/acetone (7/3) mixture and gave compound **110** (0.345 mg, 83%) as a white solid.

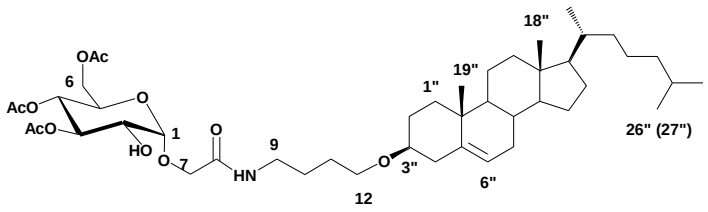

White solid

^{1}HNMR (300 MHz, $CDCl_3$) :

δ: 7.66 (t,1H, *J* = 5.4 Hz, N-H), 5.29-5.23 (m, 2H, H-6”, H-3), 4.95 (t, 1H, *J* = 9.6 Hz, H-4), 4.83 (d, 1H, *J* = 3.5 Hz, H-1), 4.28-3.99 (m, 5H, H-5, H-6a, H-6b, H-7a, H-7b), 3.76 (dd, 1H, *J* = 3.5 and 9.8 Hz, H-2), 3.51-3.38 (m, 3H, H-9a, CH_2-12), 3.14-3.06 (m, 2H, H-9b, H-3”), 2.31 (m, 1H, H-4”a), 2.10 (m, 1H, H-4”b), 2.03, 1.99, 1.98 (3s, 9H, 3 x CH_3-Ac), 1.89-0.80 (m, 43H, H-Cholesterol, CH_2-10, CH_2-11), 0.63 (s, 1H, CH_3-18”)

^{13}CNMR (75 MHz, $CDCl_3$) :

Cette thèse est accessible à l'adresse : http://theses.insa-lyon.fr/publication/2013ISAL0001/these.pdf
© [R. Xu], [2013], INSA de Lyon, tous droits réservés

δ: 170.6, 170.5, 169.5, 169.2 (3x***C***=O in Ac, C8), 140.3 (C5"), 121.8 (C6"), 99.4 (C1), 79.2 (C3"), 72.7 (C3), 69.3 (C2), 68.1 (C5), 67.9 (C4), 67.4 (C12, C7), 61.6 (C6), 56.6 (C14"), 56.0 (C17"), 50.0 (C9"), 42.2 (C13"), 39.6 (C9), 39.4 (C16"), 38.8 (C24"), 38.5 (C4"), 37.1 (C1"), 36.7 (C10"), 36.1 (C22"), 35.7 (C20"), 31.8 (C7"), 31.7 (C8"), 28.3 (C2"), 28.1 (C12"), 27.9 (C25"), 27.1 (C11), 25.7 (C10), 24.1 (C15"), 23.7 (C23"), 22.7 (C26"), 22.5 (C27"), 20.9 (C11"), 20.7, 20.6, 20.5 (3***C***H_3CO), 19.3 (C18"), 18.6 (C21"), 11.7 (C19")

m/z :

826.0 ($M + Na^+$)

$[\alpha]_D^{20}$

+55 (c 0.5 in CH_3Cl)

Elemental analysis:

Found: C, 67.21; H, 9.20; N, 2.01. $C_{45}H_{73}O_{11}N$ requires C, 67.22; H, 9.15; N, 1.74

D. 2. 2 Synthese of C6, C8, C10, C12 linker

D.2.2.1 Synthesis for cholest-5-en-3β-yl ω-azidoalkyl ether

To a solution of cholest-5-en-3β-yl ω-hydroxyalkyl ether and Et_3N (1.2 eq.) in CH_2Cl_2 (20 mL) 0°C, MsCl (1.2 eq.) was added. The mixture was maintained at 0°C for 10 min and was then stirred at RT for 15h. Water (20 mL) was added and the mixture was extracted with CH_2Cl_2 (3x15 mL). The organic layers were combined, washed with H_2O (2x20 mL) and dried over Na_2SO_4. After evaporation, the obtained crude residue was dissolved in DMF (20 mL) and NaN_3 (1.3 eq.) was added and the solution was stirred at 60°C for 15h. Water (10 mL) was added and the mixture was extracted with CH_2Cl_2 (3x10 mL). The organic layers were combined, washed with H_2O (2x20mL) and dried over Na_2SO_4. After evaporation, the obtained crude residue was chromatographied on silica gel using a pentane/CH_2Cl_2 (3/2) mixture and gave corresponding cholest-5-en-3β-yl ω-azidoalkyl ether

Cholest-5-en-3β-yl 6-azidohexyl ether (114a)

Cette thèse est accessible à l'adresse : http://theses.insa-lyon.fr/publication/2013ISAL0001/these.pdf
© [R. Xu], [2013], INSA de Lyon, tous droits réservés

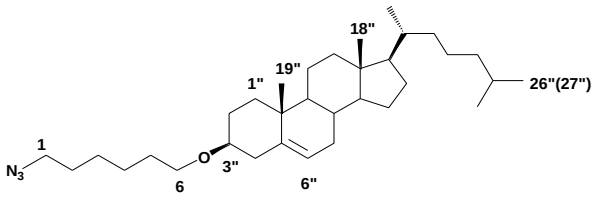

80%, White solid

^{1}HNMR (300 MHz, $CDCl_3$) :

δ : 5.30 (m,1H, H-6”), 3.45 (t, 2H, *J* = 6.7 Hz, H-6), 3.26 (t, 2H, *J* = 6.9 Hz, H-1), 3.14 (m, 1H, H-3”), 2.38-2.10 (m, 2H, H-4”), 2.00-0.80 (m, 47H, H-Cholesterol, CH_2-2 to CH_2-5), 0.64 (s, 3H, CH_3-18”);

^{13}CNMR (75 MHz, $CDCl_3$) :

δ: 141.3 (C5”), 121.6 (C6”), 79.2 (C3”), 68.0 (C6), 56.9 (C14”), 56.3 (C17”), 51.6 (C1), 50.4 (C9”), 42.5 (C13”), 40.0 (C16”), 39.7 (C24”), 39.4 (C4”), 37.4 (C1”), 37.1(C10”), 36.3 (C22”), 35.9 (C20”), 32.1 (C7”), 32.0 (C8”), 30.2, 29.0 (*C*-hexyl), 28.6 (C2”), 28.4 (C12”), 28.2 (25”), 26.7, 26.0 (*C*-hexyl), 24.4 (C15”), 24.0 (C23”), 23.0 (C26”), 22.7 (C27”), 21.2 (C11”), 19.5 (C19”), 18.9 (C21”), 12.0 (C18”)

m/z (HRMS):

534.4398 ($M + Na^+$, $C_{33}H_{57}ON_3Na$ requires 534.4394).

$[\alpha]_D^{20}$

-23 (c 0.9 in CH_2Cl_2)

Cholest-5-en-3β-yl 8-azidooctyl ether (114b)

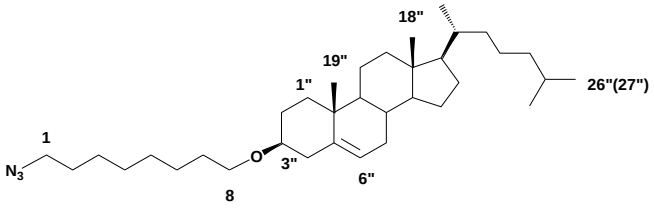

White solid

Cette thèse est accessible à l'adresse : http://theses.insa-lyon.fr/publication/2013ISAL0001/these.pdf
© [R. Xu], [2013], INSA de Lyon, tous droits réservés

^{1}HNMR (300 MHz, $CDCl_3$) :

δ: 5.34 (m, 1H, H-6”), 3.45 (t, 2H, *J* = 6.8 Hz, H-8), 3.25 (t, 2H, *J* = 6.9 Hz, H-1), 3.12 (m, 1H, H-3”), 2.35-2.05 (m, 2H, H-4”), 2.00-0.75 (m, 51H, H-Cholesterol, CH_2-2 to CH_2-7), 0.61 (s, 3H, CH_3-18”)

^{13}CNMR (75 MHz, $CDCl_3$) :

δ: 141.3 (C5”), 121.6 (C6”), 79.2 (C3”), 68.2 (C8), 56.9 (C14”), 56.3 (C17”), 51.6 (C1), 50.4 (C9”), 42.5 (C13”), 40.0 (C16”), 39.7 (C24”), 39.4 (C4”), 37.4 (C1”), 37.1 (C10”), 36.3 (C22”), 35.9 (C20”), 32.1 (C7”), 32.1 (C8”), 30.3, 29.5, 29.2, 29.0 (*C*-octyl), 28.6 (C2”), 28.4 (C12”), 28.2 (C25”), 26.7 , 26.3 (*C*-octyl), 24.4 (C15”), 24.0 (C23”), 22.7 (C26”+27”), 21.2 (C11”), 19.5 (C19”), 18.9 (C21”), 12.0 (C18”)

m/z (HRMS) :

562.4704 ($M + Na^+$, $C_{35}H_{61}ON_3Na$ requires 562.4707)

$[\alpha]_D^{20}$

-24 (*c* 0.6 in CH_2Cl_2)

FTIR :

2095 cm^{-1} (N_3)

Cholest-5-en-3β-yl 10-azidodecyl ether (114c)

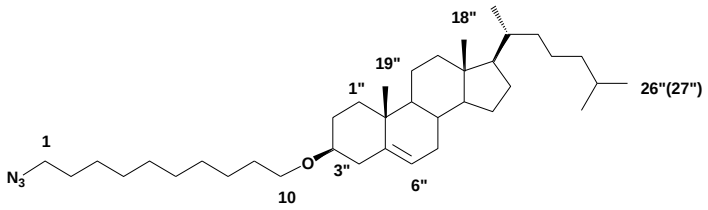

White solid

^{1}HNMR (300 MHz, $CDCl_3$) :

Cette thèse est accessible à l'adresse : http://theses.insa-lyon.fr/publication/2013ISAL0001/these.pdf
© [R. Xu], [2013], INSA de Lyon, tous droits réservés

δ: 5.27 (m, 1H, H-6”), 3.37 (t, 2H, *J* = 6.8 Hz, H-10), 3.27 (t, 2H, *J* = 7.0 Hz, H-1), 3.05 (m, 1H, H-3”), 2.34-2.06 (m, 2H, H-4”), 2.42-0.75 (m, 55H, H-Cholesterol, CH_2-2 to CH_2-9), 0.61 (s, 3H, CH_3-18”)

^{13}CNMR (75 MHz, $CDCl_3$) :

δ: 141.3 (C5”), 121.5 (C6”), 79.1 (C3”), 68.2 (C10), 56.9 (C14”), 56.3 (C17”), 51.6 (C1), 50.4 (C9”), 42.5 (C13”), 40.0 (C16”), 39.7 (C24”), 39.4 (C4”), 37.4 (C1”), 37.1 (C10”), 36.3 (C22”), 35.9 (C20”), 32.1 (C7”), 32.0 (C8”), 30.3, 29.6, 29.6, 29.5, 29.3, 29.0 (*C*-decyl), 28.6 (C12”), 28.1 (C 12+25”), 26.7, 26.3 (*C*-decyl), 24.4 (C15”), 24.0 (C23”), 23.0 (C26”), 22.7 (C26”), 21.2 (C11”), 19.5 (C19”), 18.9 (C21”), 12.0 (C18”)

m/z (HRMS) :

590.5018 ($M + Na^+$, $C_{37}H_{65}ON_3Na$ requires 590.5020)

$[\alpha]_D^{20}$

-25 (*c* 1.2 in CH_2Cl_2)

FTIR :

2095 cm^{-1} (N_3)

Cholest-5-en-3β-yl 12-azidododecyl ether (114d)

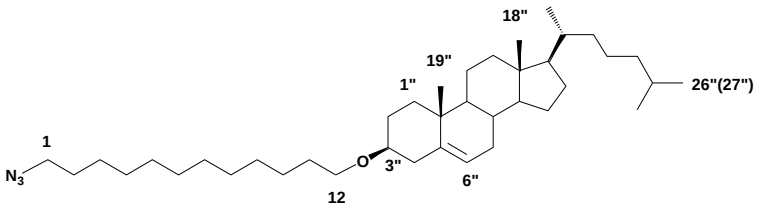

White solid

^{1}HNMR (300 MHz, $CDCl_3$) :

δ: 5.27 (m, 1H, H-6”), 3.37 (t, 2H, *J* = 6.8 Hz, H-12), 3.18 (t, 2H, *J* = 7.0 Hz, H-1), 3.05 (m, 1H, H-3”), 2.33-2.05 (m, 2H, H-4”), 1.99-0.76 (m, 59H, H-Cholesterol, CH_2-2 to CH_2-11), 0.61 (s, 3H, CH_3-18”)

Cette thèse est accessible à l'adresse : http://theses.insa-lyon.fr/publication/2013ISAL0001/these.pdf
© [R. Xu], [2013], INSA de Lyon, tous droits réservés

^{13}CNMR (75 MHz, $CDCl_3$) :

δ: 141.3 (C5”), 121.5 (C6”), 79.0 (C3”), 68.2 (C12), 56.9 (C14”), 56.3 (C17”), 51.6 (C1), 50.3 (C9”), 42.4 (C13”), 39.9 (C16”), 39.6 (C24”), 39.3 (C4”), 37.4 (C1”), 37.0 (C10”), 36.3 (C22”), 35.9 (C20”), 32.1 (C7”), 32.0 (C8”), 30.3, 29.7, 29.6, 29.6, 29.6, 29.6, 29.2, 28.9 (*C*-dodecyl), 28.6 (C2”), 28.3 (C12”), 28.1 (25”), 26.8, 26.3 (*C*-dodecyl), 24.4 (C15”), 23.9 (C23”), 22.9 (C26”), 22.7 (C27”), 21.2 (C11”), 19.5 (C19”), 18.8 (C21”), 12.0 (C18”)

m/z (ESI)

596.4 ($M+H^+$)

$[\alpha]_D^{20}$

-27 (*c* 0.5 in CH_2Cl_2)

FTIR :

2094 cm^{-1} (N_3)

D.2.2.2 Cholest-5-en-3β-yl ω-aminoalkyl ether

The cholest-5-en-3β-yl ω-azidoalkyl ether (0.1 mmol) was dissolved in THF/H_2O (2.5 ml, 4:1) and triphenylphosphine (1.1 eq.) was added. The mixture was stirred at 50℃ with addition of 0.1% of NEt_3. After completion of the reaction, monitored by TLC (9:1, DCM: MeOH), the solvent was evaporated and the crude was purified by column chromatography on silica-gel (9:1, DCM: MeOH with 0.5% vol. of NEt_3).

Cholest-5-en-3β-yl 6-aminohexyl ether (115a)

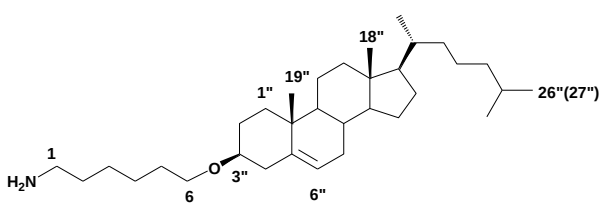

Yellow soft matter

Cette thèse est accessible à l'adresse : http://theses.insa-lyon.fr/publication/2013ISAL0001/these.pdf
© [R. Xu], [2013], INSA de Lyon, tous droits réservés

^{1}HNMR (300 MHz, $CDCl_3$) :

δ: 5.34-5.33 (m, 1H, H-6”), 3.45 (t, 2H, *J* = 6.6 Hz, H-6), 3.11 (m, 1H, H-3”), 2.71 (t, 2H, *J* = 6.9 Hz, H-1), 2.45-2.00 (m, 4H, H-4”, NH_2), 2.00-0.80 (m, 47H, H-Cholesterol, CH_2-2 to CH_2-5), 0.64 (s, 3H, CH_3-18”);

^{13}CNMR (75 MHz, $CDCl_3$) :

δ: 141.3 (C5”), 121.6 (C6”), 79.1 (C3”), 68.1 (C6), 56.9 (C14”), 56.3 (C17”), 50.4 (C9”), 42.5 (C13”), 39.9 (C1), 39.9 (C16”), 39.7 (C24”), 39.4 (C4”), 37.4 (C1”), 37.0 (C10”), 36.3 (C22”), 35.9 (C20”), 32.1 (C7”), 32.0 (C8”), 30.3, 29.6 (*C*-hexyl), 28.6 (C2”), 28.4 (C12”), 28.2 (C25”), 26.8, 26.2 (*C*-hexyl), 24.4 (C15”), 24.0 (C23”), 23.0 (C26”), 22.7 (C27”), 21.2 (C11”), 19.5 (C19”), 18.9 (C21”), 12.0 (C18”)

m/z (ESI) :

486.3 ($M+H^+$)

$[\alpha]_D^{20}$

-29 (*c* 0.8 in CH_2Cl_2)

Cholest-5-en-3β-yl 8-aminooctyl ether (115b)

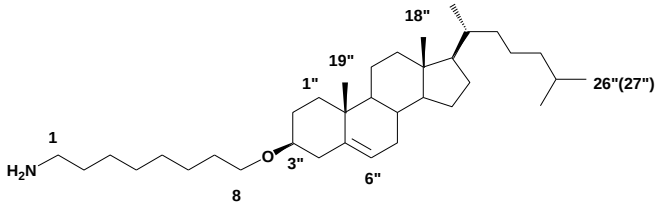

Yellow soft matter

^{1}HNMR (300 MHz, $CDCl_3$) :

δ: 5.34-5.33 (m, 1H, H-6”), 3.45 (t, 2H, *J* = 6.8 Hz, H-8), 3.12 (m, 1H, H-3”), 2.80-2.60 (m, 2H, H-1), 2.40-2.00 (m, 4H, H-4”, NH_2), 2.00-0.75 (m, 51H, H-Cholesterol, CH_2-2 to CH_2-7), 0.61 (s, 3H, CH_3-18”)

^{13}CNMR (75 MHz, $CDCl_3$) :

Cette thèse est accessible à l'adresse : http://theses.insa-lyon.fr/publication/2013ISAL0001/these.pdf
© [R. Xu], [2013], INSA de Lyon, tous droits réservés

δ: 141.3 (C5”), 121.5 (C6”), 79.1 (C3”), 68.3 (C8), 56.9 (C14”), 56.3 (C17”), 50.4 (C9”), 42.5 (C13”), 39.9 (C1+C16”), 39.7 (C24”), 39.4 (C4”), 37.4 (C1”), 37.0 (C10”), 36.3 (C22”), 35.9 (C20”), 32.1(C7”), 32.0 (C8”), 30.3, 29.6, 29.5 (*C*-octyl), 28.6 (C2”), 28.4 (C12”), 28.1(C25”), 26.9, 26.3 (*C*-octyl), 24.4 (C15”), 24.0 (C23”), 23.0 (C26”), 22.7 (C27”), 21.2 (C11”), 19.3 (C19”), 18.9 (C21”), 12.0 (C18”)

m/z (ESI):

514.3 ($M+H^+$)

Cholest-5-en-3β-yl-10-aminodecyl ether (115c)

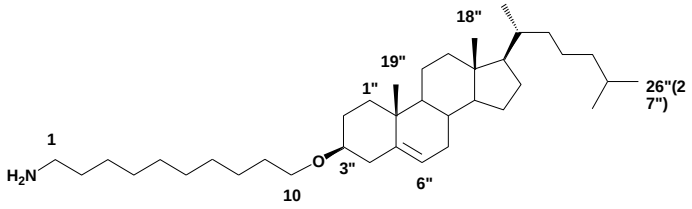

Yellow soft matter

^{1}HNMR (300 MHz, $CDCl_3$) :

δ: 8.30-7.62 (s, 2H, NH_2), 5.34-5.32 (m, 1H, H-6”), 3.43 (t, 2H, *J* = 6.8 Hz, H-10), 3.11 (m, 1H, H-3”), 3.02 (t, 2H, *J* = 7.7 Hz, H-1), 2.40-2.08 (m, 2H, H-4”), 2.08-0.75 (m, 55H, H- H-Cholesterol, CH_2-2 to CH_2-9), 0.67 (s, 3H, CH_3-18”)

Cholest-5-en-3β-yl-12-aminododecyl ether (115d)

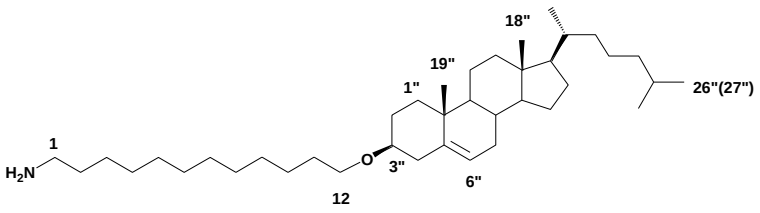

Yellow soft matter

Cette thèse est accessible à l'adresse : http://theses.insa-lyon.fr/publication/2013ISAL0001/these.pdf
© [R. Xu], [2013], INSA de Lyon, tous droits réservés

^{1}HNMR (300 MHz, $CDCl_3$) :

δ: 8.23 (s, 2H, NH_2), 5.35-5.30 (m, 1H, H-6”), 3.44 (t, 2H, *J* = 6.8 Hz, H-1), 3.11 (m, 1H, H-3”), 2.74 (s, 2H, H-12), 2.40-2.10 (m, 2H, H-4”), 2.10-0.75 (m, 59H, H-Cholesterol, CH_2-2 to CH_2-11), 0.67 (s, 3H, CH_3-18”)

^{13}CNMR (75 MHz, $CDCl_3$) :

δ: 141.6 (C5”), 121.7 (C6”), 79.3 (C3”), 68.5 (C12), 57.2 (C14”), 56.6 (C17”), 50.6 (C9”), 42.7 (C13”), 42.0 (C1), 40.1 (C16”), 39.9 (C24”), 39.6 (C4”), 37.7 (C1”), 37.3 (C10”), 36.6 (C22”), 36.2 (C20”), 32.5 (C7”), 32.3, 32.3, 30.6, 30.0, 29.8, 28.9, 28.9 (*C*- dodecyl), 28.6 (C2”), 28.6 (C12”), 28.4 (C25”), 27.2, 26.6 (*C*-dodecyl), 24.7 (C15”), 24.2 (C23”), 23.2 (C26”), 23.0 (C27”), 21.4 (C11”), 19.5 (C19”), 18.9 (C21”), 12.0 (C18”)

m/z (ESI):

584.4 ($M+Na^+$), 570.4 ($M+H^+$)

D.2.2.3 Ring opening of CMGL by cholest-5-en-3β-yl ω-aminoalkyl ether

To the cholest-5-en-3β-yl ω-aminoalkyl ether dissolved in anhydrous CH_2Cl_2 (*c* 2 M), the CMGl solid (1.3 eq.) was then added. After overnight of reaction (16h), the residue was purified by CCM using eluent of DCM/acetone (4/1) to obtain the pure compound.

Acetyl-Glu-L6-cholesterol (116)

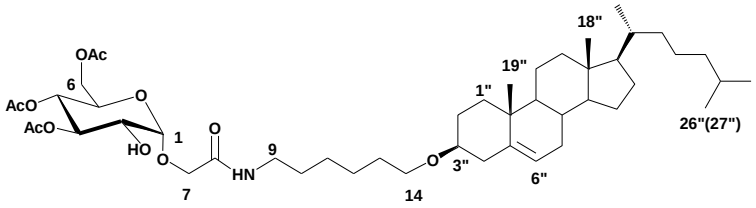

White solid

^{1}HNMR (300 MHz, $CDCl_3$) :

Cette thèse est accessible à l'adresse : http://theses.insa-lyon.fr/publication/2013ISAL0001/these.pdf
© [R. Xu], [2013], INSA de Lyon, tous droits réservés

δ: 7.44 (t, 1H, NH), 5.27 (m, 1H, H-6”), 5.21 (t, 1H, *J* = 9.8 Hz, H-3), 4.95 (t, 1H, *J* = 9.9 Hz, H-4), 4.83 (d, 1H, *J* = 3.7 Hz, H-1)，4.26-3.92 (m, 5H, H-5, H-6a, H-6b, H-7a, H-7b), 3.75 (dd, 1H, *J* = 3.8 and 9.5 Hz, H-1)，3.38 (t, 2H, *J* = 6.6 Hz, H-16), 3.20 (m, 2H, H-9), 3.06 (m, 1H, H-3”), 2.45-0.70 (m, 62H, H-Cholesterol, 3xAc, CH_2-10 to CH_2-15), 0.61 (s, 3H, CH_3-18”)

^{13}CNMR (75 MHz, $CDCl_3$) :

δ: 170.7, 169.7, 168.8 (3x***C***=O in Ac, C8), 141.1 (C5”), 121.6 (C6”), 99.2 (C1), 79.1 (C3”), 73.6 (C3), 70.4 (C2), 68.2 (C5), 67.9 (C4), 67.4 (C14, C7), 61.9 (C6), 56.8 (C14”), 56.2(C17”), 50.3 (C9”), 42.4 (C13”), 39.9 (C9), 39.6 (C16”), 39.2 (C24”), 39.2 (C4”), 37.3 (C1”), 37.0 (C10”), 36.3 (C22”), 35.9 (C20”), 32.0 (C7”), 32.0 (C8”), 30.1, 29.4 (*C*-hexyl), 28.5 (C2”), 28.3 (C12”), 28.1 (C25”), 26.8, 26.1 (*C*-hexyl), 24.4 (C15”), 23.9 (C23”), 22.9 (C26”), 22.6 (C27”), 21.1 (C11”), 21.0, 20.8, 20.7 (3***C***H_3CO), 19.5 (C19”), 18.8 (C21”), 11.9 (C18”)

m/z (HRMS):

832.5540 ($M + H^+$, $C_{47}H_{78}NO_{11}$ requires 832.5569)

$[\alpha]_D^{20}$

+40 (*c* 0.8 in CH_2Cl_2)

Acetyl-Glu-L8-cholesterol (117)

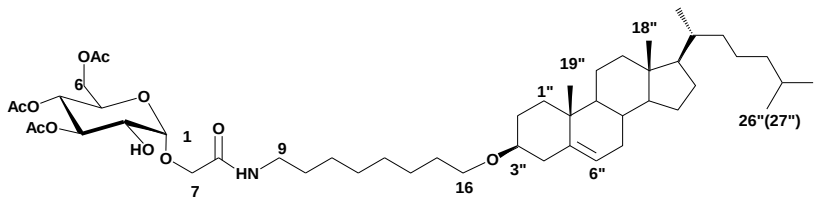

White solid

^{1}HNMR (300 MHz, $CDCl_3$) :

δ: 7.14 (t, 1H, NH), 5.28 (m, 1H, H-6”), 5.21 (t, 1H, *J* = 9.7 Hz, H-3), 4.95 (t, 1H, *J* = 9.8 Hz, H-4), 4.84 (d, 1H, *J* = 3.5 Hz, H-1)，4.26-3.92 (m, 5H, H-5, H-6a, H-6b, H-7a, H-7b), 3.75 (dd, 1H, *J* = 3.7 and 9.9 Hz, H-2)，3.37 (t, 2H, *J* = 6.7 Hz, H-18), 3.20 (m, 2H, H-9), 3.06 (m, 1H, H-3”), 2.34-0.74 (m, 66H, H-Cholesterol, 3xAc, CH_2-10 to CH_2-17), 0.61 (s, 3H, CH_3-18”)

Cette thèse est accessible à l'adresse : http://theses.insa-lyon.fr/publication/2013ISAL0001/these.pdf
© [R. Xu], [2013], INSA de Lyon, tous droits réservés

^{13}CNMR (75 MHz, $CDCl_3$) :

δ: 171.7, 170.7, 169.6, 169.5 (3x***C***=O in Ac, C8), 141.1 (C5”), 121.5 (C6”), 99.0 (C1), 79.0 (C3”), 73.7 (C3), 70.6 (C2), 68.2 (C5), 68.2 (C4), 68.0 (C16), 67.9 (C7), 61.9 (C6), 56.8 (C14”), 56.2 (C17”), 50.3 (C9”), 42.4 (C13”), 39.9 (C9), 39.6 (C16”), 39.3 (C24”), 39.3 (C4”), 37.4 (C1”), 37.0 (C10”), 36.3 (C22”), 35.9 (C20”), 32.0 (C7”), 32.0 (C8”), 30.2, 29.5, 29.5, 29.3 (*C*-octyl), 28.3 (C2”+12”), 28.1 (C25”), 26.9, 26.2 (*C*-octyl), 24.4 (C15”), 23.9 (C23”), 22.9 (C26”), 22.6 (C27”), 21.1 (C11”), 21.0, 20.8, 20.7 (3***C***H_3CO), 19.5 (C19”), 18.8 (C21”), 11.9 (C18”)

m/z (HRMS) :

860.5852 ($M + H^+$, $C_{49}H_{82}NO_{11}$ requires 860.5882)

$[\alpha]_D^{20}$

+38 (*c* 0.8 in CH_2Cl_2)

Acetyl-Glu-L10-cholesterol (118)

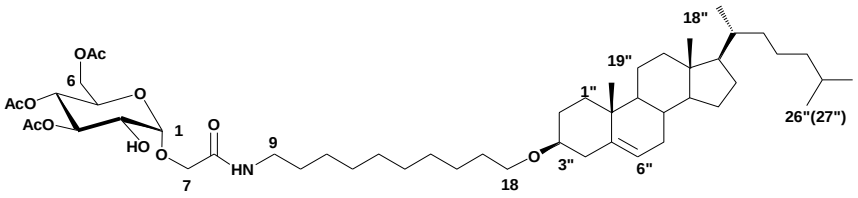

White solid

^{1}HNMR (300 MHz, $CDCl_3$) :

δ: 7.14 (t, 1H, NH), 5.28 (m, 1H, H-6”), 5.21 (t, 1H, *J* = 9.7 Hz, H-3), 4.95 (t, 1H, *J* = 9.8 Hz, H-4), 4.84 (d, 1H, *J* = 3.5 Hz, H-1)，4.26-3.92 (m, 5H, H-5, H-6a, H-6b, H-7a, H-7b), 3.75 (dd, 1H, *J* = 9.9 Hz, 3.7, H-2)，3.37 (t, 2H, *J* = 6.7 Hz, H-18), 3.20 (m, 2H, H-9), 3.06 (m, 1H, H-3”), 2.34-0.74 (m, 66H, H-Cholesterol, 3xAc, CH_2-10 to CH_2-17), 0.61 (s, 3H, s, CH_3-18”)

^{13}CNMR (75 MHz, $CDCl_3$) :

δ: 171.7, 170.7, 169.6, 169.5 (3x***C***=O in Ac, C8), 141.1 (C5”), 121.5 (C6”), 99.0 (C1), 79.0 (C3”), 73.7 (C3), 70.6 (C2), 68.2 (C5), 68.2 (C4), 67.9 (C18, C7), 61.9 (C6), 56.8 (C14”), 56.2

Cette thèse est accessible à l'adresse : http://theses.insa-lyon.fr/publication/2013ISAL0001/these.pdf
© [R. Xu], [2013], INSA de Lyon, tous droits réservés

(C17”), 50.3 (C9”), 42.4 (C13”), 39.9 (C9), 39.6 (C16”), 39.3 (C24”), 38.9 (C4”), 37.4 (C1”), 37.0 (C10”), 36.3 (C22”), 35.9 (C20”), 32.0 (C7”), 32.0 (C8”), 30.3, 29.8, 29.5, 29.6, 29.5, 29.5, 29.3 (*C*-decyl), 28.6 (C2”), 28.3 (C12”), 28.1 (C25”), 26.9, 26.2 (*C*-decyl), 24.4 (C15”), 23.9 (C23”), 22.9 (C26”), 22.6 (C27”), 21.1 (C11”), 21.0, 20.8, 20.7 (3***C***H_3CO), 19.5 (C19”), 18.8 (C21”), 11.9 (C18”)

m/z (HRMS) :

888.6162 (M + H^+, $C_{51}H_{86}NO_{11}$ requires 888.6195)

$[\alpha]_D^{20}$

+38 (c 0.8 in CH_2Cl_2)

Acetyl-Glu-L12-cholesterol (119)

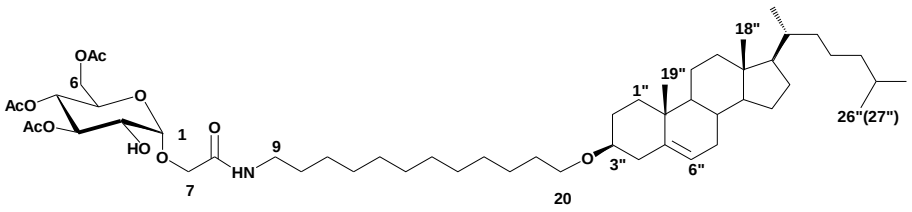

White solid

^{1}HNMR (300 MHz, $CDCl_3$) :

δ: 7.16 (t, 1H, NH), 5.34 (m, 1H, H-6”), 5.25 (t, 1H, *J* = 9.7 Hz, H-3), 5.02 (t, 1H, *J* = 9.9 Hz, H-4), 4.89 (d, 1H, *J* = 3.7 Hz, H-1)，4.32-3.97 (m, 5H, H-5, H-6a, H-6b, H-7a, H-7b), 3.80 (dd, 1H, *J* = 3.8 and 9.8 Hz, H-2)，3.43 (t, 2H, *J* = 6.8 Hz, H-20), 3.25 (m, 2H, H-9), 3.11 (m, 1H, H-3”), 2.38-0.74 (m, 70H, H-Cholesterol, 3xAc, CH_2-2 to CH_2-19), 0.66 (s, 3H, CH_3-18”)

^{13}CNMR (75 MHz, $CDCl_3$) :

δ: 171.7, 170.7, 169.6, 168.7 (3x***C***=O in Ac, C8), 141.2 (C5”), 121.5 (C6”), 99.0 (C1), 79.0 (C3”), 73.8 (C3), 70.6 (C2), 68.2 (C5), 68.2 (C4), 67.9 (C20), 67.3 (C7), 61.9 (C6), 56.9 (C14”), 56.2 (C17”), 50.3 (C9”), 42.4 (C13”), 39.9 (C9), 39.6 (C16”), 39.3 (C24”), 38.9 (C4”), 37.4 (C1”), 37.0 (C10”), 36.3 (C22”), 35.9 (C20”), 32.0 (C7”), 32.0 (C8”), 30.3, 29.9, 29.9, 29.7, 29.7, 29.6, 29.6, 29.5, 29.5, 29.4 (*C*-dodecyl), 28.6 (C2”), 28.3 (C12”), 28.1 (C25”), 27.0,

Cette thèse est accessible à l'adresse : http://theses.insa-lyon.fr/publication/2013ISAL0001/these.pdf
© [R. Xu], [2013], INSA de Lyon, tous droits réservés

26.3 (*C*-dodecyl), 24.4 (C15”), 23.9 (C23”), 22.9 (C26”), 22.6 (C27”), 21.1 (C11”), 21.0, 20.8, 20.7 (3***C***H_3CO), 19.5 (C19”), 18.8 (C21”), 11.9 (C18”)

m/z (HRMS) :

916.6475 ($M + H^+$, $C_{53}H_{90}NO_{11}$ requires 916.6508)

$[\alpha]_D^{20}$

+37 (c 1.5 in CH_2Cl_2)

D.2.2.4 Synthesis for glucosteroid amphiphiles

The partially protected compound acetyl-Glu-L_n-cholesterol (0.1mmol) was dissolved in a MeOH/Et_3N/H_2O (8/1/1, 10 mL) mixture and was further stirred at RT for 15 hours. The reaction was then coevaporated three times with water and the obtained white residue was subjected to silica gel chromatography using a CH_2Cl_2/MeOH (95/5) to give the corresponding neoglycolipid**.**

Glucosteroid L4 amphiphile (111)

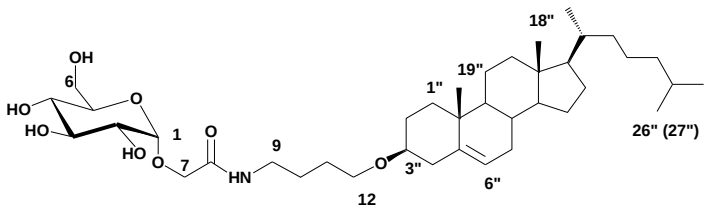

White solid

^{1}HNMR (300 MHz, $CDCl_3$/MeOD) :

δ: 5.35 (m, 1H, H-6”), 4.80 (d, 1H, *J* = 3.7 Hz, H-1), 4.17 (d, 1H, *J* = 15.8 Hz, H-7a), 4.00 (d, 1H, *J* = 15.8 Hz, H-7b), 3.83-3.68 (m, 3H, H-3, H-6a, H-6b), 3.56 (m, 1H, H-5), 3.53-3.49 (m, 3H, H-2, CH_2-12), 3.40 (m, 1H, H-4), 3.28 (m, 2H, CH_2-9), 3.17 (m, 1H, H-3”), 2.36 (m, 1H, H-4”a), 2.17 (m, 1H, H-4”b), 1.99-0.70 (m, 42H, H-Cholesterol, CH_2-10, CH_2-11), 0.69 (s, 3H, CH_3-18”)

^{13}CNMR (75 MHz, $CDCl_3$/MeOD) :

Cette thèse est accessible à l'adresse : http://theses.insa-lyon.fr/publication/2013ISAL0001/these.pdf
© [R. Xu], [2013], INSA de Lyon, tous droits réservés

δ: 170.7 (C8), 140.9 (C5”), 122.1 (C6”), 100.0 (C1), 79.6 (C3”), 73.8 (C3), 72.8 (C5), 71.9 (C2), 70.3 (C4), 67.8 (C12), 67.0 (C7), 61.6 (C6), 57.0 (C14”), 56.4 (C17”), 50.5 (C9”), 42.6 (C13”), 40.0 (C9), 39.8 (C16”), 39.3 (C24”), 39.1 (C4”), 37.4 (C1”), 37.1 (C10”), 36.4 (C22”), 36.1 (C20”), 32.2 (C7”+8”), 28.6 (C2”), 28.5 (C12”), 28.2 (25”), 27.6, 26.2 (*C*-butyl), 24.5 (C15”), 24.0 (C23”), 22.9 (C26”), 22.6 (C27”), 21.3 (C11”), 19.5 (19”), 18.8 (21”), 12.0 (18”)

m/z (ESI):

678.2 ($M+H^+$)

Elemental analysis:

Found: C, 67.30; H, 9.99; N, 2.01. $C_{39}H_{67}O_8N•H_2O$ requires C, 67.58; H, 9.77; N, 2.15

$[\alpha]_D^{20}$

+38 (*c* 0.8 in $CHCl_3$/MeOH, 7/3)

Glucosteroid L6 amphiphile (120)

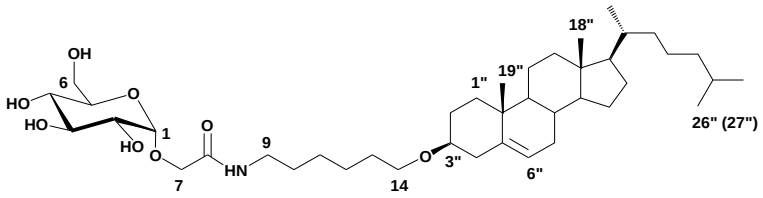

White solid

^{1}HNMR (400 MHz, $CDCl_3$/MeOD) :

δ: 5.27 (m, 1H, H-6”), 4.72 (d, 1H, *J* = 3.7 Hz, H-1), 4.08 (d, 1H, *J* = 15.9 Hz, H-7a), 3.91(d, 1H, *J* = 15.9 Hz, H-7b), 3.73-3.60 (m, 3H, H-6a, H-6b, H-3), 3.57-3.32 (m, 5H, H-2, H-4, H-5, CH_2-14), 3.22-3.01 (m, 3H, CH_2-9, H-3”), 2.32-2.03 (m, 2H, H4”), 1.96-0.77 (m, 49H, H-Cholesterol, CH_2-10 to CH_2-13), 0.60 (s, 3H, CH_3-18”)

^{13}CNMR (100 MHz, $CDCl_3$/MeOD) :

δ: 170.5 (C8), 141.1 (C5”), 122.0 (C6”), 99.8 (C1), 79.5 (C3”), 73.9 (C3), 72.6 (C5), 71.9 (C2), 70.3 (C4), 68.3 (C14), 67.1 (C7), 61.7 (C6), 57.1 (C14”), 56.4 (C17”), 50.5 (C9”), 42.6 (C13”), 40.1 (C9), 39.8 (C16”), 39.3 (C24”), 39.3 (C4”), 37.5 (C1”), 37.1 (C10”), 36.5 (C22”), 36.1

Cette thèse est accessible à l'adresse : http://theses.insa-lyon.fr/publication/2013ISAL0001/these.pdf
© [R. Xu], [2013], INSA de Lyon, tous droits réservés

(C20”), 32.2 (C7”), 32.2 (C8”), 30.2, 29.3 (*C*-hexyl), 28.7 (C2”), 28.5 (C12”), 28.3 (C25”), 27.0, 26.1 (*C*-hexyl), 24.5 (C15”), 24.1 (C23”), 23.0 (C26”), 22.8 (C27”), 21.3 (C11”), 19.6 (C18”), 19.0 (C21”), 12.1 (C18”)

m/z (HRMS) :

706.5262 ($M + H^+$, $C_{41}H_{72}O_8N$ requires 706.5252)

$[\alpha]_D^{20}$

+33 (*c* 0.5 in CH_2Cl_2/MeOH, 9/1)

Glucosteroid L8 amphiphile (121)

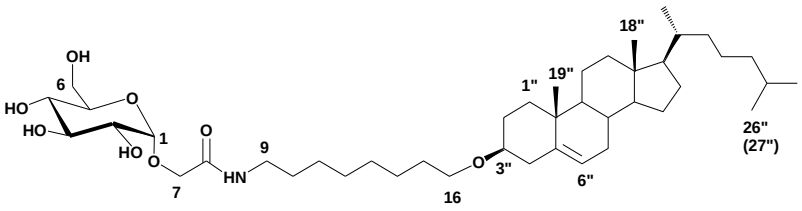

White solid

^{1}HNMR (300 MHz, $CDCl_3$/MeOD) :

δ: 5.28 (m, 1H, H-6”), 4.72 (d, 1H, *J* = 3.7 Hz, H-1), 4.08 (d, 1H, *J* = 15.9 Hz, H-7a), 3.91 (d, 1H, *J* = 15.9 Hz, H-7b), 3.74-3.60 (m, 3H, H-6a, H-6b, H-3), 3.57-3.32 (m, 5H, H-2, H-4, H-5, CH_2-14), 3.22-3.01 (m, 3H, CH_2-9, H-3”), 2.32-2.03 (m, 2H, H4”), 1.96-0.77 (m, 54H, H-Cholesterol, CH_2-10 to CH_2-13), 0.60 (s, 3H, CH_3-18”)

^{13}CNMR (75 MHz, $CDCl_3$/MeOD) :

δ: 170.1 (C8), 140.8 (C5”), 121.5 (C6”), 99.4 (C1), 79.1 (C3”), 73.6 (C3), 72.3 (C5), 71.6 (C2), 69.9 (C4), 68.1 (C16), 66.7 (C7), 61.4 (C6), 56.7 (C14”), 56.1 (C17”), 50.1 (C9”), 42.3 (C13”), 39.7 (C9), 39.5 (C16”), 39.1 (C24”), 39.0 (C4”), 37.2 (C1”), 36.8 (C10”), 36.1 (C22”), 35.7 (C20”), 31.9 (C7”), 31.8 (C8”), 30.0, 29.3, 29.2, 29.1 (*C*-octyl), 28.3 (C2”), 28.2 (C12”), 27.9 (C25”), 26.8, 26.0 (*C*-octyl), 24.2 (C15”), 23.8 (C23”), 22.7 (C26”), 22.4 (C27”), 21.0 (C11”), 19.3 (C19”), 18.6 (C21”), 11.8 (C18”)

m/z (HRMS) :

Cette thèse est accessible à l'adresse : http://theses.insa-lyon.fr/publication/2013ISAL0001/these.pdf
© [R. Xu], [2013], INSA de Lyon, tous droits réservés

734.5552 ($M + H^+$, $C_{43}H_{76}O_8N$ requires 734.5565)

$[\alpha]_D^{20}$

+34 (*c* 1.4 in CH_2Cl_2/MeOH, 9/1)

Glucosteroid L10 amphiphile (122)

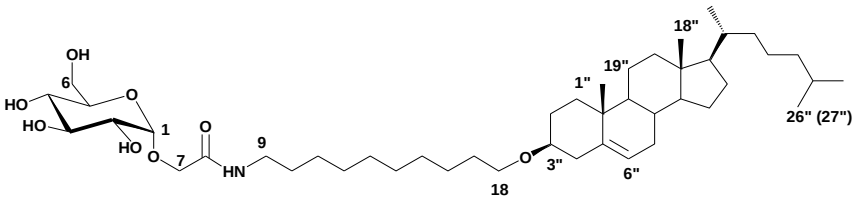

White solid

^{1}HNMR (300 MHz, $CDCl_3$/MeOD) :

δ: 5.28 (m, 1H, H-6”), 4.72 (d, 1H, *J* = 3.7 Hz, H-1), 4.09 (d, 1H, *J* = 15.9 Hz, H-7a), 3.91 (d, 1H, *J* = 15.9 Hz, H-7b), 3.74-3.60 (m, 3H, H-6a, H-6b, H-3), 3.57-3.32 (m, 5H, H-2, H-4, H-5, CH_2-14), 3.22-3.01 (m, 3H, CH_2-9, H-3”), 2.32-2.03 (m, 2H, H4”), 1.96-0.77 (m, 59H, H-Cholesterol, CH_2-10 to CH_2-13), 0.60 (s, 3H, CH_3-18”)

^{13}CNMR (75 MHz, $CDCl_3$/MeOD) :

δ: 170.0 (C8), 140.9 (C5”), 121.5 (C6”), 99.4 (C1), 79.1 (C3”), 73.5 (C3), 72.3 (C5), 71.6 (C2), 69.9 (C4), 68.2 (C18), 66.7 (C7), 61.4 (C6), 56.7 (C14”), 56.1 (C17”), 50.1 (C9”), 42.3 (C13”), 39.8 (C9), 39.7 (C16”), 39.5 (C24”), 39.5 (C4”), 39.1, 39.0, 37.2 (C10”), 36.8 (C22”), 36.1 (C20”), 31.9 (C7”), 31.8 (C8”), 29.5, 29.5, 29.4, 29.2 (*C*-decyl), 28.2 (C2”+12”), 27.9 (C25”), 26.9, 26.1 (*C*-decyl), 24.2 (C15”), 23.8 (C23”), 22.7 (C26”), 22.5 (C27”), 21.0 (C11”), 19.3 (C19”), 18.6 (C21”), 11.8 (C18”)

m/z (HRMS) :

762.5870 ($M + H^+$, $C_{45}H_{80}NO_8$ requires 762.5878)

$[\alpha]_D^{20}$

+29 (*c* 0.7 in CH_2Cl_2/MeOH, 9/1)

Cette thèse est accessible à l'adresse : http://theses.insa-lyon.fr/publication/2013ISAL0001/these.pdf
© [R. Xu], [2013], INSA de Lyon, tous droits réservés

Glucosteroid L12 amphiphile (123)

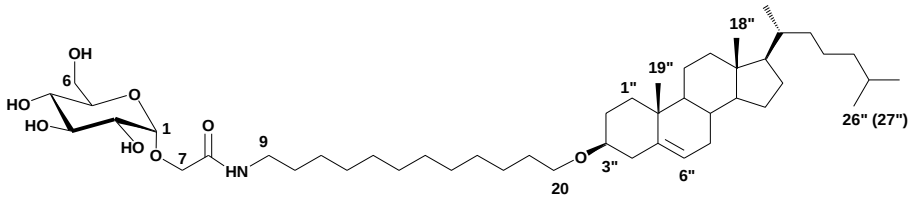

White solid

^{1}HNMR (300 MHz, $CDCl_3$/MeOD) :

δ: 5.27 (m, 1H, H-6”), 4.72 (d, 1H, *J* = 3.7 Hz, H-1), 4.09 (d, 1H, *J* = 15.9 Hz, H-7a), 3.91 (d, 1H, *J* = 15.9 Hz, H-7b), 3.72-3.60 (m, 3H, H-6a, H-6b, H-3), 3.57-3.32 (m, 5H, H-2, H-4, H-5, CH_2-14), 3.22-3.01 (m, 3H, CH_2-9, H-3”), 2.32-2.03 (m, 2H, H4”), 1.96-0.77 (m, 63H, H-Cholesterol, CH_2-10 to CH_2-13), 0.60 (s, 3H, CH_3-18”)

^{13}CNMR (75 MHz, $CDCl_3$/MeOD) :

δ: 170.0 (C8), 140.9 (C5”), 121.5 (C6”), 99.4 (C1), 79.0 (C3”), 73.5 (C3), 72.3 (C5), 71.6 (C2), 69.9 (C4), 68.2 (C20), 66.7 (C7), 61.3 (C6), 56.7 (C14”), 56.1 (C17”), 50.1 (C9”), 42.3 (C13”), 39.7 (C9), 39.4 (C16”), 39.1 (C24”), 39.0 (C4”), 37.2 (C1”), 36.8 (C10”), 36.1 (C22”), 35.7 (C20”), 31.9 (C7”), 31.8 (C8”), 30.0, 29.5, 29.5, 29.4, 29.3, 29.2 (*C*-dodecyl), 28.3 (C2”), 28.2 (C12”), 27.9 (C25”), 26.9, 26.1 (*C*-dodecyl), 24.2 (C15”), 23.8 (C23”), 22.7 (C26”), 22.4 (C27”), 21.0 (C11”), 19.3 (C19”), 18.6 (C21”), 11.8 (C18”)

m/z (HRMS) :

790.6182 ($M + H^+$, $C_{47}H_{84}NO_8$ requires 790.6191)

$[\alpha]_D^{20}$

+30 (*c* 0.8 in CH_2Cl_2/MeOH, 9/1)

D.2.2.5 Synthesis of glucosteroid bolaphiles

To a solution of acetyl-Glu-L_n-cholesterol in CH_2Cl_2 (0.1 mol L^{-1}), the proper alkyl isocyanate (10 eq.) and catalytic amounts of triethylamine (50 μL) were added under nitrogen. The mixture was stirred for 3 days at room temperature, the white solid formed during the

Cette thèse est accessible à l'adresse : http://theses.insa-lyon.fr/publication/2013ISAL0001/these.pdf
© [R. Xu], [2013], INSA de Lyon, tous droits réservés

reaction was filtrated and the solvent was evaporated. The obtained residue was dissolved in a MeOH/Et_3N/H_2O (8/1/1, 10 mL) mixture and was further stirred at 40°C for 3 hours. The reaction was then coevaporated three times with water and the obtained white residue was subjected to silica gel chromatography using a CH_2Cl_2/MeOH/Acetone/H_2O (78/5/15/2) to give the corresponding desired urethanes

Or:

To a solution of starting material in THF (0.1 mol L^{-1}), DBU (1.5 eq.) and alkyl isocyanate (1.5 eq.) were added. The mixture was stirred overnight at 45 ^oC under N_2. Then the THF was removed under vacuum, the obtained solid was purified by SiO_2 gel column chromatography (DCM/Acetone, 95:5). The obtained compound was dissolved in a mixture of MeOH/NEt/H_2O (8:1:1), stirring overnight. After evaporation, the residue was purified by SiO_2 gel column chromatography (DCM/MeOH, 95:5)

Glucosteroid L4S4 bolaphile (124a)

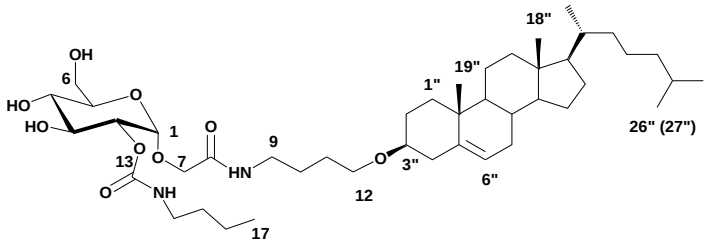

White solid

^{1}HNMR (400 MHz, $CDCl_3$/MeOD) :

δ: 7.17 (t, 1H, *J* = 5.6 Hz, NH), 6.57 (t, 1H, *J* = 5.3 Hz, NH), 5.26 (m, 1H, H-6”), 4.91 (d, 1H, *J* = 3.5 Hz, H-1), 4.45 (dd, 1H, *J* = 3.5 and 10.1 Hz, H-2), 4.07 (d, 1H, *J* = 15.4 Hz, H-7a), 3.90 (d, 1H, *J* = 15.4 Hz, H-7b), 3.80-3.71 (m, 2H, H-3, H-6a), 3.64 (dd, 1H, *J* = 5.5 and 12.3 Hz, H-6b), 3.50 (m, 1H, H-5), 3.46-3.40 (m, 2H, CH_2-12), 3.37 (t, 1H, *J* = 9.6 Hz, H-4), 3.24-3.17 (m, 2H, CH_2-9), 3.13-2.97 (m, 3H, H-3”, CH_2-14), 2.27 (ddd, 1H, *J* = 13.1 4.5 and 2.0 Hz,H-4”a), 2.09 (m, 1H, H-4”b), 1.99-0.70 (m, 49H, H-Cholesterol, CH_2-10, CH_2-11, CH_2-15 to CH_2-17), 0.61 (s, 3H, CH_3-18”)

^{13}CNMR (75 MHz, $CDCl_3$/MeOD) :

Cette thèse est accessible à l'adresse : http://theses.insa-lyon.fr/publication/2013ISAL0001/these.pdf
© [R. Xu], [2013], INSA de Lyon, tous droits réservés

δ: 169.7 (C8), 156.3 (C13), 140.1 (C5”), 121.4 (C6”), 96.9 (C1), 79.0 (C3”), 73.1 (C2), 72.4 (C5), 70.8 (C3), 69.8 (C4), 67.1 (C12), 66.1 (C7), 60.8 (C6), 56.4 (C14”), 55.8 (C17”), 49.8 (C9”), 41.9 (C13”), 40.2 (C14”), 39.4 (C24”), 39.1 (C16”), 38.6 (C9), 38.4 (C4”), 36.8 (C1”), 36.4 (C10”), 35.7 (C22”), 35.4 (C20”), 31.5 (C7”), 31.4 (C8”), 31.3, 27.9, 27.7, 27.5, 26.8, 25.8, 23.8 (C23”), 23.3 (C26”), 22.0, 21.8 (C27”), 20.6 (C11”), 19.4 (C19”), 18.7 (C21”), 18.0 (C16), 12.9 (C17), 11.2 (C18”)

m/z (HRMS) :

799.5446 ($M + Na^+$, $C_{44}H_{76}N_2O_9$ requires 799.5449)

$[\alpha]_D^{20}$

+11 (*c* 0.4 in $CHCl_3$/MeOH, 1/1)

Glucosteroid L4S8 bolaphile (124b)

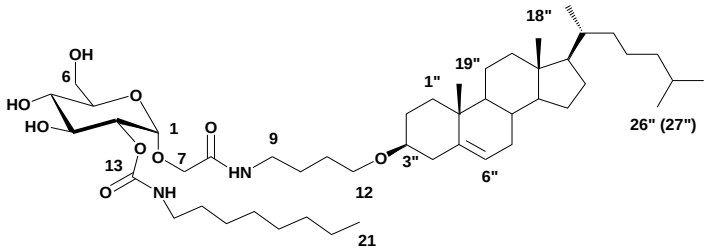

White solid

^{1}HNMR (300 MHz, $CDCl_3$/MeOD) :

δ: 7.16 (t, 1H, *J* = 5.6 Hz, NH), 6.57 (t, 1H, *J* = 5.3 Hz, NH), 5.26 (m, 1H, H-6”), 4.91 (d, 1H, *J* = 3.6 Hz, H-1), 4.91 (dd, 1H, *J* = 3.6 and 10.1 Hz, H-2), 4.06 (d, 1H, *J* = 15.6 Hz, H-7a), 3.90 (d, 1H, *J* = 15.6 Hz, H-7b), 3.79-3.71 (m, 2H, H-3, H-6a), 3.64 (dd, 1H, *J* = 4.9 and 12.0 Hz, H-6b), 3.50 (ddd, 1H, *J* = 2.3, 4.9, and 12.0 Hz, H-5), 3.42-3.34 (m, 3H, CH_2-12, H-4), 3.21-3.19 (m, 2H, CH_2-9), 3.12-2.98 (m, 3H, H-3”, CH_2-12), 2.27 (m, 1H, H-4”a), 2.09 (m, 1H, H-4”b), 1.96-0.76 (m, 57 H, H-Cholesterol, CH_2-10, CH_2-11, CH_2-15 to CH_2-20, CH_3-21), 0.60 (s, 3H, CH_3-18”)

^{13}CNMR (75 MHz, $CDCl_3$/MeOD) :

Cette thèse est accessible à l'adresse : http://theses.insa-lyon.fr/publication/2013ISAL0001/these.pdf
© [R. Xu], [2013], INSA de Lyon, tous droits réservés

δ: 176.4 (C8), 169.8 (C13), 140.5 (C5”), 121.4 (C6”), 97.3 (C1), 79.3 (C3”), 73.4 (C2), 72.5 (C5), 71.2 (C3), 70.1 (C4), 67.5 (C12), 66.5 (C7), 61.2 (C6), 56.7 (C14”), 56.1 (C17”), 50.2 (C9”), 42.3 (C13”), 41.0 (C14), 39.7 (C24”), 39.5 (C16”), 39.0 (C9), 38.8 (C4”), 37.2 (C1”), 36.8 (C10”), 36.1 (C22”), 35.7 (C20”), 31.9 (C7”), 31.8 (C8”), 29.7 , 29.7, 29.6, 29.3, 28.3 (C2”), 28.2 (C12”), 27.9 (C25”), 27.2, 26.8, 26.2 , 24.2 (C15”), 23.8 (C23”), 22.6 (C26”), 22.6 , 22.4 (C27”), 21.0 (C11”), 19.1 (C19”), 18.0 (C21”), 13.4 (C21), 11.2 (C18)

m/z (ESI) :

856.7 ($M + Na^+$)

$[\alpha]_D^{20}$

+52 (*c* 0.5 in $CHCl_3$/MeOH, 1/1)

Elemental analysis:

Found: C 68.45; H 10.17; N 3.33. $C_{45}H_{73}O_{11}N + 0.5\ H_2O$ requires C 68.72; H 10.15; N 3.23

Glucosteroid L4S10 bolaphile (124c)

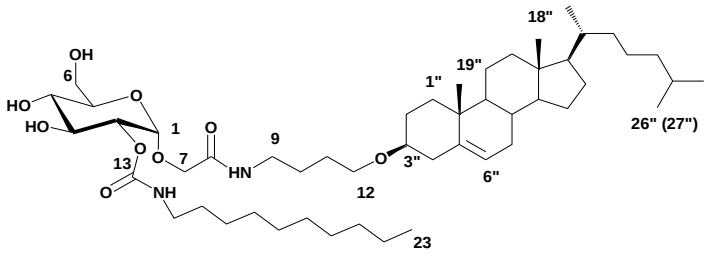

White solid

^{1}HNMR (400 MHz, $CDCl_3$/MeOD) :

δ: 7.03 (t, 1H, NH), 6.26 (t, 1H, NH), 5.25 (m, 1H, H-6”), 4.92 (d, 1H, *J* = 3.7 Hz, H-1), 4.46 (dd, 1H, *J* = 3.7 and 10.1 Hz, H-2), 4.06 (d, 1H, *J* = 15.5 Hz, H-7a), 3.89 (d, 1H, *J* = 15.6 Hz, H-7b), 3.80-3.70 (m, 2H, H-3, H-6a), 3.67 (m, 1H, H-6b), 3.50 (m, 1H, H-5), 3.46-3.36 (m, 3H, CH_2-12, H-4), 3.24-3.17 (m, 2H, CH_2-9), 3.13-2.97 (m, 3H, H-3”, CH_2-12), 2.27 (m, 1H, H-4”a), 2.10 (m, 1H, H-4”b), 2.00-0.73 (m, 61 H, H-Cholesterol, CH_2-10, CH_2-11, CH_2-15 to CH_2-20, CH_3-21), 0.61 (s, 3H, CH_3-18”)

^{13}CNMR (75 MHz, $CDCl_3$/MeOD :

Cette thèse est accessible à l'adresse : http://theses.insa-lyon.fr/publication/2013ISAL0001/these.pdf
© [R. Xu], [2013], INSA de Lyon, tous droits réservés

δ: 169.8 (C8), 156.3 (C13), 140.4 (C5”), 121.7 (C6”), 97.2 (C1), 79.2 (C3”), 73.3 (C2), 72.3 (C5), 71.1 (C3), 70.5 (C4), 67.4 (C12), 66.4 (C7), 61.1 (C6), 56.6 (C14”), 56.0 (C17”), 50.1 (C9”), 42.2 (C13”), 40.9 (C9), 39.6 (C16”), 39.3 (C24”), 38.9 (C4”), 38.8, 38.7, 37.0 (C1”), 36.7 (C10”), 36.0 (C22”), 35.6 (C20”), 31.7 (C7”), 29.6 (C8”), 29.5, 29.4, 29.2, 29.2, 28.2 (C2”), 28.0 (C12”), 27.8 (C25”), 27.1, 26.7, 26.1, 24.1 (C15”), 23.6 (C23”), 22.5 (C26”), 22.2 (C27”), 20.9 (C11”), 19.1 (C19”), 18.4 (C21”), 13.8 (C23), 11.6 (C18”)

m/z (HRMS) :

883.6390 (M + Na^+, $C_{50}H_{88}N_2O_9$ requires 883.6388)

$[\alpha]_D^{20}$

+25 (*c* 0.5 in $CHCl_3$/MeOH, 1/1)

Glucosteroid L4S12 bolaphile (124d)

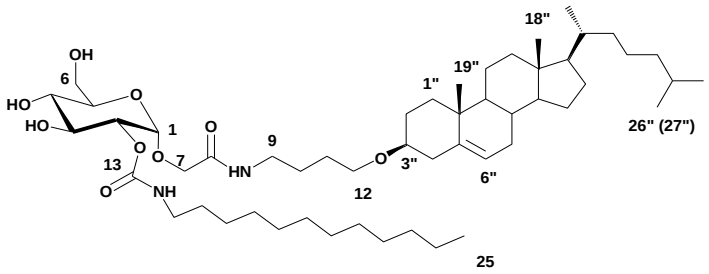

White solid

^{1}HNMR (300 MHz, $CDCl_3$/MeOD) :

δ: 5.28 (m, 1H, H6”), 4.91 (d, 1H, *J* = 3.6 Hz; H-1), 4.45 (dd, 1H, *J* = 10.1 Hz, H-2), 4,06 (d, 1H, *J* = 15.6 Hz, H-7a), 3.88 (d; 1H, *J* = 15.6 Hz, H-7b), 3.76-3.68 (m, 3H, H-3, H-6a, H-6b), 3.52-3.37 (m, 4 H, H-5, H-4, $CH_2$12), 3.20 (m, 2 H, CH_2 -9), 3.08-2.98(m, 3 H, H-3”, $CH_2$14), 2.26 (m, 1 H, H-4”a), 2.09 (m, 1 H, H4”b), 1.96-0.77 (m, 65 H, H-Cholesterol, CH_2-10, CH_2-11, CH_2-15 à CH_2-24, CH_3- 25), 0.60 (s; 3 H, CH_3-18”)

^{13}CNMR (75 MHz, $CDCl_3$/MeOD) :

δ: 169.8 (C8), 156.5 (C13), 140.6 (C5”), 121.8 (C6”), 97.3 (C1), 79.4 (C3”), 73.4 (C2), 72.4 (C5), 71.2 (C3), 70.1 (C4), 67.5 (C12), 66.5 (C7), 61.2 (C6), 56.7 (C14’’), 56.1 (C17’’), 50.2 (C9’’), 42.3 (C13’’), 41.0 (C14), 39.7 (C24’’), 39.5 (C16’’), 39.0 (C9), 38.8 (C4’’), 37.2 (C1’’),

Cette thèse est accessible à l'adresse : http://theses.insa-lyon.fr/publication/2013ISAL0001/these.pdf
© [R. Xu], [2013], INSA de Lyon, tous droits réservés

36.8 (C10’’); 36.2 (C22”), 35.7 (C20’’), 31.9 (C7’’), 31.8 (C8’’), 29.7, 29.7, 29.7, 29.7, 29.6, 29.6, 29.3, 29.3, 28.3 (C2’’), 28.2 (C12”), 27.9 (C25”), 27.2 (C11), 26.8 (C23), 26.2 (C10), 24.2 (C15”), 23.7 (C23”), 22.7 (C26”), 22.6 (C24), 22.4 (C27”), 21.0 (C11”), 19.2 (C19”), 18.6 (C21”), 13.9 (C25), 11.7 (C18”)

m/z (ESI) :

912.7 ($M + Na^+$)

$[\alpha]_D^{20}$

+41 (*c* 0.4 in $CHCl_3$/MeOH, 1/1)

Elemental analysis:

Found: C 69.57; H 10.44; N 3.12. $C_{52}H_{92}O_9N_2$ +0.5 H_2O requires C 69.66; H 10.44; N 3.16

Glucosteroid L4S14 bolaphile (124e)

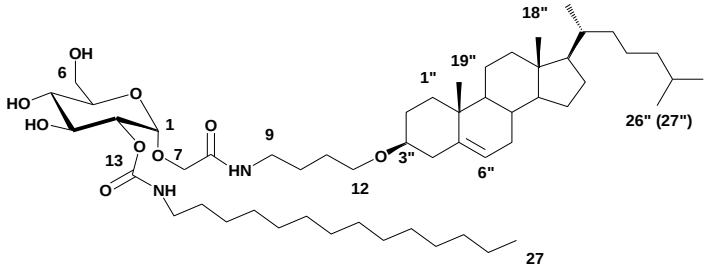

White solid

^{1}HNMR (300 MHz, $CDCl_3$/MeOD) :

δ: 7.03 (t, 1H, NH), 6.17 (t, 1H, NH), 5.35 (m, 1H, H-6”), 4.98 (d, 1H, *J* = 3.5 Hz, H-1), 4.54 (dd, 1H, *J* = 3.5 and 10.1 Hz, H-2), 4.14 (d, 1H, *J* = 15.6 Hz, H-7a), 3.96 (d, 1H, *J* = 15.6 Hz, H-7b), 3.87-3.77 (m, 3H, H-3, H-6a, H-6b), 3.60-3.47 (m, 4H, CH_2-12, H-4, H-5), 3.28 (m, 2H, CH_2-9), 3.21-3.04 (m, 3H, H-3”, CH_2-14), 2.34 (m, 1H, H-4”a), 2.17 (m, 1H, H-4”b), 2.03-0.80 (m, 69 H, H-Cholesterol, CH_2-10, CH_2-11, CH_2-15 to CH_2-26, CH_3-27), 0.68 (s, 3 H, CH_3-18”)

^{13}CNMR (125 MHz, $CDCl_3$/MeOD) :

δ: 169.6 (C8), 156.4 (C13), 140.7 (C5”), 121.9 (C6”), 97.4 (C1), 79.4 (C3”), 73.5 (C2), 72.3 (C5), 71.4 (C3), 70.3 (C4), 67.6 (C12), 66.7 (C7), 61.4 (C6), 56.8 (C14”), 56.2 (C17”), 50.2

Cette thèse est accessible à l'adresse : http://theses.insa-lyon.fr/publication/2013ISAL0001/these.pdf
© [R. Xu], [2013], INSA de Lyon, tous droits réservés

(C9”), 42.4 (C13”), 41.2 (C9), 39.8 (C16”), 39.6 (C24”), 39.1 (C4”), 38.8, 37.3 (C1”), 36.9 (C10”), 36.2 (C22”), 35.8 (C20”), 32.0 (C7”), 31.9 (C8”), 29.8-29.2, 28.4 (C2”), 28.3 (C12”), 28.0 (C25”), 27.3, 26.9, 26.3, 24.3 (C15”), 23.9 (C23”), 22.8 (C26”), 22.7, 22.5 (C27”), 21.1 (C11”), 19.4 (C19”), 18.7 (C21”), 14.1 (C27), 11.9 (C18”)

m/z (HRMS) :

939.7013 (M + Na^+, $C_{54}H_{96}N_2O_9$ requires 939.7014)

$[\alpha]_D^{20}$

+29 (*c* 0.4 in $CHCl_3$/MeOH 5/1)

Glucosteroid L4S16 bolaphile (124f)

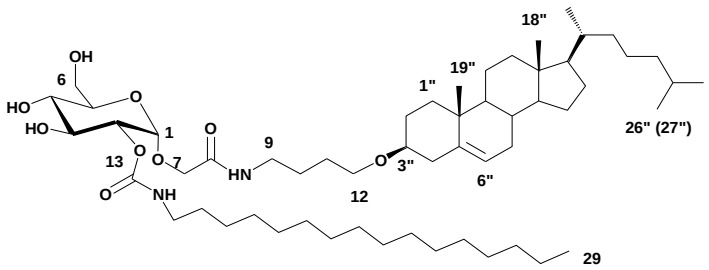

White solid

^{1}HNMR (500 MHz, $CDCl_3$/MeOD) :

δ: 5.35 (m, 1 H, H-6”), 4.92 (d, 1H, *J* = 3.0 Hz, H-1), 4.54 (dd, 1H, *J* = 3.0 and 9.9 Hz, H-2), 4.15 (d, 1H, *J* = 15.8 Hz, H-7a), 3.95 (d, 1H, *J* = 15.8 Hz, H-7b), 3.80-3.74 (m, 3H, H-3, H-6a, H-6b), 3.58-3.49 (m, 4H, CH_2-12, H-4, H-5), 3.28 (m, 2H, CH_2-9), 3.16-3.09 (m, 3H, H-3”, CH_2-14), 2.36 (m, 1H, H-4”a), 2.18 (m, 1H, H-4”b), 2.05-0.80 (m, 63H, H-Cholesterol, CH_2-10, CH_2-11, CH_2-15 to CH_2-28, CH_3-29), 0.68 (s, 3H, CH_3-18”)

^{13}CNMR (75 MHz, $CDCl_3$/MeOD) :

δ: 169.9 (C8), 156.5 (C13), 140. 7 (C5”), 122.9 (C6”), 97.4 (C1), 79.5 (C3”), 73.5 (C2), 72.5 (C5), 71.4 (C3), 70.2 (C4), 67.7 (C12), 66.7 (C7), 61.3 (C6), 56.9 (C14”), 56.3 (C17”), 50.3 (C9”), 42.4 (C13”), 41.2 (C9), 39.9 (C16”), 39.6 (C24”), 39.2 (C4”), 38.9, 37.3 (C1”), 36.9 (C10”), 36.3 (C22”), 35.8 (C20”), 32.0 (C7”), 32.0 (C8”), 29.9-29.5 (12 x CH_2), 28.5 (C2”),

Cette thèse est accessible à l'adresse : http://theses.insa-lyon.fr/publication/2013ISAL0001/these.pdf
© [R. Xu], [2013], INSA de Lyon, tous droits réservés

28.3 (C12”), 28.1 (C25”), 27.4, 27.0, 26.4, 24.4 (C15”), 23.9 (C23”), 22.9 (C26”), 22.8, 22.6 (C27”), 21.2 (11”), 19.4 (C19”), 18.8 (C21”), 14.2 (C29), 11.9 (C18”)

m/z (HRMS) :

967.7329 ($M + Na^+$, $C_{56}H_{100}O_9N_2$ requires 967.7327)

$[\alpha]_D^{20}$

+38 (*c* 0.4 in $CHCl_3$/MeOH, 5/1)

Elemental analysis:

Found: C 71.42; H 10.66; N 3.13. $C_{56}H_{100}O_9N_2$ requires C 71.14; H 10.66; N 2.96

Glucosteroid L4S18 bolaphile (124g)

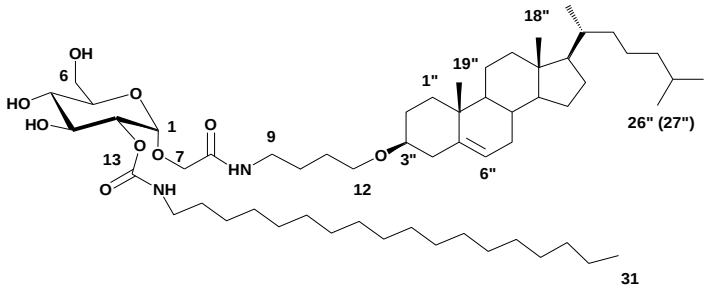

White solid

^{1}HNMR (300 MHz, $CDCl_3$/MeOD) :

δ: 7.16 (t, 1H, NH), 6.46 (t, 1H, NH), 5.35 (m, 1H, H-6”), 5.01 (d, 1H, *J* = 3.6 Hz, H-1), 4.54 (dd, 1H, *J* = 3.6 and 10.1 Hz, H-2), 4.15 (d, 1H, *J* = 15.6 Hz, H-7a), 3.97 (d, 1H, *J* = 15.6 Hz, H-7b), 3.88-3.77 (m, 3H, H-3, H-6a, H-6b), 3.61-3.45 (m, 4H, CH_2-12, H-4, H-5), 3.29 (m, 2H, CH_2-9), 3.13 (m, 3H, H-3”, CH_2-14), 2.36 (m, 1H, H-4”a), 2.20 (m, 1H, H-4”b), 2.05-0.85 (m, 77 H, H-Cholesterol, CH_2-10, CH_2-11, CH_2-15 to CH_2-30, CH_3-31), 0.68 (s, 3H, CH_3-18”)

^{13}CNMR (125 MHz, $CDCl_3$/MeOD) :

δ: 169.6 (C8), 156.3 (C13), 140. 7 (C5”), 121.9 (C6”), 97.4 (C1), 79.4 (C3”), 73.4 (C2), 72.3 (C5), 71.4 (C3), 70.2 (C4), 67.6 (C12), 66.7 (C7), 61.4 (C6), 56.8 (C14”), 56.2 (C17”), 50.2 (C9”), 42.4 (C13”), 41.2 (C9), 39.8 (C16”), 39.5 (C24”), 39.1 (C4”), 38.8, 37.2 (C1”), 36.9 (C10”), 36.2 (C22”), 35.8 (C20”), 32.0 (C7”), 32.0 (C8”), 29.8-29.4 (14 x CH_2), 28.4 (C2”),

Cette thèse est accessible à l'adresse : http://theses.insa-lyon.fr/publication/2013ISAL0001/these.pdf
© [R. Xu], [2013], INSA de Lyon, tous droits réservés

28.3 (C12”), 28.0 (C25”), 27.3, 27.3, 26.3, 24.3 (C15”), 23.9 (C23”), 22.8 (C26”), 22.7, 22.5 (C27”), 21.1 (C11”), 19.4 (C19”), 18.7 (C21”), 14.1 (C31), 11.9 (C18”)

m/z (HRMS) :

995.7641 ($M + Na^+$, $C_{56}H_{100}O_9N_2$ requires 995.7640)

$[\alpha]_D^{20}$

+28 (*c* 1.0 in $CHCl_3$/MeOH, 8/1)

Glucosteroid L6S6 bolaphile (125a)

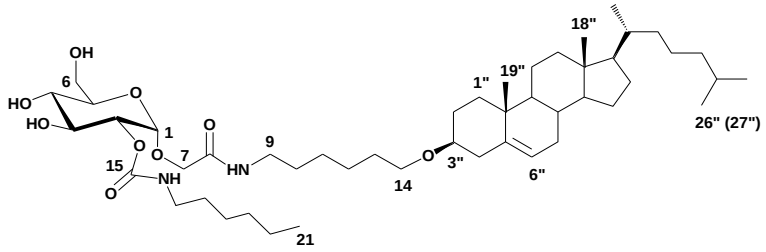

White solid

^{1}HNMR (400 MHz, $CDCl_3$/MeOD) :

δ: 5.35 (m, 1H, H-6”), 5.01 (d, 1H, *J* = 3.7 Hz, H-1), 4.55 (dd, 1H, *J* = 3.6, 10.2 Hz, H-2), 4.14 (d, 1H, *J* = 15.6 Hz, H-7a), 4.00 (d, 1H, *J* = 15.6 Hz, H-7b), 3.90-3.75 (m, 3H, H-6a, H-6b, H-3), 3.61-3.52 (m, 4H, H-5, H-4, CH_2-14), 3.25 (t, 2H, *J* = 7.3 Hz, CH_2-9), 3.19-3.04 (m, 3H, CH_2-16, H-3”), 2.40-2.10 (m, 2H, H-4”), 2.08-0.80 (m, 57 H, H-Cholesterol, CH_2-10 to CH_2-13, CH_2-17 to CH_3-21), 0.68 (s, 3 H, CH_3-18”)

^{13}CNMR (100 MHz, $CDCl_3$/MeOD) :

δ: 169.5 (C8), 156.4 (C15), 140.9 (C5”), 121.7 (C6”), 97.3 (C1), 79.2 (C3”), 73.5 (C2), 72.3 (C5), 71.3 (C3), 70.3 (C4), 68.0(C14), 66.6 (C7), 61.4 (C6), 56.8 (C14”), 56.2 (C17”), 50.3 (C9”), 42.4 (C13”), 41.2 (C9), 39.8 (C16”), 39.6 (C24”), 39.1 (C4”), 39.1, 37.3 (C1”), 36.9 (C10”), 36.2 (C22”), 35.8 (20”), 32.0 (C7”), 31.9 (C8”), 31.5, 30.0, 29.7, 29.5, 28.5 (C2”), 28.3 (C12”), 28.1 (C25”), 26.8, 26.5, 25.9, 24.3 (C15”), 23.9 (C23”), 22.8 (C26”), 22.6, 22.6 (C27”), 21.1 (C11”), 19.4 (C19”), 18.7 (C21”), 14.0 (C21), 11.9 (C18”)

m/z (ESI) :

Cette thèse est accessible à l'adresse : http://theses.insa-lyon.fr/publication/2013ISAL0001/these.pdf
© [R. Xu], [2013], INSA de Lyon, tous droits réservés

833.6 ($M+H^+$), 885.6 ($M+Na^+$)

$[\alpha]_D^{20}$

+36 (*c* 0.7 in CH_2Cl_2/MeOH (9/1))

Elemental analysis:

Found: C 68.60, H 10.45, N 3.25. $C_{48}H_{84}N_2O_9+H_2O$ requires C 68.45, H 10.17, N 3.33

Glucosteroid L6S8 bolaphile (125b)

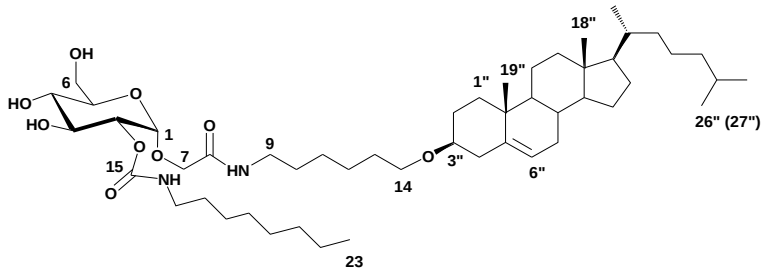

White solid

^{1}HNMR (400 MHz, $CDCl_3$/MeOD) :

δ: 5.35 (m, 1 H, H-6”), 5.01 (d, 1 H, *J* = 3.7 Hz, H-1), 4.55 (dd, 1H, *J* = 3.6 and 10.1 Hz, H-2), 4.14 (d, 1 H, *J* = 15.6 Hz, H-7a), 3.98 (d, 1H, *J* = 15.6 Hz, H-7b), 3.88-3.74 (m, 3H, H-6a, H-6b, H-3), 3.61-3.52 (m, 4H, H-5, H-4, CH_2-14), 3.25 (t, 2 H, *J* = 7.3 Hz, CH_2-9), 3.19-3.04 (m, 3 H, CH_2-16, H-3”), 2.40-2.10 (m, 2 H, H-4”), 2.08-0.80 (m, 61 H, H-Cholesterol, CH_2-10 to CH_2-13, CH_2-17 to CH_3-23), 0.68 (s, 3 H, CH_3-18”)

^{13}CNMR (100 MHz, $CDCl_3$/MeOD) :

δ: 169.5 (C8), 156.3 (C15), 140.8 (C5”), 121.6 (C6”), 97.2 (C1), 79.1 (C3”), 73.5 (C2), 72.3 (C5), 71.2 (C3), 70.1 (C4), 67.9 (C14), 66.5 (C7), 61.3 (C6), 56.7 (C14”), 56.1 (C17”), 50.2 (C9”), 42.3 (C13”), 41.1 (C9), 39.7 (C16”), 39.5 (C24”), 39.0 (C4”), 39.0, 37.2 (C1”), 36.8 (C10”), 36.1 (C22”), 35.7 (C20”), 31.9 (C7”), 31.8 (C8”), 31.7 , 29.9, 29.7, 29.3, 29.2, 29.2, 28.3 (C2”), 28.2 (C12”), 27.9 (C25”), 26.8, 26.7, 25.8, 24.2 (C15”), 23.8 (C23”), 22.7 (C26”), 22.6 (C), 22.4 (C27”), 21.0 (C11”), 19.3 (C19”), 18.6 (C21”), 14.0 (C23), 11.8 (C18”)

m/z (ESI) :

Cette thèse est accessible à l'adresse : http://theses.insa-lyon.fr/publication/2013ISAL0001/these.pdf
© [R. Xu], [2013], INSA de Lyon, tous droits réservés

861.7 ($M+H^+$), 883.7 ($M+Na^+$)

$[\alpha]_D^{20}$

+33 (*c* 0.7 in CH_2Cl_2/MeOH, 9/1)

Elemental analysis:

Found: C 69.01, H 10.31, N 3.22. $C_{50}H_{88}N_2O_9+0.5H_2O$ requires C 69.12, H 10.56, N 3.07

Glucosteroid L6S12 bolaphile (125c)

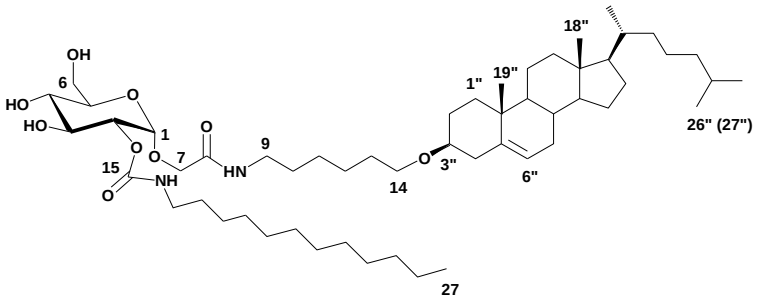

White solid

^{1}HNMR (400 MHz, $CDCl_3$/ MeOD) :

δ: 5.35 (m, 1 H, H-6”), 5.01 (d, 1H, *J* = 3.6 Hz, H-1), 4.55 (dd, 1 H, *J* = 3.6 and 10.0 Hz, H-2), 4.13 (d, 1 H, *J* = 15.6 Hz , H-7a), 3.98 (d, 1 H, *J* = 15.6 Hz, H-7b), 3.88-3.74 (m, 3 H, H-6a, H-6b, H-3), 3.61-3.44 (m, 4 H, H-5, H-4, CH_2-14), 3.25 (t, 2 H, *J* = 7.3 Hz, CH_2-9), 3.19-3.04 (m, 3 H, CH_2-16, H-3”), 2.40-2.10 (m, 2 H, H-4”), 2.08-0.80 (m, 69 H, H-Cholesterol, CH_2-10 to CH_2-13, CH_2-17 to CH_3-27), 0.68 (s, 3 H, $CH_3$18”)

^{13}CNMR (100 MHz, $CDCl_3$/MeOD) :

δ: 169.5 (C8), 156.3, 140.8 (C5”), 121.6 (C6”), 97.2 (C1), 79.1 (C3”), 73.5 (C2), 72.3 (C5), 71.2 (C3), 70.2 (C4), 67.9, 66.5 (C7), 61.3 (C6), 56.7 (C14”), 56.1 (C17”), 50.2 (C9”), 42.3 (C13”), 41.1 (C9), 39.7 (C16”), 39.5 (C24”), 39.0 (C4”), 39.0, 37.2 (C1”), 36.8 (C10”), 36.1 (C22”), 35.7 (C20”), 31.9 (C7”), 31.8 (C8”), 29.9, 29.7, 29.7, 29.6, 29.6, 29.6, 29.4, 29.3, 28.4 (C2”), 28.2 (C12”), 28.0 (C25”), 26.8, 26.7, 25.8, 24.2 (C15”), 23.8 (C23”), 22.7 (C26”), 22.6, 22.4 (C27”), 21.0 (C11”), 19.3 (C19”), 18.6 (C21”), 14.0 (C27), 11.8 (C18”)

m/z (ESI) :

Cette thèse est accessible à l'adresse : http://theses.insa-lyon.fr/publication/2013ISAL0001/these.pdf
© [R. Xu], [2013], INSA de Lyon, tous droits réservés

917.7 ($M+H^+$), 939.6 ($M+Na^+$)

$[\alpha]_D^{20}$

+34 (*c* 0.7 in CH_2Cl_2/MeOH, 9/1))

Elemental analysis:

Found: C 70.49, H 10.76, N 2.96. $C_{54}H_{96}N_2O_9$ requires C 70.70, H 10.55, N 3.05

Glucosteroid L6S14 bolaphile (125d)

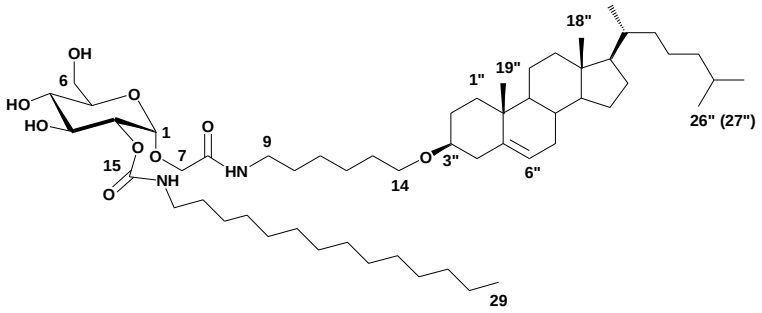

White solid

^{1}HNMR (400 MHz, $CDCl_3$/ MeOD) :

δ : 5.21 (m, 1 H, H-6”), 4.86 (d, 1 H, *J* = 3.5 Hz, H-1), 4.39 (dd, 1 H, *J* = 3.4 and 10.0 Hz, H-2), 4.00 (d, 1 H, *J* = 15.5 Hz, H-7a), 3.83 (d, 1 H, *J* = 15.6 Hz, H-7b), 3.74-3.60 (m, 3 H, H-6a, H-6b, H-3), 3.50-3.30 (m, 4 H, H-5, H-4, CH_2-14), 3.11 (t, 2 H, *J* = 7.3 Hz, CH_2-9), 3.08-2.92 (m, 3 H, CH_2-16, H-3”), 2.30-2.00 (m, 2 H, H4”), 1.96-0.77(m, 73 H, H-Cholesterol, CH_2-10 to CH_2-13, CH_2-17 to CH_3-29), 0.54 (s, 3 H, CH_3-18”)

^{13}CNMR (100 MHz, $CDCl_3$/MeOD) :

δ : 169.5 (C8), 156.3, 140.7 (C5”), 121.6 (C6”), 97.2 (C1), 79.1 (C3”), 73.4 (C2), 72.3 (C5), 71.2 (C3), 70.1 (C4), 67.9, 66.4 (C7), 61.2 (C6), 56.7 (C14”), 56.1 (C17”), 50.1 (C9”), 42.3 (C13”), 41.1 (C9), 39.7 (C16”), 39.4 (C24”), 39.0 (C4”), 39.0, 37.2 (C1”), 36.8 (C10”), 36.1 (C22”), 35.7 (C20”), 31.9 (C7”), 31.8 (C8”), 29.9, 29.7, 29.6, 29.6, 29.6, 29.3, 28.3 (C2”), 28.2 (C12”), 27.9 (C25”), 26.8, 26.7, 25.8, 24.2 (C15”), 23.7 (C23”), 22.7 (C26”), 22.6, 22.4 (C27”), 21.0 (C11”), 19.3 (C19”), 18.6 (C21”), 14.0 (C29), 11.7 (C18”)

Cette thèse est accessible à l'adresse : http://theses.insa-lyon.fr/publication/2013ISAL0001/these.pdf
© [R. Xu], [2013], INSA de Lyon, tous droits réservés

m/z (ESI) :

946.5 ($M+H^+$), 968.5 ($M+Na^+$)

$[\alpha]_D^{20}$

+29 (*c* 0.9 in CH_2Cl_2/MeOH, 9/1)

Elemental analysis:

Found: C 70.41; H 10.59; N 2.91. $C_{56}H_{100}N_2O_9+0.5H_2O$ requires C 70.41; H 10.59; N 2.94

Glucosteroid L6S16 bolaphile (125e)

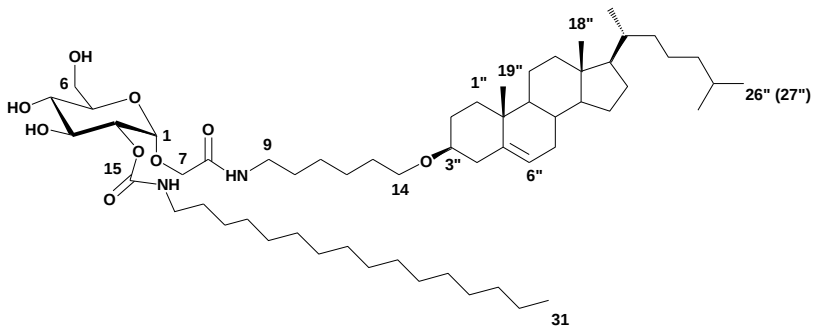

White solid

^{1}HNMR (400 MHz, $CDCl_3$/ MeOD) :

δ: 5.21 (m, 1 H, H-6”), 4.86 (d, 1 H, *J* = 3.5 Hz, H-1), 4.39 (dd, 1 H,, *J* = 3.4 and 10.0 Hz, H-2), 4.04 (d, 1 H, *J* = 15.6 Hz, H-7a), 3.88 (d, 1 H, *J* = 15.6 Hz, H-7b), 3.74-3.60 (m, 3 H, H-6a, H-6b, H-3), 3.50-3.30 (m, 4 H, H-5, H-4, CH_2-14), 3.11 (t, 2 H, *J* = 7.3 Hz, CH_2-9), 3.04-2.92 (m, 3 H, CH_2-16, H-3”), 2.30-2.00 (m, 2 H, H-4”), 1.96-0.77 (m, 77 H, H-Cholesterol, CH_2-10 to CH_2-13, CH_2-17 to CH_3-31), 0.54 (s, 3 H, CH_3-18”)

^{13}CNMR (100 MHz, $CDCl_3$/MeOD) :

δ: 169.5 (C8), 156.3 (C15), 140.7 (C5”), 121.6 (C6”), 97.1 (C1), 79.1 (C3”), 73.4 (C2), 72.3 (C5), 71.2 (C3), 70.0 (C4), 67.9 (C14), 66.4 (C7), 61.2 (C6), 56.7 (C14”), 56.1 (C17”), 50.1 (C9”), 42.2 (C13”), 41.1 (C9), 39.7 (C16”), 39.4 (C24”), 39.0 (C4”), 39.0, 37.2 (C1”), 36.8 (C10”), 36.1 (C22”), 35.7 (C20”), 31.9 (C7”), 31.8 (C8”), 29.9, 29.7, 29.7, 29.6, 29.6, 29.3,

Cette thèse est accessible à l'adresse : http://theses.insa-lyon.fr/publication/2013ISAL0001/these.pdf
© [R. Xu], [2013], INSA de Lyon, tous droits réservés

28.3 (C2”), 28.2 (C12”), 27.9 (C25”), 26.8, 26.7, 25.8, 24.2 (C15”), 23.7 (C23”), 22.7 (C26”), 22.6, 22.4 (C27”), 21.0 (C11”), 19.3 (C19”), 18.6 (C21”), 14.0 (C31), 11.8 (C18”)

m/z (ESI) :

973.8 ($M+H^+$), 995.8 ($M+Na^+$)

$[\alpha]_D^{20}$

+27 (*c* 1 in $CHCl_3$/MeOH, 9/1)

Elemental analysis:

Found: C 69.05; H 10.51; N 2.65. $C_{58}H_{104}N_2O_9+2H_2O$ requires C 69.05; H 10.70; N 2.78

Glucosteroid L6S18 bolaphile (125f)

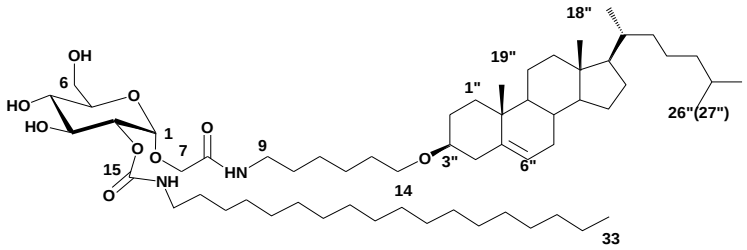

White solid

^{1}HNMR (400 MHz, $CDCl_3$/ MeOD) :

δ: 5.23 (m, 1 H, H-6”), 4.86 (d, 1 H, *J* = 3.5 Hz, H-1), 4.40 (dd, 1 H, *J* = 3.4 and 10.1 Hz, H-2), 3.98 (d, 1 H, *J* = 15.6 Hz, H-7a), 3.82 (d, 1 H, *J* = 15.6 Hz, H-7b), 3.74-3.60 (m, 3 H, H-6a, H-6b, H-3), 3.50-3.30 (m, 4 H, H-5, H-4, CH_2-14), 3.11 (t, 2 H, *J* = 7.3 Hz, CH_2-9), 3.05-2.90 (m, 3 H, CH_2-16, H-3”), 2.30-2.00 (m, 2 H, H-4”), 1.96-0.77 (m, 81H, H-Cholesterol, CH_2-10 to CH_2-13, CH_2-17 to CH_3-33), 0.53 (s, 3 H, CH_3-18”)

^{13}CNMR (100 MHz, $CDCl_3$/ MeOD) :

δ: 169.5 (C8), 156.3 (C15), 140.7 (C5”), 121.6 (C6”), 97.2 (C1), 79.1 (C3”), 73.4 (C2), 72.3 (C5), 71.2 (C3), 70.1 (C4), 67.9 (C14), 66.4 (C7), 61.2 (C6), 56.7 (C14”), 56.1 (C17”), 50.1 (C9”), 42.3 (C13”), 41.1 (C9), 39.7 (C16”), 39.4 (C24”), 39.0 (C4”), 39.0, 37.2 (C1”), 36.8 (C10”), 36.1 (C22”), 35.7 (C20”), 31.9 (C7”), 31.8 (C8”), 29.9, 29.7, 29.7, 29.6, 29.6, 29.5,

Cette thèse est accessible à l'adresse : http://theses.insa-lyon.fr/publication/2013ISAL0001/these.pdf
© [R. Xu], [2013], INSA de Lyon, tous droits réservés

29.5, 29.3, 29.3, 28.3 (C2”), 28.2 (C12”), 27.9 (C25”), 26.8, 26.7, 25.8, 24.2 (C15”), 23.8 (C23”), 22.7 (C26”), 22.6, 22.4 (C27”), 21.0 (C11”), 19.3 (C19”), 18.6 (C21”), 14.0 (C33), 11.8 (C18”)

m/z (HRMS) :

1001.8($M+H^+$), 1023.8 ($M + Na^+$)

$[\alpha]_D^{20}$

+30 (*c* 0.5 in CH_2Cl_2/MeOH, 9/1)

Elemental analysis:

Found: C 70.86; H 10.73; N 2.66. $C_{60}H_{108}N_2O_9+H_2O$ requires C 70.72; H, 10.80; N, 2.75

Glucosteroid L8S6 bolaphile (126a)

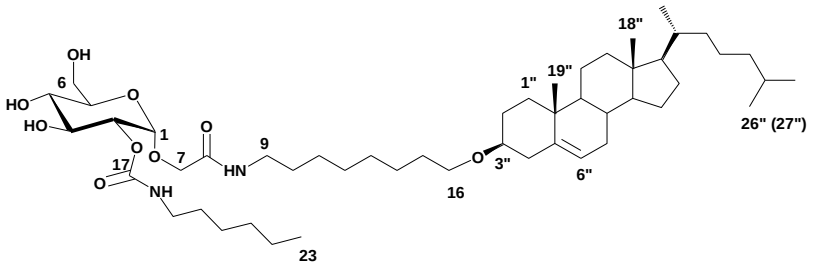

White solid

^{1}HNMR (400 MHz, $CDCl_3$/ MeOD) :

δ: 5.21 (m, 1 H, H-6”), 4.86 (d, 1 H, *J* = 3.5 Hz, H-1), 4.39 (dd, 1 H, *J* = 3.4 and 10.0 Hz, H-2), 4.04 (d, 1 H, *J* = 15.6, H-7a), 3.88 (d, 1 H, *J* = 15.6 Hz, H-7b), 3.74-3.60 (m, 3 H, H-6a, H-6b, H-3), 3.50-3.30 (m, 4 H, H-5, H-4, CH_2-14), 3.11 (t, 2 H, *J* = 7.3 Hz, CH_2-9), 3.04-2.92 (m, 3 H, CH_2-16, H-3”), 2.30-2.00 (m, 2 H, H-4”), 1.96-0.77 (m, 77 H, H-Cholesterol, CH_2-10 to CH_2-13, CH_2-17 to CH_3-31), 0.54 (s, 3 H, CH_3-18”)

^{13}CNMR (100 MHz, $CDCl_3$/ MeOD) :

δ: 169.5 (C8), 156.3 (C17), 140.7 (C5”), 121.6 (C6”), 97.1 (C1), 79.1 (C3”), 73.4 (C2), 72.3 (C5), 71.2 (C3), 70.0 (C4), 67.9 (C16), 66.4 (C7), 61.2 (C6), 56.7 (C14”), 56.1 (C17”), 50.1 (C9”), 42.2 (C13”), 41.1 (C9), 39.7 (C16”), 39.4 (C24”), 39.0 (C4”), 39.0, 37.2 (C1”), 36.8

Cette thèse est accessible à l'adresse : http://theses.insa-lyon.fr/publication/2013ISAL0001/these.pdf
© [R. Xu], [2013], INSA de Lyon, tous droits réservés

(C10”), 36.1 (C22”), 35.7 (C20”), 31.9 (C7”), 31.8 (C8”), 29.9, 29.7, 29.7, 29.6, 29.6, 29.3, 28.3 (C2”), 28.2 (C12”), 27.9 (C25”), 26.8, 26.7, 25.8, 24.2 (C15”), 23.7 (C23”), 22.7 (C26”), 22.6, 22.4 (C27”), 21.0 (C11”), 19.3 (C19”), 18.6 (C21”), 14.0 (C23), 11.8 (C18”)

m/z (ESI) :

973.8 ($M+H^+$), 995.8 ($M+Na^+$)

$[\alpha]_D^{20}$

+34 (*c* 0.6 in CH_2Cl_2/MeOH, 9/1)

Elemental analysis:

Found: C 68.27, H 10.47, N 3.03. $C_{50}H_{88}N_2O_9+H_2O$ requires C 68.30, H 10.32, N 3.19

Glucosteroid L8S8 bolaphile (126b)

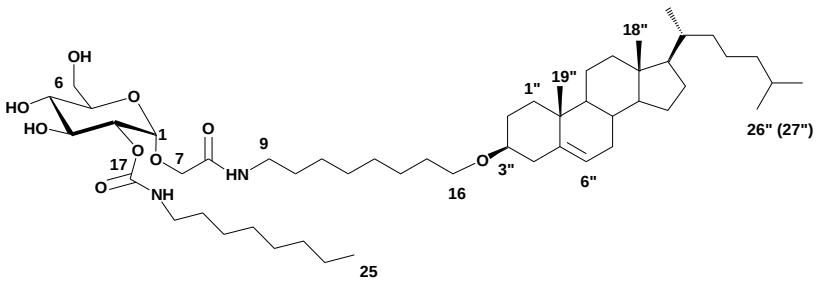

White solid

^{1}HNMR (400 MHz, $CDCl_3$/ MeOD) :

δ: 5.35 (m, 1 H, H-6”), 5.01 (d, 1 H, *J* = 3.6 Hz, H-1), 4.53 (dd, 1 H, *J* = 3.4 and 10.0 Hz, H-2), 4.13 (d, 1 H, *J* = 15.6 Hz, H-7a), 3.91(d, 1 H, *J* = 15.6 Hz, H-7b), 3.88-3.73 (m, 3 H, H-6a, H-6b, H-3), 3.61-3.44 (m, 4 H, H-5, H-4, CH_2-16), 3.25 (t, 2 H, *J* = 7.2 Hz, CH_2-9), 3.19-3.04 (m, 3 H, CH_2-18, H-3”), 2.39-2.13 (m, 2 H, H-4”), 2.08-0.80 (m, 65 H, H-Cholesterol, CH_2-10 to CH_2-15, CH_2-19 to CH_3-23), 0.68 (s, 3 H, CH_3-18”)

^{13}CNMR (100 MHz, $CDCl_3$/ MeOD) :

δ: 169.4 (C8), 156.3 (C17), 140.9 (C5”), 121.6 (C6”), 97.2 (C1), 79.1 (C3”), 73.5 (C2), 72.3 (C5), 71.2 (C3), 70.1 (C4), 68.1 (C16), 66.4 (C7), 61.3 (C6), 56.7 (C14”), 56.1 (C17”), 50.2 (C9”), 42.3 (C13”), 41.1 (C9), 39.7 (C16”), 39.5 (C24”), 39.1 (C4”), 39.0, 37.2 (C1”), 36.8

Cette thèse est accessible à l'adresse : http://theses.insa-lyon.fr/publication/2013ISAL0001/these.pdf
© [R. Xu], [2013], INSA de Lyon, tous droits réservés

(C10”), 36.1 (C22”), 35.7 (C20”), 31.9 (C7”), 31.8 (C8”), 31.7, 30.0, 29.7, 29.5, 29.4, 29.2, 29.2, 28.4 (C2”), 28.2 (C12”), 27.9 (C25”), 26.8, 26.8, 26.1, 24.2 (C15”), 23.8 (C23”), 22.7 (C26”), 22.6, 22.4 (C27”), 21.0 (C11”), 19.3 (C19”), 18.6 (C21”), 14.0 (C25), 11.8 (C18”)

m/z (ESI) :

889.7 ($M+H^+$), 911.7 ($M+Na^+$)

$[\alpha]_D^{20}$

+36 (*c* 0.7 in CH_2Cl_2/MeOH, 9/1)

Elemental analysis:

Found: C 68.93, H 10.46, N 3.06. $C_{52}H_{92}N_2O_9+H_2O$ requires C 68.84, H 10.44, N 3.09

Glucosteroid L8S12 bolaphile (126c)

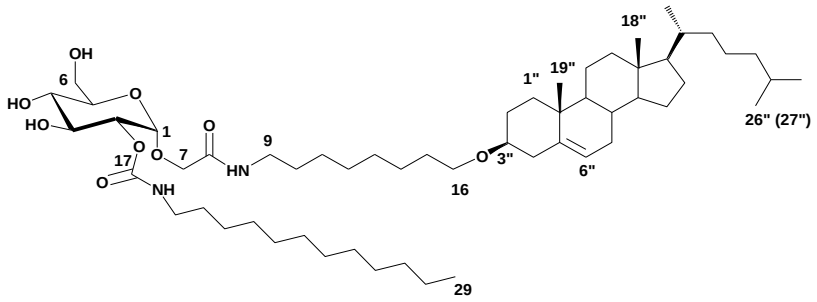

White solid

^{1}HNMR (400 MHz, $CDCl_3$/ MeOD) :

δ: 5.35 (m, 1 H, H-6”), 5.01 (d, 1 H, *J* = 3.6 Hz, H-1), 4.55 (dd, 1 H, *J* = 3.6 and 10.1 Hz, H-2), 4.13 (d, 1 H, *J* = 15.6 Hz, H-7a), 3.96 (d, 1 H, *J* = 15.6 Hz, H-7b), 3.87-3.74 (m, 3 H, H-6a, H-6b, H-3), 3.61-3.52 (m, 4 H, H-5, H-4, CH_2-16), 3.25 (t, 2 H, *J* = 7.4 Hz, CH_2-9), 3.19-3.04 (m, 3 H, CH_2-18, H-3”), 2.39-2.13 (m, 2 H, H-4”), 2.08-0.80 (m, 73 H, H-Cholesterol, CH_2-10 to CH_2-15, CH_2-19 to CH_3-27), 0.68 (s, 3 H, CH_3-18”)

^{13}CNMR (75 MHz, $CDCl_3$/ MeOD) :

δ: 169.5 (C8), 156.3 (C17), 140.8 (C5”), 121.6 (C6”), 97.1 (C1), 79.1 (C3”), 73.4 (C2), 72.3 (C5), 71.2 (C3), 70.0 (C4), 68.1 (C16), 66.4 (C7), 61.2 (C6), 56.7 (C14”), 56.1 (C17”), 50.1

Cette thèse est accessible à l'adresse : http://theses.insa-lyon.fr/publication/2013ISAL0001/these.pdf
© [R. Xu], [2013], INSA de Lyon, tous droits réservés

(C9”), 42.3 (C13”), 41.0 (C9), 39.7 (C16”), 39.4 (C24”), 39.1 (C4”), 39.0, 37.2 (C1”), 36.8 (C10”), 36.1 (C22”), 35.7 (C20”), 31.9 (C7”), 31.8 (C8”), 31.4, 30.0, 29.6, 29.4, 29.4, 29.2, 28.3 (C2”), 28.2 (C12”), 27.9 (C25”), 26.8, 26.4, 26.0, 24.2 (C15”), 23.7 (C23”), 22.7 (C26”), 22.5, 22.4 (C27”), 21.0 (C11”), 19.3 (C19”), 18.6 (C21”), 13.9 (C29), 11.8 (C18”)

m/z (ESI) :

945.7 ($M+H^+$), 967.7 ($M+Na^+$)

$[\alpha]_D^{20}$

+35 (*c* 0.7 in CH_2Cl_2/MeOH (9/1))

Elemental analysis:

Found: C 71.14, H 10.66, N 2.96. $C_{56}H_{100}N_2O_9$ requires C 71.14, H 10.66, N 2.96

Glucosteroid L8S14 bolaphile (126d)

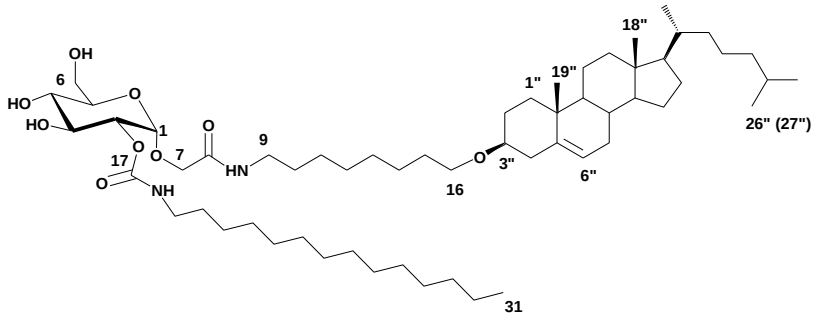

White solid

^{1}HNMR (400 MHz, $CDCl_3$/ MeOD) :

δ: 5.21 (m, 1 H, H-6”), 4.86 (d, 1 H, *J* = 3.5 Hz, H-1), 4.40 (dd, 1 H, *J* = 3.4 and 10.1 Hz, H-2), 4.00 (d, 1 H, *J* = 15.6 Hz, H-7a), 3.83 (d, 1 H, *J* = 15.6 Hz, H-7b), 3.74-3.60 (m, 3 H, H-6a, H-6b, H-3), 3.50-3.30 (m, 4 H, H-5, H-4, CH_2-16), 3.11 (t, 2 H, *J* = 7.3 Hz, CH_2-9), 3.06-2.93 (m, 3 H, CH_2-18, H-3”), 2.26-2.00 (m, 2 H, H4”), 1.96-0.77 (m, 77 H, H-Cholesterol, CH_2-10 to CH_2-15, CH_2-19 to CH_3-31), 0.54 (s, 3 H, CH_3-18”)

^{13}CNMR (100 MHz, $CDCl_3$/ MeOD) :

Cette thèse est accessible à l'adresse : http://theses.insa-lyon.fr/publication/2013ISAL0001/these.pdf
© [R. Xu], [2013], INSA de Lyon, tous droits réservés

δ: 169.5 (C8), 156.2 (C17), 140.8 (C5”), 121.5 (C6”), 97.1 (C1), 79.1 (C3”), 73.4 (C2), 72.3 (C5), 71.2 (C3), 70.1 (C4), 68.1 (C16), 66.4 (C7), 61.2 (C6), 56.7 (C14”), 56.1 (C17”), 50.1 (C9”), 42.3 (C13”), 41.1 (C9), 39.7 (C16”), 39.4 (C24”), 39.1 (C4”), 39.0, 37.2 (C1”), 36.8 (C10”), 36.1 (C22”), 35.7 (C20”), 31.9 (C7”), 31.8 (C8”), 30.0, 29.7, 29.6, 29.6, 29.6, 29.6, 29.5, 29.4, 29.4, 29.3, 29.2, 28.3 (C2”), 28.2 (C12”), 27.9 (C25”), 26.8, 26.8, 26.0, 24.2 (C15”), 23.7 (C23”), 22.7 (C26”), 22.6 , 22.4 (C27”), 21.0 (C11”), 19.3 (C19”), 18.6 (C21”), 14.0 (C31), 11.8 (C18”)

m/z (ESI) :

973.8 ($M+H^+$), 995.8 ($M+Na^+$)

$[\alpha]_D^{20}$

+30 (*c* 0.9 in CH_2Cl_2/MeOH (9/1))

Elemental analysis:

Found: C 70.66, H 10.71, N 2.71. $C_{58}H_{104}N_2O_9+H_2O$ requires C 70.30, H 10.71, N 2.83

Glucosteroid L8S16 bolaphile (126e)

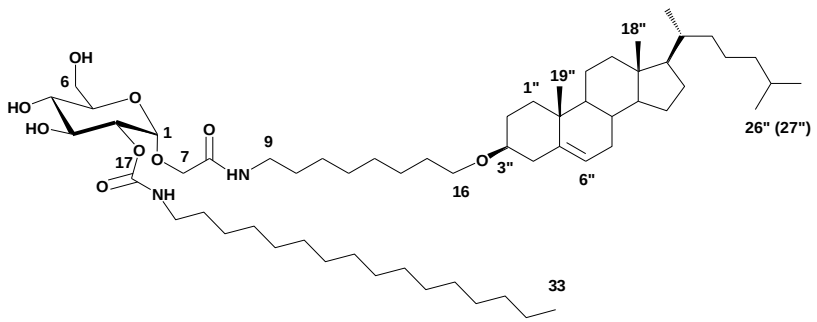

White solid

^{1}HNMR (400 MHz, $CDCl_3$/ MeOD) :

δ: 5.23 (m, 1 H, H-6”), 4.86 (d, 1 H, *J* = 3.5 Hz, H-1), 4.40 (dd, 1 H, *J* = 3.4 and 10.1 Hz, H-2), 3.98 (d, 1 H, *J* = 15.6 Hz, H-7a), 3.83 (d, 1 H, *J* = 15.6 Hz, H-7b), 3.74-3.60 (m, 3 H, H-6a, H-6b, H-3), 3.50-3.30 (m, 4 H, H-5, H-4, CH_2-16), 3.11 (t, 2 H, *J* = 7.3 Hz, CH_2-9), 3.05-2.93 (m, 3 H, CH_2-18, H-3”), 2.25-2.00 (m, 2 H, H-4”), 1.96-0.67 (m, 81 H, H-Cholesterol, CH_2-10 to CH_2-15, CH_2-19 to CH_3-33), 0.54 (s, 3 H, CH_3-18”)

Cette thèse est accessible à l'adresse : http://theses.insa-lyon.fr/publication/2013ISAL0001/these.pdf
© [R. Xu], [2013], INSA de Lyon, tous droits réservés

^{13}CNMR (100 MHz, $CDCl_3$/ MeOD) :

δ: 169.5 (C8), 156.2 (C17), 140.8 (C5”), 121.6 (C6”), 97.1 (C1), 79.1 (C3”), 73.4 (C2), 72.3 (C5), 71.2 (C3), 70.1 (C4), 68.1 (C16), 66.4 (C7), 61.2 (C6), 56.7 (C14”), 56.1 (C17”), 50.2 (C9”), 42.3 (C13”), 41.1 (C9), 39.7 (C16”), 39.4 (C24”), 39.1 (C4”), 39.0, 37.2 (C1”), 36.8 (C10”), 36.1 (C22”), 35.7 (C20”), 31.9 (C7”), 31.8 (C8”), 30.0, 29.7, 29.7, 29.6, 29.6, 29.5, 29.5, 29.4, 29.4, 29.3, 29.2, 28.3 (C2”), 28.2 (C12”), 27.9 (C25”), 26.8, 26.8, 26.0, 24.2 (C15”), 23.7 (C23”), 22.7 (C26”), 22.6, 22.4, 22.3 (C27”), 21.0 (C11”), 19.3 (C19”), 18.6 (C21”), 14.0, 13.9 (C33), 11.8 (C18”)

m/z (ESI) :

1001.8($M+H^+$), 1023.8 ($M + Na^+$)

$[\alpha]_D^{20}$

+26 (*c* 1 in CH_2Cl_2/MeOH, 9/1)

Elemental analysis:

Found: C 70.42, H 10.70, N 2.68. $C_{60}H_{108}N_2O_9+H_2O$ requires C 70.72, H 10.80, N 2.75

Glucosteroid L8S18 bolaphile (126f)

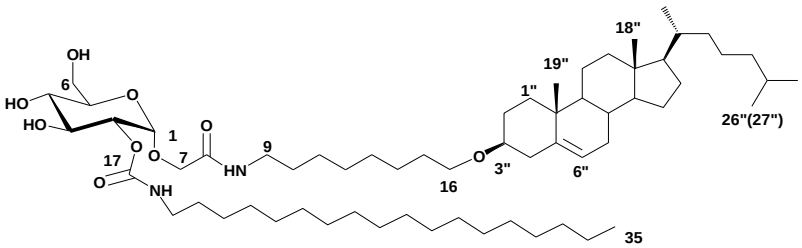

White solid

^{1}HNMR (300 MHz, $CDCl_3$/ MeOD) :

δ: 5.23 (m, 1 H, H-6”), 4.86 (d, 1 H, *J* = 3.6 Hz, H-1), 4.40 (dd, 1 H, *J* = 3.6, 10.1 Hz, H-2), 4.00 (d, 1 H, *J* = 15.6 Hz, H-7a), 3.83 (d, 1 H, *J* = 15.3 Hz, H-7b), 3.74-3.60 (m, 3 H, H-6a, H-6b, H-3) 3.50-3.30 (m, 4 H, H-5, H-4, CH_2-16), 3.11 (t, 2 H, *J* = 7.3 Hz, CH_2-9), 3.05-2.90 (m, 3 H, CH_2-18, H-3”), 2.30-2.00 (m, 2 H, H-4”), 1.96-0.67 (m, 85 H, H-Cholesterol, CH_2-10 to CH_2-15, CH_2-19 to CH_3-35), 0.53 (s, 3 H, CH_3-18”)

Cette thèse est accessible à l'adresse : http://theses.insa-lyon.fr/publication/2013ISAL0001/these.pdf
© [R. Xu], [2013], INSA de Lyon, tous droits réservés

^{13}CNMR (75 MHz, $CDCl_3$/ MeOD) :

δ: 169.5 (C8), 156.2 (C17), 140.8 (C5”), 121.5 (C6”), 97.1 (C1), 79.1 (C3”), 73.5 (C2), 72.3 (C5), 71.2 (C3), 70.1 (C4), 68.1 (C16), 66.4 (C7), 61.2 (C6), 56.7 (C14”), 56.1 (C17”), 50.2 (C9”), 42.3 (C13”), 41.1 (C9), 39.7 (C16”), 39.4 (C24”), 39.1 (C4”), 39.0, 37.2 (C1”), 36.8 (C10”), 36.1 (C22”), 35.7 (C20”), 31.9 (C7”), 31.8 (C8”), 30.0, 29.7, 29.6, 29.6, 29.4, 29.4, 29.3, 29.2, 28.3 (C2”), 28.2 (C12”), 27.9 (C25”), 26.8, 26.8, 26.1, 24.2 (C15”), 23.7 (C23”), 22.7 (C26”), 22.6, 22.4 (C27”), 21.0 (C11”), 19.3 (C19”), 18.6 (C21”), 14.0 (C35), 11.8 (C18”)

m/z (ESI) :

1029.8 ($M+H^+$), 1051.8 ($M + Na^+$)

$[\alpha]_D^{20}$

+29 (*c* 0.9 in CH_2Cl_2/MeOH, 9/1)

Elemental analysis:

Found: C 71.72, H 10.87, N 2.61. $C_{62}H_{112}N_2O_9$+0.5H_2O requires C 71.68, H, 10.98, N 2.70

Glucosteroid L10S6 bolaphile (127a)

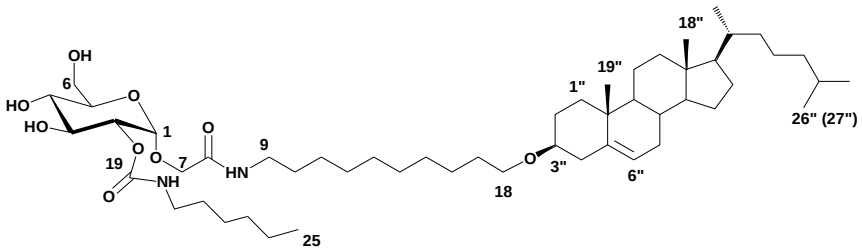

White solid

^{1}HNMR (400 MHz, $CDCl_3$/ MeOD) :

δ: 5.35 (m, 1H, H-6”), 5.02 (d, 1H, *J* = 3.6 Hz, H-1), 4.55 (dd, 1H, *J* = 3.5 and 10.1 Hz, H-2), 4.15 (d, 1H, *J* = 15.6 Hz, H-7a), 3.98 (d, 1H, *J* = 15.6 Hz, H-7b), 3.89-3.75 (m, 3H, H-6a, H-6b, H-3), 3.61-3.52 (m, 4H, H-5, H-4, CH_2-18), 3.25 (t, 2H, *J* = 7.2 Hz, CH_2-9), 3.19-3.04 (m, 3H, CH_2-20, H-3”), 2.40-2.10 (m, 2H, H-4”), 2.08-0.80 (m, 67H, H-Cholesterol, CH_2-10 to CH_2-17, CH_2-21 to CH_3-23), 0.69 (s, 3H, CH_3-18”)

Cette thèse est accessible à l'adresse : http://theses.insa-lyon.fr/publication/2013ISAL0001/these.pdf
© [R. Xu], [2013], INSA de Lyon, tous droits réservés

^{13}CNMR (100 MHz, $CDCl_3$/ MeOD) :

δ: 169.5 (C8), 156.3 (C19), 140.9 (C5”), 121.5 (C6”), 97.1 (C1), 79.0 (C3”), 73.4 (C2), 72.3 (C5), 71.2 (C3), 70.0 (C4), 68.1 (C18), 66.4 (C7), 61.2 (C6), 56.7 (C14”), 56.1 (C17”), 50.2 (C19”), 42.3 (C13”), 41.0 (C9), 39.7 (C16”), 39.4 (C24”), 39.1 (C4”), 39.0, 37.2 (C1”), 36.8 (C10”), 36.1 (C22”), 35.7 (C20”), 31.9 (C7”), 31.8 (C8”), 31.4, 30.0, 29.6, 29.5, 29.5, 29.5, 29.4, 29.3, 29.3, 28.3 (C2”), 28.2 (C12”), 27.9 (C25”), 26.9, 26.4, 26.1, 24.2 (C15”), 23.7 (C23”), 22.7 (C26”), 22.5, 22.4 (C27”), 21.0 (C11”), 19.3 (C19”), 18.6 (C21”), 13.9 (C25), 11.8 (C18”)

m/z (HRMS) :

889.6868 ($M + H^+$, $C_{52}H_{93}N_2O_9$ requires 889.6876)

$[\alpha]_D^{20}$

+34 (*c* 0.7 in CH_2Cl_2/MeOH, 9/1)

Elemental analysis:

Found: C 70.22, H 10.78, N 3.00. $C_{52}H_{92}N_2O_9$ requires C 70.23, H 10.43, N 3.15

Glucosteroid L10S8 bolaphile (127b)

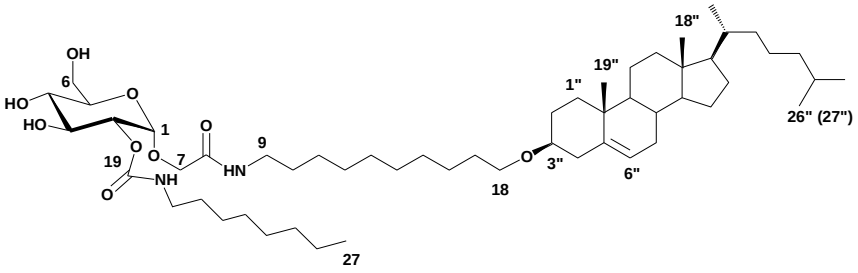

White solid

^{1}HNMR (400 MHz, $CDCl_3$/ MeOD) :

δ: 5.35 (m, 1H, H-6”), 5.01 (d, 1H, *J* = 3.5 Hz, H-1), 4.55 (dd, 1H, *J* = 3.3 and 10.1 Hz, H-2), 4.13 (d, 1H, *J* = 15.7 Hz, H-7a), 3.97 (d, 1H, *J* = 15.6 Hz, H-7b), 3.89-3.71 (m, 3H, H-6a, H-6b, H-3), 3.61-3.52 (m, 4H, H-4, H-5, CH_2-18), 3.25 (t, 2H, *J* = 7.3 Hz, CH_2-9), 3.19-3.04 (m,

Cette thèse est accessible à l'adresse : http://theses.insa-lyon.fr/publication/2013ISAL0001/these.pdf
© [R. Xu], [2013], INSA de Lyon, tous droits réservés

3H, CH_2-20, H-3"), 2.40-2.10 (m, 2H, H-4"), 2.08-0.80 (m, 71H, H-Cholesterol, CH_2-10 to CH_2-17, CH_2-21 to CH_3-25), 0.68 (s, 3H, CH_3-18")

^{13}CNMR (100 MHz, $CDCl_3$/ MeOD) :

δ: 169.6 (C8), 156.4 (C19), 141.0 (C5"), 121.6, 97.3 (C1), 79.2 (C3"), 73.6 (C2), 72.4 (C5), 71.3 (C3), 70.3 (C4), 68.3 (C18), 66.6 (C7), 61.4 (C6), 56.9 (C14"), 56.2 (C17"), 50.3 (C9"), 42.4 (C13"), 41.2 (C9), 39.9 (C16"), 39.6 (C24"), 39.2 (C4"), 39.2, 37.3 (C1"), 37.0 (C10"), 36.3 (C22"), 35.9 (C20"), 32.0 (C7"), 32.0 (C8"), 31.9, 30.1, 29.8, 29.6, 29.6, 29.6, 29.4, 29.3, 29.3, 28.5 (C2"), 28.3 (C12"), 28.1 (C25"), 27.0, 26.9, 26.2, 24.4 (C15"), 23.9 (C23"), 22.8 (C26"), 22.7, 22.6 (C27"), 21.1 (C11"), 19.4 (C19"), 18.8 (C21"), 14.1 (C27), 11.9 (C18")

m/z (ESI) :

917.7 ($M+H^+$), 939.7 ($M+Na^+$)

$[\alpha]_D^{20}$

+30 (*c* 0.8 in CH_2Cl_2/MeOH, 9/1)

Elemental analysis:

Found: C 69.48, H 10.65, N 2.95. $C_{54}H_{96}N_2O_9+H_2O$ requires C 69.34, H 10.56, N 2.99

Glucosteroid L10S12 bolaphile (127c)

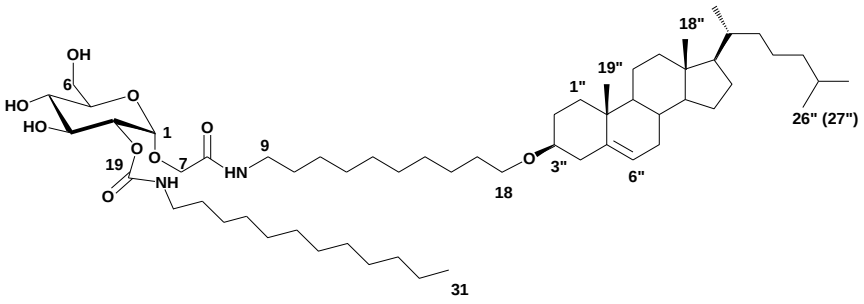

White solid

^{1}HNMR (400 MHz, $CDCl_3$/ MeOD) :

δ: 5.35 (m, 1H, H-6"), 5.01 (d, 1H, *J* = 3.6 Hz, H-1), 4.55 (dd, 1H, *J* = 3.4 and 10.0 Hz, H-2), 4.13 (d, 1H, *J* = 15.6 Hz, H-7a), 3.97 (d, 1H, *J* = 15.6 Hz, H-7b), 3.88-3.74 (m, 3H, H-6a, H-

Cette thèse est accessible à l'adresse : http://theses.insa-lyon.fr/publication/2013ISAL0001/these.pdf
© [R. Xu], [2013], INSA de Lyon, tous droits réservés

6b, H-3), 3.61-3.52 (m, 4H, H-4, H-5, CH_2-18), 3.25 (t, 2H, *J* = 7.4 Hz, CH_2-9), 3.19-3.04 (m, 3H, CH_2-20, H-3"), 2.40-2.10 (m, 2H, H-4"), 2.08-0.80 (m, 79H, H-Cholesterol, CH_2-10 to CH_2-17, CH_2-21 to CH_3-29), 0.68 (s, 3H, CH_3-18")

^{13}CNMR (100 MHz, $CDCl_3$/ MeOD) :

δ: 169.6 (C8), 156.4 (C19), 141.0 (C5"), 121.7 (C6"), 97.3 (C1), 79.2 (C3"), 73.6 (C2), 72.4 (C5), 71.4 (C3), 70.3 (C4), 68.3 (C18), 66.6 (C7), 61.4 (C6), 56.9 (C14"), 56.2 (C17"), 50.3 (C9"), 42.4 (C13"), 41.2 (C9), 39.9 (C16"), 39.6 (C24"), 39.2 (C4"), 39.2, 37.3 (C1"), 37.0 (C10"), 36.3 (C22"), 35.9 (C20"), 32.0, 32.0, 30.2, 29.8, 29.7, 29.7, 29.7, 29.6, 29.6, 29.6, 29.4, 28.5 (C2"), 28.3 (C12"), 28.1 (C25"), 27.0, 26.9, 26.2, 24.4 (C15"), 23.9 (C23"), 22.8 (C26"), 22.7, 22.6 (C27"), 21.1 (C11"), 19.4 (C19"), 18.8 (C21"), 14.1 (C31), 11.9 (C18")

m/z (HRMS) :

973.8 ($M+H^+$), 995.8 ($M+Na^+$)

$[\alpha]_D^{20}$

+31 (*c* 0.8 in CH_2Cl_2/MeOH, 9/1)

Elemental analysis:

Found: C 71.37, H 10.96, N 2.71. $C_{58}H_{104}N_2O_9$ requires C 71.56, H 10.77, N 2.88

Glucosteroid L12S6 bolaphile (128a)

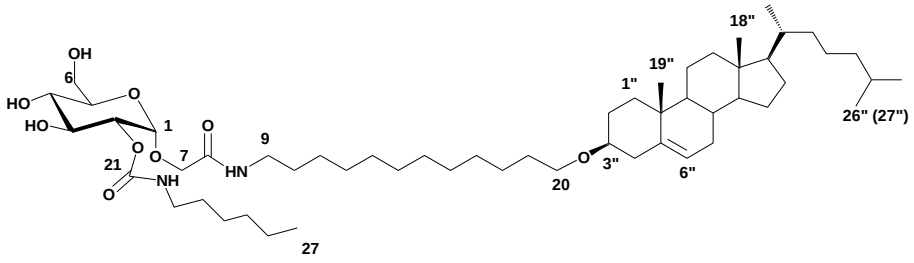

White solid

^{1}HNMR (400 MHz, $CDCl_3$/ MeOD) :

δ: 5.35 (m, 1H, H-6"), 5.01 (d, 1H, *J* = 3.7 Hz, H-1), 4.54 (dd, 1H, *J* = 3.5 and 10.1 Hz, H-2), 4.13 (d, 1H, *J* = 15.6 Hz, H-7a), 3.98 (d, 1H, *J* = 15.6 Hz, H-7b), 3.88-3.74 (m, 3H, H-6a, H-

Cette thèse est accessible à l'adresse : http://theses.insa-lyon.fr/publication/2013ISAL0001/these.pdf
© [R. Xu], [2013], INSA de Lyon, tous droits réservés

6b, H-3), 3.61-3.52 (m, 4H, H-5, H-4, CH_2-20), 3.25 (t, 2H, *J* = 7.5 Hz, CH_2-9), 3.19-3.08 (m, 3H, CH_2-22, H-3"), 2.39-2.14 (m, 2H, H-4"), 2.08-0.80 (m, 71H, H-Cholesterol, CH_2-10 to CH_2-19, CH_2-23 to CH_3-27), 0.68 (s, 3H, CH_3-18")

^{13}CNMR (100 MHz, $CDCl_3$/ MeOD) :

δ: 169.6 (C8), 156.4 (C21), 141.0 (C5"), 121.6 (C6"), 97.3 (C1), 79.2 (C3"), 73.6 (C2), 72.4 (C5), 71.4 (C3), 70.2 (C4), 68.3 (C20), 66.6 (C7), 61.4 (C6), 56.9 (C14"), 56.2 (C17"), 50.3 (C9"), 42.4 (C13"), 41.2 (C9), 39.9 (C16"), 39.6 (C24"), 39.2 (C4"), 39.2, 37.3 (C1"), 37.0 (C10"), 36.3 (C22"), 35.9 (C20"), 32.0 (C7"), 32.0 (C8"), 31.9, 31.5, 30.1, 29.8, 29.8, 29.7, 29.6, 29.6, 29.4, 29.3, 29.3, 28.5 (C2"), 28.3 (C12"), 28.1 (C25"), 27.0, 26.9, 26.5, 26.2, 24.4 (C15"), 23.9 (C23"), 22.8 (C26"), 22.7, 22.6, 22.6 (C27"), 21.1 (C11"), 19.4 (C19"), 18.8 (C21"), 14.1, 14.0 (C27), 11.9 (C18")

m/z (HRMS) :

917.7 ($M+H^+$), 939.7 ($M+Na^+$)

$[\alpha]_D^{20}$

+31 (*c* 0.7 in CH_2Cl_2/MeOH, 9/1)

Elemental analysis:

Found: C 70.67, H 10.73, N 2.88. $C_{54}H_{96}N_2O_9$ requires C 70.70, H 10.55, N 3.05

Glucosteroid L12S8 bolaphile (128b)

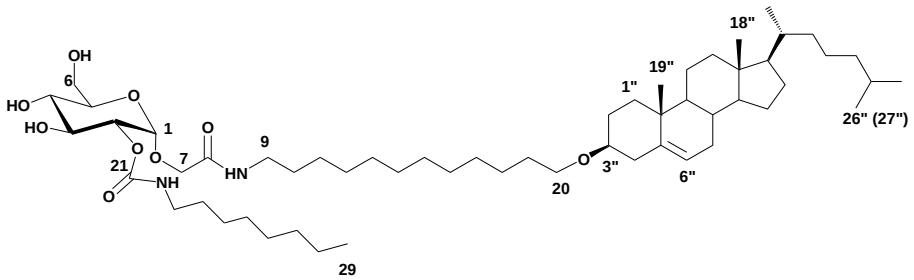

White solid

^{1}HNMR (400 MHz, $CDCl_3$/ MeOD) :

Cette thèse est accessible à l'adresse : http://theses.insa-lyon.fr/publication/2013ISAL0001/these.pdf
© [R. Xu], [2013], INSA de Lyon, tous droits réservés

δ: 5.34 (m, 1H, H-6”), 5.00 (d, 1H, *J* = 3.6 Hz, H-1), 4.52 (dd, 1H, *J* = 3.6 and 10.1 Hz, H-2), 4.12 (d, 1H, *J* =15.6 Hz, H-7a), 3.96 (d, 1H, *J* = 15.6 Hz, H-7b), 3.87-3.73 (m, 3H, H-6a, H-6b, H-3), 3.59-3.50 (m, 4H, H-5, H-4, CH_2-20), 3.23 (m, 2H, CH_2-9), 3.17-3.06 (m, 3H, CH_2-22, H-3”), 2.37-2.12 (m, 2H, H-4”), 2.06-0.78 (m, 75H, H-Cholesterol, CH_2-10 to CH_2-19, CH_2-23 to CH_3-29), 0.66 (s, 3H, CH_3-18”)

^{13}CNMR (100 MHz, $CDCl_3$/ MeOD) :

δ: 169.6 (C8), 156.3 (C21), 140.9 (C5”), 121.5 (C6”), 97.1 (C1), 79.0 (C3”), 73.4 (C2), 72.3 (C5), 71.2 (C3), 70.1 (C4), 68.2 (C20), 66.4 (C7), 61.2 (C6), 56.7 (C14”), 56.1 (C17”), 50.2 (C9”), 42.3 (C13”), 41.1 (C9), 39.7 (C16”), 39.4 (C24”), 39.1 (C4”), 39.0, 37.2 (C1”), 36.8 (C10”), 36.1 (C22”), 35.7 (C20”), 31.9 (C7”), 31.8 (C8”), 31.7, 30.0, 29.7, 29.6, 29.6, 29.5, 29.5, 29.4, 29.3, 29.2, 29.2, 28.3 (C2”), 28.2 (C12”), 27.9 (C25”), 26.9, 26.8, 26.1, 24.2 (C15”), 23.7 (C23”), 22.7 (C26”), 22.5, 22.4 (C27”), 21.0 (C11”), 19.3 (C19”), 18.6 (C21”), 13.9 (C29), 11.8 (C18”)

m/z (HRMS) :

967.7290 ($M + Na^+$, $C_{56}H_{100}N_2O_9$ requires 967.7321)

$[\alpha]_D^{20}$

+31 (*c* 0.7 in CH_2Cl_2/MeOH, 9/1)

Elemental analysis:

Found: C 69.84, H 10.85, N 2.83. $C_{56}H_{100}N_2O_9+H_2O$ requires C 69.81, H 10.67, N 2.91

Glucosteroid L12S12 bolaphile (128c)

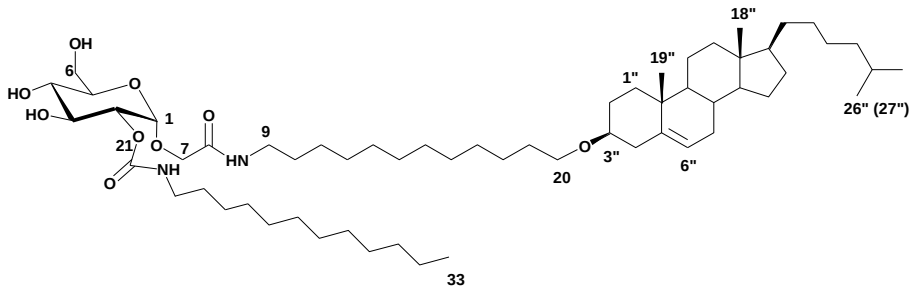

White solid

Cette thèse est accessible à l'adresse : http://theses.insa-lyon.fr/publication/2013ISAL0001/these.pdf
© [R. Xu], [2013], INSA de Lyon, tous droits réservés

^{1}HNMR (400 MHz, $CDCl_3$/ MeOD) :

δ: 5.36 (m, 1H, H-6”), 5.02 (d, 1H, *J* = 3.6 Hz, H-1), 4.55 (dd, 1H, *J* = 3.5 Hz, 10.1, H-2), 4.13 (d, 1H, *J* = 15.6 Hz, H-7a), 3.98 (d, 1H, *J* = 15.6 Hz, H-7b), 3.88-3.74 (m, 3H, H-6a, H-6b, H-3), 3.61-3.52 (m, 4H, H-5, H-4, CH_2-20), 3.25 (t, 2H, *J* = 7.5 Hz, CH_2-9), 3.19-3.08 (m, 3H, CH_2-22, H-3”), 2.39-2.14 (m, 2H, H-4”), 2.08-0.80 (m, 83H, H-Cholesterol, CH_2-10 to CH_2-19, CH_2-23 to CH_3-33), 0.68 (s, 3H, CH_3-18”)

^{13}CNMR (100 MHz, $CDCl_3$/ MeOD) :

δ: 169.4 (C8), 156.2 (C21), 141.0 (C5”), 121.5 (C6”), 97.2 (C1), 79.1 (C3”), 73.5 (C2), 72.2 (C5), 71.3 (C3), 70.2 (C4), 68.2 (C20), 66.5 (C7), 61.3 (C6), 56.8 (C14”), 56.2 (C17”), 50.2 (C9”), 42.3 (C13”), 41.1 (C9), 39.8 (C16”), 39.5 (C24”), 39.1 (C4”+), 37.3 (C1”), 36.9 (C10”), 36.2 (C22”), 35.8 (C20”), 31.9 (C7”), 31.9 (C8”), 30.1, 29.7, 29.6, 29.5, 29.4, 29.3, 29.2, 29.1, 28.4 (C2”), 28.2 (C12”), 28.0 (C25”), 26.9, 26.8, 26.1, 24.3 (C15”), 23.8 (C23”), 22.7 (C26”), 22.6, 22.5 (C27”), 21.0 (C11”), 19.3 (C19”), 18.7 (C21”), 14.0 (C33), 11.8 (C18”)

m/z (ESI) :

1001.8 ($M+H^+$)

$[\alpha]_D^{20}$

+25 (*c* 0.4 in CH_2Cl_2/MeOH, 9/1)

Elemental analysis:

Found: C 71.15, H 11.12, N 2.64. $C_{60}H_{108}N_2O_9$+0.5H_2O requires C 71.31, H 10.87, N 2.77

D.3 Synthesis of glucosyl and cellobiosyl probes

D.3.1 Synthesis for 6-dodecanoyl-2-bromonaphthalene (138)

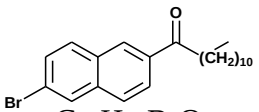

$C_{22}H_{29}BrO$
Exact Mass: 388.14
Mol. Wt.: 389.37

Cette thèse est accessible à l'adresse : http://theses.insa-lyon.fr/publication/2013ISAL0001/these.pdf
© [R. Xu], [2013], INSA de Lyon, tous droits réservés

2-bromonaphthalene (2.0 g, 1mmol) was dissolved in 9.6 ml of nitrobenzene under Ar, which was placed in an ice bath. Lauroylchloride (2.8 mol, 11.64 mL) was then added dropwised. After the addition, the reaction mixture was added by 1.4 g of $AlCl_3$. At this stage, the ice bath was removed and the reaction continued at room temperature for 2 h, which was quenched with 40 ml of distilled water. Extracted 3 times with ethyl acetate (30 mL), the organic phases were combined and washed with brine (30 mL) 3 times. Then the organic phases were dried over Na_2SO_4 and concentrated under reduced pressure. The desired compound were then obtained by recrystalizing in cold ethanol as white solid (1.1 g, 30 % of yield)

White solid

^{1} HNMR (300MHz, $CDCl_3$)

δ: 8.42 (s, 1H, H-9''), 8.05 (m, 2H, H-7'', H-1''), 7.81 (m, 2H, H-6'', H-2''), 7.62 (s, 1H, H-4''), 3.07 (t, 2H, *J* = 7.5 Hz, H-12''), 1.79 (m, 2H, H-13''), 1.37-1.26 (m, 16H, H-14''-21''), 0.88 (t, 3H, *J* = 6.6 Hz, H-22'')

^{13} CNMR (75MHz, $CDCl_3$)

δ: 200.3 (C-11''), 136.5 (C-3''), 134.9 (C-5''), 131.2 (C-1''), 131.2 (C-8''), 130.4(C-9''), 130.1 (C-6''), 129.5 (C-10''), 127.6 (C-7''), 125.3 (C-2''), 122.8 (C-4''), 38.8, 32.0 , 29.7, 29.8, 29.8, 29.7, 29.6, 29.5, 27.2, 22.8, 14.2 (C-lauroyl)

m/z (HRMS) :

389.1471 ($M + H^+$, $C_{22}H_{30}BrO$ requires 389.1475)

D.3.2 Synthesis for *N*^{1}-Boc-*N*^{2}-laurdan-*N*^{2}-methyl-diaminopropane (141)

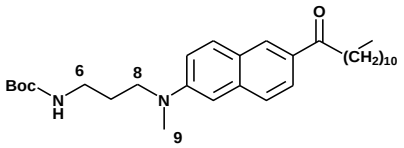

$C_{31}H_{48}N_2O_3$
Exact Mass: 496.37
Mol. Wt.: 496.72

Cette thèse est accessible à l'adresse : http://theses.insa-lyon.fr/publication/2013ISAL0001/these.pdf
© [R. Xu], [2013], INSA de Lyon, tous droits réservés

In a Schlenk tube was added 100 mg of compound **138**, 69 mg of N^1-Boc-N^2-methyl-1,3-aminopropane, 18.7 mg of $Pd_2(dba)_3$, 18.2 mg of S-Phos and 300 mg of Cs_2CO_3. The tube was then degassed by classic process, followed by enveloping the tube with Ar. After injection of 1 mL of anhydrous dioxine, the tube was heat up to 105 ^oC and stirred for 16h. The product was purified by silica gel using the eluent of ethyl acetate/ petroleum ether (5/95).

Yellow solid

^{1} HNMR (400MHz, $CDCl_3$)

δ: 8.22 (s, 1H, H-9''), 7.92 (d, 1H, *J* = 7.9 Hz, H-7''), 7.80 (d, 1H, *J* = 9.1 Hz, H-1''), 7.62 (d, 1H, *J* = 8.3 Hz, H-6''), 7.17 (s, 1H, H-2''), 6.89 (s, 1H, H-4''), 4.65 (s, 1H, H-N*H*), 3.52 (t, 2H, *J* = 7.2 Hz, H-8), 3.32-3.15 (m, 2H, H-6), 3.08 (s, 3H, H-9), 3.03 (t, 2H, *J* = 7.4, H-12''), 1.84 (m, 2H, H-7), 1.77 (m, 2H, H-13''), 1.45 (s, 9H, H-CH_3X3), 1.49-1.13 (m, 16H, H-14''-21''), 0.88 (t, 3H, *J* = 7.4 Hz, H-22'')

^{13} CNMR (100MHz, $CDCl_3$)

δ: 200.3 (C-11''), 156.2 (C-5), 148.8 (C-3''), 137.6 (C-5''), 131.1 (C-1''), 130.9 (C-8''), 129.8 (C-9''), 126.4 (C-6''), 125.5 (C-10''), 125.0 (C-7''), 116.3 (C-2''), 105.3 (C-4''), 79.6 (C-4), 50.4 (C-8), 38.8 (C-6), 38.6 (C-9), 38.5 (C-12''), 32.0 , 29.8, 29.8, 29.8, 29.7, 29.6, 29.5 (C-lauroyl), 28.5 (C-CH_3 Boc), 27.2 (C-21''), 25.0 (C-7), 22.8 (C-13''), 14.2 (C-22'')

m/z (HRMS) :

497.3721 ($M + H^+$, $C_{31}H_{49}N_2O_3$ requires 497.3738)

D.3.3 Synthesis of partially protected glucosyl and cellobiosyl laurdan probes (142, 143)

The **141** was *N*-deprotected in DCM (1 mL) using TFA (1 mL). The mixture was stirred at room temperature for 16h, followed by evoparation of solvent in vacuum. A small amount of toluene (1 mL) was then added and the solution was evaporated in vacuum and this process was repeated 3 times to remove the trace of TFA. After that, the residue was dissolved in anhydrous DCM (3 mL), which was added the solid of CMGLs. The reaction was carried on

Cette thèse est accessible à l'adresse : http://theses.insa-lyon.fr/publication/2013ISAL0001/these.pdf
© [R. Xu], [2013], INSA de Lyon, tous droits réservés

for 16h at room temperature. Then the product was purified by silica gel chromatography using the eluent of DCM/acetone (8/2).

Acetyl-Glu-laurdan (142)

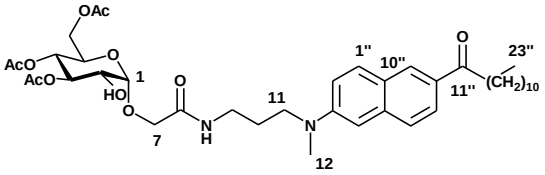

$C_{40}H_{58}N_2O_{11}$
Exact Mass: 742.4
Mol. Wt.: 742.9

^{1} HNMR (500MHz, $CDCl_3$)

δ: 8.31 (s, 1H, H-9''), 7.93 (s, 1H, H-7''), 7.79 (s, 1H, H-1''), 7.62 (s, 1H, H-6''), 7.45-7.30 (s, 1H, H-N*H*), 7.14 (s, 1H, H-2''), 6.83 (s, 1H, H-4''), 5.30 (s, 1H, H-3), 5.03 (t, 1H, *J* = 9.8 Hz, H-4), 4.91 (d, 1H, *J* = 3.6 Hz, H-1), 4.30-4.00 (m, 5H, H-5, H-6a, H-6b, H-7a, H-7b), 3.83 (m, 1H, H-2), 3.50 (m, 2H, H-11), 3.46-3.24 (m, 2H, H-9), 3.08 (s, 3H, H-12), 3.02 (t, 2H, *J* = 7.3 Hz, H-12''), 2.09-2.04 (m, 9H, H-Ac), 1.86 (m, 2H, H-10), 1.75 (m, 2H, H-13''), 1.48-1.20 (m, 16H, H-14''-21''), 0.81 (t, 3H, *J* = 6.9 Hz, H-22'')

^{13} CNMR (125MHz, $CDCl_3$)

δ: 200.5 (C-11''), 171.9, 170.8, 169.5 (C-*C*=OCH_3), 169.2 (C-8), 152.9 (C-3''), 137.7 (C-5''), 130.9 (C-1''), 130.5 (C-8''), 129.8 (C-9''), 126.2 (C-6''), 125.1 (C-10''), 124.9 (C-7''), 116.2 (C-2''), 105.1 (C-4''), 99.2 (C-1), 73.7 (C-3), 69.9 (C-2), 68.2 (C-4), 67.9 (C-5), 67.4 (C-7), 61.7 (C-6), 50.5 (C-11), 39.0 (C-12), 38.6 (C-12''), 37.1 (C-9), 32.0 (C-20''), 29.8, 29.8, 29.8, 29.7, 29.6, 29.5 (C-lauroyl), 25.0 (C-10), 24.9 (C-13''), 22.8 (C-21''), 21.1, 20.9, 20.8, (C-C=O*C*H_3), 14.3 (C-22'')

m/z (HRMS) :

743.419 ($M + H^+$, $C_{40}H_{59}N_2O_{11}$ requires 743.4113)

$[\alpha]_D^{20}$

+58 (*c* 0.7 in CH_2Cl_2)

Cette thèse est accessible à l'adresse : http://theses.insa-lyon.fr/publication/2013ISAL0001/these.pdf
© [R. Xu], [2013], INSA de Lyon, tous droits réservés

Acetyl-Cello-laurdan (143)

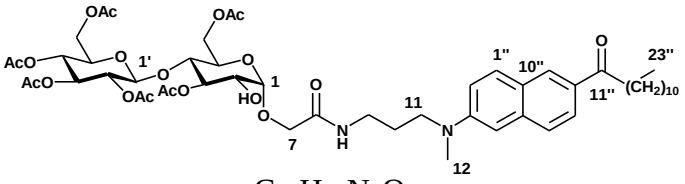

$C_{52}H_{74}N_2O_{19}$
Exact Mass: 1030.49
Mol. Wt.: 1031.15

^{1} HNMR (500MHz, $CDCl_3$)

δ: 8.22 (s, 1H, H-9''), 7.83 (d, 1H, *J* = 8.5 Hz, H-7''), 7.70 (d, 1H, *J* = 8.8 Hz, H-1''), 7.55 (d, 1H, *J* = 8.4 Hz, H-6''), 7.30-7.25 (s, 1H, H-N*H*), 7.05 (d, 1H, *J* = 8.2 Hz, H-2''), 6.76 (s, 1H, H-4''), 5.14 (t, 1H, *J* = 9.5 Hz, H-3), 5.08 (t, 1H, *J* = 9.4 Hz, H-3'), 5.02 (t, 1H, *J* = 9.6 Hz, H-4'), 4.87 (t, 1H, *J* = 8.1 Hz, H-2'), 4.75 (d, 1H, *J* = 3.8 Hz, H-1), 4.45 (d, 1H, *J* = 7.9 Hz, H-1'), 4.32 (dd, 1H, *J* = 1.9, 12.0 Hz, H-6a), 4.13 (dd, 1H, *J* = 4.1, 12.4 Hz, H-6'a), 4.13 (d, 1H, *J* = 15.9 Hz, H-7a), 4.13 (dd, 1H, *J* = 5.0, 12.0 Hz, H-6b), 4.01-3.92 (m, 2H, H-7b, H-6'b), 3.81 (m, 1H, H-5), 3.65-3.56 (m, 3H, H-2, H-4, H-5'), 3.43 (m, 2H, H-11), 3.40-3.16 (m, 2H, H-9), 2.99 (s, 3H, H-12), 2.94 (t, 2H, *J* = 7.4 Hz, H-12''), 2.05-1.92 (m, 18H, H-Ac), 1.80 (m, 2H, H-10), 1.69 (m, 2H, H-13''), 1.37-1.13 (m, 16H, H-14''-21''), 0.81 (t, 3H, *J* = 6.9 Hz, H-22'')

^{13} CNMR (125MHz, $CDCl_3$)

δ: 200.5 (C-11''), 172.0, 170.6, 170.4, 170.3, 169.5, 169.3 (C-*C*=OCH_3), 169.0 (C-8), 152.9 (C-3''), 137.7 (C-5''), 131.0 (C-1''), 130.7 (C-8''), 129.9 (C-9''), 126.2 (C-6''), 125.2 (C-10''), 124.8 (C-7''), 116.2 (C-2''), 105.4 (C-4''), 101.0 (C-1'), 98.9 (C-1), 76.1 (C-2), 73.6 (C-3), 73.0 (C-3'), 72.0 (C-5'), 71.7 (C-2'), 71.0 (C-4), 69.1 (C-5), 67.9 (C-4'), 67.4 (C-7), 61.9 (C-6), 61.8 (C-6'), 50.4 (C-11), 38.5 (C-12), 38.5 (C-12''), 37.1 (C-9), 32.0 (C-30''), 29.8, 29.8, 29.8, 29.7, 29.6, 29.5 (C-lauroyl), 27.2 (C-10), 25.0 (C-13''), 22.8 (C-21''), 21.0, 20.9, 20.8, 20.7, 20.7 (C-C=O*C*H_3), 14.2 (C-22'')

m/z (HRMS) :

1031.4937 ($M + H^+$, $C_{52}H_{75}N_2O_{19}$ requires 1031.4959), 1053.4753 ($M + Na^+$, $C_{52}H_{75}N_2NaO_{19}$ requires 1053.4778)

$[\alpha]_D^{20}$

+31 (*c* 0.8 in CH_2Cl_2)

Cette thèse est accessible à l'adresse : http://theses.insa-lyon.fr/publication/2013ISAL0001/these.pdf
© [R. Xu], [2013], INSA de Lyon, tous droits réservés

D.3.4 Synthesis of glucosyl and cellobiosyl laurdan probes (144, 145)

The deactylation of compounds **142** and **143** was carried out in MeOH/H_2O/NEt_3 (8/1/1) for 16h. The reaction was then coevaporated three times with water (10 mL) and the obtained residue was subjected to silica gel chromatography using a CH_2Cl_2/MeOH (95/5) to give the corresponding products.

Glu-laurdan probe (144)

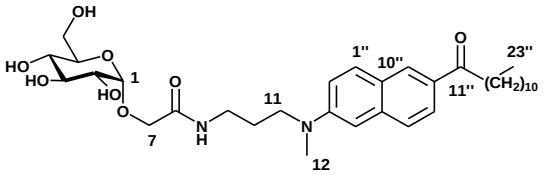

$C_{40}H_{58}N_2O_{11}$
Exact Mass: 742.4
Mol. Wt.: 742.9

^{1} HNMR (400MHz, $CDCl_3$+MeOD)

δ: 8.32 (s, 1H, H-9''), 7.87-7.78 (m, 2H, H-1'', H-7''), 7.62 (d, 1H, *J* = 8.8 Hz, H-6''), 7.30-7.66 (m, 1H, H-N*H*), 7.20 (dd, 1H, *J* = 2.4, 9.2 Hz, H-2''), 6.76 (s, 1H, H-4''), 4.84 (m, 1H, H-1), 4.20 (d, 1H, *J* = 15.8 Hz, H-7a), 4.02 (d, 1H, *J* = 15.8 Hz, H-b), 3.82 (dd, 1H, *J* = 2.2, 12.0 Hz, 6a), 3.76-3.68 (m, 2H, H-3, H-6b), 3.63-3.49 (m, 4H, H-2, H-5, H-11), 3.40-3.31 (m, 3H, H-4, H-9), 3.09 (s, 3H, H-12), 3.04 (t, 2H, *J* = 7.4 Hz, H-12''), 1.90 (m, 2H, H-10), 1.73 (m, 2H, H-13''), 1.46-1.18 (m, 16H, H-14''-21''), 0.86 (t, 3H, *J* = 6.8 Hz, H-22'')

^{13}C NMR (101 MHz, $CDCl_3$+MeOD)

δ: 203.9 (C-11''), 172.7 (C-8), 151.1 (C-3''), 139.8 (C-5''), 132.6 (C-1''), 132.0 (C-8''), 131.8 (C-9''), 127.9 (C-6''), 126.8 (C-10''), 126.0 (C-7''), 118.0 (C-2''), 106.8 (C-4''), 101.4 (C-1), 75.3 (C-3), 74.5 (C-4), 73.5 (C-2), 71.7 (C-5), 68.4 (C-7), 62.8 (C-6), 51.6 (C-9), 40.0 (C-12), 39.8 (C-12''), 38.6 (C-11), 33.6, 31.2, 31.1, 31.1, 31.0, 31.0 (lauroyl), 28.4 (C-10), 26.8 (C-13''), 24.3 (C-21''), 15.4 (C-22'').

Cette thèse est accessible à l'adresse : http://theses.insa-lyon.fr/publication/2013ISAL0001/these.pdf
© [R. Xu], [2013], INSA de Lyon, tous droits réservés

m/z (HRMS) :

617.3778 ($M + H^+$, $C_{34}H_{53}N_2O_8$ requires 617.3796)

$[\alpha]_D^{20}$

+36 (*c* 0.6 in CH_2Cl_2/MeOH, 4/1)

Cello-laurdan (145)

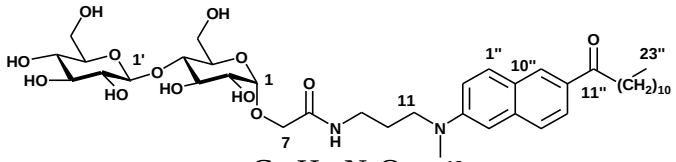

$C_{40}H_{62}N_2O_{13}$
Exact Mass: 778.43
Mol. Wt.: 778.93

Yellow solid

^{1} HNMR (500MHz, CDCl3 /MeOD= 9/1)

δ: 8.24 (s, 1H, H-9''), 7.81 (d, 1H, *J* = 1.6, 8.7 Hz, H-7''), 7.73 (d, 1H, *J* = 9.2 Hz, H-1''), 7.55 (d, 1H, *J* = 8.7 Hz, H-6''), 7.10 (dd, 1H, *J* = 2.2, 9.1 Hz, H-2''), 6.80 (s, 1H, H-4''), 4.73 (d, 1H, *J* = 3.7 Hz, H-1), 4.34 (d, 1H, *J* = 7.9 Hz, H-1'), 4.08 (d, 1H, *J* = 15.9 Hz, H-7a), 3.93 (d, 1H, *J* = 16.0 Hz, H-7b), 3.85-3.78 (m, 2H, H-6a, H-6'a), 3.82 (t, 1H, *J* = 9.2 Hz, H-3), 3.70 (dd, 1H, *J* = 2.6, 12.2 Hz, H-6b), 3.65-3.58 (m, 2H, H-5, H-6'b), 3.54-3.45 (m, 4H, H-2, H-4, H-11), 3.36-3.20 (m, 6H, H-9, H-2', H-3', H-4', H-5'), 3.02 (s, 3H, H-12), 2.97 (t, 2H, *J* = 7.5 Hz, H-12''), 1.83 (m, 2H, H-10), 1.68 (m, 2H, H-13''), 1.37-1.13 (m, 16H, H-14''-21''), 0.80 (t, 3H, *J* = 6.9 Hz, H-22'')

^{13} CNMR (125MHz, CDCl3 /MeOD= 9/1)

δ: 203.0 (C-11''), 171.8 (C-8), 150.6 (C-3''), 139.2 (C-5''), 132.3 (C-1''), 131.9 (C-8''), 131.5 (C-9''), 127.6 (C-6''), 126.7 (C-10''), 125.9 (C-7''), 117.5 (C-2''), 106.8 (C-4''), 104.5 (C-1'), 100.8 (C-1), 80.9 (C-4), 77.9 (C-3'), 77.8 (C-4'), 73.5 (C-2'), 73.0 (C-3), 72.9 (C-2), 72.5 (C-5), 71.2 (C-5'), 68.3 (C-7), 62.6 (C-6'), 62.0 (C-6), 51.5 (C-9), 39.8 (C-12), 39.8 (C-12''), 38.2 (C-11), 33.2, 31.0, 30.9, 30.8, 30.8, 30.7 (lauroyl), 28.1 (C-10), 26.4 (C-13''), 24.0 (C-21''), 15.3 (C-22'')

Cette thèse est accessible à l'adresse : http://theses.insa-lyon.fr/publication/2013ISAL0001/these.pdf
© [R. Xu], [2013], INSA de Lyon, tous droits réservés

m/z (ESI) :

779.4 ($M + H^+$), 802.4 ($M + Na^+$)

$[\alpha]_D^{20}$

+27 (*c* 0.4 in MeOH)

Cette thèse est accessible à l'adresse : http://theses.insa-lyon.fr/publication/2013ISAL0001/these.pdf
© [R. Xu], [2013], INSA de Lyon, tous droits réservés

Appendix

A. DSC curves of n-*O*-(2-hydroxyalkyl)-α-D-glucopyranosides

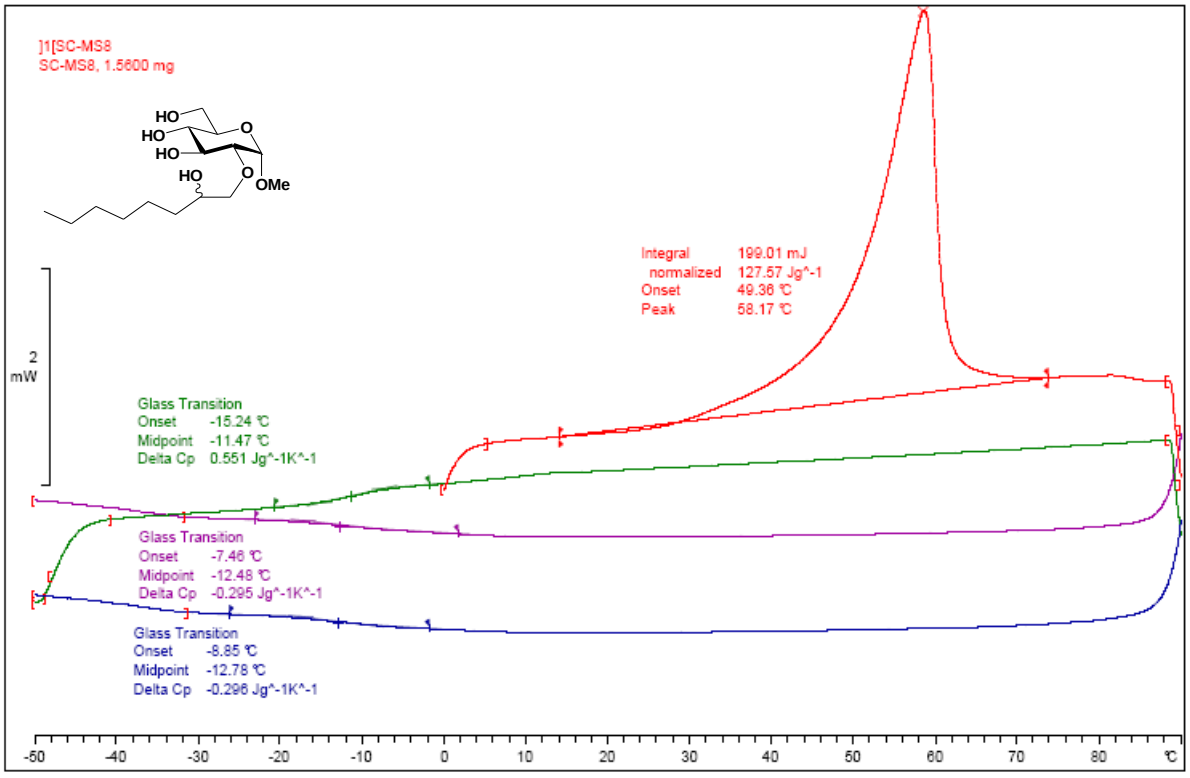

A.1: DSC curve of methyl 2-O-(2-hydroxyoctyl)-α-D-glucopyranosides (**97a**)

Cette thèse est accessible à l'adresse : http://theses.insa-lyon.fr/publication/2013ISAL0001/these.pdf
© [R. Xu], [2013], INSA de Lyon, tous droits réservés

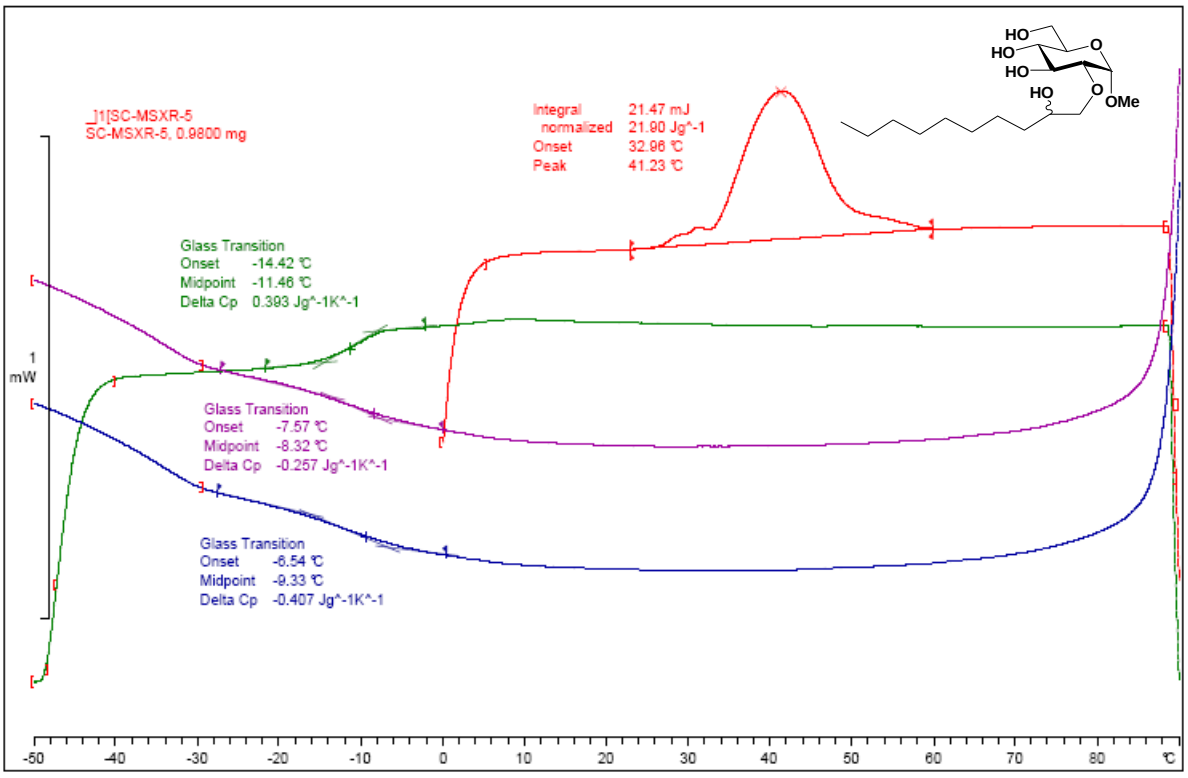

A.2: DSC curve of methyl 2-O-(2-hydroxydecyl)-α-D-glucopyranosides (**97b**)

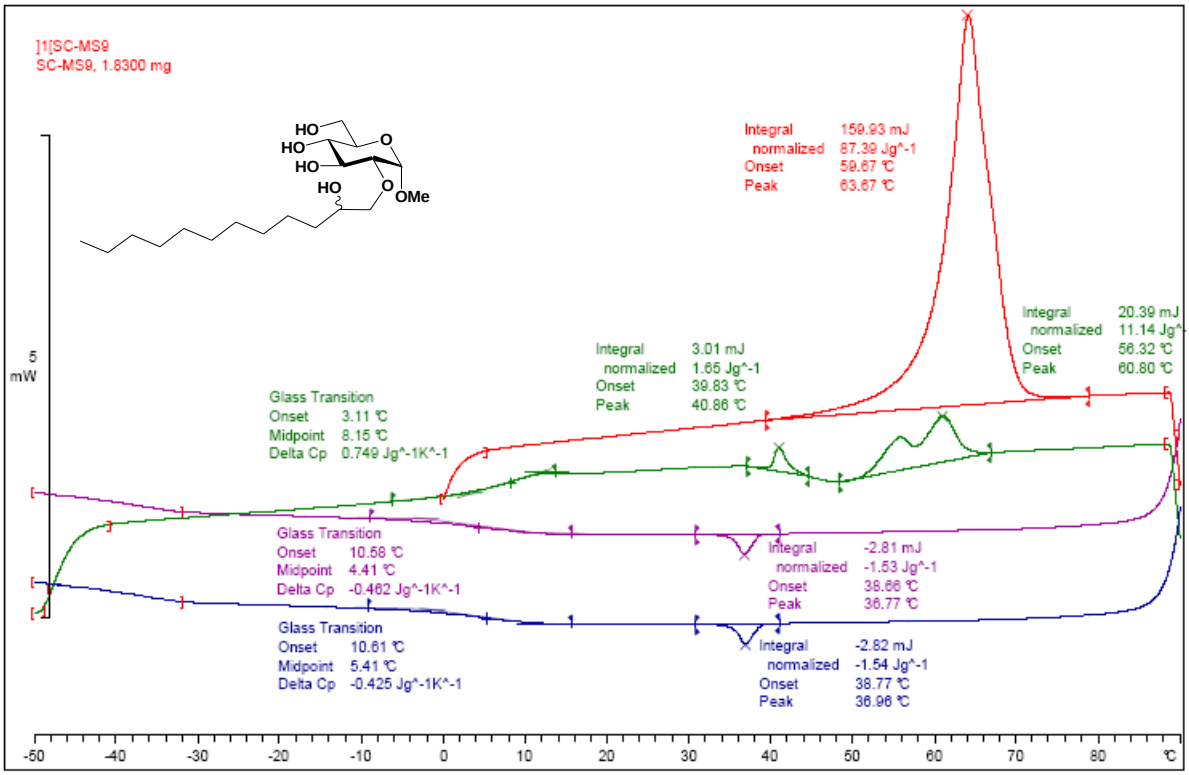

A.3: DSC curve of methyl 2-O-(2-hydroxydodecyl)-α-D-glucopyranosides (**97c**)

Cette thèse est accessible à l'adresse : http://theses.insa-lyon.fr/publication/2013ISAL0001/these.pdf
© [R. Xu], [2013], INSA de Lyon, tous droits réservés

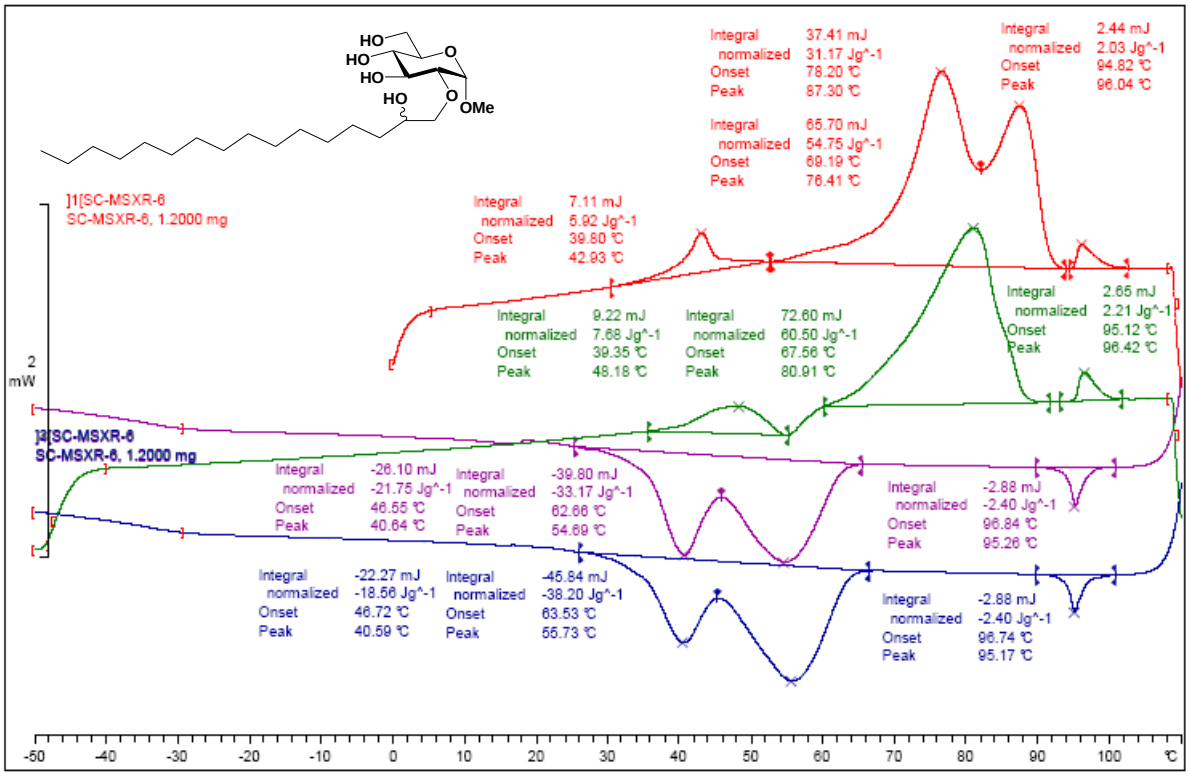

A.4: DSC curve of methyl 2-O-(2-hydroxyhexadecyl)-α-D-glucopyranosides (**97e**)

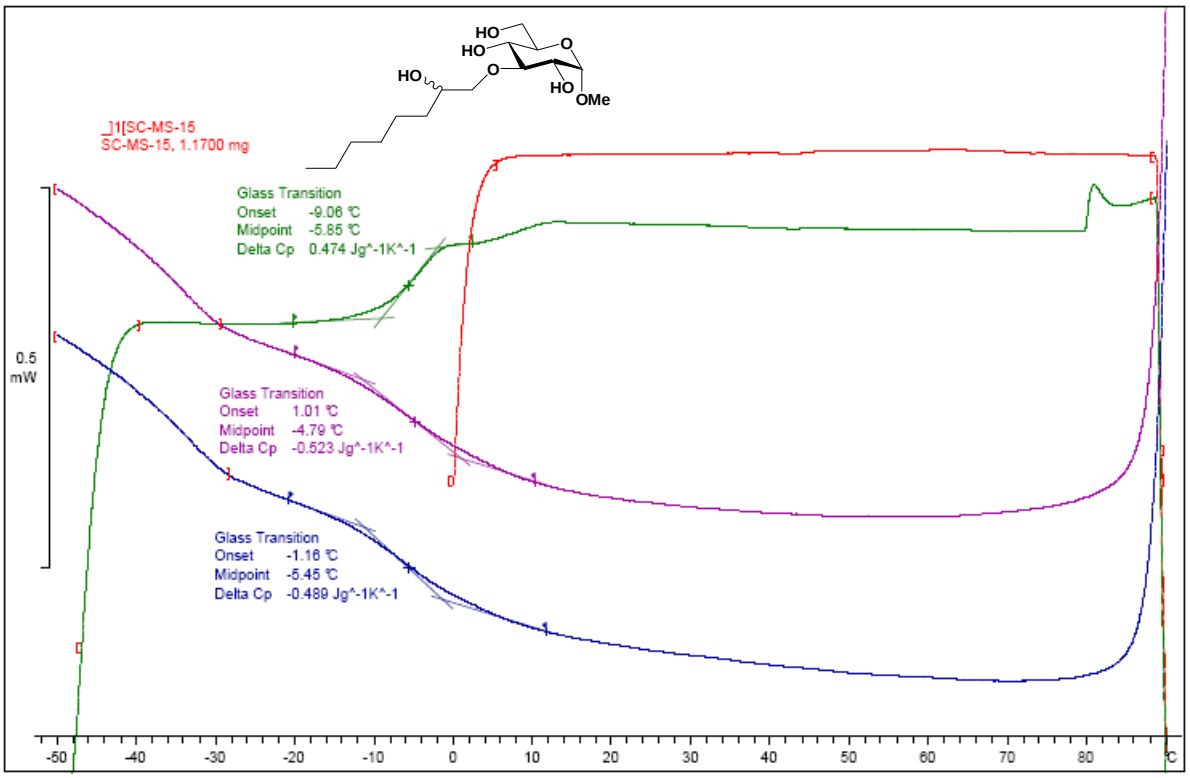

A.5: DSC curve of methyl 3-O-(2-hydroxyoctyl)-α-D-glucopyranosides (**99a**)

Cette thèse est accessible à l'adresse : http://theses.insa-lyon.fr/publication/2013ISAL0001/these.pdf
© [R. Xu], [2013], INSA de Lyon, tous droits réservés

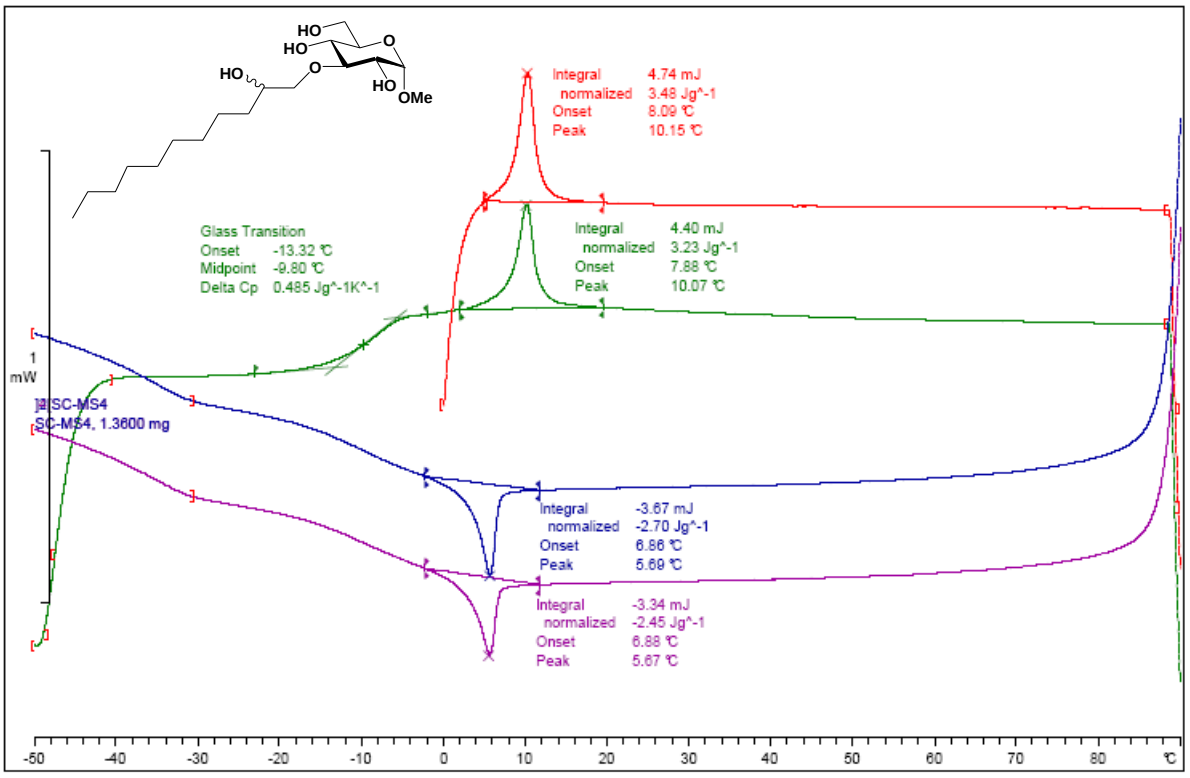

A.6: DSC curve of methyl 3-O-(2-hydroxydecyl)-α-D-glucopyranosides (**99b**)

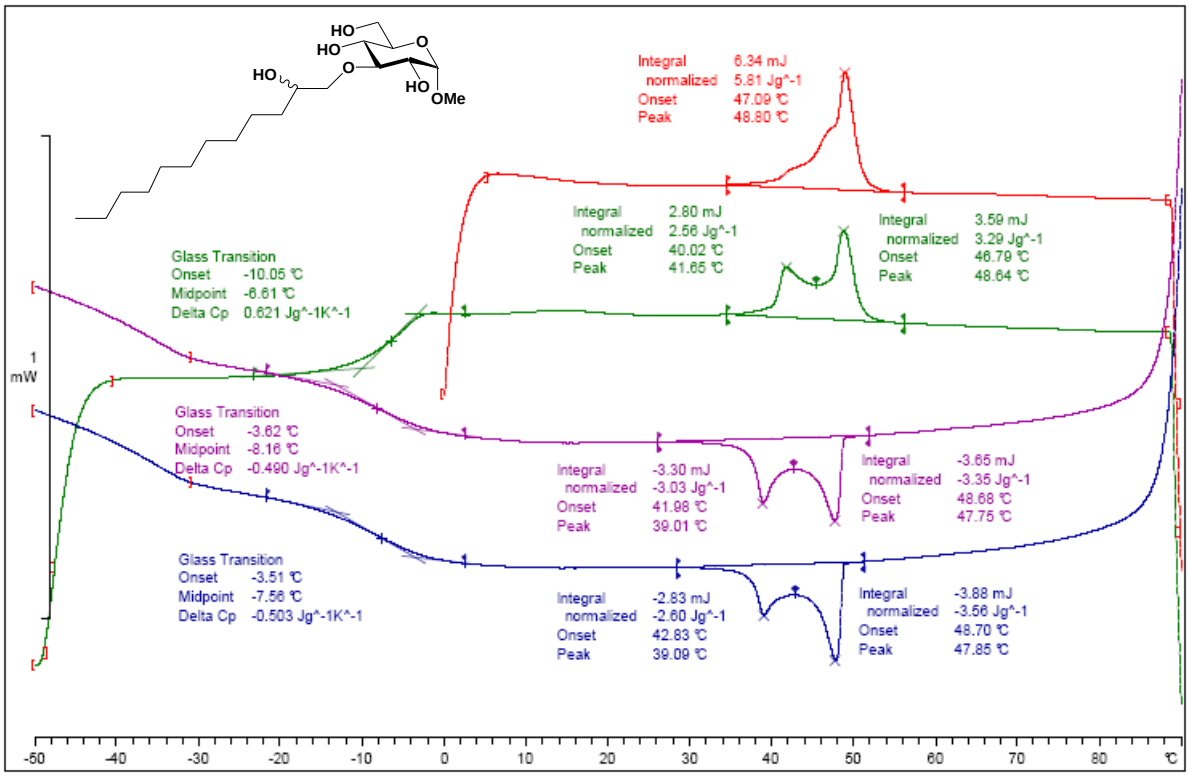

A.7: DSC curve of methyl 3-O-(2-hydroxydodecyl)-α-D-glucopyranosides (**99c**)

Cette thèse est accessible à l'adresse : http://theses.insa-lyon.fr/publication/2013ISAL0001/these.pdf
© [R. Xu], [2013], INSA de Lyon, tous droits réservés

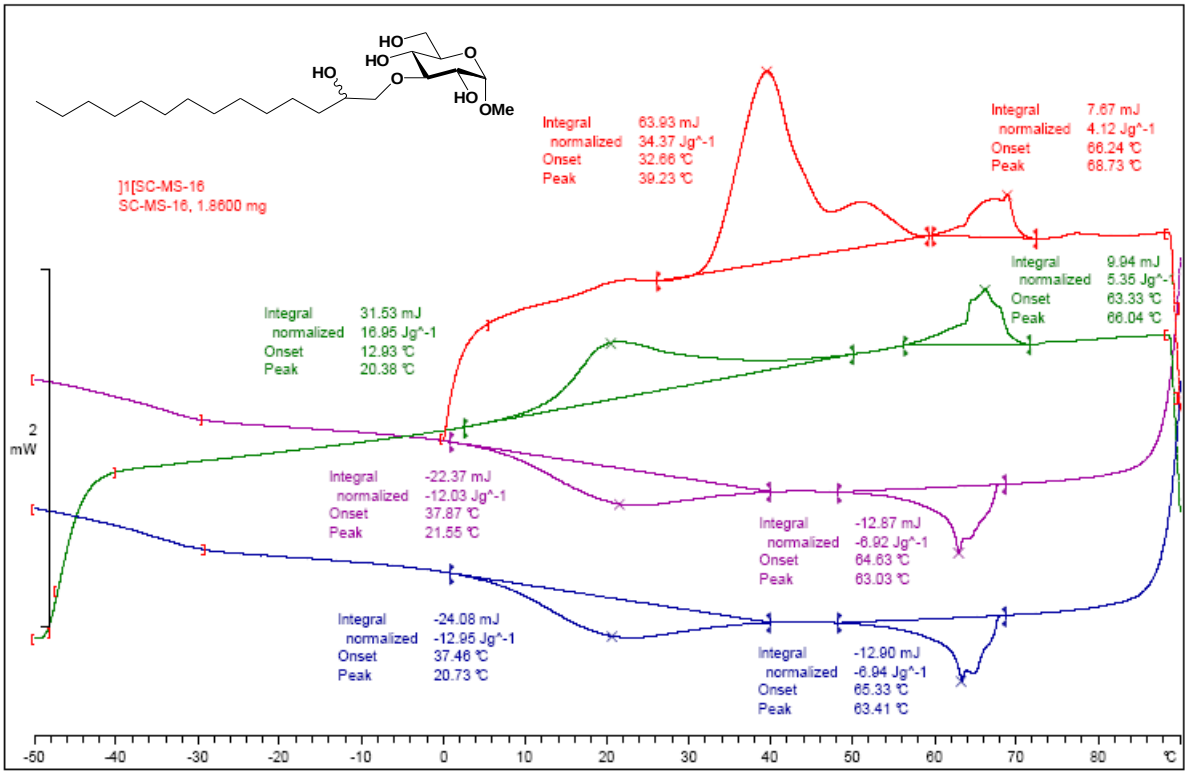

A.8: DSC curve of methyl 3-O-(2-hydroxytetradecyl)-α-D-glucopyranosides (**99d**)

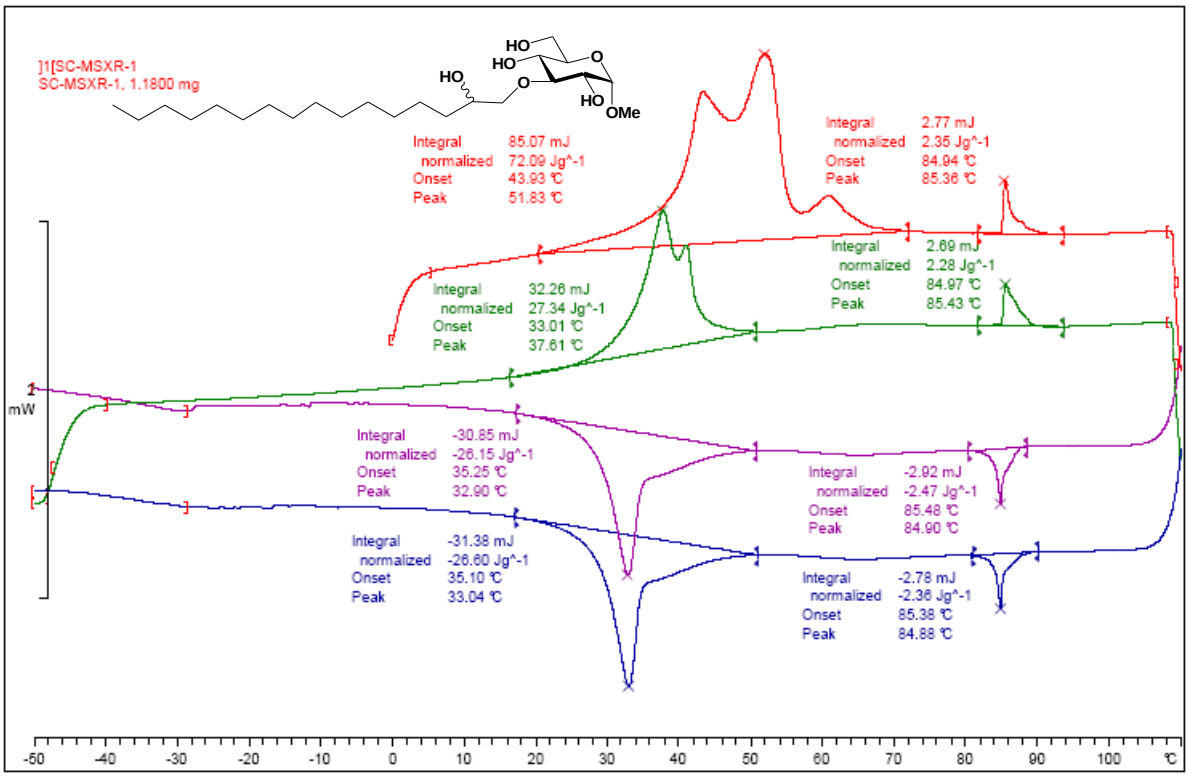

A.9: DSC curve of methyl 3-O-(2-hydroxyhexadecyl)-α-D-glucopyranosides (**99e**)

Cette thèse est accessible à l'adresse : http://theses.insa-lyon.fr/publication/2013ISAL0001/these.pdf
© [R. Xu], [2013], INSA de Lyon, tous droits réservés

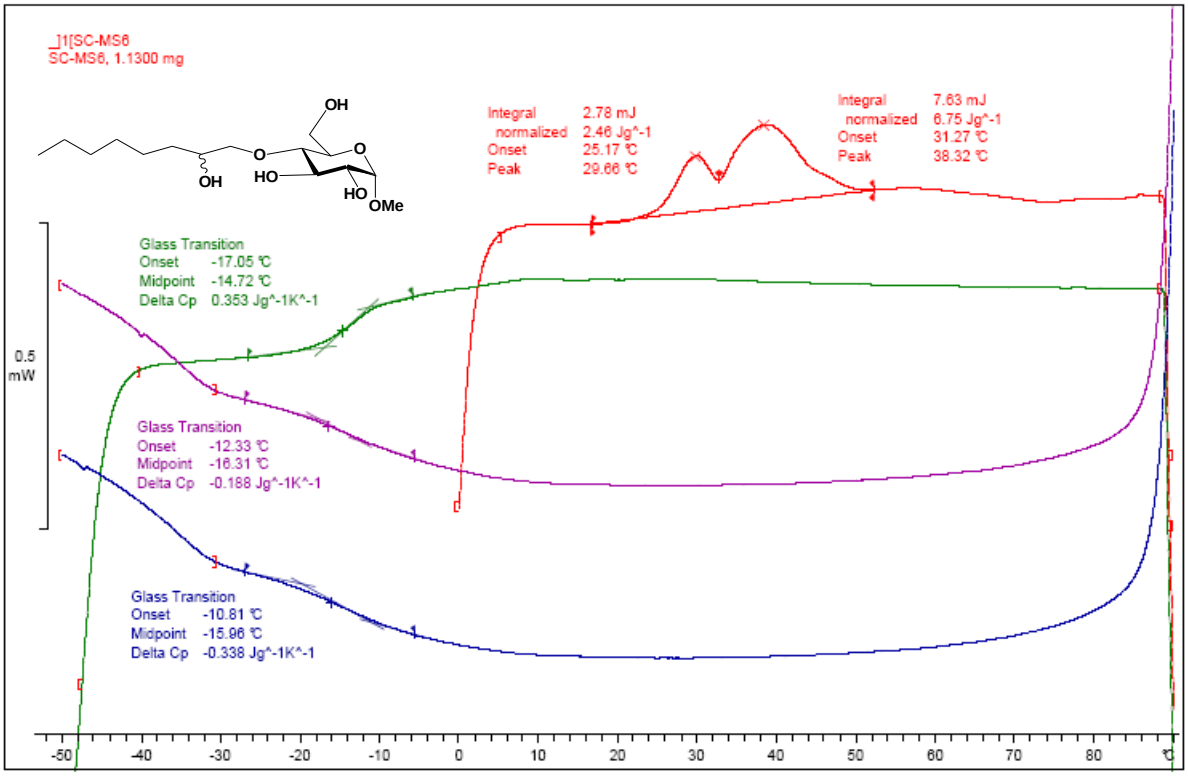

A.10: DSC curve of methyl 4-O-(2-hydroxyoctyl)-α-D-glucopyranosides (**101a**)

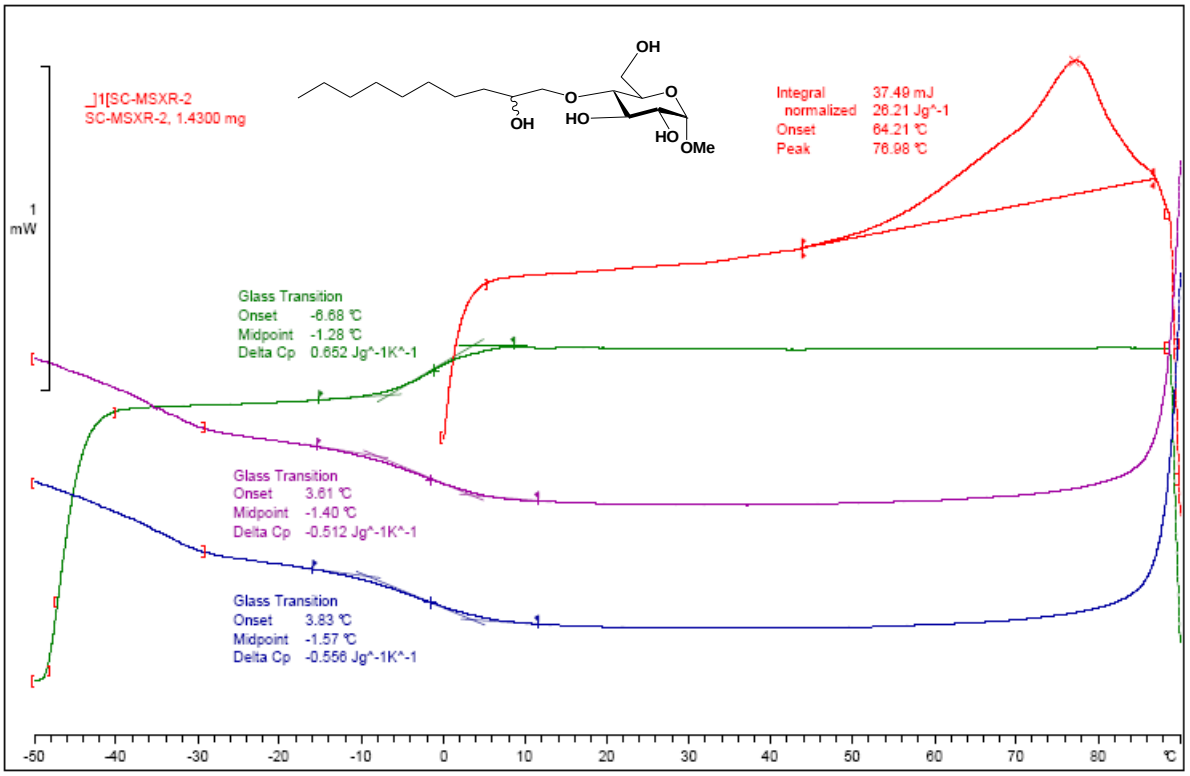

A.11: DSC curve of methyl 4-O-(2-hydroxydecyl)-α-D-glucopyranosides (**101b**)

Cette thèse est accessible à l'adresse : http://theses.insa-lyon.fr/publication/2013ISAL0001/these.pdf
© [R. Xu], [2013], INSA de Lyon, tous droits réservés

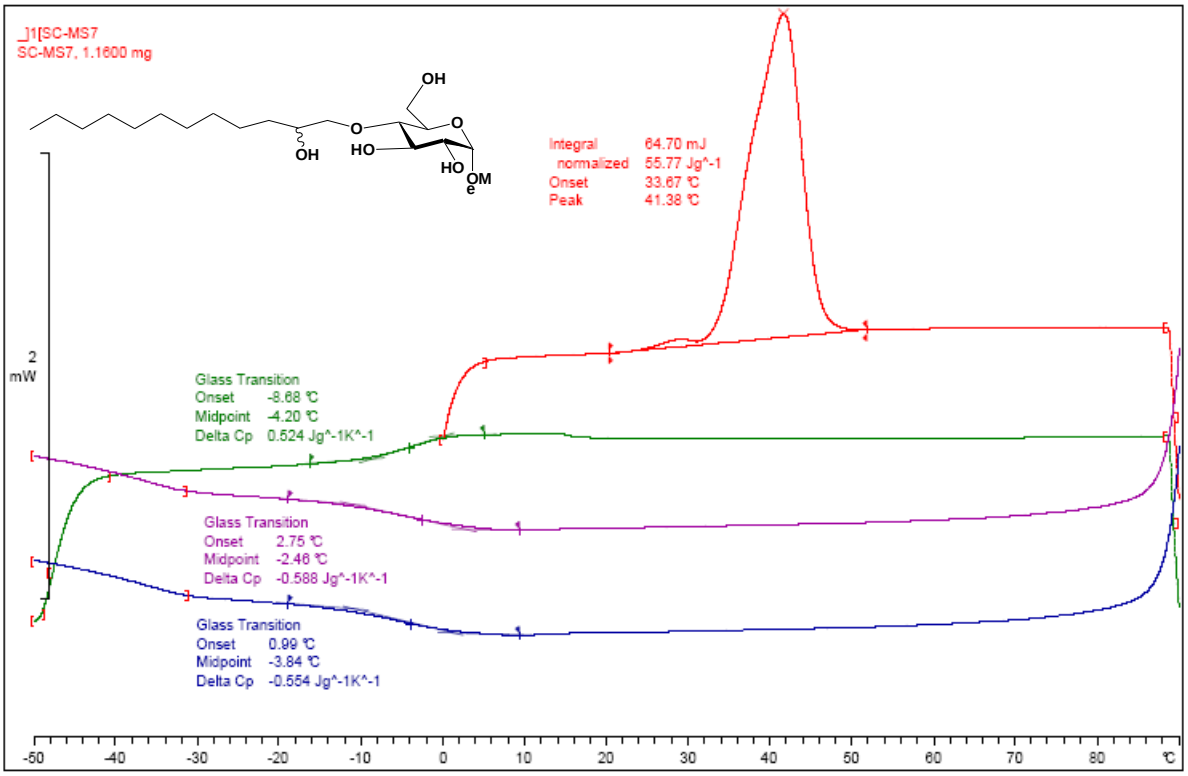

A.12: DSC curve of methyl 4-O-(2-hydroxydodecyl)-α-D-glucopyranosides (**101c**)

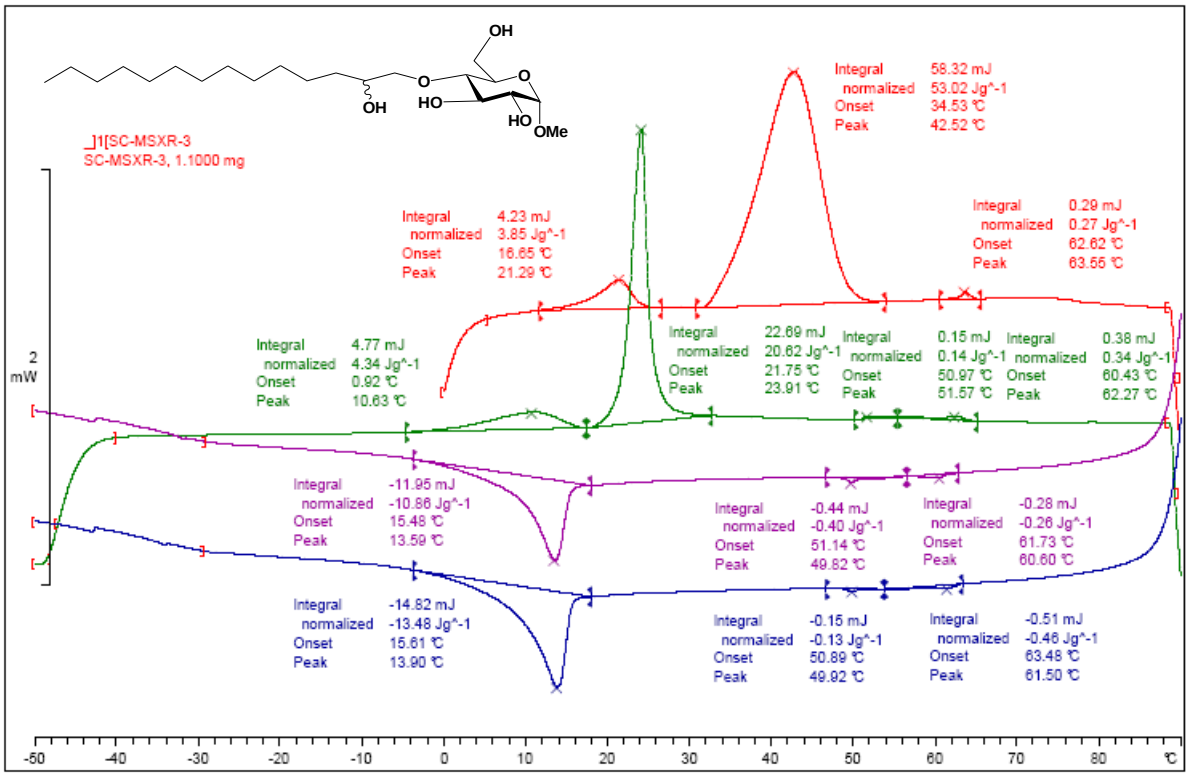

A.13: DSC curve of methyl 4-O-(2-hydroxytetradecyl)-α-D-glucopyranosides (**101d**)

Cette thèse est accessible à l'adresse : http://theses.insa-lyon.fr/publication/2013ISAL0001/these.pdf
© [R. Xu], [2013], INSA de Lyon, tous droits réservés

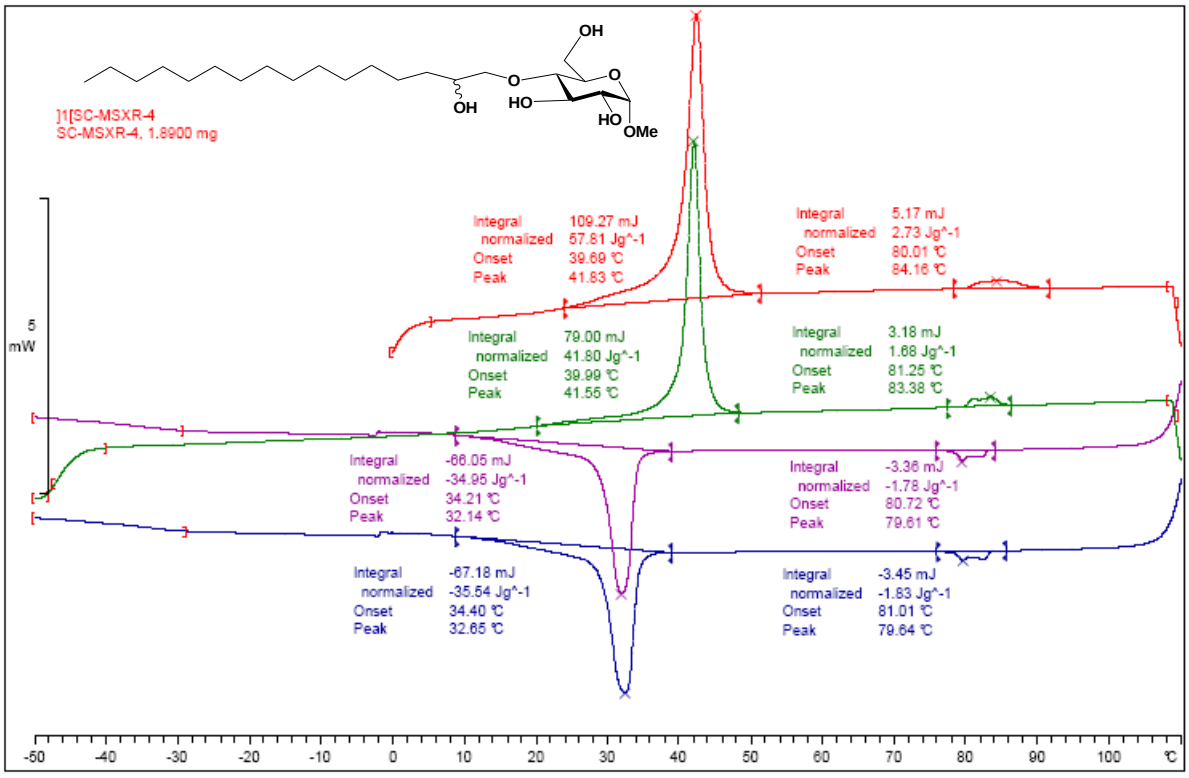

A.14: DSC curve of methyl 4-O-(2-hydroxyhexadecyl)-α-D-glucopyranosides (**101e**)

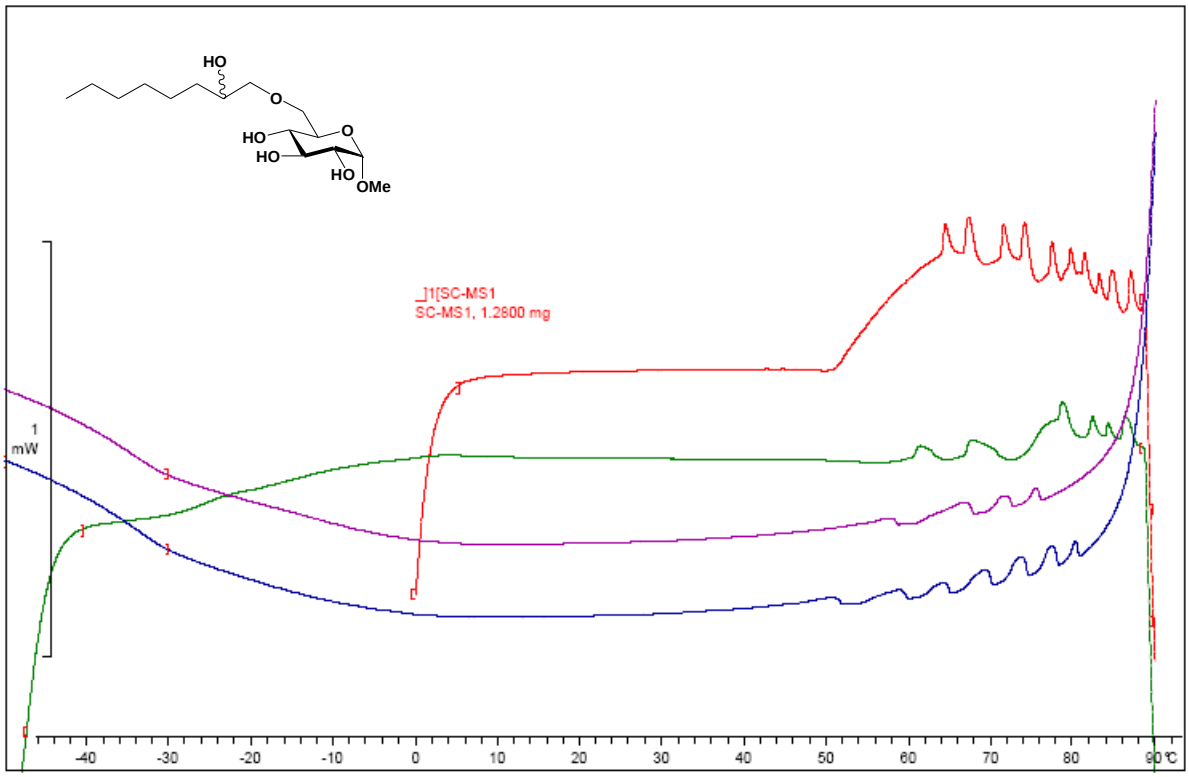

A.15: DSC curve of methyl 6-O-(2-hydroxyoctyl)-α-D-glucopyranosides (**105a**)

Cette thèse est accessible à l'adresse : http://theses.insa-lyon.fr/publication/2013ISAL0001/these.pdf
© [R. Xu], [2013], INSA de Lyon, tous droits réservés

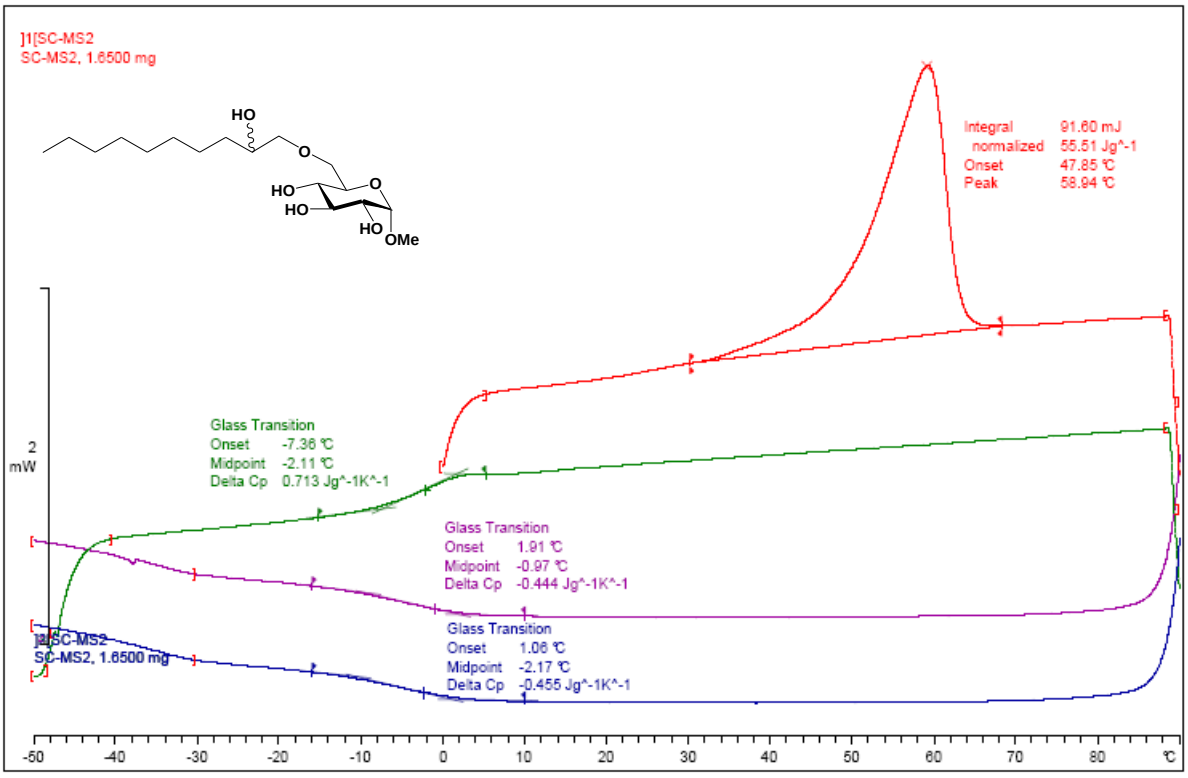

A.16: DSC curve of methyl 6-O-(2-hydroxydecyl)-α-D-glucopyranosides (**105b**)

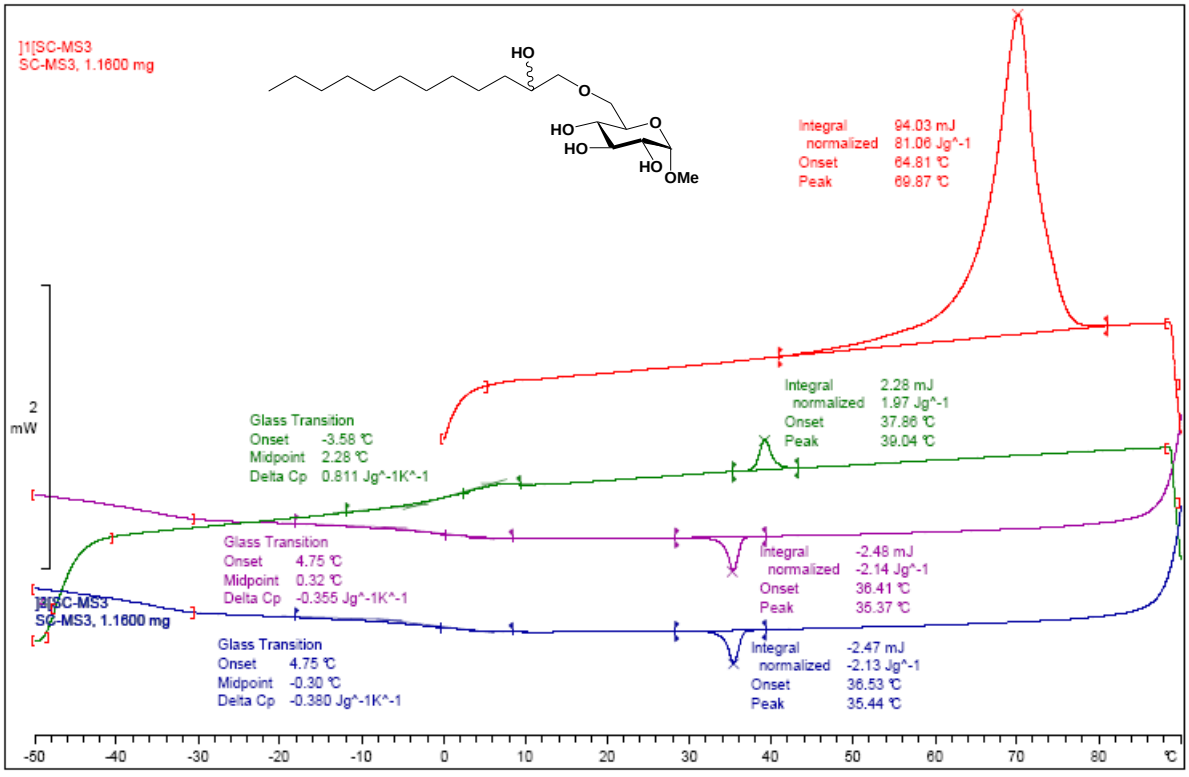

A.17: DSC curve of methyl 6-O-(2-hydroxydodecyl)-α-D-glucopyranosides (**105c**)

Cette thèse est accessible à l'adresse : http://theses.insa-lyon.fr/publication/2013ISAL0001/these.pdf
© [R. Xu], [2013], INSA de Lyon, tous droits réservés

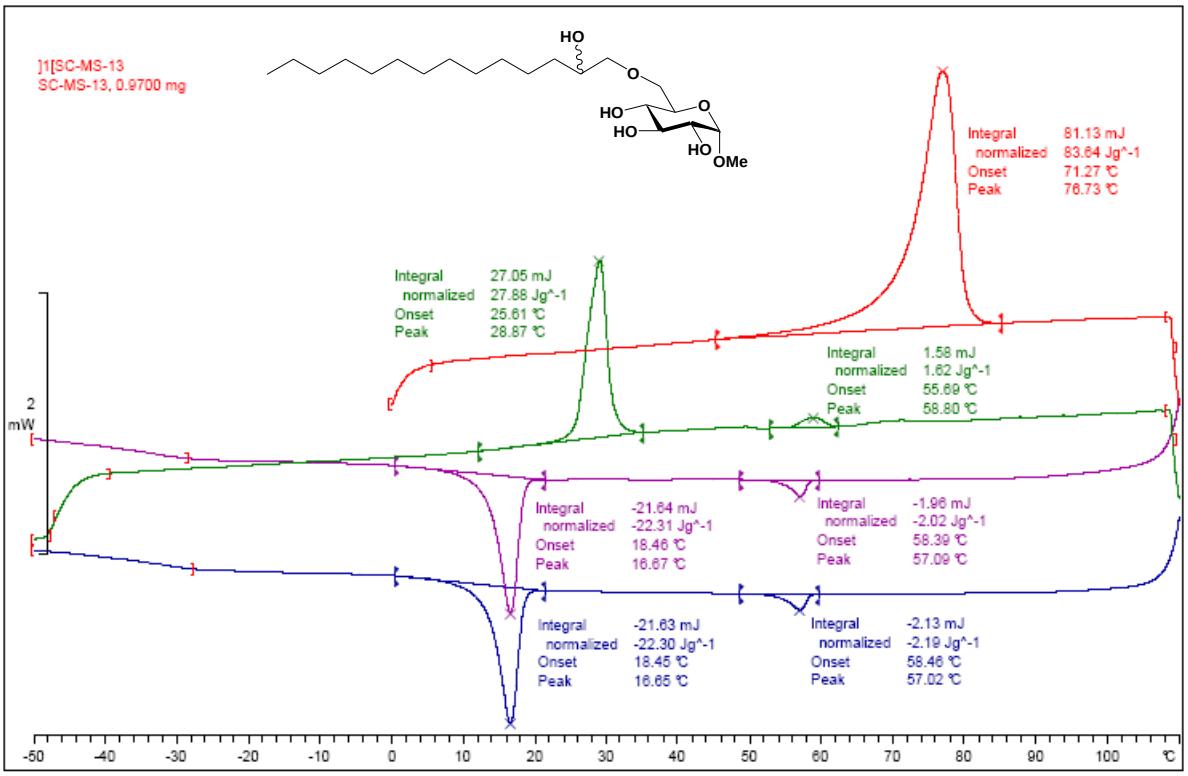

A.18: DSC curve of methyl 6-O-(2-hydroxytetradecyl)-α-D-glucopyranosides (**105d**)

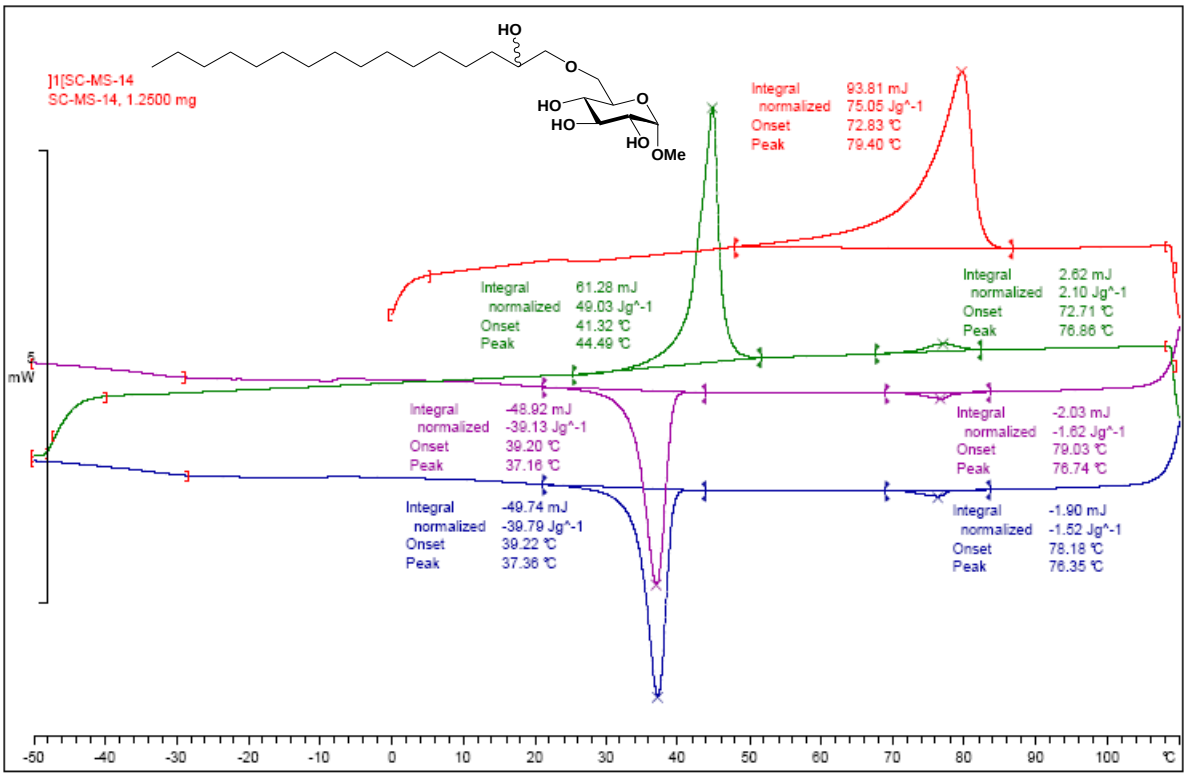

A.19: DSC curve of methyl 6-O-(2-hydroxyhexa decyl)-α-D-glucopyranosides (**105e**)

Cette thèse est accessible à l'adresse : http://theses.insa-lyon.fr/publication/2013ISAL0001/these.pdf
© [R. Xu], [2013], INSA de Lyon, tous droits réservés

B. DSC curves of glucosteroids

B. 1 Glucosteroidic amphiphiles

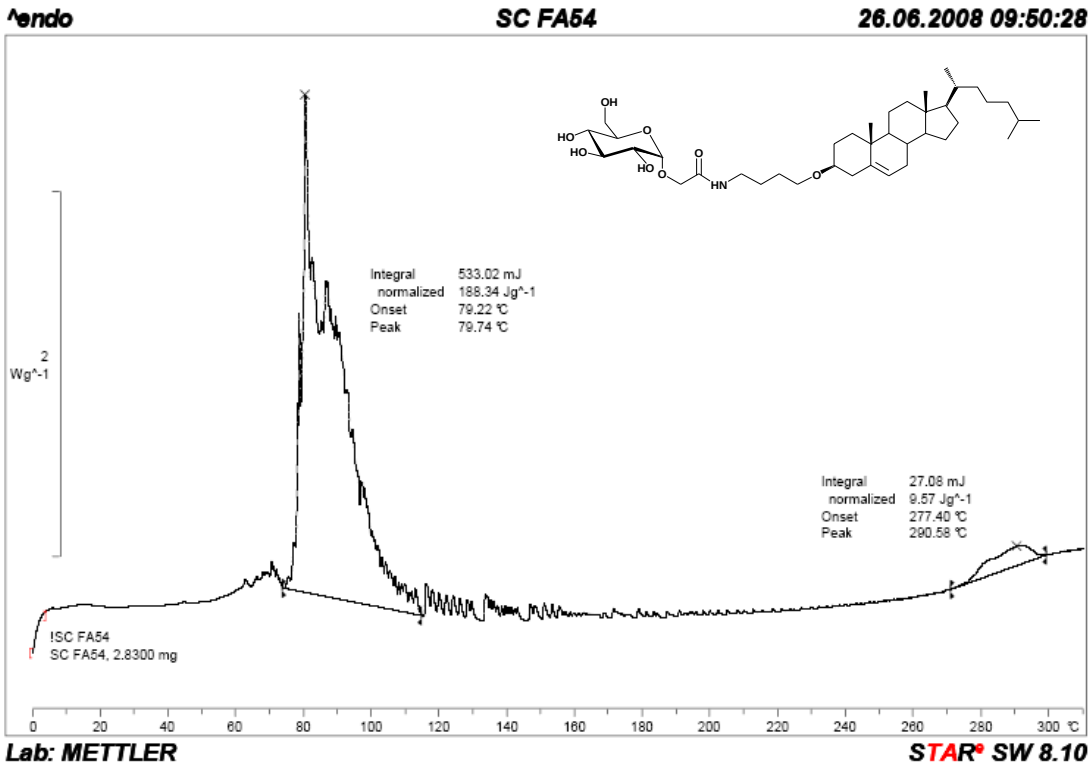

B.1.1: DSC curve of amphiphile L4 (**111)**

Cette thèse est accessible à l'adresse : http://theses.insa-lyon.fr/publication/2013ISAL0001/these.pdf
© [R. Xu], [2013], INSA de Lyon, tous droits réservés

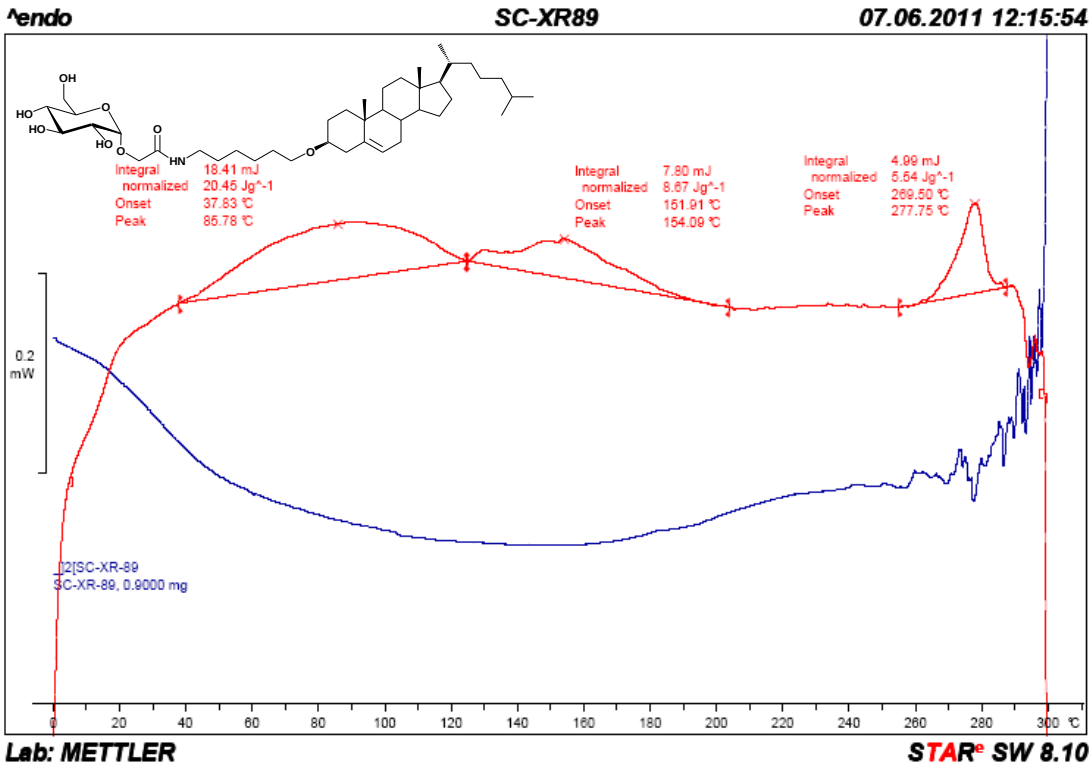

B.1.2: DSC curve of amphiphile L6 **(120)**

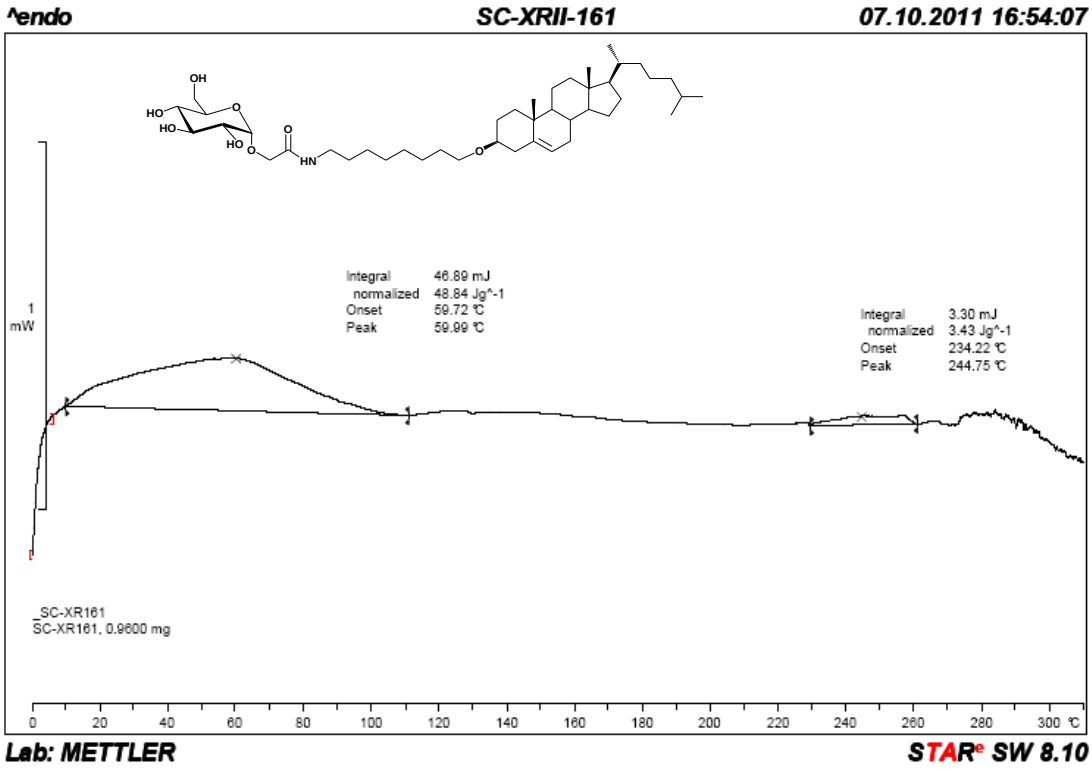

B.1.2: DSC curve of amphiphile L8 (**121)**

Cette thèse est accessible à l'adresse : http://theses.insa-lyon.fr/publication/2013ISAL0001/these.pdf
© [R. Xu], [2013], INSA de Lyon, tous droits réservés

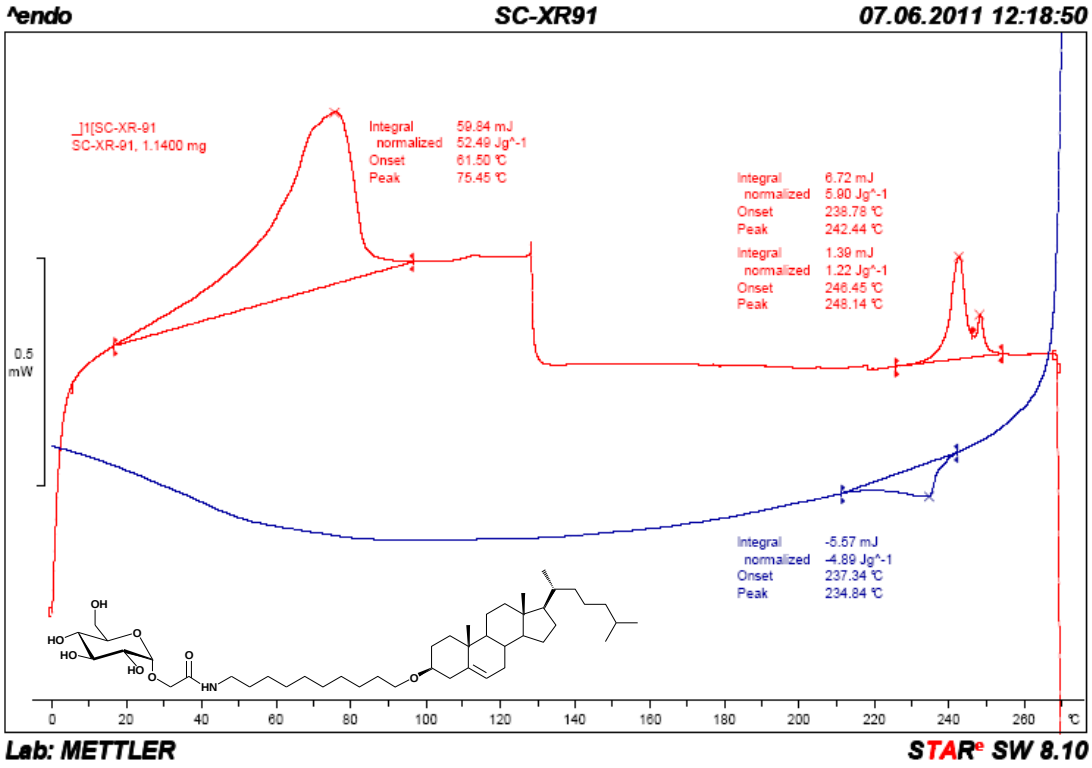

B.1.3: DSC curve of amphiphile L10 **(122)**

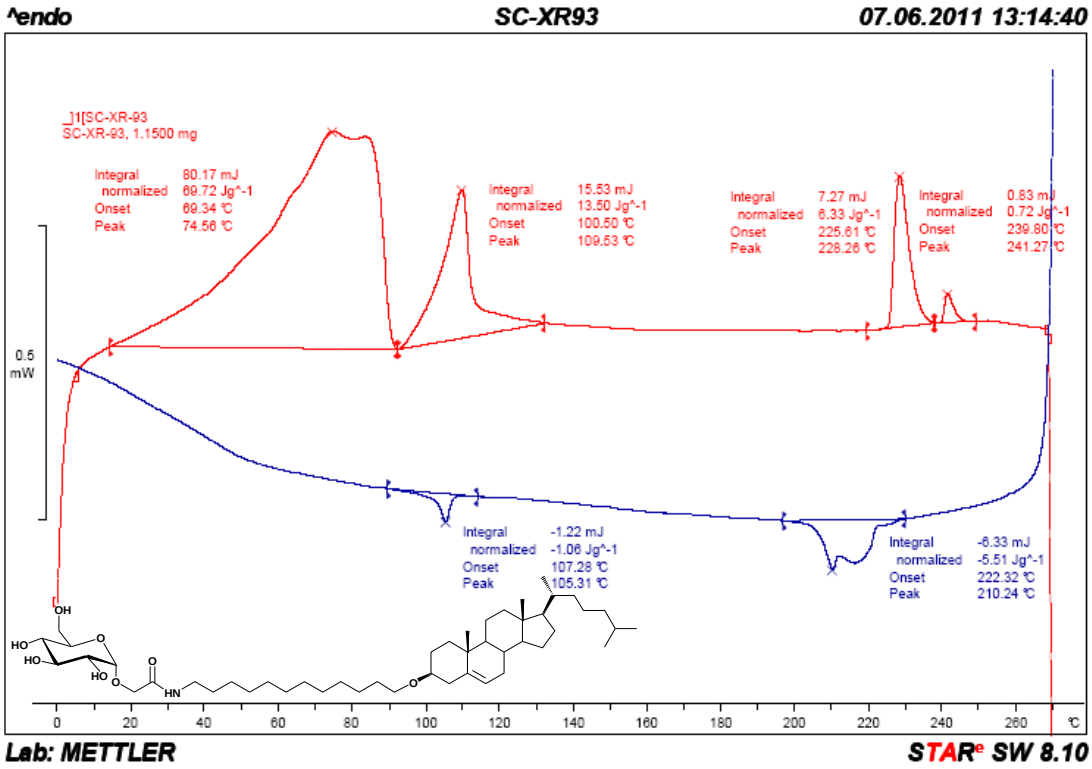

B.1.4: DSC curve of amphiphile L12 **(123)**

Cette thèse est accessible à l'adresse : http://theses.insa-lyon.fr/publication/2013ISAL0001/these.pdf
© [R. Xu], [2013], INSA de Lyon, tous droits réservés

B. 2 Glucosteroidic bolaphiles

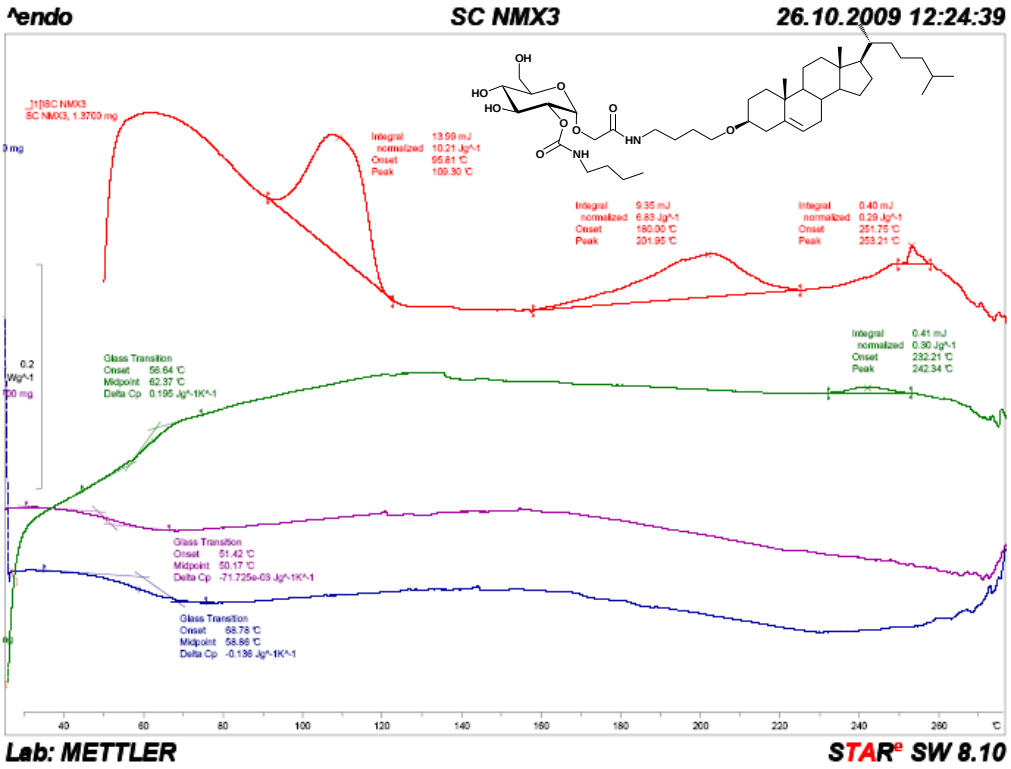

B.2.1: DSC curve of bolaphile L4S4 **(124a)**

Cette thèse est accessible à l'adresse : http://theses.insa-lyon.fr/publication/2013ISAL0001/these.pdf
© [R. Xu], [2013], INSA de Lyon, tous droits réservés

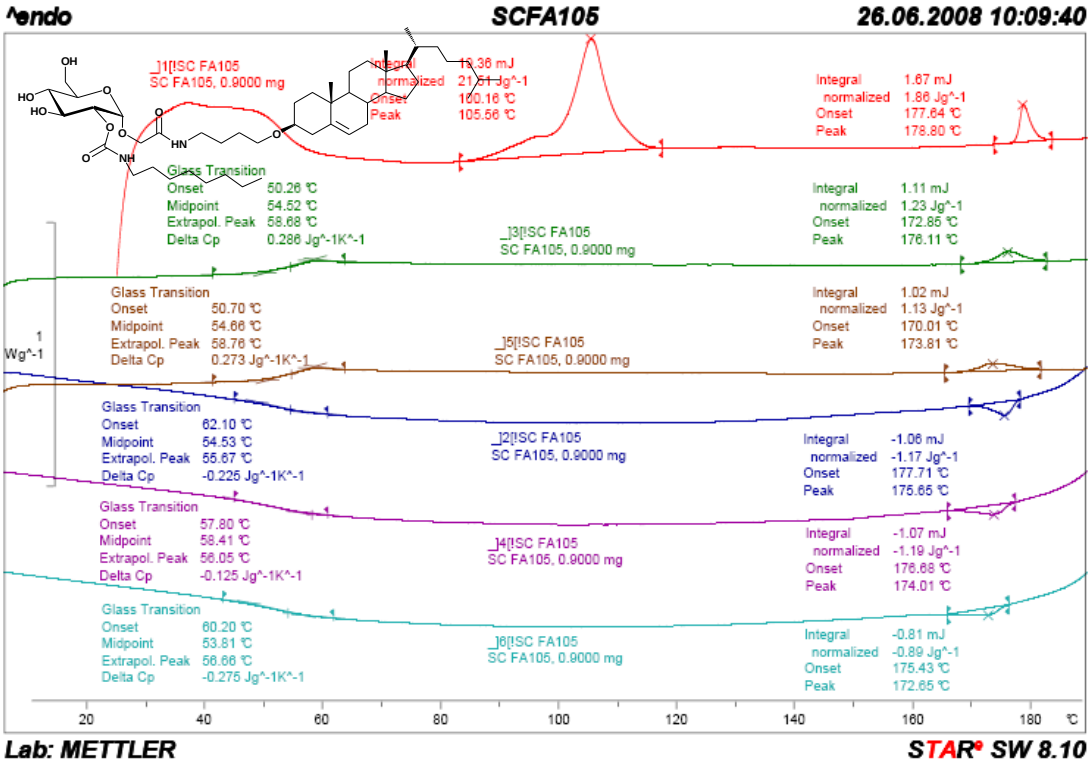

B.2.2: DSC curve of bolaphile L4S8 **(124b)**

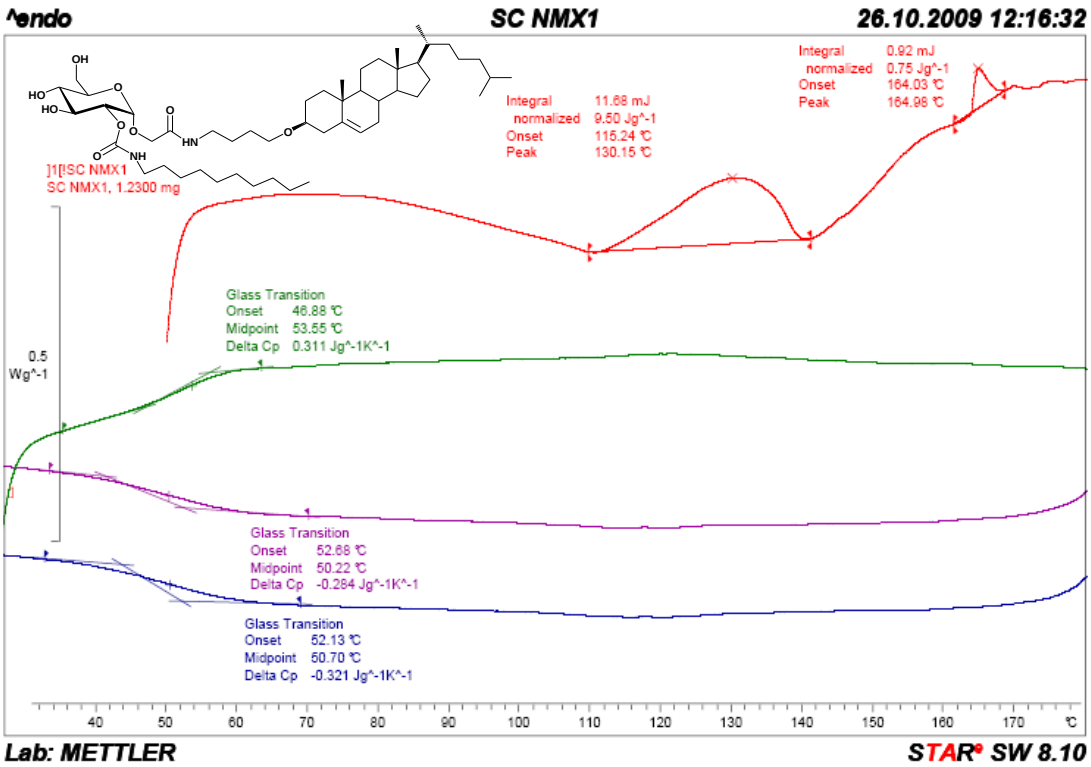

B.2.3: DSC curve of bolaphile L4S10 **(124c)**

Cette thèse est accessible à l'adresse : http://theses.insa-lyon.fr/publication/2013ISAL0001/these.pdf
© [R. Xu], [2013], INSA de Lyon, tous droits réservés

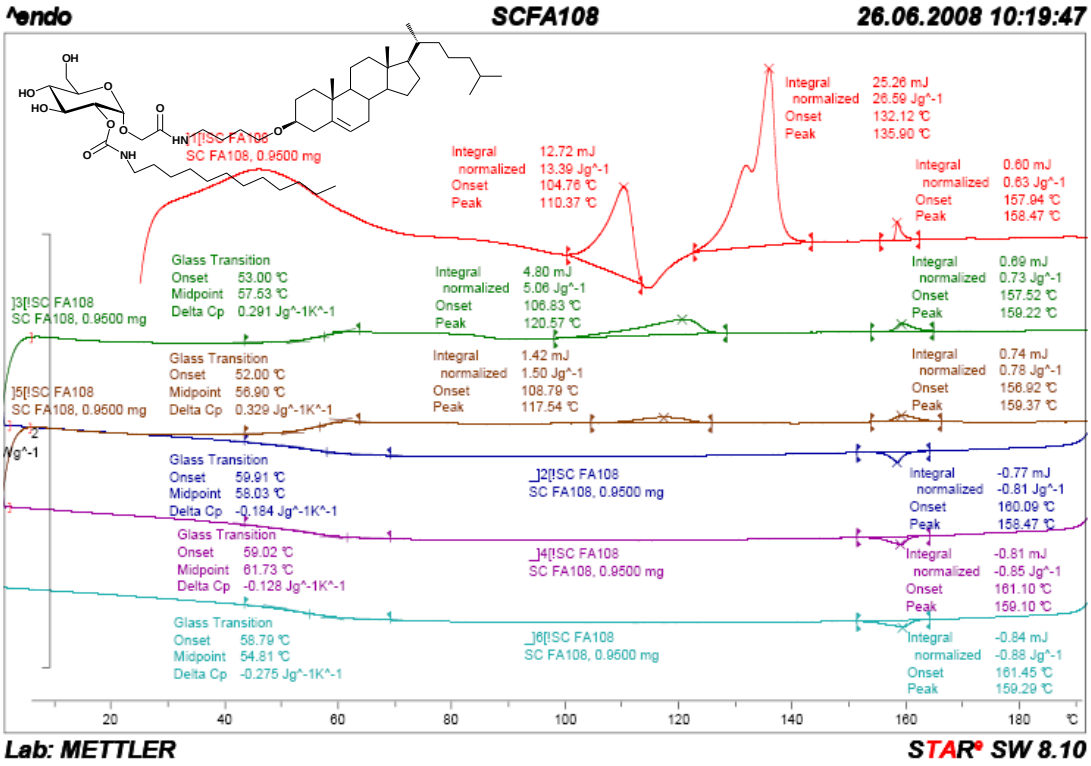

B.2.4: DSC curve of bolaphile L4S12 **(124d)**

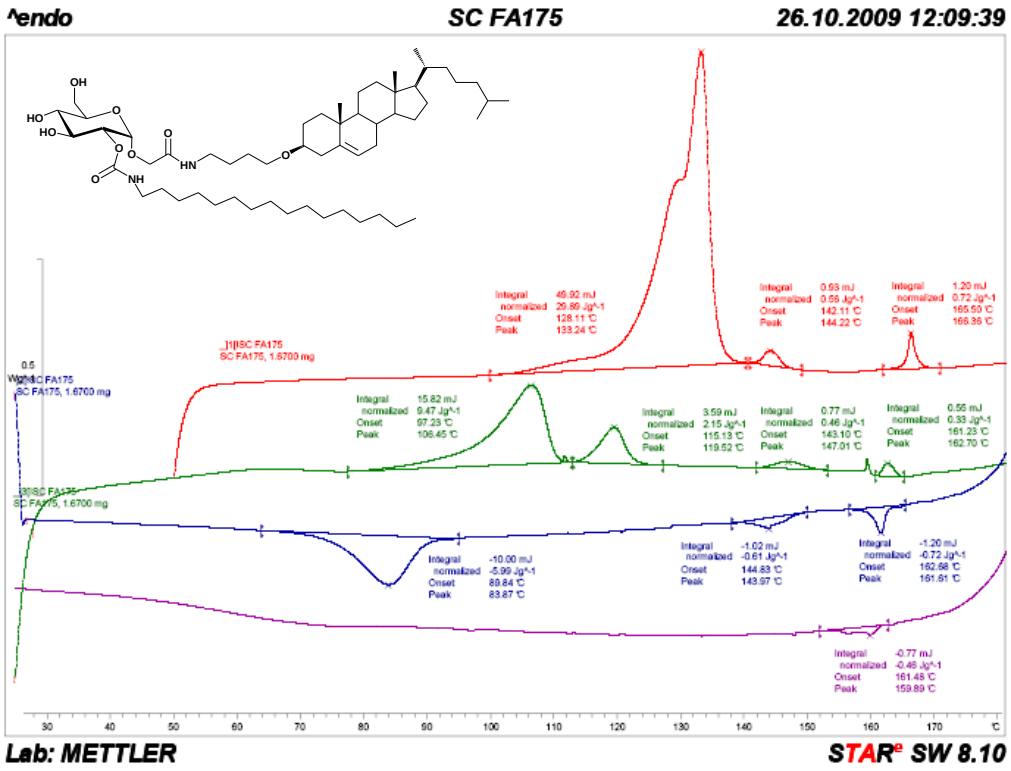

B.2.5: DSC curve of bolaphile L4S16 **(124f)**

Cette thèse est accessible à l'adresse : http://theses.insa-lyon.fr/publication/2013ISAL0001/these.pdf
© [R. Xu], [2013], INSA de Lyon, tous droits réservés

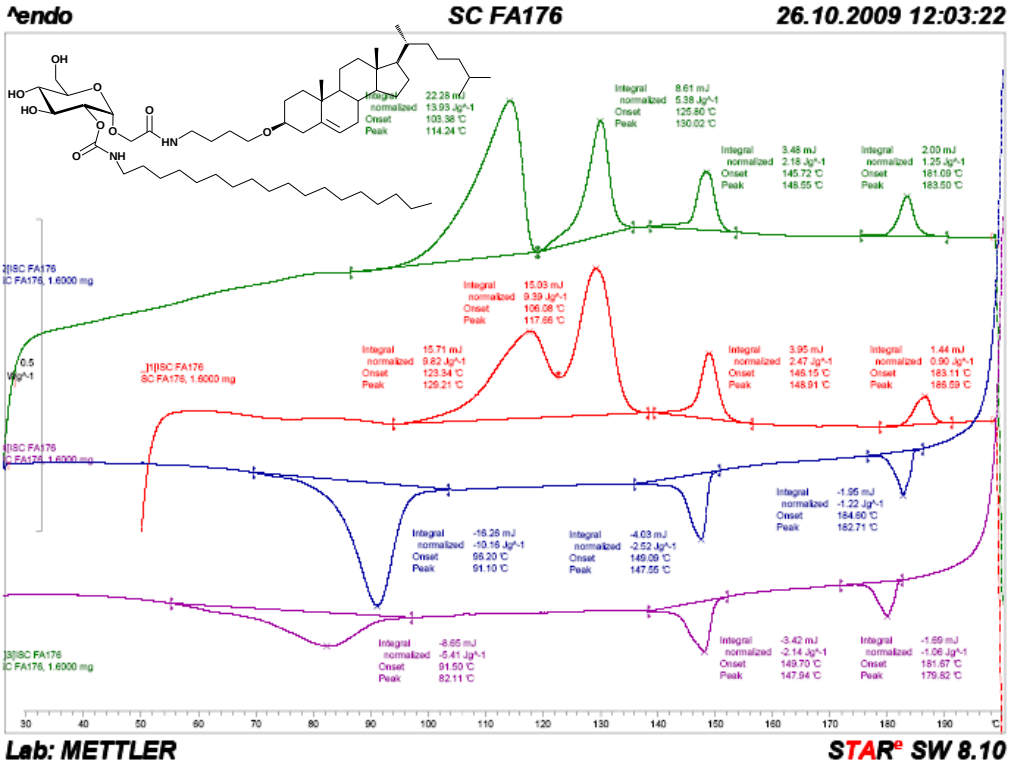

B.2.6: DSC curve of bolaphile L4S18 **(124g)**

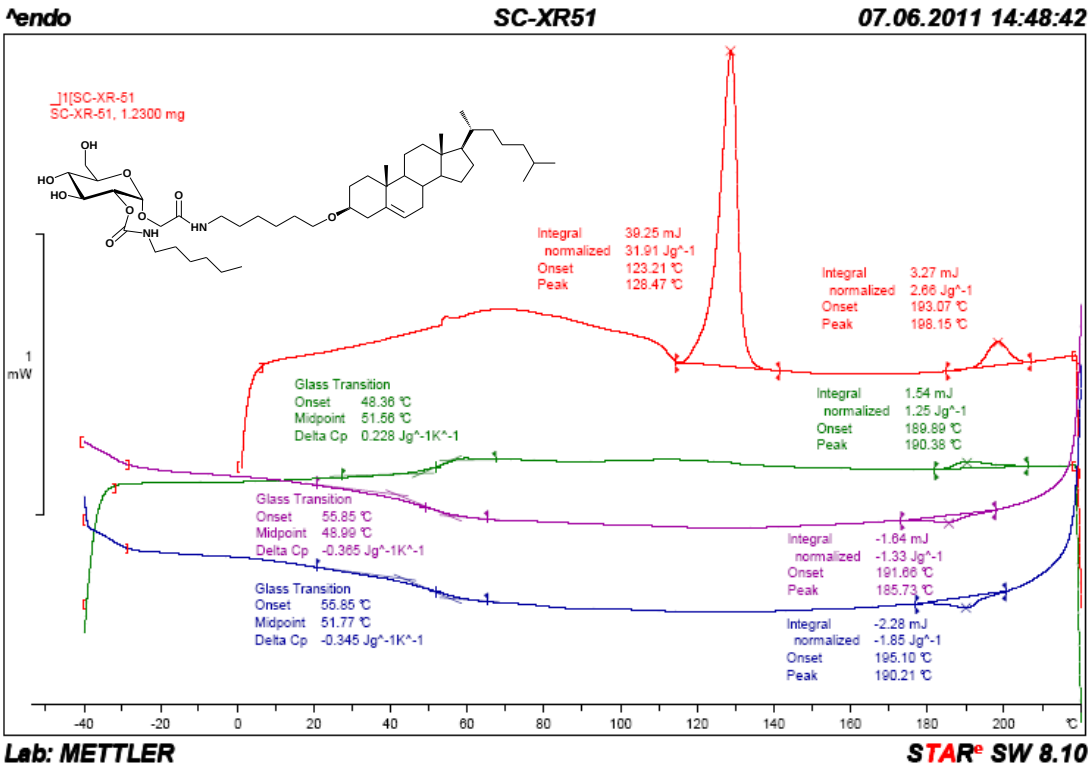

B.2.7: DSC curve of bolaphile L6S6 **(125a)**

Cette thèse est accessible à l'adresse : http://theses.insa-lyon.fr/publication/2013ISAL0001/these.pdf
© [R. Xu], [2013], INSA de Lyon, tous droits réservés

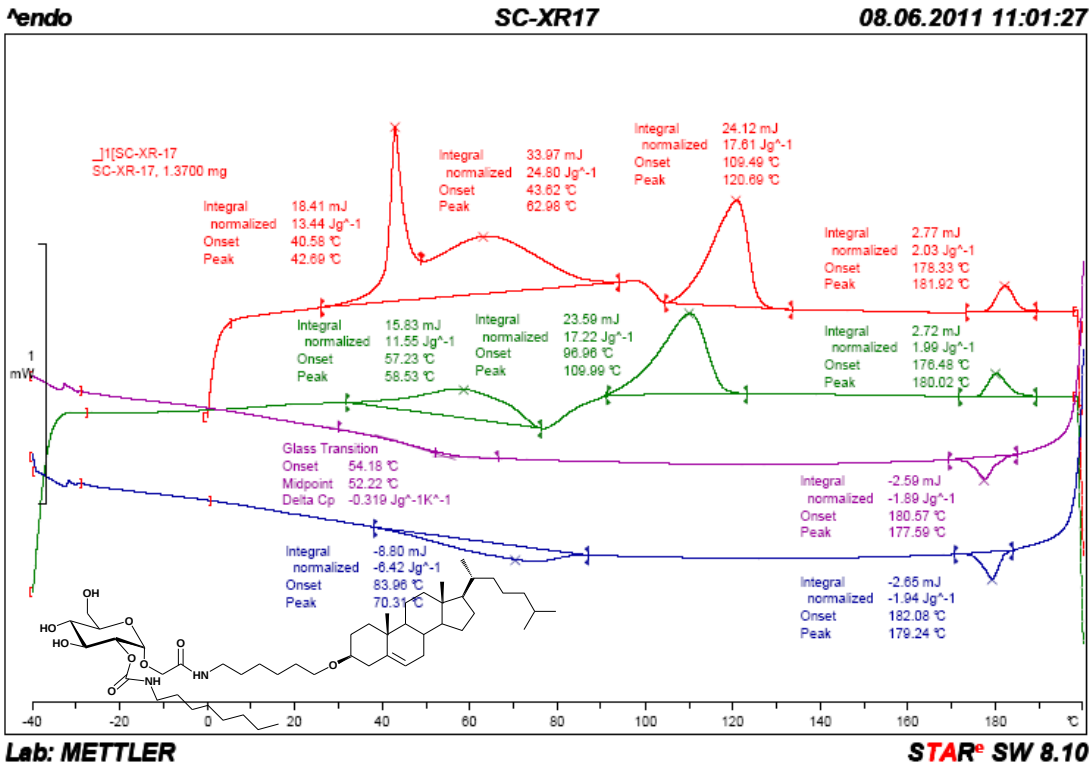

B.2.8: DSC curve of bolaphile L6S8 **(125b)**

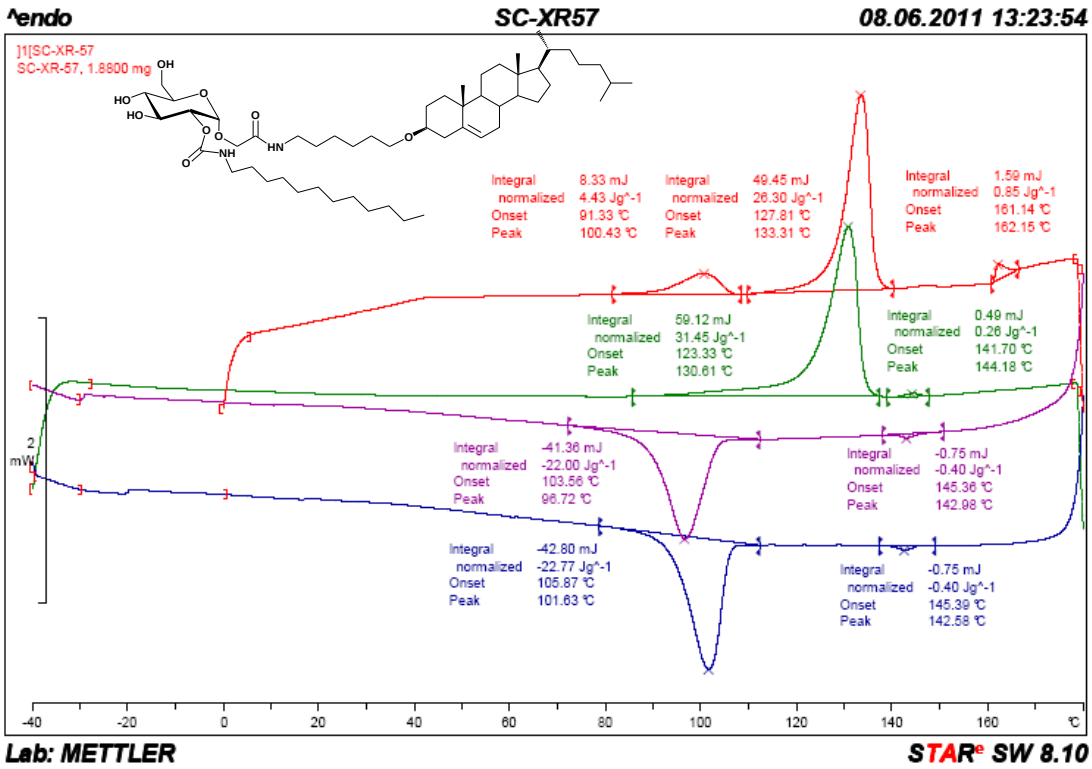

B.2.9: DSC curve of bolaphile L6S12 **(125c)**

Cette thèse est accessible à l'adresse : http://theses.insa-lyon.fr/publication/2013ISAL0001/these.pdf
© [R. Xu], [2013], INSA de Lyon, tous droits réservés

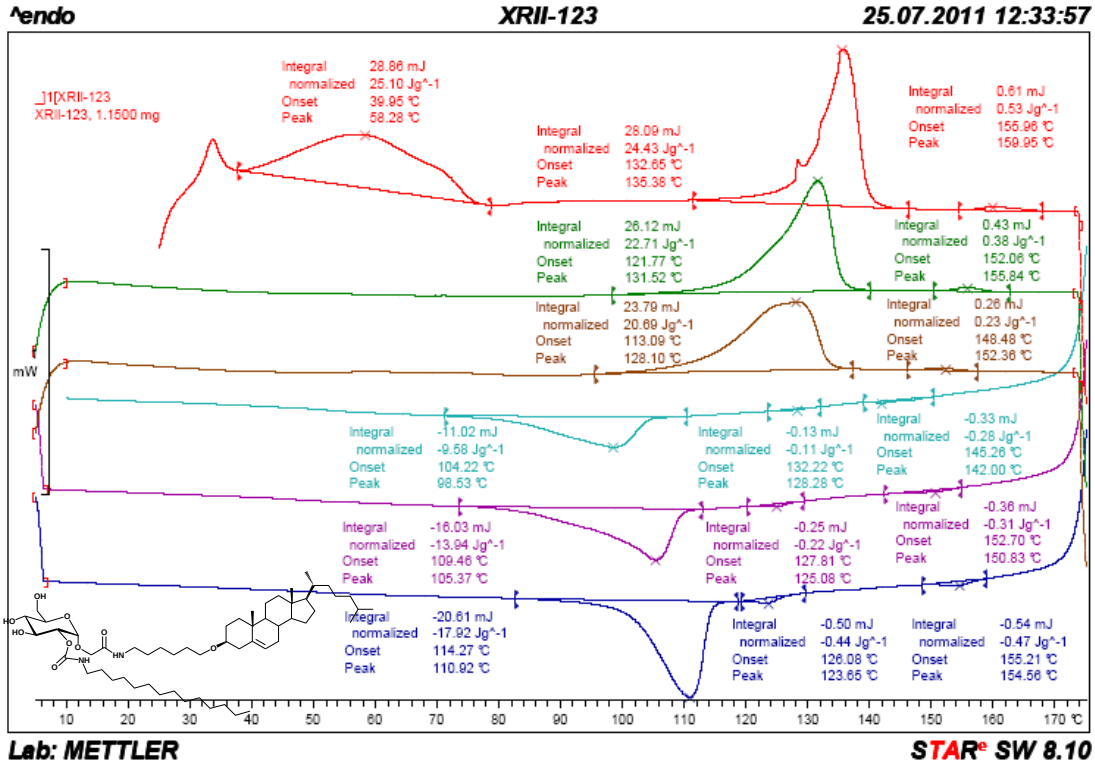

B.2.10: DSC curve of bolaphile L6S14 **(125d)**

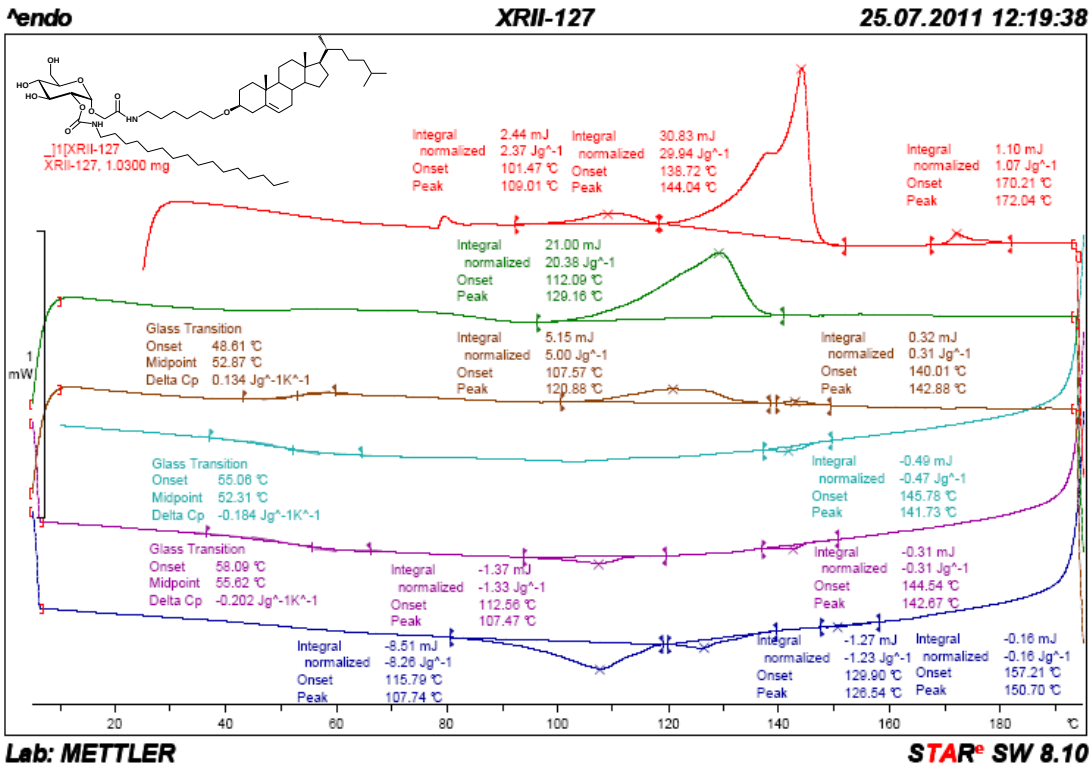

B.2.11: DSC curve of bolaphile L6S16 **(125e)**

Cette thèse est accessible à l'adresse : http://theses.insa-lyon.fr/publication/2013ISAL0001/these.pdf
© [R. Xu], [2013], INSA de Lyon, tous droits réservés

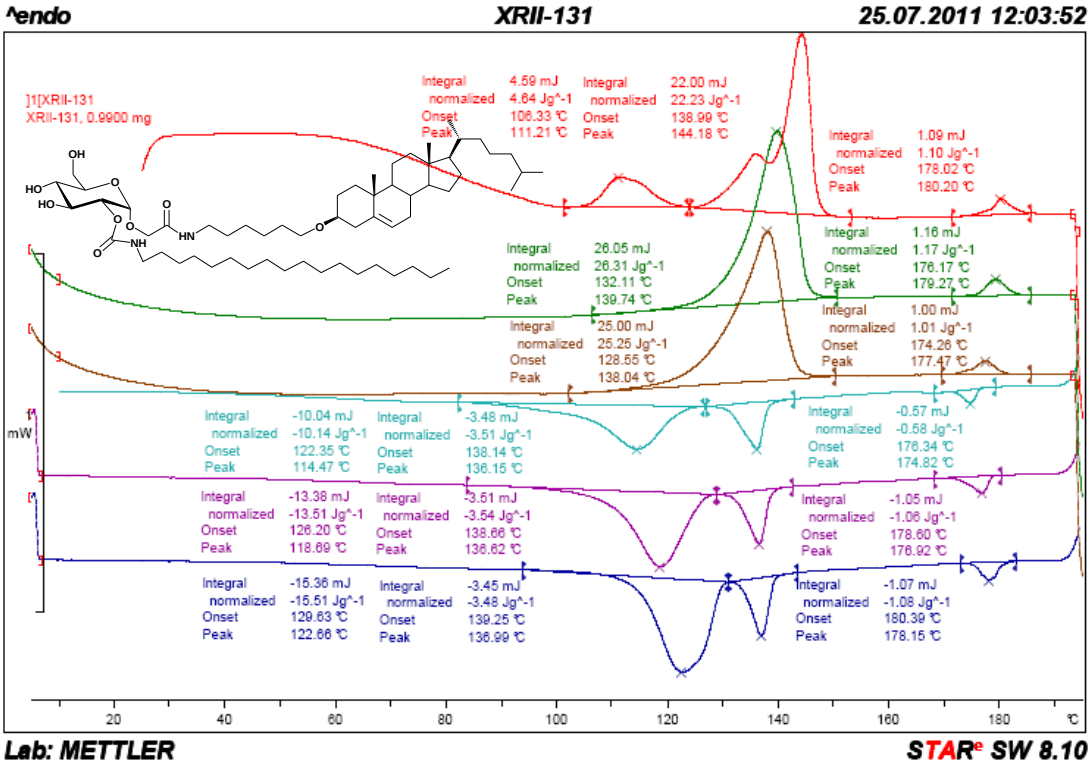

B.2.12: DSC curve of bolaphile L6S18 **(125f)**

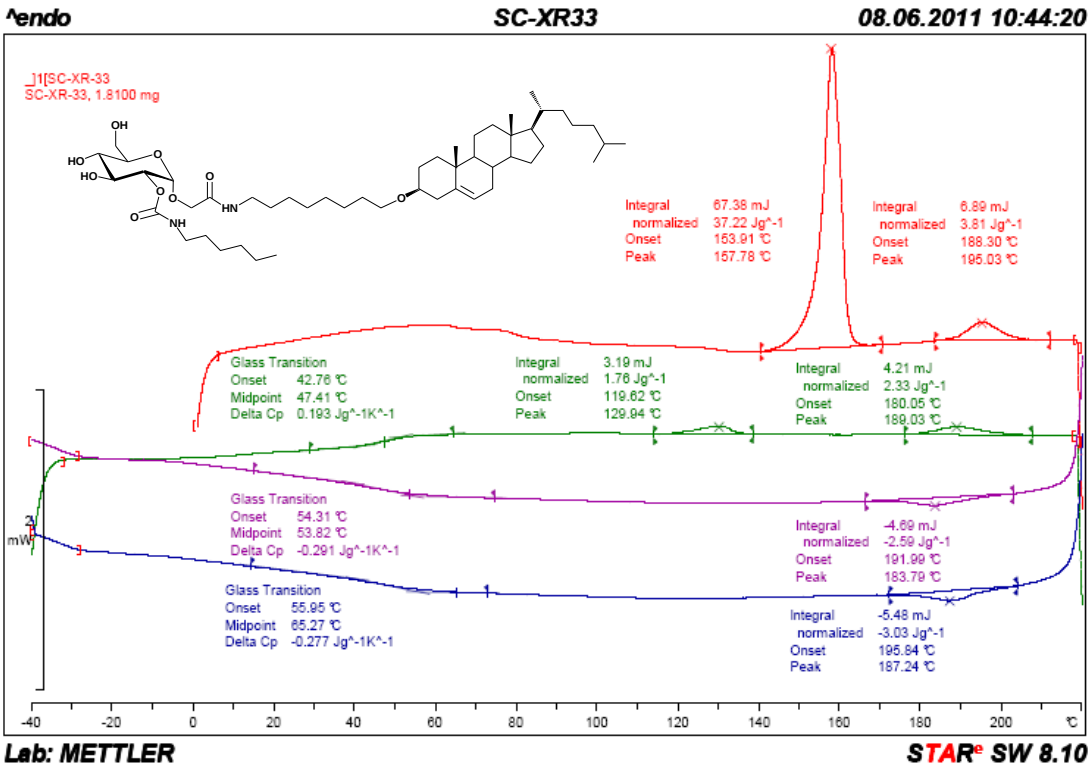

B.2.13: DSC curve of bolaphile L8S6 **(126a)**

Cette thèse est accessible à l'adresse : http://theses.insa-lyon.fr/publication/2013ISAL0001/these.pdf
© [R. Xu], [2013], INSA de Lyon, tous droits réservés

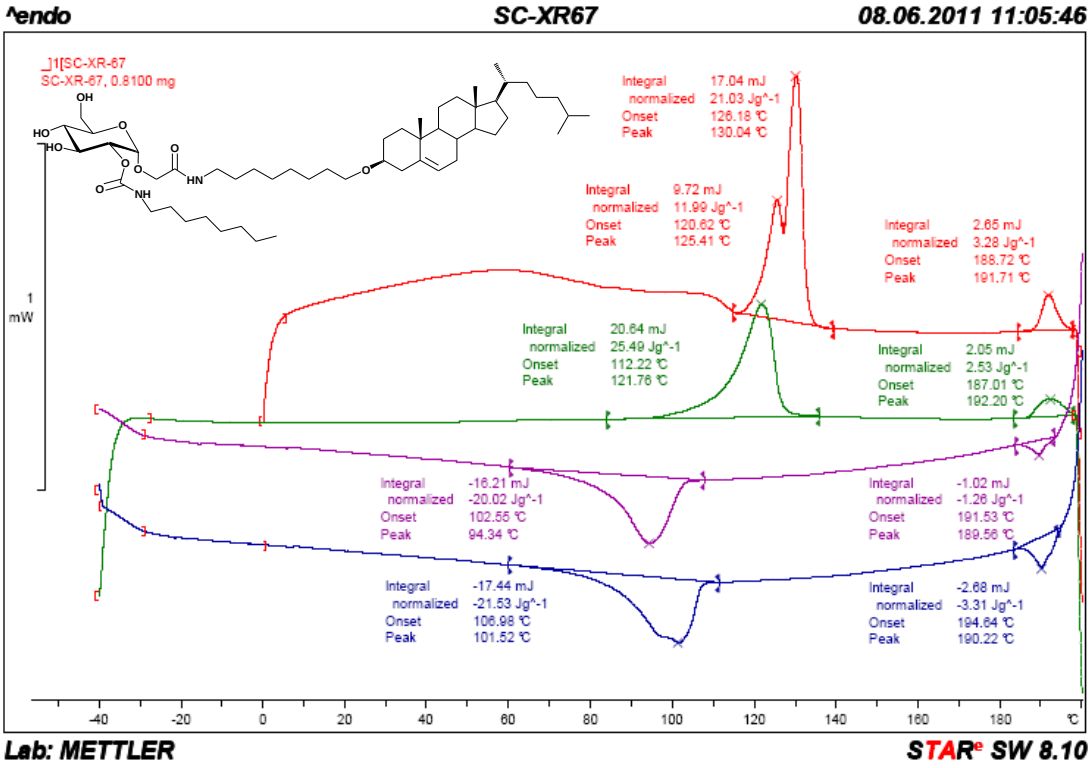

B.2.14: DSC curve of bolaphile L8S8 **(126b)**

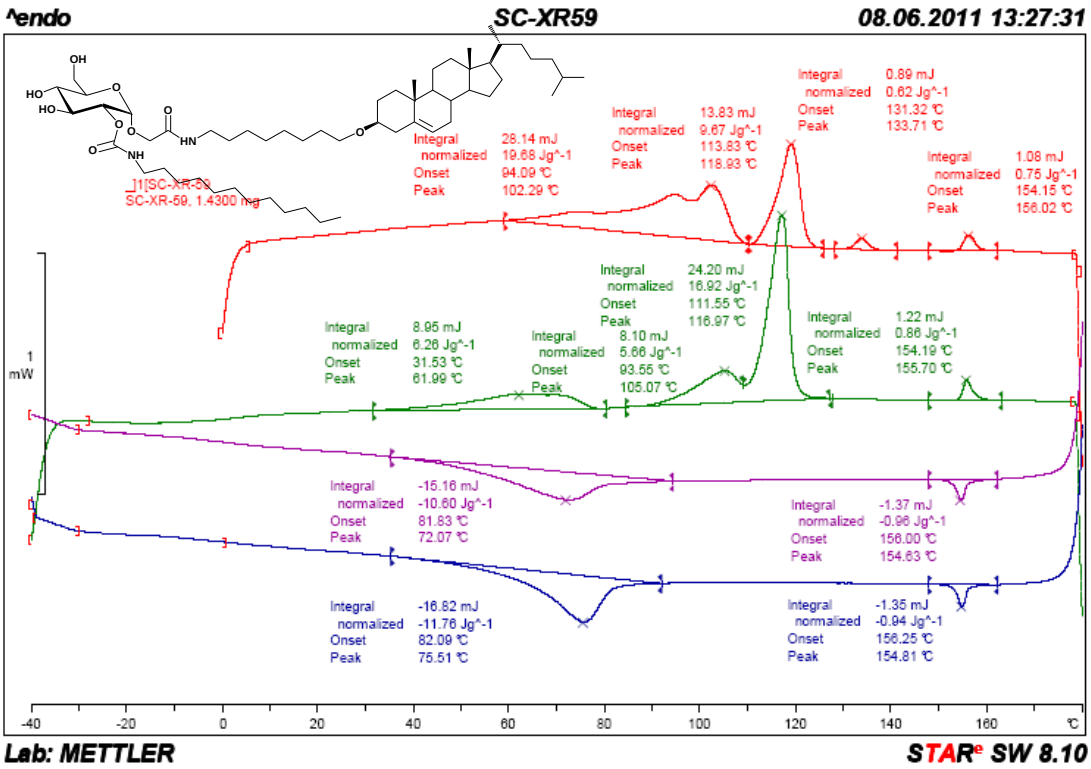

B.2.14: DSC curve of bolaphile L8S12 **(126c)**

Cette thèse est accessible à l'adresse : http://theses.insa-lyon.fr/publication/2013ISAL0001/these.pdf
© [R. Xu], [2013], INSA de Lyon, tous droits réservés

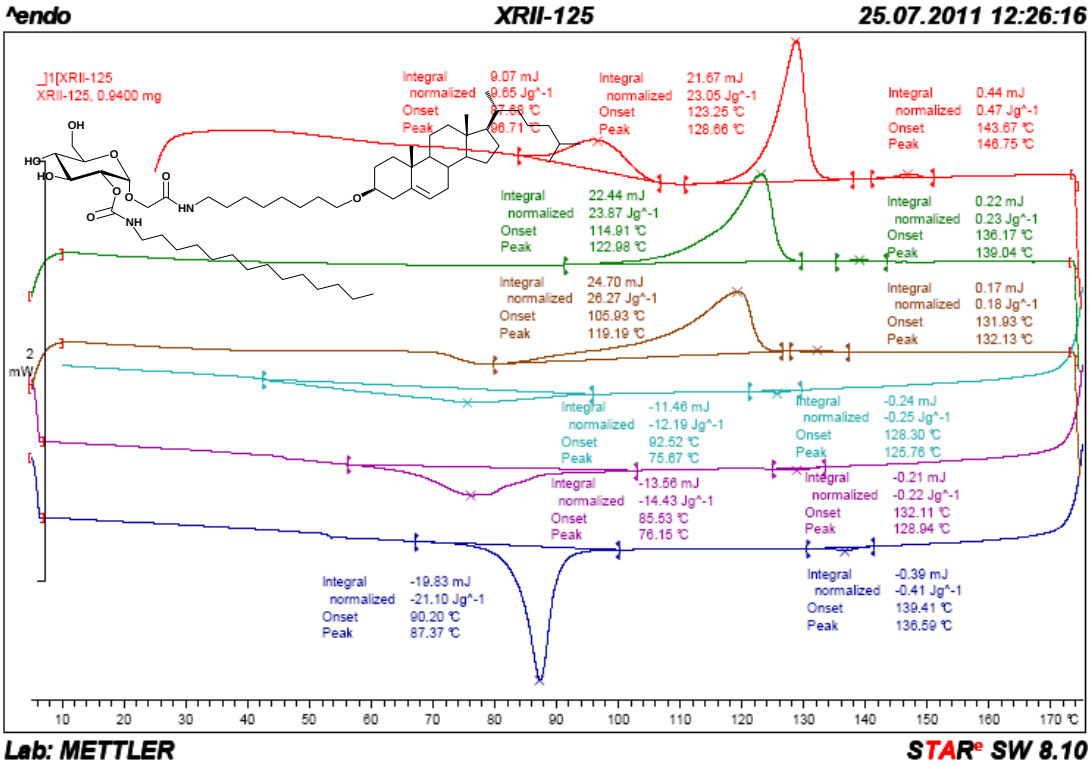

B.2.15: DSC curve of bolaphile L8S14 **(126d)**

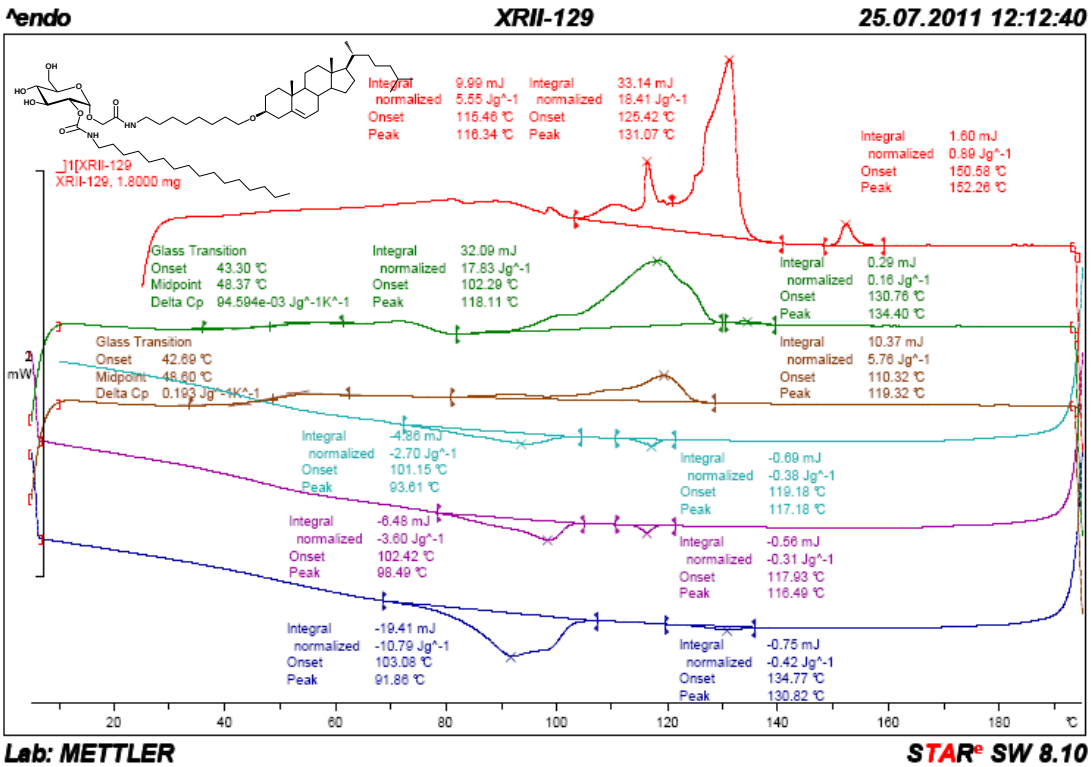

B.2.16: DSC curve of bolaphile L8S16 **(126e)**

Cette thèse est accessible à l'adresse : http://theses.insa-lyon.fr/publication/2013ISAL0001/these.pdf
© [R. Xu], [2013], INSA de Lyon, tous droits réservés

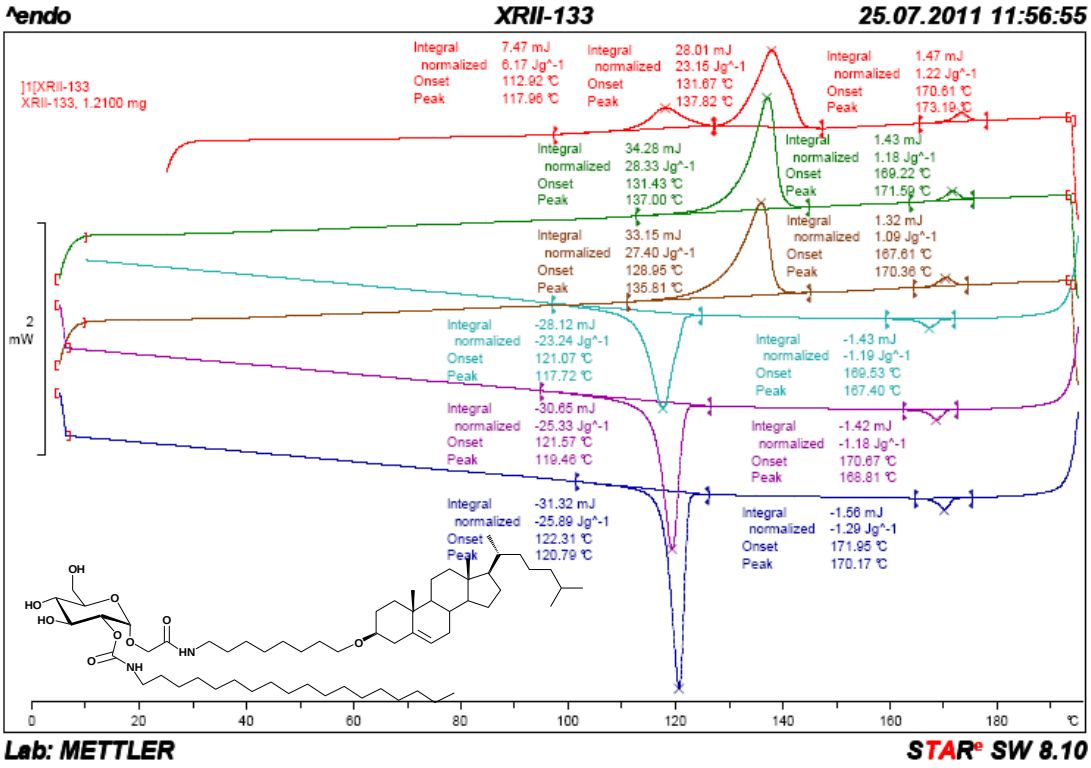

B.2.17: DSC curve of bolaphile L8S18 **(126f)**

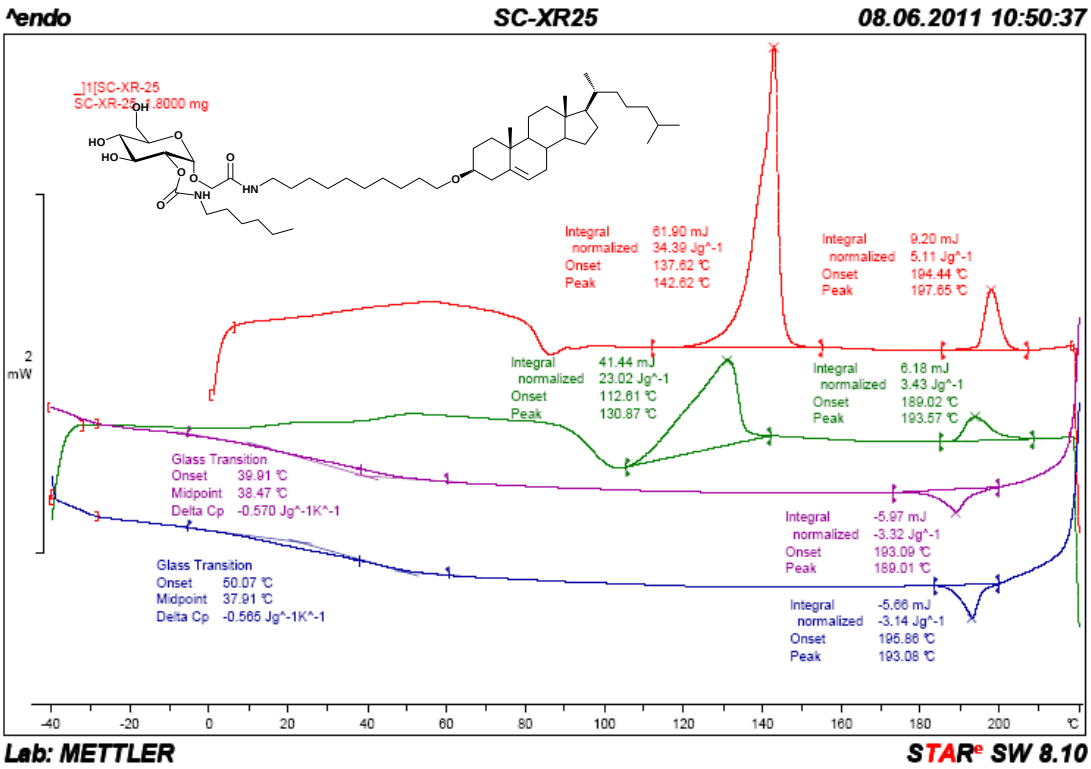

B.2.18: DSC curve of bolaphile L10S6 **(127a)**

Cette thèse est accessible à l'adresse : http://theses.insa-lyon.fr/publication/2013ISAL0001/these.pdf
© [R. Xu], [2013], INSA de Lyon, tous droits réservés

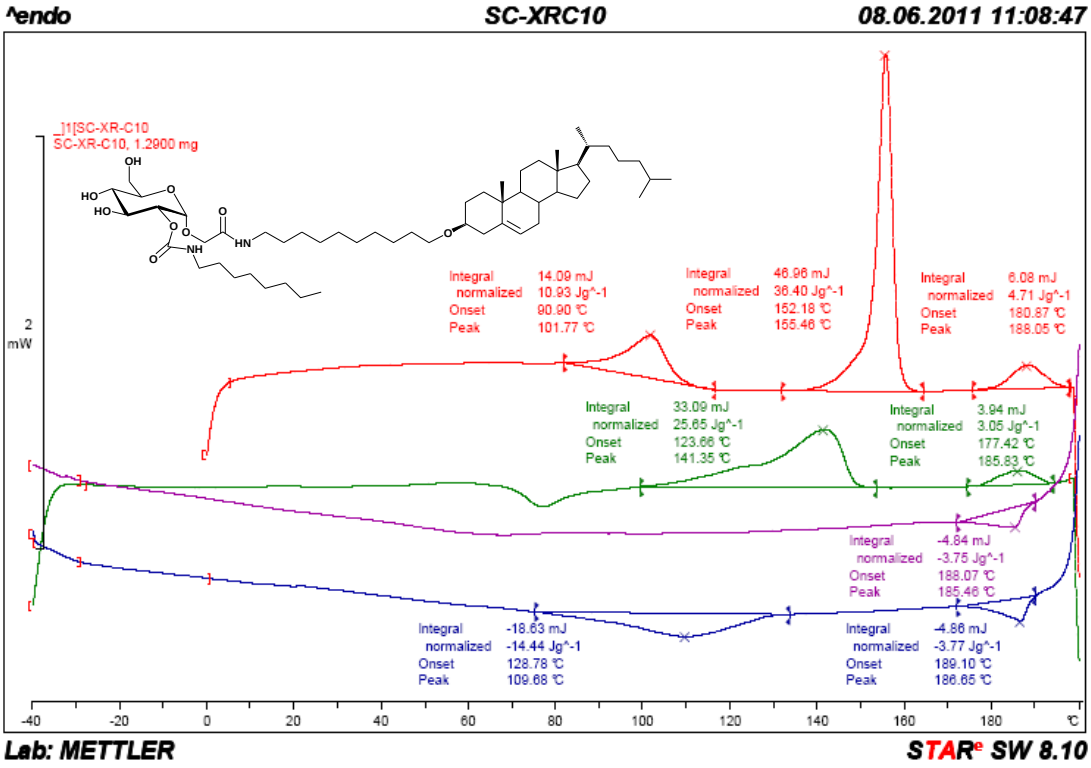

B.2.19: DSC curve of bolaphile L10S8 **(127b)**

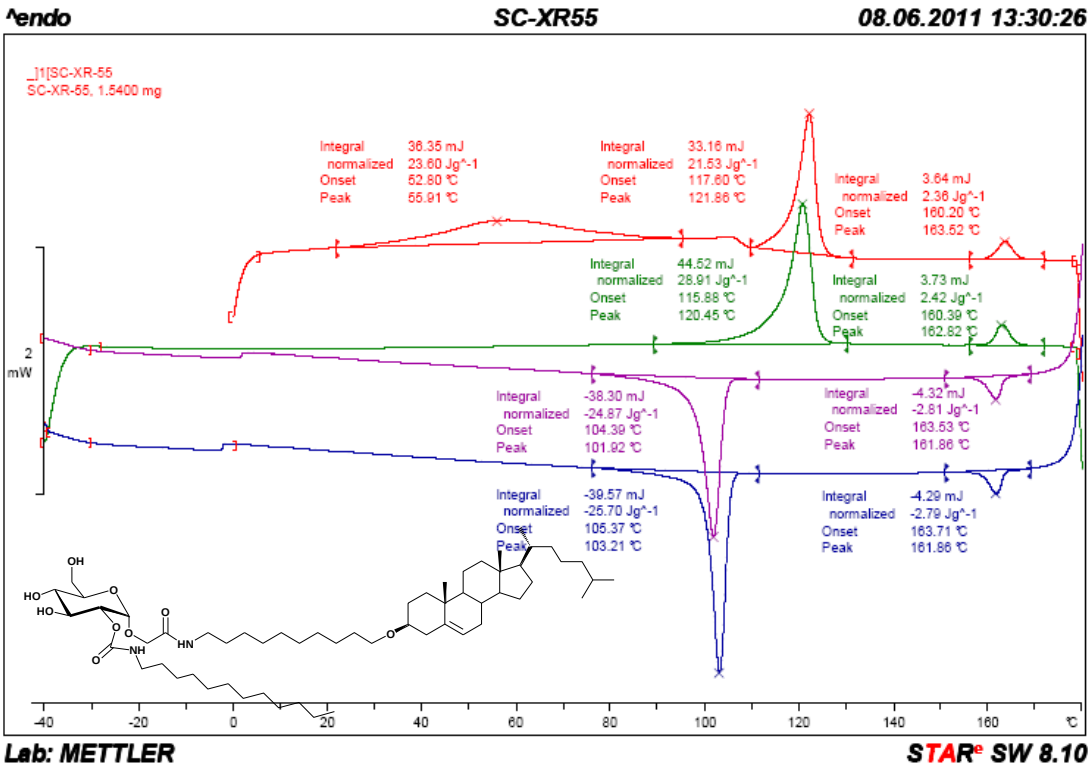

B.2.20: DSC curve of bolaphile L10S12 **(127c)**

Cette thèse est accessible à l'adresse : http://theses.insa-lyon.fr/publication/2013ISAL0001/these.pdf
© [R. Xu], [2013], INSA de Lyon, tous droits réservés

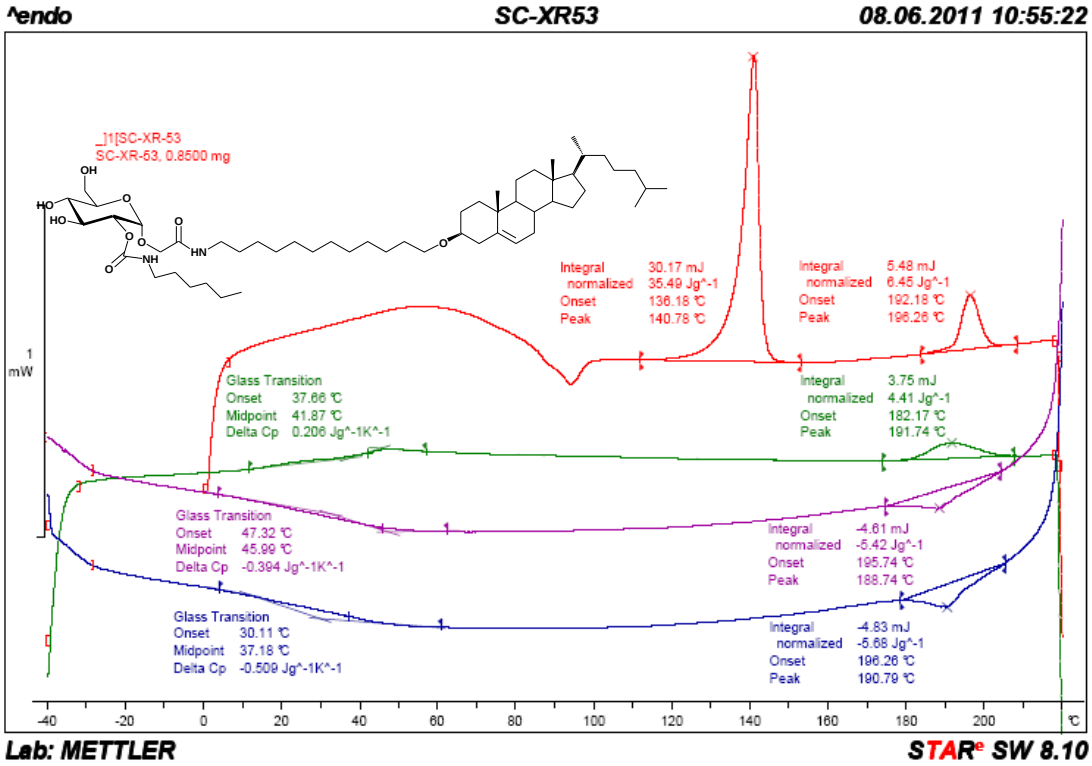

B.2.21: DSC curve of bolaphile L12S6 **(128a)**

Cette thèse est accessible à l'adresse : http://theses.insa-lyon.fr/publication/2013ISAL0001/these.pdf
© [R. Xu], [2013], INSA de Lyon, tous droits réservés

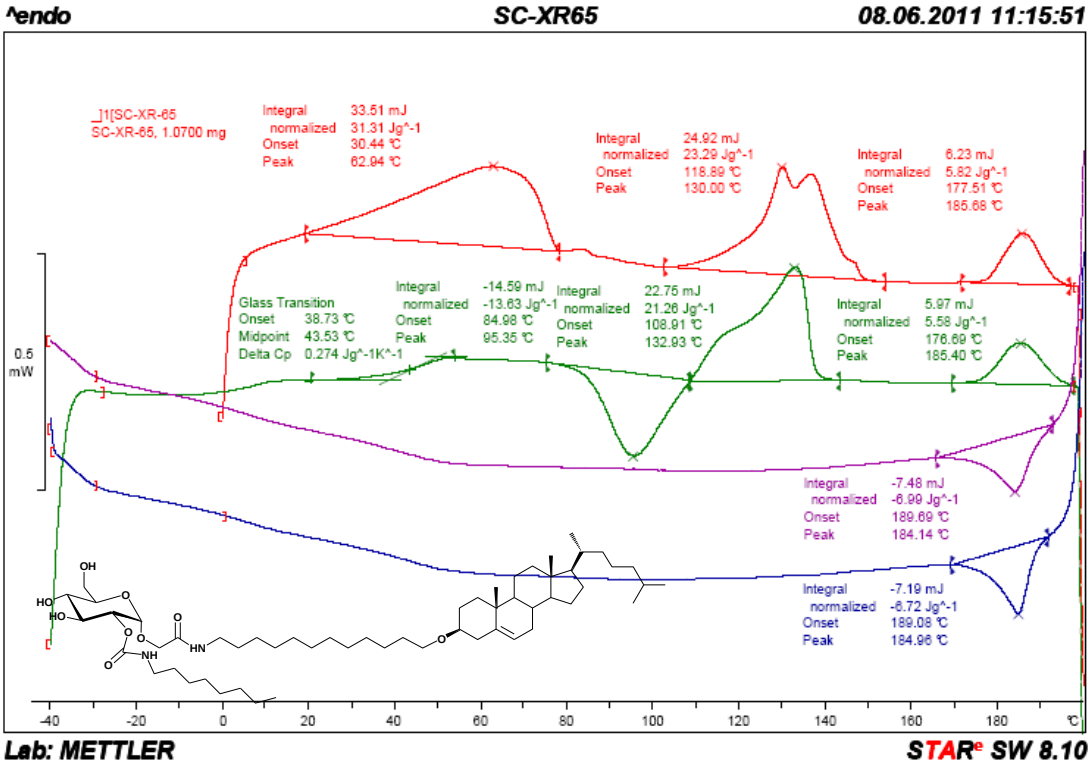

B.2.22: DSC curve of bolaphile L12S8 **(128b)**

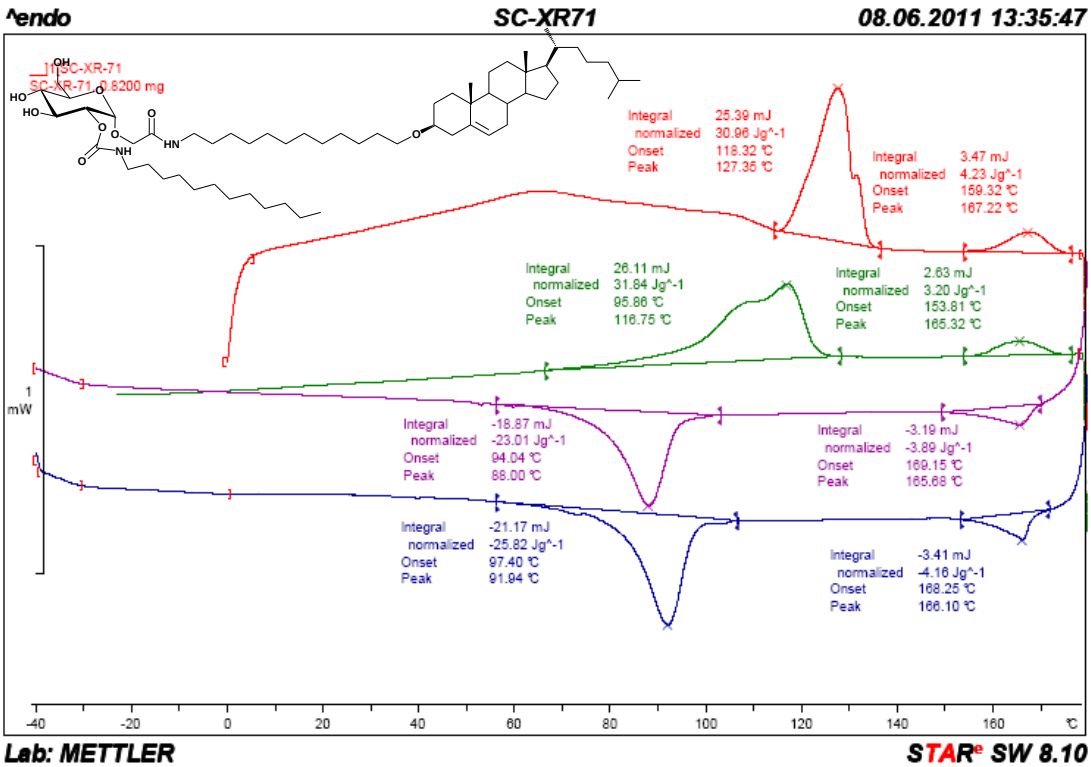

B.2.23: DSC curve of bolaphile L12S12 **(128c)**

Cette thèse est accessible à l'adresse : http://theses.insa-lyon.fr/publication/2013ISAL0001/these.pdf
© [R. Xu], [2013], INSA de Lyon, tous droits réservés

References

1. D. Myers, *Surfactant Science and Technology*. 3rd ed2005: John Wiley & Sons.
2. Dwight R. and S. W., *Surfactants-A Market Opportunity Study Update*, 2008, OMNI TECH INTERNATIONAL, LTD.
3. Y. Inami, T. Andoh, A. Sasaki, and Y. Kuraishi, *Surfactant-induced Itching and the Involvement of Histamine Released from Keratinocytes.* Yakugaku Zasshi-Journal of the Pharmaceutical Society of Japan, 2012. **132**(11): p. 1225-1230.
4. S.K. Satpute, I.M. Banat, P.K. Dhakephalkar, A.G. Banpurkar, and B.A. Chopade, *Biosurfactants, bioemulsifiers and exopolysaccharides from marine microorganisms.* Biotechnology Advances, 2010. **28**(4): p. 436-450.
5. V. Pruthi and S. Cameotra, *Novel sucrose lipid produced by Serratia marcescens and its application in enhanced oil recovery.* Journal of Surfactants and Detergents, 2000. **3**(4): p. 533-537.
6. A. Szűts and P. Szabó-Révész, *Sucrose esters as natural surfactants in drug delivery systems—A mini-review.* International Journal of Pharmaceutics, 2012. **433**(1–2): p. 1-9.
7. A.M. Lowe and N.L. Abbott, *Liquid Crystalline Materials for Biological Applications.* Chemistry of Materials, 2012. **24**(5): p. 746-758.
8. M. Pierre and I. Santos Miranda Costa, *Liposomal systems as drug delivery vehicles for dermal and transdermal applications.* Arch Dermatol Res, 2011. **303**(9): p. 607-621.
9. G.K. Ziyatdinova, E.R. Ziganshina, and H.C. Budnikov, *Application of surfactants in voltammetric analysis.* J Anal Chem, 2012. **67**(11): p. 869-879.
10. E.E. Tkalya, M. Ghislandi, G. de With, and C.E. Koning, *The use of surfactants for dispersing carbon nanotubes and graphene to make conductive nanocomposites.* Curr. Opin. Colloid Interface Sci., 2012. **17**(4): p. 225-232.
11. V. Dornburg, I. Lewandowski, and M. Patel, *Comparing the Land Requirements, Energy Savings, and Greenhouse Gas Emissions Reduction of Biobased Polymers and Bioenergy.* Journal of Industrial Ecology, 2003. **7**(3-4): p. 93-116.
12. *CESIO statistics 2011*, E.C.o.O.S.a.t. Intermediates, Editor 2011.
13. K. Hill and C. LeHen-Ferrenbach, *Sugar-Based Surfactants for Consumer Products and Technical Applications*, in *Sugar-Based Surfactants: Fundamentals and Applications*, C.C. Ruiz, Editor 2008, CRC Press.
14. P. Foley, A.K. Pour, E.S. Beach, and J.B. Zimmerman, *Derivation and synthesis of renewable surfactants.* Chemical Society Reviews, 2012. **41**(4): p. 1499-1518.
15. Y. Queneau, S. Chambert, C. Besset, and R. Cheaib, *Recent progress in the synthesis of carbohydrate-based amphiphilic materials: the examples of sucrose and isomaltulose.* Carbohydr Res, 2008. **343**(12): p. 1999-2009.
16. K. Holmberg, *Natural surfactants.* Current Opinion in Colloid & Interface Science, 2001. **6**(2): p. 148-159.
17. R. Marchant and I.M. Banat, *Microbial biosurfactants: challenges and opportunities for future exploitation.* Trends in Biotechnology, 2012. **30**(11): p. 558-565.
18. R. Marchant and I. Banat, *Biosurfactants: a sustainable replacement for chemical surfactants?* Biotechnology Letters, 2012. **34**(9): p. 1597-1605.
19. D. Kitamoto, T. Morita, T. Fukuoka, M. Konishi, and T. Imura, *Self-assembling properties of glycolipid biosurfactants and their potential applications.* Curr. Opin. Colloid Interface Sci., 2009. **14**(5): p. 315-328.

Cette thèse est accessible à l'adresse : http://theses.insa-lyon.fr/publication/2013ISAL0001/these.pdf
© [R. Xu], [2013], INSA de Lyon, tous droits réservés

20. D. Kitamoto, H. Isoda, and T. Nakahara, *Functions and potential applications of glycolipid biosurfactants — from energy-saving materials to gene delivery carriers —.* Journal of Bioscience and Bioengineering, 2002. **94**(3): p. 187-201.
21. S.-i. Hakomori, *The glycosynapse.* Proceedings of the National Academy of Sciences, 2002. **99**(1): p. 225-232.
22. R.K. Yu, Y. Suzuki, and M. Yanagisawa, *Membrane glycolipids in stem cells.* Febs Letters, 2010. **584**(9): p. 1694-1699.
23. J.W. Goodby, V. Gortz, S.J. Cowling, G. Mackenzie, P. Martin, D. Plusquellec, T. Benvegnu, P. Boullanger, D. Lafont, Y. Queneau, S. Chambert, and J. Fitremann, *Thermotropic liquid crystalline glycolipids.* Chemical Society Reviews, 2007. **36**(12): p. 1971-2032.
24. G.A. Jeffrey, *Carbohydrate liquid crystals.* Accounts of Chemical Research, 1986. **19**(6): p. 168-173.
25. G.A. Jeffrey and L.M. Wingert, *Carbohydrate liquid crystals.* Liq. Cryst., 1992. **12**(2): p. 179-202.
26. V. Vill and R. Hashim, *Carbohydrate liquid crystals: structure–property relationship of thermotropic and lyotropic glycolipids.* Curr. Opin. Colloid Interface Sci., 2002. **7**(5–6): p. 395-409.
27. O. Gronwald, E. Snip, and S. Shinkai, *Gelators for organic liquids based on self-assembly: a new facet of supramolecular and combinatorial chemistry.* Current Opinion in Colloid & Interface Science, 2002. **7**(1–2): p. 148-156.
28. C.J. Capicciotti, M. Leclere, F.A. Perras, D.L. Bryce, H. Paulin, J. Harden, Y. Liu, and R.N. Ben, *Potent inhibition of ice recrystallization by low molecular weight carbohydrate-based surfactants and hydrogelators.* Chem. Sci., 2012. **3**(5): p. 1408-1416.
29. D.R. Trivedi, A. Ballabh, and P. Dastidar, *Noncovalent syntheses of supramolecular organo gelators.* Crystal Growth & Design, 2006. **6**(3): p. 763-768.
30. L.E. Buerkle, R. Galleguillos, and S.J. Rowan, *Nonionic surfactant-induced stabilization and tailorability of sugar-amphiphile hydrogels.* Soft Matter, 2011. **7**(15): p. 6984-6990.
31. J.X. Zhang and P.X. Ma, *Host-guest interactions mediated nano-assemblies using cyclodextrin-containing hydrophilic polymers and their biomedical applications.* Nano Today, 2010. **5**(4): p. 337-350.
32. A. Diaz-Moscoso, N. Guilloteau, C. Bienvenu, A. Mendez-Ardoy, J.L.J. Blanco, J.M. Benito, L. Le Gourrierec, C. Di Giorgio, P. Vierling, J. Defaye, C.O. Mellet, and J.M.G. Fernandez, *Mannosyl-coated nanocomplexes from amphiphilic cyclodextrins and pDNA for site-specific gene delivery.* Biomaterials, 2011. **32**(29): p. 7263-7273.
33. M. Assali, M.P. Leal, I. Fernandez, P. Romero-Gomez, R. Baati, and N. Khiar, *Improved Non-Covalent Biofunctionalization of Multi-Walled Carbon Nanotubes Using Carbohydrate Amphiphiles with a Butterfly-Like Polyaromatic Tail.* Nano Research, 2010. **3**(11): p. 764-778.
34. M.J. Lawrence and G.D. Rees, *Microemulsion-based media as novel drug delivery systems.* Advanced Drug Delivery Reviews, 2000. **45**(1): p. 89-121.
35. K. Hill and O. Rhode, *Sugar-based surfactants for consumer products and technical applications.* Fett-Lipid, 1999. **101**(1): p. 25-33.
36. J. HernandezBarajas and D.J. Hunkeler, *Inverse-emulsion polymerization of acrylamide using block copolymeric surfactants: Mechanism, kinetics and modelling.* Polymer, 1997. **38**(2): p. 437-447.
37. H. Omidian, M.J. Zohuriaan-Mehr, and H. Bouhendi, *Polymerization of sodium acrylate in inverse-suspension stabilized by sorbitan fatty esters.* European Polymer Journal, 2003. **39**(5): p. 1013-1018.
38. G.J. Stockburger, *Process for preparing sorbitan esters*, USPTO, Editor 1981: USA.
39. V. Molinier, P.H.J. Kouwer, J. Fitremann, A. Bouchu, G. Mackenzie, Y. Queneau, and J.W. Goodby, *Self-organizing properties of monosubstituted sucrose fatty acid esters: The effects of chain length and unsaturation.* Chem.-Eur. J., 2006. **12**(13): p. 3547-3557.

Cette thèse est accessible à l'adresse : http://theses.insa-lyon.fr/publication/2013ISAL0001/these.pdf
© [R. Xu], [2013], INSA de Lyon, tous droits réservés

40. W. von Rybinski and K. Hill, *Alkyl Polyglycosides—Properties and Applications of a new Class of Surfactants.* Angewandte Chemie International Edition, 1998. **37**(10): p. 1328-1345.
41. D.A. Mannock and R.N. McElhaney, *Thermotropic and lyotropic phase properties of glycolipid diastereomers: role of headgroup and interfacial interactions in determining phase behaviour.* Current Opinion in Colloid & Interface Science, 2004. **8**(6): p. 426-447.
42. S.-i. Hakomori, *Structure and function of glycosphingolipids and sphingolipids: Recollections and future trends.* Biochimica et Biophysica Acta (BBA) - General Subjects, 2008. **1780**(3): p. 325-346.
43. S. Degroote, J. Wolthoorn, and G. van Meer, *The cell biology of glycosphingolipids.* Seminars in Cell & Developmental Biology, 2004. **15**(4): p. 375-387.
44. J.W. Goodby, *Liquid crystals and life.* Liq. Cryst., 1998. **24**(1): p. 25-38.
45. U.L. Khatun, S.K. Goswami, and C. Mukhopadhyay, *Modulation of the neurotensin solution structure in the presence of ganglioside GM1 bicelle.* Biophysical Chemistry, 2012. **168–169**(0): p. 48-59.
46. W.L. Smith and A.H. Merrill, *Sphingolipid Metabolism and Signaling Minireview Series.* Journal of Biological Chemistry, 2002. **277**(29): p. 25841-25842.
47. Lingwood D. and K. Simons, *Lipid Rafts As a Membrane-Organizing Principle.* Science 2010. **327**: p. 46-50.
48. A. Fujita and T. Fujimoto, *Nanoscale Analysis of Glycolipid Distribution in the Cell Membrane.* Trends in Glycoscience and Glycotechnology. **22**(126-28): p. 173-181.
49. V. Michel and M. Bakovic, *Lipid rafts in health and disease.* Biology of the Cell, 2007. **99**(3): p. 129-140.
50. Staubach S and H. F.G, *Lipid rafts: signaling and sorting platforms of cells and their roles in cancer.* Expert Rev. Proteomics, 2011. **8**(2): p. 263-277.
51. D.A. Brown and E. London, *Structure and Function of Sphingolipid- and Cholesterol-rich Membrane Rafts.* Journal of Biological Chemistry, 2000. **275**(23): p. 17221-17224.
52. E.M. Danielsen and G.H. Hansen, *Lipid raft organization and function in the small intestinal brush border.* J. Physiol. Biochem., 2008. **64**(4): p. 377-382.
53. D. A. and B.E. London, *Structure and Function of Sphingolipid- and Cholesterol-rich Membrane Rafts.* THE JOURNAL OF BIOLOGICAL CHEMISTRY, 2000. **275**(23): p. 17221–17224.
54. G. Hölzl and P. Dörmann, *Structure and function of glycoglycerolipids in plants and bacteria.* Progress in Lipid Research, 2007. **46**(5): p. 225-243.
55. D.A. Mannock, M.D. Collins, M. Kreichbaum, P.E. Harper, S.M. Gruner, and R.N. McElhaney, *The thermotropic phase behaviour and phase structure of a homologous series of racemic β-d-galactosyl dialkylglycerols studied by differential scanning calorimetry and X-ray diffraction.* Chemistry and Physics of Lipids, 2007. **148**(1): p. 26-50.
56. A.V. Popova and D.K. Hincha, *Effects of the sugar headgroup of a glycoglycerolipid on the phase behavior of phospholipid model membranes in the dry state.* Glycobiology, 2005. **15**(11): p. 1150-1155.
57. D.A. Mannock, P.E. Harper, S.M. Gruner, and R.N. McElhaney, *The physical properties of glycosyl diacylglycerols. Calorimetric, X-ray diffraction and Fourier transform spectroscopic studies of a homologous series of 1,2-di-O-acyl-3-O-(β-d-galactopyranosyl)-sn-glycerols.* Chemistry and Physics of Lipids, 2001. **111**(2): p. 139-161.
58. M. Hamberg, E. Liepinsh, G. Otting, and W. Griffiths, *Isolation and structure of a new galactolipid from oat seeds.* Lipids, 1998. **33**(4): p. 355-363.
59. S. Grille, A. Zaslawski, S. Thiele, J. Plat, and D. Warnecke, *The functions of steryl glycosides come to those who wait: Recent advances in plants, fungi, bacteria and animals.* Progress in Lipid Research, 2010. **49**(3): p. 262-288.
60. T. Ikeda, H. Miyashita, T. Kajimoto, and T. Nohara, *Synthesis of neosaponins having an α-l-rhamnopyranosyl-(1→4)-[α-l-rhamnopyranosyl-(1→2)]-d-glucopyranosyl glyco-linkage.* Tetrahedron Lett., 2001. **42**(12): p. 2353-2356.

Cette thèse est accessible à l'adresse : http://theses.insa-lyon.fr/publication/2013ISAL0001/these.pdf
© [R. Xu], [2013], INSA de Lyon, tous droits réservés

61. B. Yu, J. Sun, and X. Yang, *Assembly of Naturally Occurring Glycosides, Evolved Tactics, and Glycosylation Methods.* Accounts of Chemical Research, 2012. **45**(8): p. 1227-1236.
62. F.S. Ekholm, G. Schneider, J. Wölfling, and R. Leino, *Synthesis of a Small Library of Estradiol-Based Glycosteroid Mimics Containing a Modified D-Ring.* European Journal of Organic Chemistry, 2011. **2011**(6): p. 1064-1077.
63. Y. Zhou, C. Garcia-Prieto, D.A. Carney, R.-h. Xu, H. Pelicano, Y. Kang, W. Yu, C. Lou, S. Kondo, J. Liu, D.M. Harris, Z. Estrov, M.J. Keating, Z. Jin, and P. Huang, *OSW-1: a Natural Compound With Potent Anticancer Activity and a Novel Mechanism of Action.* Journal of the National Cancer Institute, 2005. **97**(23): p. 1781-1785.
64. K. Schrick, S. Shiva, J. Arpin, N. Delimont, G. Isaac, P. Tamura, and R. Welti, *Steryl Glucoside and Acyl Steryl Glucoside Analysis of Arabidopsis Seeds by Electrospray Ionization Tandem Mass Spectrometry.* Lipids, 2012. **47**(2): p. 185-193.
65. G. Ben-Menachem, J. Kubler-Kielb, B. Coxon, A. Yergey, and R. Schneerson, *A newly discovered cholesteryl galactoside from Borrelia burgdorferi.* Proceedings of the National Academy of Sciences of the United States of America, 2003. **100**(13): p. 7913-7918.
66. D.J. McGee, A.E. George, E.A. Trainor, K.E. Horton, E. Hildebrandt, and T.L. Testerman, *Cholesterol Enhances Helicobacter pylori Resistance to Antibiotics and LL-37.* Antimicrobial Agents and Chemotherapy, 2011. **55**(6): p. 2897-2904.
67. M.Y.Y.M.K.S.M.N.F.M.T.J. Kawakubo, *Natural Antibiotic Function of a Human Gastric Mucin Against Helicobacter pylon Infection.* Science, 2004. **305**(5686): p. 1003-1006.
68. T. Morita, T. Fukuoka, T. Imura, and D. Kitamoto, *Production of glycolipid biosurfactants by basidiomycetous yeasts.* Biotechnol. Appl. Biochem., 2009. **53**: p. 39-49.
69. T. Morita, M. Konishi, T. Fukuoka, T. Imura, S. Yamamoto, M. Kitagawa, A. Sogabe, and D. Kitamoto, *Identification of Pseudozyma graminicola CBS 10092 as a Producer of Glycolipid Biosurfactants, Mannosylerythritol Lipids.* Journal of Oleo Science, 2008. **57**(2): p. 123-131.
70. I.N.A. Van Bogaert, J. Zhang, and W. Soetaert, *Microbial synthesis of sophorolipids.* Process Biochemistry, 2011. **46**(4): p. 821-833.
71. M. Henkel, M.M. Müller, J.H. Kügler, R.B. Lovaglio, J. Contiero, C. Syldatk, and R. Hausmann, *Rhamnolipids as biosurfactants from renewable resources: Concepts for next-generation rhamnolipid production.* Process Biochemistry, 2012. **47**(8): p. 1207-1219.
72. A. Franzetti, I. Gandolfi, G. Bestetti, T.J.P. Smyth, and I.M. Banat, *Production and applications of trehalose lipid biosurfactants.* European Journal of Lipid Science and Technology, 2010. **112**(6): p. 617-627.
73. V. Haesendonck;, I.P. Hilda;, B. (Mechelen, Vanzeveren;, and E.C. Albert, *Rhamnolipids in bakery products*, 2003.
74. M. Pacwa-Plociniczak, G.A. Plaza, Z. Piotrowska-Seget, and S.S. Cameotra, *Environmental Applications of Biosurfactants: Recent Advances.* International Journal of Molecular Sciences, 2011. **12**(1): p. 633-654.
75. K.S.M. Rahman, T.J. Rahman, P. Lakshmanaperumalsamy, R. Marchant, and I.M. Banat, *The Potential of Bacterial Isolates for Emulsification with a Range of Hydrocarbons.* Acta Biotechnologica, 2003. **23**(4): p. 335-345.
76. D.H. Dusane, Y.V. Nancharaiah, S.S. Zinjarde, and V.P. Venugopalan, *Rhamnolipid mediated disruption of marine Bacillus pumilus biofilms.* Colloids and Surfaces B: Biointerfaces, 2010. **81**(1): p. 242-248.
77. C.-M. Lo and L.-K. Ju, *Sophorolipids-induced cellulase production in cocultures of Hypocrea jecorina Rut C30 and Candida bombicola.* Enzyme and Microbial Technology, 2009. **44**(2): p. 107-111.
78. S. Singh, P. Patel, S. Jaiswal, A.A. Prabhune, C.V. Ramana, and B.L.V. Prasad, *A direct method for the preparation of glycolipid-metal nanoparticle conjugates: sophorolipids as reducing and capping agents for the synthesis of water re-dispersible silver nanoparticles and their antibacterial activity.* New Journal of Chemistry, 2009. **33**(3): p. 646-652.

Cette thèse est accessible à l'adresse : http://theses.insa-lyon.fr/publication/2013ISAL0001/these.pdf
© [R. Xu], [2013], INSA de Lyon, tous droits réservés

79. N. Baccile, N. Nassif, L. Malfatti, I.N.A. Van Bogaert, W. Soetaert, G. Pehau-Arnaudet, and F. Babonneau, *Sophorolipids: a yeast-derived glycolipid as greener structure directing agents for self-assembled nanomaterials.* Green Chemistry, 2010. **12**(9): p. 1564-1567.
80. Y. Inoh, T. Furuno, N. Hirashima, D. Kitamoto, and M. Nakanishi, *Rapid delivery of small interfering RNA by biosurfactant MEL-A-containing liposomes.* Biochemical and Biophysical Research Communications, 2011. **414**(3): p. 635-640.
81. T. Fukuoka, T. Yanagihara, T. Imura, T. Morita, H. Sakai, M. Abe, and D. Kitamoto, *The diastereomers of mannosylerythritol lipids have different interfacial properties and aqueous phase behavior, reflecting the erythritol configuration.* Carbohydrate Research, 2012. **351**: p. 81-86.
82. P. Yan, M. Lu, Q. Yang, H.L. Zhang, Z.Z. Zhang, and R. Chen, *Oil recovery from refinery oily sludge using a rhamnolipid biosurfactant-producing Pseudomonas.* Bioresource Technology, 2012. **116**: p. 24-28.
83. I.M. Banat, A. Franzetti, I. Gandolfi, G. Bestetti, M.G. Martinotti, L. Fracchia, T.J. Smyth, and R. Marchant, *Microbial biosurfactants production, applications and future potential.* Applied Microbiology and Biotechnology, 2010. **87**(2): p. 427-444.
84. A. Piljac, T. Stipcˇevic´, J. Piljac-Zˇegarac, and G. Piljac, *Successful Treatment of Chronic Decubitus Ulcer with 0.1% Dirhamnolipid Ointment.* Journal of Cutaneous Medicine and Surgery, 2008. **12**: p. 1-5.
85. T. Stipcevic, A. Piljac, and G. Piljac, *Enhanced healing of full-thickness burn wounds using dirhamnolipid.* Burns, 2006. **32**(1): p. 24-34.
86. A. Vintiloiu and J.C. Leroux, *Organogels and their use in drug delivery - A review.* Journal of Controlled Release, 2008. **125**(3): p. 179-192.
87. D. Gao, M. Xue, J. Peng, J. Liu, N. Yan, P. He, and Y. Fang, *Preparation and gelling properties of sugar-contained low-molecular-mass gelators: Combination of cholesterol and linear glucose.* Tetrahedron, 2010. **66**(16): p. 2961-2968.
88. Y. Gao, Y. Kuang, Z.-F. Guo, Z. Guo, I.J. Krauss, and B. Xu, *Enzyme-Instructed Molecular Self-assembly Confers Nanofibers and a Supramolecular Hydrogel of Taxol Derivative.* Journal of the American Chemical Society, 2009. **131**(38): p. 13576-13577.
89. P. Li, X.-Q. Dou, Y.-T. Tang, S. Zhu, J. Gu, C.-L. Feng, and D. Zhang, *Gelator-polysaccharide hybrid hydrogel for selective and controllable dye release.* Journal of Colloid and Interface Science, 2012. **387**(1): p. 115-122.
90. K. Iwanaga, M. Kawai, M. Miyazaki, and M. Kakemi, *Application of organogels as oral controlled release formulations of hydrophilic drugs.* International Journal of Pharmaceutics, 2012. **436**(1–2): p. 869-872.
91. S. Mukherjee and B. Mukhopadhyay, *Phase selective carbohydrate gelator.* Rsc Advances, 2012. **2**(6): p. 2270-2273.
92. W. Feng, R. Luo, J. Xiao, P. Ji, and Z. Zheng, *Self-assembly of sugar-based amphiphile on carbon nanotubes for protein adsorption.* Chemical Engineering Science, 2011. **66**(20): p. 4807-4813.
93. S. Bhattacharya and S.N.G. Acharya, *Pronounced Hydrogel Formation by the Self-Assembled Aggregates of N-Alkyl Disaccharide Amphiphiles.* Chemistry of Materials, 1999. **11**(12): p. 3504-3511.
94. P. Cherukuri, S.M. Bachilo, S.H. Litovsky, and R.B. Weisman, *Near-Infrared Fluorescence Microscopy of Single-Walled Carbon Nanotubes in Phagocytic Cells.* Journal of the American Chemical Society, 2004. **126**(48): p. 15638-15639.
95. P. Chakravarty, R. Marches, N.S. Zimmerman, A.D.-E. Swafford, P. Bajaj, I.H. Musselman, P. Pantano, R.K. Draper, and E.S. Vitetta, *Thermal ablation of tumor cells with antibody-functionalized single-walled carbon nanotubes.* Proceedings of the National Academy of Sciences, 2008.
96. D. Tasis, N. Tagmatarchis, A. Bianco, and M. Prato, *Chemistry of Carbon Nanotubes.* Chemical Reviews, 2006. **106**(3): p. 1105-1136.

Cette thèse est accessible à l'adresse : http://theses.insa-lyon.fr/publication/2013ISAL0001/these.pdf
© [R. Xu], [2013], INSA de Lyon, tous droits réservés

97. D.A. Tsyboulski, E.L. Bakota, L.S. Witus, J.-D.R. Rocha, J.D. Hartgerink, and R.B. Weisman, *Self-Assembling Peptide Coatings Designed for Highly Luminescent Suspension of Single-Walled Carbon Nanotubes.* Journal of the American Chemical Society, 2008. **130**(50): p. 17134-17140.
98. M. Corti, L. Cantu, P. Brocca, and E. Del Favero, *Self-assembly in glycolipids.* Curr. Opin. Colloid Interface Sci., 2007. **12**(3): p. 148-154.
99. H.A. van Doren, E. Smits, J.M. Pestman, J.B.F.N. Engberts, and R.M. Kellogg, *Mesogenic sugars. From aldoses to liquid crystals and surfactants.* Chemical Society Reviews, 2000. **29**(3): p. 183-199.
100. C.M. Paleos and D. Tsiourvas, *Thermotropic Liquid Crystals Formed by Intermolecular Hydrogen Bonding Interactions.* Angewandte Chemie International Edition in English, 1995. **34**(16): p. 1696-1711.
101. C.R. Noller and W.C. Rockwell, *The Preparation of Some Higher Alkylglucosides.* Journal of the American Chemical Society, 1938. **60**(9): p. 2076-2077.
102. T. Imura, Y. Hikosaka, W. Worakitkanchanakul, H. Sakai, M. Abe, M. Konishi, H. Minamikawa, and D. Kitamoto, *Aqueous-Phase Behavior of Natural Glycolipid Biosurfactant Mannosylerythritol Lipid A: Sponge, Cubic, and Lamellar Phases.* Langmuir, 2007. **23**(4): p. 1659-1663.
103. B. Donnio, S. Buathong, I. Bury, and D. Guillon, *Liquid crystalline dendrimers.* Chemical Society Reviews, 2007. **36**(9): p. 1495-1513.
104. C. Fong, T. Le, and C.J. Drummond, *Lyotropic liquid crystal engineering-ordered nanostructured small molecule amphiphile self-assembly materials by design.* Chemical Society Reviews, 2012. **41**(3): p. 1297-1322.
105. R. Hashim, A. Sugimura, H. Minamikawa, and T. Heidelberg, *Nature-like synthetic alkyl branched-chain glycolipids: a review on chemical structure and self-assembly properties.* Liq. Cryst., 2012. **39**(1): p. 1-17.
106. D. Philp and J.F. Stoddart, *Self-Assembly in Natural and Unnatural Systems.* Angewandte Chemie International Edition in English, 1996. **35**(11): p. 1154-1196.
107. H.M. von Minden, G. Milkereit, and V. Vill, *Effects of carbohydrate headgroups on the stability of induced cubic phases in binary mixtures of glycolipids.* Chemistry and Physics of Lipids, 2002. **120**(1–2): p. 45-56.
108. F. Dumoulin, D. Lafont, T.-L. Huynh, P. Boullanger, G. Mackenzie, J.J. West, and J.W. Goodby, *Synthesis and Liquid Crystalline Properties of Mono-, Di- and Tri-O-alkyl Pentaerythritol Derivatives Bearing Tri-, Di- or Monogalactosyl Heads: The Effects of Curvature of Molecular Packing on Mesophase Formation.* Chemistry – A European Journal, 2007. **13**(19): p. 5585-5600.
109. E. Fischer and B. Helferich, Liebigs Ann. Chem., 1911. **383**: p. 68.
110. P. Bault, P. Gode, G. Goethals, J.W. Goodby, J.A. Haley, S.M. Kelly, G.H. Mehl, G. Ronco, and P. Villa, *Liquid crystalline derivatives of galactose and galactitol: dependence of thermotropic mesomorphism on carbohydrate form.* Liq. Cryst., 1998. **25**(1): p. 31-45.
111. F. Dumoulin, D. Lafont, P. Boullanger, G. Mackenzie, G.H. Mehl, and J.W. Goodby, *Self-Organizing Properties of Natural and Related Synthetic Glycolipids.* Journal of the American Chemical Society, 2002. **124**(46): p. 13737-13748.
112. J.W. Goodby, J.A. Haley, M.J. Watson, G. Mackenzie, S.M. Kelly, and P. Letellier, *The effect of substituent position on the liquid crystalline properties of dodecyl-D-xylitols.* Liq. Cryst., 1997. **22**(4): p. 497-508.
113. Queneau Y., Juliette Gagnaire, Jon J West, G. Mackenziec, and a. JohnWGoodby, *The effect of molecular shape on the liquid crystal properties of the mono-O-(2-hydroxydodecyl) sucroses.* J. Mater. Chem., 2001. **11**: p. 2839-2844.
114. N. Laurent, D. Lafont, F. Dumoulin, P. Boullanger, G. Mackenzie, P.H.J. Kouwer, and J.W. Goodby, *Synthesis of Amphiphilic Phenylazophenyl Glycosides and a Study of Their Liquid Crystal Properties.* Journal of the American Chemical Society, 2003. **125**(50): p. 15499-15506.

Cette thèse est accessible à l'adresse : http://theses.insa-lyon.fr/publication/2013ISAL0001/these.pdf
© [R. Xu], [2013], INSA de Lyon, tous droits réservés

115. J.W. Goodby, J.A. Haley, G. Mackenzie, M.J. Watson, D. Plusquellec, and V. Ferrieres, *Amphitropic liquid-crystalline properties of some novel alkyl furanosides.* Journal of Materials Chemistry, 1995. **5**(12): p. 2209-2220.
116. J.W. Goodby, J.A. Haley, M.J. Watson, G. Mackenzie, S.M. Kelly, P. Letellier, O. Douillet, P. Gode, G. Goethals, G. Ronco, and P. Villa, *Substitution effects on the liquid crystalline properties of D,L-xylitol amphiphiles.* Liq. Cryst., 1997. **22**(3): p. 367-378.
117. R. Auzély-Velty, T. Benvegnu, D. Plusquellec, G. Mackenzie, J.A. Haley, and J.W. Goodby, *Self-Organization and Formation of Liquid Crystal Phases by Molecular Templates Related to Membrane Components of Archaebacteria.* Angewandte Chemie International Edition, 1998. **37**(18): p. 2511-2515.
118. S.T. Hyde, *Identification of lyotropic liquid crystalline mesophases.* 2001. **Handbook of Applied Surface and Colloid Chemistry, (K. Holmberg, ed.)**: p. 299-332.
119. N.M. Xavier and A.P. Rauter, *Sugars containing α,β-unsaturated carbonyl systems: synthesis and their usefulness as scaffolds in carbohydrate chemistry.* Carbohydrate Research, 2008. **343**(10–11): p. 1523-1539.
120. N.M. Xavier, A.P. Rauter, and Y. Queneau, *Carbohydrate-Based Lactones: Synthesis and Applications*, in *Carbohydrates in Sustainable Development Ii: A Mine for Functional Molecules and Materials*, A.P. Rauter, P. Vogel, and Y. Queneau, Editors. 2010, Springer-Verlag Berlin: Berlin. p. 19-62.
121. A. Furstner, *Total syntheses and biological assessment of macrocyclic glycolipids.* European Journal of Organic Chemistry, 2004(5): p. 943-958.
122. C. Taillefumier and Y. Chapleur, *Synthesis and Uses of exo-Glycals.* Chemical Reviews, 2004. **104**(1): p. 263-292.
123. D.J. Ager and M.B. East, *The synthesis of carbohydrate derivatives from acyclic precursors.* Tetrahedron, 1993. **49**(26): p. 5683-5765.
124. I. Lundt, *Aldonolactones as chiral synthons*, in *Glycoscience Synthesis of Substrate Analogs and Mimetics*, H. Driguez and J. Thiem, Editors. 1997. p. 117-156.
125. M. Bierenstiel and M. Schlaf, *delta-galactonolactone: Synthesis, isolation, and comparative structure and stability analysis of an elusive sugar derivative.* European Journal of Organic Chemistry, 2004(7): p. 1474-1481.
126. I. Isaac, I. Staslk, D. Beaupère, and R. Uzan, *A new and direct access to glycono-1,4-lactones from glycopyranoses by regioselective oxidation and subsequent ring restriction.* Tetrahedron Lett., 1995. **36**(3): p. 383-386.
127. M.M. Ahmed, B.P. Berry, T.J. Hunter, D.J. Tomcik, and G.A. O'Doherty, *De Novo Enantioselective Syntheses of Galacto-Sugars and Deoxy Sugars via the Iterative Dihydroxylation of Dienoate.* Organic Letters, 2005. **7**(4): p. 745-748.
128. M.M. Ahmed and G.A. O'Doherty, *De novo asymmetric syntheses of C-4-substituted sugars via an iterative dihydroxylation strategy.* Carbohydrate Research, 2006. **341**(10): p. 1505-1521.
129. S. Ramachandran, P. Fontanille, A. Pandey, and L. C, *Gluconic Acid: Properties, Applications and Microbial Production.* Food Technol. Biotechnol., 2006. **44**(2): p. 185-195.
130. V. Ferrières, J.-N. Bertho, and D. Plusquellec, *A convenient synthesis of alkyl d-glycofuranosiduronic acids and alkyl d-glycofuranosides from unprotected carbohydrates.* Carbohydrate Research, 1998. **311**(1–2): p. 25-35.
131. M. Roussel, S. Moutard, B. Perly, M. Lefeuvre, T. Benvegnu, and D. Plusquellec, *β-Anomeric selectivity in the glycosidation of d-mannofuranurono-6,3-lactone catalyzed by boron trifluoride diethyl etherate.* Carbohydrate Research, 2003. **338**(4): p. 375-378.
132. R. Colombo, M. Anastasia, P. Rota, and P. Allevi, *The first synthesis of N-acetylneuraminic acid 1,7-lactone.* Chemical Communications, 2008. **0**(43): p. 5517-5519.
133. J. Yin and T. Linker, *Convenient Synthesis of Bicyclic Carbohydrate 1,2-Lactones and Their Stereoselective Opening to 1-Functionalized Glucose Derivatives.* Chemistry – A European Journal, 2009. **15**(1): p. 49-52.

Cette thèse est accessible à l'adresse : http://theses.insa-lyon.fr/publication/2013ISAL0001/these.pdf
© [R. Xu], [2013], INSA de Lyon, tous droits réservés

134. J.P. Gesson, J.C. Jacquesy, and M. Mondon, *Enantiodivergent synthesis of (+) and (−) altholactone from D-glucose. Preparation and cytotoxic activity of analogs.* Tetrahedron, 1989. **45**(9): p. 2627-2640.
135. L. Andersson and L. Kenne, *Lactones of methyl 3-O-[(R)- and (S)-1-carboxyethyl]-α-d-gluco-, galacto-, and manno-pyranosides.* Carbohydrate Research, 2000. **329**(2): p. 257-268.
136. S. Trombotto, A. Bouchu, G. Descotes, and Y. Queneau, *Hydrogen peroxide oxidation of palatinose and trehalulose: direct preparation of carboxymethyl α-d-glucopyranoside.* Tetrahedron Lett., 2000. **41**(43): p. 8273-8277.
137. S. Trombotto, M. Danel, J. Fitremann, A. Bouchu, and Y. Queneau, *Straightforward Route for Anchoring a Glucosyl Moiety onto Nucleophilic Species: Reaction of Amines and Alcohols with Carboxymethyl 3,4,6-Tri-O-acetyl-α-d-glucopyranoside 2-O-Lactone.* The Journal of Organic Chemistry, 2003. **68**(17): p. 6672-6678.
138. R. Pierre, S. Chambert, F. Alirachedi, M. Danel, S. Trombotto, A. Doutheau, and Y. Queneau, *Carboxymethyl glucosides and carboxymethyl glucoside lactones: A detailed study of their preparation by oxidative degradation of disaccharides.* Comptes Rendus Chimie, 2008. **11**(1–2): p. 61-66.
139. A. Listkowski, P. Ing, R. Cheaib, S. Chambert, A. Doutheau, and Y. Queneau, *Carboxymethylglycoside lactones (CMGLs): structural variations on the carbohydrate moiety.* Tetrahedron: Asymmetry, 2007. **18**(18): p. 2201-2210.
140. R. Cheaib, A. Listkowski, S. Chambert, A. Doutheau, and Y. Queneau, *Synthesis of new mono- and disaccharidic carboxymethylglycoside lactones (CMGLs) and their use toward 1,2-bisfunctionalized carbohydrate synthons.* Tetrahedron: Asymmetry, 2008. **19**(16): p. 1919-1933.
141. A. Le Chevalier, R. Pierre, R. Kanso, S. Chambert, A. Doutheau, and Y. Queneau, *Preparation of new amide-linked pseudodisaccharides by the carboxymethylglycoside lactone (CMGL) strategy.* Tetrahedron Lett., 2006. **47**(14): p. 2431-2434.
142. F. Ménard, V. Sol, C. Ringot, R. Granet, S. Alves, C.L. Morvan, Y. Queneau, N. Ono, and P. Krausz, *Synthesis of tetraglucosyl- and tetrapolyamine–tetrabenzoporphyrin conjugates for an application in PDT.* Bioorganic & Medicinal Chemistry, 2009. **17**(22): p. 7647-7657.
143. C. Barsu, R. Cheaib, S. Chambert, Y. Queneau, O. Maury, D. Cottet, H. Wege, J. Douady, Y. Bretonniere, and C. Andraud, *Neutral push-pull chromophores for nonlinear optical imaging of cell membranes.* Organic & Biomolecular Chemistry, 2010. **8**(1): p. 142-150.
144. N.M. Xavier, Y. Queneau, and A.P. Rauter, *Exploitation of Furanoid 5-Azido-3-C-Branched-Chain Sugars Towards Highly Functionalized Nitrogen-Containing Carbohydrate Derivatives.* European Journal of Organic Chemistry, 2011(4): p. 713-720.
145. O. Abdelkader, S. Moebs-Sanchez, Y. Queneau, J. Bernard, and E. Fleury, *Generation of well-defined clickable glycopolymers from aqueous RAFT polymerization of isomaltulose-derived acrylamides.* Journal of Polymer Science Part A: Polymer Chemistry, 2011. **49**(6): p. 1309-1318.
146. J. Chen, Y. Miao, S. Chambert, J. Bernard, E. Fleury, and Y. Queneau, *Carboxymethyl glycoside lactone (CMGL) synthons: Scope of the method and preliminary results on step growth polymerization of α-azide-ω-alkyne glycomonomers.* Science China: Chemistry, 2010. **53**(9): p. 1880-1887.
147. Chambert S., Alain Doutheau, and a.Y. Queneau, *Synthesis and Thermotropic Behavior of Simple New Glucolipid Amides.* J. Carbohydr. Chem 2007. **26**: p. 27-39.
148. J. Xue, J. Wu, and Z. Guo, *A New Reaction for the Direct Conversion of 4-Azido-4-deoxy-d-galactoside into a 4-Deoxy-d-erythro-hexos-3-ulose.* Organic Letters, 2004. **6**(9): p. 1365-1368.
149. P.V. Murphy, J.L. O'Brien, L.J. Gorey-Feret, and A.B. Smith Iii, *Synthesis of novel HIV-1 protease inhibitors based on carbohydrate scaffolds.* Tetrahedron, 2003. **59**(13): p. 2259-2271.

Cette thèse est accessible à l'adresse : http://theses.insa-lyon.fr/publication/2013ISAL0001/these.pdf
© [R. Xu], [2013], INSA de Lyon, tous droits réservés

150. N. Tanaka, I. Ogawa, S. Yoshigase, and J. Nokami, *Regioselective ring opening of benzylidene acetal protecting group(s) of hexopyranoside derivatives by DIBAL-H.* Carbohydrate Research, 2008. **343**(15): p. 2675-2679.
151. S. Hanessian and A.P.A. Staub, *Le fluoroborate de tritylpyridinium : un reactif efficace de tritylation.* Tetrahedron Lett., 1973. **14**(37): p. 3555-3558.
152. A. Smith, P. Nobmann, G. Henehan, P. Bourke, and J. Dunne, *Synthesis and antimicrobial evaluation of carbohydrate and polyhydroxylated non-carbohydrate fatty acid ester and ether derivatives.* Carbohydrate Research, 2008. **343**(15): p. 2557-2566.
153. C. Bayle and A. Gadelle, *An easy route to methyl 6-O-alkyl glycosides.* Tetrahedron Lett., 1994. **35**(15): p. 2335-2336.
154. R. Miethchen, J. Holz, H. Prade, and A. Liptak, *Amphiphilic and mesogenic carbohydrates - II. sysnthesis and Characterisation of mono-o-(n-alkyl)-d-glucose derivates.* Tetrahedron, 1992. **48**(15): p. 3061-3068.
155. D.L. Dorset and J.P. Rosenbusch, *Solid state properties of anomeric 1-O-n-octyl-d-glucopyranosides.* Chemistry and Physics of Lipids, 1981. **29**(4): p. 299-307.
156. D.C. Carter, J.R. Ruble, and G.A. Jeffrey, *The crystal structure of heptyl 1-thio-α-d-mannopyranoside, a liquid-crystal precursor.* Carbohydrate Research, 1982. **102**(1): p. 59-67.
157. G. Gimpl and K. Gehrig-Burger, *Cholesterol Reporter Molecules.* Bioscience Reports, 2007. **27**(6): p. 335-358.
158. K. Urata and N. Takaishi, *Cholesterol as synthetic building blocks for artificial lipids with characteristic physical, chemical and biological properties.* European Journal of Lipid Science and Technology, 2001. **103**(1): p. 29-39.
159. V. Rondelli, G. Fragneto, S. Motta, E. Del Favero, P. Brocca, S. Sonnino, and L. Cantù, *Ganglioside GM1 forces the redistribution of cholesterol in a biomimetic membrane.* Biochimica et Biophysica Acta (BBA) - Biomembranes, 2012. **1818**(11): p. 2860-2867.
160. R. Gniadecki, N. Christoffersen, and H.C. Wulf, *Cholesterol-rich plasma membrane domains (lipid rafts) in keratinocytes: Importance in the baseline and UVA-induced generation of reactive oxygen species.* J. Invest. Dermatol., 2002. **118**(4): p. 582-588.
161. J. Fantini and F.J. Barrantes, *Sphingolipid/cholesterol regulation of neurotransmitter receptor conformation and function.* Biochimica et Biophysica Acta (BBA) - Biomembranes, 2009. **1788**(11): p. 2345-2361.
162. V.A. Mallia and N. Tamaoki, *Design of chiral dimesogens containing cholesteryl groups; formation of new molecular organizations and their application to molecular photonics.* Chemical Society Reviews, 2004. **33**(2): p. 76-84.
163. C.V. Yelamaggad, G. Shanker, U.S. Hiremath, and S.K. Prasad, *Cholesterol-based nonsymmetric liquid crystal dimers: an overview.* Journal of Materials Chemistry, 2008. **18**(25): p. 2927-2949.
164. V. Faivre, P.-L. Bardonnet, P. Boullanger, H. Amenitsch, M. Ollivon, and F.o. Falson, *Self-Organization of Synthetic Cholesteryl Oligoethyleneglycol Glycosides in Water.* Langmuir, 2009. **25**(16): p. 9424-9431.
165. G.C. Vougioukalakis and R.H. Grubbs, *Ruthenium-Based Heterocyclic Carbene-Coordinated Olefin Metathesis Catalysts.* Chemical Reviews, 2010. **110**(3): p. 1746-1787.
166. A. Kurek-Tyrlik, J. Wicha, A. Zarecki, and G. Snatzke, *Methylation and hydroxymethylation of allylic alcohols via radical cyclization. Methodology for stereoselective construction of an aliphatic chain in application to sterol synthesis.* The Journal of Organic Chemistry, 1990. **55**(11): p. 3484-3492.
167. S.W. Cha, J.-I. Jin, D.-C. Kim, and W.-C. Zin, *Combined Type Liquid Crystalline Poly(oxy-1,4-phenyleneoxyterephthaloyl)s Bearing Cholesterol Pendants Attached through Polymethylene Spacers.* Macromolecules, 2001. **34**(15): p. 5342-5348.
168. J.W. Morzycki, Z. Łotowski, L. Siergiejczyk, P. Wałejko, S. Witkowski, J. Kowalski, J. Płoszyńska, and A. Sobkowiak, *A selective electrochemical method of glycosylation of 3β-hydroxy-Δ5-steroids.* Carbohydrate Research, 2010. **345**(8): p. 1051-1055.

Cette thèse est accessible à l'adresse : http://theses.insa-lyon.fr/publication/2013ISAL0001/these.pdf
© [R. Xu], [2013], INSA de Lyon, tous droits réservés

169. A. Zimmer, S. Atmaca-Abdel Aziz, M. Gilbert, D. Werner, and C.R. Noe, *Synthesis of cholesterol modified cationic lipids for liposomal drug delivery of antisense oligonucleotides.* European Journal of Pharmaceutics and Biopharmaceutics, 1999. **47**(2): p. 175-178.
170. M. Vendrell, D. Zhai, J.C. Er, and Y.-T. Chang, *Combinatorial Strategies in Fluorescent Probe Development.* Chemical Reviews, 2012. **112**(8): p. 4391-4420.
171. O. Maier, V. Oberle, and D. Hoekstra, *Fluorescent lipid probes: some properties and applications (a review).* Chemistry and Physics of Lipids, 2002. **116**(1-2): p. 3-18.
172. R.W. Sinkeldam, N.J. Greco, and Y. Tor, *Fluorescent Analogs of Biomolecular Building Blocks: Design, Properties, and Applications.* Chemical Reviews, 2010. **110**(5): p. 2579-2619.
173. H. Kobayashi, M. Ogawa, R. Alford, P.L. Choyke, and Y. Urano, *New Strategies for Fluorescent Probe Design in Medical Diagnostic Imaging.* Chemical Reviews, 2009. **110**(5): p. 2620-2640.
174. H. Chen, C. Bai, and X. Wang, *Application of probes in live cell imaging.* Journal of Epithelial Biology & Pharmacology, 2010. **3**: p. 40-48.
175. A.M. Scutaru, M. Krüger, M. Wenzel, J. Richter, and R. Gust, *Investigations on the Use of Fluorescence Dyes for Labeling Dendrimers: Cytotoxicity, Accumulation Kinetics, and Intracellular Distribution.* Bioconjugate Chemistry, 2010. **21**(12): p. 2222-2226.
176. R. Ishitsuka, T. Saito, H. Osada, Y. Ohno-Iwashita, and T. Kobayashi, *Fluorescence image screening for chemical compounds modifying cholesterol metabolism and distribution.* J. Lipid Res. **52**(11): p. 2084-2094.
177. D. W¨ustner, *Fluorescent sterols as tools in membrane biophysics and cell biology.* Chemistry and Physics of Lipids, 2007. **146**: p. 1–25.
178. L.A. Bagatolli, *To see or not to see: Lateral organization of biological membranes and fluorescence microscopy.* Biochim. Biophys. Acta-Biomembr., 2006. **1758**(10): p. 1541-1556.
179. L.D. Lavis and R.T. Raines, *Bright Ideas for Chemical Biology.* ACS Chemical Biology, 2008. **3**(3): p. 142-155.
180. T. Parasassi, E. Krasnowska, L. Bagatolli, and E. Gratton, *Laurdan and Prodan as Polarity-Sensitive Fluorescent Membrane Probes.* Journal of Fluorescence, 1998. **8**(4): p. 365-373.
181. L.A. Bagatolli, S.A. Sanchez, T. Hazlett, and E. Gratton, *Giant vesicles, laurdan, and two-photon fluorescence microscopy: Evidence of lipid lateral separation in bilayers.* Biophotonics, Pt A, 2003. **360**: p. 481-500.
182. H.M. Kim, H.-J. Choo, S.-Y. Jung, Y.-G. Ko, W.-H. Park, S.-J. Jeon, C.H. Kim, T. Joo, and B.R. Cho, *A Two-Photon Fluorescent Probe for Lipid Raft Imaging: C-Laurdan.* ChemBioChem, 2007. **8**(5): p. 553-559.
183. H.M. Kim, B.R. Kim, H.-J. Choo, Y.-G. Ko, S.-J. Jeon, C.H. Kim, T. Joo, and B.R. Cho, *Two-Photon Fluorescent Probes for Biomembrane Imaging: Effect of Chain Length.* ChemBioChem, 2008. **9**(17): p. 2830-2838.
184. M. Cheniour, *étude de l'inteaction de la créatine kinase mitochondrial avec des membranes biomimétiques et développement de sondes de fluorescence en vue d'une caracterisation fine de l'organisation latérale des lipids membranaires*, 2012, Universite Lyon 1.
185. S.P. Rannard and N.J. Davis, *The Selective Reaction of Primary Amines with Carbonyl Imidazole Containing Compounds: Selective Amide and Carbamate Synthesis.* Organic Letters, 2000. **2**(14): p. 2117-2120.
186. H. Li, M.-a. Hao, L. Wang, W. Liang, and K. Chen, *Preparation of Mono Boc-Protected Unsymmetrical Diamines.* Organic Preparations and Procedures International, 2009. **41**(4): p. 301-307.
187. C.M. So and F.Y. Kwong, *Palladium-catalyzed cross-coupling reactions of aryl mesylates.* Chemical Society Reviews, 2011. **40**(10): p. 4963-4972.
188. H. Li, C.C.C. Johansson Seechurn, and T.J. Colacot, *Development of Preformed Pd Catalysts for Cross-Coupling Reactions, Beyond the 2010 Nobel Prize.* ACS Catalysis, 2012. **2**(6): p. 1147-1164.

Cette thèse est accessible à l'adresse : http://theses.insa-lyon.fr/publication/2013ISAL0001/these.pdf
© [R. Xu], [2013], INSA de Lyon, tous droits réservés

189. B.H. Lipshutz, D.W. Chung, and B. Rich, *Aminations of Aryl Bromides in Water at Room Temperature.* Advanced Synthesis & Catalysis, 2009. **351**(11-12): p. 1717-1721.
190. T. Granjon, M.-J. Vacheron, C. Vial, and R. Buchet, *Mitochondrial Creatine Kinase Binding to Phospholipids Decreases Fluidity of Membranes and Promotes New Lipid-Induced β Structures As Monitored by Red Edge Excitation Shift, Laurdan Fluorescence, and FTIR†.* Biochemistry, 2001. **40**(20): p. 6016-6026.

Cette thèse est accessible à l'adresse : http://theses.insa-lyon.fr/publication/2013ISAL0001/these.pdf
© [R. Xu], [2013], INSA de Lyon, tous droits réservés